

Synthesis of α -Aminoboronates and PBP Pincer Palladium Boryl Complexes



Dissertation zur Erlangung des naturwissenschaftlichen Doktorgrades
der Julius-Maximilians-Universität Würzburg

Wenbo Ming

aus Jinan, V.R. China

Würzburg 2020



Eingereicht bei der Fakultät für Chemie und Pharmazie am

Gutachter der schriftlichen Arbeit

1. Gutachter: Prof. Dr. Dr. h. c. Todd B. Marder
2. Gutachter: Prof. Dr. rer. nat. habil. Udo Radius

Prüfer des öffentlichen Promotionskolloquiums

1. Prüfer: Prof. Dr. Dr. h. c. Todd B. Marder
2. Prüfer: Prof. Dr. rer. nat. habil. Udo Radius
3. Prüfer: Priv.-Doz. Dr. Florian Beuerle

Datum des öffentlichen Promotionskolloquiums

Doktorurkunde ausgehändigt am

谨此献给我的家人
Für meine Familie

stay hungry. stay foolish.

Steve Jobs

Die Experimente zur vorliegenden Arbeit wurden in der Zeit von Oktober 2015 bis Januar 2020 am Institut für Anorganische Chemie der Julius - Maximilians - Universität Würzburg unter der Aufsicht von Prof. Dr. Dr. h. c. Todd B. Marder durchgeführt.

Acknowledgements

First and foremost, I thank **Prof. Dr. Dr. h. c. Todd B. Marder** for this great opportunity that he provided me to do my doctoral research here at the University of Würzburg. I want to thank him for his great help to apply for a scholarship from the China Scholarship Council (CSC). I also appreciate that he encouraged me to communicate with others. During the past four years, he helped me with patient discussions, great ideas and useful suggestions in science and life.

I would like to thank the CSC and the Chinese government for their kind and generous financial support of my studies in Germany. I also thank the staffs of the CSC and the Generalkonsulat der Volksrepublik China in München who helped me during my time in Germany.

I would like to thank Dr. Rüdiger Bertermann and Marie-Luise Schäfer for their kind help with NMR spectroscopy. I want to thank Sabine Timmroth and Liselotte Michels for the elemental analysis measurements. I want to thank Dr. Stephan Wagner for teaching me to do the routine maintenance of the GC-MS, and the massive number of GC-MS repair services. I am very grateful to Christoph Mahler for countless HRMS measurements and general support in the laboratory. I would like to thank Sabine Lorenzen for the SPS solvent supply and teaching me many experimental skills and about safety. I would like to thank Hildegard Holzinger and Sarina Berger for their assistance in ordering chemicals and general lab supply. I would like to thank Maria Eckhardt and Cornelia Walter for their assistance during my PhD study.

I would like to thank Prof. Dr. Andrei Yudin and his group (University of Toronto) for their helpful discussions and suggestions for chapter one. I would like to thank Dr. Zhenguo Huang (University of Technology Sydney), Prof. Dr. Zhaoyang Wang (South China Normal

Acknowledgements

University), and Prof. Dr. Shasha Li (The First Affiliated Hospital of Jinan University) for their encouragement and suggestions.

To all my laboratory colleagues, I want to thank them for their help and a lot of fun. I would like to thank Dr. Alexandra Friedrich, Johannes Krebs, Florian Kerner, Zhu Wu, and Yudha Prawira Budiman for measuring and solving crystal structures. I would like to thank Jan Maier for helping to draw cover art for my papers, and many discussions about NMR spectroscopy. I would like to thank Matthias Ferger for helping to translate the thesis summary into German. I would like to thank Prof. Dr. Xiaoning Guo, Prof. Dr. Xiaoling Luo, Dr. Stefanie Griesbeck, Dr. Jörn Nitsh, Dr. Jian Zhao, Dr. Xiangqing Jia, Xiaocui Liu, and Zhu Wu for their numerous helpful discussions and suggestions regarding my research work. Dr. Julia Merz, thank you for giving important information about writing this thesis, its submission, and defense. Florian Rauch, thank you for giving me tons of suggestions about the defense. I want to thank Dr. Martin Eck for teaching me how to do quantitation by GC-MS as well as the introduction to using the glove box. I want to thank Jiang He for helping me so much with SPS solvents and many scientific discussions. Special thanks to Prof. Lei Ji, Prof. Qing Ye, Prof. Changjiang Yao, Dr. Jing Zhou, Dr. Lujia Mao, Dr. Shubhankar Kumar Bose, Dr. Shishir Ghosh, Dr. Goutam Kumar Kole, Dr. Hua Wang, Dr. Ying Ying Chia, Mingming Huang, Zhiqiang Liu, Robert Ricker, Yaming Tian, for their infinite help.

I want to thank all of the people from the Inorganic Chemistry Institute for making my time here really enjoyable.

To all my Chinese friends (Kun Peng, Xiaodong Duan, Shouguang Huang, Siyuan Liu, Dr. Meng Qu, Kang Du, Ruiqi Liu, Yuehui Tian, Ting Gao, Mo Zhu, Fang Wu, Kang Cui, Jingjing Meng, Peipei Fei, and Shitong Du), I want to thank you graciously for making me feel at home in this foreign country. I will never forget the happy times we have had during the past four years.

Last but not least, I would like to thank the members of my family, as they were and will always be the greatest source of power in my life. I thank my parents for raising me and for

Acknowledgements

their support, no matter what I do. No words can be used to express my appreciation to them what they did for me. I want to thank my parents-in-law for the care and support they have given me and my wife through the years we have been abroad. Thanks to my brother-in-law (Junwei Liu) and sister-in-law (Zhangmei Cao) for always encouraging me and having an open ear. I want to thank my wife (Xiaocui Liu) for her support and discussions in science and life. She is always there when I need her. Finally, I just want to say to the members of my family: "I love you forever!"

Thanks

List of Publications

The publications listed below are partly reproduced in this dissertation with permission from American Chemical Society. The table itemizes at which position in this work the paper has been reproduced.

Publication	Position
W. Ming, H. Soor, X. Liu, A. Trofimova, A. K. Yudin*, T. B. Marder*, <i>Chem. Soc. Rev.</i> , submitted.	Chapter 1
W. Ming, X. Liu, A. Friedrich, J. Krebs, and T. B. Marder*, <i>Org. Lett.</i> , 2019, DOI: 10.1021/acs.orglett.9b03773.	Chapter 2

Further publications:

1. X. Liu, W. Ming, A. Friedrich, F. Kerner, T. B. Marder*, *Angew. Chem. Int. Ed.*, 2019, DOI: 10.1002/anie.201908466.
2. X. Liu, W. Ming, Y. Zhang, A. Friedrich, T. B. Marder*, *Angew. Chem. Int. Ed.*, 2019, DOI: 10.1002/anie.201909376.

List of Abbreviations

acac	Acetylacetonate
aq.	Aqueous
B ₂ cat ₂	Bis(catecholato)diboron
B ₂ (OH) ₄	Tetrahydroxydiboron
B ₂ pin ₂	Bis(pinacolato)diboron
bpy	2,2'-Bipyridine
cod	1,5-Cyclooctadiene
CPME	Cyclopentyl methyl ether
DABCO	1,4-Diazabicyclo[2.2.2]octane
dan	1,8-Diaminonaphthalene
dba	Dibenzylideneacetone
DBU	1,8-Diazabicyclo(5.4.0)undec-7-ene
DCM	Dichloromethane
DFT	Density functional theory
DMAP	4-Dimethylaminopyridine
DMF	<i>N,N</i> -Dimethylformamide
DPEphos	<i>bis</i> [(2-Diphenylphosphino)phenyl] ether
dppp	1,3-Bis(diphenylphosphino)propane
dtbbpy	4,4'-Di- <i>tert</i> -butyl-2,2'-dipyridyl
equiv	Equivalents
FDA	Food and Drug Administration
GC-MS	Gas chromatography-mass spectrometry
ICy	1,3-Dicyclohexylimidazol-2-ylidene
IMes	1,3-Dimesitylimidazol-2-ylidene
IPr	1,3- <i>bis</i> (2,6-Diisopropylphenyl)imidazol-2-ylidene

List of Abbreviations

LDA	Lithium diisopropylamide
LiHMDS	Lithium bis(trimethylsilyl)amide
MIDA	Trivalent <i>N</i> -methyliminodiacetic acid
MTBE	Methyl <i>tert</i> -butyl ether
NBS	<i>N</i> -Bromosuccinimide
NHC	<i>N</i> -Heterocyclic carbene
NMR	Nuclear magnetic resonance
PCy ₃	Tricyclohexylphosphine
phen	1,10-Phenanthroline
Piv	Pivaloyl
Qphos	1,2,3,4,5-Pentaphenyl-1'-(di- <i>tert</i> -butylphosphino)ferrocene
rt	Room temperature
TBAF	Tetra- <i>n</i> -butylammonium fluoride
TEA	Triethylamine
TFA	Trifluoroacetic acid
THF	Tetrahydrofuran
TMSCl	Trimethylsilyl chloride
Xphos	2-Dicyclohexylphosphino-2',4',6'-triisopropylbiphenyl

Table of Contents

1	α -Aminoboronates: Recent advances in their preparation and synthetic applications ..3	
1.1	Abstract	3
1.2	General introduction to α -aminoboronates	3
1.3	Development of synthetic routes	7
1.3.1	From α -haloboronic esters	7
1.3.2	From imines	8
1.3.3	From alkenes	14
1.3.4	From alkynes	17
1.3.5	From indoles	18
1.3.6	Via C-H bond functionalization	20
1.3.7	Miscellaneous routes	23
1.4	Synthetic applications	27
1.4.1	Retaining the α -aminoboronate core structure	28
1.4.2	Not retaining the α -aminoboronate core structure	29
1.5	Summary and outlook	39
2	The Borono-Strecker reaction: Synthesis of α -aminoboronates <i>via</i> a multicomponent reaction of carbonyl compounds, amines and B ₂ pin ₂	43
2.1	Abstract	43
2.2	Introduction	43
2.3	Results and discussions	45
2.3.1	Optimization of reaction conditions	45
2.3.2	Investigation of reaction scope	49
2.4	Mechanistic studies	53
2.4.1	Role of Ti(OEt) ₄ in the formation of imines	53
2.4.2	Role of Ti(OEt) ₄ and protons in the hydroboration process	55
2.4.3	Stepwise reaction	56

Table of Contents

2.4.4	Interaction of products 2-3a and 2-3y with DMAP	57
2.4.5	Proposed mechanism	59
2.5	Synthetic applications of α -aminoboronates	60
2.6	Summary	60
2.7	Experimental procedures and characterization data.....	61
2.7.1	General information	61
2.7.2	Experimental procedures	62
2.7.3	Compound characterization	64
2.7.4	Single-crystal X-ray diffraction studies	86
3	Concise synthesis of α -amino cyclic boronates <i>via</i> multicomponent coupling of salicylaldehydes, amines, and $B_2(OH)_4$	93
3.1	Abstract	93
3.2	Introduction.....	93
3.3	Results and discussions	95
3.3.1	Optimization of reaction conditions	95
3.3.2	Investigation of reaction scope.....	96
3.4	Mechanistic studies.....	99
3.4.1	Stepwise reaction	99
3.4.2	Reaction of salicylaldehyde 3-1a with different ratios of morpholine 3-2a	101
3.4.3	Reaction conducted in ethanol.....	104
3.4.4	Proposed mechanism	107
3.5	Summary	107
3.6	Experimental procedures and characterization data.....	108
3.6.1	General information	108
3.6.2	Experimental procedures	109
3.6.3	Compound characterization	110
3.6.4	Single-crystal X-ray diffraction studies	126
4	PBP pincer palladium boryl complexes: synthesis, structures, and catalytic activity	133

Table of Contents

4.1	Abstract	133
4.2	Introduction	133
4.3	Results and discussion	135
4.4	Catalytic activity test	137
4.5	Summary	138
4.6	Experimental procedures and characterization data	138
4.6.1	General information	138
4.6.2	Experimental procedures	140
4.6.3	Compound characterization	142
4.6.4	Single-crystal X-ray diffraction studies	147
	Summary	151
	Zusammenfassung	159
	Notes and references	167
	Appendix	179
	Affidavit	291
	Eidesstaatliche Erklärung	291

1 α -Aminoboronates: Recent advances in their preparation and synthetic applications

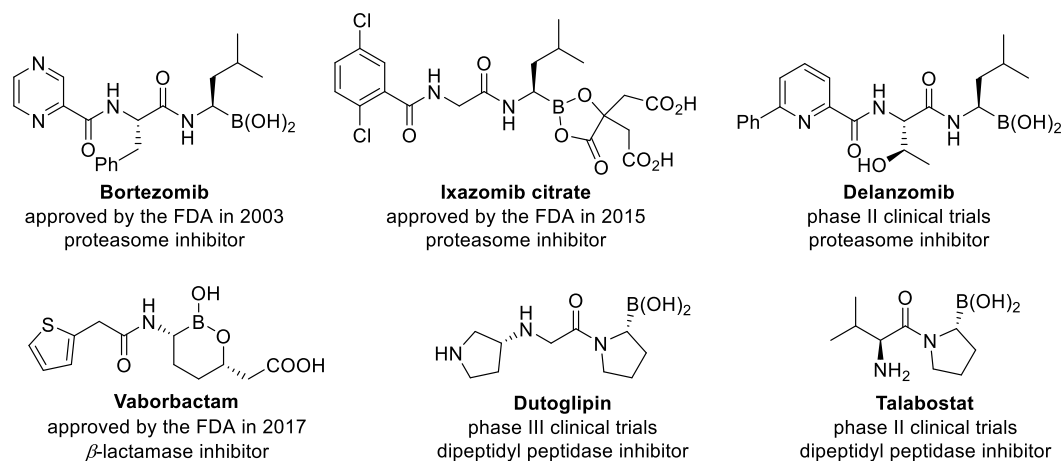
1.1 Abstract

As analogues of α -amino acids, α -aminoboronic acids and their derivatives are especially useful as bioactive agents. Thus far, three compounds containing an α -aminoboronate motif have been approved by the FDA as enzyme inhibitors, and more are currently undergoing clinical trials. In addition, α -aminoboronic acids and their derivatives have various applications in organic synthesis, *e.g.* as α -aminomethylation reagents for the synthesis of chiral nitrogen-containing molecules, as nucleophiles for preparing valuable vicinal amino alcohols, and as bis-nucleophiles in the construction of isoindolinones, *etc.* This chapter summarizes new methodology for the preparation of α -aminoboronates, including highlights of the asymmetric synthetic methods and explanations of the stereoselective manners. Their applications as versatile synthetic building blocks are also discussed.

1.2 General introduction to α -aminoboronates

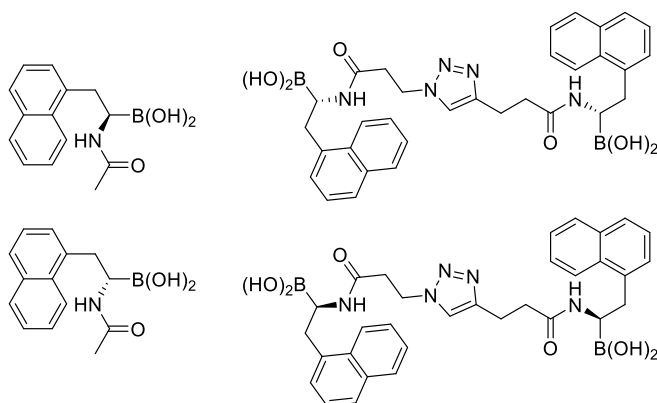
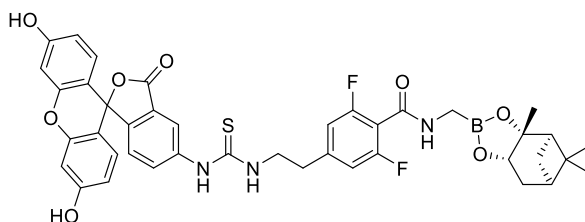
Without doubt, organoboron compounds have become among of the most useful species in chemistry due to their ease of preparation, and numerous applications in organic synthesis, pharmaceuticals and materials science.¹ In particular, as analogues of α -amino acids, α -aminoboronic acids and their derivatives are especially useful as bioactive agents, functional materials, and synthetic building blocks.² Bortezomib (trade name Velcade[®]) (Scheme 1-1) is the first boronic acid-containing compound and the first proteasome inhibitor to gain approval by the FDA in 2003 and by European authorities in 2004. It is used for the treatment of multiple myeloma (a cancer of the plasma cells), and mantle cell lymphoma (a cancer of the lymph nodes).³ Vaborbactam (Scheme 1-1) is a β -lactamase inhibitor based on a cyclic boronic acid pharmacophore. It has been used in trials investigating the treatment of bacterial infections in subjects with varying degrees of renal insufficiency.⁴ Over the past few years, a rise in the number of therapeutics based on the

α -aminoboronate motif has been accompanied by increasing efforts towards their efficient synthesis.^{1f,2e,2f,5} Some exemplary structures are drawn in Scheme 1-1.



Scheme 1-1 Examples of bioactive compounds possessing an α -aminoboronate motif.

In materials science, the Wang group reported the first water-soluble and stable α -aminoboronic acid carbohydrate sensors which showed a significant fluorescence change upon binding with three representative sugars, fructose, glucose, and sorbitol.⁶ Later, they synthesized two bis- α -aminoboronic acids using click chemistry, which significantly enhanced the binding ability with oligosaccharides as compared to their mono- α -aminoboronic acid counterparts (Scheme 1-2a).⁷ In 2012, Schofield and co-workers developed a fluorescence polarization assay for penicillin-binding proteins (PBPs) and “serine” β -lactamases using an α -aminoboronic-acid-based, reversibly binding “tracer”.⁸ The tracer bound to three different PBPs with modest affinity and more tightly to the TEM1 serine β -lactamase. In addition, the tracer can be displaced by both β -lactams and boronic acids, which indicated its suitability for use in competition binding assays (Scheme 1-2b).

(a) Wang, 2009 and 2010**(b) Schofield, 2012**

Scheme 1-2 α -Aminoboronic acids and their derivatives which serve as carbohydrate sensors, and PBPs and serine β -lactamase tracers.

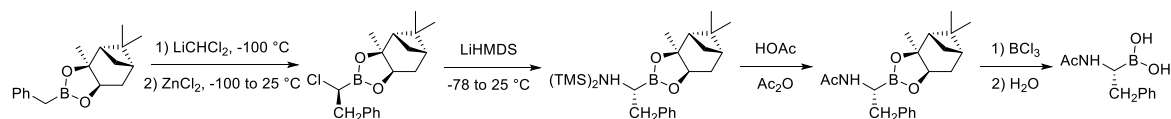
α -Aminoboronic acids and derivatives were first synthesized by Matteson and co-workers in the 1960s.⁹ Recent years have seen a rapid rise in the synthesis of diverse α -aminoboronates. This chapter summarizes the development of the methodology for the synthesis of α -aminoboronates. Different synthetic routes are categorized by different starting materials, e.g. alkylboronates, imines, alkenes, α -boryl isocyanates, α -amino acids, etc. Not all examples are illustrated; only those representing a milestone were selected (Scheme 1-3).^{2c,2g,10} In addition to their significant applications in drug discovery and materials science, α -aminoboronic acids and their derivatives have various applications in organic synthesis, e.g. as α -aminomethylation reagents for the synthesis of nitrogen-containing molecules which are found in a wide variety of alkaloid natural products and pharmaceuticals, as bis-nucleophiles in the construction of isoindolinones, and as nucleophiles for addition to ketones and aldehydes to form valuable vicinal amino alcohols, etc. Their applications as versatile synthons are summarized in Scheme 1-4, and are also discussed in this chapter.

1.3 Development of synthetic routes

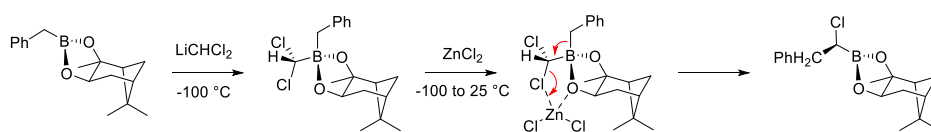
1.3.1 From α -haloboronic esters

The conventional method for preparing α -aminoboronic acids was developed by the Matteson group, and it has been used extensively in both academia and industry.¹¹ Boronic esters, containing a chiral pinanediol auxiliary, can undergo a diastereoselective homologation with dichloromethyl lithium to produce chiral α -chloroboronic esters, and further undergo stereospecific substitution with LiHMDS yielding α -aminoboronic esters (Scheme 1-5a).¹² The stereochemistry is controlled by the substrate. The carbon nucleophile attacks from the convex side of the alkyl boronate. The Lewis acid ZnCl_2 then binds to the less hindered oxygen atom facilitating the 1,2-rearrangement depicted in Scheme 1-5b.¹³ This protocol was successfully utilized in the enantioselective preparation of Bortezomib from isobutylboronic acid (Scheme 1-5c).¹⁴ Although Matteson's protocol afforded chiral α -aminoboronic esters in good yields, this procedure required several steps (Matteson's homologation, nucleophilic amination, deprotection of nitrogen, and deprotection of boron) and was synthetically challenging to execute.^{2c,12,15}

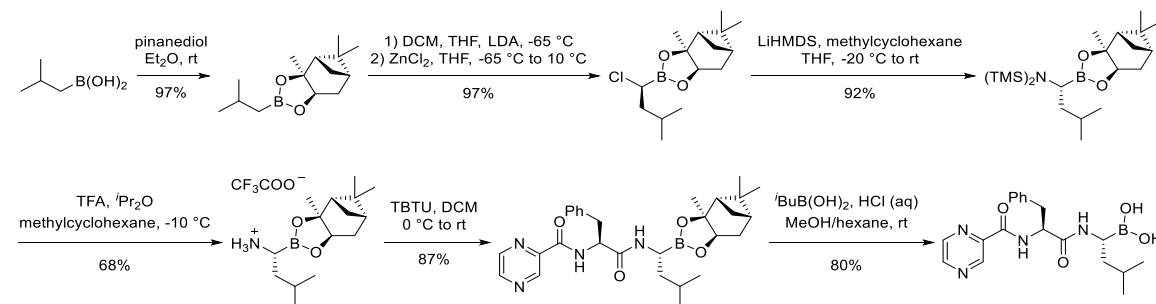
(a) Matteson, 1981



(b)



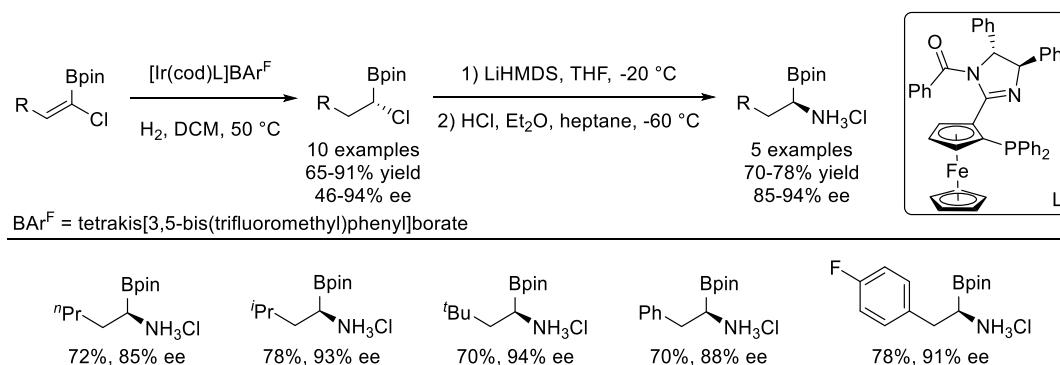
(c)



Scheme 1-5 Matteson's protocol for the synthesis of chiral α -aminoboronic acids, its stereochemistry, and application to the synthesis of Bortezomib.

Časar and co-workers reported an Ir-catalyzed chemoselective homogeneous asymmetric hydrogenation of (1-chloro-1-alkenyl)boronic esters to chiral (α -chloroalkyl)boronic esters.¹⁶ Using a modification of Matteson's method, nucleophilic substitution of chloride in (α -chloroalkyl)boronic esters with an equivalent of LiHMDS gave access to chiral α -aminoboronic esters (Scheme 1-6).¹⁷ The main drawback of this method is that tedious steps are required to prepare the starting (1-chloro-1-alkenyl)boronic esters from alkynes, including lithiation with ⁿBuLi, borylation with 2-isopropoxy-4,4,5,5-tetramethyl-1,3,2-dioxaborolane, hydrozirconation with Schwartz's reagent, and electrophilic chlorination with *N*-chlorosuccinimide.¹⁸

Časar, 2012 and 2013

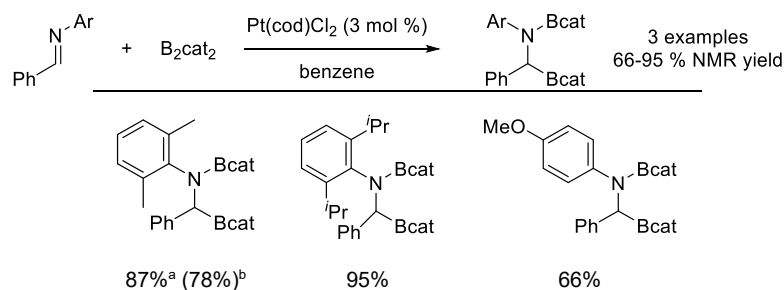


Scheme 1-6 Hydrogenation of (1-chloro-1-alkenyl)boronic esters, followed by C–Cl amination for the synthesis of chiral α -aminoboronic esters.

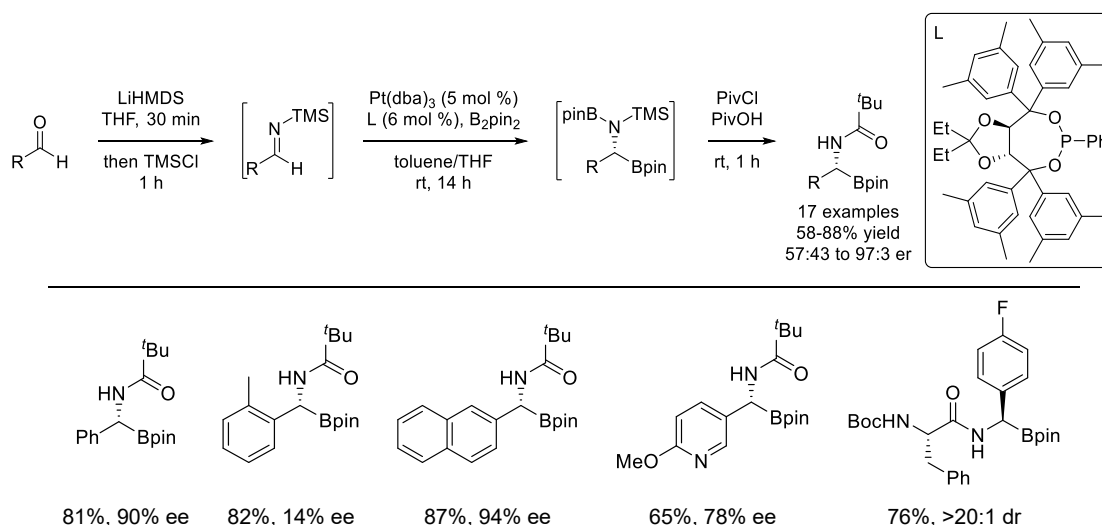
1.3.2 From imines

1.3.2.1 Pt-catalyzed diboration of aldimines

Platinum catalysts have been widely used for the diboration of unsaturated molecules, *e.g.* alkenes and alkynes.^{1d,19} In 2000, Baker and co-workers reported the diboration of aldimines using bis(catecholato)diboron (B_2cat_2) catalyzed by commercially available $\text{Pt}(\text{cod})\text{Cl}_2$.²⁰ This was the first catalytic synthesis of α -aminoboronate esters, even though this method was only suitable for aryl aldimines containing bulky or electron-donating substituents on the aryl group linked to the nitrogen atom (only three phenylaldimines were suitable substrates) (Scheme 1-7a).

(a) Baker, 2000

a) ¹H NMR yields; b) isolated yields are given in parentheses.

(b) Morcken, 2013

Scheme 1-7 Platinum-catalyzed diboration of aldimines.

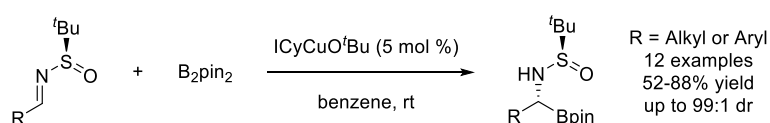
Morcken *et al.* found that enantioselective diboration of π -systems can be catalyzed by a chiral platinum-phosphonite complex.²¹ In 2013, they achieved the enantioselective addition of bis(pinacolato)diboron (B_2pin_2) to silylimines, which were generated *in situ* from aldehydes, LiHMDS, and TMSCl with the chiral platinum-phosphonite complex as catalyst.²² Desired chiral α -aminoboronate esters were obtained in moderate to good yields (58–88%), while several steps were needed, and aliphatic aldehydes were not suitable for this transformation (Scheme 1-7b).

1.3.2.2 Cu-catalyzed hydroboration of imines

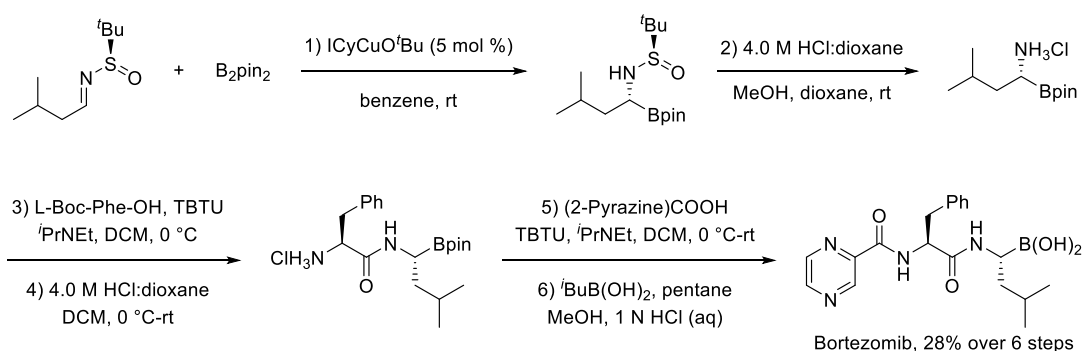
In 2008, Ellman and co-workers reported the first example of a copper-catalyzed hydroboration of *N-tert*-butanesulfinyl aldimines for the asymmetric synthesis of α -amino boronates,²³ but aryl imine substrates gave the desired products in only moderate yields

(52–61%) (Scheme 1-8a). The versatility of the *N*-sulfinyl α -amino boronate esters was demonstrated by their application in the efficient synthesis of Bortezomib (28% yield, 6 steps from *N*-sulfinyl aldimines) (Scheme 1-8b). Later, Sun and co-workers reported an improved protocol for the catalytic hydroboration of imines using benzimidazole-based *N*-heterocyclic carbenes (NHCs) as ligands.²⁴ One of the significant advantages of this approach is that the synthesis of α -amino boronic esters does not require operations to be carried out in a glovebox.

(a) Ellman, 2008



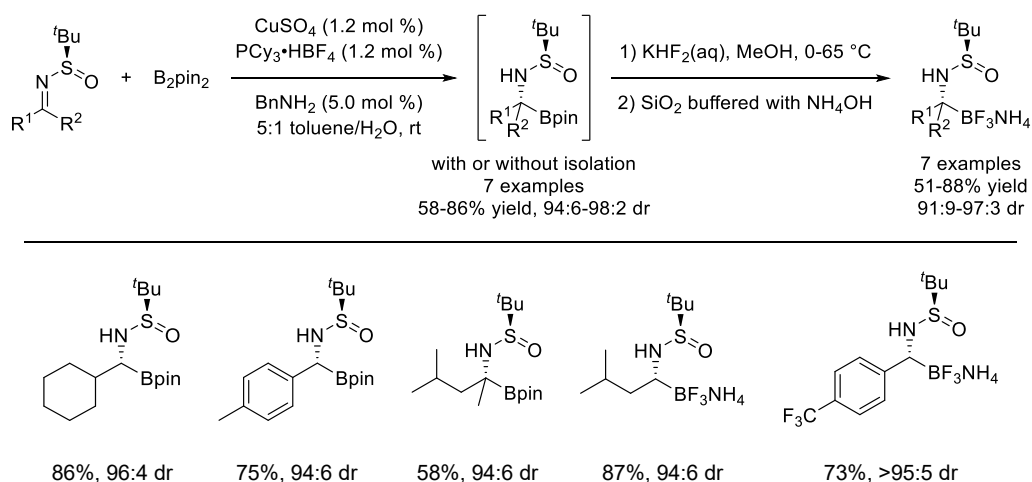
(b)



Scheme 1-8 Copper-catalyzed enantioselective hydroboration of aldimines, and its application to the synthesis of Bortezomib.

The Ellman group subsequently developed the asymmetric synthesis of α -amino boronates using an air- and moisture-stable Cu(II) catalyst.²⁵ A variety of *N*-*tert*-butanesulfinyl imines, including ketimines, react readily to provide α -sulfinamido boronic esters in moderate to good yields and with high stereoselectivities. In addition, the corresponding α -sulfinylamido trifluoroborates can be achieved in good yields *via* a sequential process (Scheme 1-9).

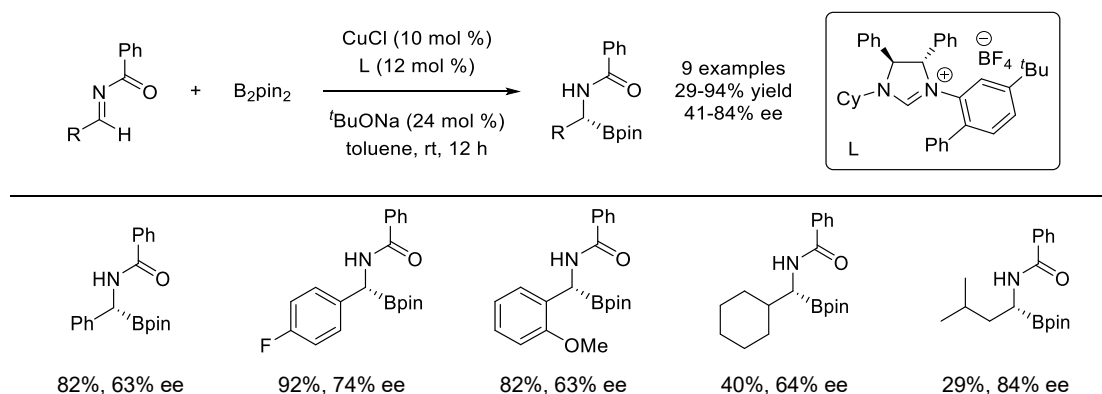
Ellman, 2014



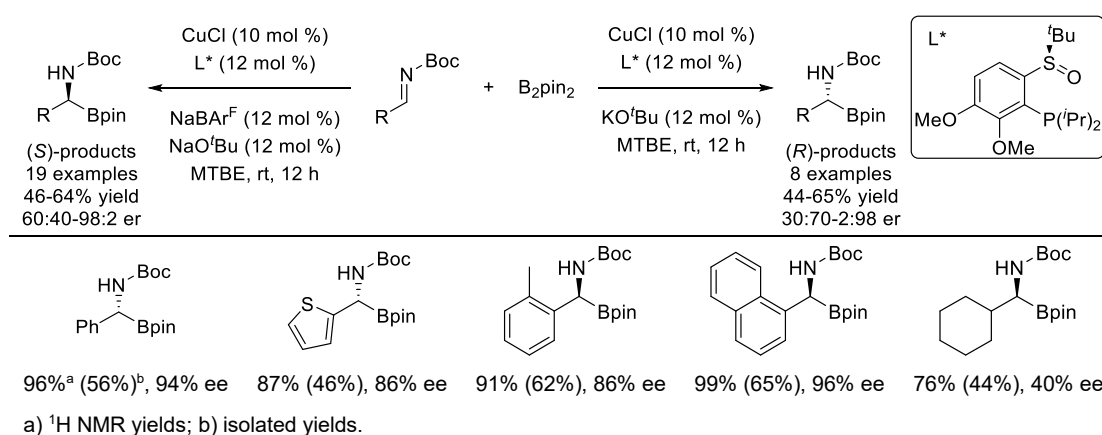
Scheme 1-9 Cu(II)-catalyzed asymmetric hydroboration of imines.

In 2013, Tian, Lin and co-workers developed a chiral NHC/Cu(I) system which can be used in the preparation of enantiomerically pure α -aminoboronic esters *via* an asymmetric hydroboration of aldimines.²⁶ However, when alkyl aldimines were selected as substrates, the corresponding products were obtained in low yields (29–40%), which the authors suggested may be because the starting materials decomposed during the reaction. (Scheme 1-10a). Later, using a chiral sulfoxide-phosphine ligand, the Liao group achieved a Cu(I)-catalyzed asymmetric pinacolboronyl addition to *N*-Boc-aldimines.²⁷ A dramatic counteranion effect (Cl^- vs $\text{BAr}^{\text{F}-}$, tetrakis[3,5-bis(trifluoromethyl)phenyl]borate) on the stereochemical course of the reaction was observed, and both enantiomers of the amino boronic esters were obtained with high enantioselectivities. However, only one example of an alkyl aldimine was reported, with low conversion and enantioselectivity (Scheme 1-10b).

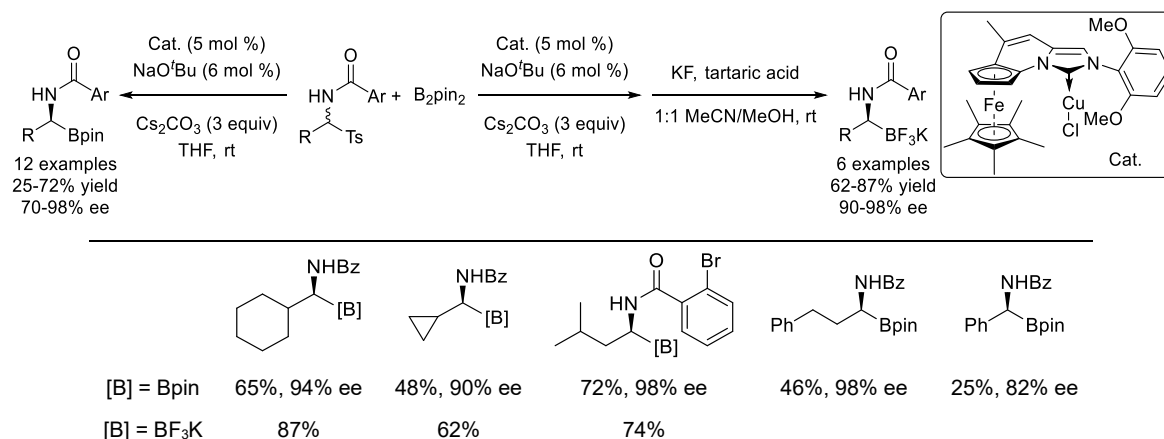
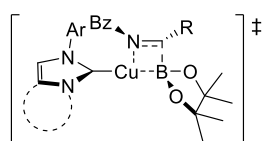
(a) Tian and Lin, 2013



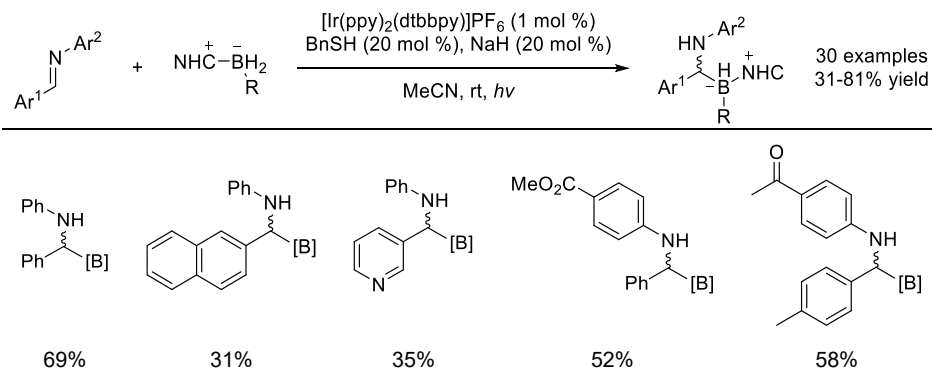
(b) Liao, 2015

**Scheme 1-10** Copper-catalyzed asymmetric hydroboration of aldimines.

In 2018, Cheong, Scheidt and co-workers reported a highly selective catalytic hydroboration of *N*-benzoyl alkyl-substituted aldimines generated *in situ* via deprotonation of imine precursors, namely *N*-benzoyl-protected α -tosylamines, with excess Cs_2CO_3 (Scheme 1-11a).²⁸ This borylation was proposed to proceed *via* a four-membered transition state, in which *in situ* formed imines underwent σ -bond metathesis with a Cu-B bond. In addition, DFT computations suggested that interactions between the oxygen in Bpin and the ferrocene in the planar-chiral catalyst were responsible for the observed stereoselectivity (Scheme 1-11b). This method gave desired α -aminoboronates in modest yields (25-72%) or α -amino trifluoroborates in good yields (62-87%).

(a) Cheong and Scheidt, 2018**(b) Proposed four-membered transition state****Scheme 1-11** Chiral NHC/Cu-catalyzed synthesis of α -aminoboronates.**1.3.2.3 Cooperative organocatalysis and photocatalysis**

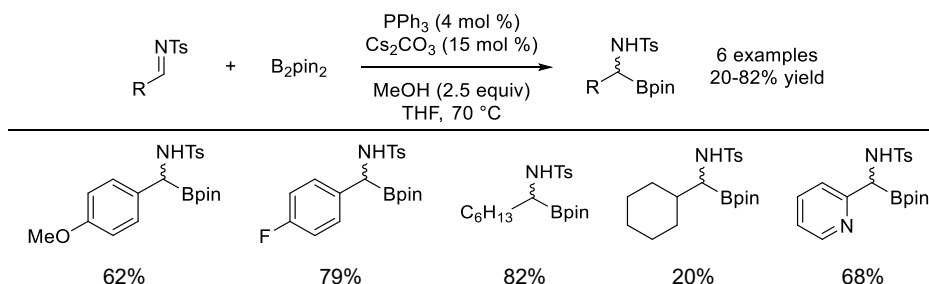
In 2018, Xie, Zhu and co-workers reported the inverse hydroboration of aryl aldimines with NHC boranes by means of photoredox/organocatalyst cooperative catalysis.²⁹ Mild reaction conditions and good functional group tolerance make this protocol practical, although only *N*-aryl substituted aryl aldimines are suitable substrates. There were no sterically congested α -amino tertiary boronates reported, and the synthesis of enantiopure α -aminoboron compounds was not achieved (Scheme 1-12).

Xie and Zhu, 2018**Scheme 1-12** Cooperative organocatalysis and photocatalysis for hydroboration of aldimines.

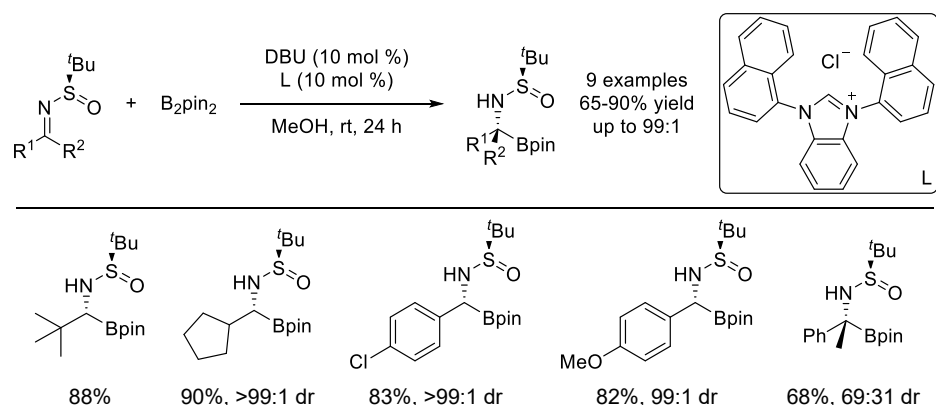
1.3.2.4 Transition-metal-free hydroboration of imines

Alkoxide anions were reported to activate B_2pin_2 to form a nucleophilic boron center.^{1d,30} In 2012, Fernández and co-workers reported the asymmetric synthesis of α -aminoboronate esters *via* a organocatalytic process.³¹ In their study, an *in situ* formed adduct^{30a} $MeO^- \rightarrow B_2pin_2$ added to the C=N double bond in tosylaldimines to produce α -aminoboronate esters. However, the role of phosphine additives, especially chiral phosphines, in the enantioselective C–B bond formation process has not been clarified (Scheme 1-13a). In addition, NHCs can activate B–B bonds.³² The Sun group reported a facile metal-free NHC-catalyzed hydroboration of *N-tert*-butanesulfinyl aldimines.³³ This method has several inherent advantages including simple operational procedure without requiring a stringent oxygen/moisture-free environment (Scheme 1-13b).

(a) Fernández, 2012



(b) Sun, 2013



Scheme 1-13 Transition-metal-free hydroboration of imines.

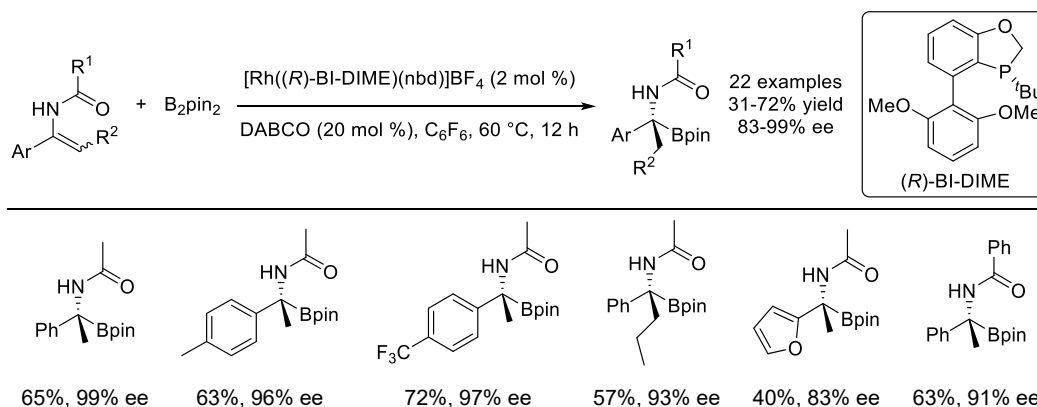
1.3.3 From alkenes

1.3.3.1 Rh-catalyzed hydroboration of enamides

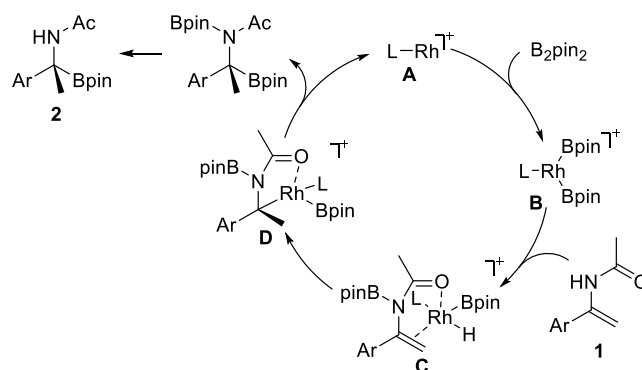
Rhodium-catalyzed hydroboration of alkenes is becoming an increasingly versatile method

for the preparation of organoboron compounds.³⁴ In 2015, Tang and co-workers reported an enantioselective synthesis of chiral α -amino tertiary boronic esters by Rh-catalyzed hydroboration of α -arylenamides (Scheme 1-14a).³⁵ Preliminary mechanistic studies indicated that this transformation proceeds *via* hydroboration rather than diboration of the acyl imine. Reaction of bis(boryl) Rh(III) species **B** with the N-H group in the substrate **1** leads to a boryl Rh(III) hydride complex **C**. Subsequent alkene insertion into the Rh(III)–H bond and reductive elimination affords product **2** (Scheme 1-14b). The yields were relatively low (31–72%), even though good to excellent enantioselectivities (83–99% ee) were achieved.

(a) Tang, 2015



(b) Proposed mechanism



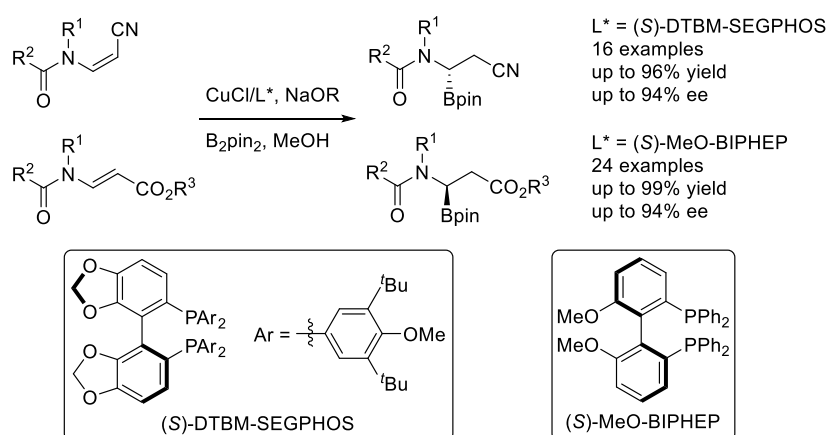
Scheme 1-14 Rh-catalyzed hydroboration of enamides.

1.3.3.2 Cu-catalyzed hydroboration of enamides

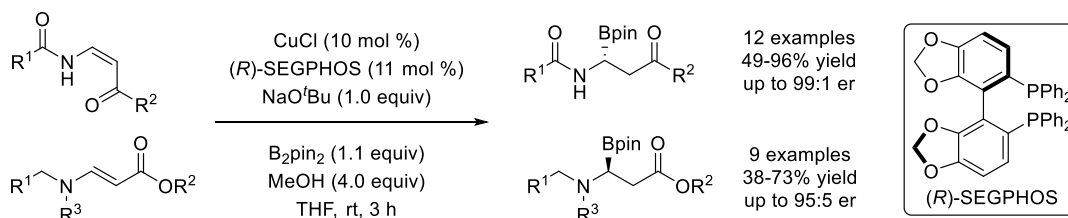
Copper-catalyzed enantioselective hydroboration of α,β -unsaturated compounds, known as β -borylation, is becoming a competent strategy to prepare chiral α -boronate esters.³⁶ In 2017, the groups of Xu, and Parra and Tortosa, independently and almost simultaneously

reported the Cu-catalyzed asymmetric hydroboration of *Z*- β -amidoacrylonitriles, *E*- β -amidoacrylates and *Z*- β -amidoacrylates using B_2pin_2 with good enantioselectivities. Enantioselectivities of the products can be effectively controlled by the configuration of the substrates and selected chiral ligands (Scheme 1-15).³⁷ In addition, Xu's method was applicable to the preparation of chiral α -aminoboronates on a gram-scale without erosion of enantioselectivities. Parra and Tortosa's method was utilized to synthesize boron-containing dipeptides and hemiboronates.

(a) Xu, 2017



(b) Parra and Tortosa, 2017



Scheme 1-15 Cu-catalyzed hydroboration of enamides.

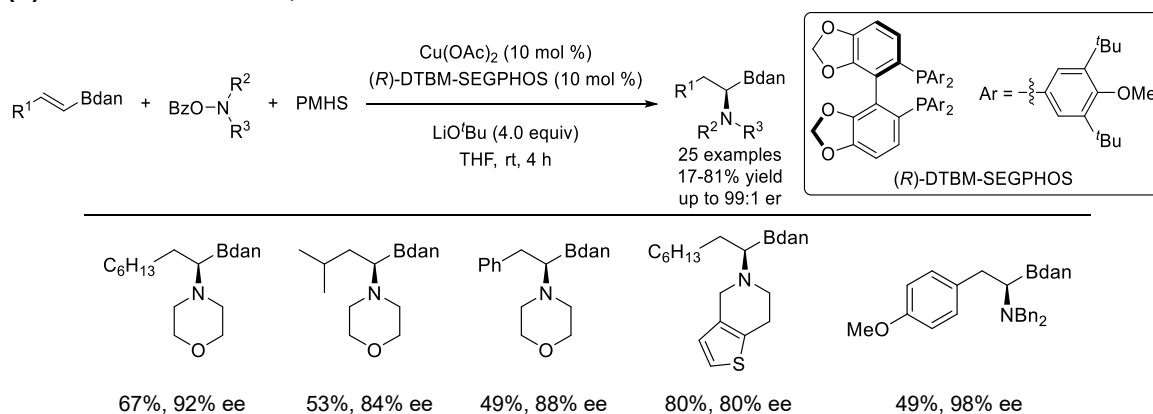
1.3.3.3 Cu-catalyzed hydroamination or aminoboration of alkenyl Bdan compounds

In 2015, Hirano, Miura and co-workers reported the synthesis of alkyl-substituted optically active α -aminoboronic acid derivatives by a copper-catalyzed regio- and enantioselective hydroamination of alkenyl Bdan compounds (dan = 1,8-diaminonaphthyl) with hydrosilanes and hydroxylamines (Scheme 1-16a).³⁸

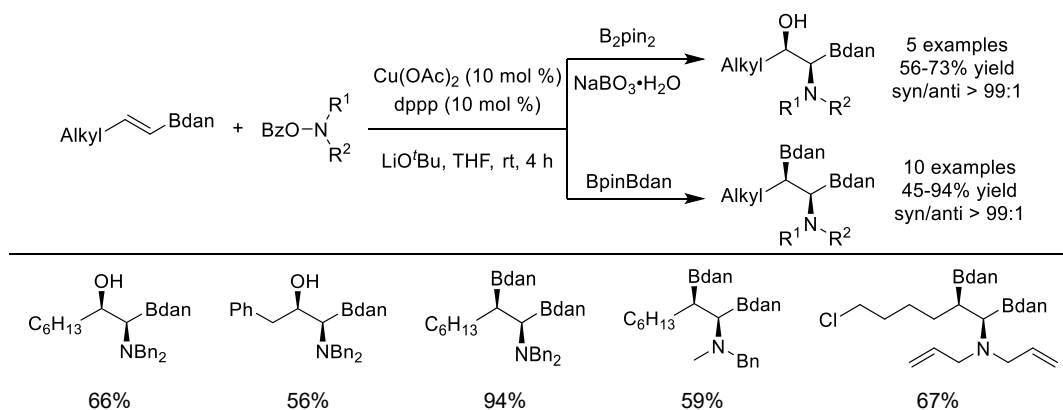
Later, the same group developed the asymmetric synthesis of β -boryl- α -aminoboronates

via a copper-catalyzed regio- and stereoselective aminoboration of alkenyl Bdan compounds with diboron reagents (B_2pin_2 or $BpinBdan$) and hydroxylamines.³⁹ The boryl group at the β position can be readily oxidized to the hydroxy group upon treatment with $NaBO_3 \cdot H_2O$ affording β -hydroxyl- α -aminoboronates, which were previously difficult to prepare (Scheme 1-16b).

(a) Hirano and Miura, 2015



(b) Hirano and Miura, 2016



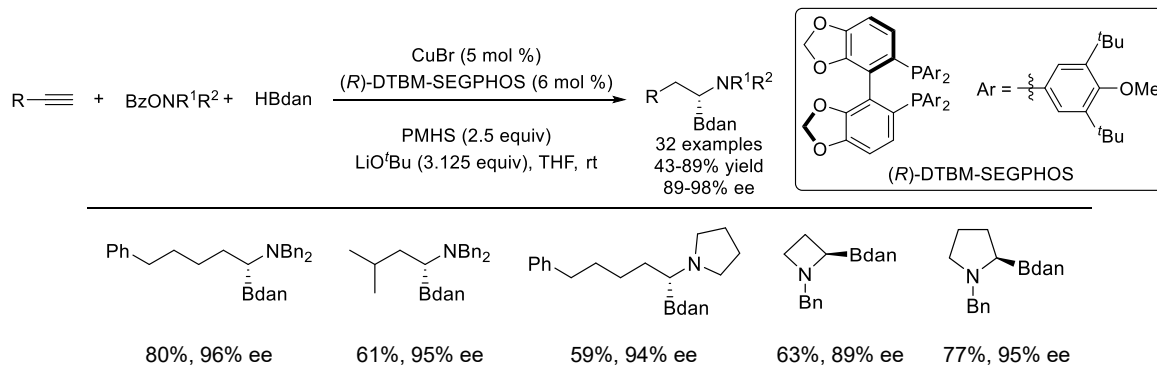
Scheme 1-16 Cu-catalyzed hydroamination or aminoboration of alkenyl Bdan compounds.

1.3.4 From alkynes

Very recently, Liu, Engle and co-workers reported the preparation of chiral α -aminoboronates via a CuH-catalyzed cascade hydroboration and hydroamination of terminal alkynes with high chemo-, regio- and enantioselectivities.⁴⁰ Mechanistic studies showed that an alkenyl Bdan compound was a competent intermediate in this reaction, whereas an enamine was not. This novel CuH-catalyzed asymmetric reductive 1,1-

difunctionalization can be expected to be applied to an array of different transformations (Scheme 1-17).

Liu and Engle, 2019

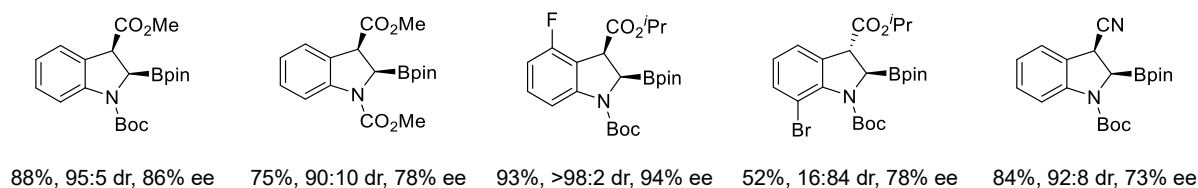
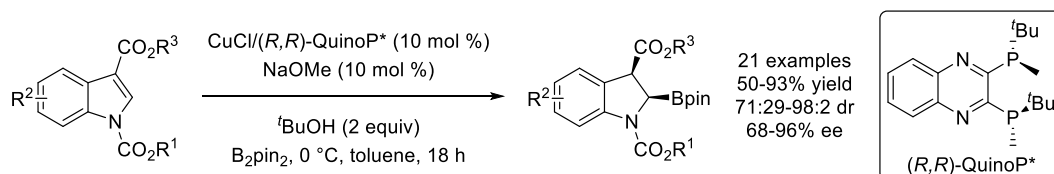


Scheme 1-17 Copper-catalyzed sequential hydroboration and hydroamination of alkynes.

1.3.5 From indoles

Enantioselective dearomatization reactions have proved to be powerful and direct approaches to access a wide variety of chiral saturated heterocycles.⁴¹ In 2018, the Xu group reported a Cu-catalyzed asymmetric dearomative borylation of *N*-alkoxycarbonyl-protected indole-3-carboxylates.⁴² The asymmetric nucleophilic addition of the boryl group occurred regioselectively at the *N*-adjacent carbon. A variety of cyclic chiral α -aminoboronates can be prepared in moderate to good yields with excellent diastereo- and enantioselectivities (Scheme 1-18).

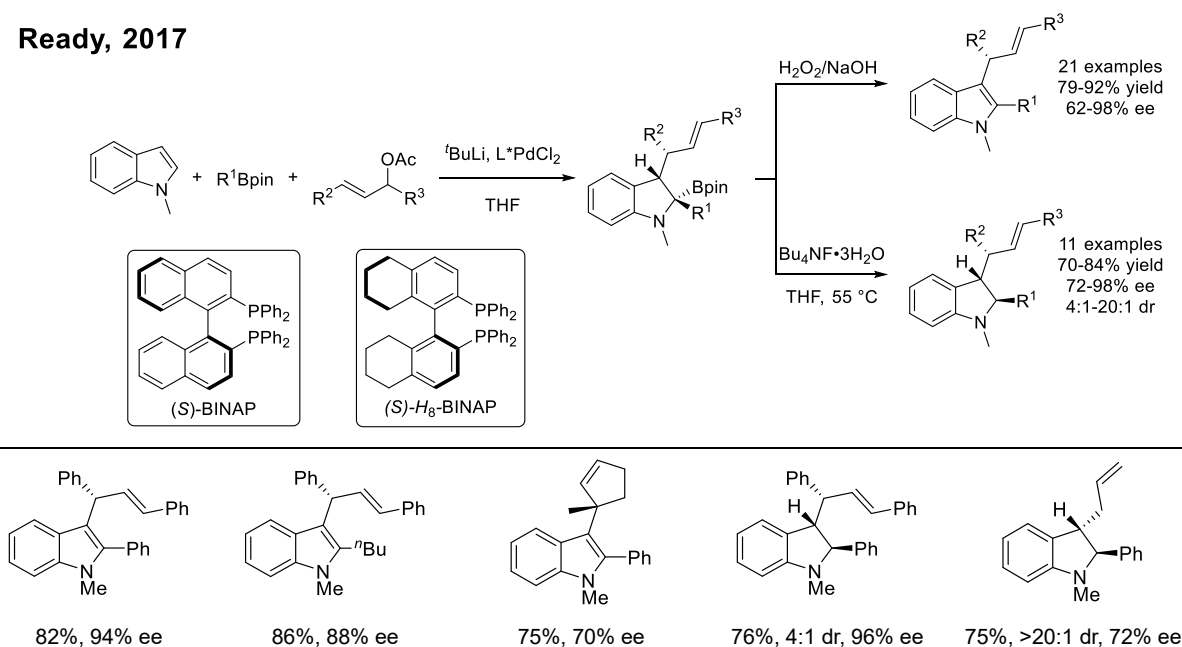
Xu, 2018



Scheme 1-18 Cu-catalyzed asymmetric dearomative hydroboration of indoles.

The reactivity of 2-indolylboron ate complexes in coupling reactions was initially studied in the 1990s by the Ishikura group.⁴³ In the presence of a Pd catalyst, 2-lithiated indoles were coupled with trialkyl boranes and allylic acetates to give 2,3-difunctionalized indoles after oxidative aromatization. In 2017, Ready and co-workers reported a Pd-catalyzed asymmetric three-component coupling of boronic esters, indoles and allylic acetates, which provided valuable heterocyclic products, namely indoles and indolines, and generated up to three new and contiguous stereocenters.⁴⁴ As key intermediates, tertiary α -aminoboronic esters were directly oxidized to the allylated indoles. These intermediates were also deborylated with $\text{Bu}_4\text{NF}\cdot 3\text{H}_2\text{O}$ affording optically active indolines (Scheme 1-19).

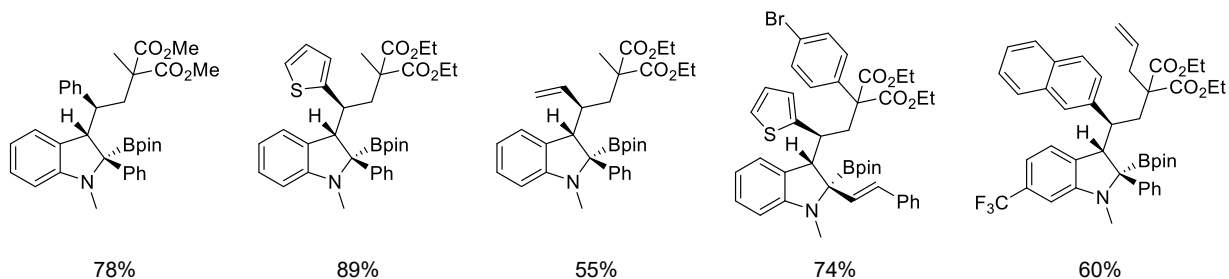
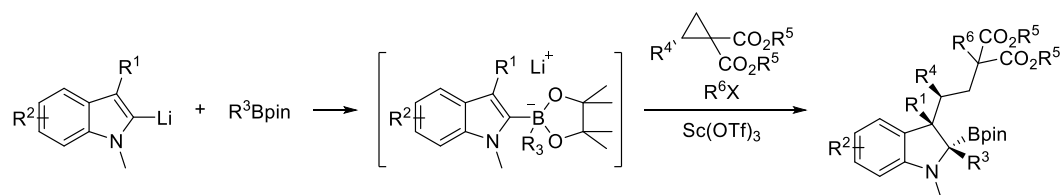
Ready, 2017



Scheme 1-19 Pd-catalyzed asymmetric three-component coupling of boronic esters, indoles, and allylic acetates.

Studer and co-workers reported a similar multicomponent dearomative coupling of indolylboron ate complexes, donor-acceptor cyclopropanes and alkyl halides with the Lewis acid catalyst $\text{Sc}(\text{OTf})_3$, giving indolines containing three contiguous stereocenters.⁴⁵ These products retained the valuable boryl functional group, making subsequent functionalization possible (Scheme 1-20).

Studer, 2018



Scheme 1-20 Lewis acid-catalyzed dearomative coupling of indolylboron ate complex, donor-acceptor cyclopropanes, and alkyl halides.

1.3.6 Via C–H bond functionalization

A long-standing challenge in synthetic chemistry is the direct, selective functionalization of alkyl, alkenyl, and aryl C–H bonds, which allows the construction of C–C as well as C–heteroatom bonds in an atom- and step-economical manner.^{1a}

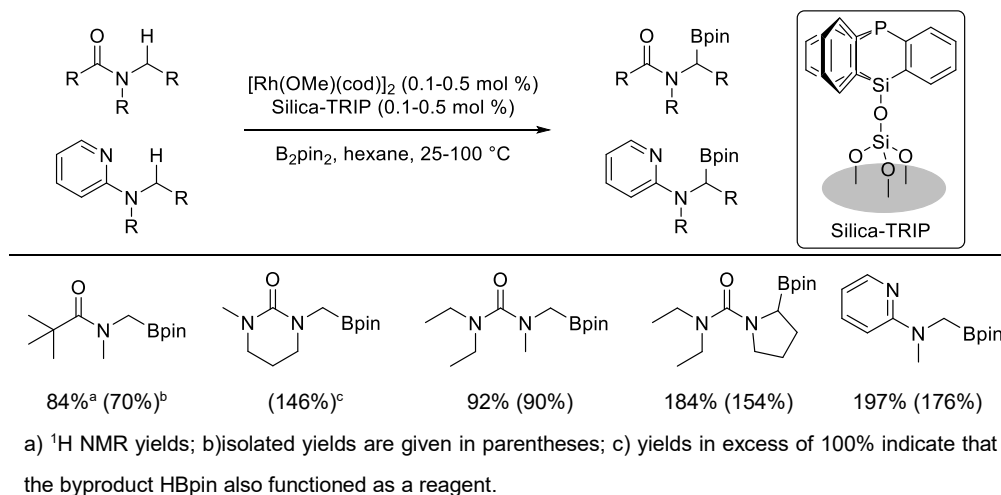
1.3.6.1 Rh- or Ir-catalyzed C–H borylation

In 2012, Sawamura and co-workers developed a heterogeneous catalyst system consisting of $[\text{Rh}(\text{OMe})(\text{cod})]_2$ and a silica-supported triarylphosphine ligand (Silica-TRIP) that features an immobilized triptycene-type cage structure with a bridgehead P atom.⁴⁶ Using this system, α -aminoalkylboronates were prepared *via* a site-selective borylation of *N*-adjacent $\text{C}(\text{sp}^3)\text{--H}$ bonds of amides, ureas and 2-aminopyridines under mild conditions. In their subsequent work, threefold cross-linked polystyrene-triphenylphosphine hybrids and silica-supported tripodal triarylphosphine Silica-3p-TPP were also found to be useful supported ligands, although the desired products were formed in low yields and the reaction had a narrow substrate scope (Scheme 1-21a).⁴⁷

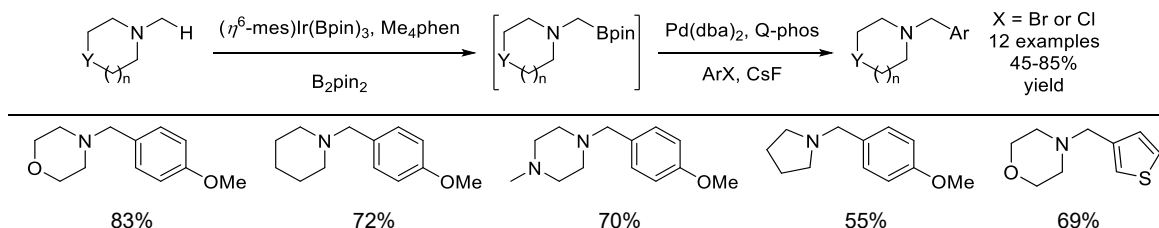
Hartwig and co-workers reported an Ir-catalyzed borylation of aliphatic C–H bonds in alkylamines offering access to α -aminoboronate esters, which were used directly in

Suzuki–Miyaura cross-coupling reactions.⁴⁸ Synthesis of α -aminoboronate esters *via* Ir-catalyzed C–H borylation was also achieved by the Li group,⁴⁹ the Suzuki and Yamashita group,⁵⁰ and the Clark group.⁵¹ Although the desired α -aminoboronate esters can be obtained in good yields and high selectivities, the substrate scope is limited (Scheme 1-21b).

(a) Sawamura, 2012



(b) Hartwig, 2014

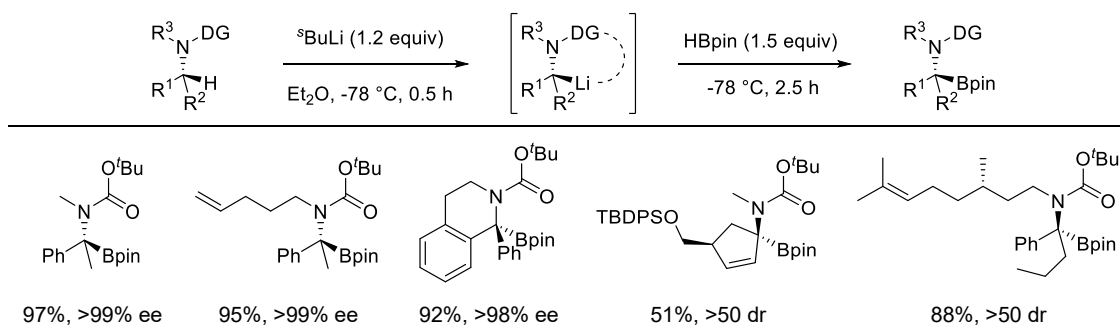


Scheme 1-21 Rh- or Ir-catalyzed C–H borylation for the synthesis of α -aminoboronates.

1.3.6.2 Base-mediated C–H borylation

In 2018, Negishi, Xu and co-workers reported a highly efficient and enantiospecific borylation method to synthesize a wide range of enantiopure (> 99% ee) tertiary α -amino boronic esters.⁵² This protocol has several advantages, including high enantiospecificity, complete retention of configuration, and gram-scale synthesis without erosion of enantiospecificity. While effective, the strongly basic conditions presented chemoselectivity issues and limited the functional group compatibility. In addition, chiral substrates are required for this two-step reaction (Scheme 1-22).

Xu and Negishi, 2018

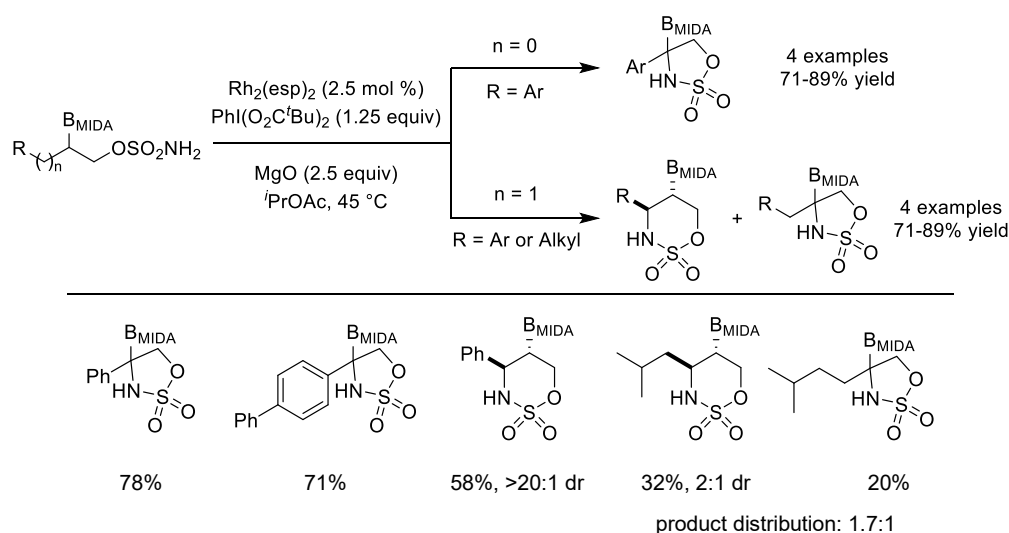


Scheme 1-22 Base-mediated stereoselective C–H borylation for enantiopure α -amino tertiary boronic esters.

1.3.6.3 Rh-catalyzed intramolecular C–H amination

Yudin and co-workers reported a rhodium-catalyzed intramolecular C–H amination of alkyl MIDA boronates for the preparation of cyclic α -amino boronates.⁵³ In the case of aryl boryl sulfamates, a single regioisomer was isolated, whereas alkyl sulfamate esters provided a mixture of five- and six-membered ring products (Scheme 1-23).

Yudin, 2015



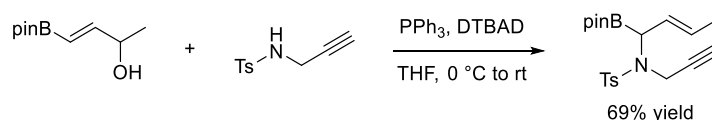
Scheme 1-23 Rh-catalyzed intramolecular C–H amination.

1.3.7 Miscellaneous routes

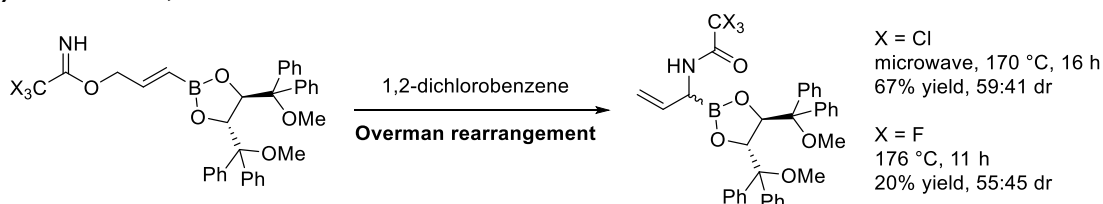
1.3.7.1 Allylic amination

Berrée *et al.* developed a regiocontrolled Mitsunobu reaction converting (3-hydroxy-1-propen-1-yl)boronates to α -aminoboronic esters, which can be used in the allylboration of aldehydes (Scheme 1-24a).⁵⁴ The Overman rearrangement is another route to synthesize allyl α -aminoboronates, which was achieved by Pietruszka and co-workers in 2008 (Scheme 1-24b).⁵⁵ Later, Carreaux *et al.* reported a novel route to α -isocyanato allylboronic esters *via* a [3,3]-sigmatropic cyanate-isocyanate rearrangement giving access to α -aminoboronic esters (Scheme 1-24c).⁵⁶

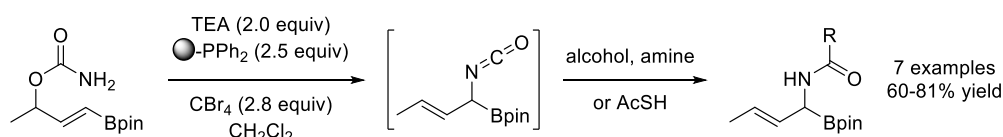
(a) Berrée, 2009



(b) Pietruszka, 2008



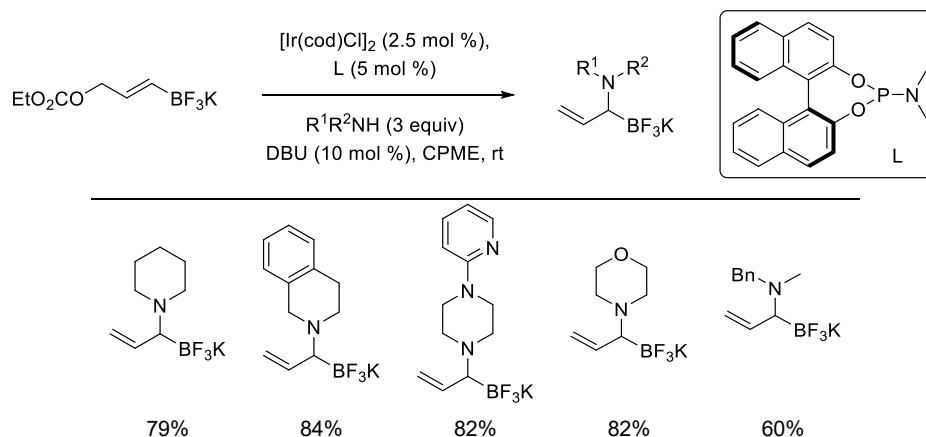
(c) Carreaux, 2013



Scheme 1-24 Synthesis of allyl α -aminoboronates *via* Mitsunobu reaction or Overman rearrangement.

Ir-catalyzed allylic amination of 3-hydroxy-1-propenylboronate derivatives was developed by Carreaux and co-workers for the preparation of allyl α -aminoboronates. Organotrifluoroborate substrates were found to be better than their boronic ester analogues in controlling the regioselectivity exclusively in favor of branched products (Scheme 1-25).⁵⁷

Carreaux, 2011

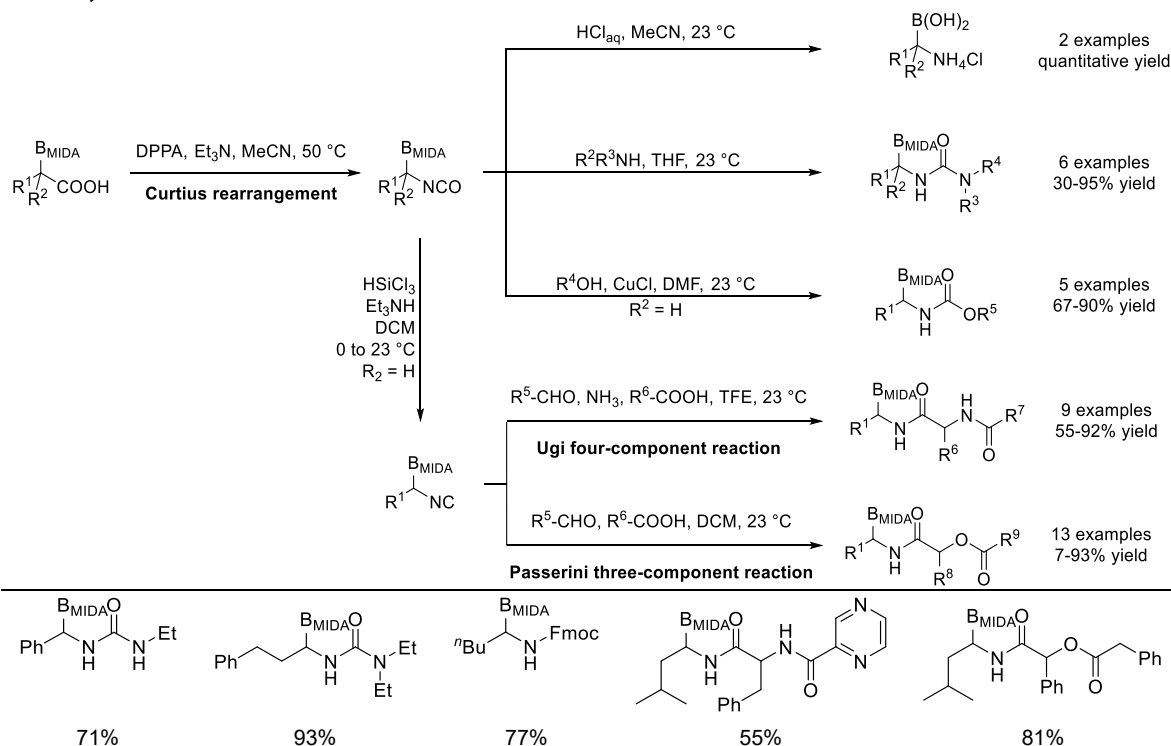


Scheme 1-25 Ir-catalyzed allylic amination strategy to allyl α -aminoboronates.

1.3.7.2 Curtius rearrangement

In 2012, Yudin and co-workers reported a Et_3N -mediated Curtius rearrangement. This process allows access to a new class of molecules, namely α -boryl isocyanates, from α -borylcarboxylic acid precursors and diphenylphosphoryl azide (DPPA). These novel, bench-stable molecules enabled mild and convenient access to a wide range of α -aminoboronic acid derivatives, including carbamates, ureas, and peptides. Additionally, this methodology allows for the facile preparation of α,α -disubstituted analogues.⁵⁸ The fact that the starting materials require multiple steps to prepare is a weakness of this protocol. The same group subsequently prepared bench-stable α -boryl isocyanides from corresponding α -isocyanates. These novel amphoteric reagents can be used in a one-step synthesis of boroalkyl-functionalized heterocycles as well as biologically active boropeptides *via* an Ugi four-component reaction and Passerini three-component reaction (Scheme 1-26).⁵⁹

Yudin, 2012 to 2014

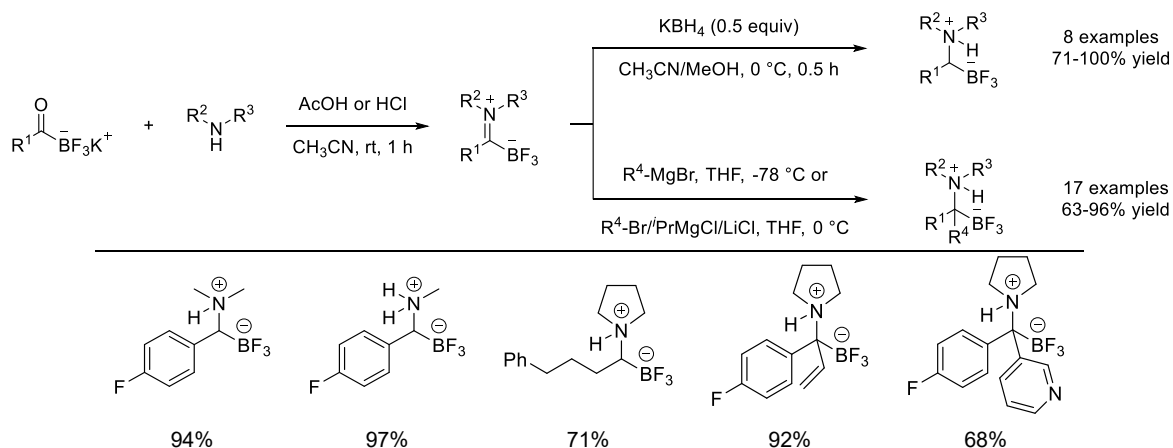


Scheme 1-26 Yudin's protocols for facile synthesis of α -aminoboronic acid derivatives.

1.3.7.3 Reductive amination of acyl boronates

Acyl boronates have been proved as important intermediates in several transformations.⁶⁰ In 2016, the Yudin group reported the synthesis of α -aminoboronates from acyl boronates *via* previously unknown boron-containing iminium ions.⁶¹ Using α -boryl aldehydes as substrates, the corresponding β -amino boronic acid derivatives can be prepared under mild conditions. In 2018, Bode and co-workers improved this reductive amination of acyl boronates. Potassium acyltrifluoroborates (KATs) were utilized in Bode's method. *Via* Grignard addition, intermediate trifluoroborate-iminiums (TIMs) were transformed into sterically demanding α -aminoboronic acids that were difficult to synthesize before (Scheme 1-27).⁶²

Yudin, 2016 and Bode, 2018

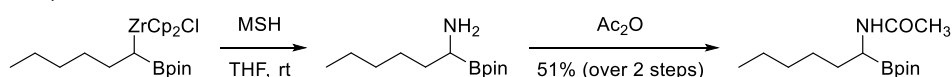


Scheme 1-27 Reductive amination of acyl boronates.

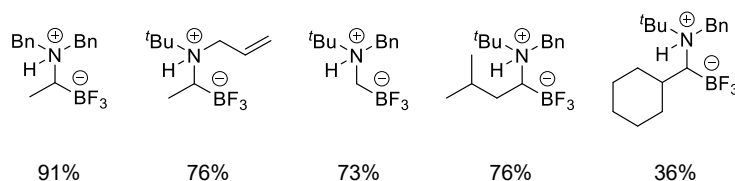
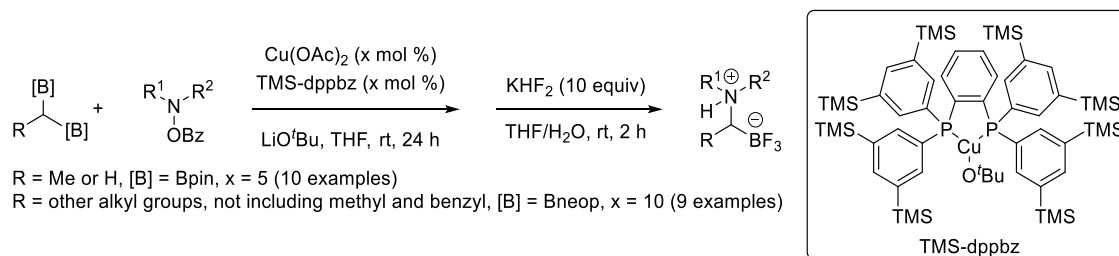
1.3.7.4 Electrophilic aminations of *gem*-borazirconocene alkanes or *gem*-diborylalkanes

In 1996, Srebnik and co-workers reported the selective and electrophilic amination of *gem*-borazirconocene alkanes with *O*-mesitylsulfonyl hydroxylamine (MSH) under mild conditions (THF as solvent, and ambient temperature), giving an α -aminoboronic ester in a reasonable yield (51% over 2 steps) (Scheme 1-28a).⁶³

(a) Srebnik, 1996



(b) Hirano and Miura, 2019

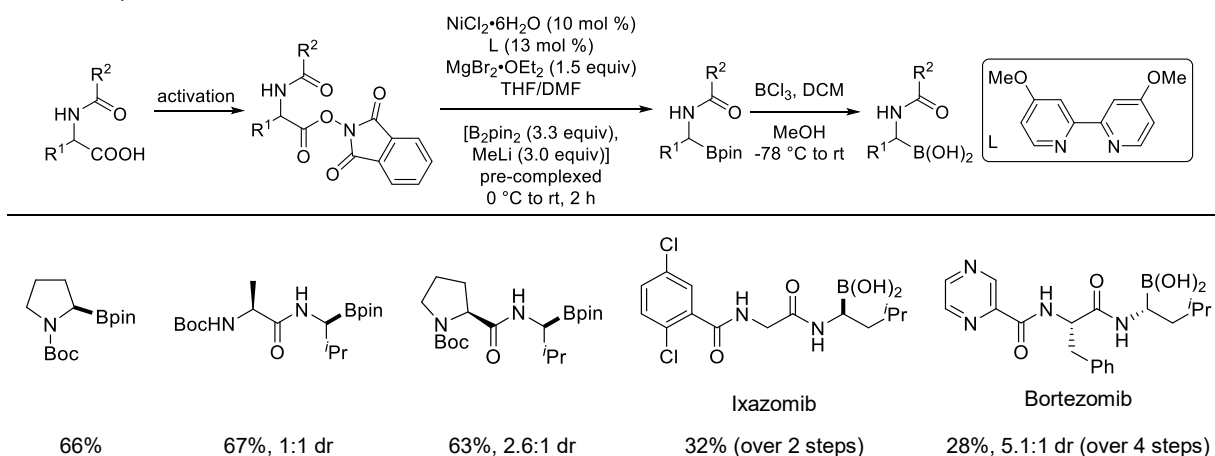
Scheme 1-28 Electrophilic aminations of *gem*-borazirconocene alkanes and *gem*-diborylalkanes.

Very recently, Hirano, Miura and co-workers reported the preparation of α -aminoboronates via a Cu-catalyzed electrophilic amination of *gem*-diborylalkanes with hydroxylamines.⁶⁴ The reactivity of neopentylglycol boronate esters is higher than that of pinacolate analogues (Scheme 1-28b).

1.3.7.5 Decarboxylative borylation

Alkyl carboxylic acids represent an ideal precursor to boronic acids, because they are present in a myriad of natural products and medicines. In 2017, Baran and co-workers reported a Ni-catalyzed decarboxylative borylation of *N*-hydroxyphthalimide redox-active esters giving high-value alkyl boronic esters. Using native peptides as starting materials, diverse α -aminoboronic acids and derivatives, including bioactive Ixazomib and Bortezomib, can be prepared smoothly (Scheme 1-29).⁶⁵ In addition, three α -aminoboronic acids synthesized by that group are human neutrophil elastase inhibitors.

Baran, 2017



Scheme 1-29 Decarboxylative borylation.

1.4 Synthetic applications

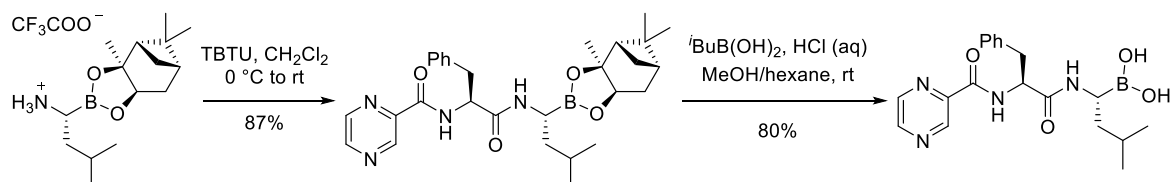
α -Aminoboronic acids and their derivatives also represent synthetically useful building blocks in organic synthesis. Rapid development has taken place in the past few years, as summarized in Scheme 1-4.

1.4.1 Retaining the α -aminoboronate core structure

α -Aminoboronic acids and their derivatives have played a unique role in drug discovery and have emerged as privileged pharmacophores in proteasome inhibitors. Thus, functionalization of α -aminoboronates at the N or B atom represents potentially powerful means by which to enrich the library of aminoboronic acids.

1.4.1.1 Functionalization at the N atom

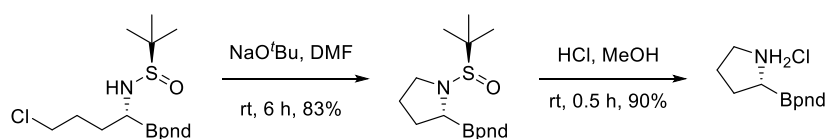
Facile and mild condensation of α -aminoboronates with peptides offers access to bioactive peptide chain-containing α -aminoboronates. The concise synthesis of Bortezomib exemplified the versatility of this strategy (Scheme 1-30).^{14a}



Scheme 1-30 Synthesis of peptide chain-containing α -aminoboronic acid derivatives.

Sun *et al.* synthesized a series of stable α -aminoboronic esters using bis(pinanediolato)diboron (B_2pnd_2) as the boron reagent, catalyzed by a triazole-based NHC and copper(I) chloride. Functional groups such as chloride were tolerated. Treatment of a chloride-substituted α -aminoboronic ester with base led to cyclization and gave the *N*-cyclic product. After a mild deprotection, a proline equivalent of an aminoboronic ester was obtained in 90% yield. Thus, a convenient method for preparing *N*-cyclic aminoboronic acid derivatives was presented. (Scheme 1-31).⁶⁶

Sun, 2014



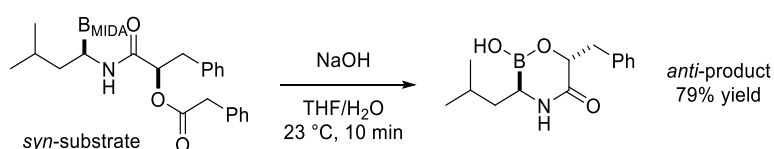
Scheme 1-31 Synthesis of *N*-cyclic aminoboronic acid derivatives.

1.4.1.2 Functionalization at the B atom

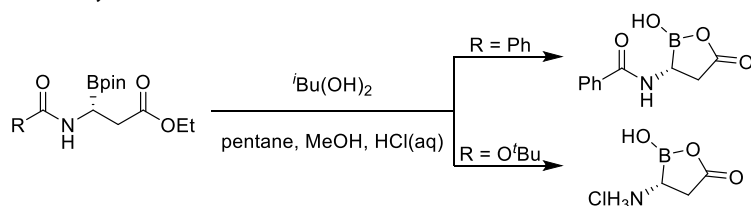
Yudin and co-workers reported that the MIDA group can be removed from α -aminoboronates under aqueous basic conditions to afford the corresponding boronic acids. Under the deprotection conditions, hydrolysis of the ester also occurred, followed by condensation of the resulting hydroxyl group with the newly formed boronic acid. This process provided access to the disubstituted hemiboronate 6-boromorpholinone, which was found to inhibit chymotrypsin-like enzymes selectively with an IC_{50} value of 19 nm (Scheme 1-32a).⁵⁹

In 2017, Parra, Tortosa and co-workers synthesized a series of chiral α -aminoboronic esters *via* the asymmetric hydroboration of alkenes. With these products in hand, hemiboronates can be prepared by hydrolysis of the pinacol boronic ester. An *N*-Boc-protected derivative was transformed into a primary α -aminoboronate, which was used to synthesize various of functionalized hemiboronates (Scheme 1-32b).^{37b}

(a) Yudin, 2013



(b) Parra and Tortosa, 2017



Scheme 1-32 Deprotection for the preparation of hemiboronates.

1.4.2 Not retaining the α -aminoboronate core structure

1.4.2.1 Suzuki–Miyaura cross-coupling

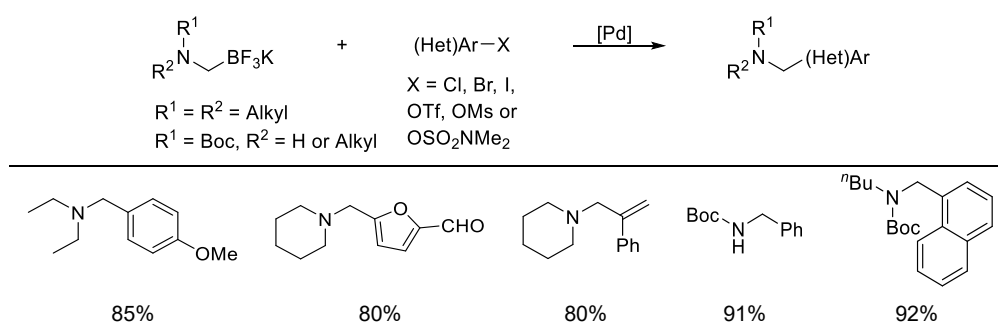
In 2007, Molander and co-workers described the Suzuki–Miyaura cross-coupling reaction of *N,N*-dialkylaminomethyltrifluoroborates with both electron-rich and electron-poor aryl bromides yielding a variety of useful nitrogen-containing molecules.⁶⁷ However, this

Suzuki–Miyaura reaction has a limited aminomethyltrifluoroborate substrate scope, as only unbranched potassium dialkylaminomethyltrifluoroborates are suitable coupling partners.

Later, the same group extended their aminomethylation reaction to more stable and less expensive aryl and heteroaryl chloride electrophilic partners.⁶⁸ The generality of this reaction with aryl iodides, triflates and alkenyl bromides was also examined.

Aminomethyl moieties appear in many biologically active molecules, so the Molander group synthesized potassium Boc-protected aminomethyltrifluoroborate, which is air-stable and can be considered as a primary aminomethyl equivalent. Using this trifluoroborate, and aryl or heteroaryl chlorides, a wide variety of aminomethylarenes can be prepared *via* Pd-catalyzed Suzuki–Miyaura cross-coupling in good to excellent yields.⁶⁹ This reaction was expanded to other electrophiles, *e.g.* aryl and heteroaryl mesylates⁷⁰ and sulfamates.⁷¹ Potassium Boc-protected secondary aminomethyltrifluoroborates were synthesized and utilized in Suzuki–Miyaura cross-coupling reactions giving access to secondary aminomethylated arenes after Boc removal (Scheme 1-33).⁷²

Molander, from 2007 to 2013

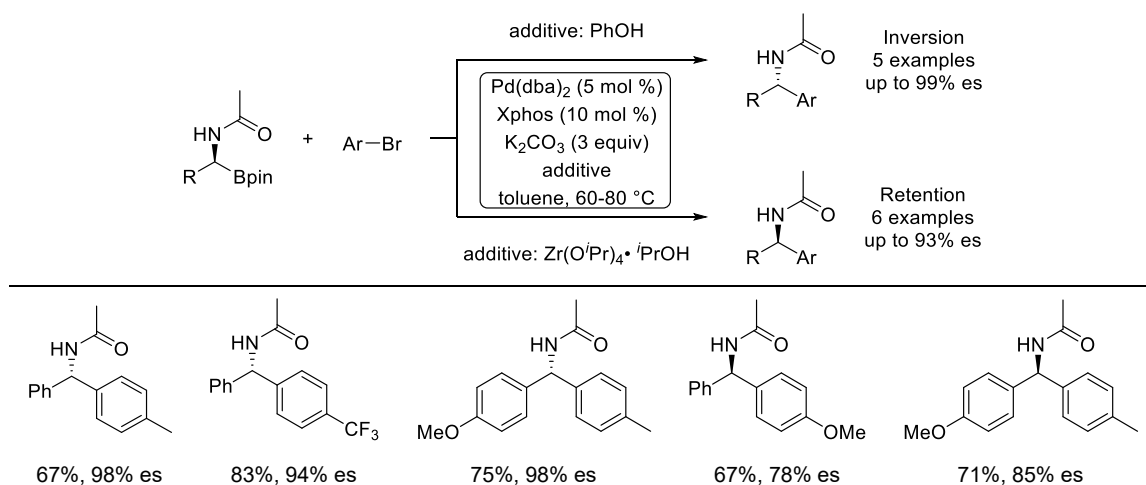


Scheme 1-33 Suzuki–Miyaura cross-coupling for the synthesis of diverse amines.

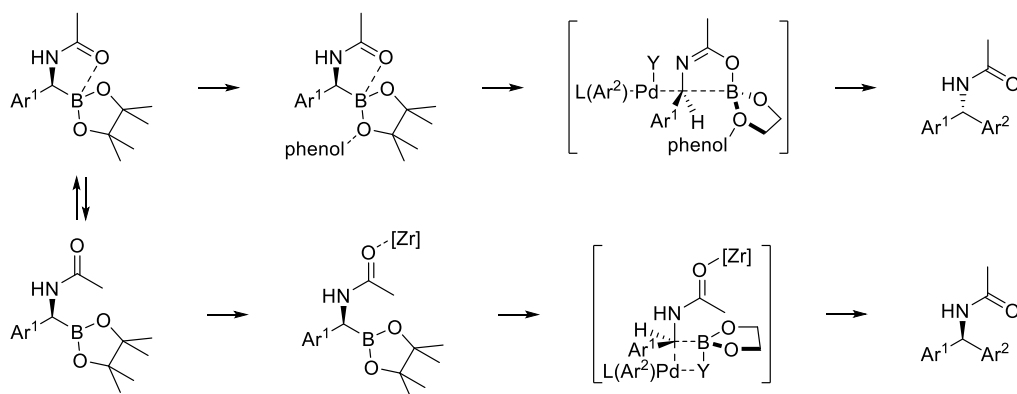
In 2010, Ohmura, Sugimoto and co-workers developed a highly stereospecific Suzuki–Miyaura coupling of enantiopure α -aminoboronic esters with aryl bromides and chlorides.⁷³ This coupling proceeds with inversion of configuration, which is unusual. It was proposed that backside attack of the palladium complex on the α -carbon atom of α -aminoboronic ester is preferred because of strong intramolecular coordination of the amide oxygen atom

to the boron center (Scheme 1-34a).

(a) Ohmura and Suginome, from 2009 to 2018



(b)



Scheme 1-34 Palladium-catalyzed asymmetric Suzuki-Miyaura coupling of α -(acylamino)boronic esters, and effects of acidic additives on the stereochemical course of the reaction.

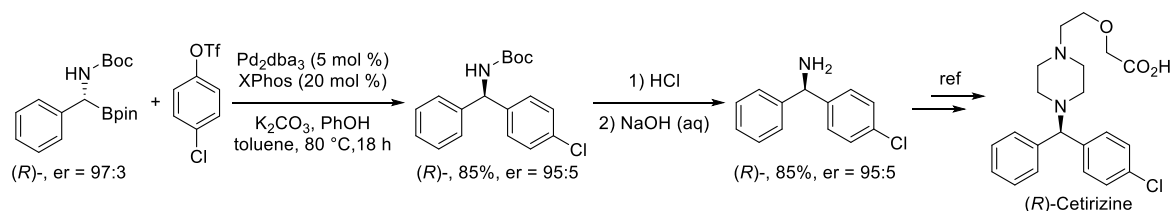
Soon after, they reported remarkable effects of acidic additives on the stereochemical course of the Suzuki–Miyaura coupling of enantioenriched α -aminoboronic esters.⁷⁴ Addition of phenol made this coupling highly enantiospecific (inversion), while in the presence of $Zr(O^iPr)_4 \cdot iPrOH$, the stereochemistry was retained. In their proposed mechanism, the coordination of phenol to the oxygen atom of the pinacol ligand enhanced the intramolecular amide O–B coordination, which enhanced enantioselectivity in the coupling which proceeded with inversion. In contrast, cleavage of the intramolecular coordination by competitive coordination of $Zr(O^iPr)_4 \cdot iPrOH$ to the amide oxygen atom

resulted in the formation of a conventional transition state, which led to a stereoretentive transmetalation (Scheme 1-34b).

Recently, the same group achieved the Suzuki–Miyaura cross-coupling of nonbenzylic α -(acylamino)alkylboron compounds with aryl halides.⁷⁵ Chiral 1-arylalkyl amides were prepared with inversion of configuration promoted by a Pd/PCy₂Ph catalytic system.

α -Aminoboronic esters have been shown to be competent coupling partners in transition metal-catalyzed reactions, allowing convergent, asymmetric assembly of chiral amine products. In Liao's work, an aryl trifluoromethanesulfonate coupled stereoselectively with a chiral α -aminoboronic ester to yield a Boc-protected chiral amine in a high yield and a good enantiomeric ratio.²⁷ An effective and mild deprotection process gave access to a chiral amine, which can be used in the synthesis of (*R*)-Cetirizine, a histamine H1 antagonist (Scheme 1-35).⁷⁶

Liao, 2015

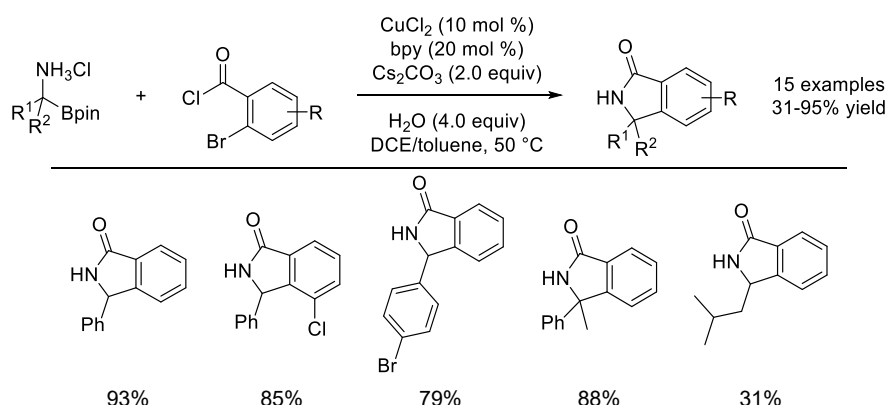


Scheme 1-35 Suzuki–Miyaura coupling of α -(acylamino)benzylboronic esters, and its application to the preparation of (*R*)-Cetirizine.

1.4.2.2 As bis-nucleophiles for the synthesis of isoindolinones

α -Aminoboronates are interesting compounds as they contain geminal nucleophilic centers. To utilize the bis-nucleophilicity of both the nitrogen atom and the C–B bond, Dumas and co-workers achieved one-pot amination/arylation of α -aminoboronates with 2-bromobenzoyl chlorides leading to isoindolinones.⁷⁷ This reaction was performed in the presence of a catalytic amount of CuCl₂. However, using chiral α -aminoboronates as substrates, only racemic products were obtained (Scheme 1-36).

Dumas, 2016

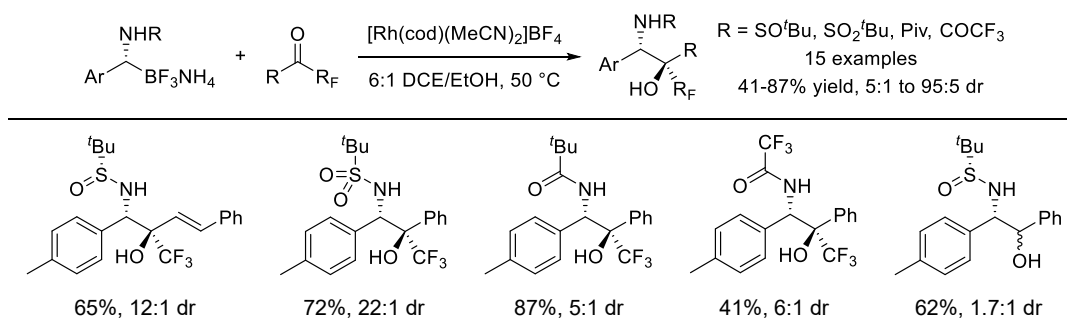


Scheme 1-36 As bis-nucleophiles for the synthesis of isoindolinones.

1.4.2.3 Addition to C=O double bonds

Ellman and co-workers reported the first Rh-catalyzed addition of α -amino trifluoroborates to aryl and alkenyl trifluoromethyl ketones for the asymmetric synthesis of vicinal amino alcohols, which are common in drugs and natural products as well as ligands for asymmetric synthesis (Scheme 1-37).⁷⁸

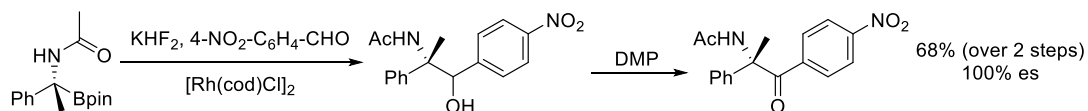
Ellman, 2014

Scheme 1-37 Addition of α -amino trifluoroborates to ketones and aldehydes for the asymmetric synthesis of vicinal amino alcohols.

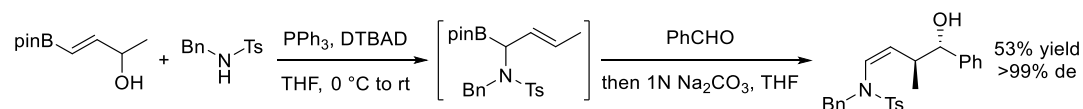
In 2015, Tang and co-workers reported that an α -aminoboronic pinacol ester reacted with 4-nitrobenzaldehyde in the presence of KHF_2 and a rhodium catalyst, followed by DMP oxidation, producing an α -acetylamino ketone in 68% overall yield with 99% ee (Scheme 1-38a).³⁵ Berrée *et al.* reported the synthesis of allyl α -aminoboronates, which then added to aldehydes to give homoallylic alcohols (Scheme 1-38b).⁵⁴ Additionally, trisubstituted

tetrahydrofurans were prepared *via* an allyl addition/intramolecular cyclization sequence (Scheme 1-38c).⁵⁶

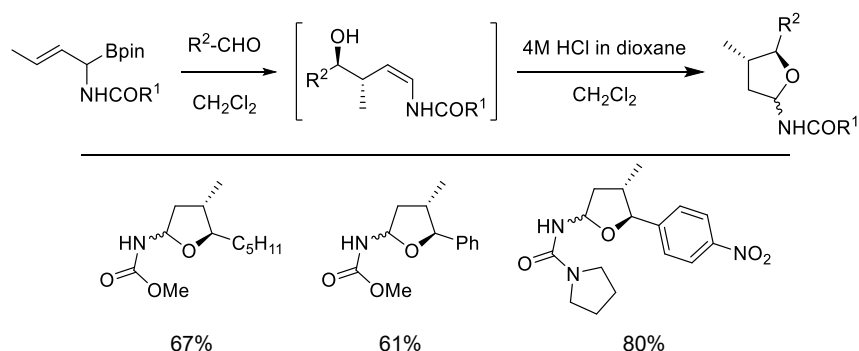
(a) Tang, 2015



(b) Berrée, 2009



(c) Carreaux, 2013

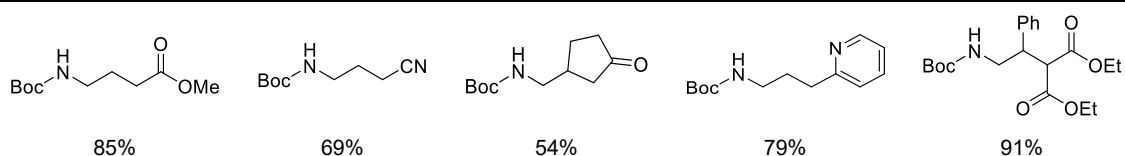
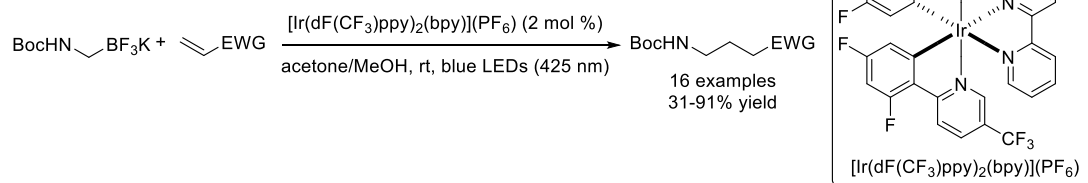


Scheme 1-38 Addition to C=O double bonds for the synthesis of α -acetylamino ketones, homoallylic alcohols, and trisubstituted tetrahydrofurans. es = enantiospecificity, [ee of product / ee of starting material] \times 100%.

1.4.2.4 α -Aminomethyl radicals generated under photoredox conditions

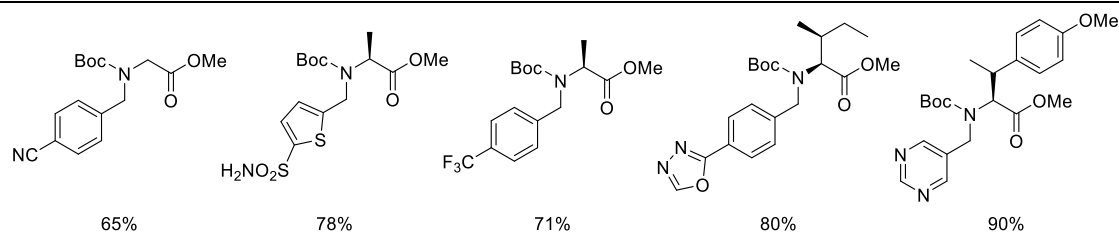
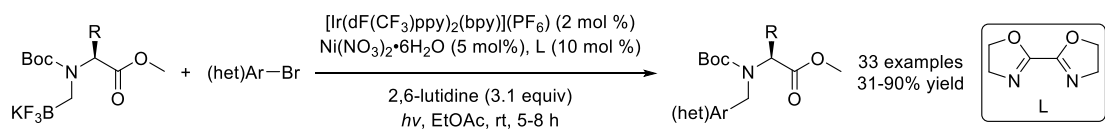
Organotrifluoroborate derivatives are excellent radical precursors because of their high stability, low toxicity, and functional group tolerance.⁷⁹ In 2014, Koike, Akita and co-workers described the photocatalytic aminomethylation of electron-deficient alkenes with α -amino trifluoroborates giving access to biologically active γ -aminobutyric acid (GABA) derivatives (Scheme 1-39).⁸⁰

Koike and Akita, 2014

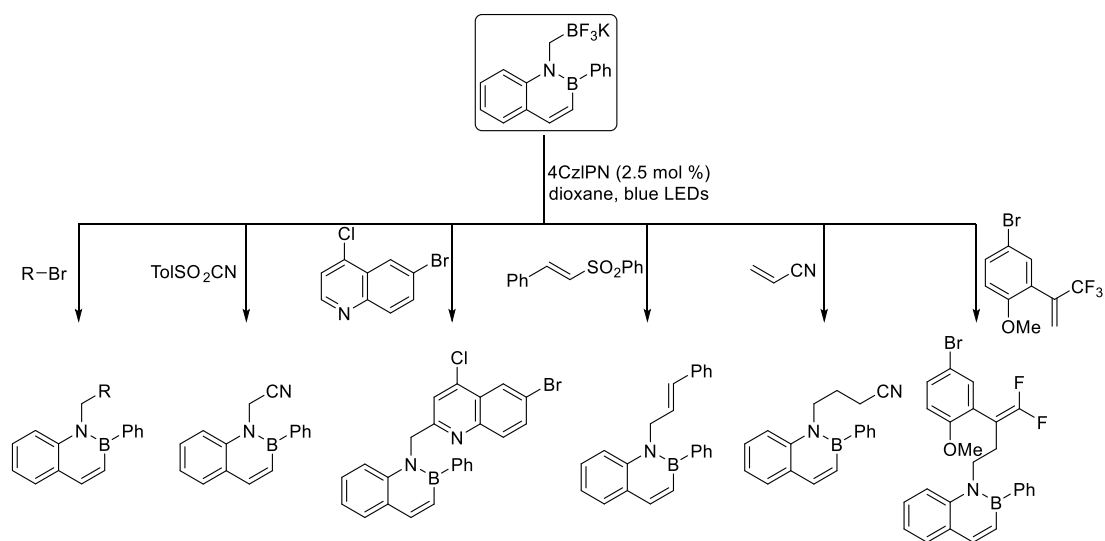


Scheme 1-39 Photocatalytic aminomethylation of electron-deficient alkenes with α -amino trifluoroborates.

(a) Molander, 2016

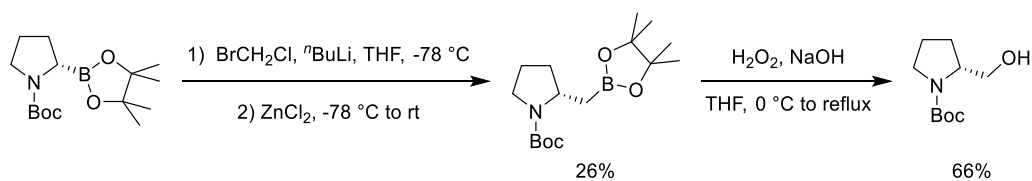


(b) Molander, 2019

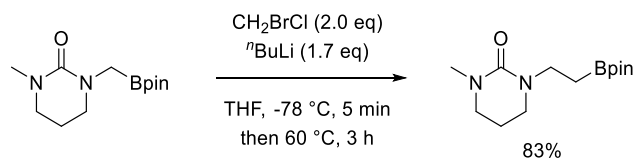


Scheme 1-40 Photocatalytic aminomethylation for the synthesis of chiral benzylamines, and the functionalization of 2,1-borazaronaphthalenes.

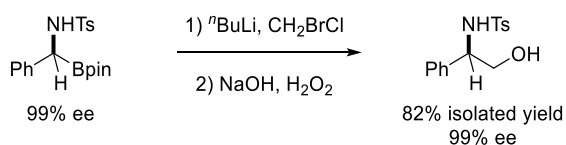
(a) Whiting, 2008



(b) Sawamura, 2012



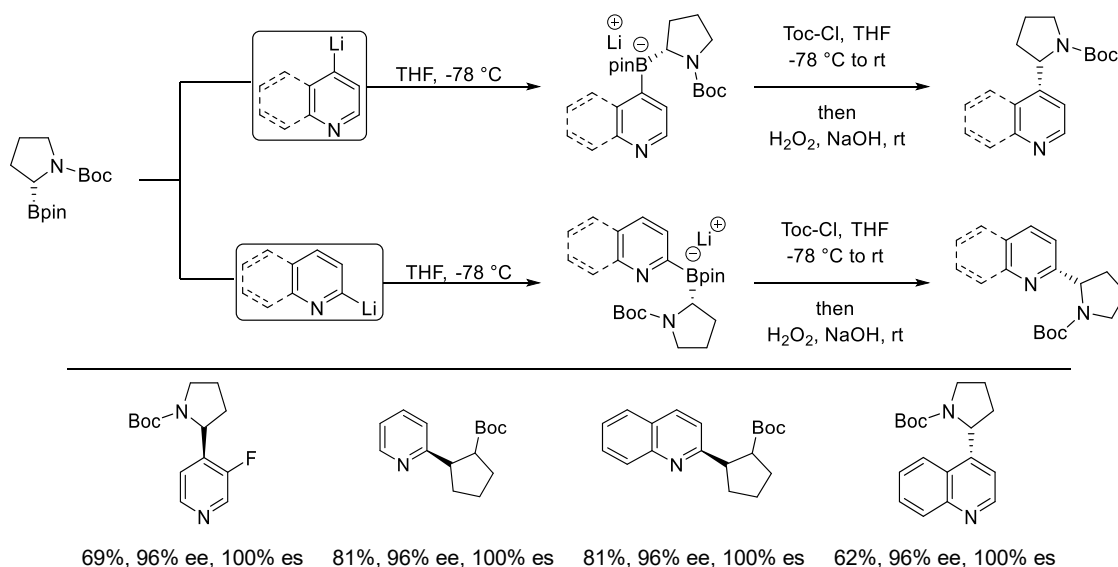
(c) Fernández, 2012



Scheme 1-42 Homologation for the synthesis of β -aminoboronates and 1,2-amino alcohols.

1.4.2.7 Reactions with R-Li or R-MgBr

Aggarwal, 2015



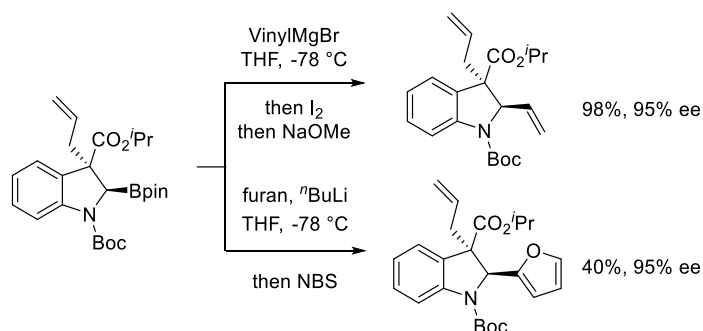
Scheme 1-43 Enantioselective coupling of α -aminoboronic esters with *N*-heteroaromatic compounds.

Transitional-metal-free stereospecific coupling of chiral cyclic α -aminoboronates with lithiated *N*-heteroaromatic compounds was reported by Aggarwal and co-workers.⁸⁵ This

protocol consists of the formation of boronate complexes by addition of α -aminoboronates to lithiated pyridines or quinolines. Subsequent 1,2-migration, induced by addition of ToC-Cl , activated the N -heterocycles by acylation. Finally, oxidative workup gave access to coupling products with excellent stereospecificity (Scheme 1-43).

Recently, Xu synthesized cyclic chiral α -aminoboronic esters and applied them in stereoselective C–C bond formation.⁴² For example, a cyclic chiral α -aminoboronic ester reacted with vinylmagnesium bromide, followed by sequential addition of I_2 and NaOMe , to afford a 2-vinylindoline. In addition, arylation with 2-lithiofuran followed by addition of NBS , gave access to 2-(2-furyl)-indoline (Scheme 1-44).

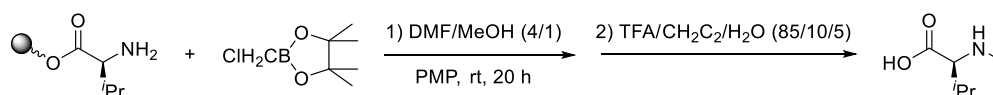
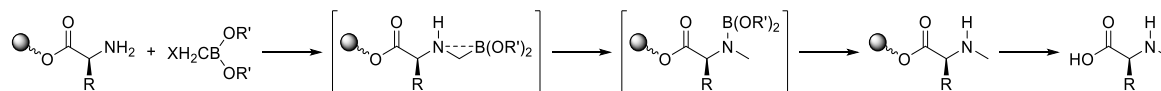
Xu, 2018



Scheme 1-44 Reaction of α -aminoboronic esters with Grignard or organolithium reagents for stereoselective C–C bonds formation.

1.4.2.8 Matteson's 1,2-carbon-to-nitrogen rearrangement of boron

Matteson *et al.* found that the instability of α -aminoboronic acids is mainly due to the migration of boron from carbon to nitrogen yielding the corresponding amines in protic solvents.^{2a,11b,86} On this basis, the Hall group reported a solid-phase method for the mono- N -methylation of resin-supported amino acids.⁸⁷ Amino acids supported on either Wang resin or the highly acid-sensitive SASRIN resin can be methylated by reaction with pinacol chloromethylboronic ester, followed by rearrangement of the resulting aminomethylboronate and subsequent cleavage of the boronate group. It constituted a useful application of the Matteson rearrangement (Scheme 1-45).

(a) Hall, 2001**(b) Proposed mechanism**

Scheme 1-45 Matteson's 1,2-carbon-to-nitrogen rearrangement of boron, and its application to direct mono-*N*-methylation of solid-supported amino acids.

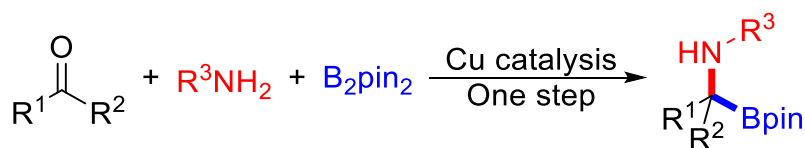
1.5 Summary and outlook

The development of synthetic methods for preparing α -aminoboronic acids and their derivatives, especially those reported in the past five years is reviewed. Their significant synthetic applications are also summarized and highlighted. For example, maintaining the α -aminoboronate core structure, peptide chain-containing α -aminoboronic acid derivatives, proline-derived α -aminoboronates, and hemiboronates were prepared. α -Aminoboronates have been widely used in the synthesis of chiral amines, isoindolinones, vicinal amino alcohols, *N*-functionalized 2,1-borazaronaphthalenes and β -aminoalkylboronic acid derivatives.

Considering their importance in the pharmaceutical industry, materials science, as well as organic synthesis, there is a driving force to develop greener, milder and more atom-economical methods for the efficient synthesis of α -aminoboronates in bulk quantities. The methods reported for their preparation *via* C-H functionalization are mainly based on precious metal catalysts, *e.g.* iridium and rhodium, or involve low temperatures ($-78\text{ }^{\circ}\text{C}$); therefore, it is expected that catalysts based on earth-abundant and low toxicity metals under milder conditions will be developed in the future. Greener synthetic methods using photocatalysis and electrocatalysis also can be expected. Moreover, novel methodologies based on α -aminoboronates for the construction of valuable compounds will no doubt continue to develop.

Chapter Two

The Borono-Strecker reaction: Synthesis of α -aminoboronates *via* a multicomponent reaction of carbonyl compounds, amines and B_2pin_2



- Multicomponent one-pot coupling
- Readily available starting materials
- Mild reaction conditions
- High functional group tolerance
- Gram-scale synthesis

36 examples
up to 95% yield

2 The Borono–Strecker reaction: Synthesis of α -aminoboronates *via* a multicomponent reaction of carbonyl compounds, amines and B_2pin_2

2.1 Abstract

This chapter developed the first Borono–Strecker reaction, a multicomponent reaction for the synthesis of α -aminoboronic acid derivatives from readily available carbonyl compounds, amines and B_2pin_2 . Diverse α -aminoboronates, including aryl-substituted and tertiary examples, were synthesized in moderate to high isolated yields. Compounds were prepared bearing *N*-(2-pyridyl) groups, which form five-membered rings *via* N–B coordination, as well as systems bearing non-coordinating *N*-aryl groups, the latter being isolated and fully characterized for the first time.

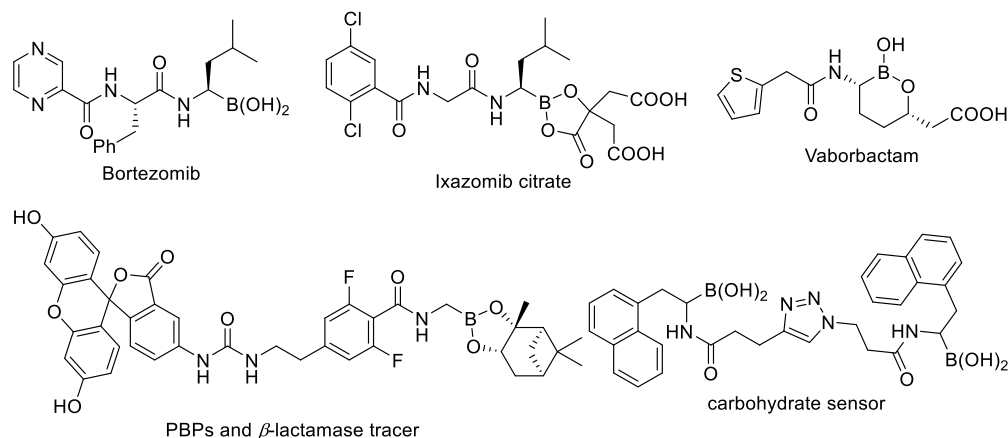
2.2 Introduction

Organoboron compounds have become increasingly of interest due to their numerous applications in organic synthesis, the pharmaceutical industry and materials science.^{1a,1b,1d,88} In particular, α -aminoboronic acids and their derivatives are important bioactive agents,^{1g,2f,89} functional materials,^{6–8} and synthetic building blocks.^{73b,74} For example, Bortezomib (trade name Velcade®) was approved by the FDA in 2003 for the treatment of multiple myeloma (a cancer of the plasma cells) and mantle cell lymphoma (a cancer of the lymph nodes).^{3,90} Wang and co-workers reported the first water-soluble and stable α -aminoboronic acid-based carbohydrate sensors which show useful fluorescence changes upon binding with three representative sugars, fructose, glucose, and sorbitol (Scheme 2-1a).^{6–7}

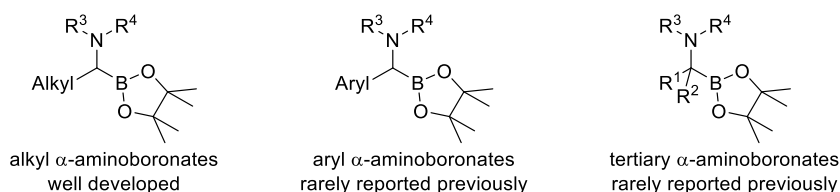
Growing interest in the therapeutic potential of α -aminoboronic acids provides the driving force to develop and refine efficient methods for their synthesis. However, only a few methods are currently available.^{2a,2c,2d,2g,12c} Synthetic approaches have focused on

Matteson's boronic ester homologation,^{11a,11b} diboration or hydroboration of imines,^{20,22–23,27–28} hydroboration of enamides,^{35,37} hydroamination or aminoboration of alkenyl Bdan compounds (dan = 1,8-diaminonaphthyl),^{38–39} decarboxylative borylation,⁶⁵ and others.^{42,44–46,48,53,57–58,59,62,64} All of these methods, though useful, have some drawbacks, such as poor functional group tolerance, tedious procedures or expensive catalysts. The synthesis of alkyl α -aminoboronic acid derivatives has been well studied, whereas aryl-substituted and sterically hindered tertiary species, though valuable, are rare (Scheme 2-1b). Development of efficient and versatile chemical transformations for synthesizing α -aminoboronates from readily available starting materials is thus highly desirable.

(a) Examples of bioactive compounds and sensors possessing an α -aminoboronate motif.



(b) Diverse α -aminoboronates reported.

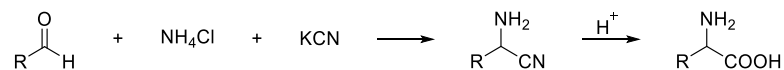


Scheme 2-1 Previously reported α -aminoboronates.

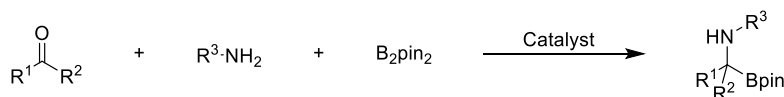
Carbonyl compounds and amines are ideal starting materials as they are inexpensive and readily available from commercial suppliers. The Strecker reaction is an efficient method for the synthesis of α -amino acids by the reaction of an aldehyde with ammonium chloride in the presence of potassium cyanide. Taking advantage of multicomponent reactions, it

can bypass the synthesis and isolation of imine intermediates, which increases product scope, reduces the number of steps, and improves atom economy (Scheme 2-2a).

(a) Strecker reaction for the synthesis of α -amino acids.



(b) Borono-Strecker reaction for the synthesis of α -aminoboronates (this work).



Scheme 2-2 Synthesis of α -amino acids and α -aminoboronates.

Herein, this chapter reports a multicomponent coupling for the synthesis of diverse α -aminoboronic acid derivatives from inexpensive and readily available starting materials, *i.e.* aldehydes or ketones, amines, and bis(pinacolato)diboron (B_2pin_2), which has the advantages of operational simplicity, low cost, and a lower likelihood of cross-compatibility problems (Scheme 2-2b). The key challenge is chemoselectivity in multicomponent reactions, and avoidance of side reactions between B_2pin_2 and aldehydes⁹¹ or amines.⁹²

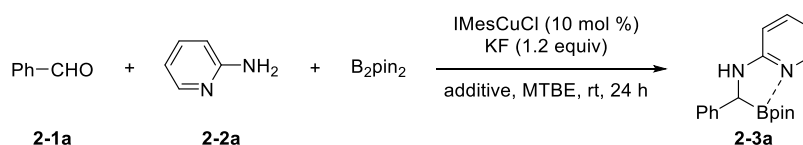
2.3 Results and discussions

2.3.1 Optimization of reaction conditions

I examined possible reaction conditions using benzaldehyde **2-1a** and 2-aminopyridine **2-2a** as the model substrates, B_2pin_2 as the boron reagent, KF as the base, and (IMes)CuCl as the catalyst.^{36b,36i,91,93} The desired α -aminoboronate **2-3a** was obtained, but only in 21% yield (Table 2-1, Entry 1). Addition of $\text{Ti}(\text{OEt})_4$ as a Lewis acid significantly improved the yield to 79% without any observation of the imine intermediate or other byproducts (Table 2-1, Entries 2–8). Use of 0.8 equiv of $\text{Ti}(\text{OEt})_4$ gave the highest yield (Table 2-1, Entry 6). Various catalysts and ligands, including NHC-copper complexes and various phosphine or nitrogen ligands, were examined, and CuCl/bpy (2,2'-bipyridine) proved to be the best combination, giving the product in 90% yield (Tables 2-3 and 2-4). Different solvents were tested, and MTBE (methyl *t*-butyl ether) was found to be the best (Table 2-5). The catalytic

efficiency was further improved by screening the amounts of CuCl and bpy, increasing the yield of the desired α -aminoboronates to 98% (Table 2-6, Entries 1–4). When KF was omitted from the reaction, the yield decreased significantly (Table 2-2), but some turnover occurred, possibly promoted by EtO⁻ as the base (*vide infra*). In the absence of catalyst or ligand, strikingly decreased yields were observed (Table 2-6, Entries 5 and 6).

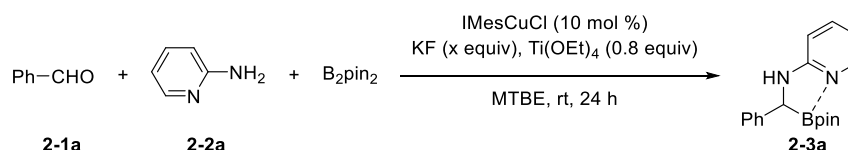
Table 2-1 Screening of additives for the Borono–Strecker reaction^a



Entry	Additive	Yield (%) ^b
1	–	21
2 ^c	4 Å molecular sieves	36
3	MgSO ₄	10
4	NaSO ₄	29
5	Ti(OEt) ₄	79 (74)
6^d	Ti(OEt)₄	78 (74)
7 ^e	Ti(OEt) ₄	62
8 ^f	Ti(OEt) ₄	62

^aReaction conditions: **2-1a** (0.5 mmol), **2-2a** (0.6 mmol, 1.2 equiv), B₂pin₂ (0.6 mmol, 1.2 equiv), KF (0.6 mmol, 1.2 equiv), additive (0.5 mmol, 1.0 equiv), I-MesCuCl (10 mol %), MTBE (2 mL) in an argon-filled glovebox, then reacted at ambient temperature unless otherwise specified. ^bThe product yields were determined by GC-MS using *n*-dodecane as the internal calibration standard. Isolated yields are given in parentheses. ^c40 mg of 4 Å molecular sieves was used as additive. ^dTi(OEt)₄ (0.4 mmol, 0.8 equiv). ^eTi(OEt)₄ (0.3 mmol, 0.6 equiv). ^fTi(OEt)₄ (0.25 mmol, 0.5 equiv).

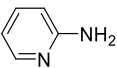
Table 2-2 Screening of the amount of KF for the Borono–Strecker reaction^a



Entry	x	Yield (%) ^b
1	1.2	78 (74)
2	0.1	55
3	0	34

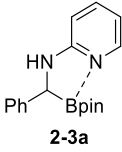
^aReaction conditions: **2-1a** (0.5 mmol), **2-2a** (0.6 mmol, 1.2 equiv), B₂pin₂ (0.6 mmol, 1.2 equiv), KF (0.6 mmol, 1.2 equiv), Ti(OEt)₄ (0.4 mmol, 0.8 equiv), I-MesCuCl (10 mol %), MTBE (2 mL) in an argon-filled glovebox, then reacted at ambient temperature unless otherwise specified. ^bThe product yields were determined by GC-MS using *n*-dodecane as the internal calibration standard. Isolated yields are given in parentheses.

Table 2-4 Screening of other metal catalysts for the Borono–Strecker reaction^a

Ph-CHO +  + B_2pin_2

catalyst (10 mol %), ligand (10 mol %)
 KF (1.2 equiv), Ti(OEt)₄ (0.8 equiv)

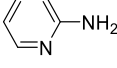
$\xrightarrow{\text{MTBE, rt, 24 h}}$



Entry	Catalyst	Ligand	Yield (%) ^b
1	MgBr ₂ ·Et ₂ O	bpy	0
2	MgCl ₂	bpy	0
3	FeCl ₂	bpy	0
4	FeCl ₃	bpy	0
5	Zn(OTf) ₂	bpy	0
6	Zn(acac) ₂	bpy	10
7	ZnCl ₂	bpy	19
8	Mn(OAc) ₂ ·4H ₂ O	bpy	9
9	Mn(OAc) ₃ ·2H ₂ O	bpy	36

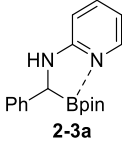
^aReaction conditions: **2-1a** (0.5 mmol), **2-2a** (0.6 mmol, 1.2 equiv), B₂pin₂ (0.6 mmol, 1.2 equiv), KF (0.6 mmol, 1.2 equiv), Ti(OEt)₄ (0.4 mmol, 0.8 equiv), catalyst (10 mol %), ligand (10 mol %), MTBE (2 mL) in an argon-filled glovebox, then reacted at ambient temperature unless otherwise specified. ^bThe product yields were determined by GC-MS using *n*-dodecane as the internal calibration standard. Isolated yields are given in parentheses.

Table 2-5 Screening of solvents for the Borono–Strecker reaction^a

Ph-CHO +  + B_2pin_2

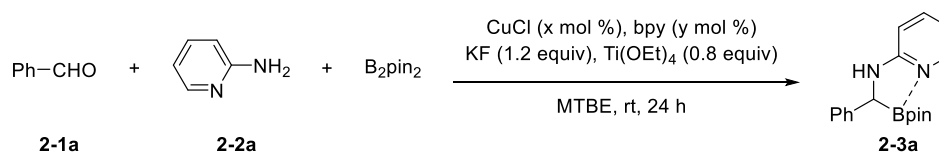
CuCl (10 mol %), bpy (10 mol %)
 KF (1.2 equiv), Ti(OEt)₄ (0.8 equiv)

$\xrightarrow{\text{solvent, rt, 24 h}}$



Entry	Solvent	Yield (%) ^b
1	MTBE	90 (85)
2	THF	60
3	Et ₂ O	40
4	CH ₂ Cl ₂	40
5	chloroform	47
6	ethyl acetate	62
7	acetone	0
8	CH ₃ CN	51
9	toluene	60
10	hexane	33
11	DMF	57

^aReaction conditions: **2-1a** (0.5 mmol), **2-2a** (0.6 mmol, 1.2 equiv), B₂pin₂ (0.6 mmol, 1.2 equiv), KF (0.6 mmol, 1.2 equiv), Ti(OEt)₄ (0.4 mmol, 0.8 equiv), CuCl (10 mol %), bpy (10 mol %), solvent (2 mL) in an argon-filled glovebox, then reacted at ambient temperature unless otherwise specified. ^bThe product yields were determined by GC-MS using *n*-dodecane as the internal calibration standard. Isolated yields are given in parentheses.

Table 2-6 Screening of the amount of catalyst and ligand for the Borono–Strecker reaction^a

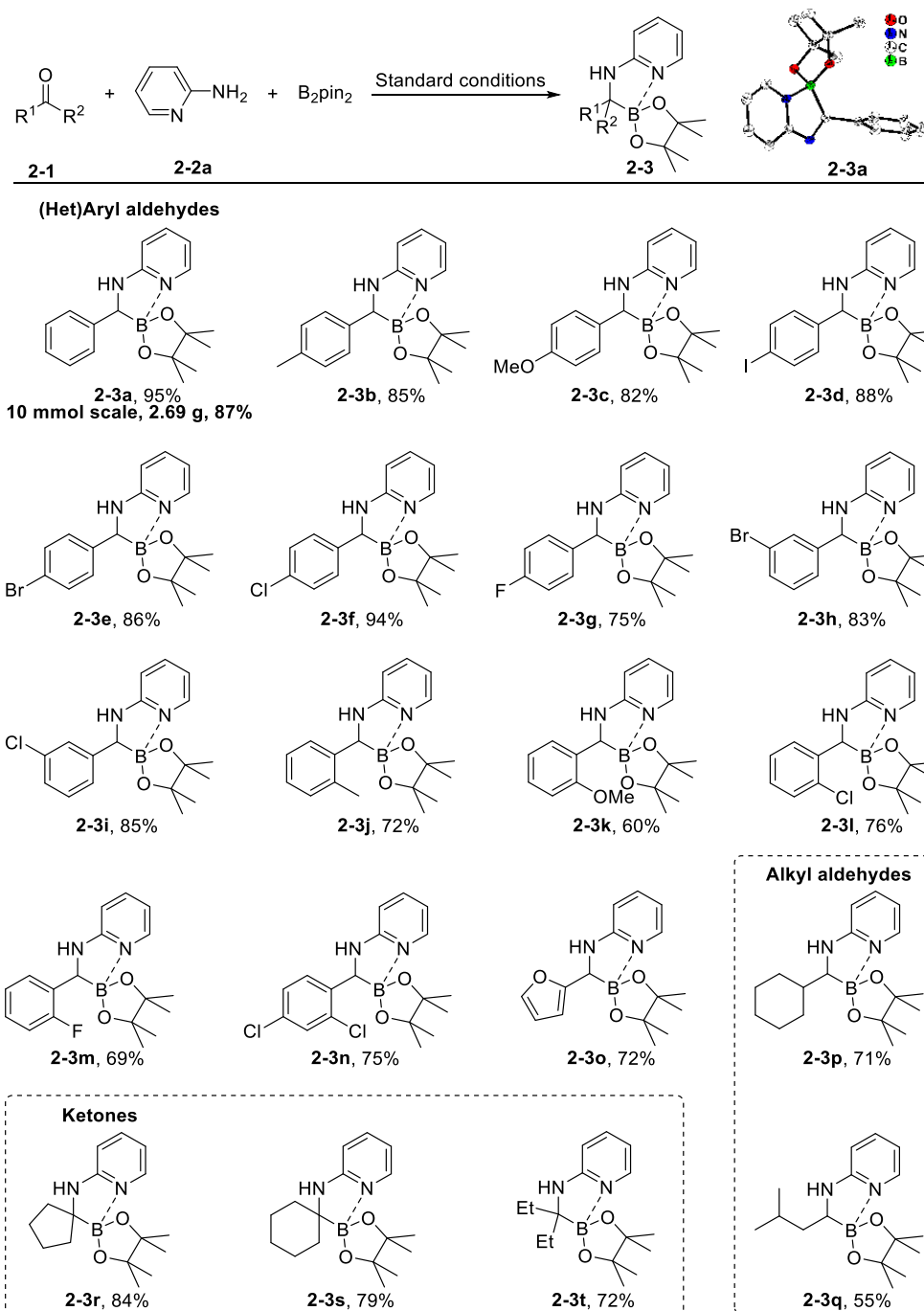
Entry	CuCl (x mol%)	bpy (y mol%)	Yield (%) ^b
1	10	10	90 (85)
2	5	5	92 (88)
3	2	2	98 (95)
4	1	1	89
5	2	0	50
6	0	2	0

^aReaction conditions: **2-1a** (0.5 mmol), **2-2a** (0.6 mmol, 1.2 equiv), B_2pin_2 (0.6 mmol, 1.2 equiv), KF (0.6 mmol, 1.2 equiv), $\text{Ti}(\text{OEt})_4$ (0.4 mmol, 0.8 equiv), CuCl (10 mol %), bpy (10 mol %), MTBE (2 mL) in an argon-filled glovebox, then reacted at ambient temperature unless otherwise specified. ^bThe product yields were determined by GC-MS using *n*-dodecane as the internal calibration standard. Isolated yields are given in parentheses.

2.3.2 Investigation of reaction scope

The substrate scope was investigated (Scheme 2-3) and both donor- and acceptor-substituted aromatic aldehydes were successfully transformed with modest to excellent isolated yields. Aryl aldehydes bearing electron-donating functionalities, such as Me and OMe, worked well, affording the corresponding α -aminoboronates in modest to good yields (**2-3b**, **2-3c**, **2-3j**, and **2-3k**, 60–85%), possibly because the electron-donating groups made the intermediate imines more resistant to boryl anion addition. Halogen-substituted aryl aldehydes were *viable* substrates giving the products in good yields. Iodide and bromide substituents on the phenyl ring were tolerated with this copper catalyst system, and no C–I or C–Br borylation product was observed during the reaction, which indicated the high chemoselectivity of this catalytic system.^{30c,94} Tolerance to halide substituents provides possibilities for further functionalization. The isolated yields obtained for *para*-substituted aryl aldehydes were slightly higher than those for *meta*- and *ortho*-aryl substrates (e.g. compare **2-3b/2-3j**, **2-3c/2-3k**, and **2-3f/2-3i/2-3l**). The heteroaromatic substrate furfural gave the desired α -aminoboronate **2-3o** in 72% yield. This method enables a convenient gram-scale synthesis (10 mmol) without significant loss of yield, as demonstrated for **2-1a** (**2-3a**: 2.69 g, 87%). The structure of product **2-3a** was confirmed by single-crystal X-ray

diffraction (Scheme 2-3). Coordination of the pyridine nitrogen to boron provides suitable stability for purification by column chromatography and isolation in air (*vide infra*).



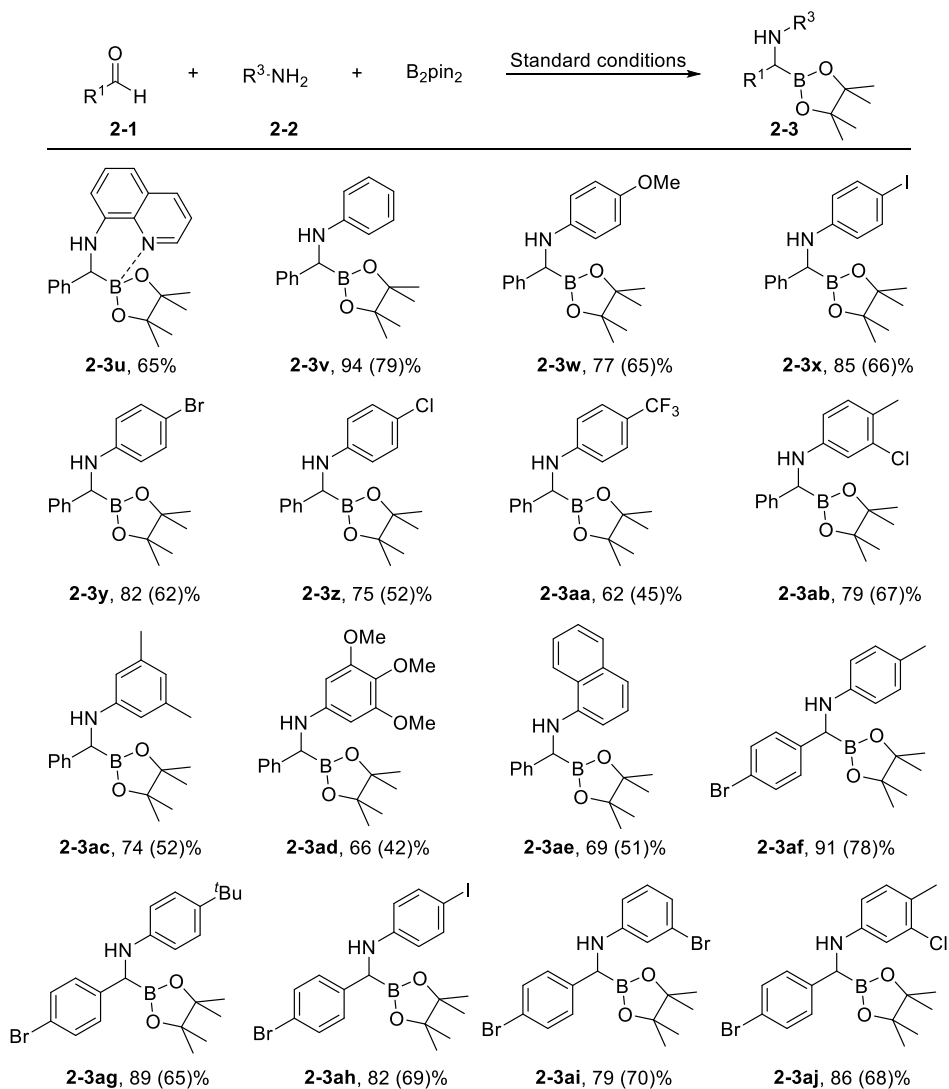
^aStandard conditions: **2-1** (0.5 mmol), **2-2a** (0.6 mmol, 1.2 equiv), B₂pin₂ (0.6 mmol, 1.2 equiv), KF (0.6 mmol, 1.2 equiv), Ti(OEt)₄ (0.4 mmol, 0.8 equiv), CuCl (2 mol %), bpy (2 mol %), MTBE (2 mL), rt, 24 h, with isolated yields.

Scheme 2-3 Synthesis of α -aminoboronates *via* the multicomponent coupling of 2-aminopyridine, B₂pin₂ and various carbonyl compounds^a

The majority of therapeutically relevant α -aminoboronates bear an α -alkyl functionality, but

surprisingly few methods to produce these compounds in a catalytic manner were reported.^{23,28,35,38,59} Under standard conditions, alkyl aldehydes also reacted with amines and B₂pin₂ to produce the target products. Cyclohexanecarboxaldehyde and isovaleraldehyde were converted in moderate to good yields (**2-3p**, 71%, and **2-3q**, 55%, respectively). Sterically congested tertiary α -aminoboronates are rare,^{24–25,35,52,62} but we note that they can be obtained using this multicomponent reaction of ketones, amines and B₂pin₂. Both cyclic (cyclopentanone **2-1v** and cyclohexanone **2-1s**) and acyclic ketones (3-pentanone **2-1t**) were suitable substrates, producing the corresponding tertiary α -aminoboronates in good yields (72–84%) (Scheme 2-3).

This multicomponent reaction can be extended to other amines (Scheme 2-4). Thus, α -aminoboronate **2-3u** was obtained from 8-aminoquinoline in 65% isolated yield. Additionally, α -aminoboronic pinacol esters not bearing a coordinating secondary α -amino group are unstable and have not been reported. Migration of boron from carbon to nitrogen in α -aminoboronates to yield the corresponding amines in protic solvents was suggested to be the main cause of their instability.^{2a,11b,86a,87} In this study, a series of aryl amines were employed (**2-2v–2-2aj**), and the desired α -aminoboronates were detected by GCMS. However, they decomposed when exposed to air, or on attempted purification by column chromatography on silica gel, but the target products can be crystallized at low temperature after filtration. A wide range of aromatic amines, containing both electron-donating (e.g. Me, OMe and ^tBu, **2-3w**, **2-3af**, and **2-3ag**) and electron-withdrawing functional groups (e.g. halides and CF₃, **2-3x**, **2-3y**, **2-3z**, **2-3aa**, **2-3ah**, and **2-3ai**), were thus successfully transformed into the target products in moderate to good yields. Both multi-substituted aryl amines (**2-2ab**, **2-2ac**, **2-2ad**, and **2-2aj**) and sterically hindered 1-naphthylamine (**2-2ae**) were also suitable substrates, giving the desired products in moderate yields. The structures of the α -aminoboronate products were confirmed as exemplified by single-crystal X-ray diffraction studies of **2-3v** and **2-3y** (Figure 2-1).



^aStandard conditions: **2-1** (0.5 mmol), **2-2** (0.6 mmol, 1.2 equiv), B_2pin_2 (0.6 mmol, 1.2 equiv), KF (0.6 mmol, 1.2 equiv), $\text{Ti}(\text{OEt})_4$ (0.4 mmol, 0.8 equiv), IMesCuCl (2 mol %), MTBE (2 mL), rt, 24 h. Yields were determined by NMR using 1,3,5-trimethoxybenzene as the internal calibration standard, with isolated yields in parentheses.

Scheme 2-4 Synthesis of α -aminoboronates *via* the multicomponent coupling of aldehydes, B_2pin_2 and various aryl amines^a

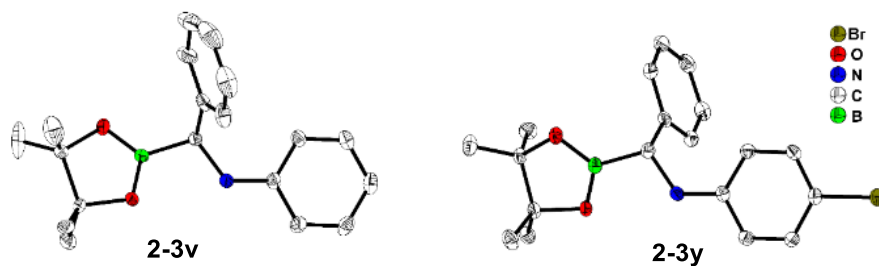
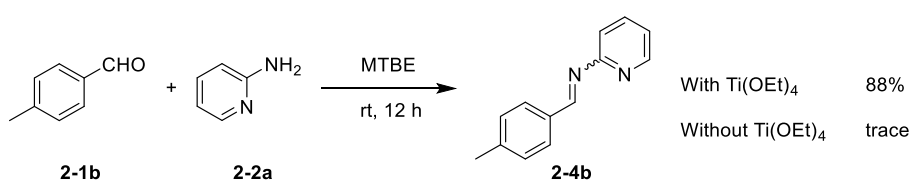


Figure 2-1 Molecular structures of **2-3v** and **2-3y**.

2.4 Mechanistic studies

2.4.1 Role of $\text{Ti}(\text{OEt})_4$ in the formation of imines

To gain insight into the mechanism of this Borono–Strecker reaction, a series of studies were carried out. Intermediate imine **2-4b** was formed in a high yield when *p*-tolualdehyde **2-1b** and 2-aminopyridine **2-2a** were mixed in the presence of $\text{Ti}(\text{OEt})_4$ (Scheme 2-5, Figure 2-2). In the absence of $\text{Ti}(\text{OEt})_4$, there was no imine detected, which indicated the important role of the Lewis acid in its formation (Scheme 2-5, Figure 2-3).



Scheme 2-5 Role of $\text{Ti}(\text{OEt})_4$ in the formation of imines.

Experimental procedure

In a 10 mL thick-walled reaction tube equipped with a magnetic stirring bar, 2-aminopyridine **2-2a** (1.2 equiv, 56.5 mg, 0.6 mmol) and MTBE (2 mL) were added. Then, *p*-tolualdehyde **2-1b** (1.0 equiv, 59 μL , 0.5 mmol) was added, and the tube was sealed with a crimped septum cap. The reaction was stirred at room temperature for 12 h, and 1,3,5-trimethoxybenzene (0.5 equiv, 42.0 mg) was then added as the internal calibration standard. The resulting mixture was analyzed by ^1H NMR spectroscopy in CDCl_3 solution. The ^1H NMR spectrum is shown below (Figure 2-2). Only a trace of the desired imine **2-4b** was observed, and most of the starting materials, **2-1b** and **2-2a**, remained.

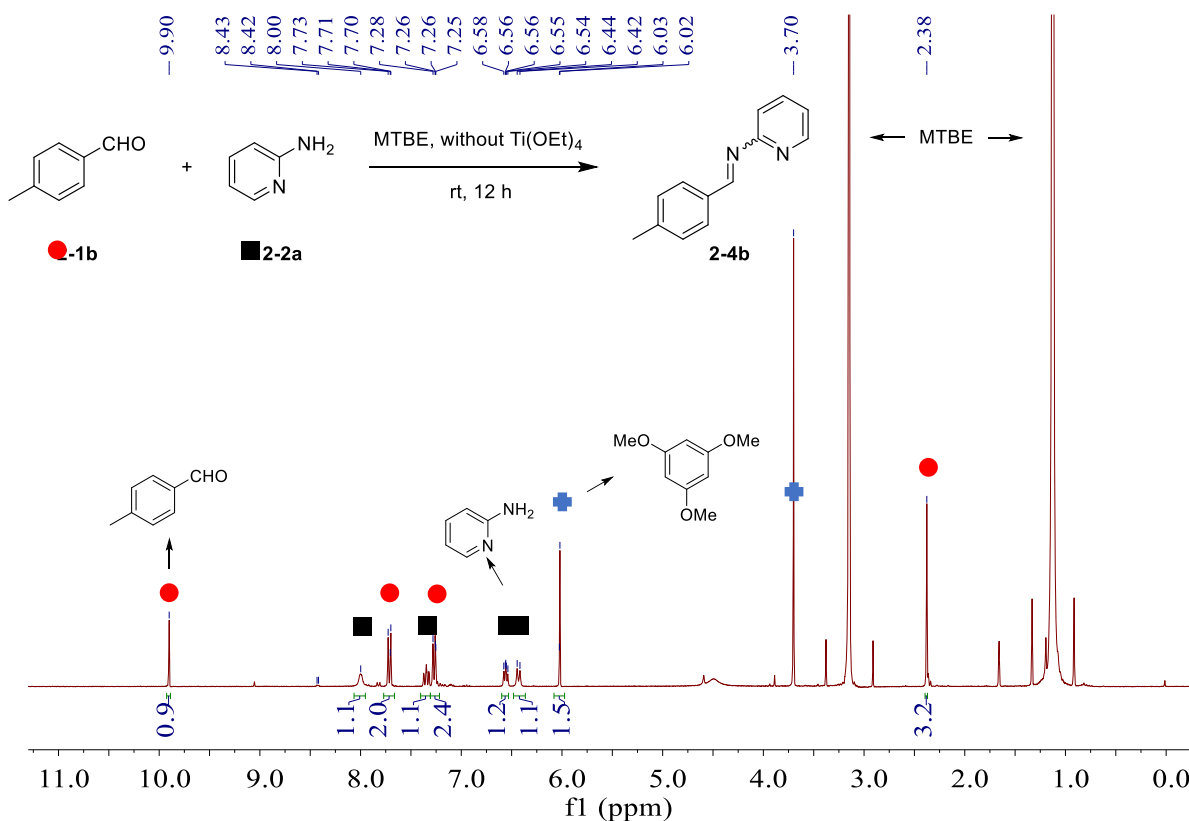


Figure 2-2 ^1H NMR spectrum of the reaction mixture in the absence of $\text{Ti}(\text{OEt})_4$ (300 MHz, CDCl_3 , rt); The presence of unreacted starting materials was confirmed by ^1H NMR spectroscopy using 1,3,5-trimethoxybenzene as the internal calibration standard.

Experimental procedure

In a 10 mL thick-walled reaction tube equipped with a magnetic stirring bar, 2-aminopyridine **2-2a** (1.2 equiv, 56.5 mg, 0.6 mmol) and MTBE (2 mL) were added. Then, *p*-tolualdehyde **2-1b** (1.0 equiv, 59 μL , 0.5 mmol) and $\text{Ti}(\text{OEt})_4$ (0.8 equiv, 91.2 mg, 0.4 mmol) were added, and the tube was sealed with a crimped septum cap. The reaction was stirred at room temperature for 12 h, and 1,3,5-trimethoxybenzene (0.5 equiv, 42.0 mg) was then added as the internal calibration standard. The resulting mixture was analyzed by ^1H NMR spectroscopy in CDCl_3 solution. The ^1H NMR spectrum is shown below (Figure 2-3). The desired imine **2-4b** was obtained in a yield of 88% (NMR yield).

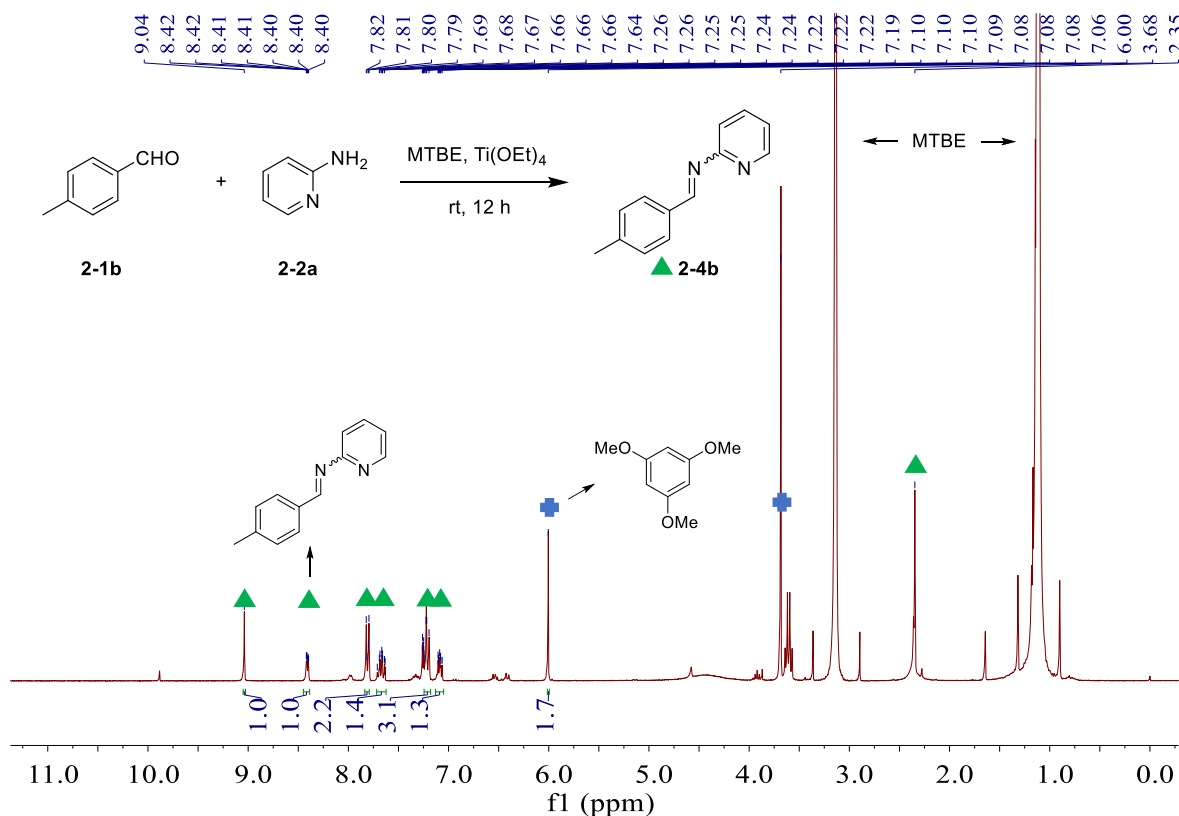
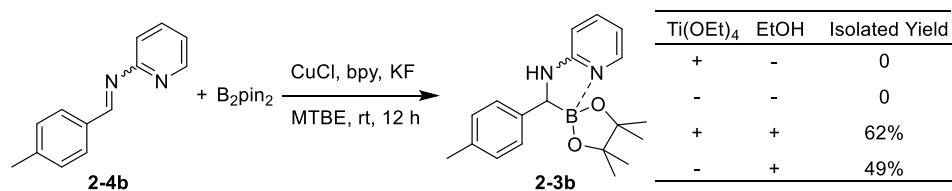


Figure 2-3 ^1H NMR spectrum of the reaction mixture in the presence of $\text{Ti}(\text{OEt})_4$ (300 MHz, CDCl_3 , rt); the product yield was determined by ^1H NMR spectroscopy using 1,3,5-trimethoxybenzene as the internal calibration standard.

2.4.2 Role of $\text{Ti}(\text{OEt})_4$ and protons in the hydroboration process

Using imine **2-4b** as the starting material, under standard conditions, α -aminoboronate **2-3b** was not formed with or without added $\text{Ti}(\text{OEt})_4$, but **2-3b** was formed under the standard conditions when 1.0 equivalent of ethanol was added, indicating that a proton source is essential for the hydroboration of imines. The slight difference in the isolated yields is probably within experimental error ($56 \pm 6\%$) (Scheme 2-6).



Scheme 2-6 Role of $\text{Ti}(\text{OEt})_4$ and protons in the hydroboration process.

2.4.3 Stepwise reaction

A stepwise reaction was conducted, in which *p*-tolualdehyde **2-1b** was first reacted with 2-aminopyridine **2-2a** in the presence of $\text{Ti}(\text{OEt})_4$ to form imine **4b** within 12 hours as the only product. CuCl , *bpy*, B_2pin_2 and KF were then added to the reaction mixture. The concentration of **2-4b** gradually decreased while the yield of **2-3b** increased. After 24 hours, imine intermediate **2-4b** was totally transformed into the α -aminoboronate **2-3b** (Figure 2-4).

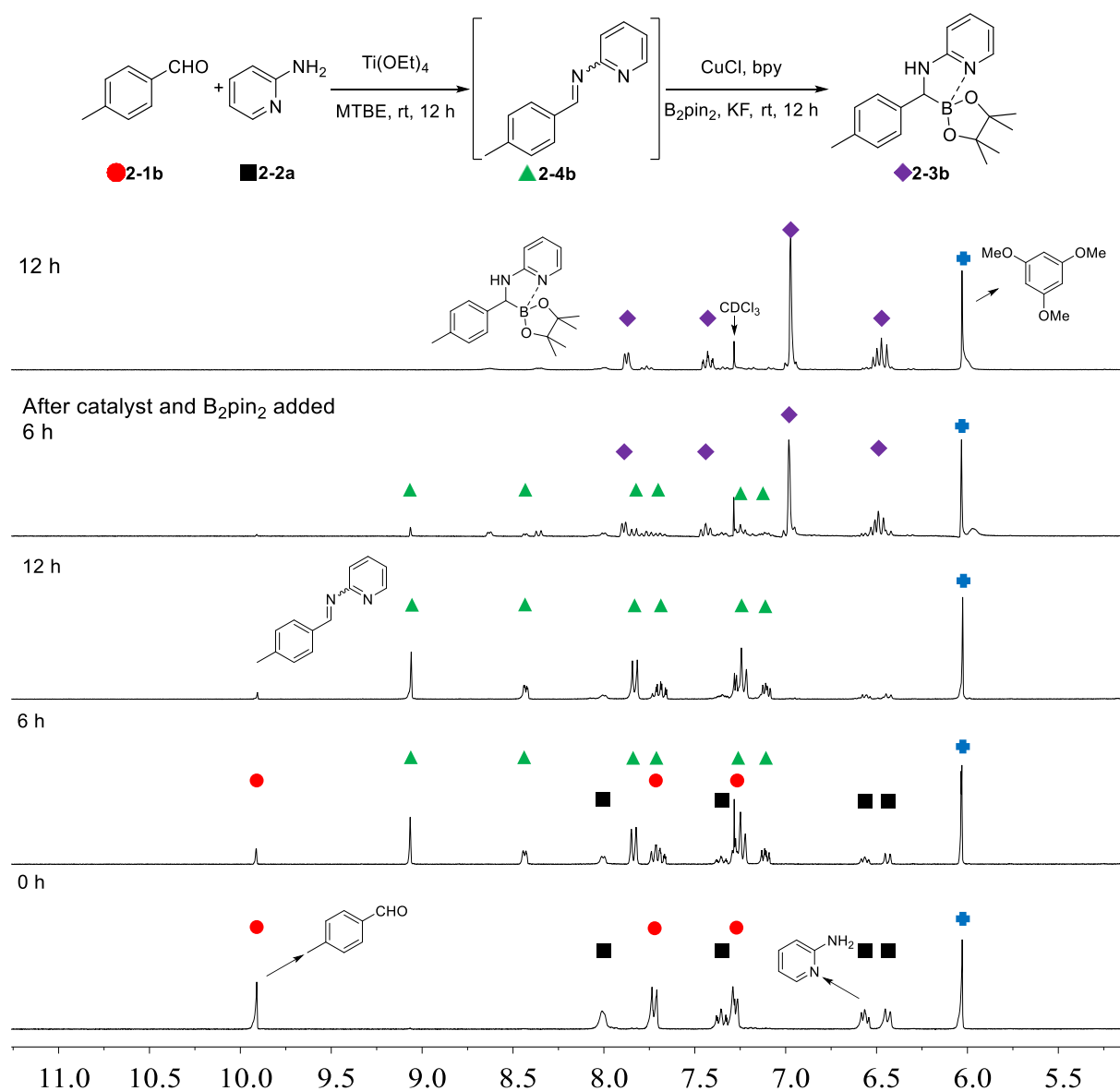


Figure 2-4 Stepwise (bottom to top) reaction process monitored by ^1H NMR spectroscopy (300 MHz, CDCl_3 , rt); 1,3,5-trimethoxybenzene (blue + sign) was used as an internal standard.

2.4.4 Interaction of products **2-3a** and **2-3y** with DMAP

Addition of 4-dimethylaminopyridine (DMAP) to **2-3a** did not lead to a significant change in the ^{11}B NMR spectrum (Figure 2-5), while the N–H proton resonance in the ^1H NMR spectrum shifted down field from 5.59 ppm to 6.65 ppm (Figure 2-6). Addition of DMAP to **2-3y** led to a significant shift of the resonance in the ^{11}B NMR spectrum from 31.8 ppm to 10.6 ppm (Figure 2-7), which indicated coordination of the DMAP to boron.

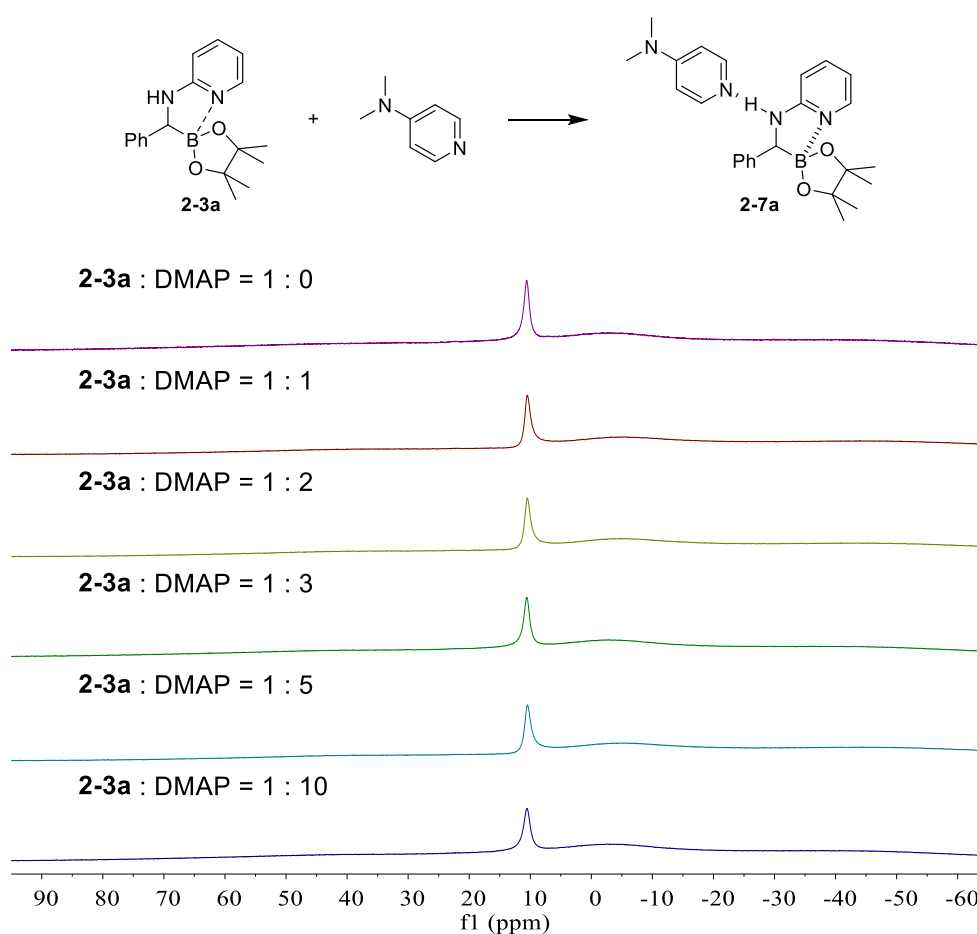


Figure 2-5 ^{11}B NMR spectrum of **2-3a** with different ratios of compound to DMAP (96 MHz, CDCl_3 , rt).

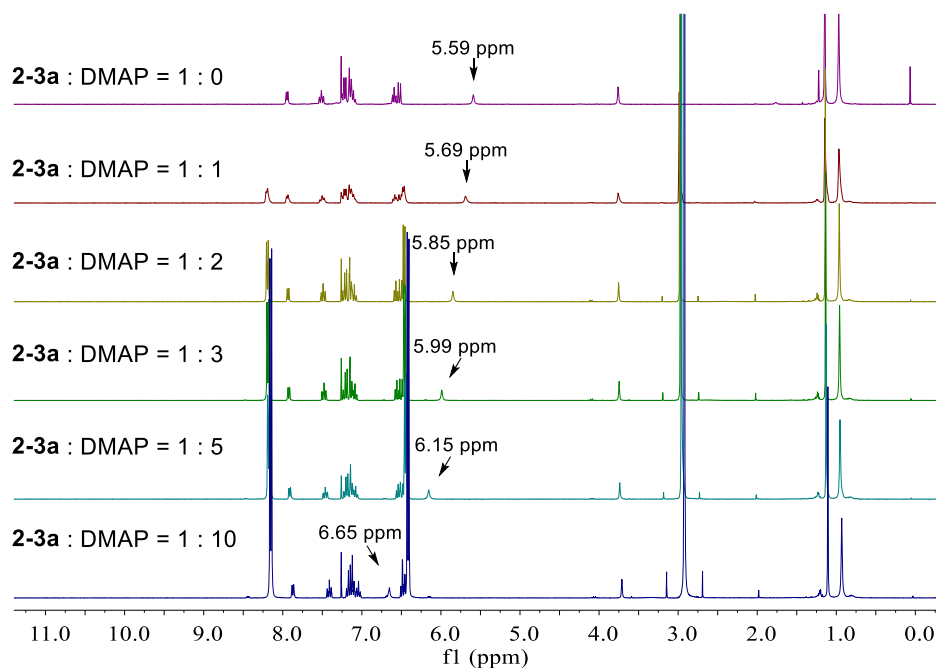


Figure 2-6 ^1H NMR spectrum of **2-3a** with different ratios of compound to DMAP (300 MHz, CDCl_3 , rt).

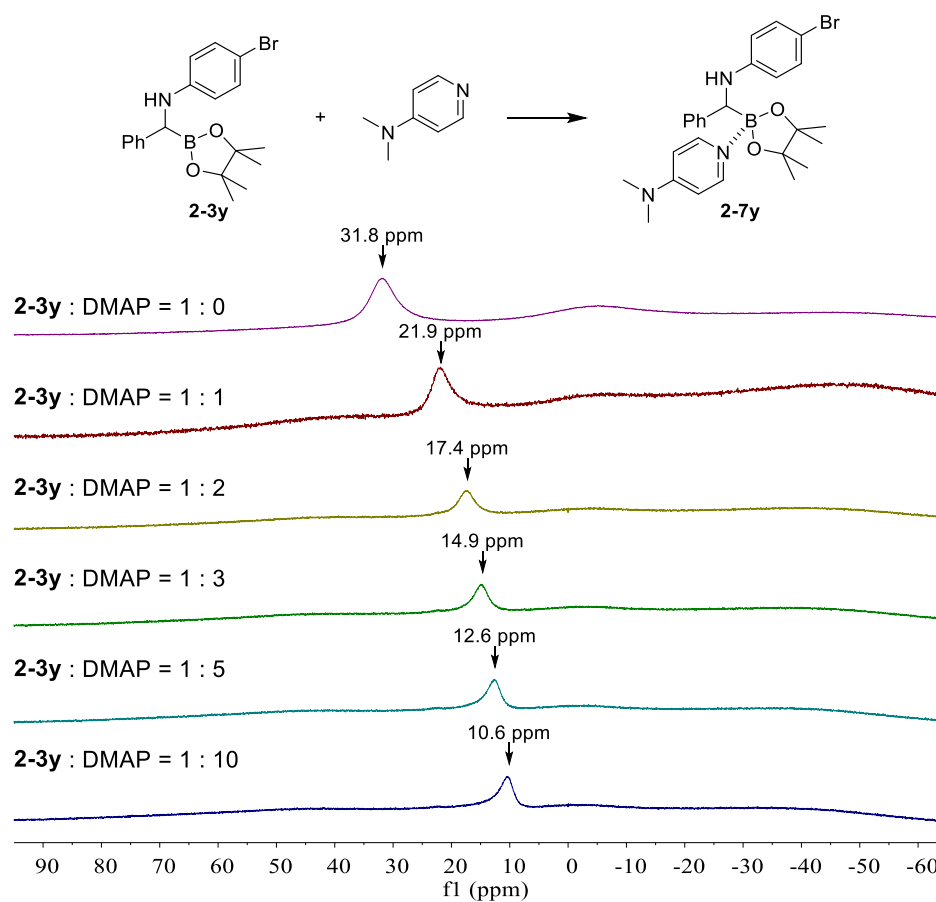


Figure 2-7 ^{11}B NMR spectrum of **2-3y** with different ratios of compound to DMAP (96 MHz, CDCl_3 , rt).

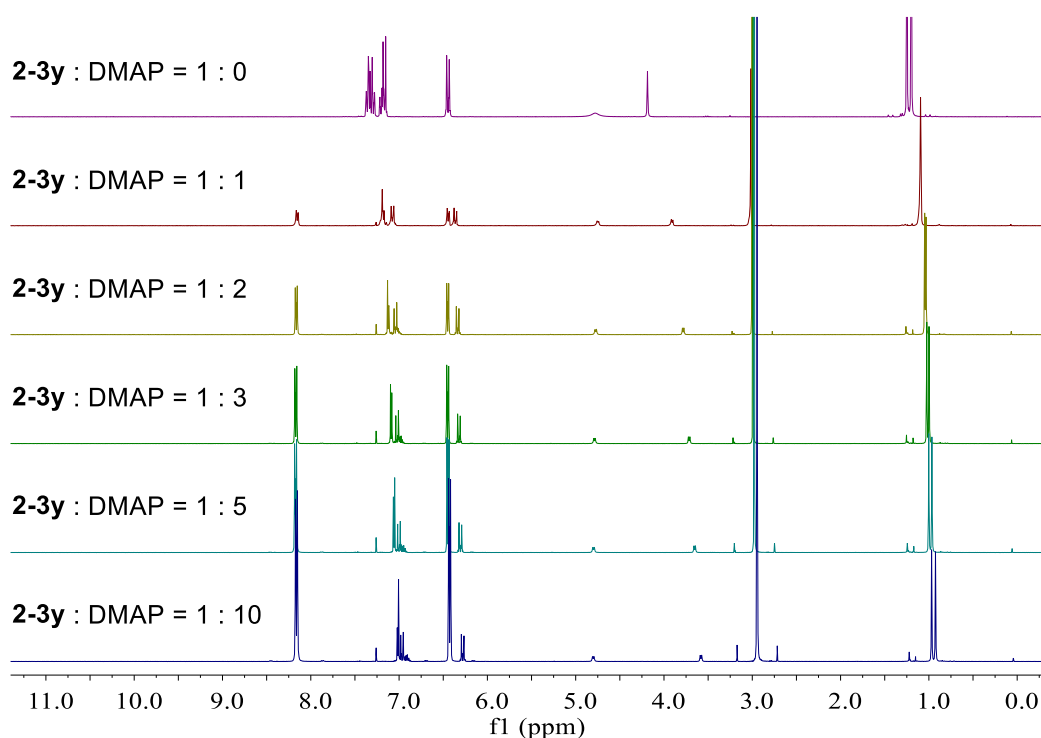
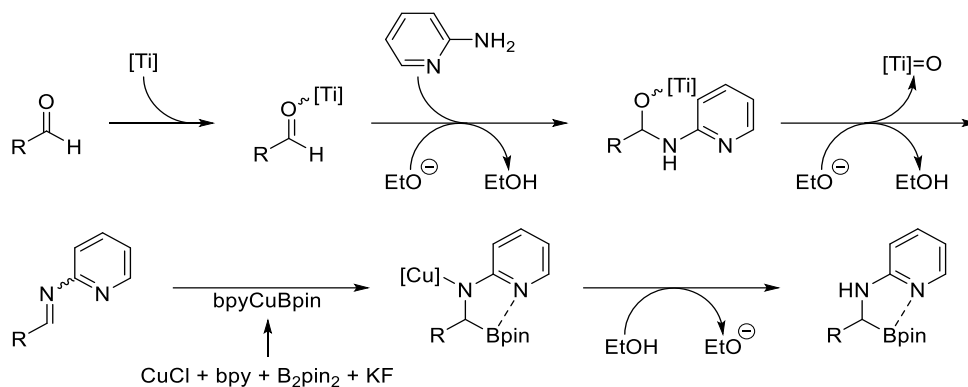


Figure 2-8 ¹H NMR spectrum of **2-3y** with different ratios of compound to DMAP (300 MHz, CDCl₃, rt).

2.4.5 Proposed mechanism

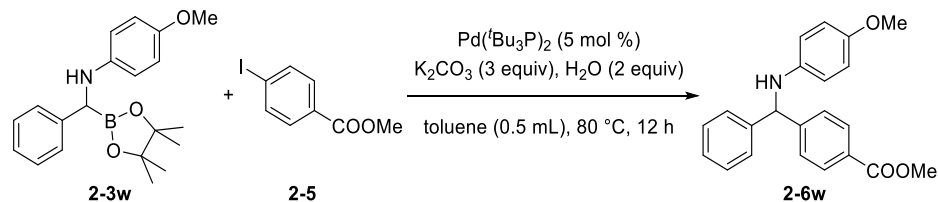
Based on our experimental observations and literature precedents,^{23,28,95} a possible mechanism for the multicomponent reaction of carbonyl compounds, amines and B₂pin₂ is shown in Scheme 2-7. Acting as a Lewis acid, Ti(OEt)₄ activates the carbonyl moiety and promotes the formation of imine intermediates. A copper-catalyzed hydroboration subsequently occurs with the assistance of a proton to yield the desired α -aminoboronates. The formation of EtO⁻ may also assist the reaction by augmenting F⁻ as a means of activating B₂pin₂ for transmetalation to copper.^{1d,30} Interestingly, under our conditions, borylation of imines⁸ is efficient, but test reactions showed that their aldehyde precursors are not borylated with our catalyst system (CuCl, bpy, and KF), either with or without Ti(OEt)₄ present, in contrast to Sadighi's (ICy)CuO-*t*-Bu catalyst for aldehyde diboration¹³ which contains a strongly σ -donating NHC ligand.



Scheme 2-7 Proposed mechanism.

2.5 Synthetic applications of α -aminoboronates

As a preliminary demonstration of the utility of our α -aminoboronates in synthesis, a Suzuki–Miyaura cross-coupling reaction of the α -aminoboronate **2-3w** with methyl 4-iodobenzoate **2-5** was conducted (Scheme 2-8).^{73b} Sterically hindered secondary amine **2-6w** was obtained in 78% isolated yield.



Scheme 2-8 Preparation of congested secondary amine **2-6w** via a Suzuki–Miyaura cross-coupling reaction.

2.6 Summary

In conclusion, this chapter report the Borono–Strecker reaction, a novel, concise multicomponent coupling reaction for the preparation of α -aminoboronates from readily available starting materials, namely carbonyl compounds, amines and B_2pin_2 . A series of α -aminoboronates, including aryl-substituted, alkyl-substituted, and more sterically congested ones, were synthesized in moderate to excellent yields. This chapter also reports the isolation and characterization of α -aminoboronates not bearing coordinating secondary α -amino groups, which are unstable and were not studied previously.

Mechanistic studies indicate the role of $\text{Ti}(\text{OEt})_4$ in the formation of imine intermediates and the role of a proton source in the subsequent hydroboration process.

2.7 Experimental procedures and characterization data

2.7.1 General information

All reagents were purchased from Alfa–Aesar, Aldrich, ABCR or VWR, and were checked for purity by GC-MS and/or ^1H NMR spectroscopy and used as received. HPLC grade solvents were argon saturated, dried using an Innovative Technology Inc. Solvent Purification System, and further deoxygenated by using the freeze-pump-thaw method. CDCl_3 was purchased from Cambridge Isotope Laboratories. All manipulations were performed in an argon-filled glove box unless otherwise stated.

Automated flash chromatography was performed using a Biotage[®] Isolera Four system, on deactivated silica gel (35% w/w H_2O). Commercially available, precoated TLC plates (Polygram[®] Sil G/UV254) were purchased from Macherey-Nagel. The removal of solvent was performed on a rotary evaporator *in vacuo* at a maximum temperature of 40 °C.

GC-MS analyses were performed using an Agilent 7890A gas chromatograph (column: HP-5MS 5% phenyl methyl siloxane, 30 m, \varnothing 0.25 mm, film 0.25 μm ; injector: 250 °C; oven: 80 °C (2 min), 80 °C to 180 °C (20 °C min^{-1}), 180 °C to 280 °C (50 °C min^{-1}), 280 °C (5 min); carrier gas: He (1.2 mL min^{-1})) equipped with an Agilent 5975C inert MSD with triple-axis detector operating in EI mode and an Agilent 7693A series auto sampler/injector. Elemental analysis was performed on a Elementar vario MICRO cube Elemental Analyzer. High-resolution mass spectra were recorded using a Thermo Fischer Scientific Exactive Plus Orbitrap MS system (ASAP probe).

NMR spectra were recorded at ambient temperature using Bruker Avance III HD 300 NMR (^1H , 300 MHz; $^{13}\text{C}\{^1\text{H}\}$, 75 MHz; ^{11}B , 96 MHz), Bruker Avance III HD 400 NMR (^1H , 400 MHz; $^{13}\text{C}\{^1\text{H}\}$, 100 MHz; ^{11}B , 128 MHz), or Bruker Avance III HD 500 NMR (^1H , 500 MHz;

$^{13}\text{C}\{^1\text{H}\}$, 126 MHz; ^{11}B , 160 MHz; ^{19}F , 471 MHz) spectrometers. ^1H NMR chemical shifts are reported relative to TMS and were referenced *via* residual proton resonance of the corresponding deuterated solvent (CDCl_3 : 7.26 ppm) whereas $^{13}\text{C}\{^1\text{H}\}$ NMR spectra are reported relative to TMS *via* the carbon signal of the deuterated solvent (CDCl_3 : 77.00 ppm). ^{11}B NMR chemical shifts are quoted relative to $\text{BF}_3 \cdot \text{Et}_2\text{O}$ as the external standard. ^{19}F NMR chemical shifts are quoted relative to CFCl_3 as the external standard.

2.7.2 Experimental procedures

General procedures for examples described in Tables 2-1 to 2-6, and Scheme 2-3 (taking 2-3a as an example).

In a 10 mL thick-walled reaction tube equipped with a magnetic stirring bar, CuCl (2 mol %, 1.0 mg, 0.01 mmol), bpy (2 mol %, 1.6 mg, 0.01 mmol), B_2pin_2 (1.2 equiv, 152.4 mg, 0.6 mmol), KF (1.2 equiv, 34.9 mg, 0.6 mmol), 2-aminopyridine **2-2a** (1.2 equiv, 56.5 mg, 0.6 mmol) and MTBE (2 mL) were added in this order. Then, benzaldehyde **2-1a** (1.0 equiv, 51 μL , 0.5 mmol) and $\text{Ti}(\text{OEt})_4$ (0.8 equiv, 91.2 mg, 0.4 mmol) were added, and the tube was sealed with a crimped septum cap. The reaction was stirred at room temperature for 24 h. The reaction mixture was then diluted with Et_2O (4 mL) and filtered through a plug of celite (\varnothing 3 mm \times 8 mm) in air with copious washing (Et_2O). The solvents were removed *in vacuo*, and the residue was purified by column chromatography on deactivated silica gel (hexane: Et_2O = 30:1).

General procedures for examples described in Scheme 2-4 (taking 2-3v as an example).

In a 10 mL thick-walled reaction tube equipped with a magnetic stirring bar, IMesCuCl (2 mol %, 4.0 mg, 0.01 mmol), B_2pin_2 (1.2 equiv, 152.4 mg, 0.6 mmol), KF (1.2 equiv, 34.9 mg, 0.6 mmol), and MTBE (2 mL) were added. Then, benzaldehyde **2-1a** (1.0 equiv, 51 μL , 0.5 mmol), aniline **2-2v** (1.2 equiv, 55 μL , 0.6 mmol) and $\text{Ti}(\text{OEt})_4$ (0.8 equiv, 91.2 mg, 0.4 mmol) were added in this order, and the tube was sealed with a crimped septum cap. The reaction was stirred at room temperature for 24 h. In an argon-filled glovebox, the reaction

mixture was then diluted with hexane (2 mL) and filtered with copious washing (hexane). The desired product crystallized overnight in a freezer (−30 °C).

Experimental procedure for the synthesis of 2-3a on a gram scale.

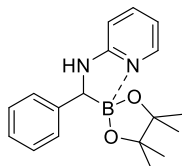
In a 25 mL thick-walled reaction tube equipped with a magnetic stirring bar, CuCl (2 mol %, 19.8 mg, 0.2 mmol), bpy (2 mol %, 31.2 mg, 0.2 mmol), B₂pin₂ (1.2 equiv, 3047.3 mg, 12.0 mmol), KF (1.2 equiv, 697.2 mg, 12.0 mmol), 2-aminopyridine **2-2a** (1.2 equiv, 1129.3 mg, 12.0 mmol) and MTBE (10 mL) were added in this order. Then, benzaldehyde **2-1a** (1.0 equiv, 1019 μL, 10.0 mmol) and Ti(OEt)₄ (0.8 equiv, 1824.9 mg, 8.0 mmol) were added, and the tube was sealed with a crimped septum cap. The reaction was stirred at room temperature for 24 h. The reaction mixture was then diluted with Et₂O (30 mL) and filtered through a plug of celite (∅ 3 mm × 8 mm) in the air with copious washing (Et₂O). The solvents were removed *in vacuo*, and the residue was purified by column chromatography on deactivated silica gel (hexane:Et₂O = 30:1) giving **2-3a** as a white solid (2.69 g, 87%).

Experimental procedures for examples described in Scheme 2-8.

In a 10 mL thick-walled reaction tube equipped with a magnetic stirring bar, α-aminoboronate **2-3w** (1.0 equiv, 67.8 mg, 0.2 mmol), methyl 4-iodobenzoate **2-5** (1.1 equiv, 57.6 mg, 0.22 mmol), Pd(^tBu₃P)₂ (5 mol %, 5.1 mg, 0.01 mmol), K₂CO₃ (3 equiv, 82.9 mg, 0.6 mmol) and toluene (0.5 mL) were added. Then, the tube was sealed with a crimped septum cap and taken out of the glovebox, and H₂O (2.0 equiv, 7.2 μL, 0.4 mmol) was added by a syringe. The reaction was stirred at 80 °C for 12 h. The reaction mixture was then diluted with CH₂Cl₂ (5 mL) and filtered through a plug of celite (∅ 3 mm × 8 mm) in air with copious washing (CH₂Cl₂). The solvents were removed *in vacuo*, and the residue was purified by column chromatography on silica gel (hexane:Et₂O = 10:1).

2.7.3 Compound characterization

N-(phenyl(4,4,5,5-tetramethyl-1,3,2-dioxaborolan-2-yl)methyl)pyridin-2-amine



Flash chromatography on deactivated silica gel (hexane:Et₂O = 30:1) afforded the product **2-3a** (147 mg, 95%), white solid, m.p. 200 °C.

¹H NMR (300 MHz, CDCl₃) δ 7.95 (d, *J* = 6 Hz, 1H), 7.51 (ddd, *J* = 9, 7, 2 Hz, 1H), 7.26–7.18 (m, 2H), 7.19–7.06 (m, 3H), 6.59 (ddd, *J* = 7, 6, 1 Hz, 1H), 6.53 (ddd, *J* = 9, 1, 1 Hz, 1H), 5.59 (s, 1H), 3.76 (s, 1H), 1.15 (s, 6H), 0.97 (s, 6H).

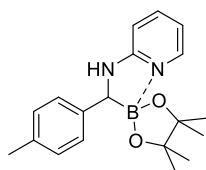
¹³C{¹H} NMR (75 MHz, CDCl₃) δ 158.7, 144.2, 141.6, 139.3, 127.9, 127.4, 125.3, 112.1, 108.5, 79.8, 56.1 (v br), 26.5, 26.3.

¹¹B NMR (96 MHz, CDCl₃) δ 10.6.

HRMS (ASAP pos): calc. for [M+H]⁺ C₁₈H₂₄BN₂O₂⁺ 311.1925; found: 311.1916.

Elem. Anal. Calc. (%) for C₁₈H₂₃BN₂O₂: C, 69.70; H, 7.47; N, 9.03; found: C, 69.74; H, 7.45; N, 8.90.

N-((4,4,5,5-tetramethyl-1,3,2-dioxaborolan-2-yl)(*p*-tolyl)methyl)pyridin-2-amine



Flash chromatography on deactivated silica gel (hexane:Et₂O = 30:1) afforded the product **2-3b** (138 mg, 85%), white solid, m.p. 203 °C.

¹H NMR (300 MHz, CDCl₃) δ 7.97–7.89 (m, 1H), 7.50 (ddd, *J* = 9, 7, 2 Hz, 1H), 7.03 (s, 4H), 6.57 (ddd, *J* = 7, 6, 1 Hz, 1H), 6.49 (ddd, *J* = 9, 1, 1 Hz, 1H), 5.50 (s, 1H), 3.72 (s, 1H), 2.29 (s, 3H), 1.15 (s, 6H), 0.98 (s, 6H).

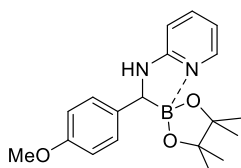
¹³C{¹H} NMR (75 MHz, CDCl₃) δ 158.5, 141.3, 140.9, 139.2, 134.5, 128.5, 127.2, 111.9, 108.3, 79.6, 55.8 (v br), 26.4, 26.1, 21.0.

^{11}B NMR (96 MHz, CDCl_3) δ 10.4.

HRMS (ASAP pos): calc. for $[\text{M}+\text{H}]^+$ $\text{C}_{19}\text{H}_{26}\text{BN}_2\text{O}_2^+$ 325.2082; found: 325.2081.

Elem. Anal. Calc. (%) for $\text{C}_{19}\text{H}_{25}\text{BN}_2\text{O}_2$: C, 70.38; H, 7.77; N, 8.64; found: C, 70.43; H, 7.84; N, 8.68.

***N*-((4-methoxyphenyl)(4,4,5,5-tetramethyl-1,3,2-dioxaborolan-2-yl)methyl)pyridin-2-amine**



Flash chromatography on deactivated silica gel (hexane: Et_2O = 30:1) afforded the product **2-3c** (139 mg, 82%), white solid, m.p. 141 °C.

^1H NMR (300 MHz, CDCl_3) δ 7.91–7.82 (m, 1H), 7.43 (ddd, J = 9, 7, 2 Hz, 1H), 7.08–6.98 (m, 2H), 6.79–6.70 (m, 2H), 6.52 (ddd, J = 7, 6, 1 Hz, 1H), 6.40 (ddd, J = 9, 1, 1 Hz, 1H), 5.88 (s, 1H), 3.73 (s, 3H), 3.63 (s, 1H), 1.10 (s, 6H), 0.94 (s, 6H).

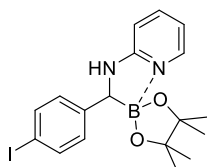
$^{13}\text{C}\{^1\text{H}\}$ NMR (75 MHz, CDCl_3) δ 158.6, 157.5, 141.2, 139.1, 136.3, 128.5, 113.3, 111.7, 108.4, 79.7, 58.3 (v br), 55.3, 26.4, 26.2.

^{11}B NMR (96 MHz, CDCl_3) δ 10.2.

HRMS (ASAP pos): calc. for $[\text{M}+\text{H}]^+$ $\text{C}_{19}\text{H}_{26}\text{BN}_2\text{O}_3^+$ 341.2031; found: 341.2032.

Elem. Anal. Calc. (%) for $\text{C}_{19}\text{H}_{25}\text{BN}_2\text{O}_3$: C, 67.07; H, 7.41; N, 8.23; found: C, 66.96; H, 7.67; N, 7.99.

***N*-((4-iodophenyl)(4,4,5,5-tetramethyl-1,3,2-dioxaborolan-2-yl)methyl)pyridin-2-amine**



Flash chromatography on deactivated silica gel (hexane: Et_2O = 30:1) afforded the product **2-3d** (192 mg, 88%), white solid, m.p. 200 °C.

¹H NMR (300 MHz, CDCl₃) δ 7.87–7.79 (m, 1H), 7.53–7.44 (m, 3H), 6.89–6.80 (m, 2H), 6.53 (ddd, *J* = 7, 6, 1 Hz, 1H), 6.39 (ddd, *J* = 9, 1, 1 Hz, 1H), 6.12 (s, 1H), 3.61 (s, 1H), 1.11 (s, 6H), 0.94 (s, 6H).

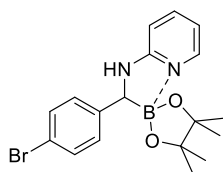
¹³C{¹H} NMR (75 MHz, CDCl₃) δ 158.6, 144.1, 141.6, 138.9, 136.8, 129.4, 112.2, 108.5, 90.0, 79.9, 55.1 (v br), 26.5, 26.2.

¹¹B NMR (96 MHz, CDCl₃) δ 10.1.

HRMS (ASAP pos): calc. for [M+H]⁺ C₁₈H₂₃BN₂O₂⁺ 437.0892; found: 437.0884.

Elem. Anal. Calc. (%) for C₁₉H₂₂BN₂O₂: C, 49.58; H, 5.09; N, 6.42; found: C, 49.77; H, 5.18; N, 6.32.

***N*-((4-bromophenyl)(4,4,5,5-tetramethyl-1,3,2-dioxaborolan-2-yl)methyl)pyridin-2-amine**



Flash chromatography on deactivated silica gel (hexane:Et₂O = 30:1) afforded the product **2-3e** (167 mg, 86%), white solid, m.p. 236 °C.

¹H NMR (500 MHz, CDCl₃) δ 7.87–7.81 (m, 1H), 7.47 (ddd, *J* = 9, 7, 2 Hz, 1H), 7.17–7.10 (m, 2H), 7.05–6.99 (m, 2H), 6.54 (ddd, *J* = 7, 6, 1 Hz, 1H), 6.40 (ddd, *J* = 9, 1, 1 Hz, 1H), 6.09 (s, 1H), 3.65 (s, 1H), 1.10 (s, 6H), 0.94 (s, 6H).

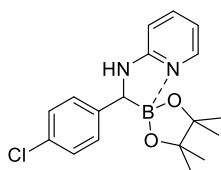
¹³C{¹H} NMR (126 MHz, CDCl₃) δ 158.5, 142.7, 141.4, 138.9, 130.6, 128.6, 127.8, 112.0, 108.4, 79.8, 54.9 (v br), 26.4, 26.1.

¹¹B NMR (160 MHz, CDCl₃) δ 10.4.

HRMS (ASAP pos): calc. for [M+H]⁺ C₁₈H₂₃BBrN₂O₂⁺ 389.1030; found: 389.1031.

Elem. Anal. Calc. (%) for C₁₈H₂₂BBrN₂O₂: C, 55.56; H, 5.70; N, 7.20; found: C, 55.60; H, 5.47; N, 7.00.

***N*-((4-chlorophenyl)(4,4,5,5-tetramethyl-1,3,2-dioxaborolan-2-yl)methyl)pyridin-2-amine**



Flash chromatography on deactivated silica gel (hexane:Et₂O = 30:1) afforded the product **2-3f** (162 mg, 94%), white solid, m.p. 223 °C.

¹H NMR (300 MHz, CDCl₃) δ 7.94-7.84 (m, 1H), 7.55-7.42 (m, 1H), 7.16 (dd, *J* = 8, 2 Hz, 2H), 7.10–6.97 (m, 2H), 6.64–6.51 (m, 1H), 6.51–6.39 (m, 1H), 5.88 (s, 1H), 3.68 (s, 1H), 1.12 (s, 6H), 0.96 (s, 6H).

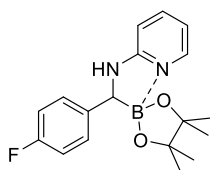
¹³C{¹H} NMR (126 MHz, CDCl₃) δ 158.6, 142.8, 141.7, 139.2, 130.8, 128.7, 128.0, 112.4, 108.5, 79.9, 54.9 (v br), 26.6, 26.3.

¹¹B NMR (96 MHz, CDCl₃) δ 10.4.

HRMS (ASAP pos): calc. for [M+H]⁺ C₁₈H₂₃BClN₂O₂⁺ 345.1536; found: 345.1533.

Elem. Anal. Calc. (%) for C₁₈H₂₂BClN₂O₂: C, 62.73; H, 6.43; N, 8.13; found: C, 62.52; H, 6.52; N, 8.02.

***N*-((4-fluorophenyl)(4,4,5,5-tetramethyl-1,3,2-dioxaborolan-2-yl)methyl)pyridin-2-amine**



Flash chromatography on deactivated silica gel (hexane:Et₂O = 30:1) afforded the product **2-3g** (123 mg, 75%), white solid, m.p. 165 °C.

¹H NMR (300 MHz, CDCl₃) δ 7.94 (d, *J* = 6 Hz, 1H), 7.52 (ddd, *J* = 9, 7, 2 Hz, 1H), 7.10 (dd, *J* = 9, 6 Hz, 2H), 6.96–6.84 (m, 2H), 6.60 (ddd, *J* = 7, 6, 1 Hz, 1H), 6.51 (dd, *J* = 9, 1 Hz, 1H), 5.65 (s, 1H), 3.73 (s, 1H), 1.13 (s, 6H), 0.96 (s, 6H).

¹³C{¹H} NMR (75 MHz, CDCl₃) δ 161.0 (d, *J* = 242 Hz), 158.4, 141.5, 139.6 (d, *J* = 3 Hz), 139.1, 128.7 (d, *J* = 8 Hz), 114.4 (d, *J* = 21 Hz), 112.2, 108.3, 79.7, 54.7 (v br), 26.4, 26.1.

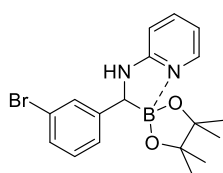
^{11}B NMR (96 MHz, CDCl_3) δ 10.4.

^{19}F NMR (471 MHz, CDCl_3) δ -118.7.

HRMS (ASAP pos): calc. for $[\text{M}+\text{H}]^+$ $\text{C}_{18}\text{H}_{23}\text{BFN}_2\text{O}_2^+$ 329.1831; found: 329.1819.

Elem. Anal. Calc. (%) for $\text{C}_{18}\text{H}_{22}\text{BFN}_2\text{O}_2$: C, 65.87; H, 6.76; N, 8.54; found: C, 65.86; H, 6.51; N, 8.89.

***N*-((3-bromophenyl)(4,4,5,5-tetramethyl-1,3,2-dioxaborolan-2-yl)methyl)pyridin-2-amine**



Flash chromatography on deactivated silica gel (hexane: Et_2O = 30:1) afforded the product **2-3h** (162 mg, 83%), white solid, m.p. 197 °C.

^1H NMR (300 MHz, CDCl_3) δ 7.85 (d, J = 6 Hz, 1H), 7.45 (ddd, J = 9, 7, 2 Hz, 1H), 7.24–7.15 (m, 2H), 7.08–6.96 (m, 2H), 6.56 (ddd, J = 7, 6, 1 Hz, 1H), 6.45 (ddd, J = 9, 1, 1 Hz, 1H), 6.19 (s, 1H), 3.62 (s, 1H), 1.10 (s, 6H), 0.93 (s, 6H).

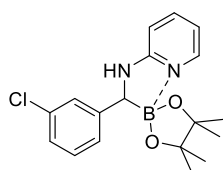
$^{13}\text{C}\{^1\text{H}\}$ NMR (75 MHz, CDCl_3) δ 158.6, 146.9, 141.6, 139.0, 130.0, 129.4, 128.2, 125.9, 122.0, 112.2, 108.6, 80.0, 55.2 (v br), 26.5, 26.3.

^{11}B NMR (96 MHz, CDCl_3) δ 10.5.

HRMS (ASAP pos): calc. for $[\text{M}+\text{H}]^+$ $\text{C}_{18}\text{H}_{23}\text{BBrN}_2\text{O}_2^+$ 389.1030; found: 389.1031.

Elem. Anal. Calc. (%) for $\text{C}_{18}\text{H}_{22}\text{BBrN}_2\text{O}_2$: C, 55.56; H, 5.70; N, 7.20; found: C, 55.59; H, 5.77; N, 7.05.

***N*-((3-chlorophenyl)(4,4,5,5-tetramethyl-1,3,2-dioxaborolan-2-yl)methyl)pyridin-2-amine**



Flash chromatography on deactivated silica gel (hexane: Et_2O = 30:1) afforded the product

2-3i (146 mg, 85%), white solid, m.p. 181 °C.

¹H NMR (300 MHz, CDCl₃) δ 7.91 (d, *J* = 6 Hz, 1H), 7.52 (ddd, *J* = 9, 7, 2 Hz, 1H), 7.18–6.95 (m, 4H), 6.60 (ddd, *J* = 7, 6, 1 Hz, 1H), 6.51 (ddd, *J* = 9, 1, 1 Hz, 1H), 5.84 (s, 1H), 3.70 (s, 1H), 1.14 (s, 6H), 0.98 (s, 6H).

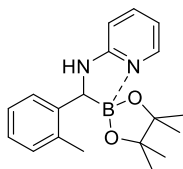
¹³C{¹H} NMR (75 MHz, CDCl₃) δ 158.6, 146.5, 141.7, 139.1, 133.7, 129.1, 127.1, 125.5, 125.4, 112.4, 108.5, 80.0, 55.2 (v br), 26.6, 26.4.

¹¹B NMR (96 MHz, CDCl₃) δ 10.4.

HRMS (ASAP pos): calc. for [M+H]⁺ C₁₈H₂₃BClN₂O₂⁺ 345.1536; found: 345.1531.

Elem. Anal. Calc. (%) for C₁₈H₂₂BClN₂O₂: C, 62.73; H, 6.43; N, 8.13; found: C, 62.82; H, 6.21; N, 8.50.

***N*-((4,4,5,5-tetramethyl-1,3,2-dioxaborolan-2-yl)(*o*-tolyl)methyl)pyridin-2-amine**



Flash chromatography on deactivated silica gel (hexane:Et₂O = 30:1) afforded the product

2-3j (117 mg, 72%), white solid, m.p. 200 °C.

¹H NMR (300 MHz, CDCl₃) δ 8.00 (d, *J* = 6 Hz, 1H), 7.52 (ddd, *J* = 9, 7, 2 Hz, 1H), 7.24–7.18 (m, 1H), 7.16–6.97 (m, 3H), 6.61 (ddd, *J* = 7, 6, 1 Hz, 1H), 6.53 (ddd, *J* = 9, 1, 1 Hz, 1H), 5.30 (s, 1H), 4.13 (s, 1H), 2.40 (s, 3H), 1.11 (s, 6H), 0.90 (s, 6H).

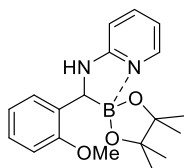
¹³C{¹H} NMR (126 MHz, CDCl₃) δ 158.8, 142.0, 141.3, 139.1, 135.2, 129.8, 128.4, 125.6, 125.1, 112.1, 108.7, 79.7, 51.0 (v br), 26.5, 26.2, 20.4.

¹¹B NMR (96 MHz, CDCl₃) δ 10.9.

HRMS (ASAP pos): calc. for [M+H]⁺ C₁₉H₂₆BN₂O₂⁺ 325.2082; found: 325.2068.

Elem. Anal. Calc. (%) for C₁₉H₂₅BN₂O₂: C, 70.38; H, 7.77; N, 8.64; found: C, 70.15; H, 7.84; N, 8.61.

***N*-((2-methoxyphenyl)(4,4,5,5-tetramethyl-1,3,2-dioxaborolan-2-yl)methyl)pyridin-2-amine**



Flash chromatography on deactivated silica gel (hexane:Et₂O = 30:1) afforded the product **2-3k** (102 mg, 60%), white solid, m.p. 180 °C.

¹H NMR (300 MHz, CDCl₃) δ 7.95 (d, *J* = 6 Hz, 1H), 7.48 (ddd, *J* = 9, 7, 2 Hz, 1H), 7.16 (dd, *J* = 8, 2 Hz, 1H), 7.09 (ddd, *J* = 8, 8, 2 Hz, 1H), 6.90–6.75 (m, 2H), 6.56 (m, 1H), 6.50 (d, *J* = 9 Hz, 1H), 5.40 (s, 1H), 4.27 (s, 1H), 3.75 (s, 3H), 1.16 (s, 6H), 0.99 (s, 6H).

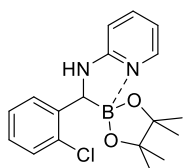
¹³C{¹H} NMR (126 MHz, CDCl₃) δ 159.0, 157.0, 141.3, 139.1, 132.8, 128.4, 126.1, 120.5, 111.8, 110.2, 108.5, 79.7, 55.3, 48.9 (v br), 26.2, 26.2.

¹¹B NMR (96 MHz, CDCl₃) δ 10.7.

HRMS (ASAP pos): calc. for [M+H]⁺ C₁₉H₂₆BN₂O₃⁺ 341.2031; found: 341.2020.

Elem. Anal. Calc. (%) for C₁₉H₂₅BN₂O₃: C, 67.07; H, 7.41; N, 8.23; found: C, 66.81; H, 7.59; N, 8.22.

***N*-((2-chlorophenyl)(4,4,5,5-tetramethyl-1,3,2-dioxaborolan-2-yl)methyl)pyridin-2-amine**



Flash chromatography on deactivated silica gel (hexane:Et₂O = 30:1) afforded the product **2-3l** (131 mg, 76%), white solid, m.p. 169 °C.

¹H NMR (300 MHz, CDCl₃) δ 7.97 (d, *J* = 6 Hz, 1H), 7.52 (ddd, *J* = 9, 7, 2 Hz, 1H), 7.33–7.21 (m, 2H), 7.13 (ddd, *J* = 8, 8, 2 Hz, 1H), 7.04 (ddd, *J* = 8, 8, 2 Hz, 1H), 6.63 (ddd, *J* = 7, 6, 1 Hz, 1H), 6.54 (dd, *J* = 9, 1 Hz, 1H), 5.57 (s, 1H), 4.40 (s, 1H), 1.14 (s, 6H), 0.95 (s, 6H).

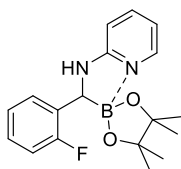
$^{13}\text{C}\{^1\text{H}\}$ NMR (126 MHz, CDCl_3) δ 158.7, 141.7, 141.6, 139.1, 133.1, 130.1, 129.0, 126.5, 126.4, 112.4, 108.6, 79.9, 50.0 (v br), 26.2, 26.2.

^{11}B NMR (160 MHz, CDCl_3) δ 10.5.

HRMS (ASAP pos): calc. for $[\text{M}+\text{H}]^+$ $\text{C}_{18}\text{H}_{23}\text{BClN}_2\text{O}_2^+$ 345.1536; found: 345.1525.

Elem. Anal. Calc. (%) for $\text{C}_{18}\text{H}_{22}\text{BClN}_2\text{O}_2$: C, 62.73; H, 6.43; N, 8.13; found: C, 62.53; H, 6.38; N, 8.50.

***N*-((2-fluorophenyl)(4,4,5,5-tetramethyl-1,3,2-dioxaborolan-2-yl)methyl)pyridin-2-amine**



Flash chromatography on deactivated silica gel (hexane: Et_2O = 30:1) afforded the product **2-3m** (113 mg, 69%), white solid, m.p. 160 °C.

^1H NMR (300 MHz, CDCl_3) δ 7.86 (dd, J = 6, 1 Hz, 1H), 7.44 (ddd, J = 9, 7, 2 Hz, 1H), 7.13–6.86 (m, 4H), 6.53 (ddd, J = 7, 6, 1 Hz, 1H), 6.44 (ddd, J = 8, 1, 1 Hz, 1H), 6.31 (s, 1H), 3.94 (s, 1H), 1.10 (s, 6H), 0.92 (s, 6H).

$^{13}\text{C}\{^1\text{H}\}$ NMR (75 MHz, CDCl_3) δ 160.7 (d, J = 244 Hz), 158.9, 141.3, 138.8, 131.4 (d, J = 14 Hz), 129.6 (d, J = 5 Hz), 126.5 (d, J = 8 Hz), 123.6 (d, J = 3 Hz), 114.9 (d, J = 22 Hz), 111.8, 108.6, 79.8, 48.5 (v br), 26.1, 26.1.

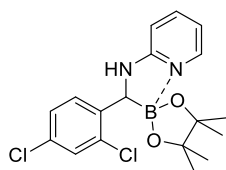
^{11}B NMR (96 MHz, CDCl_3) δ 10.4.

^{19}F NMR (471 MHz, CDCl_3) δ -117.6.

HRMS (ASAP pos): calc. for $[\text{M}+\text{H}]^+$ $\text{C}_{18}\text{H}_{23}\text{BFN}_2\text{O}_2^+$ 329.1831; found: 329.1828.

Elem. Anal. Calc. (%) for $\text{C}_{18}\text{H}_{22}\text{BFN}_2\text{O}_2$: C, 65.87; H, 6.76; N, 8.54; found: C, 65.86; H, 6.51; N, 8.89.

**2'-(2,4-dichlorophenyl)-4,4,5,5-tetramethyl-1',2'-dihydro-2λ4,4'λ4
spiro[[1,3,2]dioxaborolane-2,3'-[1,4,2]diazaborolo[1,5-a]pyridine]**



Flash chromatography on deactivated silica gel (hexane:Et₂O = 30:1) afforded the product **2-3n** (141.2 mg, 75%), white solid, m.p. 235 °C.

¹H NMR (300 MHz, CDCl₃) δ 7.97 (d, *J* = 6 Hz, 1H), 7.54 (ddd, *J* = 9, 7, 2 Hz, 1H), 7.30 (d, *J* = 2 Hz, 1H), 7.19 (d, *J* = 8 Hz, 1H), 7.10 (dd, *J* = 8, 2 Hz, 1H), 6.64 (ddd, *J* = 7, 6, 1 Hz, 1H), 6.53 (ddd, *J* = 9, 1, 1 Hz, 1H), 5.62 (s, 1H), 4.33 (d, *J* = 2 Hz, 1H), 1.13 (s, 6H), 0.96 (s, 6H).

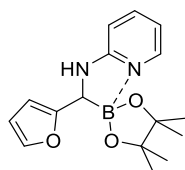
¹³C{¹H} NMR (75 MHz, CDCl₃) δ 158.7, 141.7, 140.5, 139.0, 133.6, 131.1, 131.1, 128.6, 126.7, 112.7, 108.7, 80.0, 51.1 (v br), 26.4, 26.2.

¹¹B NMR (96 MHz, CDCl₃) δ 10.4.

HRMS (ASAP pos): calc. for [M+H]⁺ C₁₈H₂₂BCl₂N₂O₂⁺ 379.1146; found: 379.1147.

Elem. Anal. Calc. (%) for C₁₈H₂₁BCl₂N₂O₂: C, 57.03; H, 5.58; N, 7.39; found: C, 56.91; H, 5.84; N, 7.62.

N-(furan-2-yl(4,4,5,5-tetramethyl-1,3,2-dioxaborolan-2-yl)methyl)pyridin-2-amine



Flash chromatography on deactivated silica gel (hexane:Et₂O = 30:1) afforded the product **2-3o** (108 mg, 72%), pale yellow solid, m.p. 193 °C.

¹H NMR (300 MHz, CDCl₃) δ 7.93 (d, *J* = 6 Hz, 1H), 7.47 (ddd, *J* = 9, 7, 2 Hz, 1H), 7.29 (dd, *J* = 2, 1 Hz, 1H), 6.57 (ddd, *J* = 7, 6, 1 Hz, 1H), 6.47 (d, *J* = 9 Hz, 1H), 6.25 (dd, *J* = 3, 2 Hz, 1H), 6.12 (d, *J* = 3 Hz, 1H), 5.73 (s, 1H), 3.80 (s, 1H), 1.21 (s, 6H), 1.09 (s, 6H).

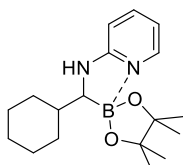
¹³C{¹H} NMR (75 MHz, CDCl₃) δ 158.4, 157.1, 141.6, 140.9, 139.1, 112.1, 110.1, 108.7, 105.0, 79.9, 48.5 (v br), 26.4, 25.9.

^{11}B NMR (96 MHz, CDCl_3) δ 10.0.

HRMS (ASAP pos): calc. for $[\text{M}+\text{H}]^+$ $\text{C}_{16}\text{H}_{22}\text{BN}_2\text{O}_3^+$ 301.1718; found: 301.1710.

Elem. Anal. Calc. (%) for $\text{C}_{16}\text{H}_{21}\text{BN}_2\text{O}_3$: C, 64.02; H, 7.05; N, 9.33; found: C, 64.14; H, 7.21; N, 9.52.

***N*-(cyclohexyl(4,4,5,5-tetramethyl-1,3,2-dioxaborolan-2-yl)methyl)pyridin-2-amine**



Flash chromatography on deactivated silica gel (hexane: Et_2O = 30:1) afforded the product **2-3p** (112 mg, 71%), white solid, m.p. 161 °C.

^1H NMR (300 MHz, CDCl_3) δ 7.88 (d, J = 6 Hz, 1H), 7.39 (ddd, J = 9, 7, 2 Hz, 1H), 6.56–6.34 (m, 2H), 5.33 (s, 1H), 2.38 (d, J = 2 Hz, 1H), 1.81–1.53 (m, 6H), 1.28–1.02 (m, 16H), 0.92–0.78 (m, 1H).

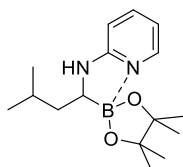
$^{13}\text{C}\{^1\text{H}\}$ NMR (75 MHz, CDCl_3) δ 158.7, 140.9, 138.6, 110.9, 108.3, 79.2, 54.5 (v br), 40.0, 32.3, 28.4, 26.9, 26.6, 26.5, 26.5, 26.2.

^{11}B NMR (96 MHz, CDCl_3) δ 10.5.

HRMS (ASAP pos): calc. for $[\text{M}+\text{H}]^+$ $\text{C}_{18}\text{H}_{30}\text{BN}_2\text{O}_2^+$ 317.2395; found: 317.2387.

Elem. Anal. Calc. (%) for $\text{C}_{18}\text{H}_{29}\text{BN}_2\text{O}_2$: C, 68.36; H, 9.24; N, 8.86; found: C, 68.54; H, 9.20; N, 8.63.

***N*-(3-methyl-1-(4,4,5,5-tetramethyl-1,3,2-dioxaborolan-2-yl)butyl)pyridin-2-amine**



Flash chromatography on deactivated silica gel (hexane: Et_2O = 30:1) afforded the product **2-3q** (80 mg, 55%), white solid, m.p. 146 °C.

¹H NMR (300 MHz, CDCl₃) δ 7.87 (d, *J* = 6 Hz, 1H), 7.34 (ddd, *J* = 9, 7, 2 Hz, 1H), 6.44 (ddd, *J* = 7, 6, 1 Hz, 1H), 6.36 (ddd, *J* = 9, 1, 1 Hz, 1H), 5.62 (s, 1H), 2.66–2.52 (m, 1H), 1.63–1.48 (m, 1H), 1.44–1.26 (m, 2H), 1.22 (s, 6H), 1.19 (s, 6H), 0.90 (d, *J* = 6 Hz, 6H).

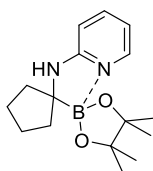
¹³C{¹H} NMR (75 MHz, CDCl₃) δ 158.3, 140.8, 138.8, 110.9, 108.6, 79.2, 47.4 (v br), 41.4, 26.5, 26.0, 26.0, 24.1, 21.1.

¹¹B NMR (96 MHz, CDCl₃) δ 10.4.

HRMS (ASAP pos): calc. for [M+H]⁺ C₁₆H₂₈BN₂O₂ 291.2238; found: 291.2227.

Elem. Anal. Calc. (%) for C₁₆H₂₇BN₂O₂: C, 66.22; H, 9.38; N, 9.65; found: C, 66.31; H, 9.23; N, 9.84.

***N*-(1-(4,4,5,5-tetramethyl-1,3,2-dioxaborolan-2-yl)cyclopentyl)pyridin-2-amine**



Flash chromatography on deactivated silica gel (hexane:Et₂O = 30:1) afforded the product **2-3r** (121 mg, 84%), white solid, m.p. 260 °C.

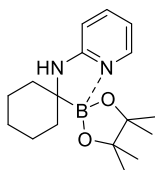
¹H NMR (400 MHz, CDCl₃) δ 7.93 (d, *J* = 6 Hz, 1H), 7.40 (ddd, *J* = 9, 7, 2 Hz, 1H), 6.48 (dd, *J* = 6, 6 Hz, 1H), 6.36 (d, *J* = 9 Hz, 1H), 5.17 (s, 1H), 2.11–1.94 (m, 2H), 1.77–1.56 (m, 4H), 1.56–1.45 (m, 2H), 1.23 (s, 12H).

¹³C{¹H} NMR (101 MHz, CDCl₃) δ 157.1, 140.9, 139.0, 111.0, 108.2, 79.3, 58.4 (v br), 36.3, 26.9, 25.2.

¹¹B NMR (128 MHz, CDCl₃) δ 10.9.

HRMS (ASAP neg): calc. for [M-H]⁻ C₁₆H₂₄BN₂O₂⁻ 287.1936; found: 287.1937.

Elem. Anal. Calc. (%) for C₁₆H₂₅BN₂O₂: C, 66.68; H, 8.74; N, 9.72; found: C, 66.77; H, 8.78; N, 9.71.

***N*-(1-(4,4,5,5-tetramethyl-1,3,2-dioxaborolan-2-yl)cyclohexyl)pyridin-2-amine**

Flash chromatography on deactivated silica gel (hexane:Et₂O = 30:1) afforded the product **2-3s** (119 mg, 79%), white solid, m.p. 248 °C.

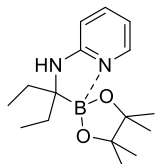
¹H NMR (400 MHz, CDCl₃) δ 7.92 (d, *J* = 6 Hz, 1H), 7.46–7.36 (m, 1H), 6.53–6.41 (m, 2H), 5.52 (s, 1H), 1.87–1.47 (m, 8H), 1.31–1.18 (m, 14H).

¹³C{¹H} NMR (101 MHz, CDCl₃) δ 157.2, 140.9, 139.1, 111.1, 108.7, 79.2, 49.2 (v br), 32.8, 27.1, 26.2, 22.8.

¹¹B NMR (128 MHz, CDCl₃) δ 10.9.

HRMS (ASAP neg): calc. for [M-H]⁻ C₁₇H₂₆BN₂O₂ 301.2093; found: 301.2093.

Elem. Anal. Calc. (%) for C₁₇H₂₇BN₂O₂: C, 67.56; H, 9.01; N, 9.27; found: C, 67.21; H, 8.87; N, 8.99.

***N*-(3-(4,4,5,5-tetramethyl-1,3,2-dioxaborolan-2-yl)pentan-3-yl)pyridin-2-amine**

Flash chromatography on deactivated silica gel (hexane:Et₂O = 30:1) afforded the product **2-3t** (104 mg, 72%), white solid, m.p. 192 °C.

¹H NMR (300 MHz, CDCl₃) δ 7.92 (d, *J* = 6 Hz, 1H), 7.42 (ddd, *J* = 9, 7, 2 Hz, 1H), 6.48 (ddd, *J* = 7, 6, 1 Hz, 1H), 6.43 (d, *J* = 9 Hz, 1H), 4.82 (s, 1H), 1.71–1.48 (m, 4H), 1.24 (s, 12H), 0.90 (t, *J* = 7 Hz, 6H).

¹³C{¹H} NMR (75 MHz, CDCl₃) δ 157.9, 141.1, 139.1, 111.2, 108.5, 79.3, 52.4 (v br), 27.9, 27.1, 9.2.

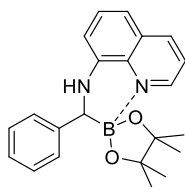
¹¹B NMR (96 MHz, CDCl₃) δ 11.1.

HRMS (ASAP pos): calc. for [M+H]⁺ C₁₆H₂₈BN₂O₂ 291.2238; found: 291.2229.

Elem. Anal. Calc. (%) for C₁₆H₂₇BN₂O₂: C, 66.22; H, 9.38; N, 9.65; found: C, 66.10; H, 9.42;

N, 9.58.

***N*-(phenyl(4,4,5,5-tetramethyl-1,3,2-dioxaborolan-2-yl)methyl)quinolin-8-amine**



Flash chromatography on deactivated silica gel (hexane:Et₂O = 30:1) afforded the product **2-3u** (117 mg, 65%), orange solid, m.p. 164 °C.

¹H NMR (300 MHz, CDCl₃) δ 9.11 (dd, *J* = 5, 2 Hz, 1H), 8.30 (dd, *J* = 8, 2 Hz, 1H), 7.46 (ddd, *J* = 8, 4, 1 Hz, 1H), 7.41 (d, *J* = 8 Hz, 1H), 7.35–7.28 (m, 2H), 7.24–7.17 (m, 2H), 7.14–7.06 (m, 2H), 6.88 (d, *J* = 8 Hz, 1H), 4.08 (s, 1H), 1.17 (s, 6H), 0.98 (s, 6H).

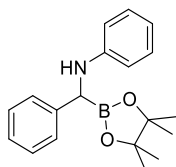
¹³C{¹H} NMR (75 MHz, CDCl₃) δ 144.9, 143.0, 141.7, 141.2, 130.6, 129.9, 129.3, 128.0, 126.9, 125.5, 120.1, 113.9, 112.4, 81.3, 53.8 (v br), 26.3, 26.2.

¹¹B NMR (96 MHz, CDCl₃) δ 10.4.

HRMS (ASAP pos): calc. for [M+H]⁺ C₂₂H₂₆BN₂O₂⁺ 361.2082; found: 361.2063.

Elem. Anal. Calc. (%) for C₂₂H₂₅BN₂O₂: C, 73.35; H, 6.99; N, 7.78; found: C, 73.08; H, 6.94; N, 7.65.

***N*-(phenyl(4,4,5,5-tetramethyl-1,3,2-dioxaborolan-2-yl)methyl)aniline**



Crystallization at –30 °C (MTBE: hexane = 1:1) afforded the product **2-3v** (122 mg, 79%), white solid.

¹H NMR (300 MHz, CDCl₃) δ 7.42–7.32 (m, 2H), 7.30–7.22 (m, 2H), 7.19–7.12 (m, 1H), 7.12–7.01 (m, 2H), 6.68–6.59 (m, 1H), 6.59–6.51 (m, 2H), 4.80 (s, 1H), 4.21 (s, 1H), 1.22 (s, 6H), 1.17 (s, 6H).

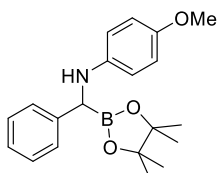
¹³C{¹H} NMR (75 MHz, CDCl₃) δ 148.0, 140.9, 129.2, 128.6, 126.5, 126.2, 117.1, 113.3, 84.6, 46.4 (v br), 24.8, 24.6.

^{11}B NMR (96 MHz, CDCl_3) δ 32.1.

HRMS (ASAP pos): calc. for $[\text{M}+\text{H}]^+$ $\text{C}_{19}\text{H}_{25}\text{BNO}_2^+$ 310.1973; found: 310.1966.

Elem. Anal. Calc. (%) for $\text{C}_{19}\text{H}_{24}\text{BNO}_2$: C, 73.80; H, 7.82; N, 4.53; found: C, 74.12; H, 7.76; N, 4.41.

4-methoxy-*N*-(phenyl(4,4,5,5-tetramethyl-1,3,2-dioxaborolan-2-yl)methyl)aniline



Crystallization at $-30\text{ }^\circ\text{C}$ (MTBE: hexane = 1:1) afforded the product **2-3w** (110 mg, 65%), white solid.

^1H NMR (300 MHz, CDCl_3) δ 7.41–7.34 (m, 2H), 7.31–7.23 (m, 2H), 7.20–7.11 (m, 1H), 6.72–6.65 (m, 2H), 6.54–6.46 (m, 2H), 4.43 (s, 1H), 4.16 (s, 1H), 3.69 (s, 3H), 1.22 (s, 6H), 1.17 (s, 6H).

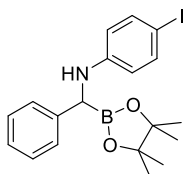
$^{13}\text{C}\{^1\text{H}\}$ NMR (75 MHz, CDCl_3) δ 151.7, 142.5, 141.3, 128.6, 126.5, 126.1, 114.9, 114.0, 84.5, 55.9, 47.0 (v br), 24.8, 24.6.

^{11}B NMR (96 MHz, CDCl_3) δ 31.5.

HRMS (ASAP pos): calc. for $[\text{M}+\text{H}]^+$ $\text{C}_{20}\text{H}_{27}\text{BNO}_3^+$ 340.2079; found: 340.2073.

Elem. Anal. Calc. (%) for $\text{C}_{20}\text{H}_{26}\text{BNO}_3$: C, 70.81; H, 7.73; N, 4.13; found: C, 70.71; H, 7.77; N, 4.08.

4-iodo-*N*-(phenyl(4,4,5,5-tetramethyl-1,3,2-dioxaborolan-2-yl)methyl)aniline



Crystallization at $-30\text{ }^\circ\text{C}$ (MTBE: hexane = 1:1) afforded the product **2-3x** (144 mg, 66%), white solid.

^1H NMR (500 MHz, CDCl_3) δ 7.34–7.25 (m, 6H), 7.16 (t, $J = 8\text{ Hz}$, 1H), 6.32 (d, $J = 8\text{ Hz}$, 2H), 4.71 (d, $J = 5\text{ Hz}$, 1H), 4.15 (d, $J = 5\text{ Hz}$, 1H), 1.22 (s, 6H), 1.17 (s, 6H).

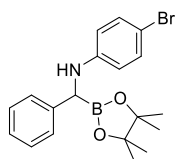
$^{13}\text{C}\{^1\text{H}\}$ NMR (126 MHz, CDCl_3) δ 147.7, 140.3, 137.7, 128.7, 126.4, 126.3, 115.4, 84.8, 77.5, 46.0 (v br), 24.8, 24.6.

^{11}B NMR (160 MHz, CDCl_3) δ 32.3.

HRMS (ASAP pos): calc. for $[\text{M}+\text{H}]^+$ $\text{C}_{19}\text{H}_{24}\text{BINO}_2^+$ 436.0939; found: 436.0931

Elem. Anal. Calc. (%) for $\text{C}_{19}\text{H}_{23}\text{BINO}_2$: C, 52.45; H, 5.33; N, 3.22; found: C, 52.36; H, 5.35; N, 3.05.

4-bromo-*N*-(phenyl(4,4,5,5-tetramethyl-1,3,2-dioxaborolan-2-yl)methyl)aniline



Crystallization at $-30\text{ }^\circ\text{C}$ (MTBE: hexane = 1:1) afforded the product **2-3y** (120 mg, 62%), white solid.

^1H NMR (300 MHz, CDCl_3) δ 7.36–7.24 (m, 4H), 7.22–7.10 (m, 3H), 6.42 (d, $J = 8\text{ Hz}$, 2H), 4.75 (s, 1H), 4.16 (s, 1H), 1.23 (s, 6H), 1.18 (s, 6H).

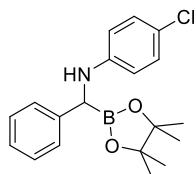
$^{13}\text{C}\{^1\text{H}\}$ NMR (75 MHz, CDCl_3) δ 147.0, 140.3, 131.8, 128.7, 126.4, 120.1, 114.7, 108.5, 84.7, 46.3 (v br), 24.8, 24.6.

^{11}B NMR (96 MHz, CDCl_3) δ 31.8.

HRMS (ASAP pos): calc. for $[\text{M}+\text{H}]^+$ $\text{C}_{19}\text{H}_{24}\text{BBrNO}_2^+$ 388.1078; found: 388.1072.

Elem. Anal. Calc. (%) for $\text{C}_{19}\text{H}_{23}\text{BBrNO}_2$: C, 58.80; H, 5.97; N, 3.61; found: C, 58.70; H, 5.95; N, 3.39.

4-chloro-*N*-(phenyl(4,4,5,5-tetramethyl-1,3,2-dioxaborolan-2-yl)methyl)aniline



Crystallization at $-30\text{ }^\circ\text{C}$ (MTBE: hexane = 1:1) afforded the product **2-3z** (89 mg, 52%), white solid.

^1H NMR (300 MHz, CDCl_3) δ 7.36–7.24 (m, 4H), 7.21–7.12 (m, 1H), 7.04–6.96 (m, 2H), 6.49–6.42 (m, 2H), 4.69 (s, 1H), 4.16 (s, 1H), 1.22 (s, 6H), 1.17 (s, 6H).

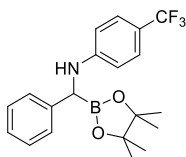
$^{13}\text{C}\{^1\text{H}\}$ NMR (75 MHz, CDCl_3) δ 146.7, 140.5, 129.0, 128.7, 126.4, 126.3, 121.5, 114.2, 84.7, 46.3 (v br), 24.8, 24.6.

^{11}B NMR (96 MHz, CDCl_3) δ 31.2.

HRMS (ASAP pos): calc. for $[\text{M}+\text{H}]^+$ $\text{C}_{19}\text{H}_{24}\text{BCINO}_2^+$ 344.1583; found: 344.1575.

Elem. Anal. Calc. (%) for $\text{C}_{19}\text{H}_{23}\text{BCINO}_2$: C, 66.41; H, 6.75; N, 4.08; found: C, 66.40; H, 6.82; N, 3.98.

***N*-(phenyl(4,4,5,5-tetramethyl-1,3,2-dioxaborolan-2-yl)methyl)-4-(trifluoromethyl)aniline**



Crystallization at $-30\text{ }^\circ\text{C}$ (MTBE: hexane = 1:1) afforded the product **2-3aa** (85 mg, 45%), white solid.

^1H NMR (300 MHz, CDCl_3) δ 7.36–7.25 (m, 6H), 7.22–7.12 (m, 1H), 6.54 (d, $J = 8$ Hz, 2H), 5.00 (s, 1H), 4.22 (s, 1H), 1.23 (s, 6H), 1.18 (s, 6H).

$^{13}\text{C}\{^1\text{H}\}$ NMR (75 MHz, CDCl_3) δ 150.6, 140.0, 128.8, 126.6, 126.5 (q, $J = 4$ Hz), 126.3, 125.2 (q, $J = 270$ Hz), 118.5 (q, $J = 32$ Hz), 112.3, 84.9, 45.9 (v br), 24.8, 24.6.

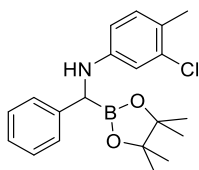
^{11}B NMR (96 MHz, CDCl_3) δ 31.6.

^{19}F NMR (471 MHz, CDCl_3) δ -60.9.

HRMS (ASAP pos): calc. for $[\text{M}+\text{H}]^+$ $\text{C}_{20}\text{H}_{24}\text{BF}_3\text{NO}_2^+$ 378.1847; found: 378.1839.

Elem. Anal. Calc. (%) for $\text{C}_{20}\text{H}_{23}\text{BF}_3\text{NO}_2$: C, 63.68; H, 6.15; N, 3.71; found: C, 63.75; H, 6.16; N, 3.71.

3-chloro-4-methyl-*N*-(phenyl(4,4,5,5-tetramethyl-1,3,2-dioxaborolan-2-yl)methyl)aniline



Crystallization at $-30\text{ }^\circ\text{C}$ (MTBE: hexane = 1:1) afforded the product **2-3ab** (120 mg, 67%),

white solid.

^1H NMR (300 MHz, CDCl_3) δ 7.36–7.22 (m, 4H), 7.16 (t, $J = 8$ Hz, 1H), 6.88 (dd, $J = 8$, 1 Hz, 1H), 6.57 (d, $J = 3$ Hz, 1H), 6.34 (dd, $J = 8$, 3 Hz, 1H), 4.59 (d, $J = 5$ Hz, 1H), 4.15 (d, $J = 5$ Hz, 1H), 2.18 (s, 3H), 1.22 (s, 6H), 1.17 (s, 6H).

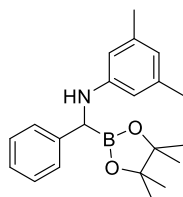
$^{13}\text{C}\{^1\text{H}\}$ NMR (75 MHz, CDCl_3) δ 147.3, 140.6, 134.7, 131.2, 128.7, 126.4, 126.3, 123.6, 113.5, 111.6, 84.7, 46.2 (v br), 24.8, 24.6, 19.0.

^{11}B NMR (96 MHz, CDCl_3) δ 32.0.

HRMS (ASAP pos): calc. for $[\text{M}+\text{H}]^+$ $\text{C}_{20}\text{H}_{26}\text{BCINO}_2^+$ 358.1740; found: 358.1729.

Elem. Anal. Calc. (%) for $\text{C}_{20}\text{H}_{25}\text{BCINO}_2$: C, 67.16; H, 7.05; N, 3.92; found: C, 67.39; H, 6.90; N, 3.54.

3,5-dimethyl-*N*-(phenyl(4,4,5,5-tetramethyl-1,3,2-dioxaborolan-2-yl)methyl)aniline



Crystallization at -30 °C (MTBE: hexane = 1:1) afforded the product **2-3ac** (88 mg, 52%), white solid.

^1H NMR (300 MHz, CDCl_3) δ 7.40–7.35 (m, 2H), 7.31–7.24 (m, 2H), 7.19–7.11 (m, 1H), 6.29 (s, 1H), 6.21 (s, 2H), 4.56 (s, 1H), 4.18 (s, 1H), 2.16 (s, 3H), 2.16 (s, 3H), 1.22 (s, 6H), 1.17 (s, 6H).

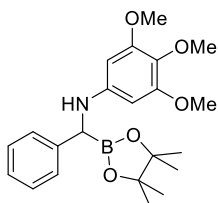
$^{13}\text{C}\{^1\text{H}\}$ NMR (75 MHz, CDCl_3) δ 148.4, 141.3, 138.8, 128.6, 126.4, 126.1, 119.0, 111.0, 84.5, 46.3 (v br), 24.8, 24.6, 21.6.

^{11}B NMR (96 MHz, CDCl_3) δ 31.6.

HRMS (ASAP pos): calc. for $[\text{M}+\text{H}]^+$ $\text{C}_{21}\text{H}_{29}\text{BNO}_2^+$ 338.2286; found: 338.2279.

Elem. Anal. Calc. (%) for $\text{C}_{21}\text{H}_{28}\text{BNO}_2$: C, 74.79; H, 8.37; N, 4.15; found: C, 74.93; H, 8.31; N, 4.17.

3,4,5-trimethoxy-*N*-(phenyl(4,4,5,5-tetramethyl-1,3,2-dioxaborolan-2-yl)methyl)aniline



Crystallization at $-30\text{ }^{\circ}\text{C}$ (MTBE: hexane = 1:1) afforded the product **2-3ad** (84 mg, 42%), white solid.

$^1\text{H NMR}$ (300 MHz, CDCl_3) δ 7.39-7.33 (m, 2H), 7.31-7.24 (m, 2H), 7.20-7.12 (m, 1H), 5.79 (s, 2H), 4.57 (d, $J = 5\text{ Hz}$, 1H), 4.15 (d, $J = 5\text{ Hz}$, 1H), 3.70 (s, 3H), 3.68 (s, 6H) 1.22 (s, 6H), 1.17 (s, 6H).

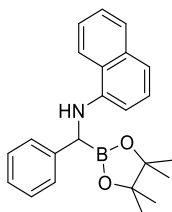
$^{13}\text{C}\{^1\text{H}\}$ NMR (75 MHz, CDCl_3) δ 153.9, 145.0, 141.3, 129.6, 128.7, 126.5, 126.3, 90.5, 84.6, 61.2, 55.8, 46.9 (v br), 24.7, 24.6.

$^{11}\text{B NMR}$ (96 MHz, CDCl_3) δ 30.2.

HRMS (ASAP pos): calc. for $[\text{M}+\text{H}]^+$ $\text{C}_{22}\text{H}_{31}\text{BNO}_5$ 400.2290; found: 400.2291.

Elem. Anal. Calc. (%) for $\text{C}_{22}\text{H}_{30}\text{BNO}_5$: C, 66.18; H, 7.57; N, 3.51; found: C, 66.41; H, 7.61; N, 3.51.

***N*-(phenyl(4,4,5,5-tetramethyl-1,3,2-dioxaborolan-2-yl)methyl)naphthalen-1-amine**



Crystallization at $-30\text{ }^{\circ}\text{C}$ (MTBE: hexane = 1:1) afforded the product **2-3ae** (92 mg, 51%), white solid.

$^1\text{H NMR}$ (300 MHz, CDCl_3) δ 8.08-7.95 (m, 1H), 7.83-7.74 (m, 1H), 7.57-7.38 (m, 4H), 7.35-7.24 (m, 2H), 7.22-7.11 (m, 3H), 6.39 (dd, $J = 7, 2\text{ Hz}$, 1H), 5.49 (s, 1H), 4.39 (s, 1H), 1.27 (s, 6H), 1.22 (s, 6H).

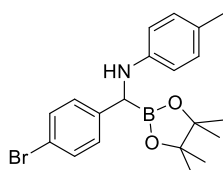
$^{13}\text{C}\{^1\text{H}\}$ NMR (75 MHz, CDCl_3) δ 143.1, 140.6, 134.5, 128.8, 128.6, 126.8, 126.4, 126.3, 125.7, 124.6, 123.4, 120.1, 116.8, 105.2, 84.8, 46.3 (v br), 24.9, 24.6.

^{11}B NMR (96 MHz, CDCl_3) δ 31.5.

HRMS (ASAP pos): calc. for $[\text{M}+\text{H}]^+$ $\text{C}_{23}\text{H}_{27}\text{BNO}_2$ 360.2129; found: 360.2135.

Elem. Anal. Calc. (%) for $\text{C}_{23}\text{H}_{26}\text{BNO}_2$: C, 76.89; H, 7.29; N, 3.90; found: C, 76.56; H, 7.27; N, 3.85.

***N*-((4-bromophenyl)(4,4,5,5-tetramethyl-1,3,2-dioxaborolan-2-yl)methyl)-4-methylaniline**



Crystallization at -30 °C (MTBE: hexane = 1:1) afforded the product **2-3af** (157 mg, 78%), white solid.

^1H NMR (300 MHz, CDCl_3) δ 7.38 (d, J = 9 Hz, 2H), 7.25 (dd, J = 9, 1 Hz, 2H), 6.89 (d, J = 8 Hz, 2H), 6.42 (d, J = 8 Hz, 2H), 4.52 (d, J = 5 Hz, 1H), 4.13 (d, J = 5 Hz, 1H), 2.18 (s, 3H), 1.22 (s, 6H), 1.18 (s, 6H).

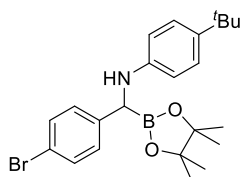
$^{13}\text{C}\{^1\text{H}\}$ NMR (75 MHz, CDCl_3) δ 145.5, 140.5, 131.6, 129.7, 128.1, 126.3, 119.7, 113.1, 84.8, 46.0 (v br), 24.8, 24.6, 20.5.

^{11}B NMR (96 MHz, CDCl_3) δ 32.0.

HRMS (ASAP pos): calc. for $[\text{M}+\text{H}]^+$ $\text{C}_{20}\text{H}_{26}\text{BBrNO}_2$ 402.1234; found: 402.1237.

Elem. Anal. Calc. (%) for $\text{C}_{20}\text{H}_{25}\text{BBrNO}_2$: C, 59.74; H, 6.27; N, 3.48; found: C, 59.96; H, 6.29; N, 3.58.

***N*-((4-bromophenyl)(4,4,5,5-tetramethyl-1,3,2-dioxaborolan-2-yl)methyl)-4-(*tert*-butyl)aniline**



Crystallization at -30 °C (MTBE: hexane = 1:1) afforded the product **2-3ag** (144 mg, 65%), white solid.

^1H NMR (300 MHz, CDCl_3) δ 7.42 (d, $J = 9$ Hz, 2H), 7.30 (dd, $J = 9, 1$ Hz, 2H), 7.14 (d, $J = 9$ Hz, 2H), 6.49 (d, $J = 9$ Hz, 2H), 4.57 (d, $J = 4$ Hz, 1H), 4.14 (d, $J = 4$ Hz, 1H), 1.26 (s, 9H), 1.24 (s, 6H), 1.20 (s, 6H).

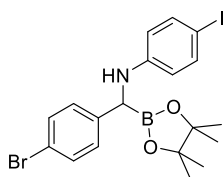
$^{13}\text{C}\{^1\text{H}\}$ NMR (75 MHz, CDCl_3) δ 145.7, 140.8, 139.9, 131.6, 128.1, 126.0, 119.7, 112.6, 84.8, 46.3 (v br), 33.9, 31.7, 24.8, 24.5.

^{11}B NMR (96 MHz, CDCl_3) δ 31.9.

HRMS (ASAP pos): calc. for $[\text{M}+\text{H}]^+$ $\text{C}_{23}\text{H}_{32}\text{BBrNO}_2$ 444.1704; found: 444.1700.

Elem. Anal. Calc. (%) for $\text{C}_{23}\text{H}_{31}\text{BBrNO}_2$: C, 62.19; H, 7.03; N, 3.15; found: C, 61.64; H, 7.02; N, 2.93.

***N*-((4-bromophenyl)(4,4,5,5-tetramethyl-1,3,2-dioxaborolan-2-yl)methyl)-4-iodoaniline**



Crystallization at -30 °C (MTBE: hexane = 1:1) afforded the product **2-3ah** (177 mg, 69%), white solid.

^1H NMR (500 MHz, CDCl_3) δ 7.38 (d, $J = 8$ Hz, 2H), 7.31 (d, $J = 8$ Hz, 2H), 7.20 (d, $J = 8$ Hz, 2H), 6.28 (d, $J = 8$ Hz, 2H), 4.69 (d, $J = 5$ Hz, 1H), 4.10 (d, $J = 5$ Hz, 1H), 1.22 (s, 6H), 1.17 (s, 6H).

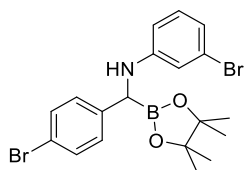
$^{13}\text{C}\{^1\text{H}\}$ NMR (126 MHz, CDCl_3) δ 147.3, 139.6, 137.8, 131.8, 128.0, 120.0, 115.4, 85.0, 77.8, 45.6 (v br), 24.8, 24.6.

^{11}B NMR (160 MHz, CDCl_3) δ 32.1.

HRMS (ASAP pos): calc. for $[\text{M}+\text{H}]^+$ $\text{C}_{19}\text{H}_{23}\text{BBrINO}_2$ 514.0044; found: 514.0031.

Elem. Anal. Calc. (%) for $\text{C}_{19}\text{H}_{23}\text{BBrINO}_2$: C, 44.40; H, 4.31; N, 2.73; found: C, 44.26; H, 4.25; N, 2.84.

3-bromo-*N*-((4-bromophenyl)(4,4,5,5-tetramethyl-1,3,2-dioxaborolan-2-yl)methyl)aniline



Crystallization at $-30\text{ }^{\circ}\text{C}$ (MTBE: hexane = 1:1) afforded the product **2-3ai** (163 mg, 70%), white solid.

$^1\text{H NMR}$ (300 MHz, CDCl_3) δ 7.40 (d, $J = 9$ Hz, 2H), 7.21 (d, $J = 9$ Hz, 2H), 6.91 (dd, $J = 8, 8$ Hz, 1H), 6.73 (ddd, $J = 8, 2, 1$ Hz, 1H), 6.67 (dd, $J = 2, 2$ Hz, 1H), 6.38 (ddd, $J = 8, 2, 1$ Hz, 1H), 4.71 (d, $J = 5$ Hz, 1H), 4.11 (d, $J = 5$ Hz, 1H), 1.22 (s, 6H), 1.17 (s, 6H).

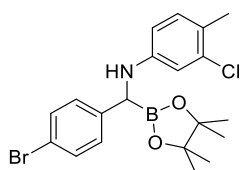
$^{13}\text{C}\{^1\text{H}\}$ NMR (75 MHz, CDCl_3) δ 149.2, 139.6, 131.8, 130.5, 128.0, 123.2, 120.1, 120.0, 115.9, 111.5, 85.0, 45.6 (v br), 24.8, 24.6.

$^{11}\text{B NMR}$ (96 MHz, CDCl_3) δ 31.6.

HRMS (ASAP pos): calc. for $[\text{M}+\text{H}]^+$ $\text{C}_{21}\text{H}_{23}\text{BBr}_2\text{NO}_2$ 466.0163; found: 466.0168.

Elem. Anal. Calc. (%) for $\text{C}_{19}\text{H}_{22}\text{BBr}_2\text{NO}_2$: C, 48.87; H, 4.75; N, 3.00; found: C, 48.84; H, 4.85; N, 2.86.

***N*-((4-bromophenyl)(4,4,5,5-tetramethyl-1,3,2-dioxaborolan-2-yl)methyl)-3-chloro-4-methylaniline**



Crystallization at $-30\text{ }^{\circ}\text{C}$ (MTBE: hexane = 1:1) afforded the product **2-3aj** (148 mg, 68%), white solid.

$^1\text{H NMR}$ (500 MHz, CDCl_3) δ 7.39 (d, $J = 7$ Hz, 2H), 7.22 (d, $J = 7$ Hz, 2H), 6.89 (d, $J = 8$ Hz, 1H), 6.53 (s, 1H), 6.30 (d, $J = 8$ Hz, 1H), 4.58 (d, $J = 5$ Hz, 1H), 4.10 (d, $J = 5$ Hz, 1H), 2.19 (s, 3H), 1.21 (s, 6H), 1.17 (s, 6H).

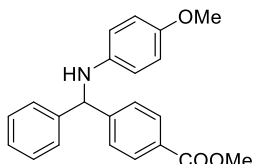
$^{13}\text{C}\{^1\text{H}\}$ NMR (126 MHz, CDCl_3) δ 146.9, 139.9, 134.8, 131.8, 131.3, 128.1, 124.0, 120.0, 113.5, 111.6, 84.9, 45.8 (v br), 24.8, 24.6, 19.0.

^{11}B NMR (160 MHz, CDCl_3) δ 32.4.

HRMS (ASAP pos): calc. for $[\text{M}+\text{H}]^+$ $\text{C}_{20}\text{H}_{25}\text{BBrClNO}_2$ 436.0845; found: 435.0849.

Elem. Anal. Calc. (%) for $\text{C}_{20}\text{H}_{24}\text{BBrClNO}_2$: C, 55.02; H, 5.54; N, 3.21; found: C, 55.06; H, 5.63; N, 3.10.

methyl 4-(((4-methoxyphenyl)amino)(phenyl)methyl)benzoate



Flash chromatography on deactivated silica gel (hexane: Et_2O = 10:1) afforded the product **2-6w** (54 mg, 78%), white solid.

^1H NMR (300 MHz, CDCl_3) δ 8.05–7.95 (m, 2H), 7.53–7.44 (m, 2H), 7.38–7.22 (m, 5H), 6.77–6.68 (m, 2H), 6.54–6.44 (m, 2H), 5.46 (s, 1H), 4.02 (s, 1H), 3.90 (s, 3H), 3.71 (s, 3H).

$^{13}\text{C}\{^1\text{H}\}$ NMR (75 MHz, CDCl_3) δ 167.0, 152.5, 148.4, 142.7, 141.4, 130.2, 129.3, 129.0, 127.8, 127.7, 127.4, 114.9, 114.9, 63.9, 55.9, 52.2.

HRMS (ASAP pos): calc. for $[\text{M}+\text{H}]^+$ $\text{C}_{22}\text{H}_{22}\text{NO}_3$ 348.1594; found: 348.1590.

2.7.4 Single-crystal X-ray diffraction studies

Crystal structure determination Crystals suitable for single-crystal X-ray diffraction were selected, coated in perfluoropolyether oil, and mounted on MiTeGen sample holders. Diffraction data of **2-3a** were collected on a BRUKER X8-APEX II diffractometer with a CCD area detector using Mo-K α radiation monochromated by multi-layer mirror. Diffraction data of **2-3v** and **2-3y** were collected on a Rigaku Oxford Diffraction XtaLAB Synergy diffractometer with a semiconductor HPA-detector (HyPix-6000) and multi-layer mirror monochromated Cu-K α radiation. The crystals were cooled using Oxford Cryostream low-temperature devices. Data were collected at 100 K. The images were processed and corrected for Lorentz-polarization effects and absorption as implemented in the Bruker software packages (**2-3a**) or using the CrysAlis^{Pro} software from Rigaku Oxford Diffraction (**2-3v** and **2-3y**). The structures were solved using the intrinsic phasing method (SHELXT)⁹⁶ and Fourier expansion technique. All non-hydrogen atoms were refined in anisotropic approximation, with most hydrogen atoms 'riding' in idealized positions, by full-matrix least squares against F^2 of all data, using SHELXL⁹⁷ software and the SHELXLE⁹⁸ graphical user interface. Only the H2 and H4N hydrogen atoms bonded to nitrogen were refined freely in compound **2-3a**, and the H2 hydrogen atoms bonded to nitrogen in compounds **2-3v** and **2-3y**. Diamond⁹⁹ software was used for graphical representation. Crystal data and experimental details are listed in Table 2-7; full structural information has been deposited with the Cambridge Crystallographic Data Centre. CCDC-1949303 (**2-3a**), 1949304 (**2-3v**), and 1949305 (**2-3y**).

Table 2-7 Single-crystal X-ray Diffraction Data and Structure Refinements of Compounds **2-3a**, **2-3v**, and **2-3y**

Data	2-3a	2-3v	2-3y
CCDC number	1949303	1949304	1949305
Empirical formula	C ₁₈ H ₂₃ BN ₂ O ₂	C ₁₉ H ₂₄ BNO ₂	C ₁₉ H ₂₃ BBrNO ₂
Formula weight / g·mol ⁻¹	310.19	309.20	388.10
<i>T</i> / K	100(2)	100(2)	100(2)
λ / Å, radiation	Mo-K α 0.71073	Cu-K α 1.54184	Cu-K α 1.54184
Crystal size / mm ³	0.30×0.27×0.13	0.13×0.07×0.03	0.21×0.12×0.09
Crystal color, habit	colorless plate	colorless block	colorless block
μ / mm ⁻¹	0.079	0.579	3.164
Crystal system	Triclinic	Monoclinic	Triclinic
Space group	<i>P</i> $\bar{1}$	<i>P</i> 2 ₁ / <i>n</i>	<i>P</i> $\bar{1}$
<i>a</i> / Å	10.953(5)	6.53430(10)	9.7994(3)
<i>b</i> / Å	11.602(6)	18.0163(4)	10.4104(2)
<i>c</i> / Å	13.554(7)	15.1210(3)	10.4227(3)
α / °	87.273(14)	90	61.181(2)
β / °	85.486(10)	98.995(2)	77.700(2)
γ / °	79.100(8)	90	88.428(2)
Volume / Å ³	1685.2(15)	1758.21(6)	906.68(5)
<i>Z</i>	4	4	2
ρ_{calc} / g·cm ⁻³	1.223	1.168	1.422
<i>F</i> (000)	664	664	400
θ range / °	2.301–26.913	3.844–72.081	4.636–72.129
Reflections collected	54592	14598	21723
Unique reflections	7255	3460	3554
Parameters / restraints	429 / 0	254 / 12	225 / 0
GooF on <i>F</i> ²	1.047	1.034	1.052
<i>R</i> ₁ [<i>I</i> >2 σ (<i>I</i>)]	0.0445	0.0468	0.0423
<i>wR</i> ² (all data)	0.1086	0.1177	0.1124
Max. / min. residual electron density / e·Å ⁻³	0.290 / -0.232	0.227 / -0.268	0.924 / -0.851

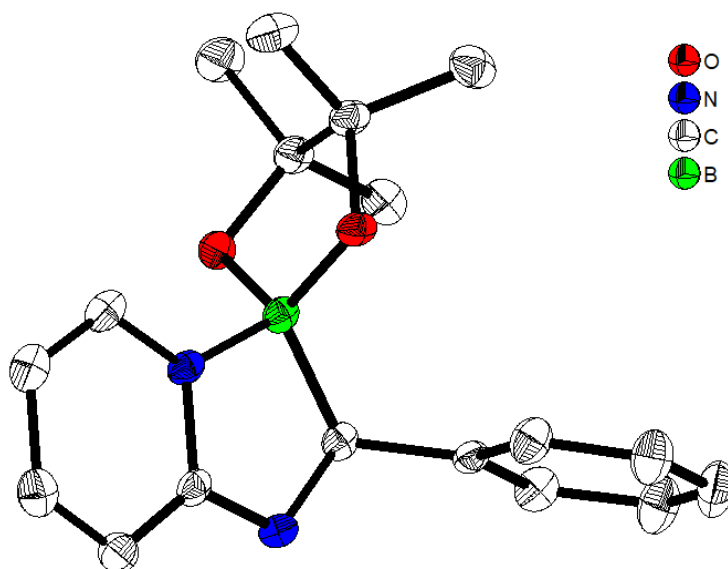


Figure 2-9 Molecular structure of **2-3a** in the solid state at 100 K. Atomic displacement ellipsoids are drawn at the 50% probability level, and H atoms are omitted for clarity. Only one of two independent molecules is drawn.

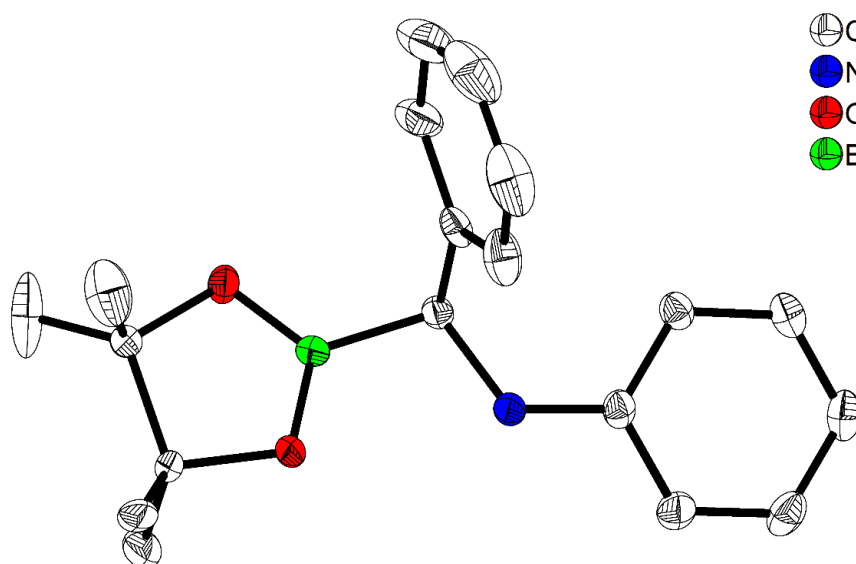


Figure 2-10 Molecular structure of **2-3v** in the solid state at 100 K. Atomic displacement ellipsoids are drawn at the 50% probability level, and H atoms are omitted for clarity. The BPin moiety is disordered and only the part with the higher occupancy (52%) is shown here.

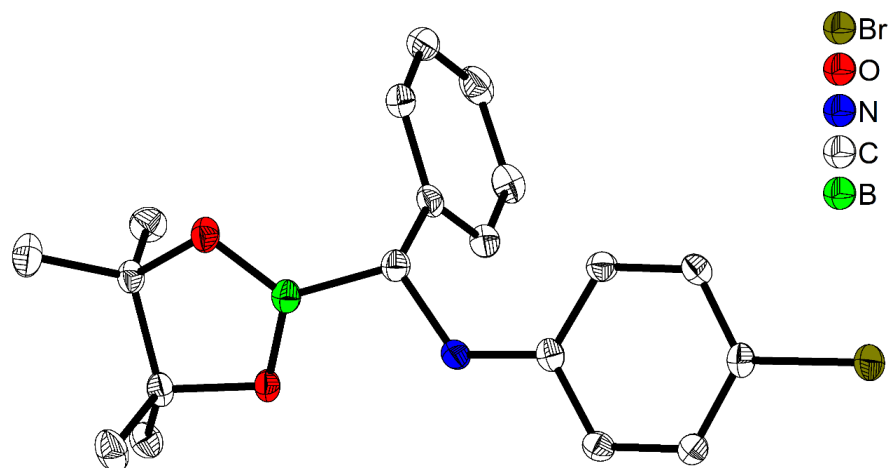
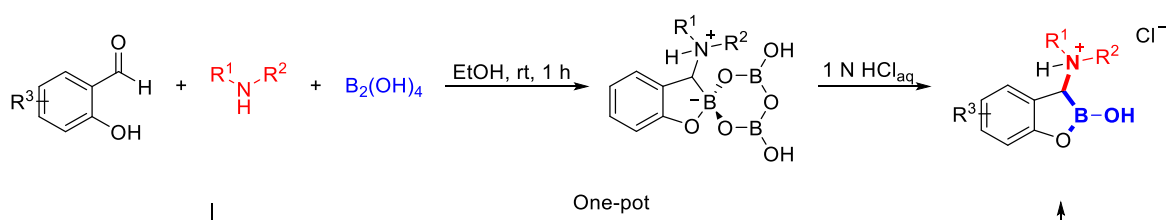


Figure 2-11 Molecular structure of **2-3y** in the solid state at 100 K. Atomic displacement ellipsoids are drawn at the 50% probability level, and H atoms are omitted for clarity.

Chapter Three

Concise synthesis of α -amino cyclic boronates *via* multicomponent coupling of salicylaldehydes, amines, and $B_2(OH)_4$



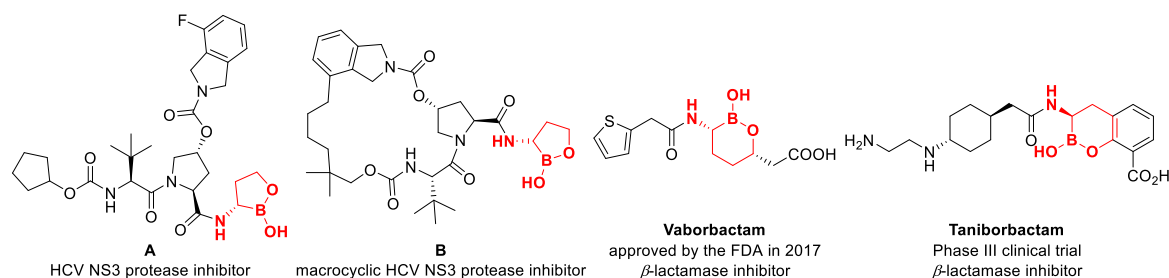
3 Concise synthesis of α -amino cyclic boronates *via* multicomponent coupling of salicylaldehydes, amines, and $B_2(OH)_4$

3.1 Abstract

A concise synthesis of α -amino cyclic boronates *via* multicomponent coupling of readily available salicylaldehydes, amines, and $B_2(OH)_4$ was achieved. The process can be carried out at room temperature in ethanol, does not require catalysts or additives, and is easy to scale up. Amins and ligated boroxines are intermediates in this reaction.

3.2 Introduction

Organoboron compounds have numerous applications in organic synthesis, pharmaceuticals and functional materials.^{1a,1b,1d,88,100} In particular, α -aminoboronic acids and their derivatives are important due to their roles as bioactive agents, functional materials, and synthetic building blocks.^{2c,2g,6-8,10,73b,74,101} For example, α -amino cyclic boronate **A**, and its macrocyclic derivative **B** (Scheme 3-1), are HCV NS3 serine protease inhibitors (IC_{50} 23 nM and 43 nM, respectively).¹⁰² Vaborbactam, approved by the FDA in 2017, is a β -lactamase inhibitor based on a cyclic boronic acid pharmacophore. It has been used in trials investigating the treatment of bacterial infections in subjects with varying degrees of renal insufficiency (Scheme 3-1, **C**).^{4,103} Taniborbactam is a new-generation cyclic boronate β -lactamase inhibitor, which has a unique broad-spectrum activity, covering both serine- β -lactamases and metallo- β -lactamases (Scheme 3-1, **D**).¹⁰⁴

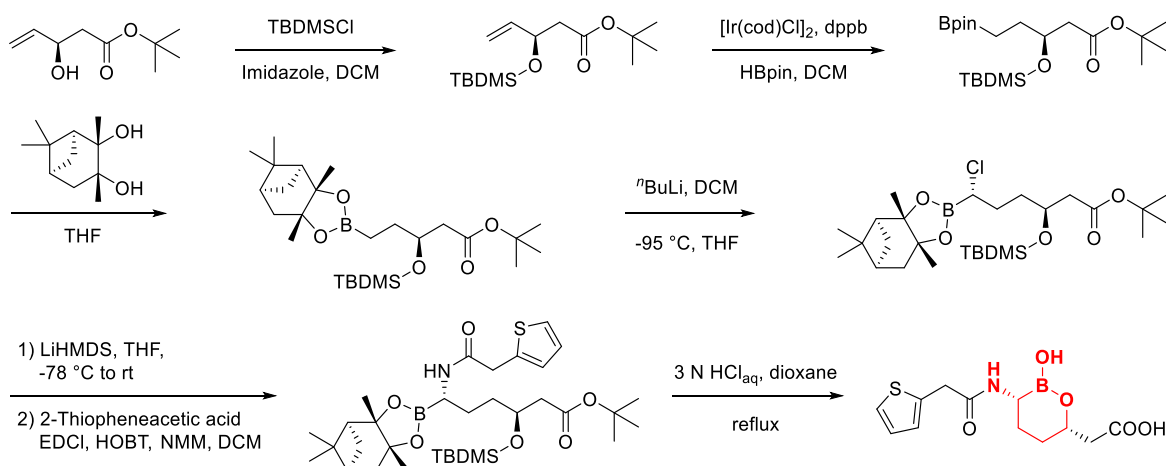
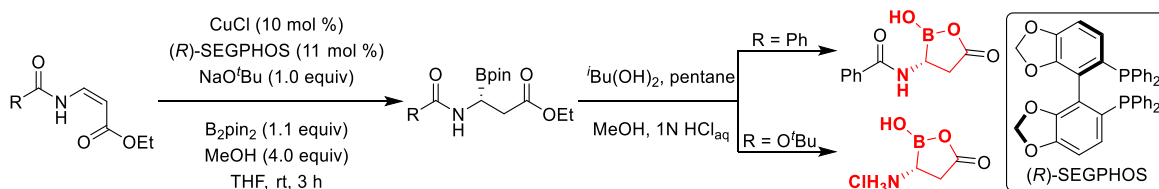
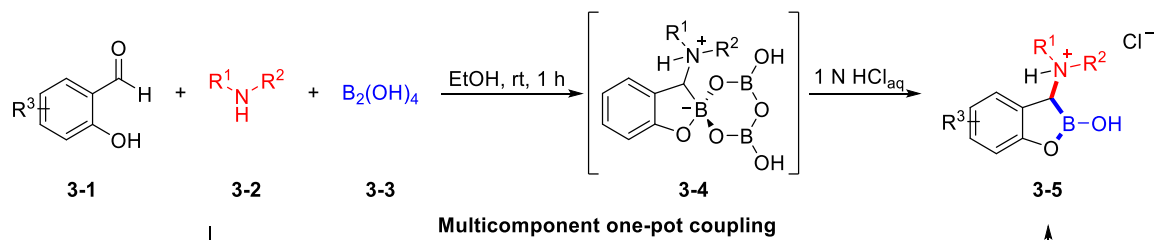


Scheme 3-1 Examples of enzyme inhibitors possessing an α -amino cyclic boronate motif.

The therapeutic potential of α -amino cyclic boronates provides a great driving force to develop and refine efficient and green methods for their synthesis. However, compared with their non-cyclic derivatives,^{12c,20,22-23,31,35,38,46,58a} relatively few methods are available for the preparation of α -amino cyclic boronates. Traditional synthetic methods are based on multi-step reactions, including Ir-catalyzed borylation, Matteson's boronic ester homologation, nucleophilic amination, cyclization, *etc.* (Scheme 3-2a).^{103,105} In 2017, Parra, Tortosa and co-workers synthesized a series of chiral α -aminoboronic esters by a Cu-catalyzed asymmetric hydroboration of β -amidoacrylates. With these borylated products in hand, hemiboronates were prepared by hydrolysis of the pinacol boronic ester, and an *N*-Boc protected derivative was transformed into a primary α -aminoboronate (Scheme 3-2b).^{37b} These useful methods require harsh conditions, multi-step procedures, and/or metal catalysts. Additionally, the starting materials usually require several steps to prepare. Thus, development of efficient and versatile chemical transformations for synthesizing α -amino cyclic boronates from readily available starting materials is highly desirable.

Aldehydes and amines have been widely utilized in multicomponent Mannich, Strecker, and Petasis reactions, *etc.*, and are ideal starting materials as they are abundant, inexpensive and readily available from commercial suppliers. Bypassing the isolation of imine or iminium intermediates increases the product scope, reduces the number of steps, and is thus more economical and sustainable.

The synthesis of diverse α -amino cyclic boronates *via* the multicomponent coupling of commercially available salicylaldehydes, amines, and tetrahydroxydiboron [B₂(OH)₄] is achieved. The process is simple, can be run in a green solvent, and does not require catalysts or additives (Scheme 3-2c).

a) Reported synthetic route to Vaborbactam.^{103,105}b) Parra and Tortosa's protocol to synthesize α -amino cyclic boronates.^{37b}c) Catalyst- and additive-free synthesis of α -amino cyclic boronates *via* multicomponent coupling (this work).

Scheme 3-2 Previously reported methods for the synthesis α -amino cyclic boronates, and our method.

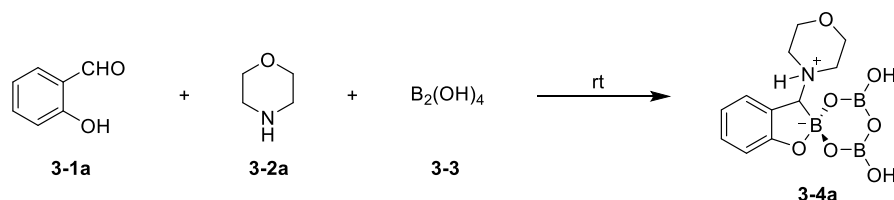
3.3 Results and discussions

3.3.1 Optimization of reaction conditions

Our initial studies showed that a novel ligated boroxine **3-4a** was formed after 24 h, when salicylaldehyde **3-1a**, morpholine **3-2a** and B₂(OH)₄ were mixed in toluene at room temperature (Table 3-1, Entry 1). Optimization of the reaction showed that polar solvents gave higher yields of product than non-polar ones, giving the product in 94% isolated yield, when CH₃CN was used (Entries 2-7). Compound **3-4a** was formed in 93% yield in only 12

h (Entry 8) and, due to its low solubility in CH₃CN, the product can be easily separated *via* filtration.

Table 3-1 The development of optimized conditions for ligated boroxine formation^a

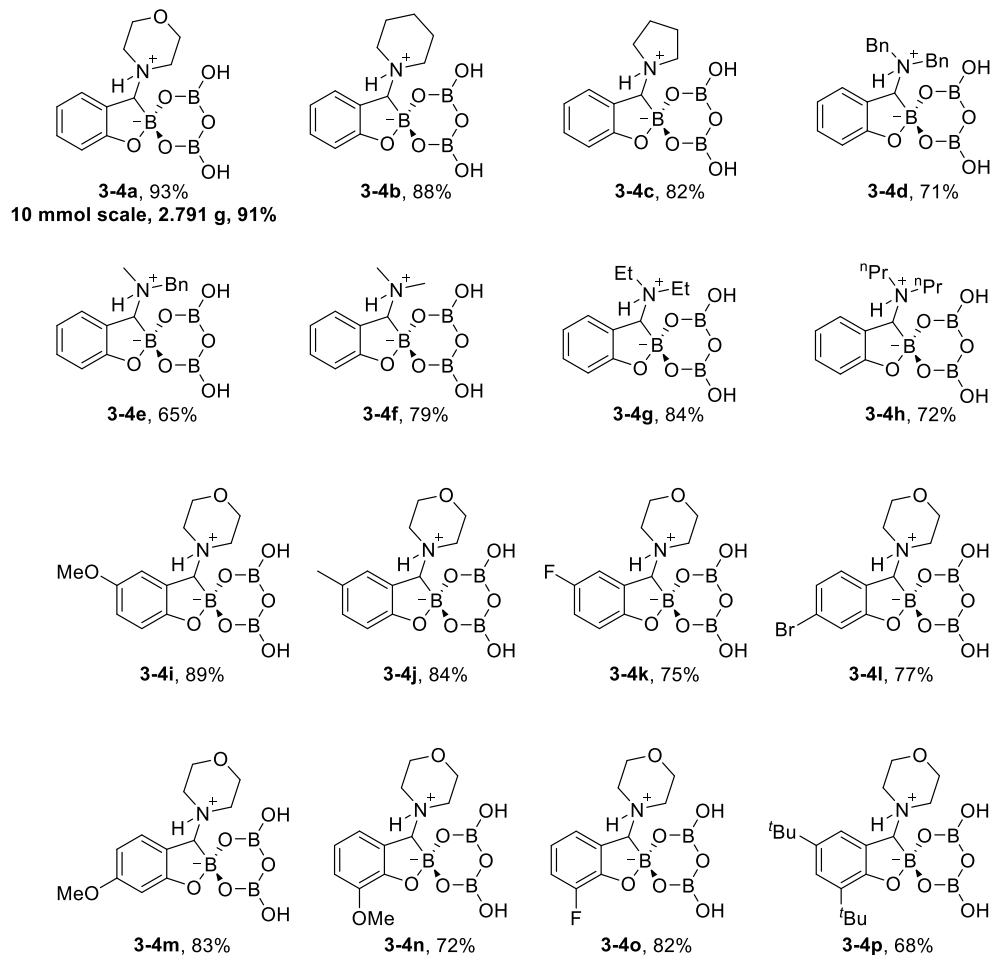
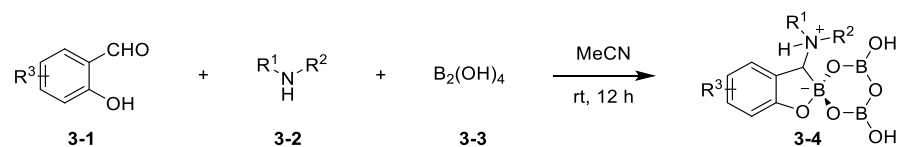


Entry	Solvent	Time (h)	Yield (%)
1	toluene	24	49
2	Et ₂ O	24	38
3	CH ₂ Cl ₂	24	65
4	THF	24	68
5	EtOAc	24	72
6	acetone	24	89
7	MeCN	24	94
8	MeCN	12	93
9	MeCN	6	72

^aReaction conditions: **3-1a** (0.5 mmol), **3-2a** (0.5 mmol, 1.0 equiv), B₂(OH)₄ (0.75 mmol, 1.5 equiv), solvent (2 mL), in air at ambient temperature, with isolated yields of product.

3.3.2 Investigation of reaction scope

With optimized conditions in hand, the substrate scope was then systematically studied, and the results are compiled in Scheme 3-3. Secondary aliphatic amines, including piperidine, pyrrolidine, Bn₂NH, BnMeNH, Me₂NH, Et₂NH, and ⁿPr₂NH were suitable substrates for this reaction. Both electron-donating methyl, methoxy, and *t*-butyl, and electron-withdrawing bromide and fluoride substituents on the salicylaldehyde were tolerated (Scheme 3-3). A convenient gram-scale reaction (10 mmol) of **3-1a** give **3-4a** in 91% yield (2.791 g). The structures of the products were exemplified by single-crystal X-ray diffraction studies of **3-4a**, **3-4d**, and **3-4p** (Figure 3-1).



Reaction conditions: **3-1** (0.5 mmol, 1.0 equiv), **3-2** (0.5 mmol, 1.0 equiv) and **3-3** (0.75 mmol, 1.5 equiv) in MeCN (2 mL) in air at ambient temperature unless otherwise specified, with isolated yields of target product.

Scheme 3-3 Substrate scope of synthesis of boroxines.

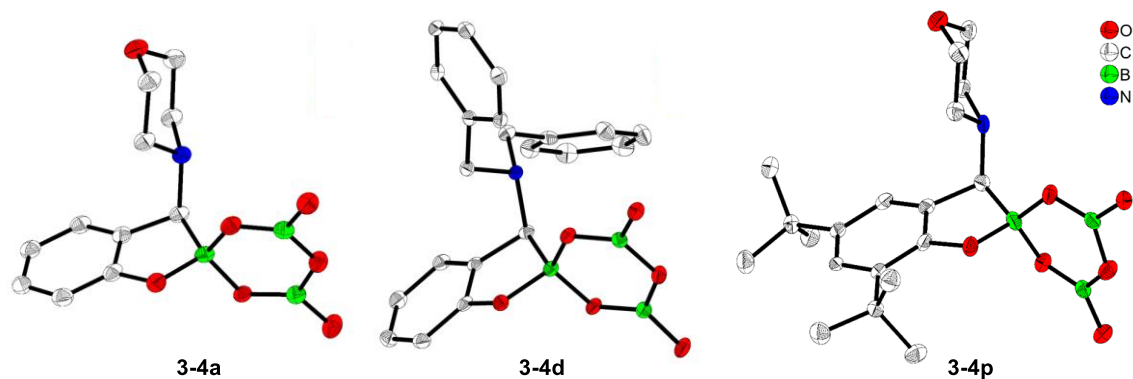
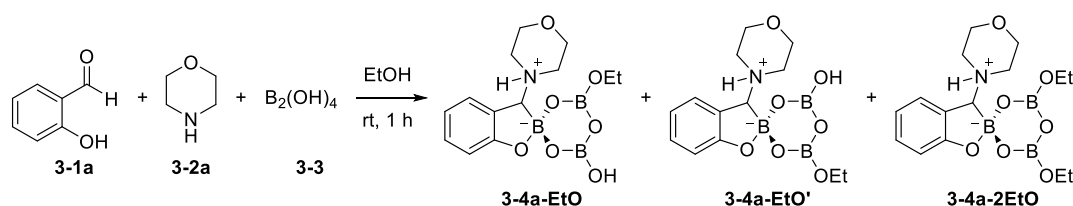
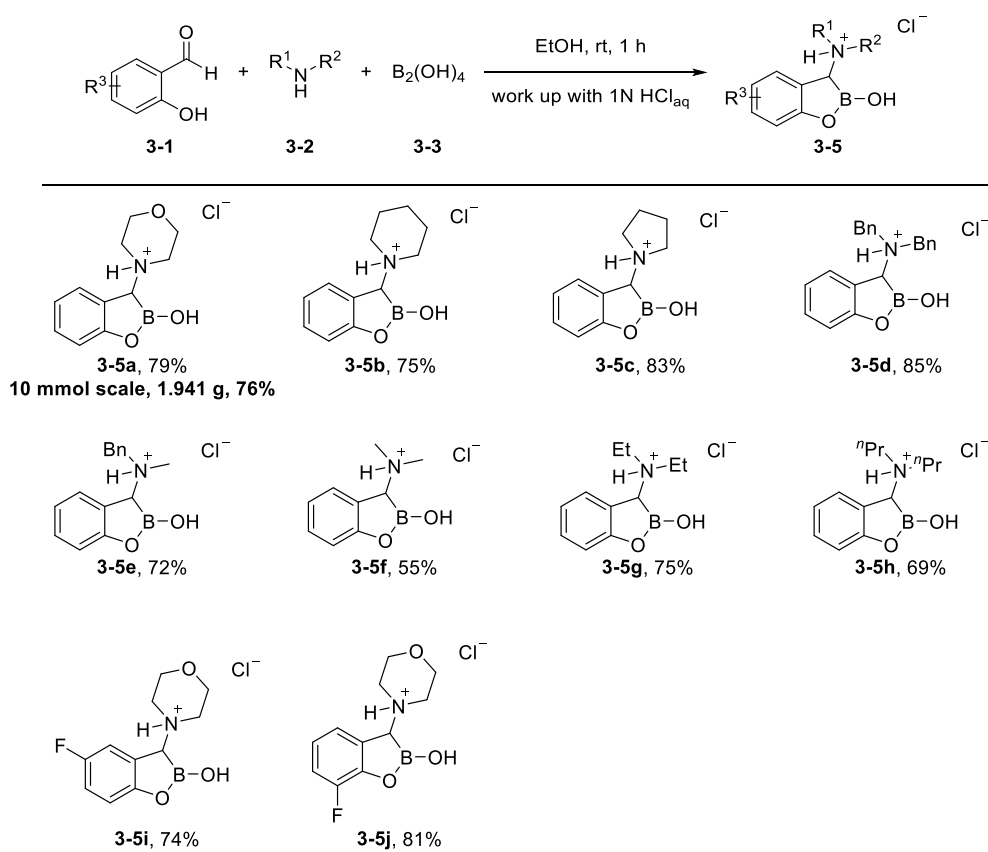


Figure 3-1 Molecular structures of **3-4a**, **3-4d**, and **3-4p**.

Given its low price, low boiling point and low toxicity, ethanol is widely used as a green solvent in organic synthesis.¹⁰⁶ With ethanol as the solvent for our reaction, one or both hydroxyls were substituted by EtO⁻, as confirmed by NMR spectroscopy and HRMS (Scheme 3-4 and Figures 3-8 to 3-12). However, the products were formed faster and in higher yields, and after work up with 1N HCl_{aq}, a benzoxaborole-derived α -amino cyclic boronate was isolated in good yield.^{107,108} As depicted in Scheme 3-5, a series of α -amino cyclic boronates were prepared *via* this multicomponent reaction.



Scheme 3-4 Reaction conducted in ethanol.



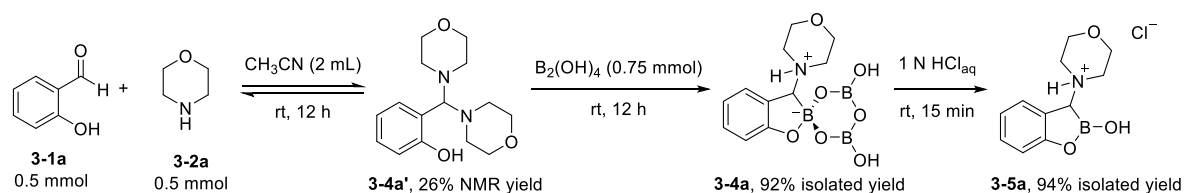
Reaction conditions: 3-1 (0.5 mmol), 3-2 (0.5 mmol, 1.0 equiv) and B₂(OH)₄ (0.75 mmol, 1.5 equiv), ethanol (2 mL), in air under ambient temperature for 1h, then 2 mL 1N HCl_{aq} was added, with isolated yields of target product.

Scheme 3-5 Substrate scope of the one-pot synthesis of α -amino cyclic boronates.

3.4 Mechanistic studies

3.4.1. Stepwise reaction

To gain insight into the mechanism, the reaction was conducted stepwise, and a minal intermediate **3-4a'** was formed in 26% yield immediately upon mixing salicylaldehyde **3-1a** and morpholine **3-1b** in CH₃CN, confirmed by ¹H NMR spectroscopy (Figure 3-2). Prolonging the reaction time to 12 h did not lead to an improvement in the yield of **3-4a'**, indicating that the formation of aminals is reversible. B₂(OH)₄ was then added to the reaction mixture, and boroxine **3-4a** was isolated in 92% yield after stirring for 12 h. Then, **3-4a** was hydrolyzed with 1N HCl_{aq} to give α-amino cyclic boronate **3-5a** in 94% yield (Scheme 3-6).



Scheme 3-6 Stepwise reaction process; the yield of intermediate **3-4a'** was monitored by ¹H NMR spectroscopy (300 MHz, CDCl₃, rt) using 1,3,5-trimethoxybenzene as an internal standard.

Experimental procedures

(1) In a 10 mL reaction tube equipped with a magnetic stirring bar, MeCN (2 mL), salicylaldehyde **3-1a** (0.5 mmol), and morpholine **3-2a** (0.5 mmol, 1.0 equiv) were added in this order, and 1,3,5-trimethoxybenzene (0.25 mmol, 0.5 equiv) was then added as an internal calibration standard. The resulting mixture was analyzed by ¹H NMR spectroscopy in CDCl₃ solution. The ¹H NMR spectrum is shown below (Figure 3-2). Amination **3-4a'** was obtained in 26% NMR yield.

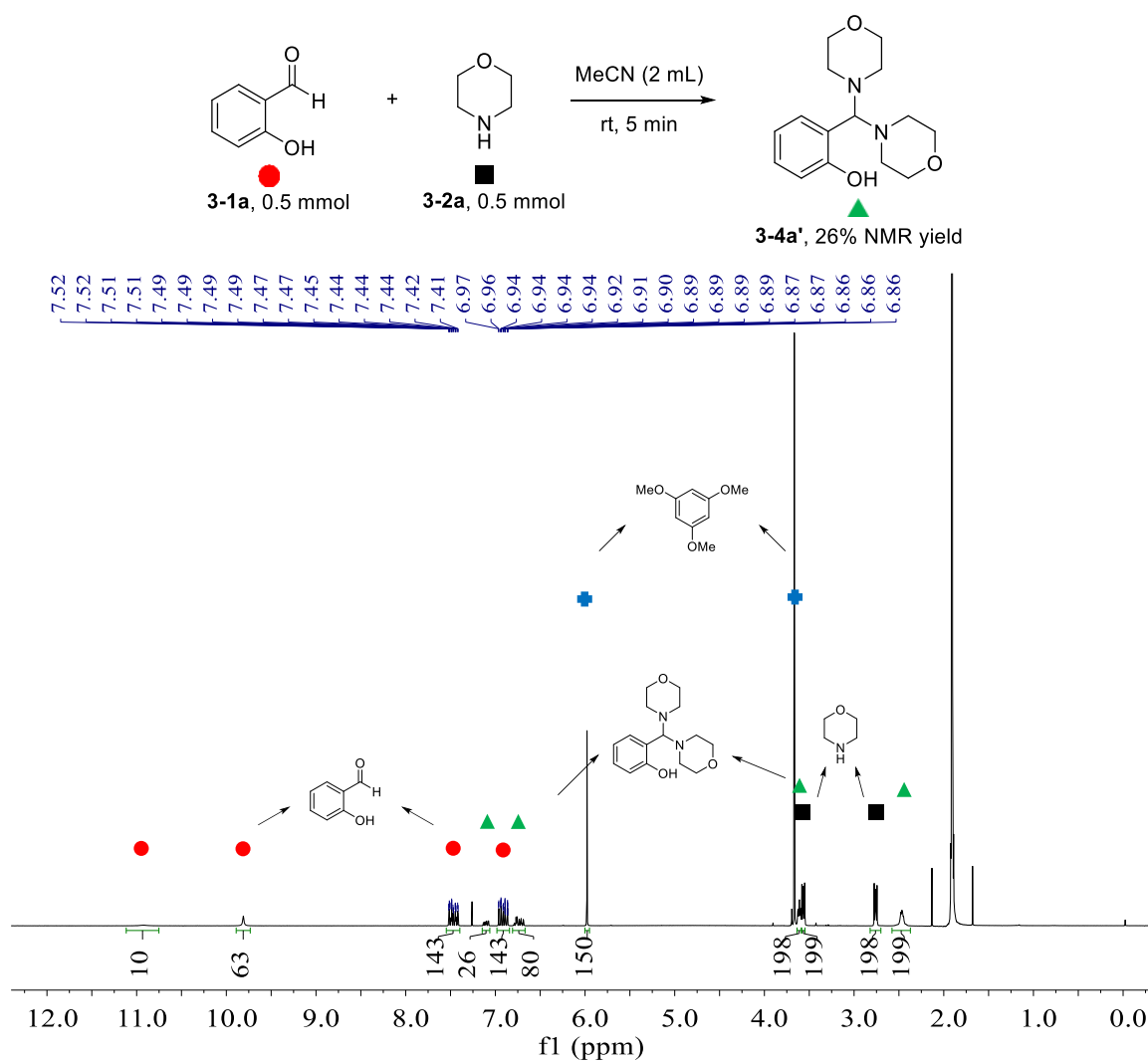


Figure 3-2 ¹H NMR spectrum (300 MHz, CDCl₃, rt) of the reaction mixture of **3-1a** and **3-2a** in MeCN; the product yield was determined by ¹H NMR spectroscopy using 1,3,5-trimethoxybenzene (blue + sign) as the internal calibration standard.

(2) To the above filtrate, B₂(OH)₄ (0.75 mmol, 1.5 equiv) was added and the reaction mixture was stirred at room temperature overnight, then filtered through filter paper and washed with MeCN (10 mL). The product was dried under vacuum to give **3-4a** as a white solid (141 mg, 92% isolated yield).

(3) To a 10 mL reaction tube equipped with a magnetic stirring bar, **3-4a** (141 mg, 0.46 mmol) and 1N HCl_{aq} (2 mL) were added. The resulting solution was stirred for 15 min, and then extracted with Et₂O (2 x 5 mL) to remove impurities. The aqueous solution was

evaporated to dryness under vacuum to obtain a white residue, which was then dissolved in CH_2Cl_2 (5 mL). Removal of CH_2Cl_2 under vacuum gave the product **5a** as white solid (94% isolated yield).

3.4.2. Reaction of salicylaldehyde **3-1a** with different ratios of morpholine **3-2a**

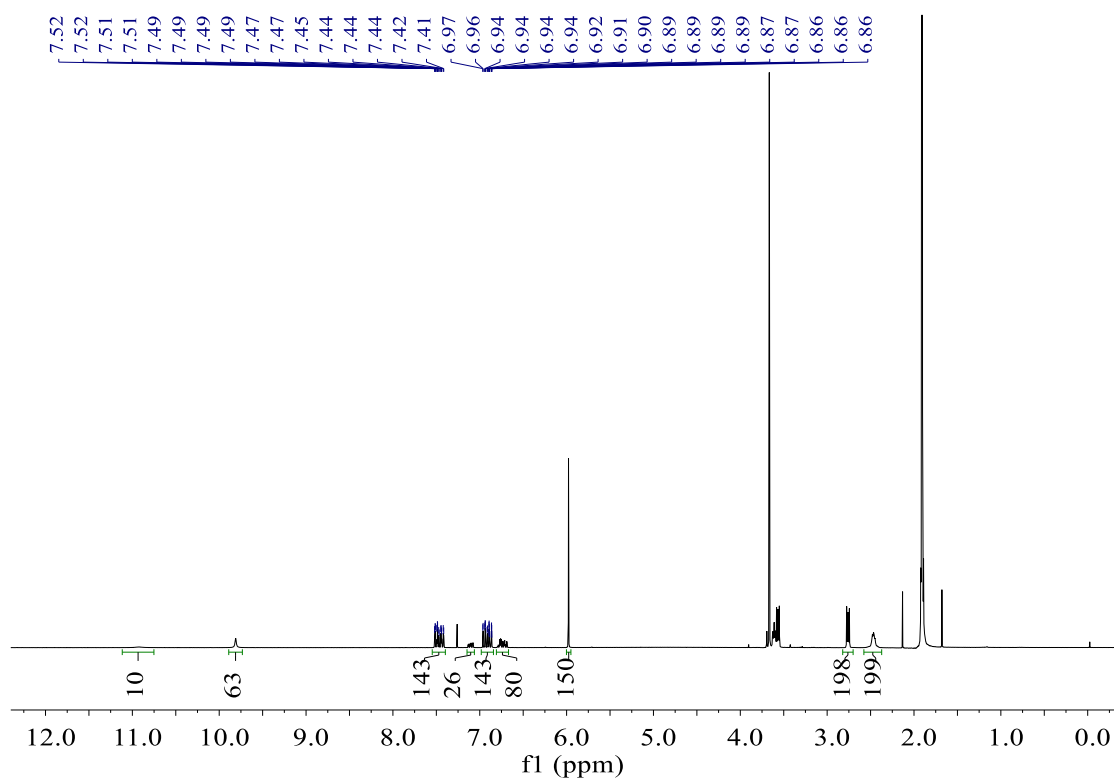


Figure 3-3 ^1H NMR spectrum of the reaction of salicylaldehyde **3-1a** with 1 equivalent of morpholine **3-2a** (300 MHz, CDCl_3 , rt); 1,3,5-trimethoxybenzene was used as an internal standard.

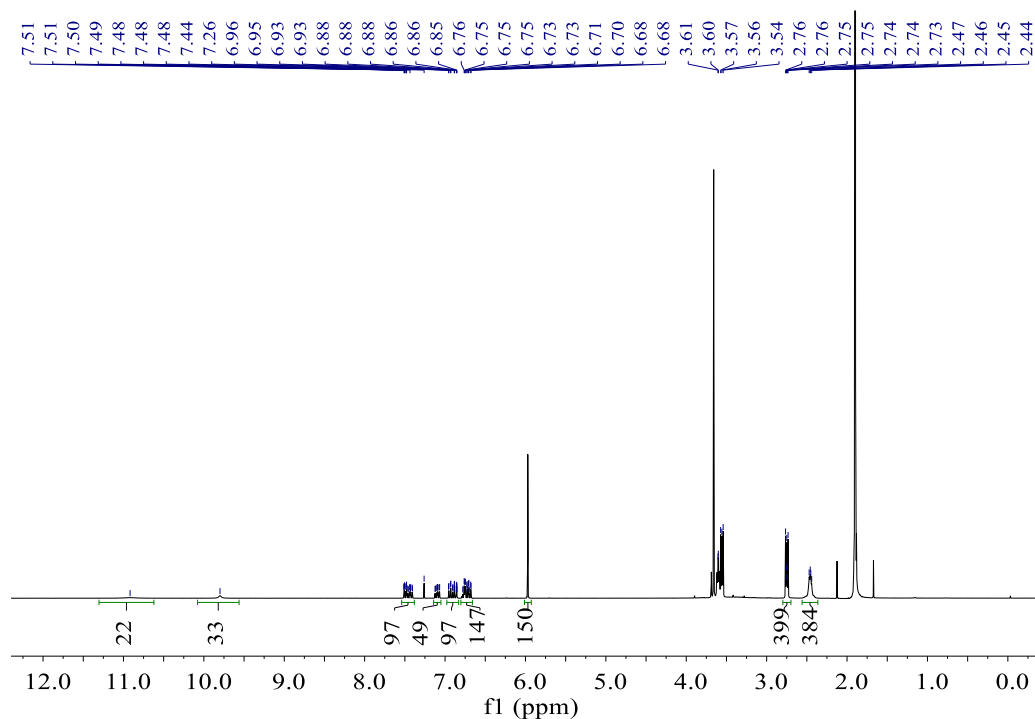


Figure 3-4 ^1H NMR spectrum of the reaction of salicylaldehyde **3-1a** with 2 equivalents of morpholine **3-2a** (300 MHz, CDCl_3 , rt); 1,3,5-trimethoxybenzene was used as an internal standard.

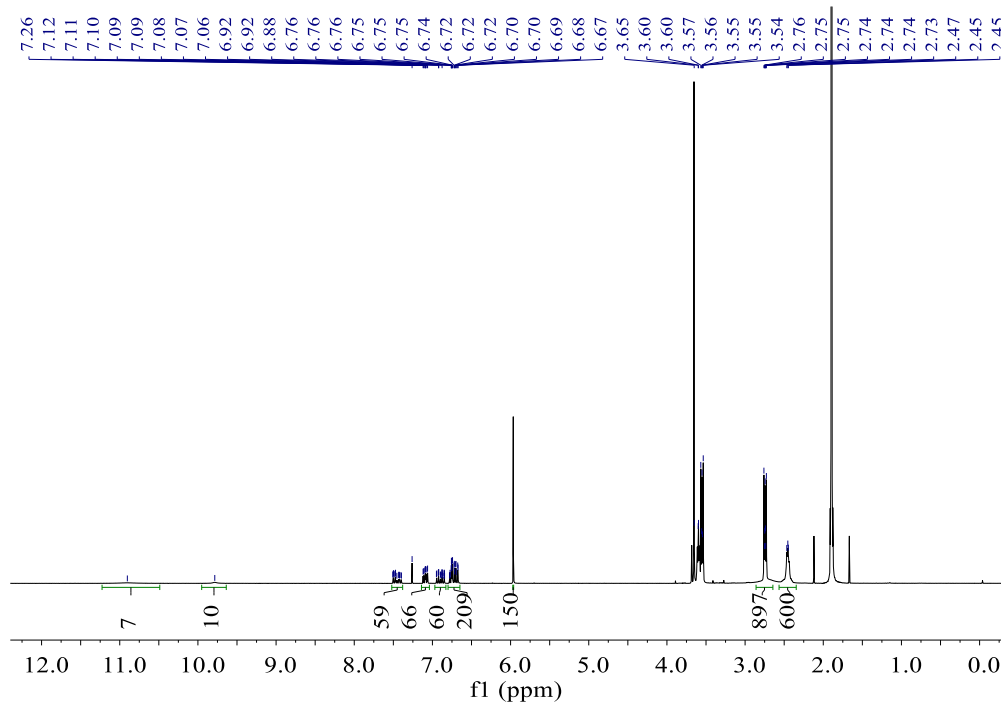


Figure 3-5 ^1H NMR spectrum of the reaction of salicylaldehyde **3-1a** with 3 equivalents of morpholine **3-2a** (300 MHz, CDCl_3 , rt); 1,3,5-trimethoxybenzene was used as an internal standard.

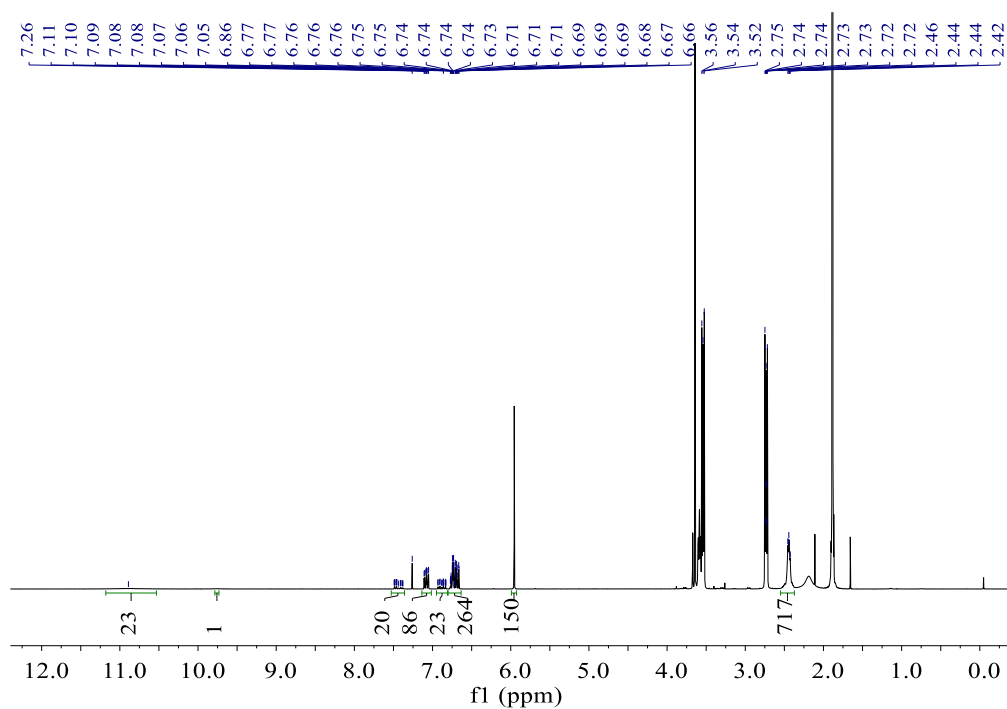


Figure 3-6 ¹H NMR spectrum of the reaction of salicylaldehyde **3-1a** with 5 equivalents of morpholine **3-2a** (300 MHz, CDCl₃, rt); 1,3,5-trimethoxybenzene was used as an internal standard.

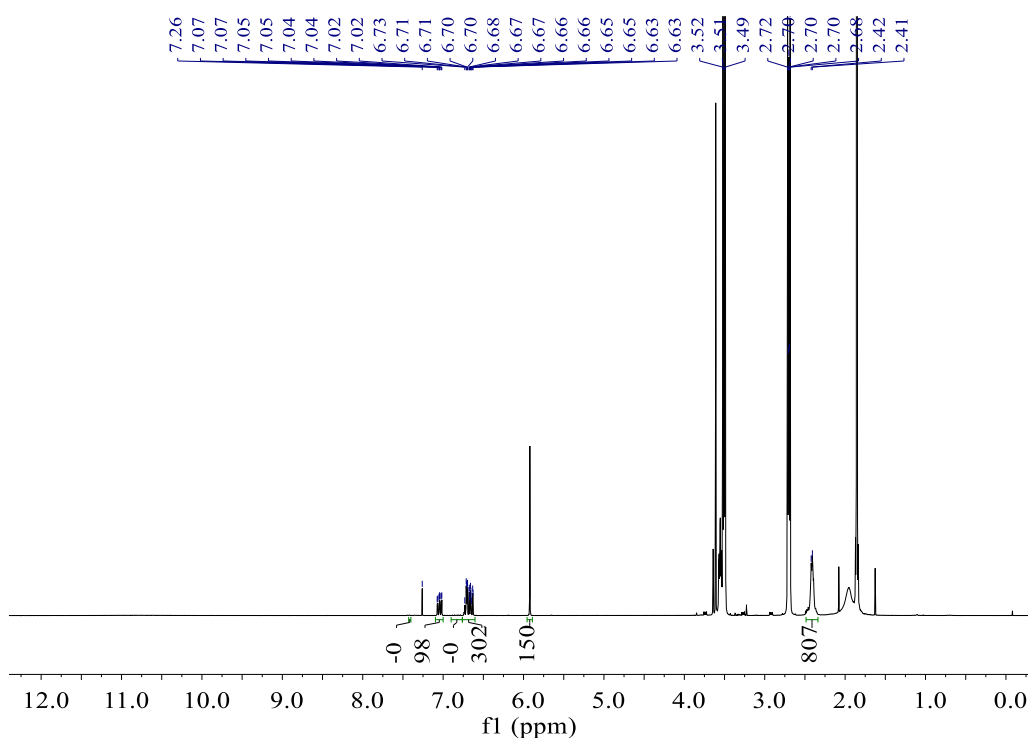


Figure 3-7 ¹H NMR spectrum of the reaction of salicylaldehyde **3-1a** with 10 equivalents of morpholine **3-2a** (300 MHz, CDCl₃, rt); 1,3,5-trimethoxybenzene was used as an internal standard.

3.4.3 Reaction conducted in ethanol

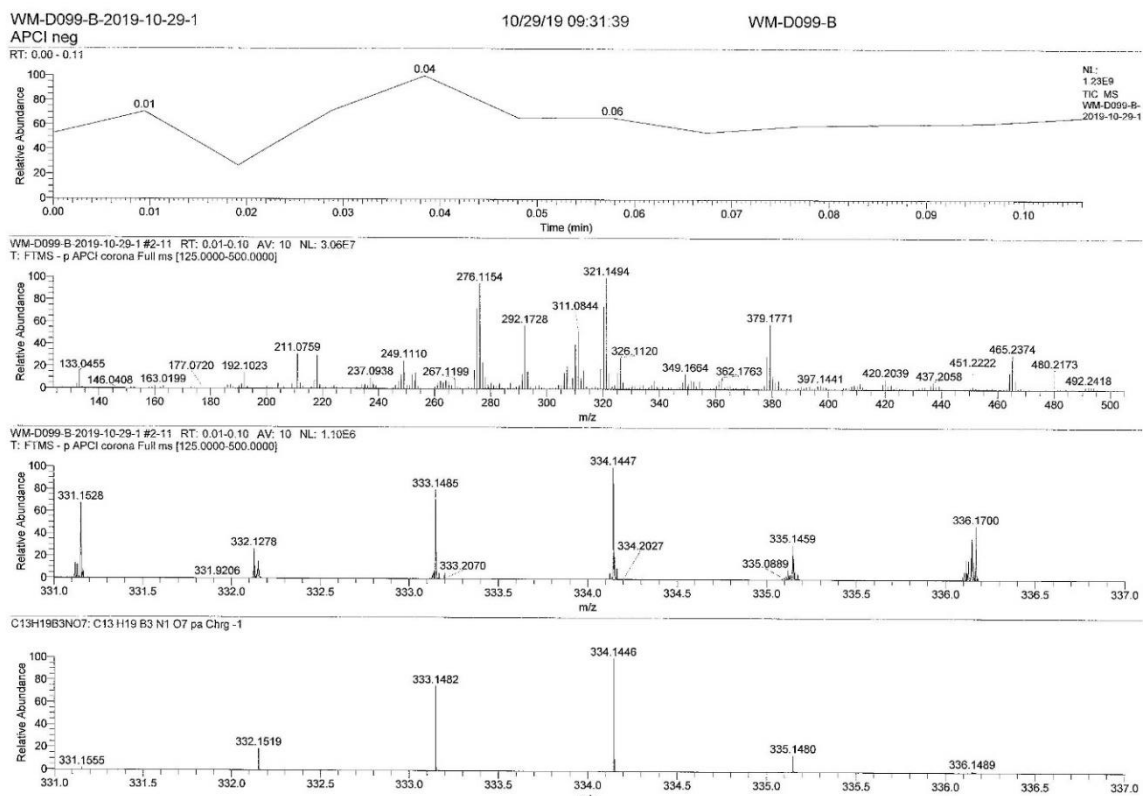
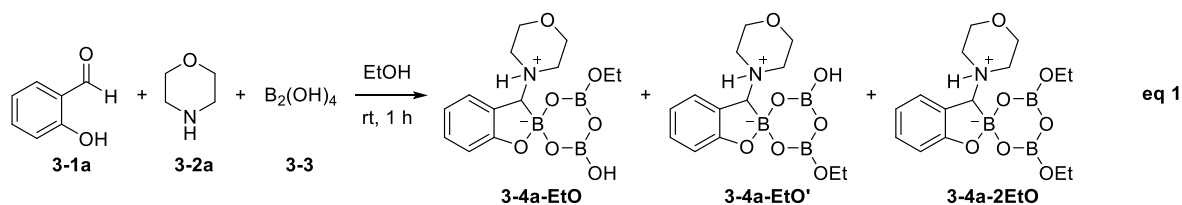


Figure 3-8 HRMS (APCI neg) of the reaction mixture in eq 1; *m/z* of **3-4a-EtO** and/or **3-4a-EtO'**: [*M*-*H*]⁻ calcd for C₁₃H₁₉B₃NO₇⁻ 334.1446, found 334.1447.

Chapter Three

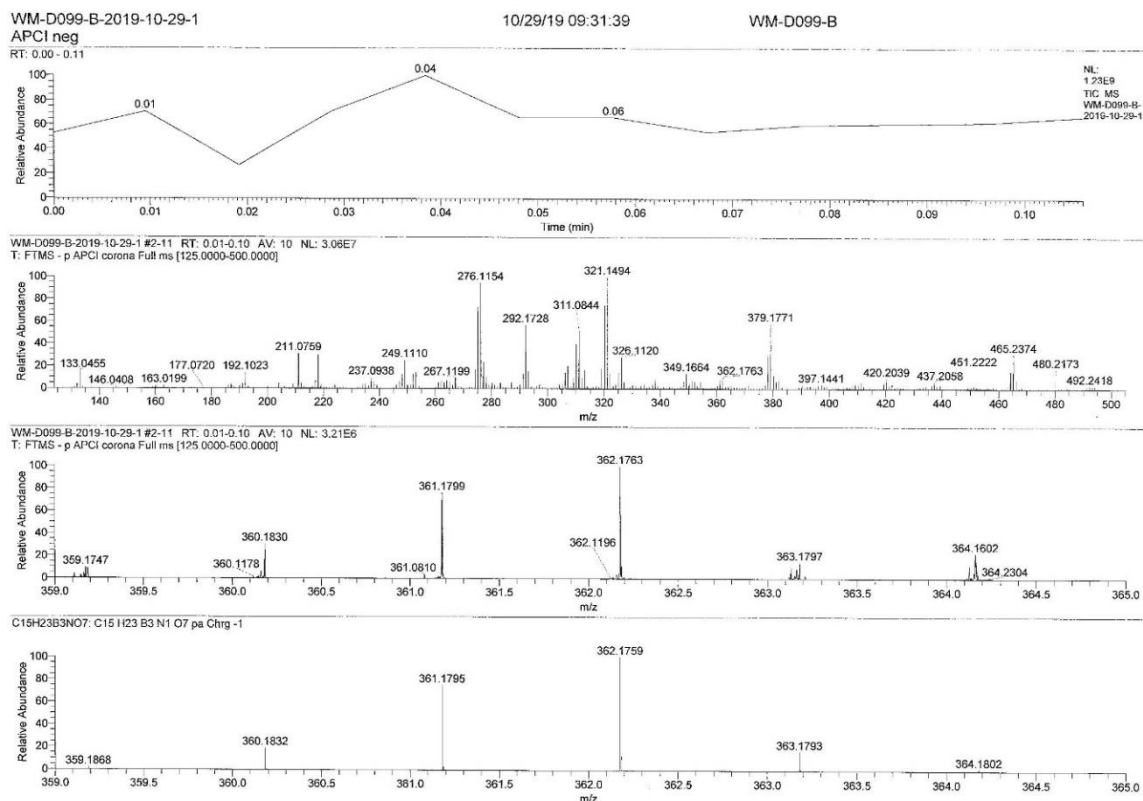


Figure 3-9 HRMS (APCI neg) of the reaction mixture in eq 1; m/z of **3-4a-2EtO**: $[M-H]^-$ calcd for $C_{15}H_{23}B_3NO_7^-$ 362.1759, found 362.1763.

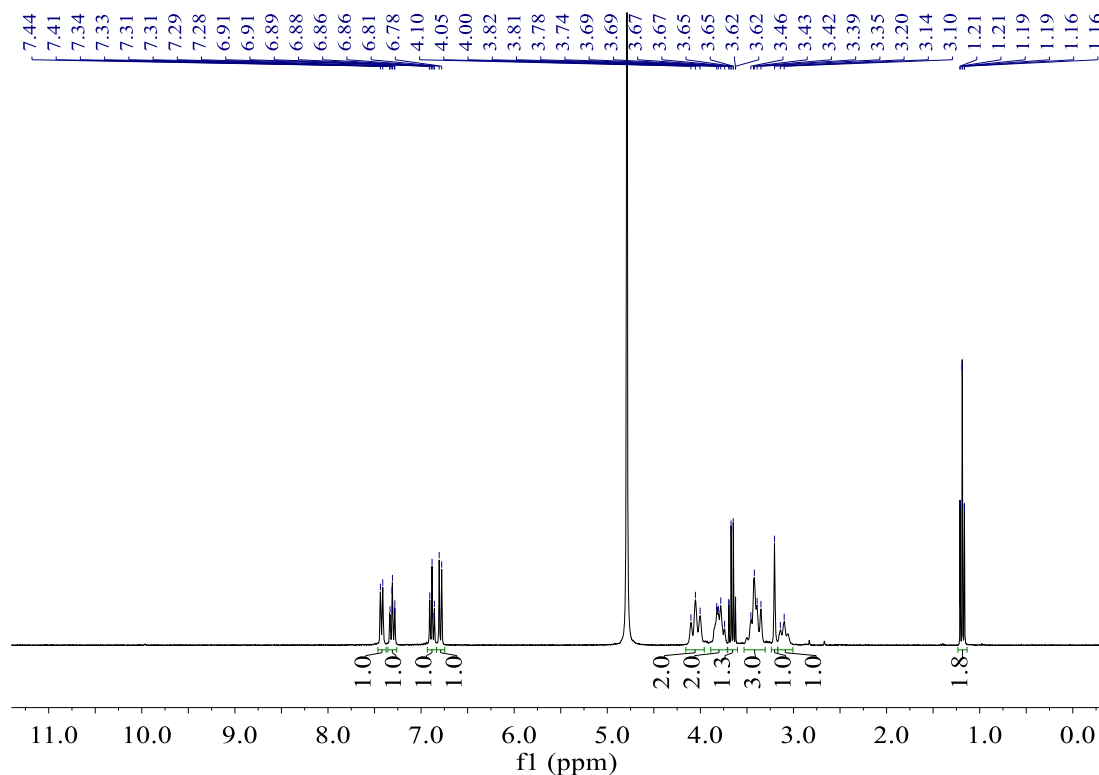


Figure 3-10 1H NMR spectrum of the reaction mixture in eq 1 (300 MHz, D_2O , rt).

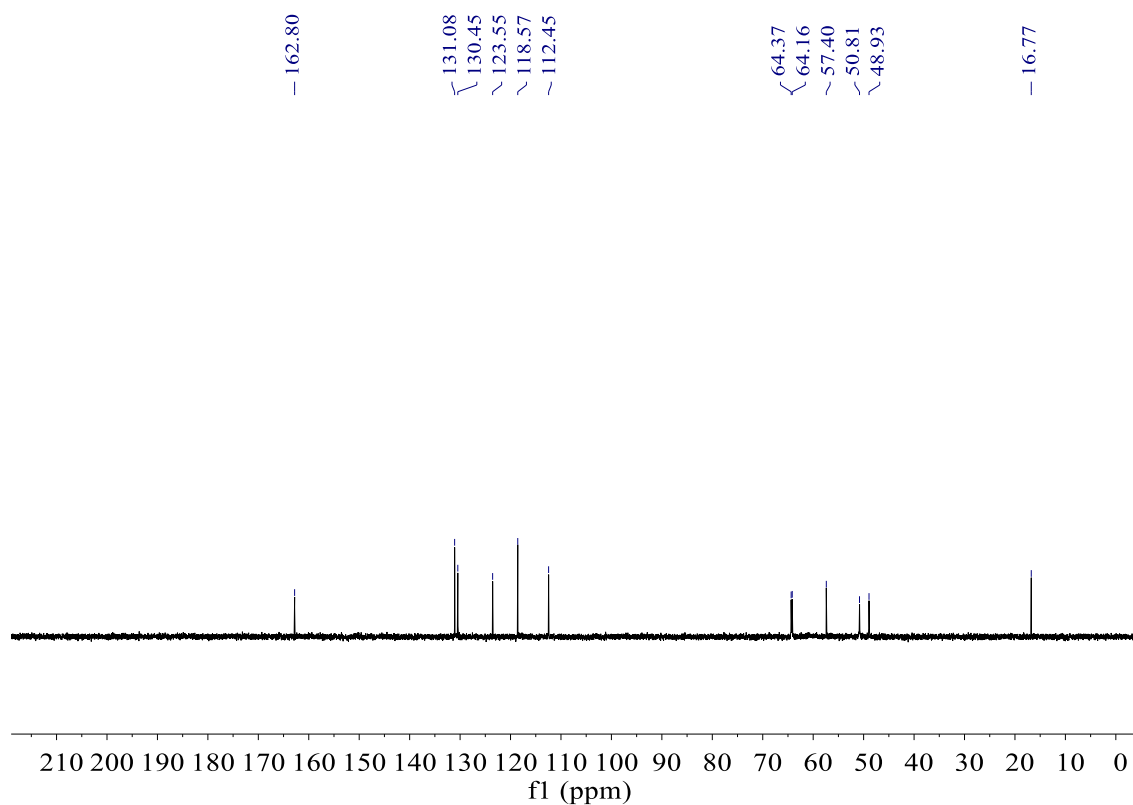


Figure 3-11 $^{13}\text{C}\{^1\text{H}\}$ NMR spectrum of the reaction mixture in eq 1 (75 MHz, D_2O , rt).

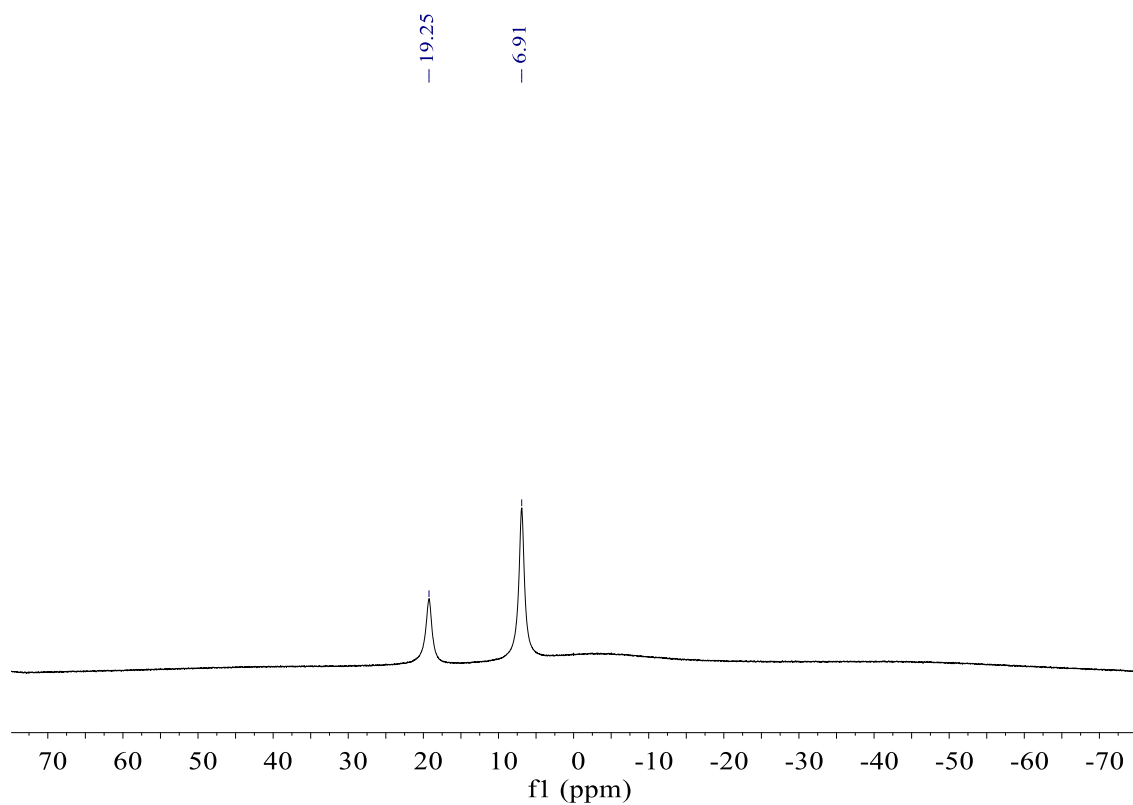
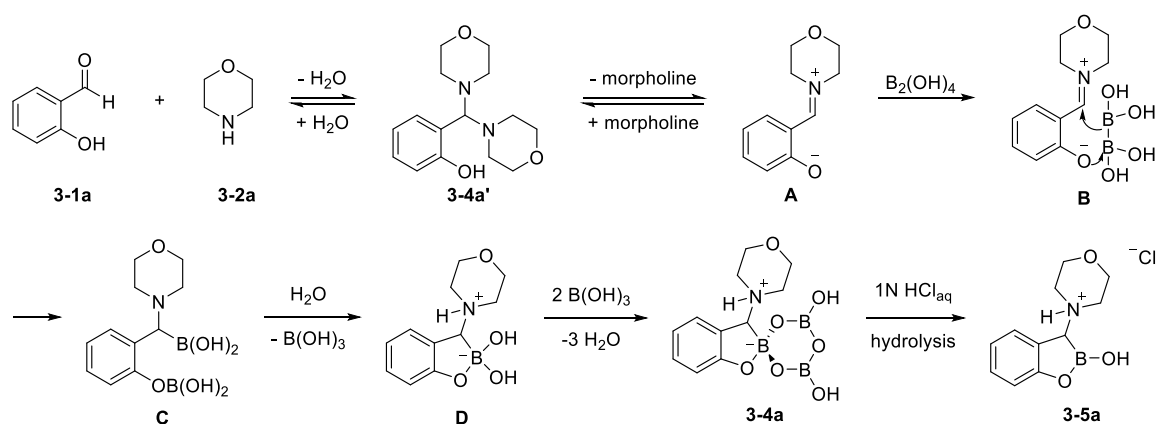


Figure 3-12 ^{11}B NMR spectrum of the reaction mixture in eq 1 (96 MHz, D_2O , rt).

3.4.4 Proposed mechanism

The Petasis three-component reaction between an amine, an aldehyde and an organoboron compound, has evolved into a versatile process for the synthesis of amino acids, amino alcohols, and various heterocycles.¹⁰⁹ In 1962, Matteson *et al.* first reported ligand-facilitated trimerization of boronic acids when they prepared the 1 : 1 pyridine complex of vinylboronic acid anhydride, the boroxine being generated spontaneously in a high yield.¹¹⁰

Based on the above, and our observations, we propose the mechanism for our multicomponent coupling reaction shown in Scheme 3-7. Salicylaldehyde **3-1a** reacts with morpholine **3-1b** to form aminal intermediate **3-4a'**. The key intermediate **B** is assembled by formation of iminium ion **A**, and coordination of its phenolate oxygen to $B_2(OH)_4$.^{1d,30} Intramolecular boryl group transfer provides **C**, the immediate precursor to ligated α -aminoboronic acid **D**, which can react with boric acid to give boroxine **3-4a**. Finally, hydrolysis with 1N HCl_{aq} affords α -amino cyclic boronate **3-5a**.



Scheme 3-7 Proposed mechanism for the formation of **3-5a**.

3.5 Summary

In conclusion, a green and economical process for the synthesis of α -amino cyclic boronates was developed. The desired products can be obtained *via* a one-step multicomponent reaction from the readily available starting materials, salicylaldehydes,

amines, and $B_2(OH)_4$. Our protocol has several advantages over previous routes including mild reaction conditions (room temperature, in air), no catalysts or additives, easy product isolation, and green solvents (ethanol and water).

3.6 Experimental procedures and characterization data

3.6.1 General information

All reagents were purchased from Alfa-Aesar, Aldrich, TCI, ABCR, VWR, or Fluorochem, and were checked for purity by GC-MS and/or 1H NMR spectroscopy and used as received. D_2O was purchased from Deutero GmbH, and CD_3OD were purchased from Sigma-Aldrich. Diboronic acid was purified by washing with dioxane following a reported method.¹¹¹

The removal of solvent was performed on a rotary evaporator *in vacuo* at a maximum temperature of 40 °C. GC-MS analyses were performed using an Agilent 7890A gas chromatograph (column: HP-5MS 5% phenyl methyl siloxane, 30 m, \varnothing 0.25 mm, film 0.25 μm ; injector: 250 °C; oven: 40 °C (2 min), 40 °C to 280 °C (20 °C·min⁻¹); carrier gas: He (1.2 mL·min⁻¹)) equipped with an Agilent 5975C inert MSD with triple-axis detector operating in EI mode and an Agilent 7693A series auto sampler/injector. Elemental analysis were performed on a Leco CHNS-932 Elemental Analyzer. High-resolution mass spectra were recorded using a Thermo Fischer Scientific Exactive Plus Orbitrap MS system (ASAP, ESI or HPCI probe). All NMR spectra were recorded at ambient temperature using Bruker DRX-300 (1H , 300 MHz; $^{13}C\{^1H\}$, 75 MHz; ^{11}B , 96 MHz) or Bruker Avance 500 NMR (1H , 500 MHz; $^{13}C\{^1H\}$, 125 MHz; ^{11}B , 160 MHz; $^{19}F\{^1H\}$, 471 MHz) spectrometers. 1H NMR chemical shifts are reported relative to TMS and were referenced *via* residual proton resonances of the corresponding deuterated solvent (D_2O , 4.79 ppm; CD_3OD , 3.31 ppm; $CDCl_3$, 7.26 ppm), whereas $^{13}C\{^1H\}$ NMR spectra are reported relative to TMS *via* the carbon signals of the deuterated solvent (CD_3OD , 49.00 ppm; $CDCl_3$, 77.16 ppm). ^{11}B NMR chemical shifts are quoted relative to $BF_3 \cdot Et_2O$ as external standard. ^{19}F NMR chemical shifts are quoted relative to $CFCl_3$ as the external standard.

3.6.2 Experimental procedures

General procedures for the preparation of boroxines (Table 3-1 and Scheme 3-3).

In a 10 mL reaction tube equipped with a magnetic stirring bar, MeCN (2 mL), salicylaldehyde **3-1** (0.5 mmol), amine **3-2** (0.5 mmol, 1.0 equiv) and $B_2(OH)_4$ (0.75 mmol, 1.5 equiv) were added in this order. The reaction mixture was stirred at room temperature overnight, then filtered through filter paper and washed with MeCN (10 mL). The product was dried under vacuum.

Preparation of **3-4f** (Scheme 3-3).

In a 10 mL reaction tube equipped with a magnetic stirring bar, dimethylamine hydrochloride **3-2f** (0.5 mmol) and $NaHCO_3$ (0.5 mmol, 1.0 equiv) were dissolved in 2 mL of MeCN. Then, salicylaldehyde **3-1a** (0.5 mmol, 1.0 equiv) was added and the reaction was stirred for 30 min. After filtration using filter paper, a clear yellow solution was obtained. To this filtrate, $B_2(OH)_4$ (0.75 mmol, 1.5 equiv) was added and the reaction mixture was stirred at room temperature overnight, then filtered through filter paper and washed with MeCN (10 mL). The product was dried under vacuum.

Experimental procedure for the synthesis of **3-4a** on a gram scale (10 mmol).

In a 25 mL reaction tube equipped with a magnetic stirring bar, MeCN (10 mL), salicylaldehyde **3-1a** (10 mmol, 1.221 g), morpholine **3-2a** (1.0 equiv, 10 mmol, 0.871 g) and $B_2(OH)_4$ (1.5 equiv, 15 mmol, 1.345 g) were added in this order. The reaction mixture was stirred at room temperature overnight, then filtered through filter paper and washed with MeCN (30 mL). The product **3-4a** was obtained as a white solid (2.791 g, 91%).

General procedures for the preparation of benzoxaborole-derived α -amino cyclic boronates.

In a 10 mL reaction tube equipped with a magnetic stirring bar, EtOH (2 mL), salicylaldehyde **3-1** (0.5 mmol), amine **3-2** (0.5 mmol, 1.0 equiv) and $B_2(OH)_4$ (0.75 mmol, 1.5 equiv) were added in this order. The reaction mixture was stirred at room temperature for 1 h. 1N HCl_{aq} (2 mL) was added to the reaction mixture, and the resulting solution was

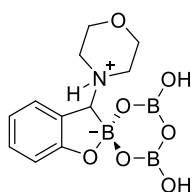
stirred for 15 min. The reaction mixture was extracted with Et₂O (2 x 5 mL) to remove impurities. The aqueous solution was evaporated to dryness to obtain a white residue, which was then dissolved in CH₂Cl₂ (5 mL). Removal of CH₂Cl₂ under vacuum gave the product.

Experimental procedure for the synthesis of 3-5a on a gram scale (10 mmol).

In a 25 mL reaction tube equipped with a magnetic stirring bar, EtOH (10 mL), salicylaldehyde **3-1a** (10 mmol, 1.221 g), morpholine **3-2a** (1.0 equiv, 10 mmol, 0.871 g) and B₂(OH)₄ (1.5 equiv, 15 mmol, 1.345 g) were added in this order. The reaction mixture was stirred at room temperature for 1 h. 1N HCl_{aq} (40 mL) was then added to the reaction mixture, and the resulting solution was stirred for 15 min. The reaction mixture was extracted with Et₂O (2 x 20 mL) to remove impurities. The aqueous solution was evaporated to dryness to obtain a white residue, which was then dissolved in CH₂Cl₂ (20 mL). Removal of CH₂Cl₂ under vacuum gave the product **3-5a** as a white solid (1.941 g, 76%).

3.6.3 Compound characterization

4',6'-dihydroxy-3-(morpholino-4-ium)-3H-spiro[benzo[d][1,2]oxaborole-2,2'-[1,3,5,2,4,6]trioxatriborinan]-2-uide



3-4a, was isolated as a white solid (143 mg, 93%), m.p. = 223 °C.

¹H NMR (300 MHz, D₂O): δ = 7.42 (d, *J* = 8 Hz, 1H), 7.31 (dd, *J* = 8, 8 Hz, 1H), 6.88 (dd, *J* = 8, 8 Hz, 1H), 6.79 (d, *J* = 8 Hz, 1H), 4.08 (d, *J* = 14 Hz, 1H), 4.03 (d, *J* = 15 Hz, 1H), 3.90-3.69 (m, 2H), 3.54-3.29 (m, 3H), 3.20 (s, 1H), 3.17-3.03 (m, 1H) ppm. Protons directly attached to nitrogen and oxygen were not detected due to exchange with D₂O.

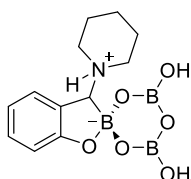
¹³C{¹H} NMR (75 MHz, D₂O): δ = 162.8, 131.1, 130.4, 123.5, 118.6, 112.4, 64.4, 64.2, 60.7 (v br), 50.8, 48.9 ppm.

^{11}B NMR (96 MHz, D_2O): $\delta = 19.4, 6.9$ ppm.

HRMS (ESI neg) m/z : $[M-H]^-$ Calcd for $\text{C}_{11}\text{H}_{15}\text{B}_3\text{NO}_7^-$ 306.1133; found: 306.1144.

Elem. Anal. Calcd (%) for $\text{C}_{11}\text{H}_{16}\text{B}_3\text{NO}_7$: C 43.08, H 5.26, N 4.57; found: C 43.02, H 5.56, N 4.57.

4',6'-dihydroxy-3-(piperidin-1-ium-1-yl)-3H-spiro[benzo[d][1,2]oxaborole-2,2'-[1,3,5,2,4,6]trioxatriborinan]-2-uide



3-4b was isolated as a white solid (134 mg, 88%), m.p. = 209 °C.

^1H NMR (300 MHz, D_2O): $\delta = 7.41$ (d, $J = 8$ Hz, 1H), 7.29 (ddd, $J = 8, 8, 1$ Hz, 1H), 6.87 (ddd, $J = 8, 8, 1$ Hz, 1H), 6.77 (d, $J = 8$ Hz, 1H), 3.47-3.28 (m, 2H), 3.21 (ddd, $J = 13, 13, 3$ Hz, 1H), 3.12 (s, 1H), 2.79-2.59 (m, 1H), 2.02-1.55 (m, 5H), 1.47-1.23 (m, 1H) ppm. Protons directly attached to nitrogen and oxygen were not detected due to exchange with D_2O .

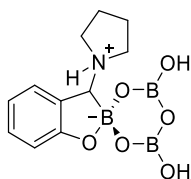
$^{13}\text{C}\{^1\text{H}\}$ NMR (75 MHz, D_2O): $\delta = 162.7, 130.7, 130.3, 124.4, 118.5, 112.3, 60.1$ (v br), 52.7, 50.0, 23.6, 23.3, 21.4 ppm.

^{11}B NMR (96 MHz, D_2O): $\delta = 19.4, 6.9$ ppm.

HRMS (ESI neg) m/z : $[M-H]^-$ Calcd for $\text{C}_{12}\text{H}_{17}\text{B}_3\text{NO}_6^-$ 304.1341; found: 304.1351.

Elem. Anal. Calcd (%) for $\text{C}_{12}\text{H}_{18}\text{B}_3\text{NO}_6$: C 47.30, H 5.95, N 4.60; found: C 47.37, H 5.96, N 4.66.

4',6'-dihydroxy-3-(pyrrolidin-1-ium-1-yl)-3H-spiro[benzo[d][1,2]oxaborole-2,2'-[1,3,5,2,4,6]trioxatriborinan]-2-uide



3-4c was isolated as a white solid (119 mg, 82%), m.p. = 230 °C.

¹H NMR (300 MHz, D₂O): δ = 7.42 (dd, J = 8, 2 Hz, 1H), 7.27 (ddd, J = 8, 8, 2 Hz, 1H), 6.85 (ddd, J = 8, 8, 1 Hz, 1H), 6.77 (d, J = 8 Hz, 1H), 3.71-3.57 (m, 1H), 3.57-3.45 (m, 1H), 3.30 (s, 1H), 3.28-3.13 (m, 1H), 3.13-2.96 (m, 1H), 2.24-1.44 (m, 4H) ppm. Protons directly attached to nitrogen and oxygen were not detected due to exchange with D₂O.

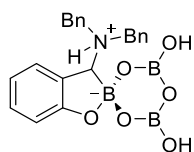
¹³C{¹H} NMR (75 MHz, D₂O): δ = 162.3, 130.6, 129.7, 125.7, 118.4, 112.3, 57.2 (v br), 53.3, 51.8, 22.9, 22.6 ppm.

¹¹B NMR (96 MHz, D₂O): δ = 19.4, 7.0 ppm.

HRMS (ESI neg) m/z : [$M-H$]⁻ Calcd for C₁₁H₁₅B₃NO₆⁻ 290.1184; found: 290.1196.

Elem. Anal. Calcd (%) for C₁₁H₁₆B₃NO₆: C 45.45, H 5.55, N 4.82; found: C 45.25, H 5.36, N 4.49.

3-(dibenzylammonio)-4',6'-dihydroxy-3H-spiro[benzo[*d*][1,2]oxaborole-2,2'-[1,3,5,2,4,6]trioxatriborinan]-2-uide



3-4d was isolated as a white solid (148 mg, 71%), m.p. = 226 °C.

¹H NMR (300 MHz, CD₃OD): δ = 7.56-7.31 (m, 9H), 7.29-7.16 (m, 3H), 6.85-6.72 (m, 2H), 4.40-4.13 (m, 3H), 3.77-3.47 (m, 2H) ppm. Protons directly attached to nitrogen and oxygen were not detected due to exchange with CD₃OD.

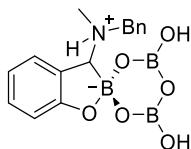
¹³C{¹H} NMR (75 MHz, CD₃OD): δ = 166.6, 133.2, 132.9, 132.1, 131.5 (2C), 131.3 (2C), 130.7(2C), 130.6, 130.4 (4C), 125.0, 119.2, 113.7, 57.3, 57.1 ppm. The carbon atom directly attached to boron was not detected, likely due to quadrupolar broadening.

¹¹B NMR (96 MHz, CD₃OD): δ = 18.4, 7.5 ppm.

HRMS (ESI neg) m/z : [$M-H$]⁻ Calcd for C₂₁H₂₁B₃NO₆⁻ 416.1654; found: 416.1668.

Elem. Anal. Calcd (%) for C₂₁H₂₂B₃NO₆: C 60.51, H 5.32, N 3.36; found: C 60.38, H 5.76, N 3.54.

3-(benzyl(methyl)ammonio)-4',6'-dihydroxy-3H-spiro[benzo[d][1,2]oxaborole-2,2'-[1,3,5,2,4,6]trioxatriborinan]-2-uide



3-4e was isolated as a white solid (111 mg, 65%), m.p. = 163 °C.

¹H NMR (300 MHz, D₂O) (mixture of diastereomers, *dr* = 55:45):

δ (major diastereomer) = 7.56–7.39 (m, 6H), 7.33 (dd, *J* = 8, 8 Hz, 1H), 6.96–6.87 (m, 1H), 6.82 (d, *J* = 8 Hz, 1H), 4.34 (d, *J* = 13 Hz, 1H), 4.18 (d, *J* = 13 Hz, 1H), 3.37 (s, 1H), 2.66 (s, 3H) ppm. Protons directly attached to nitrogen and oxygen were not detected due to exchange with D₂O.

δ (minor diastereomer) = 7.56–7.39 (m, 6H), 7.32 (dd, *J* = 8, 8 Hz, 1H), 6.96–6.87 (m, 1H), 6.82 (d, *J* = 8 Hz, 1H), 4.48 (d, *J* = 13 Hz, 1H), 3.60 (d, *J* = 13 Hz, 1H), 3.35 (s, 1H), 2.71 (s, 3H) ppm. Protons directly attached to nitrogen and oxygen were not detected due to exchange with D₂O.

¹³C{¹H} NMR (75 MHz, D₂O) (mixture of diastereomers, *dr* = 55:45):

δ (major diastereomer) = 162.8, 131.2, 131.0, 130.6 (2C), 130.0, 129.6, 129.1 (2C), 124.7, 118.7, 112.5, 59.6 (v br), 56.3, 37.5 ppm.

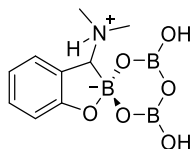
δ (minor diastereomer) = 162.9, 131.2, 131.0, 130.5 (2C), 130.0, 129.5, 129.0 (2C), 124.4, 118.6, 112.5, 59.6 (v br), 57.8, 38.6 ppm.

¹¹B NMR (96 MHz, D₂O) (mixture of diastereomers, *dr* = 55:45): δ = 19.4, 7.0 ppm.

HRMS (ESI neg) *m/z*: [*M*–H][–] Calcd for C₁₅H₁₇B₃NO₆[–] 340.1341; found: 340.1353.

Elem. Anal. Calcd (%) for C₁₅H₁₈B₃NO₆: C 52.87, H 5.32, N 4.11; found: C 52.84, H 5.33, N 4.12.

3-(dimethylammonio)-4',6'-dihydroxy-3H-spiro[benzo[d][1,2]oxaborole-2,2'-[1,3,5,2,4,6]trioxatriborinan]-2-uide



3-4f was isolated as a white solid (104 mg, 79%), m.p. = 410 °C.

¹H NMR (500 MHz, D₂O): δ = 7.43 (dd, J = 8, 1 Hz, 1H), 7.31 (ddd, J = 8, 8, 1 Hz, 1H), 6.89 (ddd, J = 8, 8, 1 Hz, 1H), 6.79 (dd, J = 8, 1 Hz, 1H), 3.21 (s, 1H), 2.83 (s, 3H), 2.67 (s, 3H) ppm. Protons directly attached to nitrogen and oxygen were not detected due to exchange with D₂O.

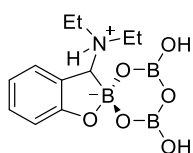
¹³C{¹H} NMR (126 MHz, D₂O): δ = 162.7, 130.9, 130.0, 124.5, 118.6, 112.4, 60.4 (v br), 41.9, 39.9 ppm.

¹¹B NMR (160 MHz, D₂O): δ = 19.5, 7.0 ppm.

HRMS (ESI neg) m/z : [$M-H$]⁻ Calcd for C₉H₁₃B₃NO₆⁻ 264.1028; found: 264.1038.

Elem. Anal. Calcd (%) for C₉H₁₄B₃NO₆: C 40.85, H 5.33, N 5.29; found: C 40.71, H 5.39, N 5.17.

3-(diethylammonio)-4',6'-dihydroxy-3H-spiro[benzo[d][1,2]oxaborole-2,2'-[1,3,5,2,4,6]trioxatriborinan]-2-uide



3-4g was isolated as a white solid (123 mg, 84%), m.p. = 230 °C.

¹H NMR (300 MHz, D₂O): δ = 7.39 (d, J = 8 Hz, 1H), 7.28 (ddd, J = 8, 8, 1 Hz, 1H), 6.87 (ddd, J = 8, 8, 1 Hz, 1H), 6.78 (d, J = 8 Hz, 1H), 3.45 (s, 1H), 3.39-2.98 (m, 3H), 2.97-2.80 (m, 1H), 1.34-1.25 (m, 6H) ppm. Protons directly attached to nitrogen and oxygen were not detected due to exchange with D₂O.

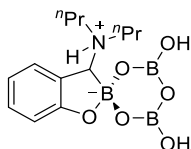
¹³C{¹H} NMR (75 MHz, D₂O): δ = 162.7, 130.6, 129.6, 124.8, 118.6, 112.3, 54.5 (v br), 46.9, 46.9, 10.1, 9.7 ppm.

¹¹B NMR (96 MHz, D₂O): δ = 19.4, 7.0 ppm.

HRMS (ESI neg) m/z : $[M-H]^-$ Calcd for $C_{11}H_{17}B_3NO_6^-$ 292.1341; found: 292.1352.

Elem. Anal. Calcd (%) for $C_{11}H_{18}B_3NO_6$: C 45.14, H 6.20, N 4.79; found: C 45.15, H 6.33, N 4.48.

3-(dipropylammonio)-4',6'-dihydroxy-3H-spiro[benzo[*d*][1,2]oxaborole-2,2'-[1,3,5,2,4,6]trioxatriborinan]-2-uide



3-4h was isolated as a white solid (115 mg, 72%), m.p. = 130 °C.

1H NMR (300 MHz, D_2O): δ = 7.39 (d, J = 8 Hz, 1H), 7.28 (dd, J = 8, 8 Hz, 1H), 6.86 (d, J = 8, 8 Hz, 1H), 6.78 (d, J = 8 Hz, 1H), 3.44 (s, 1H), 3.31-2.92 (m, 3H), 2.87-2.66 (m, 1H), 1.89-1.59 (m, 4H), 0.98-0.81 (m, 6H) ppm. Protons directly attached to nitrogen and oxygen were not detected due to exchange with D_2O .

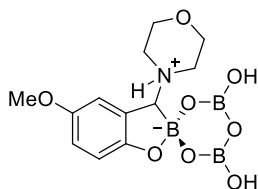
$^{13}C\{^1H\}$ NMR (75 MHz, D_2O): δ = 162.7, 130.7, 129.6, 124.9, 118.6, 112.3, 56.2 (v br), 54.2, 53.9, 18.6, 18.2, 10.2, 10.2 ppm.

^{11}B NMR (96 MHz, D_2O): δ = 19.4, 7.0 ppm.

HRMS (ESI neg) m/z : $[M-H]^-$ Calcd for $C_{13}H_{21}B_3NO_6^-$ 320.1654; found: 320.1658.

Elem. Anal. Calcd (%) for $C_{13}H_{22}B_3NO_6$: C 48.68, H 6.91, N 4.37; found: C 48.45, H 6.94, N 4.28.

4',6'-dihydroxy-6-methoxy-3-(morpholino-4-ium)-3H-spiro[benzo[*d*][1,2]oxaborole-2,2'-[1,3,5,2,4,6]trioxatriborinan]-2-uide



3-4i was isolated as a white solid (150 mg, 89%), m.p. = 262 °C.

1H NMR (300 MHz, D_2O): δ = 7.07 (d, J = 3 Hz, 1H), 6.95 (dd, J = 9, 3 Hz, 1H), 6.73 (d, J = 9 Hz, 1H), 4.08 (d, J = 14 Hz, 1H), 4.03 (d, J = 14 Hz, 1H), 3.81-3.79 (m, 5H), 3.50-3.31 (m, 3H), 3.18 (s, 1H), 3.16-3.03 (m, 1H) ppm. Protons directly attached to nitrogen and

oxygen were not detected due to exchange with D₂O.

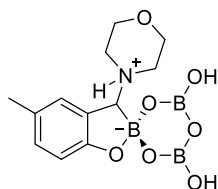
¹³C{¹H} NMR (75 MHz, D₂O): δ = 157.3, 151.4, 124.0, 116.9, 116.2, 112.5, 64.4, 64.2, 60.4 (v br), 56.3, 50.7, 48.9 ppm.

¹¹B NMR (96 MHz, D₂O): δ = 19.3, 6.9 ppm.

HRMS (ESI neg) *m/z*: [*M*-H]⁻ Calcd for C₁₂H₁₇B₃NO₈: 336.1239; found: 336.1240.

Elem. Anal. Calcd (%) for C₁₂H₁₈B₃NO₈: C 42.81, H 5.39, N 4.16; found: C 42.62, H 5.49., N 3.98.

4',6'-dihydroxy-5-methyl-3-(morpholino-4-ium)-3H-spiro[benzo[*d*][1,2]oxaborole-2,2'-[1,3,5,2,4,6]trioxatriborinan]-2-uide



3-4j was isolated as a white solid (135 mg, 84%), m.p. = 219 °C.

¹H NMR (500 MHz, D₂O): δ = 7.27 (s, 1H), 7.15 (d, *J* = 8 Hz, 1H), 6.71 (d, *J* = 8 Hz, 1H), 4.10 (d, *J* = 13 Hz, 1H), 4.04 (d, *J* = 13 Hz, 1H), 3.91-3.73 (m, 2H), 3.55-3.31 (m, 3H), 3.19 (s, 1H), 3.15-3.03 (m, 1H), 2.28 (s, 3H) ppm. Protons directly attached to nitrogen and oxygen were not detected due to exchange with D₂O.

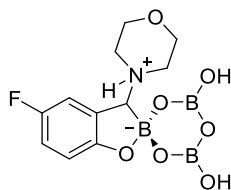
¹³C{¹H} NMR (126 MHz, D₂O): δ = 160.5, 131.3, 130.7, 128.2, 123.4, 112.1, 64.4, 64.2, 60.9 (v br), 50.9, 48.9, 19.7 ppm.

¹¹B NMR (160 MHz, D₂O): δ = 19.4, 6.9 ppm.

HRMS (APCI neg) *m/z*: [*M*-H]⁻ Calcd for C₁₂H₁₇B₃NO₇: 320.1290; found: 320.1271.

Elem. Anal. Calcd (%) for C₁₂H₁₈B₃NO₇: C 44.94, H 5.66, N 4.37; found: C 44.79, H 5.95., N 4.34.

5-fluoro-4',6'-dihydroxy-3-(morpholino-4-ium)-3H-spiro[benzo[d][1,2]oxaborole-2,2'-[1,3,5,2,4,6]trioxatriborinan]-2-uide



3-4k was isolated as a white solid (122 mg, 75%), m.p. = 295 °C.

¹H NMR (500 MHz, D₂O): δ = 7.20 (ddd, *J* = 9, 3, 1 Hz, 1H), 7.05 (ddd, *J* = 9, 9, 3 Hz, 1H), 6.73 (dd, *J* = 9, 5 Hz, 1H), 4.13-4.10 (m, 2H), 3.85–3.77 (m, 2H), 3.51–3.33 (m, 3H), 3.20 (s, 1H), 3.15 (ddd, *J* = 13, 13, 4 Hz, 1H) ppm. Protons directly attached to nitrogen and oxygen were not detected due to exchange with D₂O.

¹³C{¹H} NMR (126 MHz, D₂O): δ = 158.9 (d, *J* = 2 Hz), 155.5 (d, *J* = 234 Hz), 124.0 (d, *J* = 8 Hz), 117.2 (d, *J* = 24 Hz), 116.5 (d, *J* = 23 Hz), 112.5 (d, *J* = 9 Hz), 64.4, 64.1, 60.1 (v br), 50.7, 49.0.

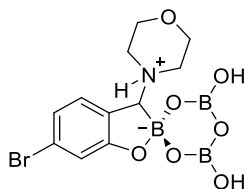
¹¹B NMR (160 MHz, D₂O): δ = 19.4, 7.1 ppm.

¹⁹F{¹H} NMR (471 MHz, D₂O): δ = -126.3 ppm.

HRMS (ESI neg) *m/z*: [*M*-H]⁻ Calcd for C₁₁H₁₄B₃FNO₇ 324.1039; found: 324.1038.

Elem. Anal. Calcd (%) for C₁₁H₁₅B₃FNO₇: C 40.69, H 4.66, N 4.31; found: C 40.58, H 4.67, N 4.30.

6-bromo-4',6'-dihydroxy-3-(morpholino-4-ium)-3H-spiro[benzo[d][1,2]oxaborole-2,2'-[1,3,5,2,4,6]trioxatriborinan]-2-uide



3-4l was isolated as a white solid (148 mg, 77%), m.p. = 272 °C.

¹H NMR (300 MHz, D₂O): δ = 7.57 (d, *J* = 2 Hz, 1H), 7.42 (dd, *J* = 9, 2 Hz, 1H), 6.70 (d, *J* = 9 Hz, 1H), 4.16-3.98 (m, 2H), 3.91-3.69 (m, 2H), 3.53-3.26 (m, 3H), 3.19 (s, 1H), 3.18-3.04 (m, 1H) ppm. Protons directly attached to nitrogen and oxygen were not detected due to exchange with D₂O.

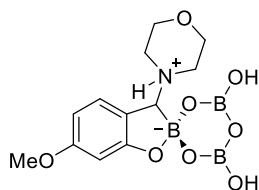
$^{13}\text{C}\{^1\text{H}\}$ NMR (126 MHz, D_2O): δ = 162.0, 133.6, 132.7, 125.7, 114.2, 109.3, 64.3, 64.1, 60.3 (v br), 50.8, 49.0 ppm.

^{11}B NMR (96 MHz, D_2O): δ = 19.4, 7.0 ppm.

HRMS (ESI neg) m/z : $[M-H]^-$ Calcd for $\text{C}_{11}\text{H}_{14}\text{B}_3\text{BrNO}_7^-$ 384.0238; found: 384.0245.

Elem. Anal. Calcd (%) for $\text{C}_{11}\text{H}_{15}\text{B}_3\text{BrNO}_7$: C 34.27, H 3.92, N 3.63; found: C 34.19, H 3.94., N 3.59.

4',6'-dihydroxy-6-methoxy-3-(morpholino-4-ium)-3H-spiro[benzo[d][1,2]oxaborole-2,2'-[1,3,5,2,4,6]trioxatriborinan]-2-uide



3-4m was isolated as a white solid (140 mg, 83%), m.p. = 260 °C.

^1H NMR (300 MHz, D_2O): δ = 7.33 (d, J = 8 Hz, 1H), 6.48 (dd, J = 8, 3 Hz, 1H), 6.39 (d, J = 3 Hz, 1H), 4.17-3.95 (m, 2H), 3.86-3.72 (m, 5H), 3.49-3.26 (m, 3H), 3.14 (s, 1H), 3.06 (ddd, J = 13, 13, 4 Hz, 1H) ppm. Protons directly attached to nitrogen and oxygen were not detected due to exchange with D_2O .

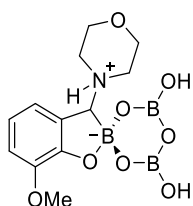
$^{13}\text{C}\{^1\text{H}\}$ NMR (126 MHz, D_2O): δ = 164.3, 161.5, 131.0, 116.2, 104.4, 98.2, 64.4, 64.2, 60.3 (v br), 55.3, 50.8, 48.7 ppm.

^{11}B NMR (160 MHz, D_2O): δ = 19.4, 7.2 ppm.

HRMS (ESI neg) m/z : $[M-H]^-$ Calcd for $\text{C}_{12}\text{H}_{17}\text{B}_3\text{NO}_8^-$ 336.1239; found: 336.1234.

Elem. Anal. Calcd (%) for $\text{C}_{12}\text{H}_{18}\text{B}_3\text{NO}_8$: C 42.81, H 5.39, N 4.16; found: C 42.62, H 5.45., N 4.11.

4',6'-dihydroxy-7-methoxy-3-(morpholino-4-ium)-3H-spiro[benzo[d][1,2]oxaborole-2,2'-[1,3,5,2,4,6]trioxatriborinan]-2-uide



3-4n was isolated as a white solid (121 mg, 72%), m.p. = 273 °C.

¹H NMR (300 MHz, D₂O): δ = 7.06 (d, J = 8 Hz, 1H), 7.02 (d, J = 8 Hz, 1H), 6.83 (dd, J = 8, 8 Hz, 1H), 4.07 (d, J = 14 Hz, 1H), 4.02 (d, J = 15 Hz, 1H), 3.92-3.72 (m, 5H), 3.52-3.31 (m, 3H), 3.20 (s, 1H), 3.08 (ddd, J = 13, 13, 4 Hz, 1H) ppm. Protons directly attached to nitrogen and oxygen were not detected due to exchange with D₂O.

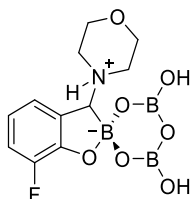
¹³C{¹H} NMR (75 MHz, D₂O): δ = 152.3, 145.9, 124.0, 122.6, 118.2, 113.6, 64.4, 64.1, 61.1 (v br), 55.7, 50.8, 48.9 ppm.

¹¹B NMR (96 MHz, D₂O): δ = 19.4, 7.1 ppm.

HRMS (ESI neg) m/z : [$M-H$]⁻ Calcd for C₁₂H₁₇B₃NO₈⁻ 336.1239; found: 336.1252.

Elem. Anal. Calcd (%) for C₁₂H₁₈B₃NO₈: C 42.81, H 5.39, N 4.16; found: C 42.71, H 5.36, N 4.09.

7-fluoro-4',6'-dihydroxy-3-(morpholino-4-ium)-3H-spiro[benzo[*d*][1,2]oxaborole-2,2'-[1,3,5,2,4,6]trioxatriborinan]-2-uide



3-4o was isolated as a white solid (133 mg, 82%), m.p. = 310 °C.

¹H NMR (500 MHz, D₂O): δ = 7.22 (d, J = 8 Hz, 1H), 7.14 (ddd, J = 11, 8, 1 Hz, 1H), 6.82 (ddd, J = 13, 8, 5 Hz, 1H), 4.12-4.00 (m, 2H), 3.86-3.75 (m, 2H), 3.50-3.35 (m, 3H), 3.24 (s, 1H), 3.12 (ddd, J = 12, 12, 4 Hz, 1H) ppm. Protons directly attached to nitrogen and oxygen were not detected due to exchange with D₂O.

¹³C{¹H} NMR (126 MHz, D₂O): δ = 150.0 (d, J = 11 Hz), 149.6 (d, J = 241 Hz), 126.5 (d, J = 5 Hz), 125.7 (d, J = 4 Hz), 118.2 (d, J = 6 Hz), 117.2 (d, J = 17 Hz), 64.4, 64.1, 60.2 (v br), 50.8, 49.0 ppm.

¹¹B NMR (160 MHz, D₂O): δ = 19.4, 7.4 ppm.

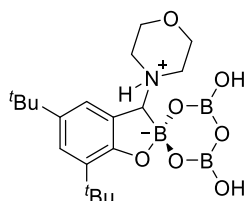
¹⁹F{¹H} NMR (471 MHz, D₂O): δ = -139.1 ppm.

HRMS (ESI neg) m/z : [$M-H$]⁻ Calcd for C₁₁H₁₄B₃FNO₇⁻ 324.1039; found: 324.1040.

Elem. Anal. Calcd (%) for C₁₁H₁₅B₃FNO₇: C 40.69, H 4.66, N 4.31; found: C 40.58, H 4.73,

N 4.32.

5,7-di-*tert*-butyl-4',6'-dihydroxy-3-(morpholino-4-ium)-3H-spiro[benzo[*d*][1,2]oxaborole-2,2'-[1,3,5,2,4,6]trioxatriborinan]-2-uide



3-4p was isolated as a white solid (142 mg, 68%), m.p. = 211 °C.

¹H NMR (300 MHz, CD₃OD): δ = 7.20-7.14 (m, 2H), 4.02-3.89 (m, 2H), 3.75-3.62 (m, 2H), 3.38-3.22 (m, 3H), 3.13 (s, 1H), 3.12-3.02 (m, 1H), 1.40 (s, 9H), 1.28 (s, 9H) ppm. Protons directly attached to nitrogen and oxygen were not detected due to exchange with CD₃OD.

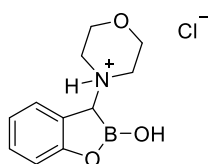
¹³C{¹H} NMR (75 MHz, CD₃OD): δ = 162.9, 140.0, 134.4, 125.0, 124.9, 124.2, 65.8, 65.6, 62.9 (v br), 52.5, 51.0, 35.4, 35.1, 32.4 (3C), 29.9 (3C) ppm.

¹¹B NMR (96 MHz, CD₃OD): δ = 18.5, 7.5 ppm.

HRMS (ESI neg) *m/z*: [*M*-H]⁻ Calcd for C₁₉H₃₁B₃NO₇ 418.2385; found: 418.2391.

Elem. Anal. Calcd (%) for C₁₉H₃₂B₃NO₇: C 54.48, H 7.70, N 3.34; found: C 54.33, H 7.69, N 3.31.

4-(2-hydroxy-2,3-dihydrobenzo[*d*][1,2]oxaborol-3-yl)morpholin-4-ium chloride



3-5a was isolated as a white solid (101 mg, 79%).

¹H NMR (300 MHz, D₂O): δ = 7.40 (d, *J* = 8 Hz, 1H), 7.33 (dd, *J* = 8, 8 Hz, 1H), 6.93 (dd, *J* = 8, 8 Hz, 1H), 6.86 (d, *J* = 8 Hz, 1H), 4.14-3.90 (m, 2H), 3.88-3.66 (m, 2H), 3.53 (s, 1H), 3.49-3.22 (m, 3H), 3.04 (dd, *J* = 13, 13 Hz, 1H) ppm. Protons directly attached to nitrogen and oxygen were not detected due to exchange with D₂O.

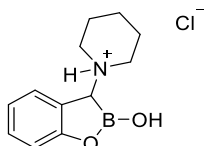
¹³C{¹H} NMR (75 MHz, D₂O): δ = 160.2, 131.5 (2C), 121.3, 119.7, 113.7, 64.0 (d, *J* = 10 Hz), 59.1 (v br), 51.3, 49.3 ppm.

¹¹B NMR (96 MHz, D₂O): δ = 14.3 ppm.

HRMS (ESI pos) m/z : $[M-Cl]^+$ Calcd for $C_{11}H_{15}BNO_3^+$ 220.1140; found: 220.1136.

Elem. Anal. Calcd (%) for $C_{11}H_{15}BCINO_3$: C 51.71, H 5.92, N 5.48; found: C 51.68, H 5.99, N 5.42.

1-(2-hydroxy-2,3-dihydrobenzo[d][1,2]oxaborol-3-yl)piperidin-1-ium chloride



3-5b was isolated as a white solid (95 mg, 75%).

1H NMR (300 MHz, CD_3OD): δ = 7.35 (dd, J = 8, 2 Hz, 1H), 7.23 (ddd, J = 8, 8, 2 Hz, 1H), 6.91-6.76 (m, 2H), 3.60 (s, 1H), 3.42 (d, J = 13 Hz, 1H), 3.38 (d, J = 13 Hz, 1H), 3.22-3.02 (m, 1H), 2.86-2.54 (m, 1H), 1.95-1.62 (m, 5H), 1.54-1.24 (m, 1H) ppm. Protons directly attached to nitrogen and oxygen were not detected due to exchange with CD_3OD .

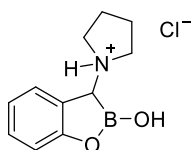
$^{13}C\{^1H\}$ NMR (75 MHz, CD_3OD): δ = 162.5, 132.2, 132.1, 122.4, 120.3, 114.9, 58.8 (v br), 54.3, 51.9, 24.7, 24.5, 23.0 ppm.

^{11}B NMR (96 MHz, CD_3OD): δ = 16.3 ppm.

HRMS (ESI pos) m/z : $[M-Cl]^+$ Calcd for $C_{12}H_{17}BNO_2^+$ 218.1347; found: 218.1342.

Elem. Anal. Calcd (%) for $C_{12}H_{17}BCINO_2$: C 56.85, H 6.76, N 5.52; found: C 56.68, H 6.88, N 5.37.

1-(2-hydroxy-2,3-dihydrobenzo[d][1,2]oxaborol-3-yl)pyrrolidin-1-ium chloride



3-5c was isolated as a white solid (99 mg, 83%).

1H NMR (300 MHz, CD_3OD): δ = 7.32 (ddd, J = 8, 2, 1 Hz, 1H), 7.23 (ddd, J = 8, 7, 2 Hz, 1H), 6.90-6.79 (m, 2H), 3.83 (s, 1H), 3.69 (ddd, J = 12, 8, 5 Hz, 1H), 3.29-3.16 (m, 2H), 3.01 (ddd, J = 11, 8, 8 Hz, 1H), 2.24-1.73 (m, 4H) ppm. Protons directly attached to nitrogen and oxygen were not detected due to exchange with CD_3OD .

$^{13}C\{^1H\}$ NMR (75 MHz, CD_3OD): δ = 161.3, 131.9, 131.9, 123.4, 120.4, 115.2, 55.4, 53.4,

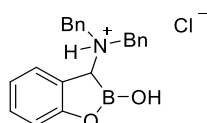
24.0 (2C) ppm. The carbon atom directly attached to boron was not detected, likely due to quadrupolar broadening.

^{11}B NMR (96 MHz, CD_3OD): $\delta = 18.5$ ppm.

HRMS (ESI pos) m/z : $[\text{M}-\text{Cl}]^+$ Calcd for $\text{C}_{11}\text{H}_{15}\text{BNO}_2^+$ 204.1190; found: 204.1187.

Elem. Anal. Calcd (%) for $\text{C}_{11}\text{H}_{15}\text{BCINO}_2$: C 55.16, H 6.31, N 5.85; found: C 54.97, H 6.29, N 5.73.

***N,N*-dibenzyl-2-hydroxy-2,3-dihydrobenzo[*d*][1,2]oxaborol-3-aminium chloride**



3-5d was isolated as a white solid (155 mg, 85%).

^1H NMR (300 MHz, CD_3OD): $\delta = 7.49\text{--}7.42$ (m, 6H), 7.39 (m, 3H), 7.23 (ddd, $J = 8, 8, 3$ Hz, 3H), 6.90–6.78 (m, 2H), 4.39 (d, $J = 13$ Hz, 1H), 4.35 (d, $J = 13$ Hz, 1H), 4.25 (d, $J = 13$ Hz, 1H), 3.77 (d, $J = 13$ Hz, 1H), 3.70 (s, 1H) ppm. Protons directly attached to nitrogen and oxygen were not detected due to exchange with CD_3OD .

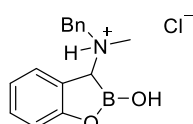
$^{13}\text{C}\{^1\text{H}\}$ NMR (75 MHz, CD_3OD): $\delta = 165.5, 132.9, 132.7, 132.3, 131.6$ (2C), 131.4 (2C), 131.1, 130.8, 130.6, 130.4 (4C), 124.2, 119.8, 114.1, 57.6, 57.2 ppm. The carbon atom directly attached to boron was not detected, likely due to quadrupolar broadening.

^{11}B NMR (96 MHz, CD_3OD): $\delta = 10.8$ ppm.

HRMS (ESI pos) m/z : $[\text{M}-\text{Cl}]^+$ Calcd for $\text{C}_{21}\text{H}_{21}\text{BNO}_2^+$ 330.1660; found: 330.1648.

Elem. Anal. Calcd (%) for $\text{C}_{21}\text{H}_{21}\text{BCINO}_2$: C 68.98, H 5.79, N 3.83; found: C 68.74, H 5.88, N 3.85.

***N*-benzyl-2-hydroxy-*N*-methyl-2,3-dihydrobenzo[*d*][1,2]oxaborol-3-aminium chloride**



3-5e was isolated as a white solid (104 mg, 72%).

^1H NMR (300 MHz, CD_3OD) (mixture of diastereomers, $dr = 55:45$):

δ (major diastereomer) = 7.51–7.36 (m, 6H), 7.34–7.20 (m, 1H), 6.94–6.81 (m, 2H), 4.44

(d, $J = 13$ Hz, 1H), 4.16 (d, $J = 13$ Hz, 1H), 3.71 (s, 1H), 2.70 (s, 3H) ppm. Protons directly attached to nitrogen and oxygen were not detected due to exchange with CD_3OD .

δ (minor diastereomer) = 7.51–7.36 (m, 6H), 7.34–7.20 (m, 1H), 6.94–6.81 (m, 2H), 4.61 (d, $J = 13$ Hz, 1H), 3.78 (s, 1H), 3.49 (d, $J = 13$ Hz, 1H), 2.59 (s, 3H) ppm. Protons directly attached to nitrogen and oxygen were not detected due to exchange with CD_3OD .

$^{13}\text{C}\{^1\text{H}\}$ NMR (75 MHz, CD_3OD) (mixture of diastereomers, $dr = 55:45$):

δ (major diastereomer) = 163.1, 132.6, 132.5, 131.8 (2C), 130.8, 130.3, 130.2 (2C), 122.2, 120.6, 114.9, 58.1, 53.6 (v br), 38.8 ppm.

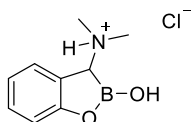
δ (minor diastereomer) = 163.1, 132.3, 132.3, 131.9 (2C), 130.9, 130.7, 130.2 (2C), 123.0, 120.4, 114.9, 60.6, 53.6 (v br), 39.9 ppm.

^{11}B NMR (96 MHz, CD_3OD) (mixture of diastereomers, $dr = 55:45$): $\delta = 15.7$ ppm.

HRMS (ESI pos) m/z : $[M-\text{Cl}]^+$ Calcd for $\text{C}_{15}\text{H}_{17}\text{BNO}_2^+$ 254.1347; found: 254.1346.

Elem. Anal. Calcd (%) for $\text{C}_{15}\text{H}_{17}\text{BCINO}_2$: C 62.22, H 5.92, N 4.84; found: C 62.01, H 5.68, N 4.81.

2-hydroxy-N,N-dimethyl-2,3-dihydrobenzo[*d*][1,2]oxaborol-3-aminium chloride



3-5f was isolated as a white solid (59 mg, 55%).

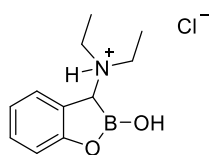
^1H NMR (300 MHz, CD_3OD): $\delta = 7.39$ – 7.32 (m, 1H), 7.31 – 7.22 (m, 1H), 6.91 – 6.81 (m, 2H), 3.67 (s, 1H), 2.85 (s, 3H), 2.65 (s, 3H) ppm. Protons directly attached to nitrogen and oxygen were not detected due to exchange with CD_3OD .

$^{13}\text{C}\{^1\text{H}\}$ NMR (75 MHz, CD_3OD): $\delta = 162.4$, 132.2, 132.1, 122.6, 120.3, 114.9, 59.3 (v br), 43.5, 41.4 ppm.

^{11}B NMR (96 MHz, CD_3OD): $\delta = 16.6$ ppm.

HRMS (ESI pos) m/z : $[M-\text{Cl}]^+$ Calcd for $\text{C}_9\text{H}_{13}\text{BNO}_2^+$ 178.1034; found: 178.1031.

Elem. Anal. Calcd (%) for $\text{C}_9\text{H}_{13}\text{BCINO}_2$: C 50.64, H 6.14, N 6.56; found: C 50.52, H 6.08, N 6.47.

***N,N*-diethyl-2-hydroxy-2,3-dihydrobenzo[*d*][1,2]oxaborol-3-aminium chloride**

3-5g was isolated as a white solid (91 mg, 75%).

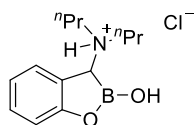
¹H NMR (300 MHz, CD₃OD): δ = 7.38–7.29 (m, 1H), 7.23 (ddd, 8, 8, 2 Hz, 1H), 6.87–6.82 (m, 2H), 3.83 (s, 1H), 3.28–3.05 (m, 3H), 2.76 (dq, J = 14, 7 Hz, 1H), 1.33 (t, J = 7 Hz, 3H), 1.25 (t, J = 7 Hz, 3H) ppm. Protons directly attached to nitrogen and oxygen were not detected due to exchange with CD₃OD.

¹³C{¹H} NMR (75 MHz, CD₃OD): δ = 162.5, 132.0, 131.5, 122.7, 120.4, 114.9, 54.0 (v br), 48.5, 47.5, 10.8, 9.8 ppm.

¹¹B NMR (96 MHz, CD₃OD): δ = 16.0 ppm.

HRMS (ESI pos) m/z : [M -Cl]⁺ Calcd for C₁₁H₁₇BNO₂⁺ 206.1347; found: 206.1344.

Elem. Anal. Calcd (%) for C₁₁H₁₇BCINO₂: C 54.70, H 7.10, N 5.80; found: C 54.55, H 7.23, N 5.78.

2-hydroxy-*N,N*-dipropyl-2,3-dihydrobenzo[*d*][1,2]oxaborol-3-aminium chloride

3-5h was isolated as a white solid (93 mg, 69%).

¹H NMR (300 MHz, CD₃OD): δ = 7.37–7.28 (m, 1H), 7.25 (ddd, J = 8, 8, 2 Hz, 1H), 6.87–6.82 (m, 2H), 3.83 (s, 1H), 3.20–2.92 (m, 3H), 2.77–2.51 (m, 1H), 1.96–1.50 (m, 4H), 0.98 (t, J = 7 Hz, 3H), 0.87 (t, J = 7 Hz, 3H) ppm. Protons directly attached to nitrogen and oxygen were not detected due to exchange with CD₃OD.

¹³C{¹H} NMR (75 MHz, CD₃OD): δ = 162.9, 132.2, 131.5, 122.8, 120.4, 114.8, 56.1, 54.9, 19.8, 18.8, 11.3, 11.3 ppm. The carbon atom directly attached to boron was not detected, likely due to quadrupolar broadening.

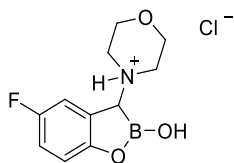
¹¹B NMR (96 MHz, CD₃OD): δ = 15.3 ppm.

HRMS (ESI pos) m/z : [M -Cl]⁺ Calcd for C₁₃H₂₁BNO₂⁺ 234.1660; found: 234.1656.

Elem. Anal. Calcd (%) for C₁₃H₂₁BCINO₂: C 57.92, H 7.85, N 5.20; found: C 57.85, H 7.81,

N 5.11.

4-(5-fluoro-2-hydroxy-2,3-dihydrobenzo[d][1,2]oxaborol-3-yl)morpholin-4-ium chloride



3-5i was isolated as a white solid (101 mg, 74%).

¹H NMR (300 MHz, CD₃OD): δ = 7.20 (dd, J = 9, 3 Hz, 1H), 7.02 (ddd, J = 9, 9, 3 Hz, 1H), 6.81 (dd, J = 9, 5 Hz, 1H), 4.06–3.93 (m, 2H), 3.84–3.69 (m, 2H), 3.67 (s, 1H), 3.48–3.33 (m, 2H), 3.27–3.22 (m, 1H), 3.16 (td, J = 12, 4 Hz, 1H) ppm. Protons directly attached to nitrogen and oxygen were not detected due to exchange with CD₃OD.

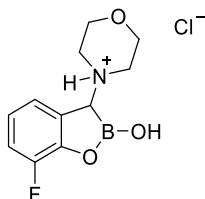
¹³C{¹H} NMR (75 MHz, CD₃OD): δ = 158.1, 155.9 (d, J = 236 Hz), 121.7 (d, J = 8 Hz), 117.2 (d, J = 23 Hz), 116.7 (d, J = 23 Hz), 113.8 (d, J = 8 Hz), 63.9, 63.8, 57.1 (v br), 51.3, 49.9 ppm.

¹¹B NMR (96 MHz, CD₃OD): δ = 14.8 ppm.

HRMS (ESI pos) m/z : [M -Cl]⁺ Calcd for C₁₁H₁₄BFNO₃⁺ 238.1045; found: 238.1041.

Elem. Anal. Calcd (%) for C₁₁H₁₄BCIFNO₃: C 48.31, H 5.16, N 5.12; found: C 48.22, H 5.29, N 5.07.

4-(7-fluoro-2-hydroxy-2,3-dihydrobenzo[d][1,2]oxaborol-3-yl)morpholin-4-ium chloride



3-5j was isolated as a white solid (111 mg, 81%).

¹H NMR (300 MHz, CD₃OD): δ = 7.19 (ddd, J = 8, 1, 1 Hz, 1H), 7.10 (ddd, J = 11, 8, 1 Hz, 1H), 6.81 (ddd, J = 8, 8, 5 Hz, 1H), 4.04–3.90 (m, 2H), 3.84–3.70 (m, 2H), 3.68 (s, 1H), 3.46–3.34 (m, 2H), 3.29–3.26 (m, 1H), 3.08 (ddd, J = 12, 12, 4 Hz, 1H) ppm. Protons directly attached to nitrogen and oxygen were not detected due to exchange with CD₃OD.

$^{13}\text{C}\{^1\text{H}\}$ NMR (75 MHz, CD_3OD): δ = 150.4 (d, J = 243 Hz), 149.4 (d, J = 12 Hz), 125.9 (d, J = 3 Hz), 124.1 (d, J = 4 Hz), 118.5 (d, J = 7 Hz), 117.1 (d, J = 18 Hz), 63.9, 63.8, 57.2 (v br), 51.5, 49.8 ppm.

^{11}B NMR (96 MHz, CD_3OD): δ = 14.6 ppm.

HRMS (ESI pos) m/z : $[\text{M}-\text{Cl}]^+$ Calcd for $\text{C}_{11}\text{H}_{14}\text{BFNO}_3^+$ 238.1045; found: 238.1041.

Elem. Anal. Calcd (%) for $\text{C}_{11}\text{H}_{14}\text{BCIFNO}_3$: C 48.31, H 5.16, N 5.12; found: C 48.12, H 5.25, N 5.26.

3.6.4 Single-crystal X-ray diffraction studies

Crystal structure determination Crystals suitable for single-crystal X-ray diffraction were selected, coated in perfluoropolyether oil, and mounted on MiTeGen sample holders. Diffraction data were collected on a BRUKER X8-APEX II diffractometer with a CCD area detector using Mo-K_α radiation monochromated by graphite (**3-4p**) or multi-layer mirror (**3-4a** and **3-4d**). The crystals were cooled using Oxford Cryostream low-temperature devices. Data were collected at 100 K. The images were processed and corrected for Lorentz-polarization effects and absorption as implemented in the Bruker software packages. The structures were solved using the intrinsic phasing method (SHELXT)⁹⁶ and Fourier expansion technique. All non-hydrogen atoms were refined in anisotropic approximation, with hydrogen atoms 'riding' in idealized positions, by full-matrix least squares against F^2 of all data, using SHELXL⁹⁷ software and the SHELXLE⁹⁸ graphical user interface. Diamond⁹⁹ software was used for graphical representation. Crystal data and experimental details are listed in Table 3-2; full structural information has been deposited with the Cambridge Crystallographic Data Centre. CCDC-1964346 (**3-4a**), 1964347 (**3-4d**), and 1964348 (**3-4p**).

Table 3-2 Single-crystal X-ray diffraction data and structure refinements of compounds **3-4a**, **3-4d**, and **3-4p**.

Data	3-4a	3-4d	3-4p
CCDC number	1964346	1964347	1964348
Empirical formula	C ₁₁ H ₁₆ B ₃ NO ₇	C ₂₁ H ₂₂ B ₃ NO ₆ · 2(C ₃ H ₆ O)	C ₁₉ H ₃₂ B ₃ NO ₇
Formula weight / g·mol ⁻¹	306.68	532.98	418.88
<i>T</i> / K	100(2)	100(2)	100(2)
λ / Å, radiation	0.71073, Mo-K α	0.71073, Mo-K α	0.71073, Mo-K α
Crystal size / mm ³	0.40×0.15×0.07	0.54 ×0.27×0.16	0.53 ×0.27×0.20
Crystal color, habit	colorless plate	colorless block	colorless plate
μ / mm ⁻¹	0.123	0.094	0.092
Crystal system	Monoclinic	Triclinic	Triclinic
Space group	<i>P</i> 2 ₁ / <i>c</i>	<i>P</i> $\bar{1}$	<i>P</i> $\bar{1}$
<i>a</i> / Å	8.430(6)	9.549(5)	11.314(7)
<i>b</i> / Å	17.184(13)	11.307(2)	11.980(8)
<i>c</i> / Å	9.073(7)	13.260(3)	17.961(10)
α / °	90	100.88(3)	72.586(9)
β / °	93.26(4)	92.261(11)	79.494(13)
γ / °	90	105.79(3)	72.755(19)
Volume / Å ³	1312.2(17)	1346.6(8)	2207(2)
<i>Z</i>	4	2	4
ρ_{calc} / g·cm ⁻³	1.552	1.314	1.261
<i>F</i> (000)	640	564	896
θ range / °	2.370–26.057	1.571–26.478	1.895–26.420
Reflections collected	10207	15073	40589
Unique reflections	2587	5534	9038
Parameters / restraints	203 / 0	399 / 162	557 / 1
GooF on <i>F</i> ²	1.032	1.048	1.016
R ₁ [<i>I</i> >2 σ (<i>I</i>)]	0.0472	0.0415	0.0718
wR ² (all data)	0.1188	0.1076	0.1569
Max. / min. residual electron density / e·Å ⁻³	0.321 / -0.220	0.295 / -0.266	0.426 / -0.291

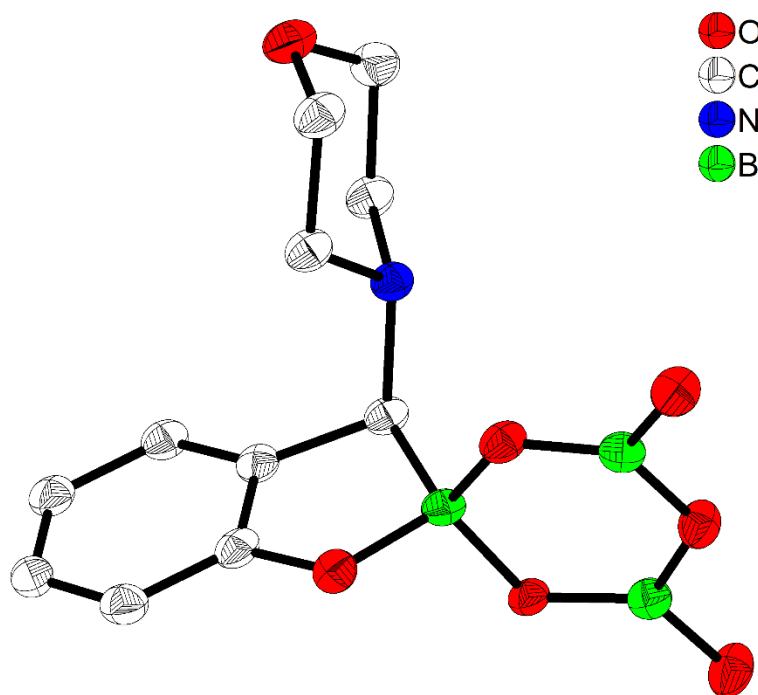


Figure 3-13 Molecular structure of **3-4a** in the solid state at 100 K. Atomic displacement ellipsoids are drawn at the 50% probability level, and H atoms are omitted for clarity.

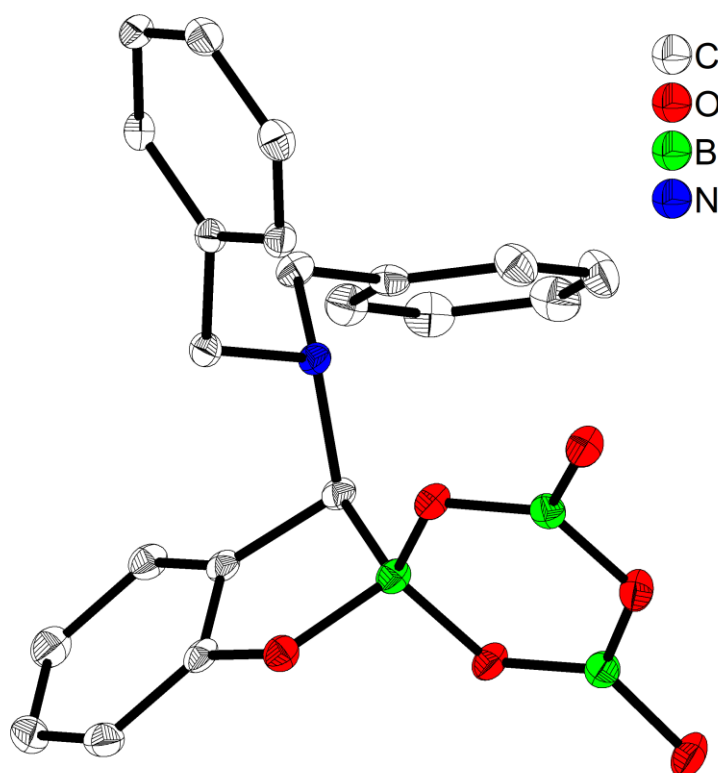


Figure 3-14 Molecular structure of **3-4d** in the solid state at 100 K. Atomic displacement ellipsoids are drawn at the 50% probability level. H atoms and solvent molecules are omitted for clarity.

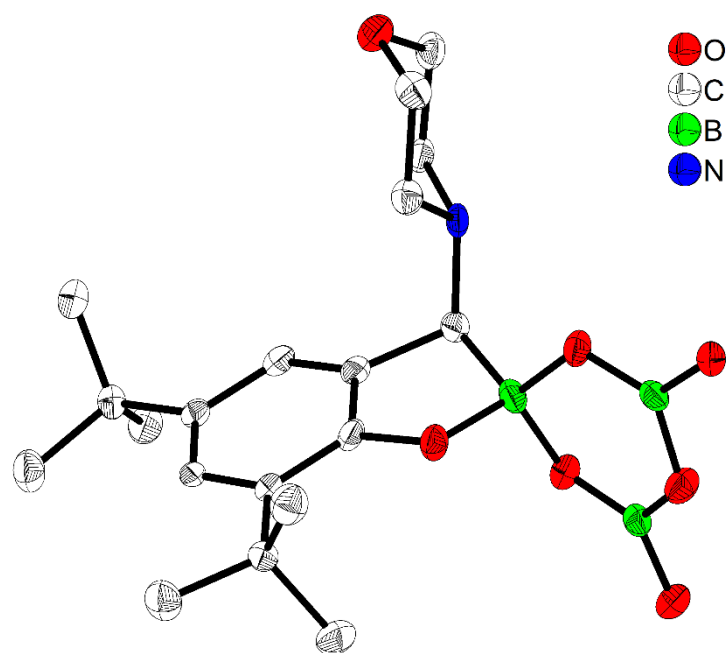


Figure 3-15 Molecular structure of **3-4p** in the solid state at 100 K. Atomic displacement ellipsoids are drawn at the 50% probability level, and H atoms are omitted for clarity. Only one of two independent molecules is shown here.

Chapter Four

PBP pincer palladium boryl complexes: synthesis, structures, and catalytic activity

4 PBP pincer palladium boryl complexes: synthesis, structures, and catalytic activity

4.1 Abstract

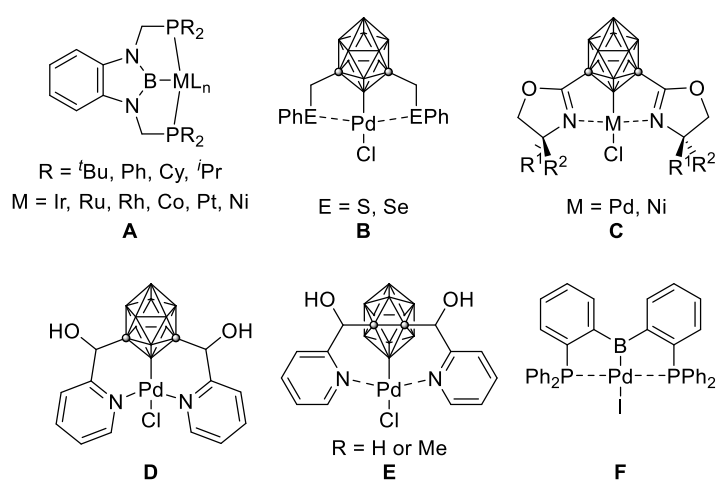
The diazaborole-based PBP pincer palladium chloride (**4-3**) and trifluoromethanesulfonate (**4-4**) complexes were synthesized and fully characterized by NMR spectrometry, HRMS, elemental analysis, and single-crystal X-ray diffraction. The Pd-Cl and Pd-O bond lengths in the compounds **4-3** and **4-4** are compared with their PNP (or NNN), PCP, and PSiP analogues. The Pd-Cl bond length of **4-3** is much longer than those in its PNP and PCP analogues, and is slightly shorter than in the PSiP complex. Compared with its NNN, PCP, and PSiP analogues, the Pd-O bond length in **4-4** is the longest, indicating the strong trans influence of the boryl moiety. Complex **4-3** catalyzed the Suzuki-Miyaura coupling of aryl iodides with phenylboronic acid.

4.2 Introduction

The first compound exhibiting an M-B σ -bond was reported in 1963 and was later classified as a metal boryl complex.¹¹² Since then, many metal boryl complexes have been reported.¹¹³ The first structurally characterized metal boryl complexes were reported in 1990 by Baker, Marder *et al.*¹¹⁴ and Merola *et al.*,¹¹⁵ and bis boryl $[(PPh_3)_2RhCl(Bcat)_2]$ ¹¹⁶ and tris boryl complexes $[(\eta^6\text{-arene})Ir(Bcat)_3]$ ¹¹⁷ were reported by Baker, Marder, Norman *et al.* The main applications of such organometallic species are in the field of catalysis, including transition metal-catalyzed hydroboration, diboration, C-H borylation, C-X (X= F, Cl, Br, and I) borylation, and others.^{93a,93b,113,118} In all of these reactions, the boryl moieties are “reactive” ligands, that is, borylation of the organic substrates occurs during the reaction.

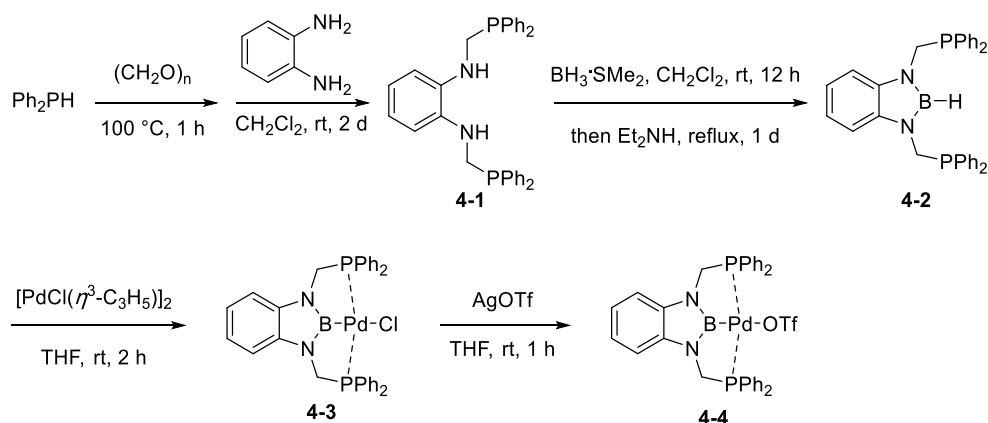
In 2009, Yamashita, Nozaki *et al.* synthesized diazaborole-based PBP pincer iridium complexes, in which the boryl group acted as a “supporting” ligand.¹¹⁹ At the same time, the Mirkin group reported the preparation of SeBSe and SBS Pd(II) complexes involving

carborane-based pincer ligands.¹²⁰ In the following years, more examples of pincer-type transition metal-boryl complexes were reported,¹²¹ and used as catalysts.¹²² Considering the strong electron-donating ability of the electropositive element boron, the electron density at metal center is enhanced significantly, which makes the oxidative addition process easier, and boryl ligands have an especially large trans influence.^{93b,123} Taking advantage of this, boryl pincer complexes have been applied in various types of catalytic reactions, including hydrosilylation of alkenes^{122c} and carbon dioxide,^{122j} dehydrogenation of alkanes^{122h,122i} and dimethylamine-borane,^{122k} C-H borylation,^{122l} etc.



Scheme 4-1 Previously reported transition metal boryl and carboranyl pincer complexes.

Herein, the synthesis of the first diazaborole-based PBP pincer palladium complexes were achieved. Their crystal and molecular structures were obtained. In addition, the PBP palladium chloride complex was used as a catalyst for Suzuki-Miyaura cross-coupling reactions.



Scheme 4-2 Synthesis of PBP pincer palladium(II) chloride (**4-3**) and trifluoromethanesulfonate (**4-4**).

4.3 Results and discussion

The known 1,3,2-benzodiazaborole¹²⁴ **4-2** was synthesized from diphenylphosphine, paraformaldehyde, *o*-phenylenediamine, and BH₃·SMe₂.^{121a} Treating **4-2** with [PdCl(η³-C₃H₅)₂] gave the diazaborole-based PBP pincer palladium chloride **4-3** in quantitative yield. The PBP pincer palladium trifluoromethanesulfonate **4-4** was then synthesized by treatment of **4-3** with AgOTf. Both **4-3** and **4-4** were characterized by NMR spectrometry, HRMS, and single-crystal X-ray diffraction studies.

The ³¹P{¹H} NMR spectrum of free ligand **4-2** shows a sharp singlet at δ = -22.3 ppm, whereas those of **4-3** and **4-4** show sharp singlets at δ = 42.1 and at δ = 42.4 ppm, respectively. The ¹¹B{¹H} NMR spectra of **4-3** and **4-4** show singlets at δ = 38.7 and at δ = 35.8 ppm, respectively. The ¹H NMR spectrum of **3** displays a virtual triplet at δ = 4.62 ppm with a coupling constant of *J* = 3 Hz, which is attributable to the methylene group attached to P. The signal assigned to the methylene unit appears as a virtual triplet at δ = 49.1 ppm with a coupling constant of *J* = 20 Hz in the ¹³C{¹H} NMR spectrum of **4-3**. The ¹H NMR and ¹³C{¹H} NMR spectra of **4-4** are similar with those of **4-3**, and the virtual triplets appear at 4.57 and 49.1 ppm, respectively.

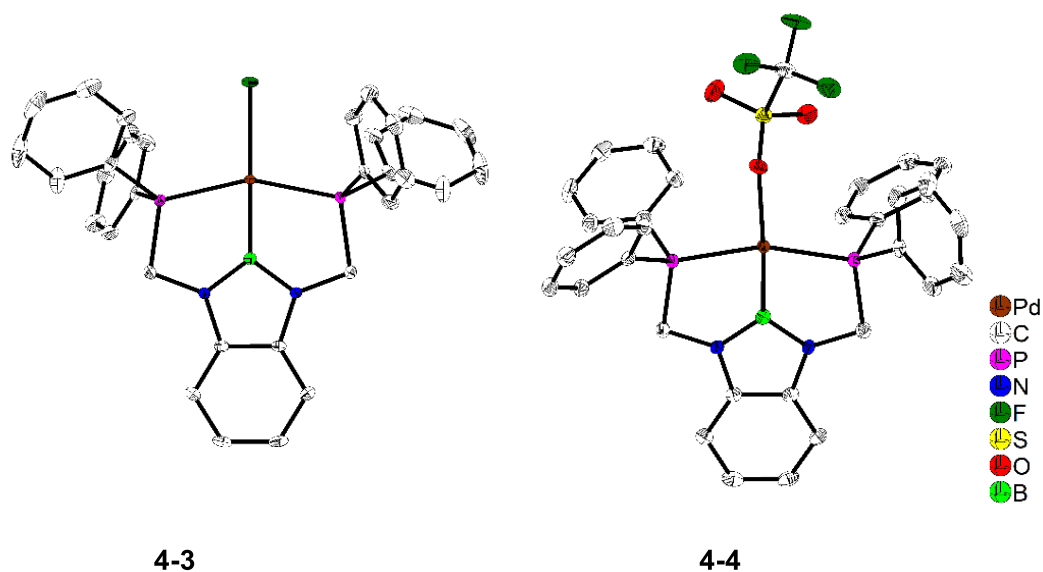
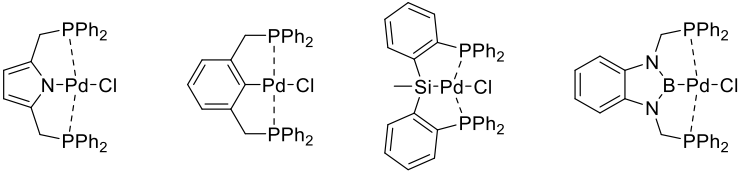
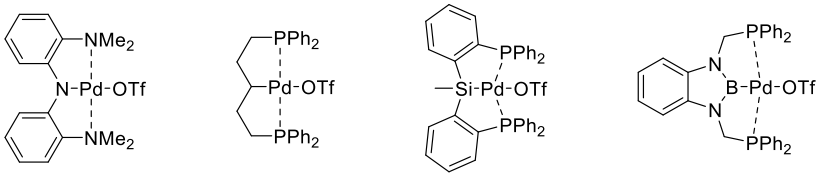


Figure 4-1 Molecular structures of **4-3** (left) and **4-4** (right) in the solid state at 100 K. Atomic displacement ellipsoids are drawn at the 50% probability level, and H atoms are omitted for clarity. Selected bond lengths [\AA] and angles [$^\circ$]: Complex **4-3**: Pd1-B1 1.978(3), Pd1-P1 2.2974(12), Pd1-Cl1 2.4283(10), P1-C4 1.864(2), P1-C5 1.812(2), P1-C11 1.820(2), P1-Pd1-P1' 155.57(3), B1-Pd1-Cl1 180.0; Complex **4-4**: Pd1-B1 1.968(3), Pd1-O1 2.2870(19), Pd1-P1 2.3208(8), Pd1-P2 2.3160(8), P1-C1 1.867(3), P1-C15 1.808(3), P1-C9 1.818(3), P2-C2 1.865(3), P2-C27 1.819(3), P2-C21 1.821(3), B1-Pd1-O1 175.64(11), P1-Pd1-P2 155.16(3).

Complexes **4-3** and **4-4** were additionally characterized by single-crystal X-ray diffraction (Figure 4-1). The solid-state structures of **4-3** and **4-4** are very similar and exhibit slightly distorted square-planar geometries around the Pd^{II} centers. The B-Pd-Cl angle in **4-3** is exactly 180° by symmetry, and the B-Pd-O angle in **4-4** is $175.64(11)^\circ$. The Pd-Cl bond length of **4-3** is $2.4283(10) \text{ \AA}$, which is much longer than those in its PNP and PCP analogues,¹²⁵ and is slightly shorter than in the PSiP complex¹²⁶ (Table 4-1). Compared with its NNN, PCP, and PSiP analogues, the Pd-O bond length in **4-4** is the longest with $2.2870(19) \text{ \AA}$ (Table 4-2).¹²⁷ All of these data underline the exceptionally strong trans influence of boron.^{123a,123c-h}

Table 4-1 Comparison of Pd-Cl Bond Lengths in Different Pd Pincer Complexes


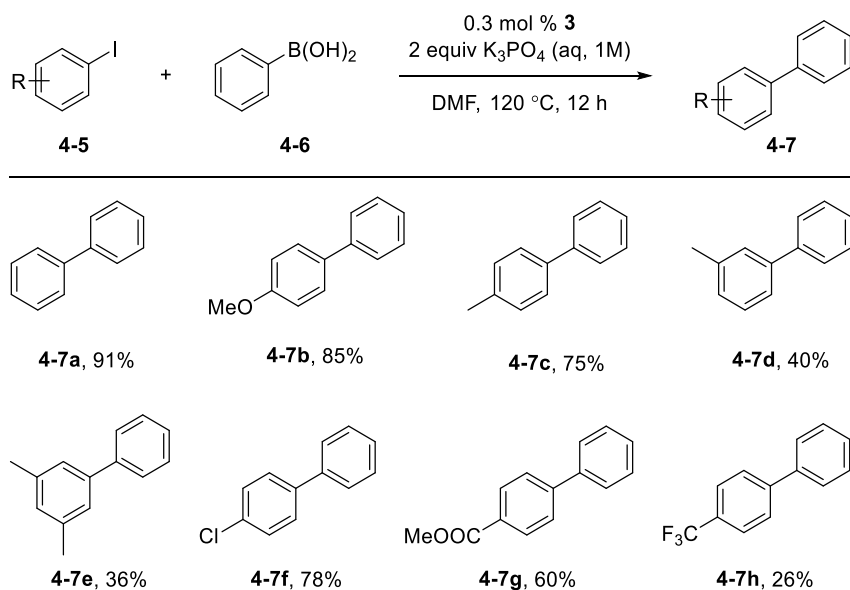
	PNP-Pd-Cl ^{125a}	PCP-Pd-Cl ^{125b}	PSiP-Pd-Cl ¹²⁶	PBP-Pd-Cl
Pd-Cl bond length (Å)	2.3136(16)	2.368(3)	2.4414(17)	2.4283(10)
X-Pd-Cl angle (°) (X = N, C, Si, B)	176.82(14)	178.8(3)	169.01(6)	180.0

Table 4-2 Comparison of Pd-O Bond Lengths in Different Pd Pincer Complexes


	NNN-Pd-OTf ^{127a}	PCP-Pd-OTf ^{127b}	PSiP-Pd-OTf ^{127c}	PBP-Pd-OTf
Bond length of Pd-O (Å)	2.1067(16)	2.2106(18)	2.260(2)	2.2870(19)
Angle of X-Pd-O (°) (X = N, C, Si, B)	174.64(7)	171.66(9)	177.86(6)	175.64(11)

4.4 Catalytic activity test

The Suzuki-Miyaura cross-coupling reaction is one of the most important C-C bond formation reactions, and is an indispensable tool in organic synthesis for the construction of symmetric and unsymmetric biaryl compounds.¹²⁸ Compound **4-3** was thus employed as a catalyst for Suzuki-Miyaura cross-coupling reactions of iodoarenes and phenylboronic acid to synthesize biaryls (Scheme 4-3).¹²⁹



Scheme 4-3 Suzuki-Miyaura cross-coupling reactions using **4-3** as a catalyst.

4.5 Summary

In summary, the first pincer-type palladium boryl complexes based on 1,3,2-diazaborole as the backbone was synthesized and fully characterized. The long Pd-Cl and Pd-O bond lengths indicate the exceptionally strong trans influence of the boryl moiety. The PBP pincer palladium chloride complex has been successfully employed as catalyst in Suzuki-Miyaura cross-coupling reactions of iodoarenes with phenylboronic acid.

4.6 Experimental procedures and characterization data

4.6.1 General information

All reagents were purchased from Alfa-Aesar, Aldrich, ABCR or VWR, and were checked for purity by GC-MS and/or 1H NMR spectroscopy and used as received. HPLC grade solvents were argon saturated, dried using an Innovative Technology Inc. Solvent Purification System, and further deoxygenated by using the freeze-pump-thaw method. $CDCl_3$, CD_2Cl_2 , and C_6D_6 were purchased from Cambridge Isotope Laboratories. All manipulations were performed in an argon-filled glove box unless otherwise stated.

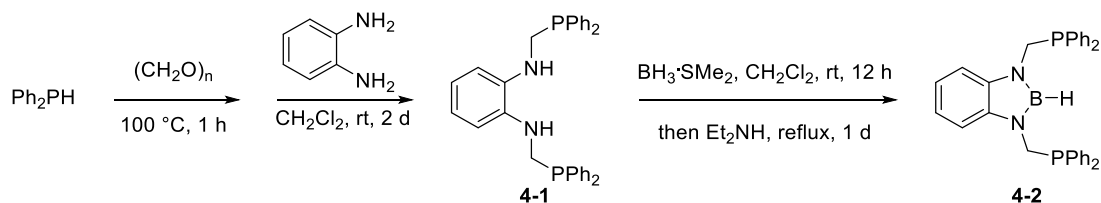
Automated flash chromatography was performed using a Biotage[®] Isolera Four system on

silica gel. Commercially available, precoated TLC plates (Polygram® Sil G/UV254) were purchased from Macherey-Nagel. The removal of solvent was performed on a rotary evaporator *in vacuo* at a maximum temperature of 40 °C.

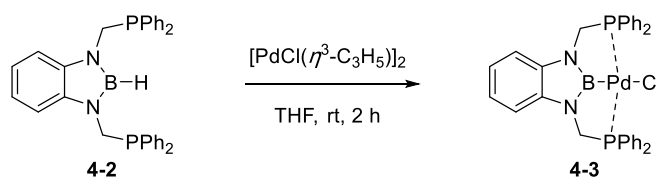
GC-MS analyses were performed using an Agilent 7890A gas chromatograph (column: HP-5MS 5% phenyl methyl siloxane, 30 m, ϕ 0.25 mm, film 0.25 μ m; injector: 250 °C; oven: 80 °C (2 min), 80 °C to 180 °C (20 °C min⁻¹), 180 °C to 280 °C (50 °C min⁻¹), 280 °C (5 min); carrier gas: He (1.2 mL min⁻¹)) equipped with an Agilent 5975C inert MSD with triple-axis detector operating in EI mode and an Agilent 7693A series auto sampler/injector. Elemental analyses were performed on a Elementar vario MICRO cube Elemental Analyzer. High-resolution mass spectra were recorded using a Thermo Fischer Scientific Exactive Plus Orbitrap MS system (ASAP and LIFDI probe).

NMR spectra were recorded at ambient temperature using Bruker Avance III HD 300 NMR (¹H, 300 MHz; ¹³C{¹H}, 75 MHz; ¹¹B, 96 MHz), or Bruker Avance III HD 500 NMR (¹H, 500 MHz; ¹³C{¹H}, 126 MHz; ¹¹B, 160 MHz; ¹⁹F, 471 MHz) spectrometers. ¹H NMR chemical shifts are reported relative to TMS and were referenced *via* residual proton resonance of the corresponding deuterated solvent (C₆D₆, 7.16 ppm; CD₂Cl₂, 5.32 ppm; CDCl₃, 7.26 ppm), whereas ¹³C{¹H} NMR spectra are reported relative to TMS *via* the carbon signal of the deuterated solvent (C₆D₆, 128.06 ppm; CD₂Cl₂, 53.84 ppm; CDCl₃, 77.00 ppm). ¹¹B NMR chemical shifts are quoted relative to BF₃·Et₂O as the external standard. ¹⁹F NMR chemical shifts are quoted relative to CFC₃ as the external standard. The following abbreviations are used in reporting NMR data: s = singlet; d = doublet; t = triplet, vt = virtual triplet; q = quartet; m = multiplet.

4.6.2 Experimental procedures

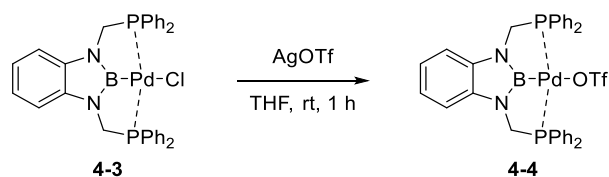
Synthesis of ligand **4-2** according to the literature procedure.^{121a}

A suspension of Ph_2PH (931 mg, 5.0 mmol, 1.0 equiv) and paraformaldehyde (150 mg, 5.0 mmol, 1.0 equiv) was stirred for 1 h at 100 °C. A solution of *o*-phenylenediamine (270 mg, 2.5 mmol, 0.25 equiv) in CH_2Cl_2 (5 mL) was added to the suspension and the resulting solution was stirred for 1 d at room temperature. The solution was filtered through a short silica column eluting with 10 mL of THF, and then the volatiles were removed under vacuum to afford **4-1** as a colorless oil. The oil was diluted with 5 mL of CH_2Cl_2 , and a solution of $\text{BH}_3\cdot\text{SMe}_2$ (1 M in CH_2Cl_2 , 17.5 mL, 3.5 equiv) was added, and the resulting solution was stirred for 12 h at room temperature. The solvent was then removed under vacuum, and THF (10 mL) and Et_2NH (5 mL) were added to the residue. The resulting solution was stirred for 12 h at reflux. The volatiles were removed under vacuum, and the resulting suspension was filtered through a silica gel column eluting with toluene (300 mL). An analytically pure sample of **4-2** was obtained by recrystallization from hexane (1.338 g, 52%). Spectroscopic data for **4-2** match those previously reported.^{121a}

Synthesis of ^{Ph}*PBP*-pincer palladium chloride complex **4-3**.

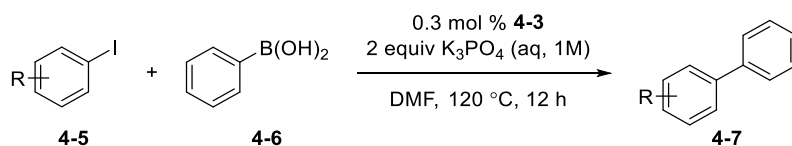
To a stirred solution of borane **4-2** (434 mg, 1.0 mmol, 1.0 equiv) in THF (10 mL) was added $[\text{PdCl}(\eta^3\text{-C}_3\text{H}_5)_2]$ (183 mg, 0.5 mmol, 0.5 equiv). The reaction was stirred at room temperature for 2 h to afford a grey suspension. The suspension was filtered, and the precipitate was washed with THF (20 mL). Removal of the solvent from the filtrate under vacuum gave **4-3** as a grey solid (642 mg, 98%). Single crystals were obtained from a concentrated CH_3CN solution of **4-3**.

Synthesis of ^{Ph}PBP-pincer palladium trifluoromethanesulfonate complex 4-4.



To a stirred solution of **4-3** (655 mg, 1.0 mmol, 1.0 equiv) in THF (5 mL) was added AgOTf (260 mg, 1.01 mmol, 1.01 equiv) at room temperature. After 1 h, the mixture was filtered through a short pad of Celite and the solvent was removed from the filtrate under vacuum. The solid obtained was purified by recrystallization from THF/pentane to give **4-4** as a red solid (715 mg, 93%).

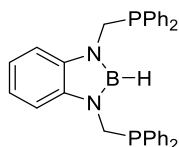
General procedure for Suzuki-Miyaura cross-coupling reaction using 4-3 as catalyst.



In a argon-filled glove box, a tube (20 mL) containing ^{Ph}PBP-PdCl **4-3** (1 mg, 0.0015 mmol, 0.3 mol %), aryl iodide **4-5** (0.5 mmol), phenylboronic acid **4-6** (92 mg, 0.75 mmol, 1.5 equiv), and dry DMF (400 μ L) was capped with a septum. Degassed aqueous K₃PO₄ (1 mL, 1 M, 1.0 mmol) was added *via* syringe, and the mixture was stirred at 120 °C for 12 h. The mixture was filtered through a pad of Celite and eluted with Et₂O (10 mL). The filtrate was concentrated under vacuum, and the residue was purified by flash column chromatography using hexane as eluent to afford the products.

4.6.3 Compound characterization

1,3-bis((diphenylphosphaneyl)methyl)-2,3-dihydro-1H-benzo[*d*][1,3,2]diazaborole



4-2, white solid, 52%. Its spectroscopic data are consistent with a literature report.^{121a}

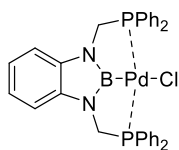
¹H NMR (300 MHz, C₆D₆) δ = 7.36–7.26 (m, 8H), 7.23 (dd, *J* = 6, 3 Hz, 2H), 7.13 (dd, *J* = 6, 3 Hz, 2H), 7.07–6.99 (m, 12H), 4.20 (d, *J* = 5 Hz, 4H) ppm. The proton directly attached to boron was not detected, likely due to quadrupolar broadening.

¹¹B{¹H} NMR (96 MHz, C₆D₆) δ = 26.0 ppm.

³¹P{¹H} NMR (122 MHz, C₆D₆) δ = -22.3 ppm.

HRMS (ASAP pos): calc. for [M+H]⁺ C₃₂H₃₀BN₂P₂⁺ 515.1972; found: 515.1967.

(1,3-bis((diphenylphosphaneyl)methyl)-1,3-dihydro-2H-benzo[*d*][1,3,2]diazaborol-2-yl)palladium(II) chloride



4-3, gray solid, 98%.

¹H NMR (500 MHz, CD₂Cl₂) δ = 7.99–7.93 (m, 8H), 7.52–7.44 (m, 12H), 7.05–7.02 (m, 2H), 7.02–6.97 (m, 2H), 4.62 (vt, *J* = 3 Hz, 4H) ppm.

¹³C{¹H} NMR (126 MHz, CD₂Cl₂) δ = 138.5 (vt, *J* = 11 Hz), 133.8 (vt, *J* = 7 Hz), 132.7 (vt, *J* = 20 Hz), 131.5, 129.6 (vt, *J* = 5 Hz), 119.8, 110.1, 49.1 (vt, *J* = 20 Hz) ppm.

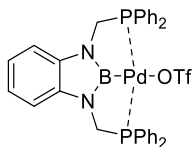
¹¹B{¹H} NMR (160 MHz, CD₂Cl₂) δ = 38.7 ppm.

³¹P{¹H} NMR (202 MHz, CD₂Cl₂) δ = 42.1 ppm.

HRMS (LIFDI): calc. for [M]⁺ C₃₂H₂₈BClN₂P₂Pd⁺ 654.0539; found: 654.0530.

Elem. Anal. Calc. (%) for C₃₂H₂₈BClN₂P₂Pd: C, 58.66; H, 4.31; N, 4.28; found: C, 58.98; H, 4.32; N, 4.29.

(1,3-bis((diphenylphosphaneyl)methyl)-1,3-dihydro-2H-benzo[d][1,3,2]diazaborol-2-yl)((trifluoromethyl)sulfonyl)oxy)palladium



4-4, red solid, 93%.

¹H NMR (500 MHz, CD₂Cl₂) δ = 7.86–7.76 (m, 8H), 7.58–7.44 (m, 12H), 7.08–6.96 (m, 4H), 4.57 (vt, J = 3, Hz, 4H) ppm.

¹³C{¹H} NMR (126 MHz, CD₂Cl₂) δ = 138.2 (vt, J = 11 Hz), 133.8 (vt, J = 7 Hz), 131.9, 131.3 (vt, J = 21 Hz), 129.6 (vt, J = 5 Hz), 120.2, 110.2, 49.1 (vt, J = 20 Hz) ppm.

¹¹B{¹H} NMR (160 MHz, CD₂Cl₂) δ = 35.8 ppm.

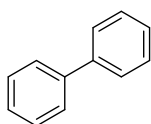
¹⁹F NMR (471 MHz, CD₂Cl₂) δ = -78.2 ppm.

³¹P{¹H} NMR (202 MHz, CD₂Cl₂) δ = 42.4 ppm.

HRMS (LIFDI): calc. for [M]⁺ C₃₃H₂₈BF₃N₂O₃P₂PdS⁺ 768.0370; found: 768.0361.

Elem. Anal. Calc. (%) for C₃₃H₂₈BF₃N₂O₃P₂PdS: C, 51.55; H, 3.67; N, 3.64; S, 4.17; found: C, 51.39; H, 3.71; N, 3.44; S, 4.38.

1,1'-biphenyl

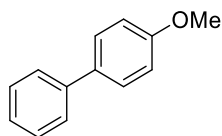


4-7a, white solid, 91%. m.p. 70.0 °C. Its spectroscopic data are consistent with a literature report.¹³⁰

¹H NMR (300 MHz, CDCl₃) δ = 7.65–7.57 (m, 4H), 7.46 (ddd, J = 8, 7, 1 Hz, 4H), 7.40–7.32 (m, 2H) ppm.

¹³C{¹H} NMR (126 MHz, CD₂Cl₂) δ = 141.4, 128.9, 127.4, 127.3 ppm.

HRMS (ASAP pos): calc. for [M+H]⁺ C₁₂H₁₁⁺ 155.0855; found: 155.0850.

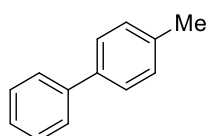
4-methoxy-1,1'-biphenyl

4-7b, white solid, 85%. m.p. 90.5 °C. Its spectroscopic data are consistent with a literature report.¹³⁰

¹H NMR (300 MHz, CDCl₃) δ = 7.64–7.51 (m, 4H), 7.49–7.40 (m, 2H), 7.38–7.29 (m, 1H), 7.06–6.97 (m, 2H), 3.87 (s, 3H) ppm.

¹³C{¹H} NMR (126 MHz, CD₂Cl₂) δ = 159.1, 140.8, 133.7, 128.7, 128.1, 126.7, 126.6, 114.2, 55.3 ppm.

HRMS (ASAP pos): calc. for [M+H]⁺ C₁₃H₁₃O⁺ 185.0961; found: 185.0957.

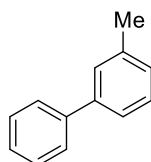
4-methyl-1,1'-biphenyl

4-7c, white solid, 75%. m.p. 73.2 °C. Its spectroscopic data are consistent with a literature report.¹³⁰

¹H NMR (300 MHz, CDCl₃) δ = 7.62–7.56 (m, 2H), 7.54–7.48 (m, 2H), 7.47–7.38 (m, 2H), 7.38–7.29 (m, 1H), 7.28–7.23 (m, 2H), 2.41 (s, 3H) ppm.

¹³C{¹H} NMR (126 MHz, CD₂Cl₂) δ = 141.3, 138.5, 137.2, 129.6, 128.8, 127.1, 127.1, 127.1, 21.2 ppm.

HRMS (ASAP pos): calc. for [M+H]⁺ C₁₃H₁₃⁺ 169.1012; found: 169.1008.

3-methyl-1,1'-biphenyl

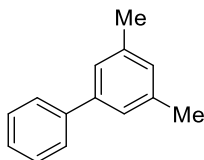
4-7d, colorless liquid, 40%. Its spectroscopic data are consistent with a literature report.¹³¹

¹H NMR (300 MHz, CDCl₃) δ = 7.65–7.57 (m, 2H), 7.52–7.39 (m, 4H), 7.38–7.30 (m, 2H), 7.25–7.14 (m, 1H), 2.44 (s, 3H) ppm.

$^{13}\text{C}\{^1\text{H}\}$ NMR (126 MHz, CD_2Cl_2) δ = 141.5, 141.4, 138.5, 128.8, 128.8, 128.1, 128.1, 127.3, 127.3, 124.4, 21.7 ppm.

HRMS (ASAP): calc. for $[\text{M}+\text{H}]^+$ $\text{C}_{13}\text{H}_{13}^+$ 169.1012; found: 169.1008.

3,5-dimethyl-1,1'-biphenyl



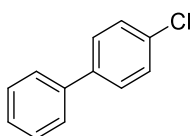
4-7e, colorless liquid, 36%. Its spectroscopic data are consistent with a literature report.¹³¹

^1H NMR (300 MHz, CDCl_3) δ = 7.62–7.55 (m, 2H), 7.47–7.39 (m, 2H), 7.37–7.30 (m, 1H), 7.23 (dt, J = 2, 1 Hz, 2H), 7.03–6.98 (m, 1H), 2.40 (s, 6H) ppm.

$^{13}\text{C}\{^1\text{H}\}$ NMR (126 MHz, CD_2Cl_2) δ = 141.6, 141.4, 138.4, 129.0, 128.8, 127.3, 127.2, 125.2, 21.6 ppm.

HRMS (ASAP pos): calc. for $[\text{M}+\text{H}]^+$ $\text{C}_{14}\text{H}_{15}^+$ 183.1168; found: 183.1164.

4-chloro-1,1'-biphenyl

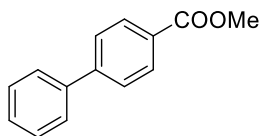


4-7f, white solid, 78%. m.p. 72.8 °C. Its spectroscopic data are consistent with a literature report.¹³⁰

^1H NMR (300 MHz, CDCl_3) δ = 7.60–7.50 (m, 4H), 7.49–7.32 (m, 5H) ppm.

$^{13}\text{C}\{^1\text{H}\}$ NMR (126 MHz, CD_2Cl_2) δ = 140.1, 139.8, 133.5, 129.0, 129.0, 128.5, 127.7, 127.1 ppm.

HRMS (ASAP pos): calc. for $[\text{M}+\text{H}]^+$ $\text{C}_{12}\text{H}_{10}\text{Cl}^+$ 189.0466; found: 189.0461.

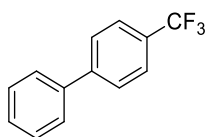
methyl [1,1'-biphenyl]-4-carboxylate

4-7g, white solid, 60%. m.p. 117.4 °C. Its spectroscopic data are consistent with a literature report.¹³²

¹H NMR (300 MHz, CDCl₃) δ = 8.11 (d, J = 9 Hz, 2H), 7.72–7.59 (m, 3H), 7.55–7.35 (m, 2H), 3.95 (s, 3H) ppm.

¹³C{¹H} NMR (126 MHz, CD₂Cl₂) δ = 167.0, 145.6, 140.0, 130.1, 128.9, 128.9, 128.1, 127.2, 127.0, 52.1 ppm.

HRMS (ASAP pos): calc. for [M+H]⁺ C₁₄H₁₃O₂⁺ 213.0910; found: 213.0906.

4-(trifluoromethyl)-1,1'-biphenyl

4-7h, white solid, 26%. m.p. 69.4 °C. Its spectroscopic data are consistent with a literature report.¹³³

¹H NMR (300 MHz, CDCl₃) δ = 7.70 (s, 4H), 7.64–7.55 (m, 2H), 7.52–7.44 (m, 2H), 7.44–7.37 (m, 1H) ppm.

¹³C{¹H} NMR (126 MHz, CDCl₃) δ = 144.9, 139.9, 129.5 (q, J = 33 Hz), 129.1, 128.3, 127.6, 127.4, 125.9 (q, J = 4 Hz), 124.4 (q, J = 272 Hz) ppm.

HRMS (ASAP pos): calc. for [M]⁺ C₁₃H₉F₃⁺ 222.0651; found: 222.0647.

4.6.4 Single-crystal X-ray diffraction studies

Crystal structure determination Crystals suitable for single-crystal X-ray diffraction were selected, coated in perfluoropolyether oil, and mounted on MiTeGen sample holders. Diffraction data were collected on a BRUKER X8-APEX II diffractometer with a CCD area detector using Mo- K_{α} radiation monochromated by graphite (**4-3**) or multi-layer mirror (**4-4**). The crystals were cooled using Oxford Cryostream low-temperature devices. Data were collected at 100 K. The images were processed and corrected for Lorentz-polarization effects and absorption as implemented in the Bruker software packages. The structures were solved using the intrinsic phasing method (SHELXT)⁹⁶ and Fourier expansion technique. All non-hydrogen atoms were refined in anisotropic approximation, with most hydrogen atoms 'riding' in idealized positions, by full-matrix least squares against F^2 of all data, using SHELXL⁹⁷ software and the SHELXLE⁹⁸ graphical user interface. Diamond⁹⁹ software was used for graphical representation. Crystal data and experimental details are listed in Table 4-3. Full structural information has been deposited with the Cambridge Crystallographic Data Centre. CCDC-1959972 (**4-3**) and 1959973 (**4-4**).

Table 4-3 Single-crystal X-ray diffraction data and structure refinements of compounds **4-3** and **4-4**.

Data	4-3	4-4
CCDC number	1959972	1959973
Empirical formula	C ₃₂ H ₂₈ BCIN ₂ P ₂ Pd	C ₃₃ H ₂₈ BF ₃ N ₂ O ₃ P ₂ PdS
Formula weight / g·mol ⁻¹	655.16	768.78
<i>T</i> / K	100(2)	100(2)
λ / Å, radiation	0.71073, Mo-K α	0.71073, Mo-K α
Crystal size / mm ³	0.24×0.19×0.10	0.19×0.18×0.14
Crystal color, habit	colorless plate	colorless block
μ / mm ⁻¹	0.876	0.825
Crystal system	Monoclinic	Orthorhombic
Space group	<i>C2/c</i>	<i>Pbca</i>
<i>a</i> / Å	16.751(9)	17.999(3)
<i>b</i> / Å	12.431(4)	17.931(4)
<i>c</i> / Å	15.975(7)	19.238(3)
α / °	90	90
β / °	120.362(13)	90
γ / °	90	90
Volume / Å ³	2870(2)	6209(2)
<i>Z</i>	4	8
ρ_{calc} / g·cm ⁻³	1.516	1.645
<i>F</i> (000)	1328	3104
θ range / °	2.179–27.525	1.921–27.484
Reflections collected	19354	116870
Unique reflections	3311	7117
Parameters / restraints	178 / 0	415 / 0
GooF on <i>F</i> ²	1.042	1.037
R ₁ [<i>I</i> >2 σ (<i>I</i>)]	0.0255	0.0351
wR ² (all data)	0.0577	0.0741
Max. / min. residual electron density / e·Å ⁻³	0.489 / -0.552	0.715 / -0.844

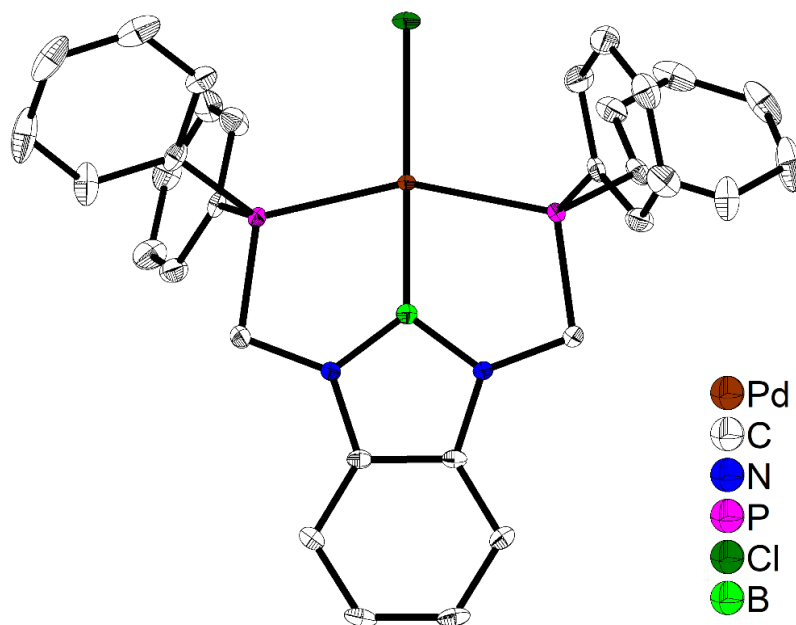


Figure 4-2 Molecular structure of **4-3** in the solid state at 100 K. Atomic displacement ellipsoids are drawn at the 50% probability level, and H atoms are omitted for clarity.

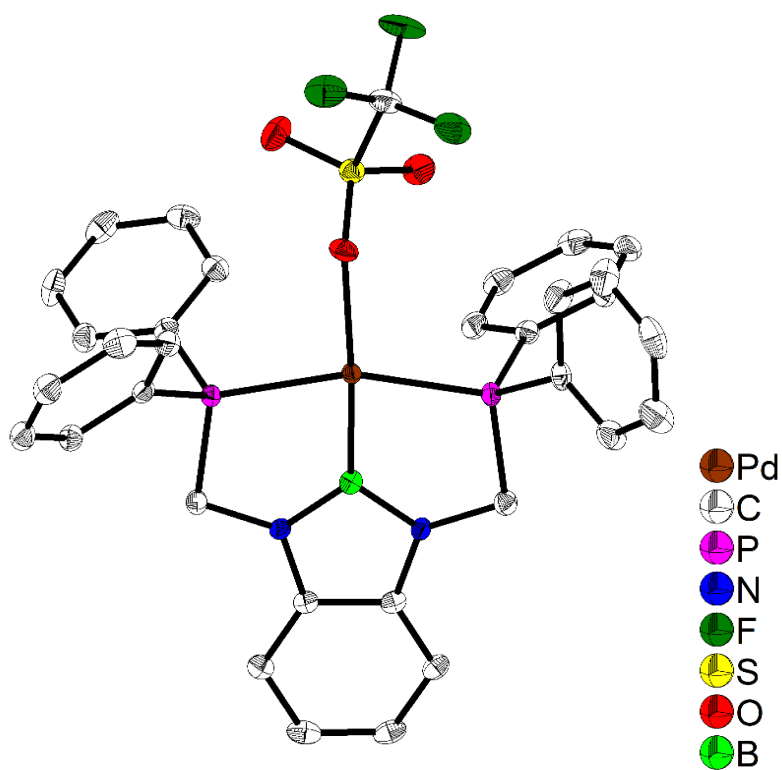


Figure 4-3 Molecular structure of **4-4** in the solid state at 100 K. Atomic displacement ellipsoids are drawn at the 50% probability level, and H atoms are omitted for clarity.

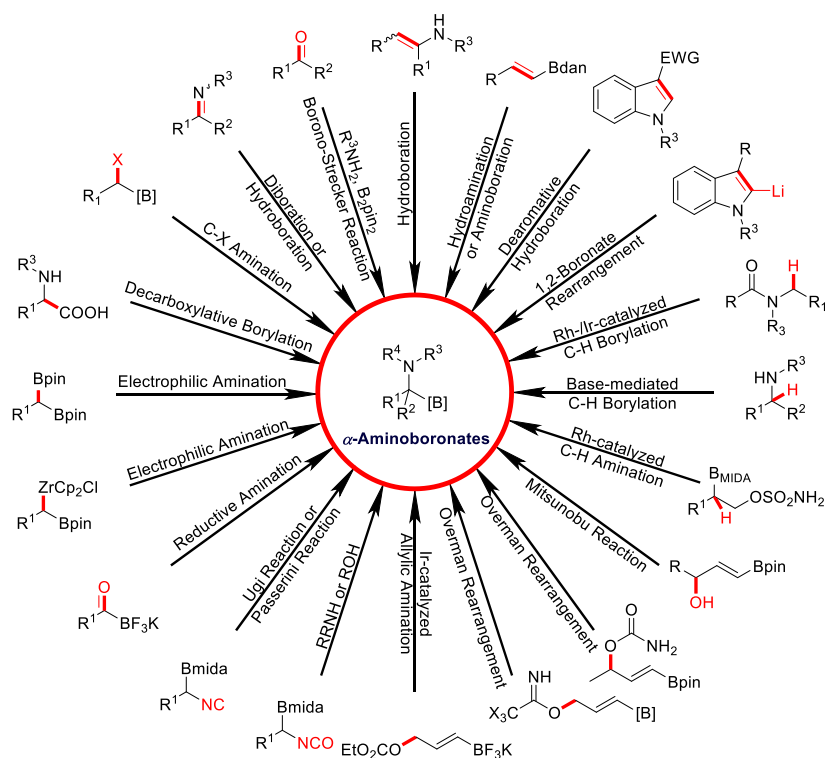
Summary

As analogues of α -amino acids, α -aminoboronic acids and their derivatives are especially useful as bioactive agents. Thus far, three compounds containing an α -aminoboronate motif have been approved by the FDA as enzyme inhibitors, and more candidates are undergoing clinical trials. In addition, α -aminoboronic acids and their derivatives have various applications in materials science, *e.g.* as carbohydrate sensors, penicillin-binding proteins tracers, and serine β -lactamase tracers.

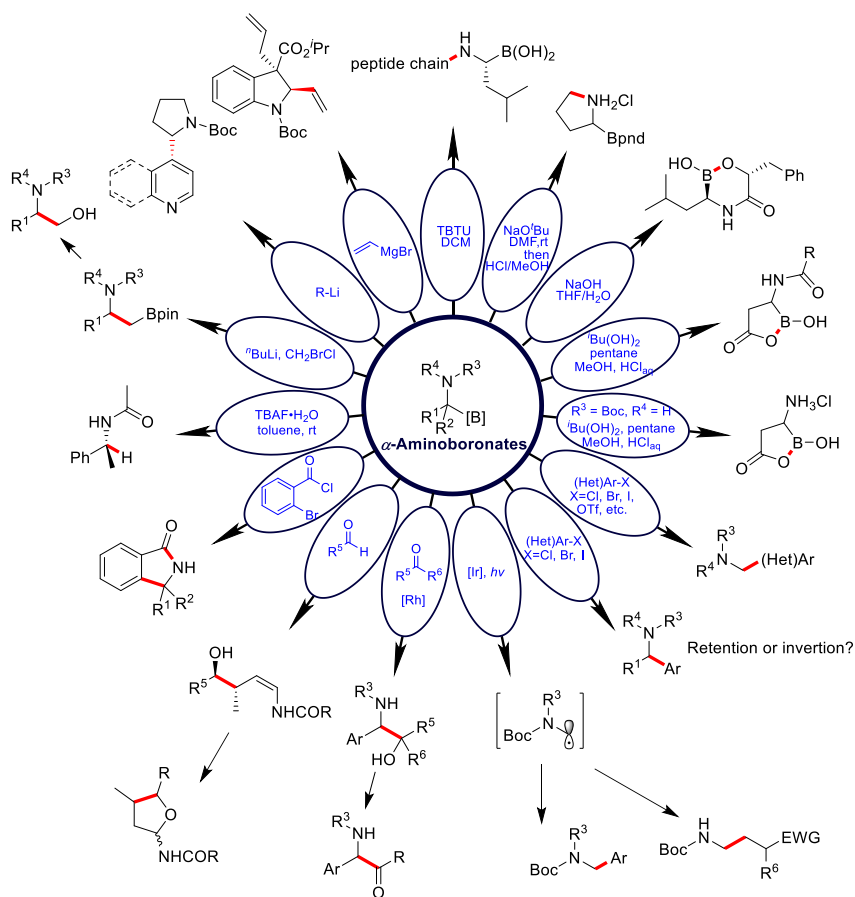
Chapter 1

In this chapter, the development of methodology for the synthesis of α -aminoboronates is summarized. Different synthetic routes are categorized by different starting materials, *e.g.* alkylboronates, imines, alkenes, α -boryl isocyanates, α -amino acids, *etc.* (Scheme S-1). In addition to their significant applications in drug discovery and materials science, α -aminoboronic acids and their derivatives have various applications in organic synthesis, *e.g.* as α -aminomethylation reagents for the synthesis of nitrogen-containing molecules which are found in a wide variety of alkaloid natural products and pharmaceuticals, as bis-nucleophiles in the construction of isoindolinones, and as nucleophiles for addition to ketones and aldehydes to form valuable vicinal amino alcohols, *etc.* Their applications as versatile synthons are also summarized in this chapter (Scheme S-2).

Summary



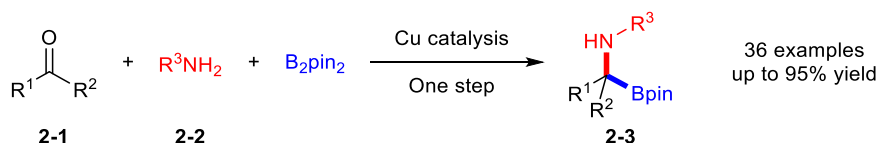
Scheme S-1 Overview of different synthetic strategies to α -aminoboronates.



Scheme S-2 Overview of applications of α -aminoboronates in organic synthesis.

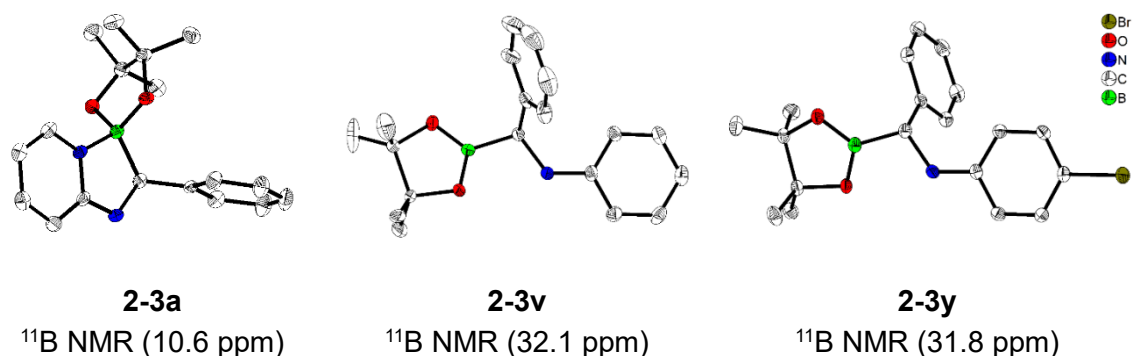
Chapter 2

In chapter 2, the first Borono-Strecker reaction is described, in which the synthesis of α -aminoboronates can be achieved *via* a novel multicomponent reaction of readily available carbonyl compounds (aldehydes and ketones), amines and B₂pin₂ (Scheme S-3).



Scheme S-3 Borono-Strecker reaction for the synthesis of α -aminoboronates.

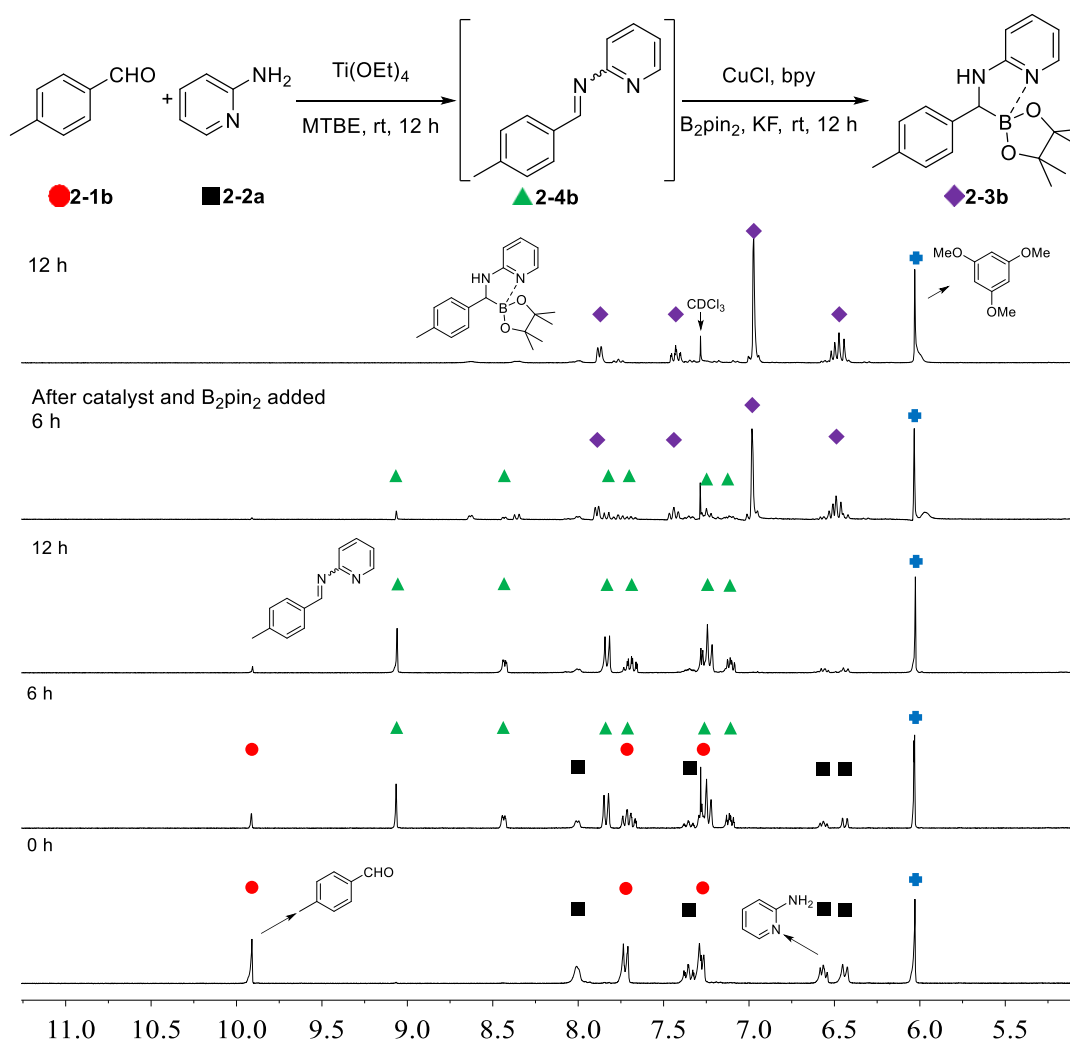
Diverse α -aminoboronates, including rare aryl-substituted and tertiary examples, were synthesized in moderate to high isolated yields (36 examples, up to 95% yield). Thus, compounds were prepared bearing *N*-(2-pyridyl) groups, which form 5-membered rings *via* N-B coordination, as well as systems bearing non-coordinating *N*-aryl groups, the latter being isolated and fully characterized for the first time. Coordination of the pyridine nitrogen to boron provides suitable stability for purification by column chromatography and isolation in air (Scheme S-4). In addition, this multicomponent reaction can be readily conducted on a gram scale to produce the corresponding α -aminoboronic esters without significant loss of yield.



Scheme S-4 Molecular structures and ¹¹B NMR chemical shifts of **2-3a**, **2-3v**, and **2-3y**.

The stepwise reaction indicates that imines are important intermediates in this

multicomponent reaction. Further mechanistic studies indicate the role of $\text{Ti}(\text{OEt})_4$ in the formation of imine intermediates, and the role of a proton source in the subsequent hydroboration process (Scheme S-5).

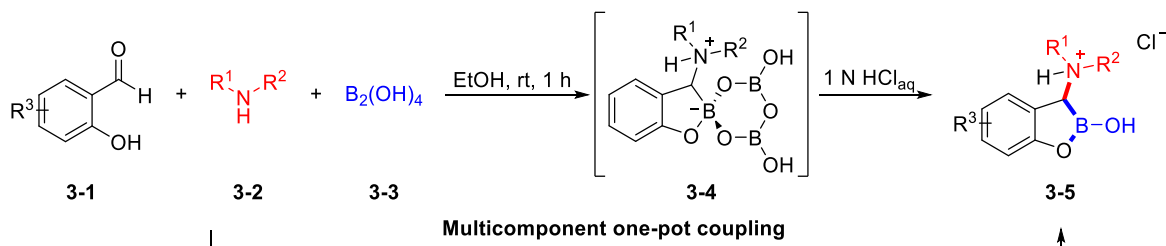


Scheme S-5 Stepwise (bottom to top) reaction process monitored by ^1H NMR spectroscopy (300 MHz, CDCl_3 , rt); 1,3,5-trimethoxybenzene (blue + sign) was used as an internal standard.

Chapter 3

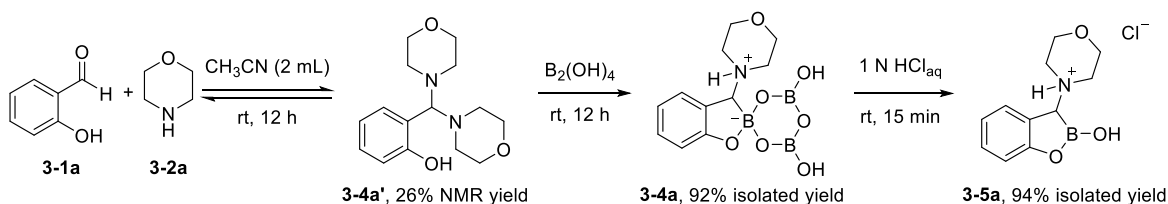
In chapter 3, a concise synthesis of α -amino cyclic boronates *via* multicomponent coupling of readily available salicylaldehydes, amines, and $\text{B}_2(\text{OH})_4$ is presented (Scheme S-6). This protocol has several advantages over previous routes including mild reaction conditions (room temperature, in air), no catalyst or additive, easy product isolation, and green

solvents (ethanol and water).



Scheme S-6 Concise synthesis of α -amino cyclic boronates *via* multicomponent coupling.

To gain further insights into the mechanism of this reaction, the reaction was conducted stepwise, and a minimal intermediate **3-4a'** was formed in 26% yield immediately upon mixing salicylaldehyde **3-1a** and morpholine **3-1b** in CH_3CN , confirmed by ^1H NMR spectroscopy. Prolonging the reaction time to 12 h did not lead to an improvement of the yield of **3-4a'**, indicating that the formation of aminated boroxines is reversible. $\text{B}_2(\text{OH})_4$ was then added to the reaction mixture, and boroxine **3-4a** was isolated in 92% yield after stirring for 12 h. Then, **3-4a** was hydrolyzed with 1N HCl_{aq} to give α -amino cyclic boronate **3-5a** in 94% yield (Scheme S-7).

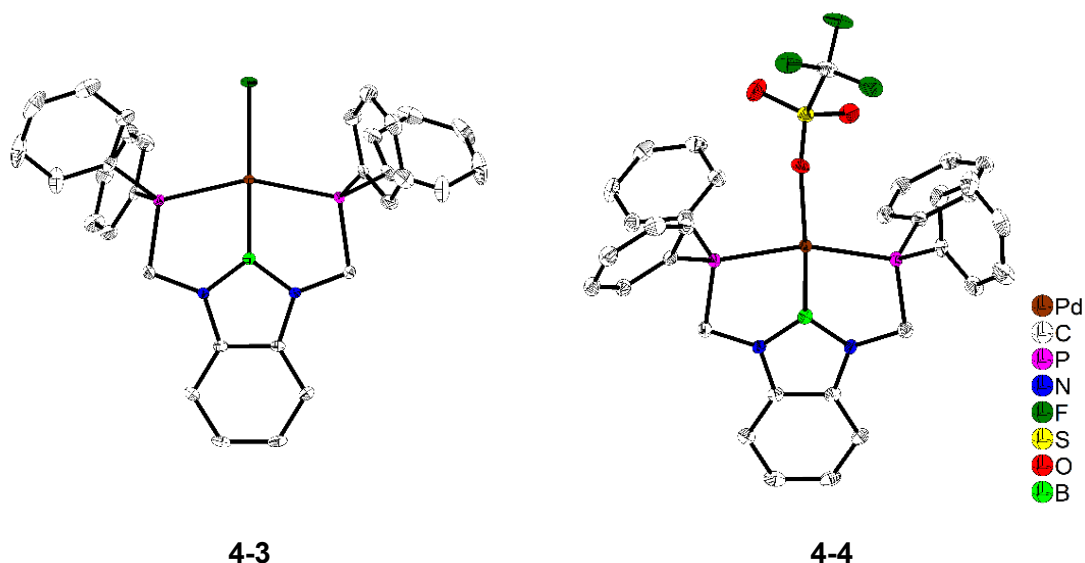


Scheme S-7 Stepwise reaction process; the yield of intermediate **3-4a'** was monitored by ^1H NMR spectroscopy (300 MHz, CDCl_3 , rt) using 1,3,5-trimethoxybenzene as an internal standard.

Chapter 4

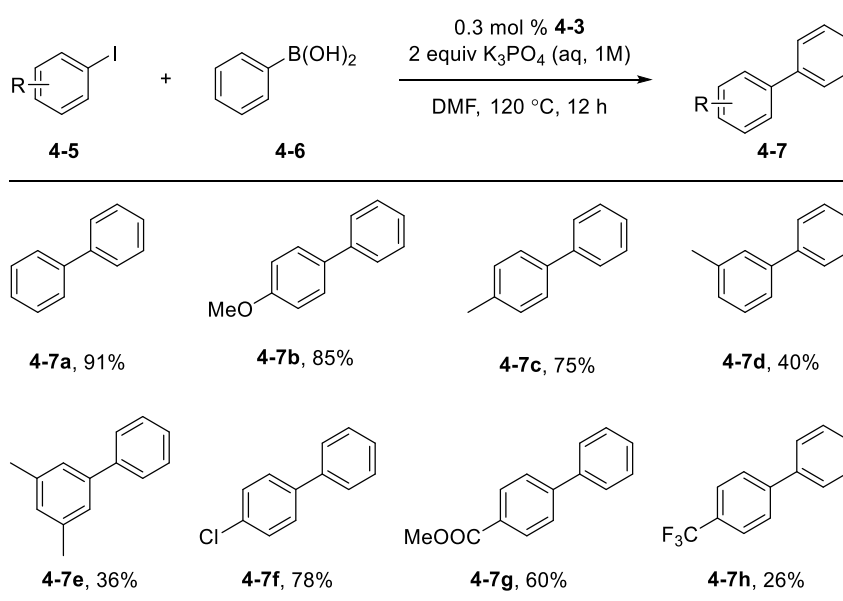
In chapter 4, the diazaborole-based PBP pincer palladium chloride (**4-3**) and the diazaborole-based PBP pincer palladium trifluoromethanesulfonate (**4-4**) complexes were synthesized and fully characterized (NMR, HRMS, elemental analysis, and single-crystal X-ray diffraction) for the first time (Scheme S-8). In their structures, the Pd-Cl bond length in **4-3** is much longer than that in its PNP and PCP analogues, and is slightly shorter than

the PSiP one. Compared with its NNN, PCP, and PSiP analogues, the Pd-O bond length in **4-4** is the longest, which indicates the strong trans influence of boron.



Scheme S-8 Molecular structures of **4-3** and **4-4**.

In addition, **4-3** showed catalytic reactivity for the Suzuki-Miyaura coupling of aryl iodides and phenylboronic acid (Scheme S-9), giving symmetric and unsymmetric biaryl compounds.



Scheme S-9 Catalytic Suzuki-Miyaura cross-coupling reaction using **4-3** as catalyst.

Conclusion

The first Borono-Strecker reaction has been developed to synthesize α -aminoboronates *via* a multicomponent reaction of readily available carbonyl compounds (aldehydes and ketones), amines and B_2pin_2 . The preparation of α -amino cyclic boronates can be achieved *via* multicomponent coupling of salicylaldehydes, amines, and $B_2(OH)_4$. In addition, the diazaborole-based PBP pincer palladium chloride and the diazaborole-based PBP pincer palladium trifluoromethanesulfonate complexes were synthesized and fully characterized for the first time, and used as catalysts for Suzuki-Miyaura cross-coupling reactions.

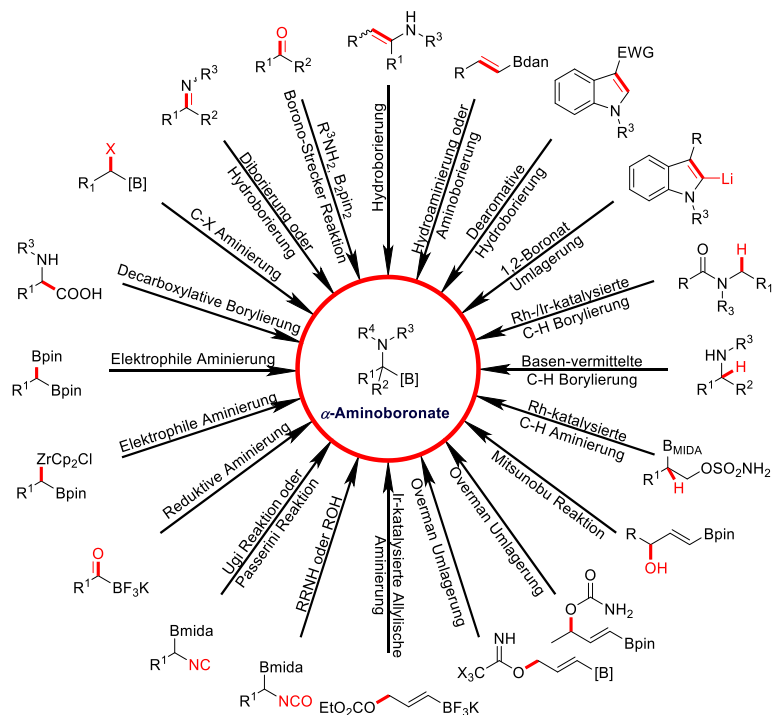
Zusammenfassung

Als Analoga der α -Aminosäuren sind α -Aminoborsäuren und ihre Derivate besonders als bioaktive Substanzen von großem Nutzen. Bisher wurden drei Verbindungen, die ein α -Aminoborat in ihrer Struktur enthielten, von der FDA als Enzymhemmstoffe zugelassen und weitere Kandidaten durchlaufen derzeit klinische Tests. Zusätzlich besitzen α -Aminoborsäuren und ihre Derivate diverse Anwendungsmöglichkeiten in den Materialwissenschaften, so zum Beispiel als Sensoren für Kohlenhydrate, als Tracer für Penicillin-bindende Proteine oder als Tracer für Serin- β -Lactamasen.

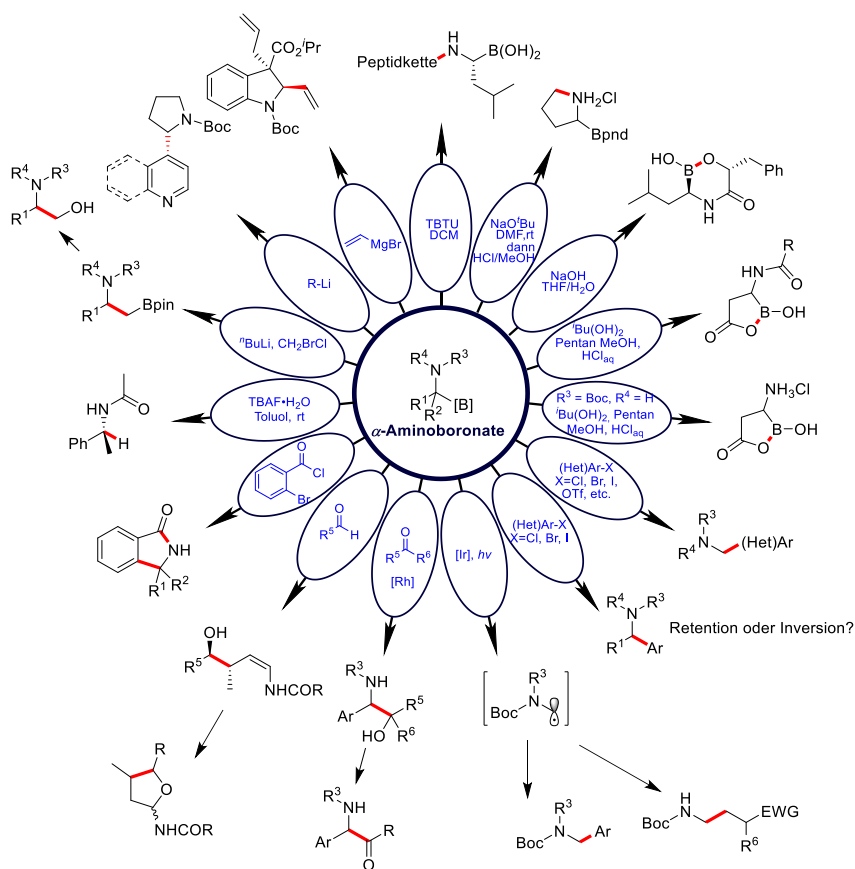
Kapitel 1

In diesem Kapitel wurde die Entwicklung der Methoden zur Synthese von α -Aminoboronaten zusammengefasst. Verschiedene Syntheserouten wurden anhand der verschiedenen Startmaterialien, z. B. Alkylboronate, Imine, Alkene, α -Borylisocyanate, α -Aminoborsäuren usw. kategorisiert (Schema S-1). Neben den medizinischen und materialwissenschaftlichen Anwendungen, besitzen α -Aminoborsäuren und ihre Derivate diverse Anwendungsmöglichkeiten in der organischen Synthese. Sie werden als α -Aminomethylierungsreagenz in der Synthese von stickstoffhaltigen Molekülen, die in vielen Alkaloiden und pharmazeutischen Wirkstoffen enthalten sind, als Bis-Nukleophile in der Synthese von Isoindolinonen und als Nukleophile in Additionsreaktionen an Ketone und Aldehyde, zur Synthese von vicinalen Aminoalkoholen usw. eingesetzt. Ihre Anwendungsmöglichkeiten als vielseitige Synthone wurden in diesem Kapitel ebenfalls zusammengefasst (Scheme S-2).

Zusammenfassung



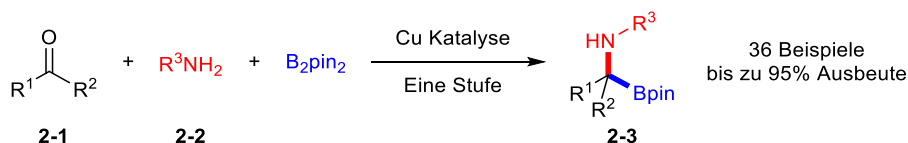
Schema S-1 Überblick über verschiedene Synthesestrategien zur Bildung von α -Aminoboraten.



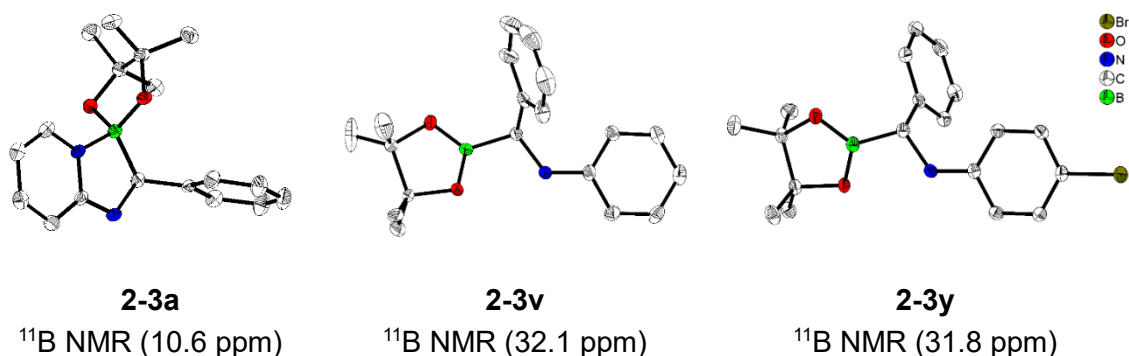
Schema S-2 Überblick über die Anwendungsmöglichkeiten von α -Aminoboraten in der organischen Synthese.

Kapitel 2

In Kapitel 2 wurde über die erste Borono-Strecker Reaktion berichtet, mit der die Synthese von α -Aminoboronaten in einer neuartigen Multikomponenten-Reaktion aus leicht zugänglichen Carbonylverbindungen (Aldehyde und Ketone), Aminen und B_2pin_2 gelingt (Scheme S-3).



Schema S-3 Borono-Strecker Reaktion zur Synthese von α -Aminoboronaten.

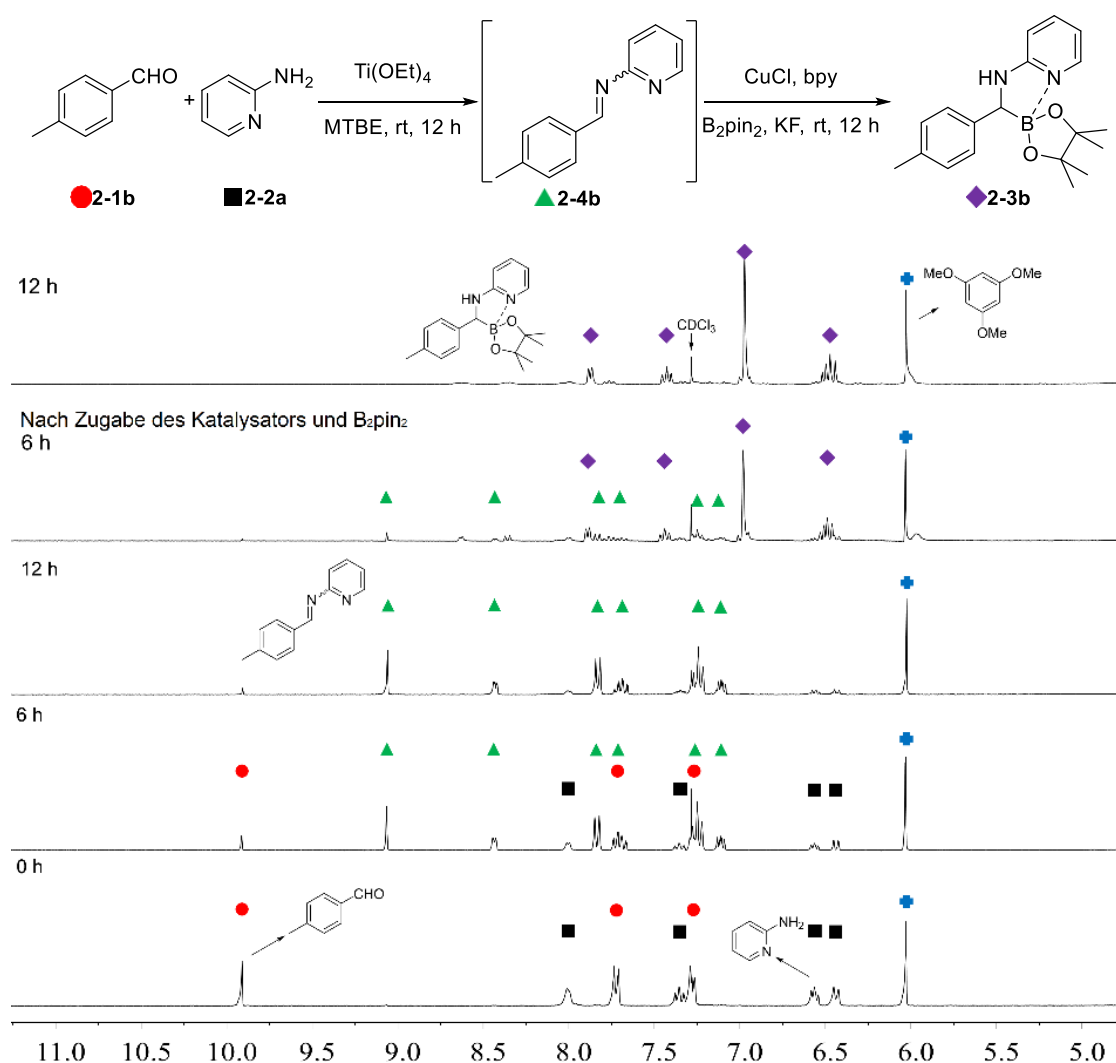


Schema S-4 Molekülstrukturen und ^{11}B NMR Verschiebungen der Verbindungen **2-3a**, **2-3v** und **2-3y**.

Verschiedene α -Aminoboronate, einschließlich seltener Aryl-substituierter und tertiärer Verbindungen, wurden in moderaten bis hohen Ausbeuten synthetisiert (36 Beispiele, bis zu 95% Ausbeute). Es wurden Verbindungen mit *N*-(2-pyridyl) Gruppen, die mittels N-B Koordination fünfgliedrige Ringe bilden, so wie Systeme mit nicht koordinierenden *N*-Aryl Gruppen dargestellt. Die letztgenannten Verbindungen konnten im Zuge dieser Arbeit erstmalig isoliert und vollständig charakterisiert werden. Die Koordination des Stickstoffatoms des Pyridins zum Bor liefert ausreichende Stabilität und erlaubt so die Aufarbeitung an Luft und die Aufreinigung mittels Säulenchromatographie (Schema S-4). Diese Multikomponenten-Reaktion konnte außerdem im Gramm-Maßstab durchgeführt

werden und liefert den jeweiligen α -Aminoborsäureester ohne nennenswerte Ausbeuteverluste.

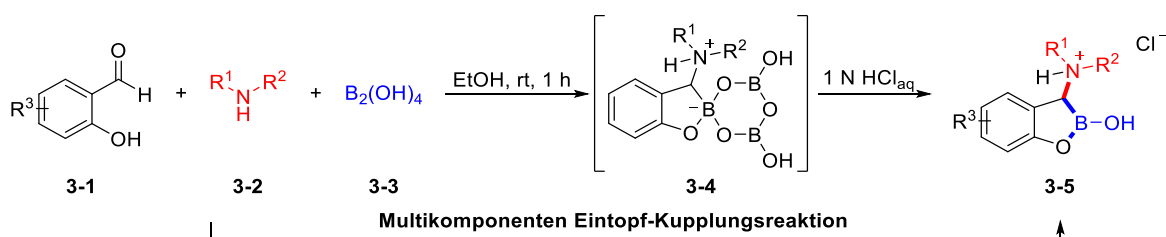
Die schrittweise Durchführung der Reaktion zeigt, dass Imine ein wichtiges Zwischenprodukt dieser Multikomponenten-Reaktion darstellen. Weitere mechanistische Studien zeigten die Funktion von $\text{Ti}(\text{OEt})_4$ in der Bildung des Imin Zwischenprodukts und die Funktion einer Protonenquelle in dem darauffolgenden Hydroborierungsprozess (Schema S-5).



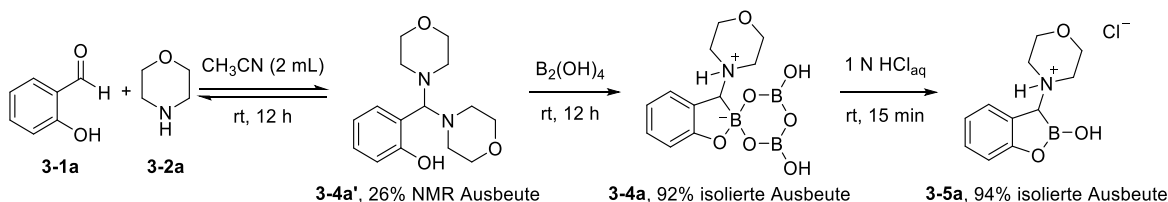
Schema S-5 Verfolgung des schrittweisen (von unten nach oben) Reaktionsverlaufs mittels ^1H NMR Spektroskopie (300 MHz, CDCl_3 , rt); 1,3,5-Trimethoxybenzol (blaue + Markierung) wurde als interner Standard verwendet.

Kapitel 3

In Kapitel 3 wurde über die Eintopfsynthese von zyklischen α -Aminoboronaten durch Multikomponenten-Kupplung von leicht zugänglichen Salicylaldehyden, Aminen und $B_2(OH)_4$ berichtet (Schema S-6). Mildere Reaktionsbedingungen (Raumtemperatur, an Luft), keine Verwendung von Katalysatoren oder Additiven, einfache Isolierung des Produkts und die Verwendung von grünen Lösemitteln (Ethanol und Wasser) gehören zu den Vorteilen, die diese Methode gegenüber vorherigen Methoden besitzt.



Schema S-6 Eintopfsynthese von zyklischen α -Aminoboronaten durch Multikomponenten-Kupplung.



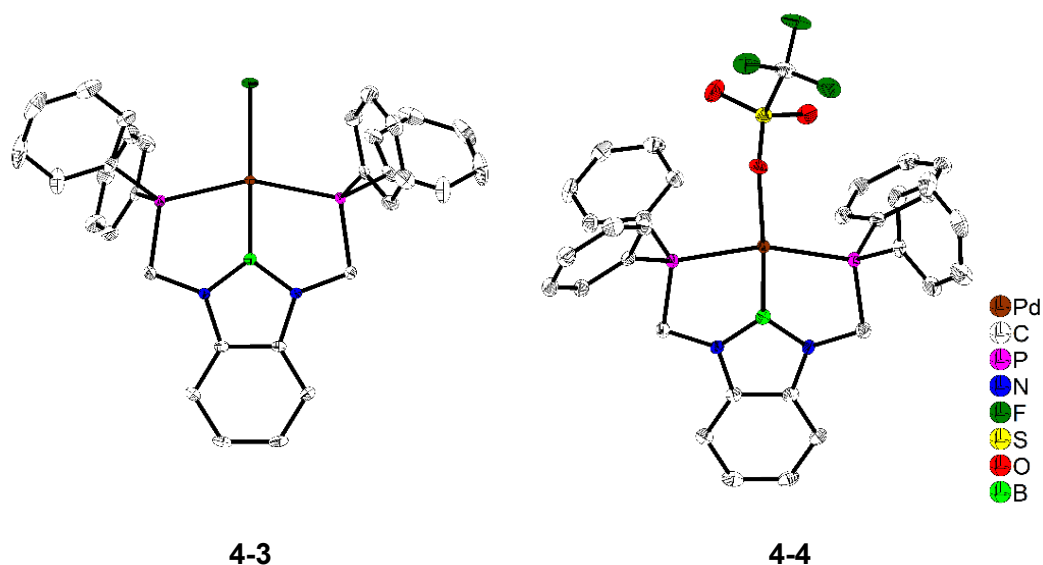
Schema S-7 Schrittweiser Reaktionsverlauf; die Ausbeute des Zwischenprodukts **3-4a'** wurde mittels ^1H NMR Spektroskopie (300 MHz, CDCl_3 , rt) bestimmt. Als interner Standard wurde 1,3,5-Trimethoxybenzol verwendet.

Um Einsicht in den Reaktionsmechanismus zu erhalten, wurde die Reaktion schrittweise durchgeführt. Das Aminal **3-4a'** wurde durch Reaktion von Salicylaldehyd **3-1a** und Morpholin **3-1b** in CH_3CN in einer ^1H NMR Ausbeute von 26% erhalten. Eine Verlängerung der Reaktionszeit auf 12 h führte zu keiner höheren Ausbeute von **3-4a'**, was auf eine reversible Aminalbildung schließen lässt. Anschließend wurde $B_2(OH)_4$ zur Reaktionsmischung hinzugegeben und nach einer Reaktionszeit von 12 h wurde das Boroxin **3-4a** in einer Ausbeute von 92% isoliert. Verbindung **3-4a** wurde mit $1\text{N HCl}_{\text{aq}}$

hydrolysiert und das zyklische α -Aminoboronat **3-5a** wurde in 94% Ausbeute erhalten (Scheme S-7).

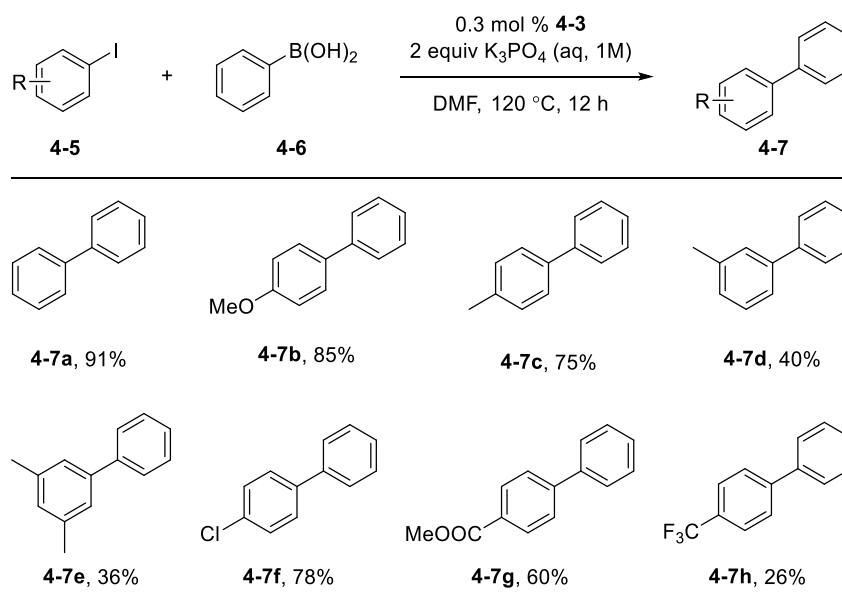
Kapitel 4

In Kapitel 4 wurden der Diazaborol-basierte PBP Pincer Palladium Chlorid Komplex (**4-3**) und der Diazaborol-basierte PBP Pincer Palladium Trifluoromethylsulfonat Komplex (**4-4**) erstmalig synthetisiert und mittels NMR, HRMS, Elementaranalyse und Einkristallstrukturanalyse vollständig charakterisiert (Schema S-8). Der Pd-Cl Bindungsabstand in Verbindung **4-3** ist deutlich länger als der in den analogen PNP und PCP Verbindungen und etwas kürzer als der in PSiP. Im Vergleich mit den NNN, PCP und PSiP Analoga, ist der Pd-O Bindungsabstand in Verbindung **4-4** am längsten, was auf den starken trans-Einfluss des Bors zurückzuführen ist.



Schema S-8 Molekülstrukturen der Verbindungen **4-3** und **4-4**.

Außerdem zeigte Verbindung **4-3** katalytische Aktivität in der Suzuki-Miyaura Kupplung von Aryliodiden und Phenylborsäure (Schema S-9) und es konnten auf diese Weise symmetrische und unsymmetrische Biarylverbindungen dargestellt werden.



Schema S-9 Verwendung von **4-3** als Katalysator in der Suzuki-Miyaura Kreuzkupplungsreaktion.

Zusammenfassend, wurde die erste Borono-Strecker Reaktion zur Synthese von α -Aminoboronaten, mittels einer Multikomponenten-Reaktion aus leicht zugänglichen Carbonylverbindungen (Aldehyde und Ketone), Aminen und B_2pin_2 , entwickelt. Außerdem gelang die Darstellung von zyklischen α -Aminoboronaten durch Multikomponenten-Kupplung von leicht zugänglichen Salicylaldehyden, Aminen und $B_2(OH)_4$. Des Weiteren wurde der Diazaborol-basierte PBP Pincer Palladium Chlorid Komplex und der Diazaborol-basierte PBP Pincer Palladium Trifluoromethylsulfonat Komplex erstmalig synthetisiert, vollständig charakterisiert und als Katalysator für Suzuki-Miyaura Kreuzkupplungen eingesetzt.

Notes and references

- (a) I. A. I. Mkhaliid, J. H. Barnard, T. B. Marder, J. M. Murphy and J. F. Hartwig, *Chem. Rev.*, 2010, **110**, 890-931; (b) *Boronic Acids: Preparation and Applications in Organic Synthesis, Medicine and Materials*, ed. D. G. Hall, Wiley-VCH, Weinheim, 2nd edn., 2011; (c) *Synthesis and Applications of Organoboron Compounds*, eds. E. Fernández and A. Whiting, Springer, Berlin, 2015; (d) E. C. Neeve, S. J. Geier, I. A. I. Mkhaliid, S. A. Westcott and T. B. Marder, *Chem. Rev.*, 2016, **116**, 9091-9161; (e) L. Ji, S. Griesbeck and T. B. Marder, *Chem. Sci.*, 2017, **8**, 846-863; (f) D. B. Diaz and A. K. Yudin, *Nat. Chem.*, 2017, **9**, 731; (g) H. S. Ban and H. Nakamura, *Chem. Rec.*, 2015, **15**, 616-635.
- (a) K. Takroui, V. M. Dembitsky and M. Srebnik, in *Contemporary Aspects of Boron: Chemistry and Biological Applications*, eds. H. Abu Ali, V. M. Dembitsky and M. Srebnik, Elsevier, Amsterdam, 2005, pp. 495-549; (b) V. M. Dembitsky and M. Srebnik, *Tetrahedron*, 2003, **59**, 579-593; (c) D. S. Matteson, *Med. Res. Rev.*, 2008, **28**, 233-246; (d) V. M. Dembitsky and M. Srebnik, in *Amino Acids, Peptides and Proteins in Organic Chemistry*, ed. A. B. Hughes, Wiley-VCH, Weinheim, 2009, pp. 145-187; (e) P. C. Trippier and C. McGuigan, *MedChemComm*, 2010, **1**, 183-198; (f) R. Smoum, A. Rubinstein, V. M. Dembitsky and M. Srebnik, *Chem. Rev.*, 2012, **112**, 4156-4220; (g) P. Andres, G. Ballano, M. I. Calaza and C. Cativiela, *Chem. Soc. Rev.*, 2016, **45**, 2291-2307.
- Bortezomib in the Treatment of Multiple Myeloma*, eds. I. M. Ghobrial, P. G. Richardson and K. C. Anderson, Springer, Basel, 2010.
- O. Lomovskaya, D. Sun, D. Rubio-Aparicio, K. Nelson, R. Tsivkovski, D. C. Griffith and M. N. Dudley, *Antimicrob. Agents Chemother.*, 2017, **61**, e01443-01417.
- (a) M. Gentile, M. Offidani, E. Vigna, L. Corvatta, A. G. Recchia, L. Morabito, F. Morabito and S. Gentili, *Expert Opin. Investig. Drugs*, 2015, **24**, 1287-1298; (b) D. T. Vogl, T. G. Martin, R. Vij, P. Hari, J. R. Mikhael, D. Siegel, K. L. Wu, M. Delforge and C. Gasparetto, *Leuk. Lymphoma*, 2017, **58**, 1872-1879; (c) K. M. S. Johnson, *Curr. Opin. Investig. Drugs*, 2010, **11**, 455-463; (d) C. C. Cunningham, *Expert Opin. Investig. Drugs*, 2007, **16**, 1459-1465; (e) S. J. Baker, J. W. Tomsho and S. J. Benkovic, *Chem. Soc. Rev.*, 2011, **40**, 4279-4285; (f) F. Yang, M. Zhu, J. Zhang and H. Zhou, *MedChemComm*, 2018, **9**, 201-211.
- S. Jin, C. Zhu, M. Li and B. Wang, *Bioorg. Med. Chem. Lett.*, 2009, **19**, 1596-1599.
- S. Jin, C. Zhu, Y. Cheng, M. Li and B. Wang, *Bioorg. Med. Chem.*, 2010, **18**, 1449-1455.
- S. R. Inglis, M. Strieker, A. M. Rydzik, A. Dessen and C. J. Schofield, *Anal. Biochem.*, 2012, **420**, 41-47.
- (a) D. S. Matteson and T.-C. Cheng, *J. Organomet. Chem.*, 1966, **6**, 100-101; (b) D.

- S. Matteson and T.-C. Cheng, *J. Org. Chem.*, 1968, **33**, 3055-3060.
10. S. Touchet, F. Carreaux, B. Carboni, A. Bouillon and J.-L. Boucher, *Chem. Soc. Rev.*, 2011, **40**, 3895-3914.
 11. (a) D. S. Matteson, K. M. Sadhu and G. E. Lienhard, *J. Am. Chem. Soc.*, 1981, **103**, 5241-5242; (b) D. S. Matteson and K. M. Sadhu, *Organometallics*, 1984, **3**, 614-618; (c) D. S. Matteson, P. K. Jesthi and K. M. Sadhu, *Organometallics*, 1984, **3**, 1284-1288; (d) D. S. Matteson, T. J. Michnick, R. D. Willett and C. D. Patterson, *Organometallics*, 1989, **8**, 726-729.
 12. (a) D. S. Matteson, *Chem. Rev.*, 1989, **89**, 1535-1551; (b) D. S. Matteson, *Tetrahedron*, 1998, **54**, 10555-10607; (c) D. S. Matteson, *J. Org. Chem.*, 2013, **78**, 10009-10023.
 13. (a) D. S. Matteson and R. Ray, *J. Am. Chem. Soc.*, 1980, **102**, 7590-7591; (b) D. S. Matteson and K. M. Sadhu, *J. Am. Chem. Soc.*, 1983, **105**, 2077-2078; (c) E. J. Corey, D. Barnes-Seeman and T. W. Lee, *Tetrahedron: Asymmetry*, 1997, **8**, 3711-3713.
 14. (a) J. Adams, M. Behnke, S. Chen, A. A. Cruickshank, L. R. Dick, L. Grenier, J. M. Klunder, Y.-T. Ma, L. Plamondon and R. L. Stein, *Bioorg. Med. Chem. Lett.*, 1998, **8**, 333-338; (b) B. S. Greener and D. S. Millan, in *Modern Drug Synthesis*, eds. J. J. Li and D. S. Johnson, John Wiley & Sons, Inc., Hoboken, 2010, ch. 8, pp. 99-110.
 15. D. S. Matteson, *Tetrahedron*, 1989, **45**, 1859-1885.
 16. (a) I. Gazić Smilović, E. Casas-Arcé, S. J. Roseblade, U. Nettekoven, A. Zanotti-Gerosa, M. Kovačević and Z. Časar, *Angew. Chem. Int. Ed.*, 2012, **51**, 1014-1018; (b) S. J. Roseblade, E. Casas-Arcé, U. Nettekoven, I. Gazić Smilović, A. Zanotti-Gerosa and Z. Časar, *Synthesis*, 2013, **45**, 2824-2831.
 17. I. Gazić Smilović and Z. Časar, *Chim. Oggi - Chem. Today*, 2013, **31**, 20-25.
 18. (a) H. C. Brown, N. G. Bhat and M. Srebnik, *Tetrahedron Lett.*, 1988, **29**, 2631-2634; (b) B. Zheng and M. Srebnik, *Tetrahedron Lett.*, 1993, **34**, 4133-4136; (c) L. Deloux, E. Skrzypczak-Jankun, B. V. Cheesman, M. Srebnik and M. Sabat, *J. Am. Chem. Soc.*, 1994, **116**, 10302-10303.
 19. (a) T. Marder and N. Norman, *Top. Catal.*, 1998, **5**, 63-73; (b) T. Ishiyama and N. Miyaoura, *Chem. Rec.*, 2004, **3**, 271-280; (c) T. B. Marder, in *Science of Synthesis, 6: Category 1, Organometallics*, eds. D. E. Kaufmann, D. S. Matteson, E. Schaumann and M. Regitz, Georg Thieme Verlag, Stuttgart, 2005, vol. 6, pp. 117-137; (d) R. D. Dewhurst and T. B. Marder, *Nat. Chem.*, 2014, **6**, 279-280.
 20. G. Mann, K. D. John and R. T. Baker, *Org. Lett.*, 2000, **2**, 2105-2108.
 21. (a) L. T. Kliman, S. N. Mlynarski and J. P. Morken, *J. Am. Chem. Soc.*, 2009, **131**, 13210-13211; (b) L. T. Kliman, S. N. Mlynarski, G. E. Ferris and J. P. Morken, *Angew. Chem. Int. Ed.*, 2012, **51**, 521-524.
 22. K. Hong and J. P. Morken, *J. Am. Chem. Soc.*, 2013, **135**, 9252-9254.
 23. M. A. Beenen, C. An and J. A. Ellman, *J. Am. Chem. Soc.*, 2008, **130**, 6910-6911.

24. K. Wen, H. Wang, J. Chen, H. Zhang, X. Cui, C. Wei, E. Fan and Z. Sun, *J. Org. Chem.*, 2013, **78**, 3405-3409.
25. A. W. Buesking, V. Bacauanu, I. Cai and J. A. Ellman, *J. Org. Chem.*, 2014, **79**, 3671-3677.
26. S. S. Zhang, Y. S. Zhao, P. Tian and G. Q. Lin, *Synlett*, 2013, **24**, 437-442.
27. D. Wang, P. Cao, B. Wang, T. Jia, Y. Lou, M. Wang and J. Liao, *Org. Lett.*, 2015, **17**, 2420-2423.
28. C. B. Schwamb, K. P. Fitzpatrick, A. C. Brueckner, H. C. Richardson, P. H. Y. Cheong and K. A. Scheidt, *J. Am. Chem. Soc.*, 2018, **140**, 10644-10648.
29. N. Zhou, X. A. Yuan, Y. Zhao, J. Xie and C. Zhu, *Angew. Chem. Int. Ed.*, 2018, **57**, 3990-3994.
30. (a) S. Pietsch, E. C. Neeve, D. C. Apperley, R. Bertermann, F. Mo, D. Qiu, M. S. Cheung, L. Dang, J. Wang, U. Radius, Z. Lin, C. Kleeberg and T. B. Marder *Chem. Eur. J.*, 2015, **21**, 7082-7098; (b) R. D. Dewhurst, E. Neeve, T. B. Marder and H. Braunschweig, *Chem. Commun.*, 2015, **51**, 9594-9607; (c) C. Kleeberg, L. Dang, Z. Lin and T. B. Marder, *Angew. Chem. Int. Ed.*, 2009, **48**, 5350-5354; (d) A. B. Cuenca, R. Shishido, H. Ito and E. Fernández, *Chem. Soc. Rev.*, 2017, **46**, 415-430.
31. C. Sole, H. Gulyas and E. Fernández, *Chem. Commun.*, 2012, **48**, 3769-3771.
32. (a) K.-s. Lee, A. R. Zhugralin and A. H. Hoveyda, *J. Am. Chem. Soc.*, 2009, **131**, 7253-7255; (b) C. Kleeberg, A. G. Crawford, A. S. Batsanov, P. Hodgkinson, D. C. Apperley, M. S. Cheung, Z. Lin and T. B. Marder, *J. Org. Chem.*, 2012, **77**, 785-789; (c) C. Kleeberg, A. G. Crawford, A. S. Batsanov, P. Hodgkinson, D. C. Apperley, M. S. Cheung, Z. Lin and T. B. Marder, *J. Org. Chem.*, 2012, **77**, 785-789; (d) I. Ibrahem, P. Breistein and A. Córdova, *Chem. Eur. J.*, 2012, **18**, 5175-5179; (e) H. Wu, S. Radomkit, J. M. O'Brien and A. H. Hoveyda, *J. Am. Chem. Soc.*, 2012, **134**, 8277-8285; (f) S. Radomkit and A. H. Hoveyda, *Angew. Chem. Int. Ed.*, 2014, **53**, 3387-3391; (g) S. Pietsch, U. Paul, I. A. Cade, M. J. Ingleson, U. Radius and T. B. Marder, *Chem. Eur. J.*, 2015, **21**, 9018-9021; (h) L. Wang, Z. Chen, M. Ma, W. Duan, C. Song and Y. Ma, *Org. Biomol. Chem.*, 2015, **13**, 10691-10698; (i) S. Würtemberger-Pietsch, U. Radius and T. B. Marder, *Dalton Trans.*, 2016, **45**, 5880-5895; (j) A. Eichhorn, L. Kuehn, T. B. Marder and U. Radius, *Chem. Commun.*, 2017, **53**, 11694-11696; (k) M. Eck, S. Würtemberger-Pietsch, A. Eichhorn, J. H. J. Berthel, R. Bertermann, U. S. D. Paul, H. Schneider, A. Friedrich, C. Kleeberg, U. Radius and T. B. Marder, *Dalton Trans.*, 2017, **46**, 3661-3680.
33. K. Wen, J. Chen, F. Gao, P. S. Bhadury, E. Fan and Z. Sun, *Org. Biomol. Chem.*, 2013, **11**, 6350-6356.
34. (a) J. D. Hewes, C. W. Kreimendahl, T. B. Marder and M. F. Hawthorne, *J. Am. Chem. Soc.*, 1984, **106**, 5757-5759; (b) D. Männig and H. Nöth, *Angew. Chem. Int. Ed.*, 1985, **24**, 878-879; (c) K. Burgess, W. A. Van der Donk, S. A. Westcott, T. B. Marder, R. T.

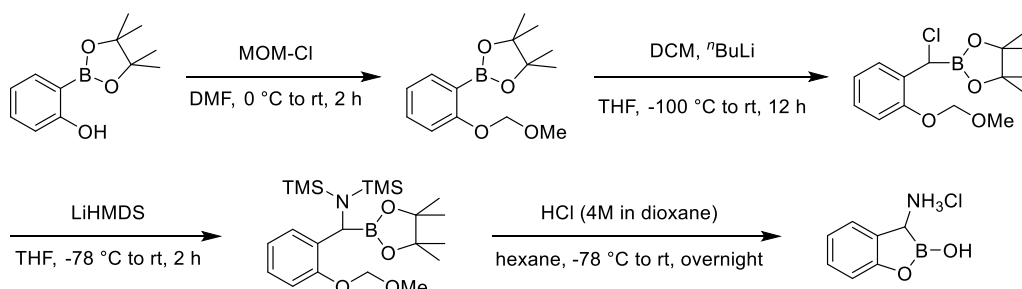
- Baker and J. C. Calabrese, *J. Am. Chem. Soc.*, 1992, **114**, 9350-9359; (d) D. A. Evans, G. C. Fu and B. A. Anderson, *J. Am. Chem. Soc.*, 1992, **114**, 6679-6685; (e) A. E. Dorigo and P. v. R. Schleyer, *Angew. Chem. Int. Ed.*, 1995, **34**, 115-118.
35. N. Hu, G. Zhao, Y. Zhang, X. Liu, G. Li and W. Tang, *J. Am. Chem. Soc.*, 2015, **137**, 6746-6749.
36. (a) J.-E. Lee and J. Yun, *Angew. Chem. Int. Ed.*, 2008, **47**, 145-147; (b) L. Dang, Z. Lin and T. B. Marder, *Organometallics*, 2008, **27**, 4443-4454; (c) I. H. Chen, L. Yin, W. Itano, M. Kanai and M. Shibasaki, *J. Am. Chem. Soc.*, 2009, **131**, 11664-11665; (d) J. M. O'Brien, K.-s. Lee and A. H. Hoveyda, *J. Am. Chem. Soc.*, 2010, **132**, 10630-10633; (e) J. C. H. Lee, R. McDonald and D. G. Hall, *Nat. Chem.*, 2011, **3**, 894-899; (f) S. Kobayashi, P. Xu, T. Endo, M. Ueno and T. Kitanosono, *Angew. Chem. Int. Ed.*, 2012, **51**, 12763-12766; (g) L. Zhu, T. Kitanosono, P. Xu and S. Kobayashi, *Chem. Commun.*, 2015, **51**, 11685-11688; (h) K. Kubota, K. Hayama, H. Iwamoto and H. Ito, *Angew. Chem. Int. Ed.*, 2015, **54**, 8809-8813; (i) D. Hemming, R. Fritzscheier, S. A. Westcott, W. L. Santos and P. G. Steel, *Chem. Soc. Rev.*, 2018, **47**, 7477-7494; (j) Y. G. Lawson, M. J. G. Lesley, N. C. Norman, C. R. Rice and T. B. Marder, *Chem. Commun.*, 1997, 2051-2052; (k) N. J. Bell, A. J. Cox, N. R. Cameron, J. S. O. Evans, T. B. Marder, M. A. Duin, C. J. Elsevier, X. Baucherel, A. A. D. Tulloch and R. P. Tooze, *Chem. Commun.*, 2004, 1854-1855; (l) B. Liu, M. Gao, L. Dang, H. Zhao, T. B. Marder and Z. Lin, *Organometallics*, 2012, **31**, 3410-3425.
37. (a) L. Chen, X. Zou, H. Zhao and S. Xu, *Org. Lett.*, 2017, **19**, 3676-3679; (b) A. López, T. B. Clark, A. Parra and M. Tortosa, *Org. Lett.*, 2017, **19**, 6272-6275.
38. D. Nishikawa, K. Hirano and M. Miura, *J. Am. Chem. Soc.*, 2015, **137**, 15620-15623.
39. D. Nishikawa, K. Hirano and M. Miura, *Org. Lett.*, 2016, **18**, 4856-4859.
40. D.-W. Gao, Y. Gao, H. Shao, T.-Z. Qiao, X. Wang, B. Sanchez, J. Chen, P. Liu and K. Engle, *ChemRxiv*, 2019, DOI: 10.26434/chemrxiv.7961633.
41. (a) C.-X. Zhuo, W. Zhang and S.-L. You, *Angew. Chem. Int. Ed.*, 2012, **51**, 12662-12686; (b) Q. Ding, X. Zhou and R. Fan, *Org. Biomol. Chem.*, 2014, **12**, 4807-4815; (c) C.-X. Zhuo, C. Zheng and S.-L. You, *Acc. Chem. Res.*, 2014, **47**, 2558-2573.
42. L. Chen, J. Shen, Q. Gao and S. Xu, *Chem. Sci.*, 2018, **9**, 5855-5859.
43. (a) M. Ishikura and M. Terashima, *J. Chem. Soc., Chem. Commun.*, 1991, 1219-1221; (b) M. Ishikura and I. Agata, *Heterocycles*, 1996, **43**, 1591-1595; (c) M. Ishikura and H. Kato, *Tetrahedron*, 2002, **58**, 9827-9838; (d) M. Ishikura, W. Ida and K. Yanada, *Tetrahedron*, 2006, **62**, 1015-1024.
44. S. Panda and J. M. Ready, *J. Am. Chem. Soc.*, 2017, **139**, 6038-6041.
45. S. Das, C. G. Daniliuc and A. Studer, *Angew. Chem. Int. Ed.*, 2018, **57**, 4053-4057.
46. S. Kawamorita, T. Miyazaki, T. Iwai, H. Ohmiya and M. Sawamura, *J. Am. Chem. Soc.*, 2012, **134**, 12924-12927.
47. (a) T. Iwai, T. Harada, K. Hara and M. Sawamura, *Angew. Chem. Int. Ed.*, 2013, **52**,

- 12322-12326; (b) T. Iwai, R. Murakami, T. Harada, S. Kawamorita and M. Sawamura, *Adv. Synth. Catal.*, 2014, **356**, 1563-1570.
48. Q. Li, C. W. Liskey and J. F. Hartwig, *J. Am. Chem. Soc.*, 2014, **136**, 8755-8765.
49. G. Wang, L. Liu, H. Wang, Y.-S. Ding, J. Zhou, S. Mao and P. Li, *J. Am. Chem. Soc.*, 2017, **139**, 91-94.
50. T. Nakamura, K. Suzuki and M. Yamashita, *J. Am. Chem. Soc.*, 2017, **139**, 17763-17766.
51. S. N. Hyland, E. A. Meck, M. Tortosa and T. B. Clark, *Tetrahedron Lett.*, 2019, **60**, 1096-1098.
52. Q. Qi, X. Yang, X. Fu, S. Xu and E. Negishi, *Angew. Chem. Int. Ed.*, 2018, **57**, 15138-15142.
53. J. D. St. Denis, C. F. Lee and A. K. Yudin, *Org. Lett.*, 2015, **17**, 5764-5767.
54. F. Berrée, N. Gernigon, A. Hercouet, C. H. Lin and B. Carboni, *Eur. J. Org. Chem.*, 2009, **2009**, 329-333.
55. J. Pietruszka, N. Schöne, W. Frey and L. Grundl, *Chem. Eur. J.*, 2008, **14**, 5178-5197.
56. S. Touchet, A. Macé, T. Roisnel, F. Carreaux, A. Bouillon and B. Carboni, *Org. Lett.*, 2013, **15**, 2712-2715.
57. S. Touchet, F. Carreaux, G. A. Molander, B. Carboni and A. Bouillon, *Adv. Synth. Catal.*, 2011, **353**, 3391-3396.
58. (a) Z. He, A. Zajdlik, J. D. St. Denis, N. Assem and A. K. Yudin, *J. Am. Chem. Soc.*, 2012, **134**, 9926-9929; (b) A. Zajdlik, Z. He, J. D. St. Denis and A. K. Yudin, *Synthesis*, 2014, **46**, 445-454.
59. A. Zajdlik, Z. Wang, J. L. Hickey, A. Aman, A. D. Schimmer and A. K. Yudin, *Angew. Chem. Int. Ed.*, 2013, **52**, 8411-8415.
60. F. K. Scharnagl, S. K. Bose and T. B. Marder, *Org. Biomol. Chem.*, 2017, **15**, 1738-1752.
61. D. B. Diaz, C. C. G. Scully, S. K. Liew, S. Adachi, P. Trinchera, J. D. St. Denis and A. K. Yudin, *Angew. Chem. Int. Ed.*, 2016, **55**, 12659-12663.
62. T. Shiro, A. Schuhmacher, M. K. Jackl and J. W. Bode, *Chem. Sci.*, 2018, **9**, 5191-5196.
63. B. Zheng, L. Deloux, S. Pereira, E. Skrzypczak-Jankun, B. V. Cheesman, M. Sabat and M. Srebnik, *Appl. Organomet. Chem.*, 1996, **10**, 267-278.
64. S. Nishino, K. Hirano and M. Miura, *Org. Lett.*, 2019, **21**, 4759-4762.
65. C. Li, J. Wang, L. M. Barton, S. Yu, M. Tian, D. S. Peters, M. Kumar, A. W. Yu, K. A. Johnson, A. K. Chatterjee, M. Yan and P. S. Baran, *Science*, 2017, **356**, eaam7355.
66. J. Chen, L.-y. Chen, Y. Zheng and Z. Sun, *RSC Adv.*, 2014, **4**, 21131-21133.
67. G. A. Molander and D. L. Sandrock, *Org. Lett.*, 2007, **9**, 1597-1600.
68. G. A. Molander, P. E. Gormisky and D. L. Sandrock, *J. Org. Chem.*, 2008, **73**, 2052-2057.

69. G. A. Molander and I. Shin, *Org. Lett.*, 2011, **13**, 3956-3959.
70. G. A. Molander and I. Shin, *Org. Lett.*, 2012, **14**, 3138-3141.
71. G. A. Molander and I. Shin, *Org. Lett.*, 2013, **15**, 2534-2537.
72. G. A. Molander and I. Shin, *Org. Lett.*, 2012, **14**, 4458-4461.
73. (a) O. Toshimichi, A. Tomotsugu and S. Michinori, *Chem. Lett.*, 2009, **38**, 664-665; (b) T. Ohmura, T. Awano and M. Sugimoto, *J. Am. Chem. Soc.*, 2010, **132**, 13191-13193.
74. T. Awano, T. Ohmura and M. Sugimoto, *J. Am. Chem. Soc.*, 2011, **133**, 20738-20741.
75. T. Ohmura, K. Miwa, T. Awano and M. Sugimoto, *Chem. Asian J.*, 2018, **13**, 2414-2417.
76. C. J. Opalka, T. E. Dambra, J. J. Faccione, G. Bodson and E. Cossement, *Synthesis*, 1995, **1995**, 766-768.
77. A. M. Dumas, A. J. Sieradzki and L. J. Donnelly, *Org. Lett.*, 2016, **18**, 1848-1851.
78. A. W. Buesking and J. A. Ellman, *Chem. Sci.*, 2014, **5**, 1983-1987.
79. J. C. Tellis, C. B. Kelly, D. N. Primer, M. Jouffroy, N. R. Patel and G. A. Molander, *Acc. Chem. Res.*, 2016, **49**, 1429-1439.
80. K. Miyazawa, T. Koike and M. Akita, *Adv. Synth. Catal.*, 2014, **356**, 2749-2755.
81. M. El Khatib, R. A. M. Serafim and G. A. Molander, *Angew. Chem. Int. Ed.*, 2016, **55**, 254-258.
82. X. Wang, G. H. M. Davies, A. Koschitzky, S. R. Wisniewski, C. B. Kelly and G. A. Molander, *Org. Lett.*, 2019, **21**, 2880-2884.
83. (a) S. Roesner, D. J. Blair and V. K. Aggarwal, *Chem. Sci.*, 2015, **6**, 3718-3723; (b) P. A. Cox, A. G. Leach, A. D. Campbell and G. C. Lloyd-Jones, *J. Am. Chem. Soc.*, 2016, **138**, 9145-9157; (c) P. A. Cox, M. Reid, A. G. Leach, A. D. Campbell, E. J. King and G. C. Lloyd-Jones, *J. Am. Chem. Soc.*, 2017, **139**, 13156-13165.
84. K. Arnold, A. S. Batsanov, B. Davies, C. Grosjean, T. Schütz, A. Whiting and K. Zawatzky, *Chem. Commun.*, 2008, 3879-3881.
85. J. Llaveria, D. Leonori and V. K. Aggarwal, *J. Am. Chem. Soc.*, 2015, **137**, 10958-10961.
86. (a) H. Witte, P. Mischke and G. Hesse, *Liebigs Ann. Chem.*, 1969, **722**, 21-28; (b) D. S. Matteson and D. Majumdar, *J. Organomet. Chem.*, 1979, **170**, 259-264; (c) G. B. Fisher, J. J. Juarez-Brambila, C. T. Goralski, W. T. Wipke and B. Singaram, *J. Am. Chem. Soc.*, 1993, **115**, 440-444.
87. C. Laplante and D. G. Hall, *Org. Lett.*, 2001, **3**, 1487-1490.
88. *Synthesis and Application of Organoboron Compounds*, eds. E. Fernández and A. Whiting, Springer, Berlin, 2015.
89. L. R. Dick and P. E. Fleming, *Drug Discovery Today*, 2010, **15**, 243-249.
90. (a) <https://www.velcade.com> (accessed November 2019); (b) R. C. Kane, P. F. Bross, A. T. Farrell and R. Pazdur, *Oncologist*, 2003, **8**, 508-513.
91. (a) D. S. Laitar, E. Y. Tsui and J. P. Sadighi, *J. Am. Chem. Soc.*, 2006, **128**, 11036-

- 11037; (b) H. Zhao, L. Dang, T. B. Marder and Z. Lin, *J. Am. Chem. Soc.*, 2008, **130**, 5586-5594.
92. During optimization of the reaction, byproducts R-NHBpin or R-N(Bpin)₂ were detected by GC-MS.
93. For experimental and DFT studies of copper(I) boryl complexes being nucleophiles, see, for examples: (a) T. B. Marder, in *Organometallic Chemistry*, The Royal Society of Chemistry, Cambridge, U.K., 2008, pp. 46-57; (b) L. Dang, Z. Lin and T. B. Marder, *Chem. Commun.*, 2009, 3987-3995; (c) D. S. Laitar, P. Muller and J. P. Sadighi, *J. Am. Chem. Soc.*, 2005, **127**, 17196-17197; (d) H. Zhao, Z. Lin and T. B. Marder, *J. Am. Chem. Soc.*, 2006, **128**, 15637-15643; (e) L. Dang, H. Zhao, Z. Lin and T. B. Marder, *Organometallics*, 2007, **26**, 2824-2832.
94. (a) W. Zhu and D. Ma, *Org. Lett.*, 2006, **8**, 261-263; (b) S. Ando, H. Matsunaga and T. Ishizuka, *J. Org. Chem.*, 2015, **80**, 9671-9681; (c) C.-T. Yang, Z.-Q. Zhang, H. Tajuddin, C.-C. Wu, J. Liang, J.-H. Liu, Y. Fu, M. Czyzewska, P. G. Steel, T. B. Marder and L. Liu, *Angew. Chem. Int. Ed.*, 2012, **51**, 528-532; (d) S. K. Bose, S. Brand, H. O. Omoregie, M. Haehnel, J. Maier, G. Bringmann and T. B. Marder, *ACS Catalysis*, 2016, **6**, 8332-8335.
95. G. Liu, D. A. Cogan, T. D. Owens, T. P. Tang and J. A. Ellman, *J. Org. Chem.*, 1999, **64**, 1278-1284.
96. G. Sheldrick, *Acta Crystallogr.*, 2015, **A71**, 3-8.
97. G. Sheldrick, *Acta Crystallogr.*, 2008, **A64**, 112-122.
98. C. B. Hübschle, G. M. Sheldrick and B. Dittrich, *J. Appl. Crystallogr.*, 2011, **44**, 1281-1284.
99. Brandenburg, K. Diamond (version 4.4.0), Crystal and Molecular Structure Visualization, Crystal Impact, H. Putz & K. Brandenburg GbR, Bonn, 2017.
100. *Handbook of Boron Science with Applications in Organometallics, Catalysis, Materials and Medicine*, World Scientific Publishing Europe Ltd., London, 2018.
101. A. Šterman, I. Sosič, S. Gobec and Z. Časar, *Org. Chem. Front.*, 2019, **6**, 2991-2998.
102. (a) X. Li, Y.-K. Zhang, Y. Liu, C. Z. Ding, Q. Li, Y. Zhou, J. J. Plattner, S. J. Baker, X. Qian, D. Fan, L. Liao, Z.-J. Ni, G. V. White, J. E. Mordaunt, L. X. Lazarides, M. J. Slater, R. L. Jarvest, P. Thommes, M. Ellis, C. M. Edge, J. A. Hubbard, D. Somers, P. Rowland, P. Nassau, B. McDowell, T. J. Skarzynski, W. M. Kazmierski, R. M. Grimes, L. L. Wright, G. K. Smith, W. Zou, J. Wright and L. E. Pennicott, *Bioorg. Med. Chem. Lett.*, 2010, **20**, 3550-3556; (b) X. Li, Y.-K. Zhang, Y. Liu, C. Z. Ding, Y. Zhou, Q. Li, J. J. Plattner, S. J. Baker, S. Zhang, W. M. Kazmierski, L. L. Wright, G. K. Smith, R. M. Grimes, R. M. Crosby, K. L. Creech, L. H. Carballo, M. J. Slater, R. L. Jarvest, P. Thommes, J. A. Hubbard, M. A. Convery, P. M. Nassau, W. McDowell, T. J. Skarzynski, X. Qian, D. Fan, L. Liao, Z.-J. Ni, L. E. Pennicott, W. Zou and J. Wright, *Bioorg. Med. Chem. Lett.*, 2010, **20**, 5695-5700.

103. S. J. Hecker, K. R. Reddy, M. Totrov, G. C. Hirst, O. Lomovskaya, D. C. Griffith, P. King, R. Tsivkovski, D. Sun, M. Sabet, Z. Tarazi, M. C. Clifton, K. Atkins, A. Raymond, K. T. Potts, J. Abendroth, S. H. Boyer, J. S. Loutit, E. E. Morgan, S. Durso and M. N. Dudley, *J. Med. Chem.*, 2015, **58**, 3682-3692.
104. (a) J. Brem, R. Cain, S. Cahill, M. A. McDonough, I. J. Clifton, J.-C. Jiménez-Castellanos, M. B. Avison, J. Spencer, C. W. G. Fishwick and C. J. Schofield, *Nat. Comm.*, 2016, **7**, 12406; (b) S. T. Cahill, R. Cain, D. Y. Wang, C. T. Lohans, D. W. Wareham, H. P. Oswin, J. Mohammed, J. Spencer, C. W. G. Fishwick, M. A. McDonough, C. J. Schofield and J. Brem, *Antimicrob. Agents Chemother.*, 2017, **61**, e02260-02216; (c) S. T. Cahill, J. M. Tyrrell, I. H. Navratilova, K. Calvopiña, S. W. Robinson, C. T. Lohans, M. A. McDonough, R. Cain, C. W. G. Fishwick, M. B. Avison, T. R. Walsh, C. J. Schofield and J. Brem, *Biochim. Biophys. Acta*, 2019, **1863**, 742-748; (d) A. Krajnc, J. Brem, P. Hinchliffe, K. Calvopiña, T. D. Panduwawala, P. A. Lang, J. J. A. G. Kamps, J. M. Tyrrell, E. Widlake, B. G. Saward, T. R. Walsh, J. Spencer and C. J. Schofield, *J. Med. Chem.*, 2019, **62**, 8544-8556; (e) G. W. Langley, R. Cain, J. M. Tyrrell, P. Hinchliffe, K. Calvopiña, C. L. Tooke, E. Widlake, C. G. Dowson, J. Spencer, T. R. Walsh, C. J. Schofield and J. Brem, *Bioorg. Med. Chem. Lett.*, 2019, **29**, 1981-1984.
105. D. Fan, R. L. Jarvest, L. Lazarides, Q. Li, X. Li, Y. Liu, L. Liao, J. E. Mordaunt, Z.-J. Ni, J. Plattner, X. Qian, M. J. Slater, G. V. White and Y. K. Zhang, *World Pat.*, WO2009046098A1, 2009.
106. C. Capello, U. Fischer and K. Hungerbühler, *Green Chem.*, 2007, **9**, 927-934.
107. Due to its physicochemical and drug-like properties, benzoxaborole is a privileged structure in medicinal chemistry, which has been widely applied as antifungal, antibacterial, antiviral, antiparasitic, and antiinflammatory agents. See: (a) S. J. Baker, Y.-K. Zhang, T. Akama, A. Lau, H. Zhou, V. Hernandez, W. Mao, M. R. K. Alley, V. Sanders and J. J. Plattner, *J. Med. Chem.*, 2006, **49**, 4447-4450; (b) F. L. Rock, W. Mao, A. Yaremchuk, M. Tukalo, T. Crépin, H. Zhou, Y.-K. Zhang, V. Hernandez, T. Akama, S. J. Baker, J. J. Plattner, L. Shapiro, S. A. Martinis, S. J. Benkovic, S. Cusack and M. R. K. Alley, *Science*, 2007, **316**, 1759-1761; (c) Q.-H. Hu, R.-J. Liu, Z.-P. Fang, J. Zhang, Y.-Y. Ding, M. Tan, M. Wang, W. Pan, H.-C. Zhou and E.-D. Wang, *Sci. Rep.*, 2013, **3**, 2475; (d) J. Zhang, M. Zhu, Y. Lin and H. Zhou, *Sci. China Chem.*, 2013, **56**, 1372-1381; (e) E. Sonoiki, C. L. Ng, M. C. S. Lee, D. Guo, Y.-K. Zhang, Y. Zhou, M. R. K. Alley, V. Ahyong, L. M. Sanz, M. J. Lafuente-Monasterio, C. Dong, P. G. Schupp, J. Gut, J. Legac, R. A. Cooper, F.-J. Gamo, J. DeRisi, Y. R. Freund, D. A. Fidock and P. J. Rosenthal, *Nat. Comm.*, 2017, **8**, 14574; (f) A. Nocentini, C. T. Supuran and J.-Y. Winum, *Expert Opin. Ther. Pat.*, 2018, **28**, 493-504.
108. A reported synthetic route¹⁰⁵ to benzoxaborole-derived α -amino cyclic boronates is outlined below.

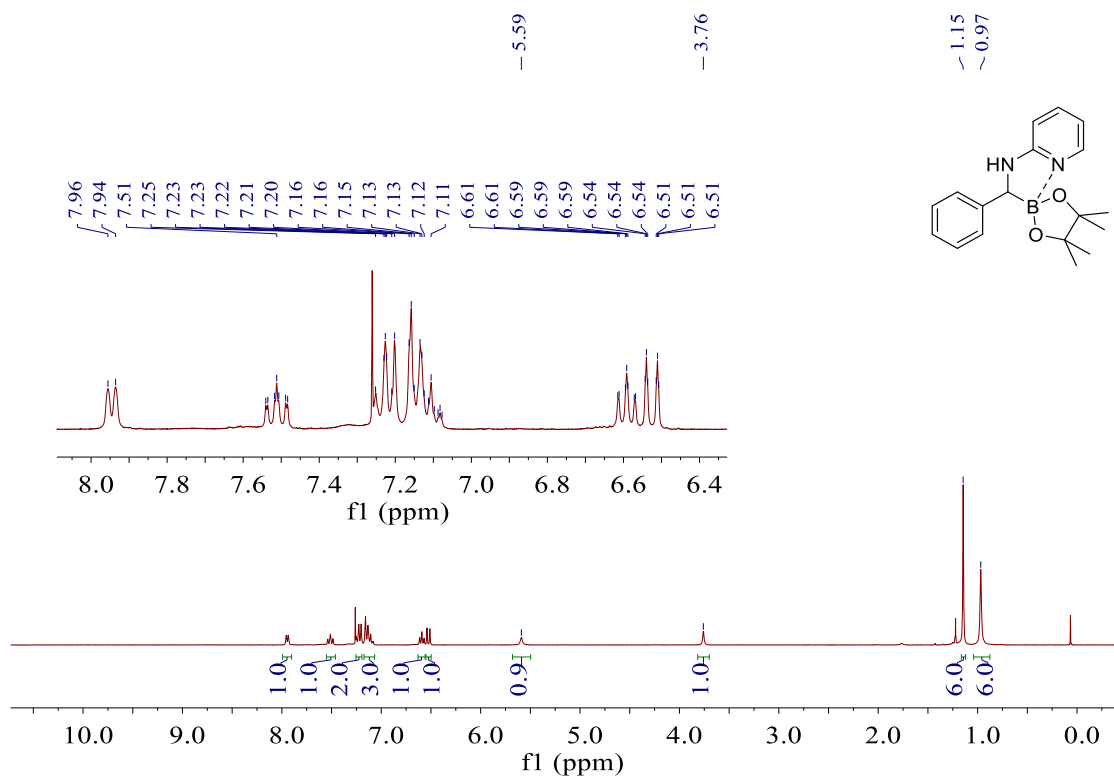
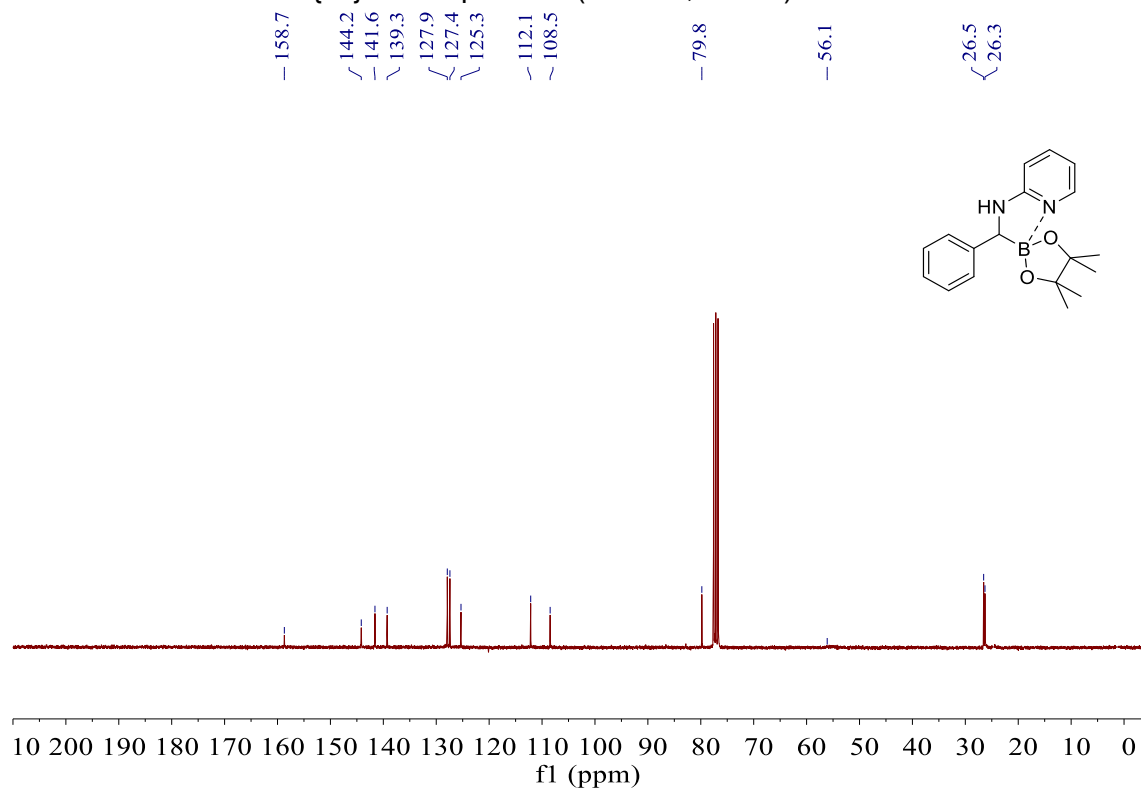


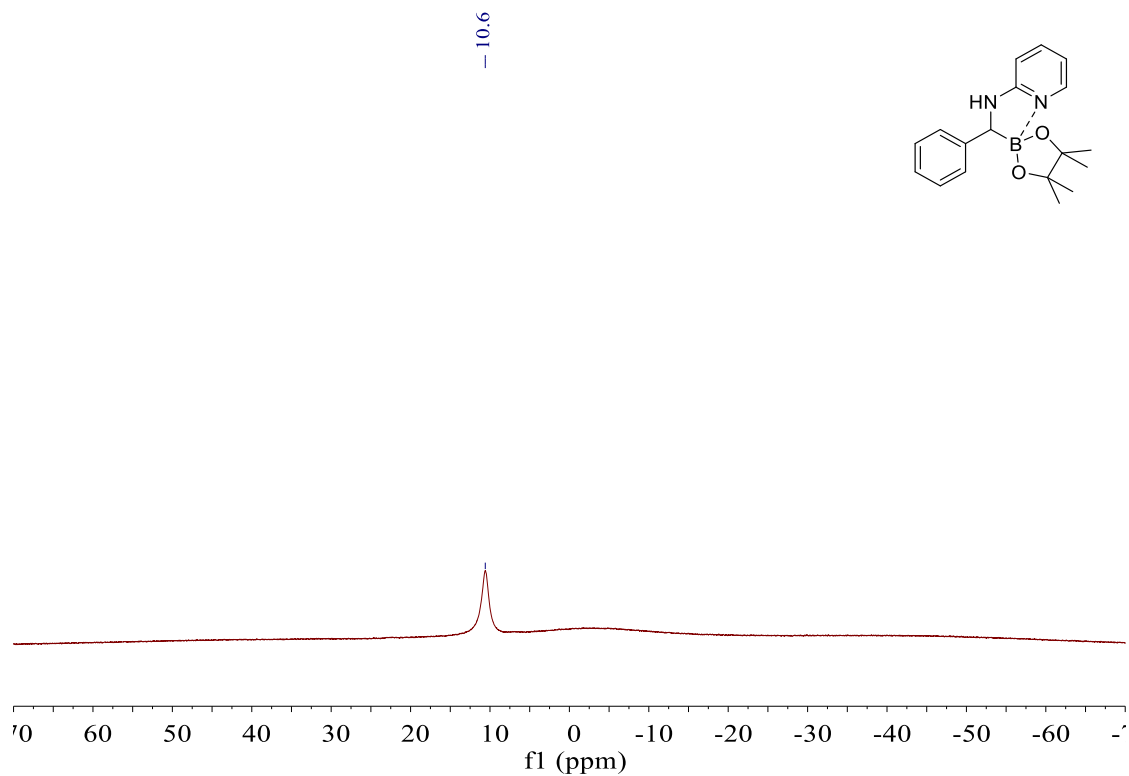
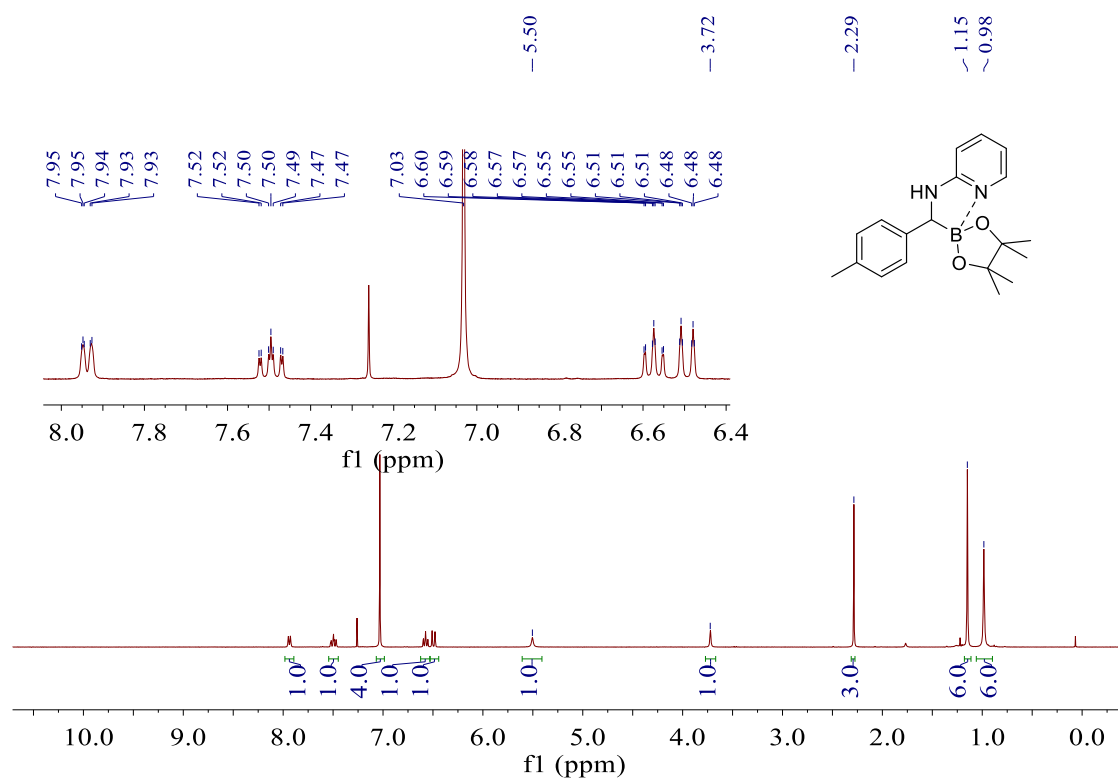
109. (a) N. A. Petasis and S. Boral, *Tetrahedron Lett.*, 2001, **42**, 539-542; (b) Q. Wang and M. G. Finn, *Org. Lett.*, 2000, **2**, 4063-4065; (c) N. R. Candeias, F. Montalbano, P. M. Cal and P. M. Gois, *Chem. Rev.*, 2010, **110**, 6169-6193; (d) C. A. Guerrero and T. R. Ryder, in *Boron Reagents in Synthesis*, ed. A. Coca, American Chemical Society, Washington DC, 2016, ch. 9, pp. 275-311; (e) P. Wu, M. Givskov and T. E. Nielsen, *Chem. Rev.*, 2019, **119**, 11245-11290.
110. D. S. Matteson, *J. Org. Chem.*, 1962, **27**, 3712-3712.
111. M. Raducan, R. Alam and K. J. Szabó, *Angew. Chem. Int. Ed.*, 2012, **51**, 13050-13053.
112. H. Nöth and G. Schmid, *Angew. Chem. Int. Ed.*, 1963, **2**, 623-623.
113. (a) S. Aldridge and D. L. Coombs, *Coord. Chem. Rev.*, 2004, **248**, 535-559; (b) H. Braunschweig and M. Colling, *Coord. Chem. Rev.*, 2001, **223**, 1-51; (c) H. Braunschweig, R. D. Dewhurst and A. Schneider, *Chem. Rev.*, 2010, **110**, 3924-3957; (d) H. Braunschweig, C. Kollann and D. Rais, *Angew. Chem. Int. Ed.*, 2006, **45**, 5254-5274; (e) G. J. Irvine, M. J. G. Lesley, T. B. Marder, N. C. Norman, C. R. Rice, E. G. Robins, W. R. Roper, G. R. Whittell and L. J. Wright, *Chem. Rev.*, 1998, **98**, 2685-2722.
114. R. T. Baker, D. W. Ovenall, J. C. Calabrese, S. A. Westcott, N. J. Taylor, I. D. Williams and T. B. Marder, *J. Am. Chem. Soc.*, 1990, **112**, 9399-9400.
115. J. R. Knorr and J. S. Merola, *Organometallics*, 1990, **9**, 3008-3010.
116. (a) R. T. Baker, J. C. Calabrese, S. A. Westcott, P. Nguyen and T. B. Marder, *J. Am. Chem. Soc.*, 1993, **115**, 4367-4368; (b) P. Nguyen, G. Lesley, N. J. Taylor, T. B. Marder, N. L. Pickett, W. Clegg, M. R. J. Elsegood and N. C. Norman, *Inorg. Chem.*, 1994, **33**, 4623-4624.
117. P. Nguyen, H. P. Blom, S. A. Westcott, N. J. Taylor and T. B. Marder, *J. Am. Chem. Soc.*, 1993, **115**, 9329-9330.
118. (a) Z. Lin, in *Computational Studies in Organometallic Chemistry*, eds. A. S. Macgregor and O. Eisenstein, Springer International Publishing, Cham, 2016, pp. 39-58; (b) G. R. Owen, *Chem. Commun.*, 2016, **52**, 10712-10726.
119. Y. Segawa, M. Yamashita and K. Nozaki, *J. Am. Chem. Soc.*, 2009, **131**, 9201-9203.
120. A. M. Spokoiny, M. G. Reuter, C. L. Stern, M. A. Ratner, T. Seideman and C. A. Mirkin, *J. Am. Chem. Soc.*, 2009, **131**, 9482-9483.
121. (a) Y. Segawa, M. Yamashita and K. Nozaki, *Organometallics*, 2009, **28**, 6234-6242;

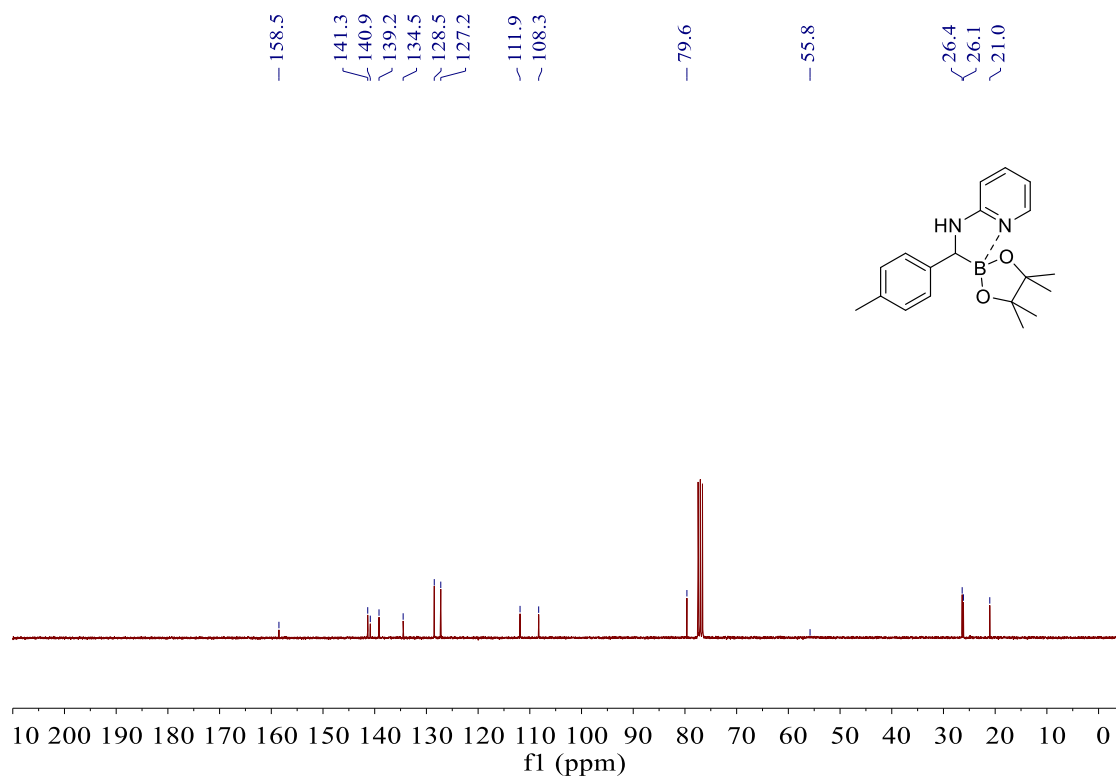
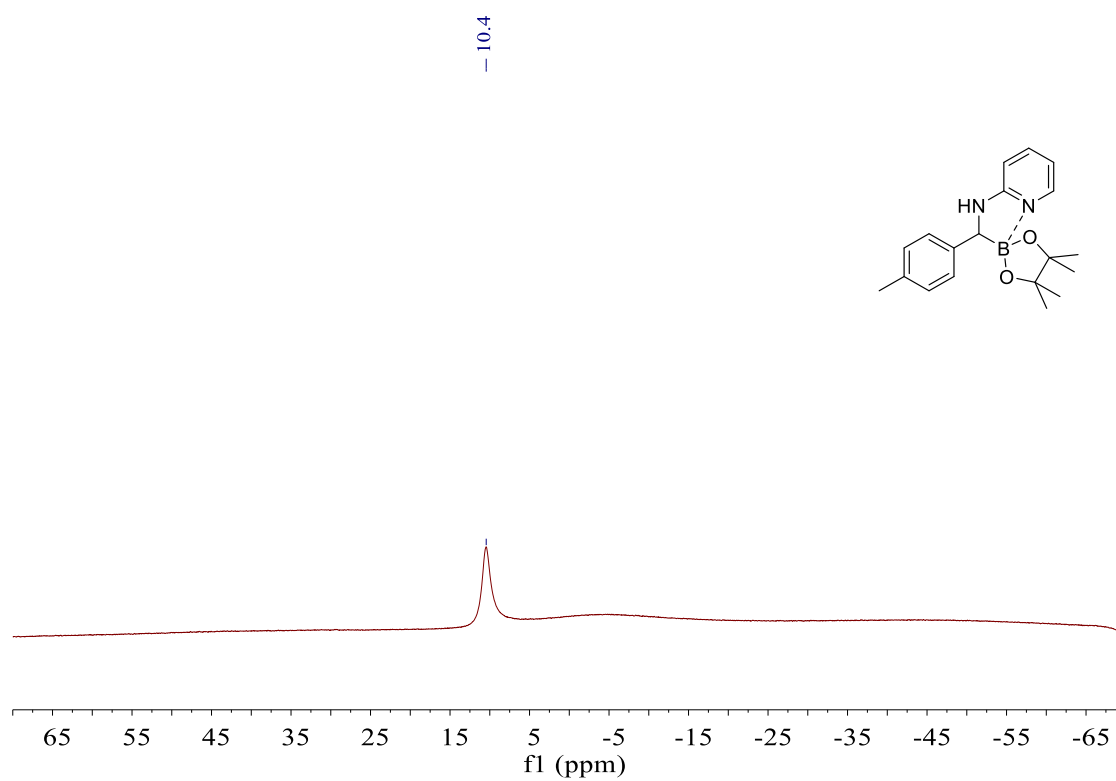
- (b) A. F. Hill, S. B. Lee, J. Park, R. Shang and A. C. Willis, *Organometallics*, 2010, **29**, 5661-5669; (c) M. Hasegawa, Y. Segawa, M. Yamashita and K. Nozaki, *Angew. Chem. Int. Ed.*, 2012, **51**, 6956-6960; (d) Y. Masuda, M. Hasegawa, M. Yamashita, K. Nozaki, N. Ishida and M. Murakami, *J. Am. Chem. Soc.*, 2013, **135**, 7142-7145; (e) T. Miyada and M. Yamashita, *Organometallics*, 2013, **32**, 5281-5284; (f) N. Curado, C. Maya, J. Lopez-Serrano and A. Rodriguez, *Chem. Commun.*, 2014, **50**, 15718-15721; (g) A. F. Hill and C. M. A. McQueen, *Organometallics*, 2014, **33**, 1977-1985; (h) D. Schuhknecht, F. Ritter and M. E. Tauchert, *Chem. Commun.*, 2016, **52**, 11823-11826; (i) W.-C. Shih, W. Gu, M. C. MacInnis, S. D. Timpa, N. Bhuvanesh, J. Zhou and O. V. Ozerov, *J. Am. Chem. Soc.*, 2016, **138**, 2086-2089.
122. (a) M. E. El-Zaria, H. Ariei and H. Nakamura, *Inorg. Chem.*, 2011, **50**, 4149-4161; (b) T.-P. Lin and J. C. Peters, *J. Am. Chem. Soc.*, 2013, **135**, 15310-15313; (c) H. Ogawa and M. Yamashita, *Dalton Trans.*, 2013, **42**, 625-629; (d) O. Hayato and Y. Makoto, *Chem. Lett.*, 2014, **43**, 664-666; (e) T.-P. Lin and J. C. Peters, *J. Am. Chem. Soc.*, 2014, **136**, 13672-13683; (f) T. Miyada, E. Huang Kwan and M. Yamashita, *Organometallics*, 2014, **33**, 6760-6770; (g) M. Y. Tsang, C. Viñas, F. Teixidor, J. G. Planas, N. Conde, R. SanMartin, M. T. Herrero, E. Domínguez, A. Lledós, P. Vidossich and D. Choquesillo-Lazarte, *Inorg. Chem.*, 2014, **53**, 9284-9295; (h) K. Tanoue and M. Yamashita, *Organometallics*, 2015, **34**, 4011-4017; (i) E. H. Kwan, Y. J. Kawai, S. Kamakura and M. Yamashita, *Dalton Trans.*, 2016, **45**, 15931-15941; (j) P. Rios, N. Curado, J. Lopez-Serrano and A. Rodriguez, *Chem. Commun.*, 2016, **52**, 2114-2117; (k) E. H. Kwan, H. Ogawa and M. Yamashita, *ChemCatChem*, 2017, **9**, 2457-2462; (l) W.-C. Shih and O. V. Ozerov, *J. Am. Chem. Soc.*, 2017, **139**, 17297-17300; (m) X. Huang, K. Zhang, Y. Shao, Y. Li, F. Gu, L.-B. Qu, C. Zhao and Z. Ke, *ACS Catalysis*, 2019, 5279-5289.
123. (a) J. Zhu, Z. Lin and T. B. Marder, *Inorg. Chem.*, 2005, **44**, 9384-9390; (b) J. Cid, J. J. Carbo and E. Fernandez, *Chem. Eur. J.*, 2012, **18**, 12794-12802; (c) H. Braunschweig, P. Brenner, A. Müller, K. Radacki, D. Rais and K. Uttinger, *Chem. Eur. J.*, 2007, **13**, 7171-7176; (d) Y. Segawa, M. Yamashita and K. Nozaki, *Angew. Chem. Int. Ed.*, 2007, **46**, 6710-6713; (e) H. Braunschweig, H. Green, K. Radacki and K. Uttinger, *Dalton Trans.*, 2008, 3531-3534; (f) H. Braunschweig, R. Leech, D. Rais, K. Radacki and K. Uttinger, *Organometallics*, 2008, **27**, 418-422; (g) H. Braunschweig, K. Radacki and K. Uttinger, *Chem. Eur. J.*, 2008, **14**, 7858-7866; (h) L. Dang, H. Zhao, Z. Lin and T. B. Marder, *Organometallics*, 2008, **27**, 1178-1186.
124. (a) L. Weber, *Coord. Chem. Rev.*, 2001, **215**, 39-77; (b) L. Weber, *Coord. Chem. Rev.*, 2008, **252**, 1-31.
125. (a) S. Kumar, G. Mani, S. Mondal and P. K. Chattaraj, *Inorg. Chem.*, 2012, **51**, 12527-12539; (b) F. Gorla, L. M. Venanzi and A. Albinati, *Organometallics*, 1994, **13**, 43-54.
126. J. Takaya, S. Nakamura and N. Iwasawa, *Chem. Lett.*, 2012, **41**, 967-969.

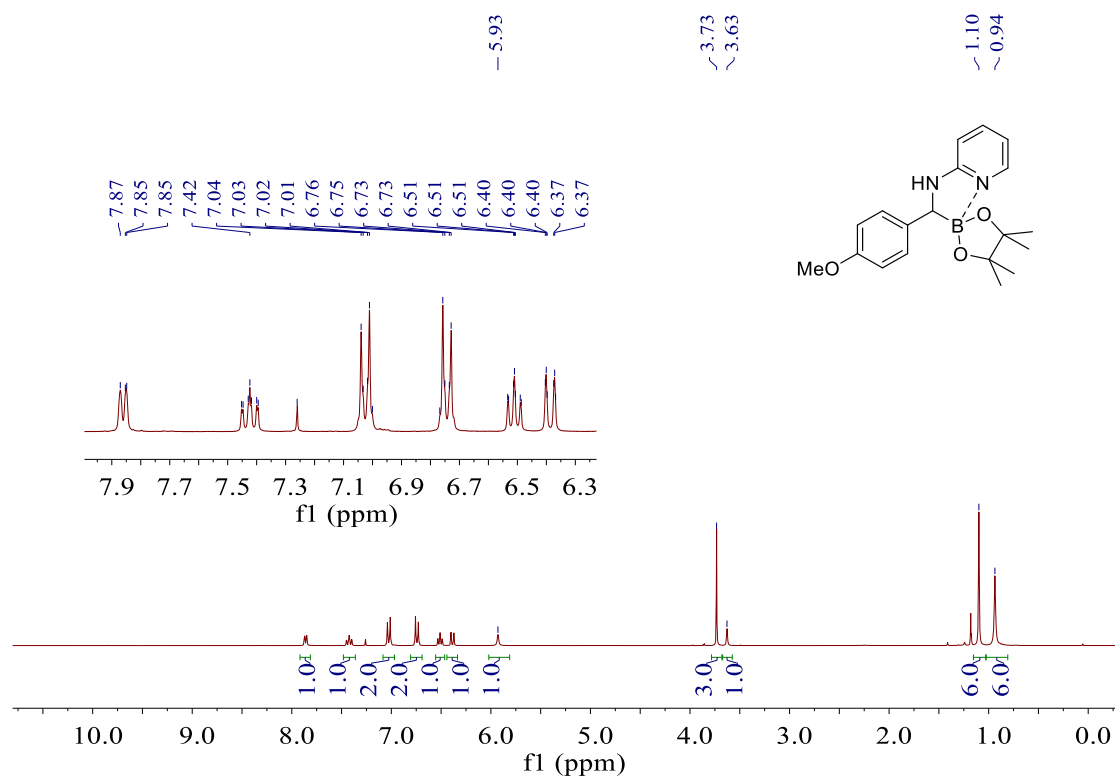
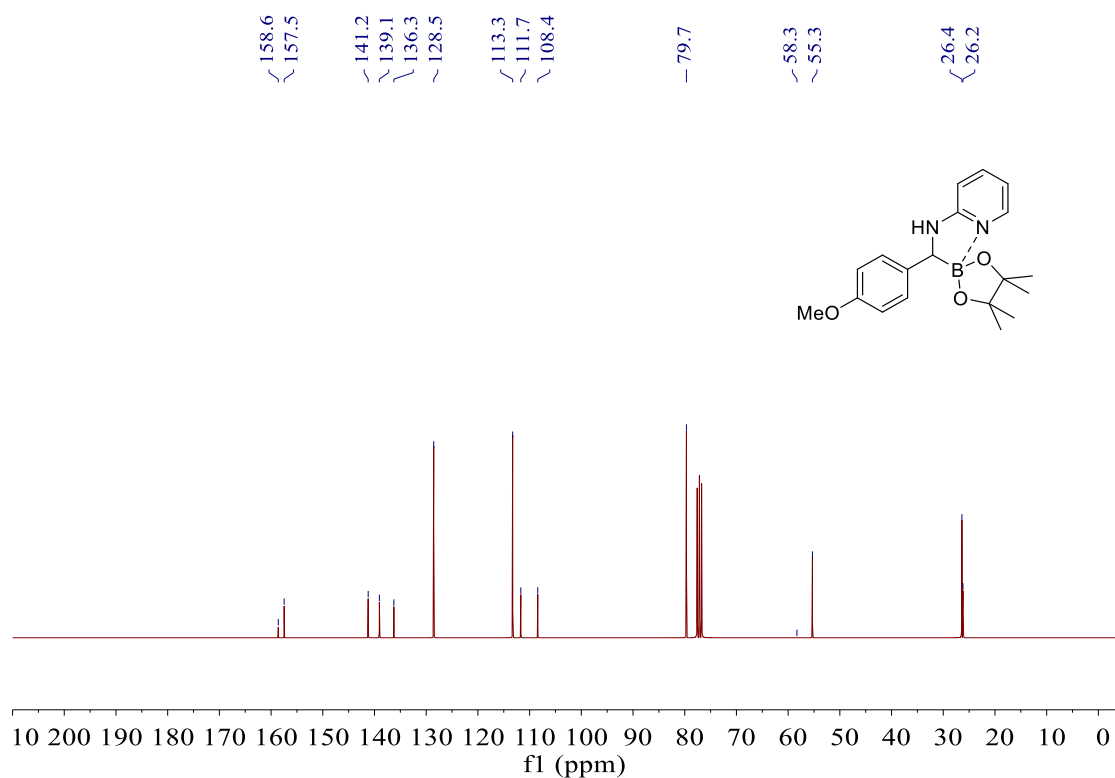
127. (a) P. Ren, O. Vechorkin, Z. Csok, I. Salihi, R. Scopelliti and X. Hu, *Dalton Trans.*, 2011, **40**, 8906-8911; (b) K. E. Neo, H. V. Huynh, L. L. Koh, W. Henderson and T. S. A. Hor, *Dalton Trans.*, 2007, 5701-5709; (c) J. Takaya and N. Iwasawa, *J. Am. Chem. Soc.*, 2008, **130**, 15254-15255.
128. N. Miyaura and A. Suzuki, *Chem. Rev.*, 1995, **95**, 2457-2483.
129. (a) N. Selander and K. J. Szabó, *Chem. Rev.*, 2011, **111**, 2048-2076; (b) D. Olsson and O. F. Wendt, *J. Organomet. Chem.*, 2009, **694**, 3112-3115; (c) J. Kjellgren, J. Aydin, O. A. Wallner, I. V. Saltanova and K. J. Szabó, *Chem. Eur. J.*, 2005, **11**, 5260-5268; (d) S. Bonnet, J. H. van Lenthe, M. A. Siegler, A. L. Spek, G. van Koten and R. J. M. K. Gebbink, *Organometallics*, 2009, **28**, 2325-2333.
130. J. Yang, Y. Wu, X. Wu, W. Liu, Y. Wang and J. Wang, *Green Chem.*, 2019, **21**, 5267-5273.
131. J. Kim and S. H. Hong, *ACS Catalysis*, 2017, **7**, 3336-3343.
132. C. Audubert and H. Lebel, *Org. Lett.*, 2017, **19**, 4407-4410.
133. C. Liu, Z.-X. Qin, C.-L. Ji, X. Hong and M. Szostak, *Chem. Sci.*, 2019, **10**, 5736-5742.

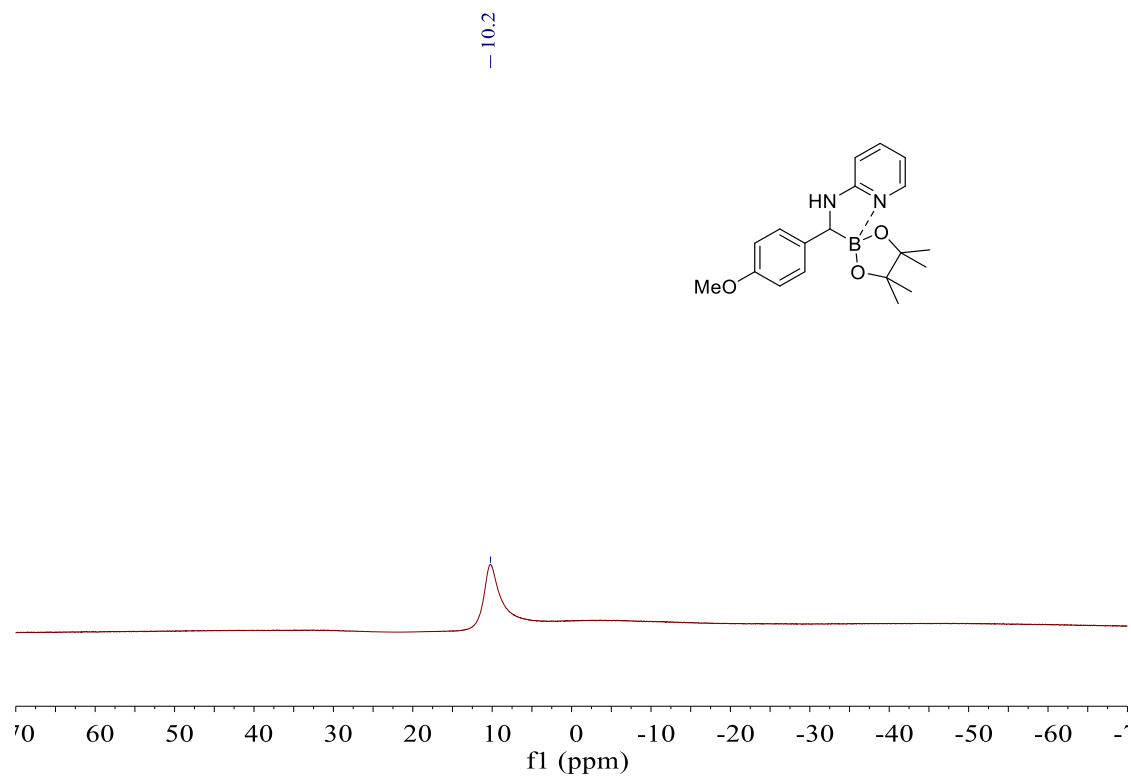
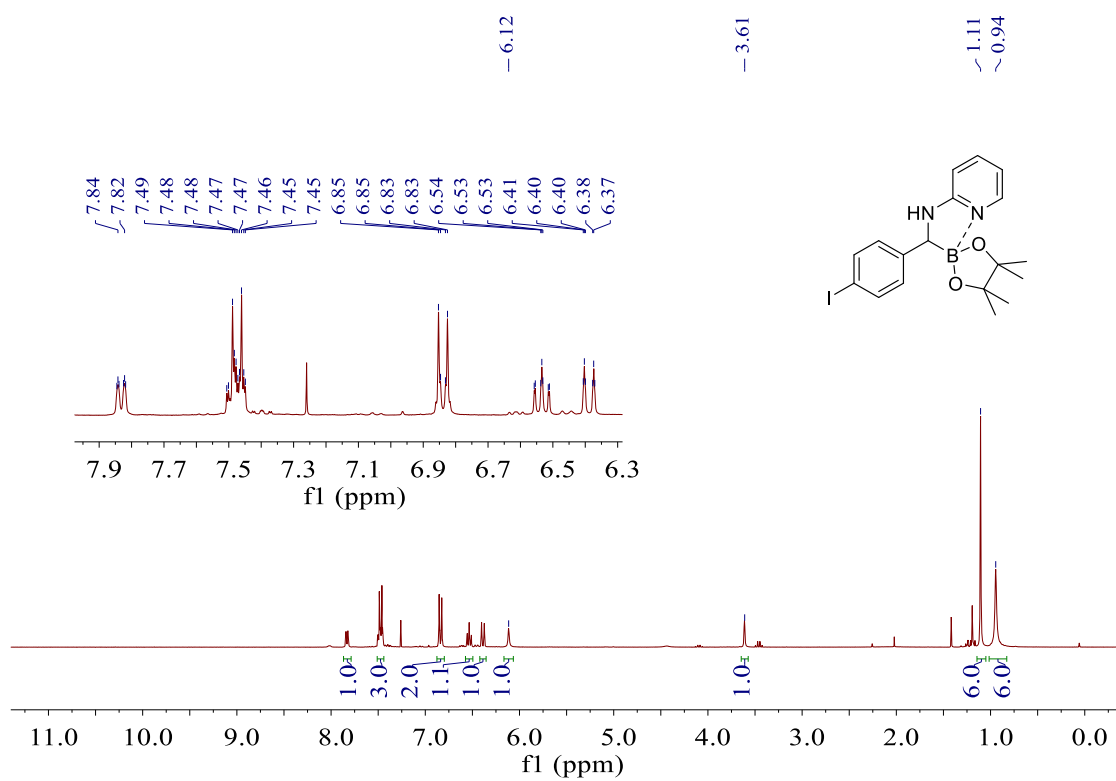
Appendix

 ^1H NMR spectrum (300 MHz, CDCl_3) of **2-3a** $^{13}\text{C}\{^1\text{H}\}$ NMR spectrum (75 MHz, CDCl_3) of **2-3a**

^{11}B NMR spectrum (96 MHz, CDCl_3) of **2-3a** ^1H NMR spectrum (300 MHz, CDCl_3) of **2-3b**

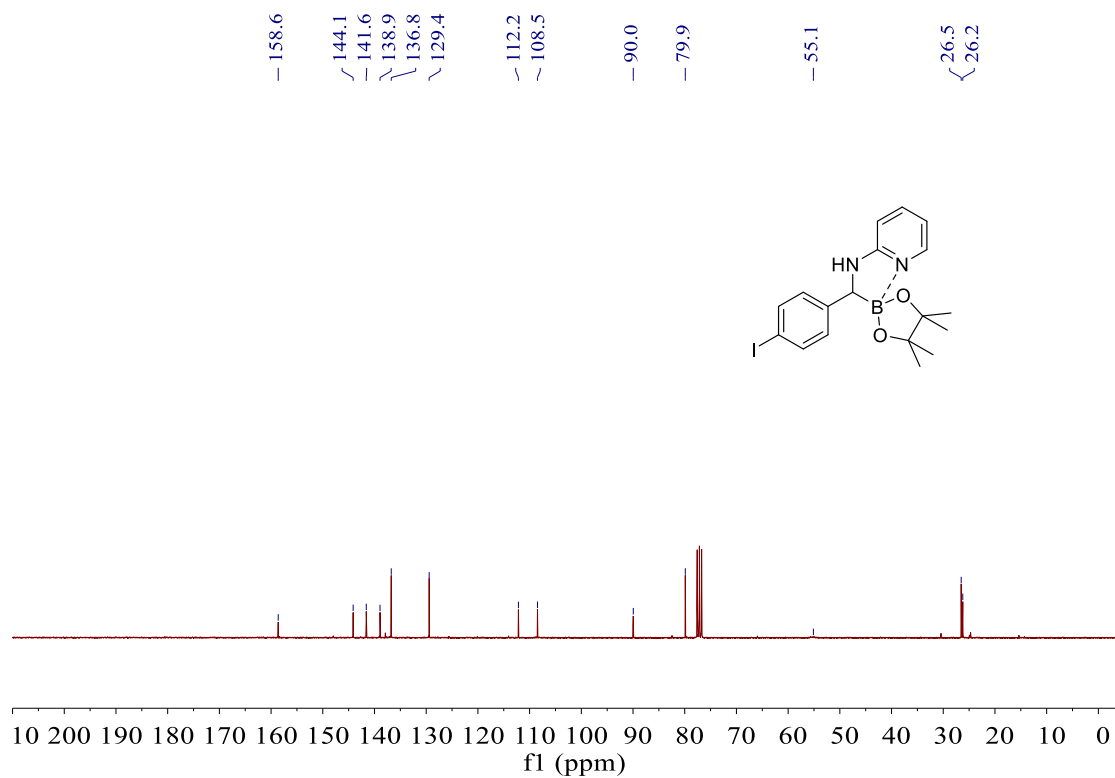
$^{13}\text{C}\{^1\text{H}\}$ NMR spectrum (75 MHz, CDCl_3) of **2-3b** ^{11}B NMR spectrum (96 MHz, CDCl_3) of **2-3b**

^1H NMR spectrum (300 MHz, CDCl_3) of **2-3c** $^{13}\text{C}\{^1\text{H}\}$ NMR spectrum (75 MHz, CDCl_3) of **2-3c**

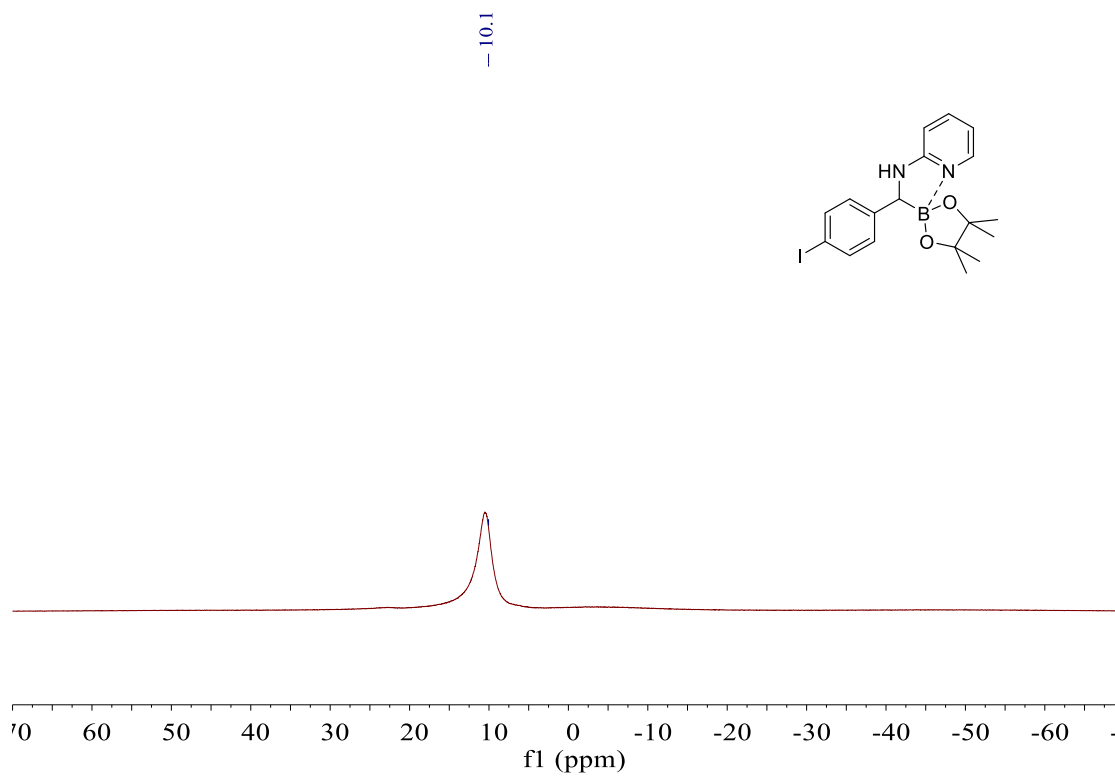
^{11}B NMR spectrum (96 MHz, CDCl_3) of **2-3c** ^1H NMR spectrum (300 MHz, CDCl_3) of **2-3d**

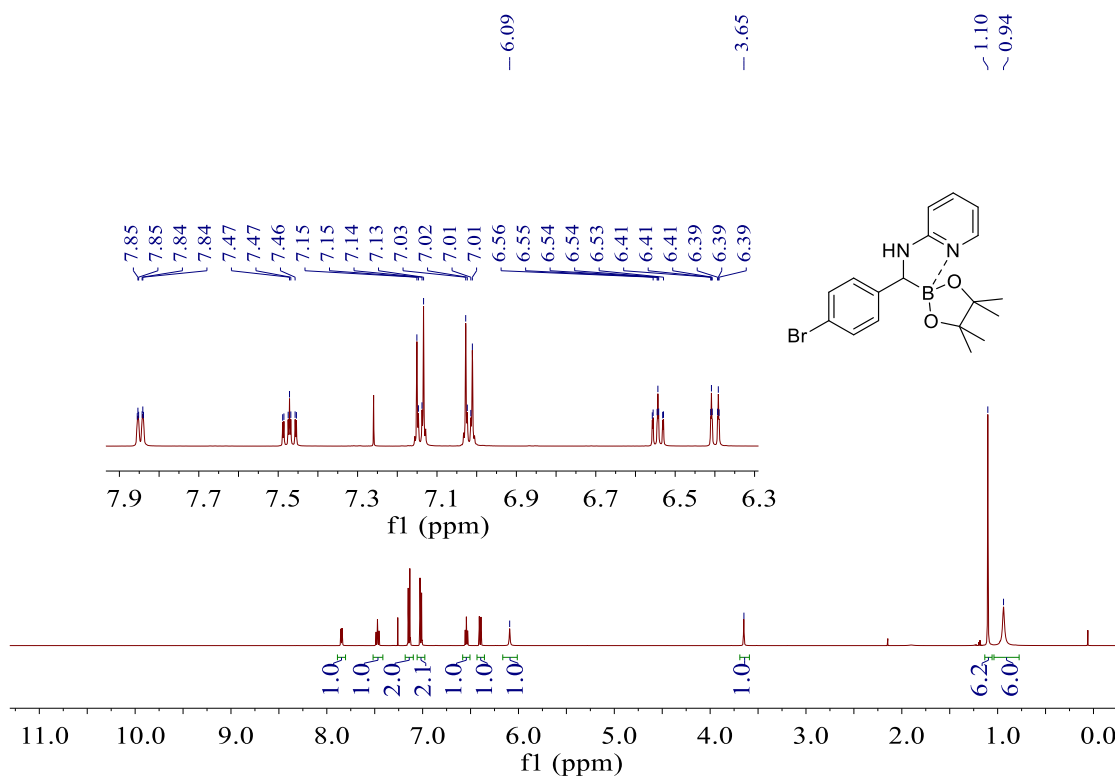
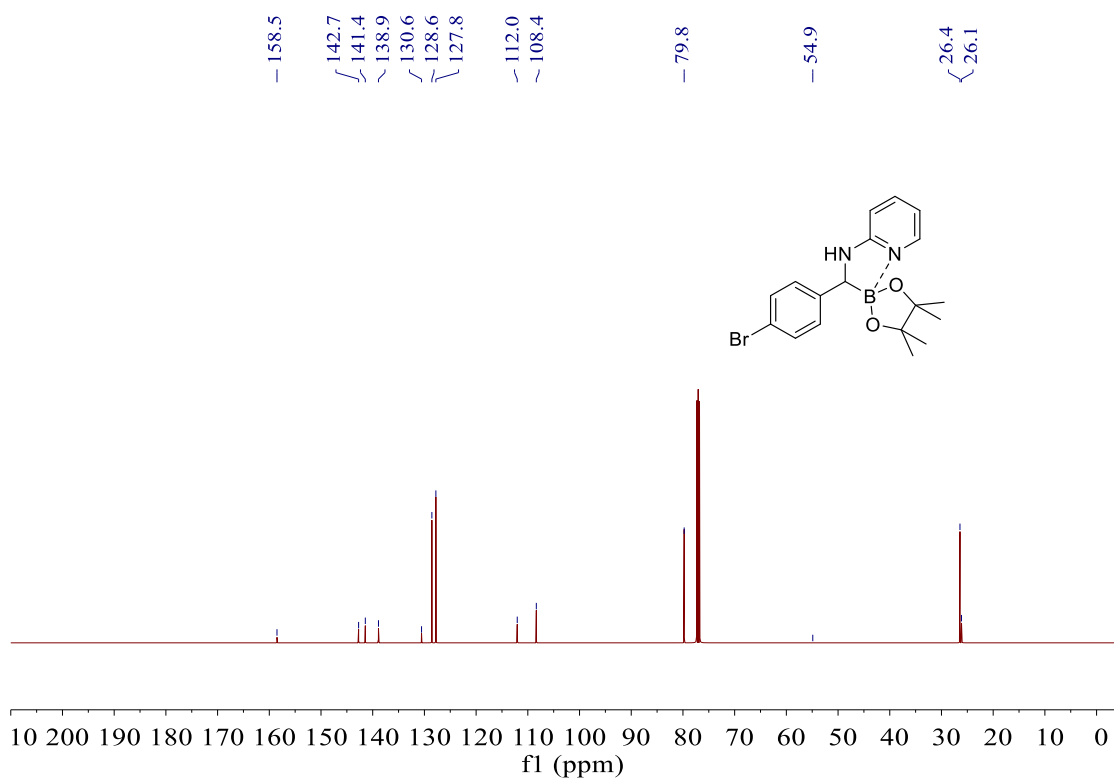
Appendix

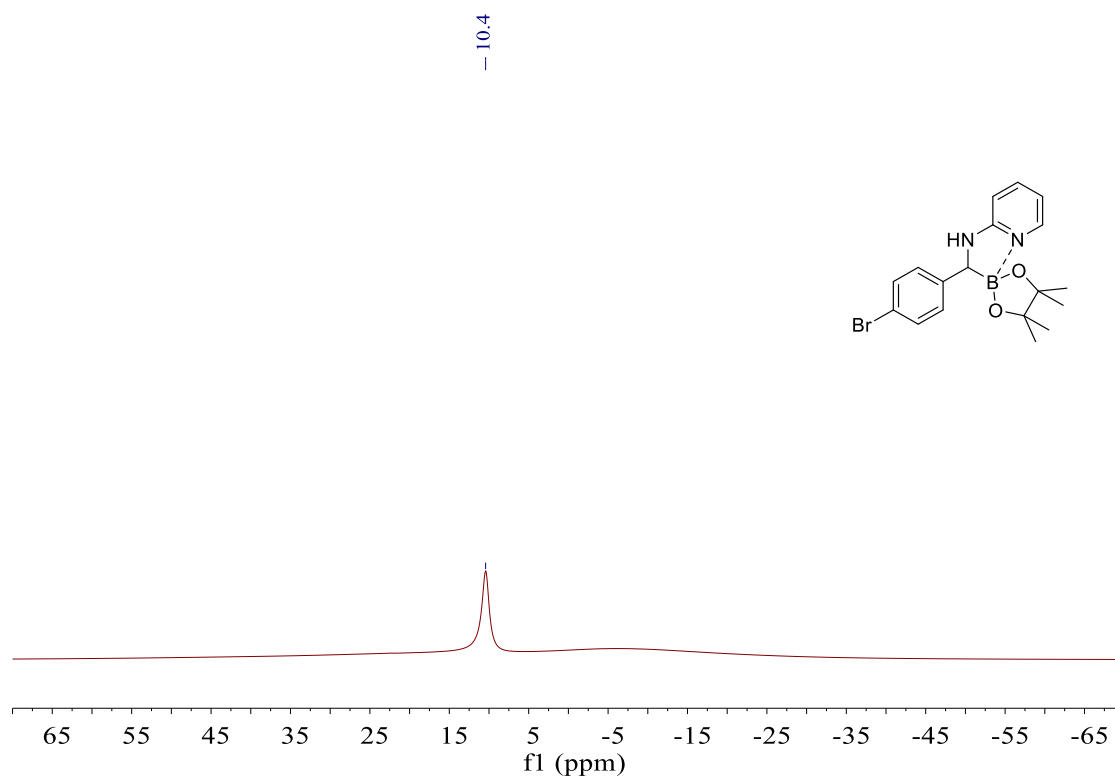
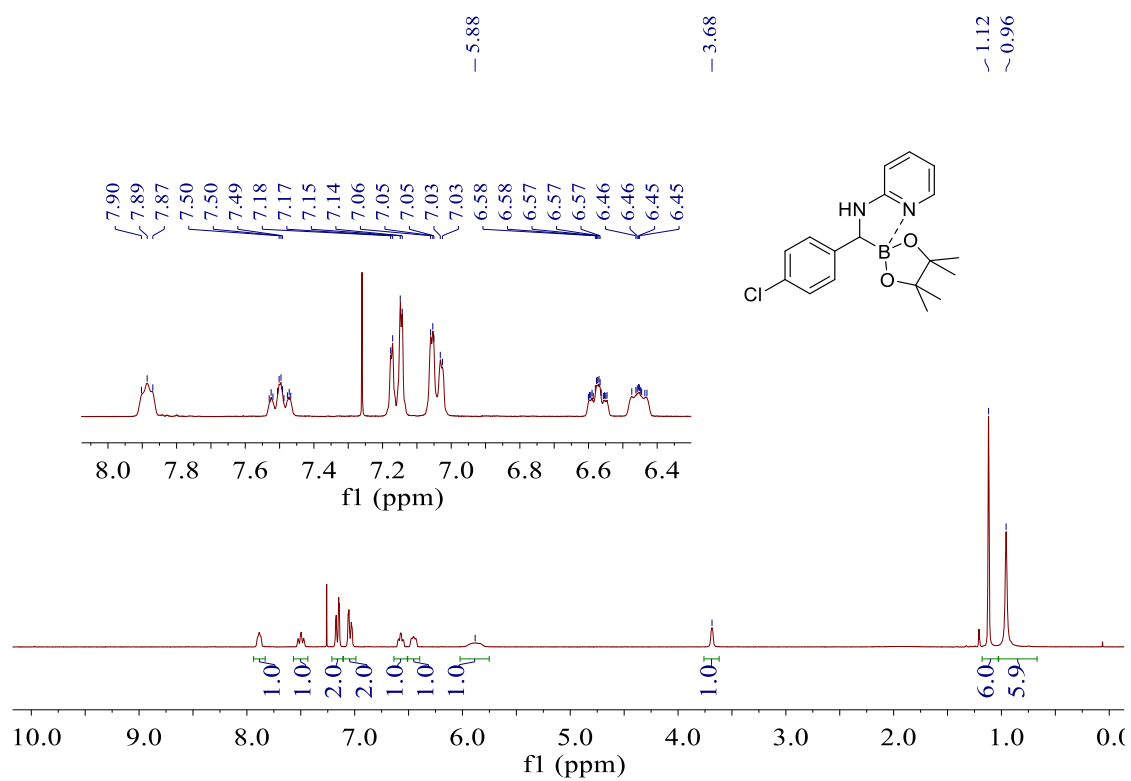
$^{13}\text{C}\{^1\text{H}\}$ NMR spectrum (75 MHz, CDCl_3) of **2-3d**

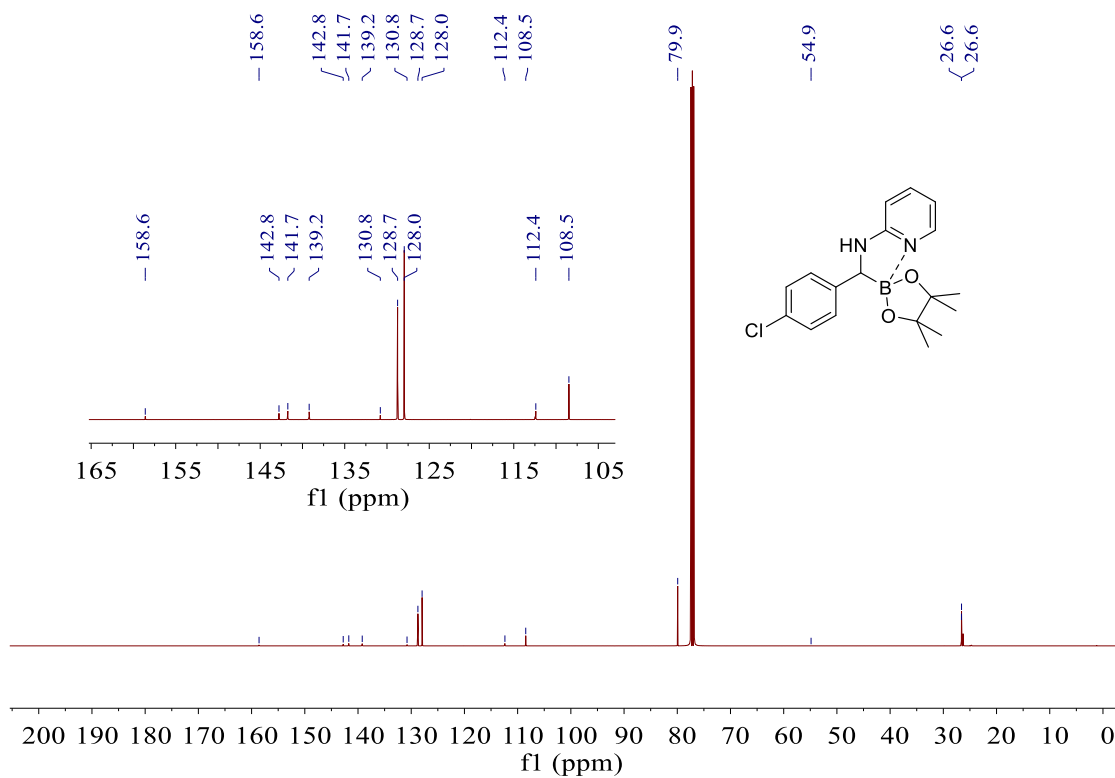
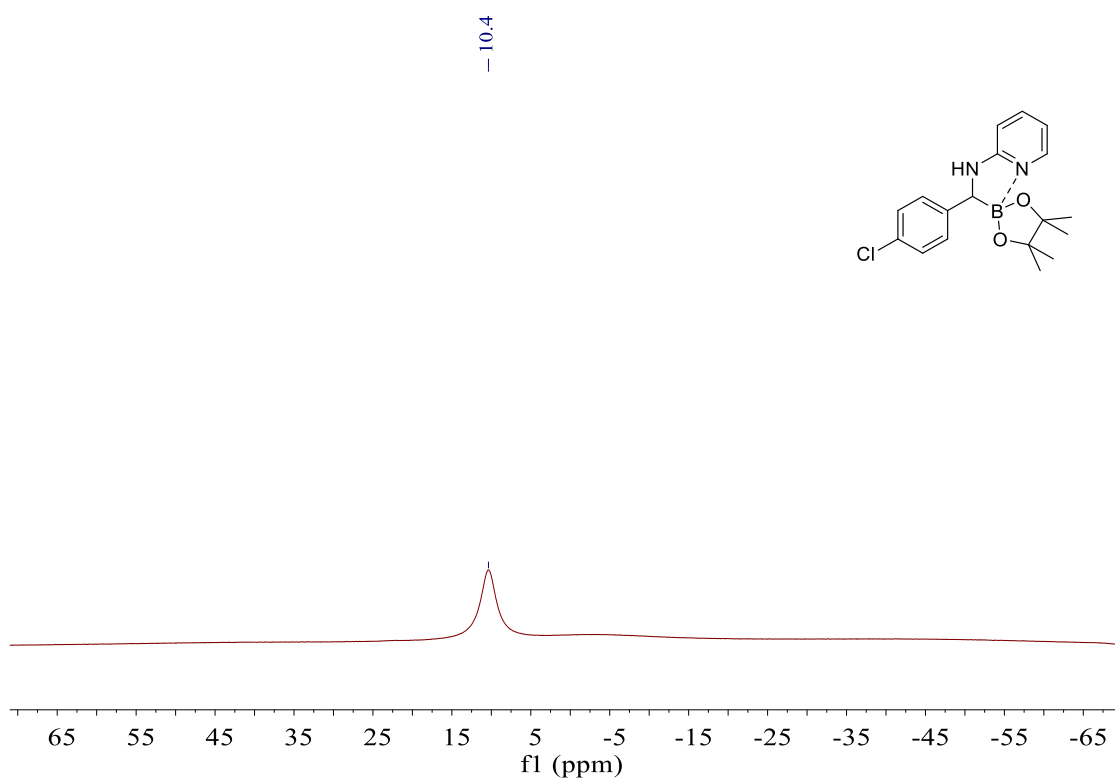


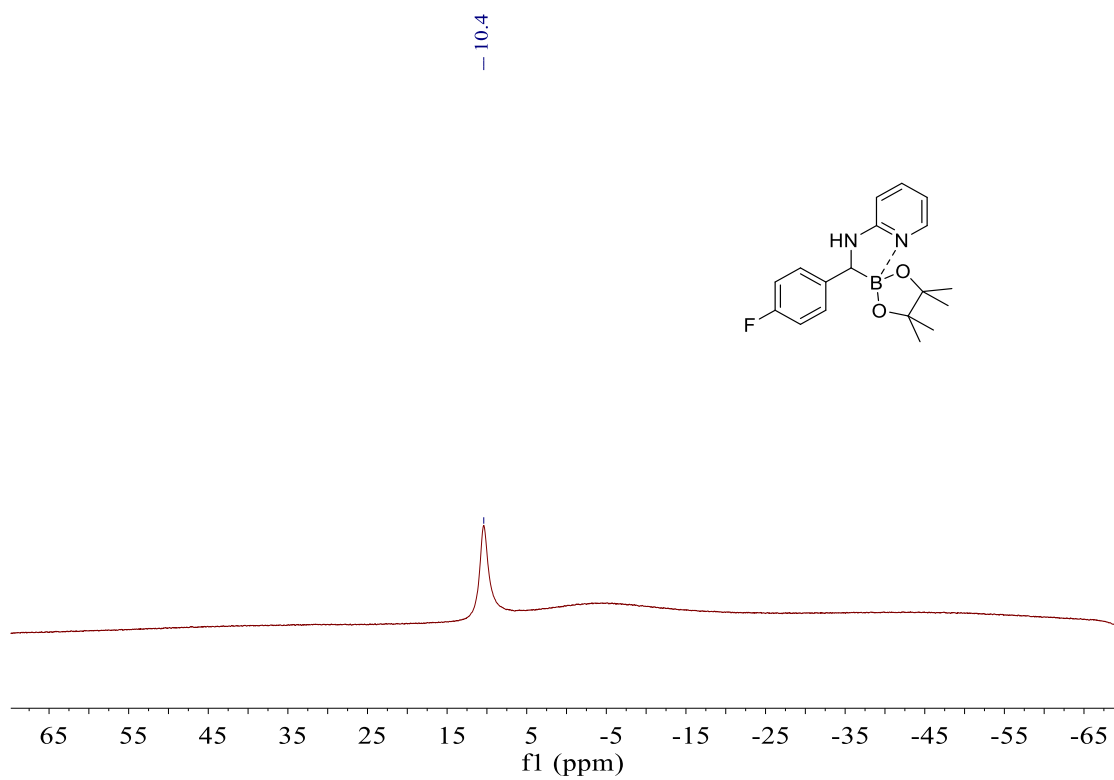
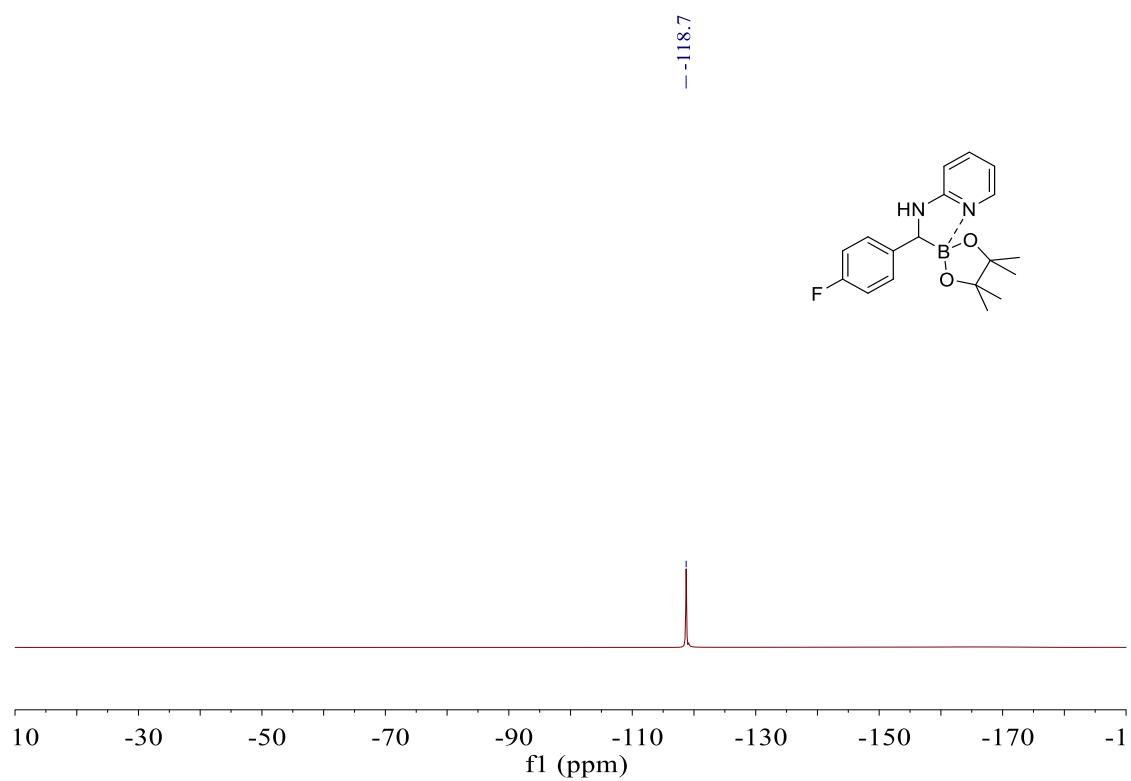
^{11}B NMR spectrum (96 MHz, CDCl_3) of **2-3d**

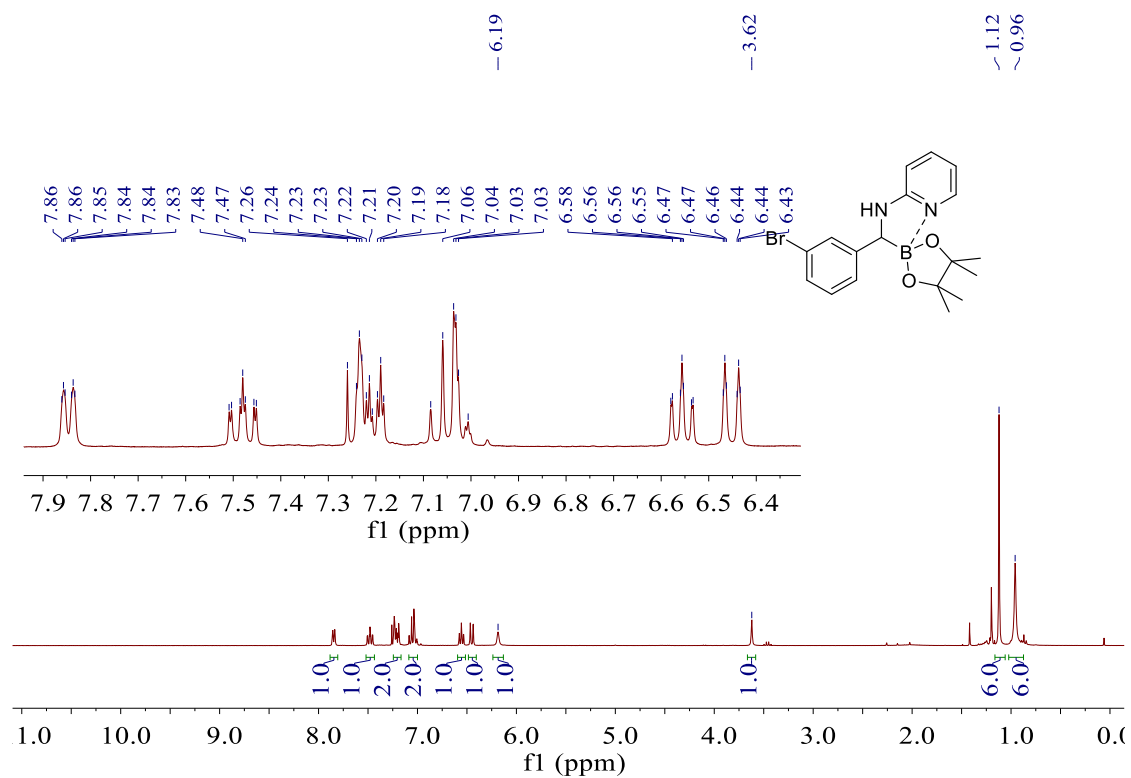
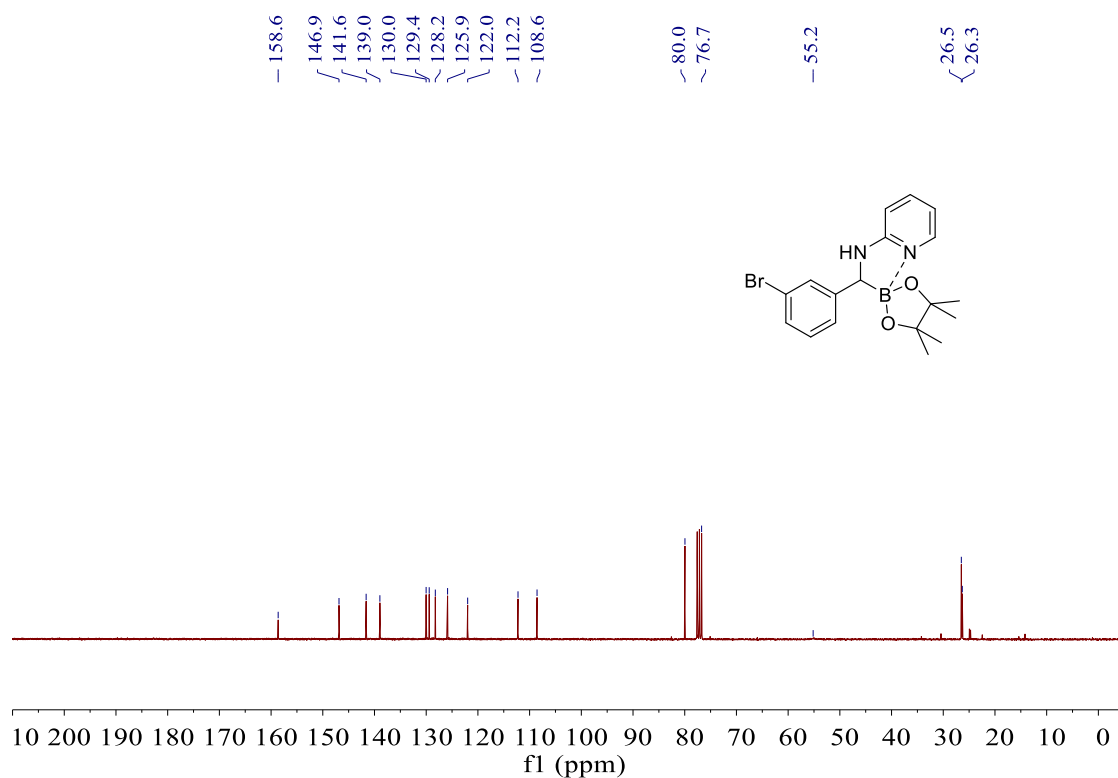


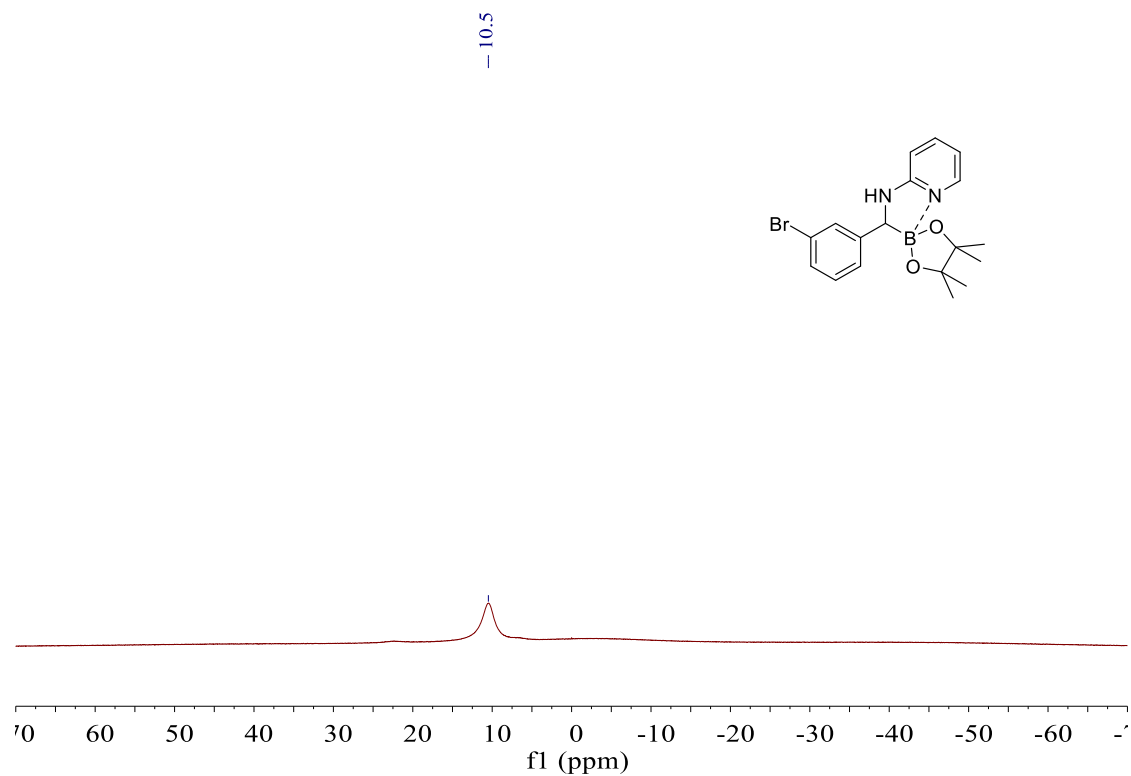
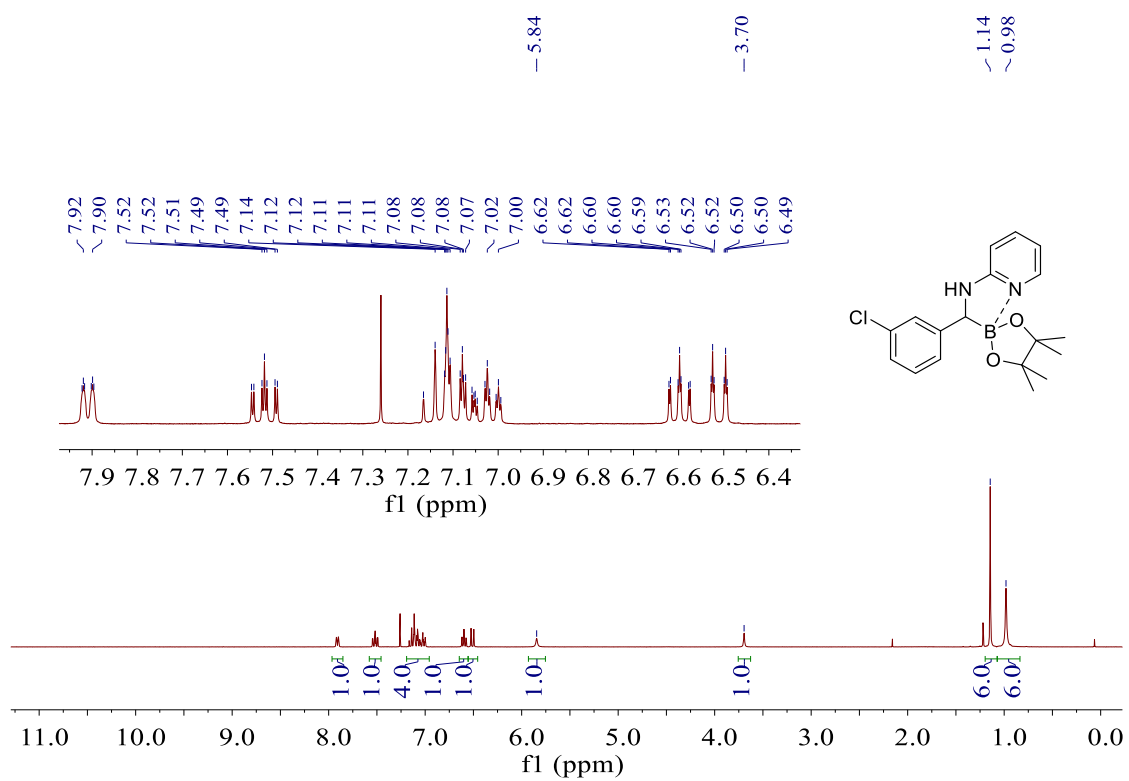
^1H NMR spectrum (500 MHz, CDCl_3) of **2-3e** $^{13}\text{C}\{^1\text{H}\}$ NMR spectrum (126 MHz, CDCl_3) of **2-3e**

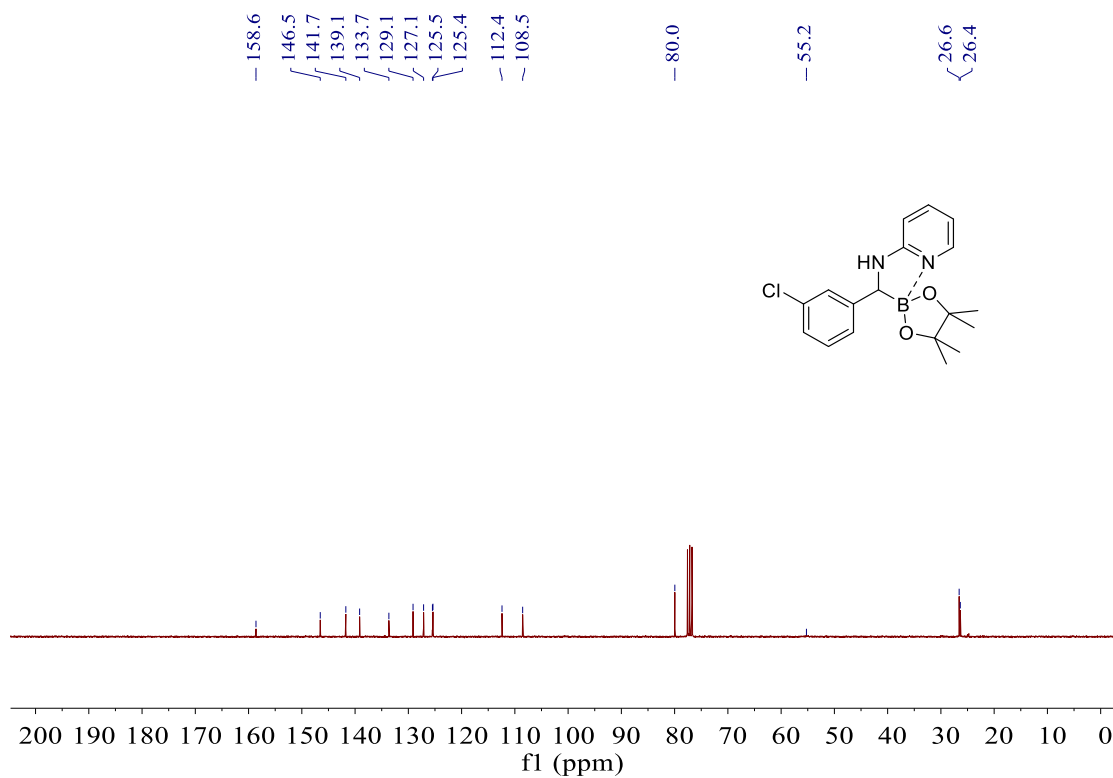
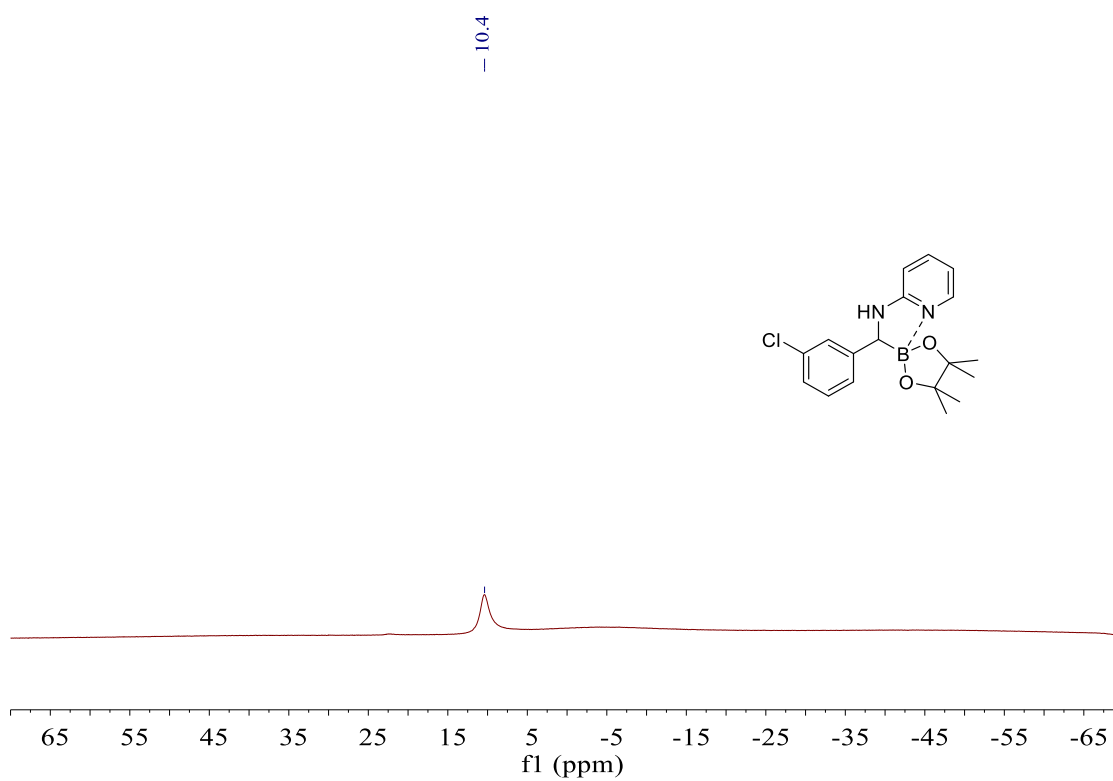
^{11}B NMR spectrum (160 MHz, CDCl_3) of **2-3e** ^1H NMR spectrum (300 MHz, CDCl_3) of **2-3f**

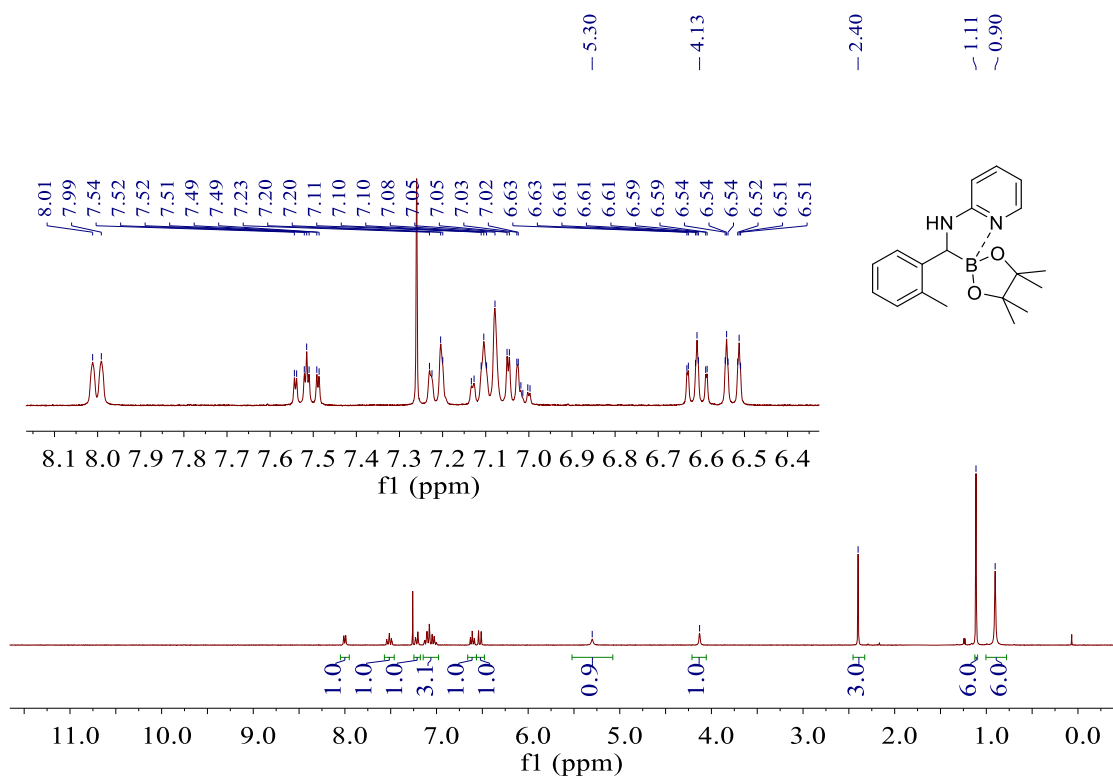
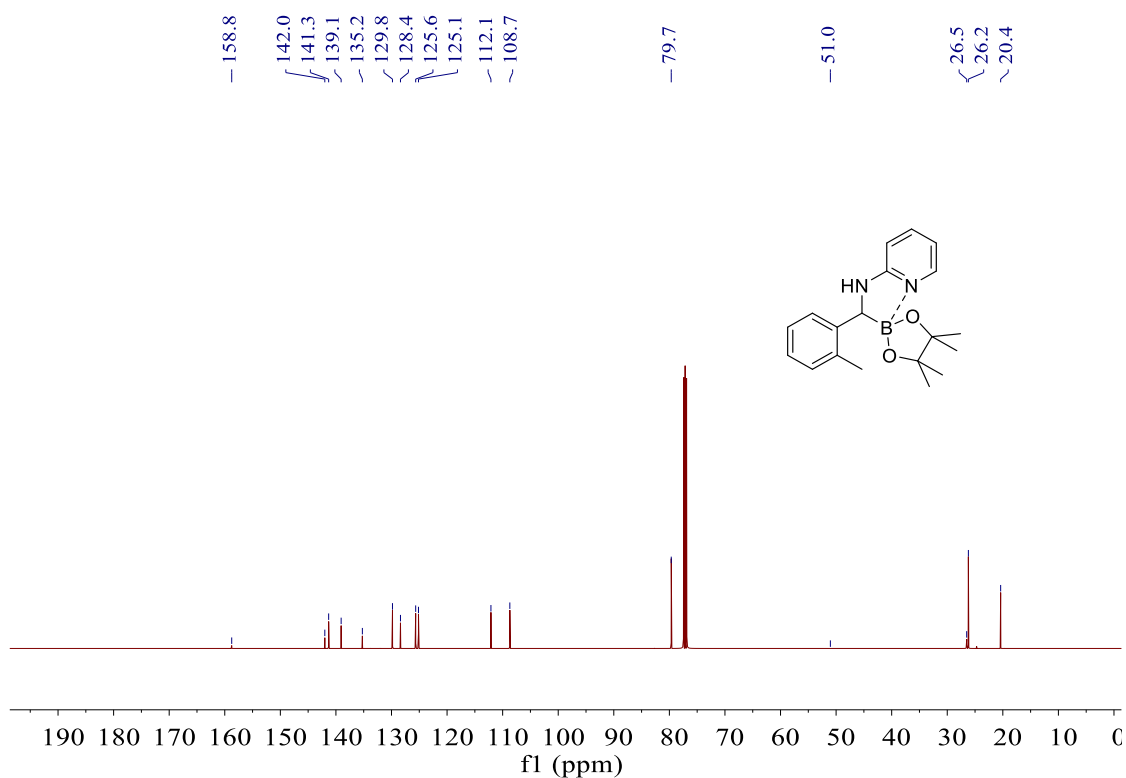
$^{13}\text{C}\{^1\text{H}\}$ NMR spectrum (126 MHz, CDCl_3) of **2-3f** ^{11}B NMR spectrum (96 MHz, CDCl_3) of **2-3f**

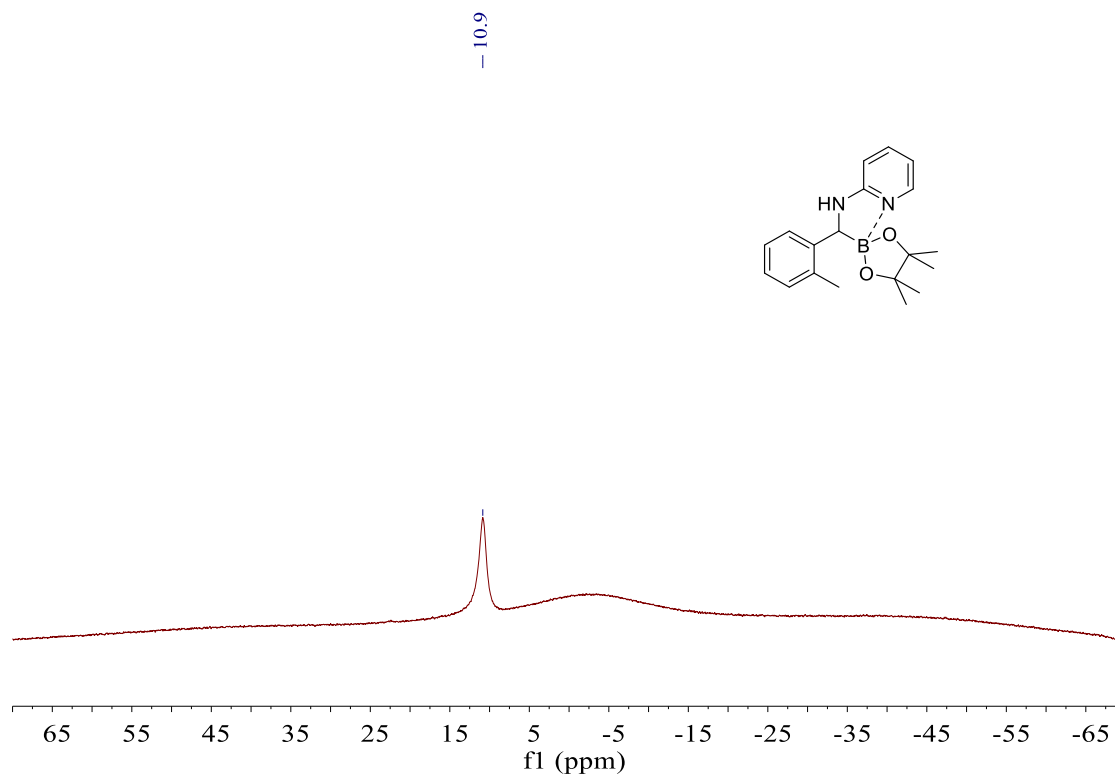
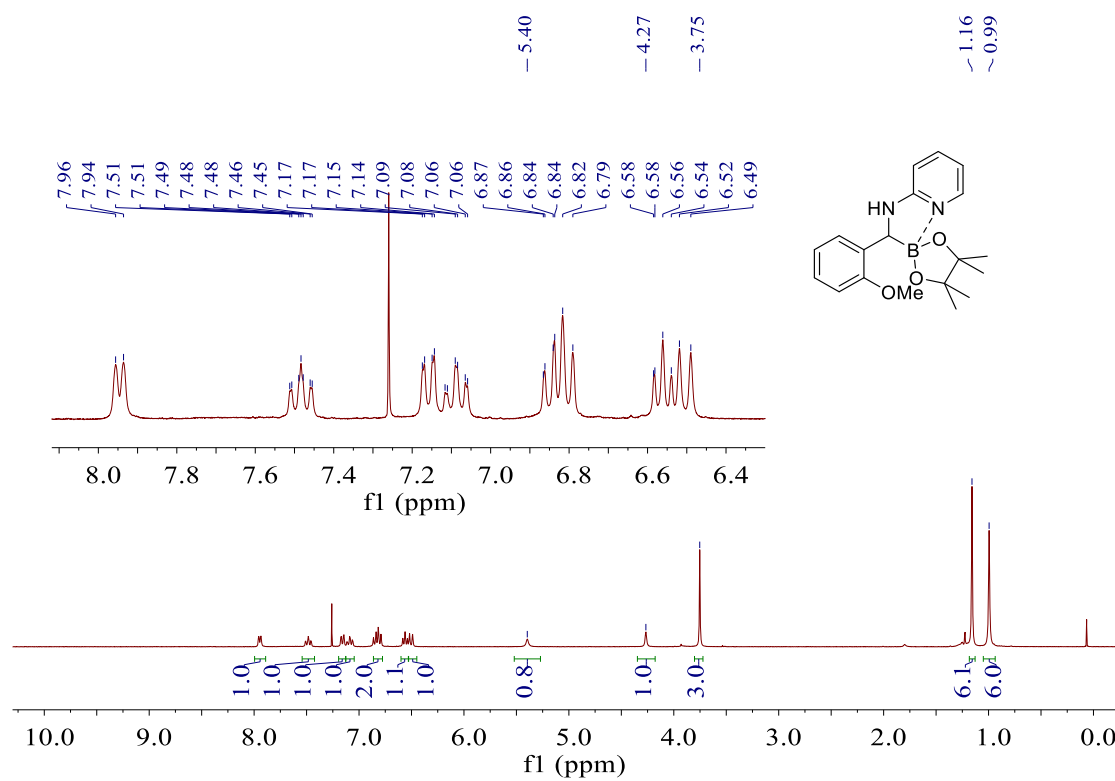
^{11}B NMR spectrum (96 MHz, CDCl_3) of **2-3g** $^{19}\text{F}\{^1\text{H}\}$ NMR spectrum (471 MHz, CDCl_3) of **2-3g**

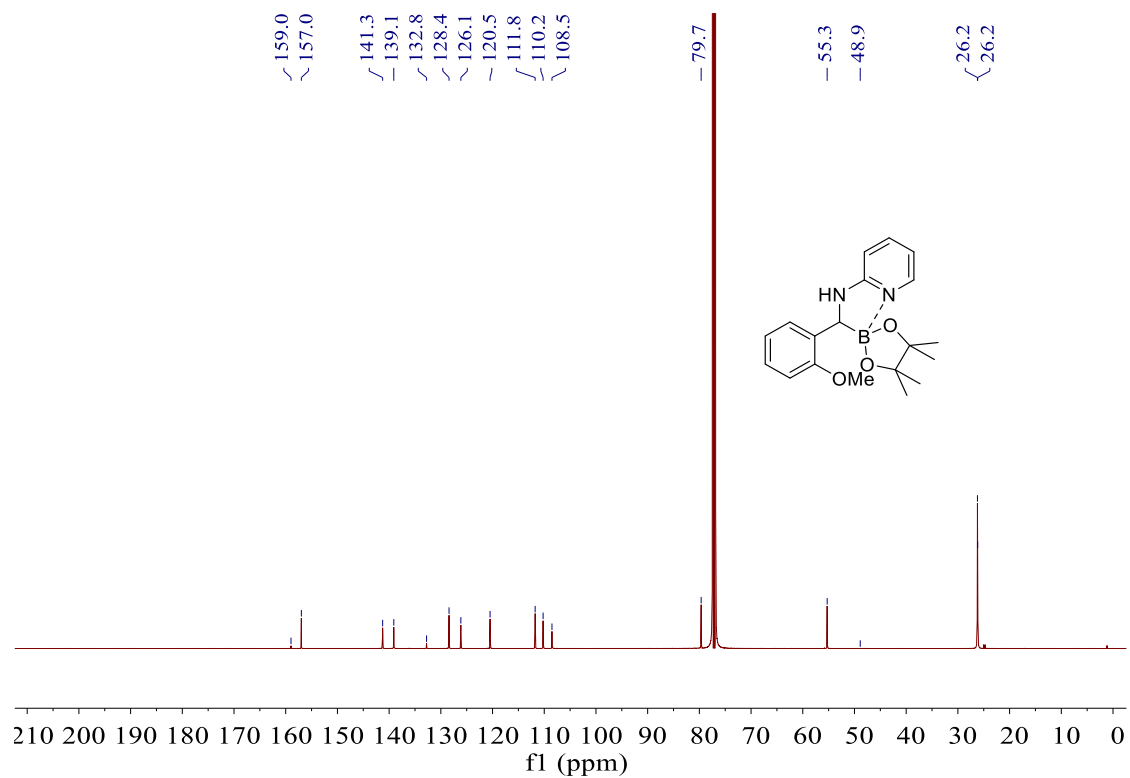
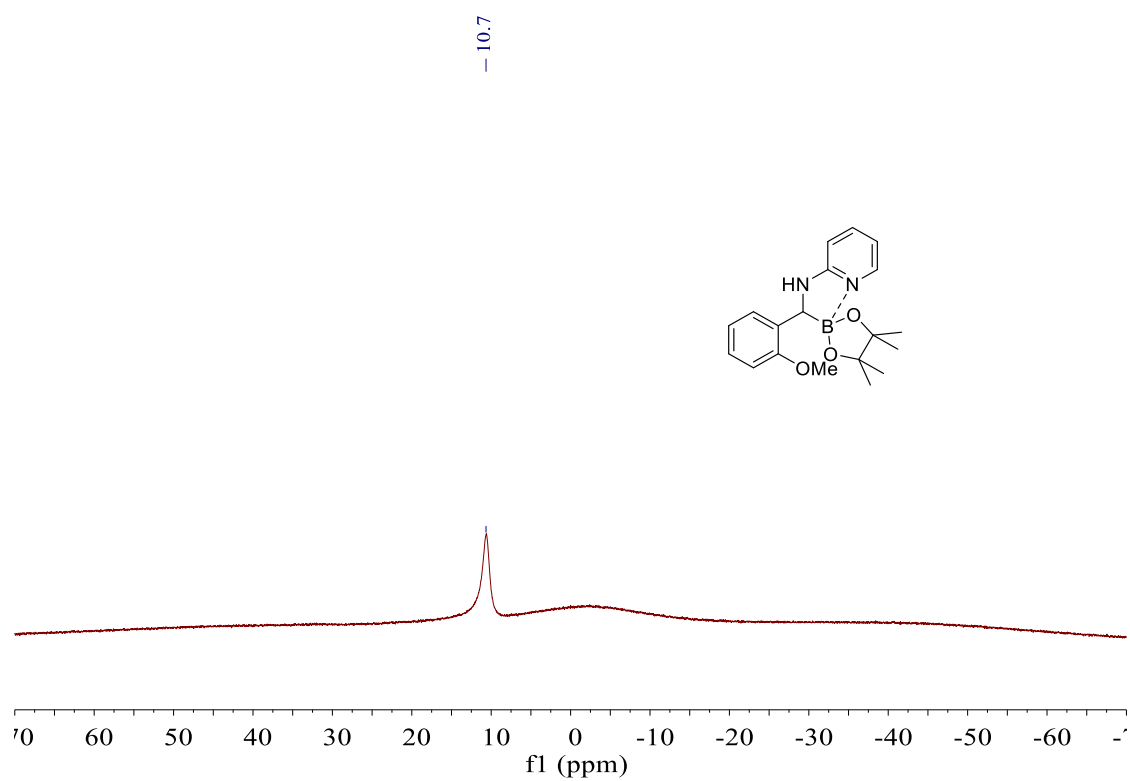
^1H NMR spectrum (300 MHz, CDCl_3) of **2-3h** $^{13}\text{C}\{^1\text{H}\}$ NMR spectrum (75 MHz, CDCl_3) of **2-3h**

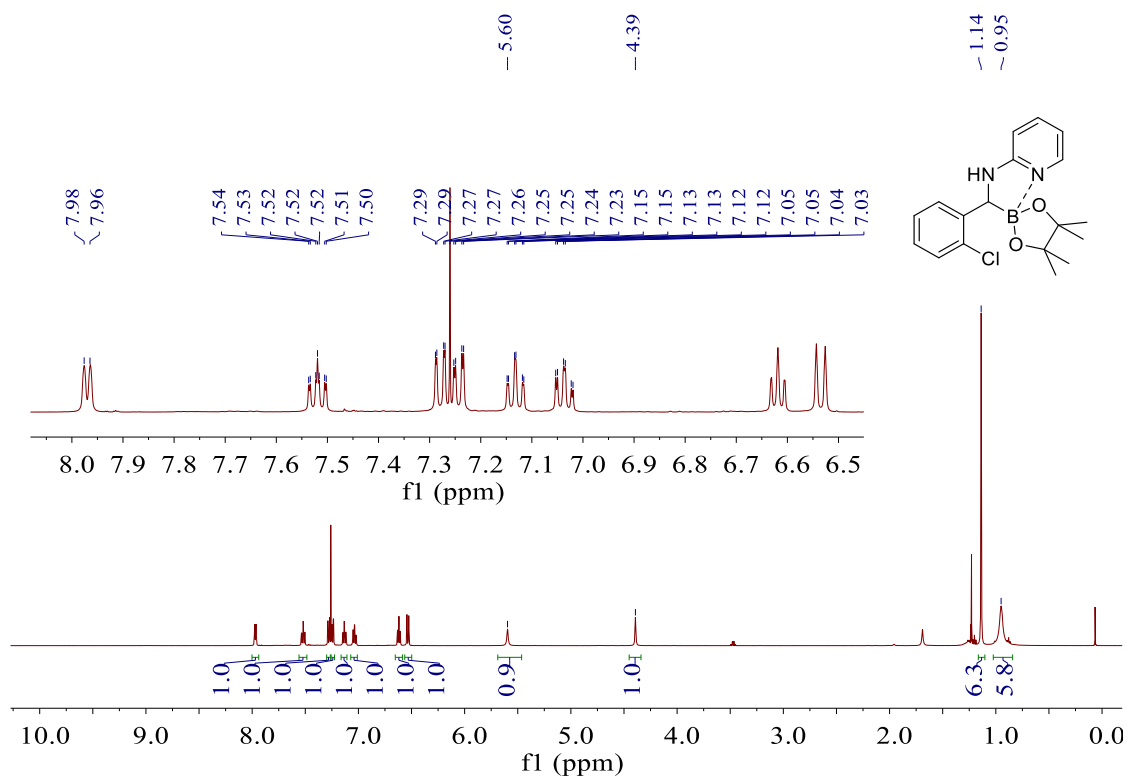
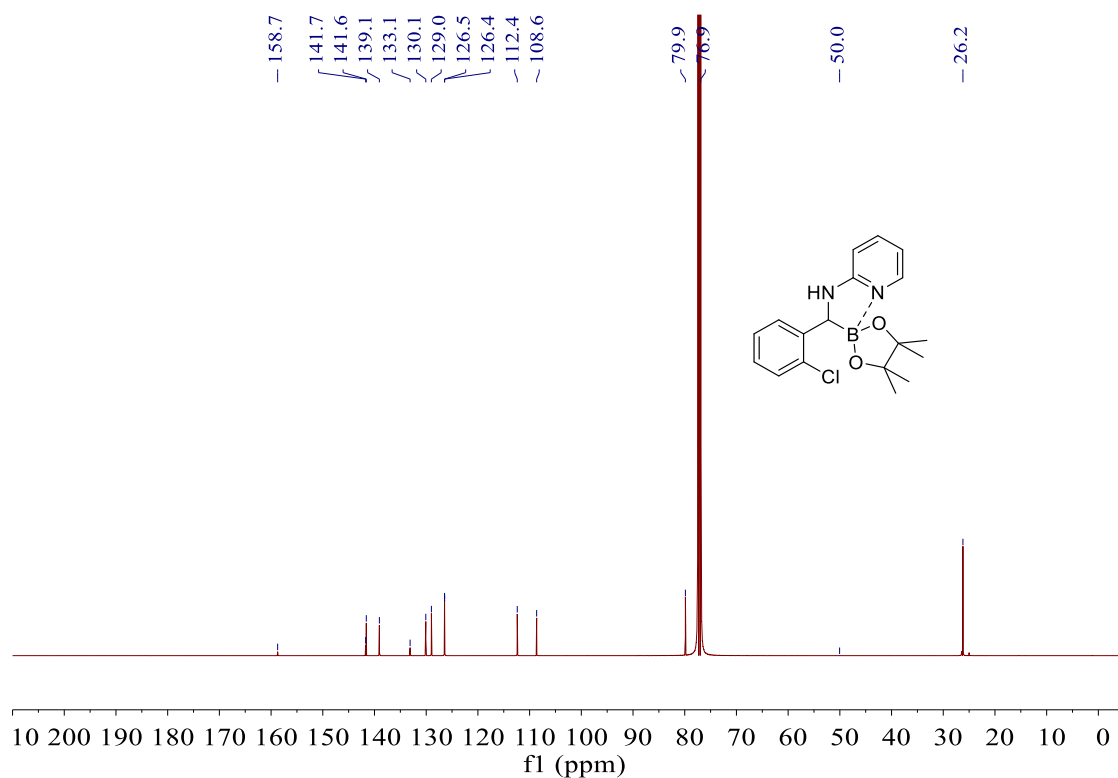
^{11}B NMR spectrum (96 MHz, CDCl_3) of **2-3h** ^1H NMR spectrum (300 MHz, CDCl_3) of **2-3i**

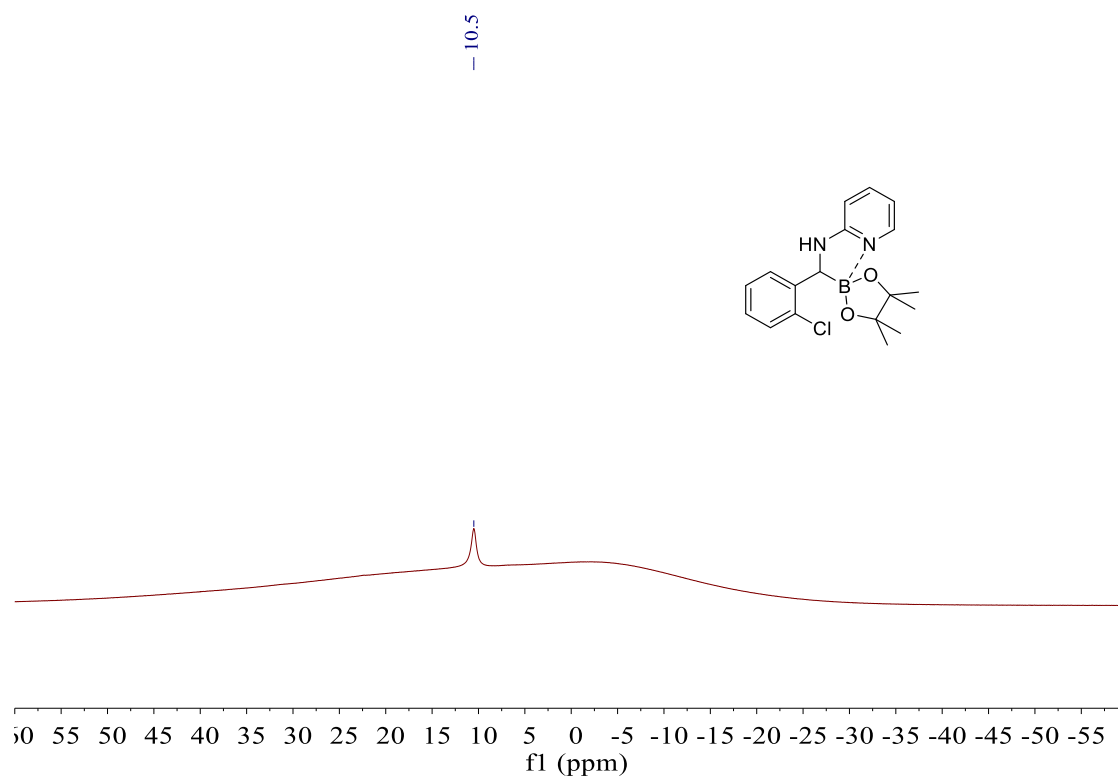
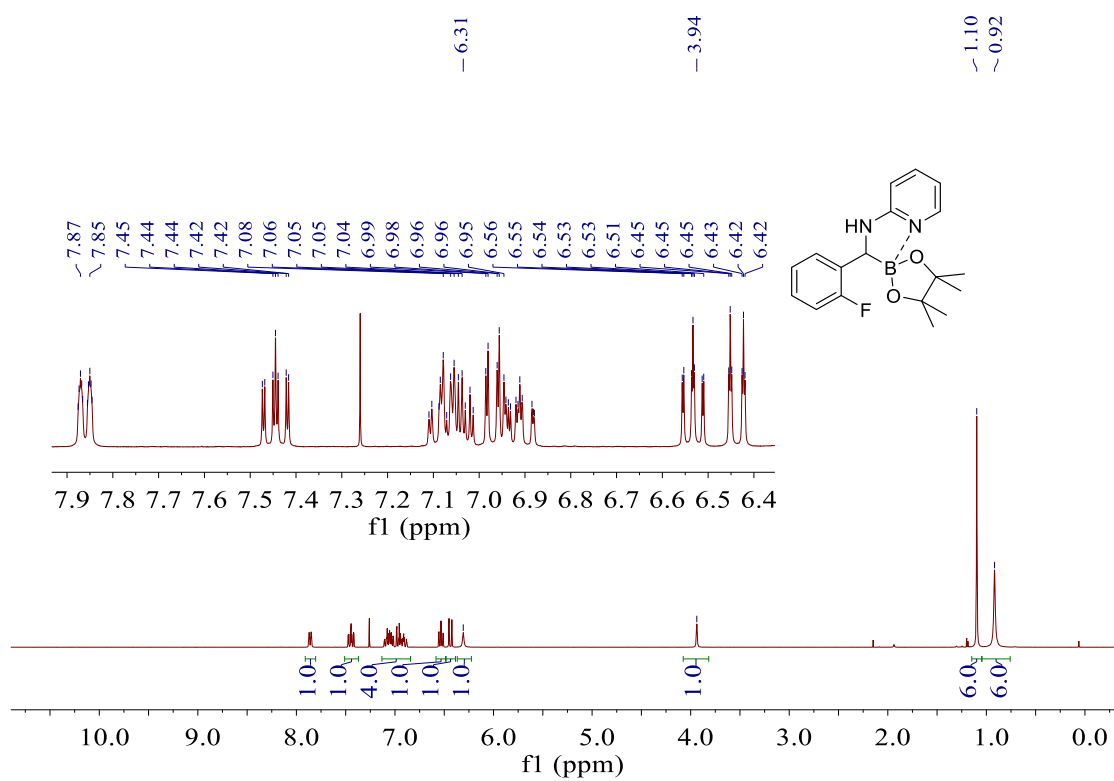
$^{13}\text{C}\{^1\text{H}\}$ NMR spectrum (75 MHz, CDCl_3) of **2-3i** ^{11}B NMR spectrum (96 MHz, CDCl_3) of **2-3i**

^1H NMR spectrum (300 MHz, CDCl_3) of **2-3j** $^{13}\text{C}\{^1\text{H}\}$ NMR spectrum (126 MHz, CDCl_3) of **2-3j**

^{11}B NMR spectrum (96 MHz, CDCl_3) of **2-3j** ^1H NMR spectrum (300 MHz, CDCl_3) of **2-3k**

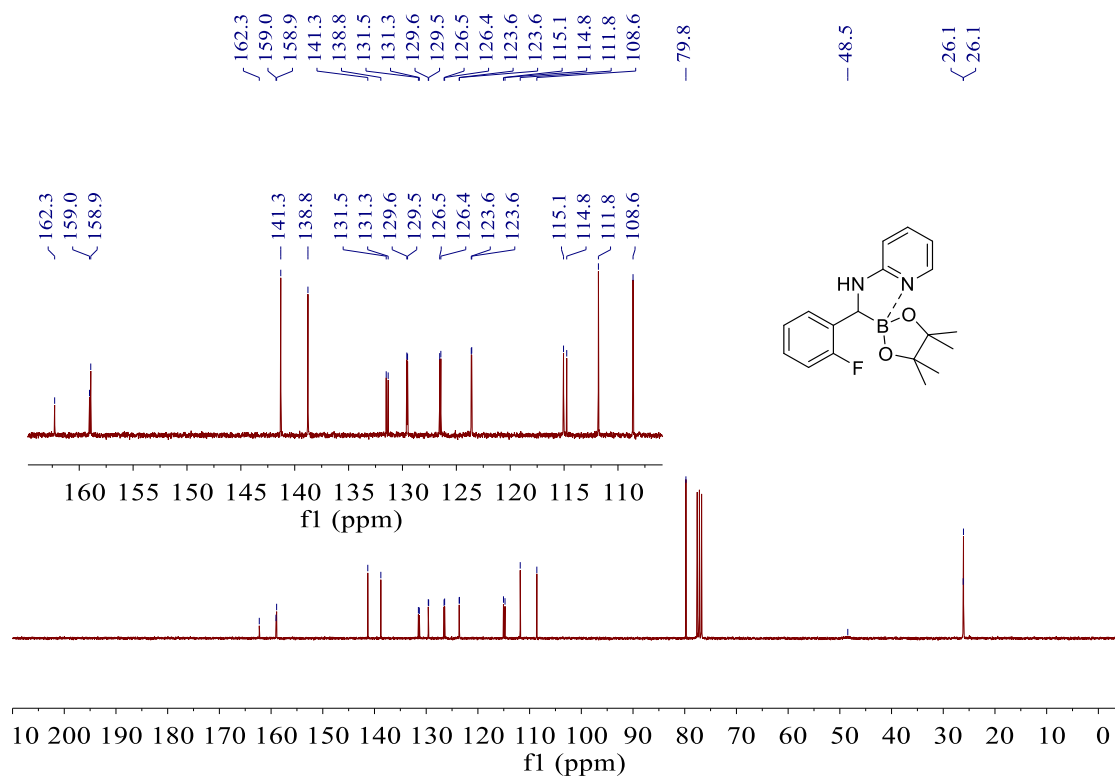
$^{13}\text{C}\{^1\text{H}\}$ NMR spectrum (126 MHz, CDCl_3) of **2-3k** ^{11}B NMR spectrum (96 MHz, CDCl_3) of **2-3k**

^1H NMR spectrum (300 MHz, CDCl_3) of **2-3I** $^{13}\text{C}\{^1\text{H}\}$ NMR spectrum (126 MHz, CDCl_3) of **2-3I**

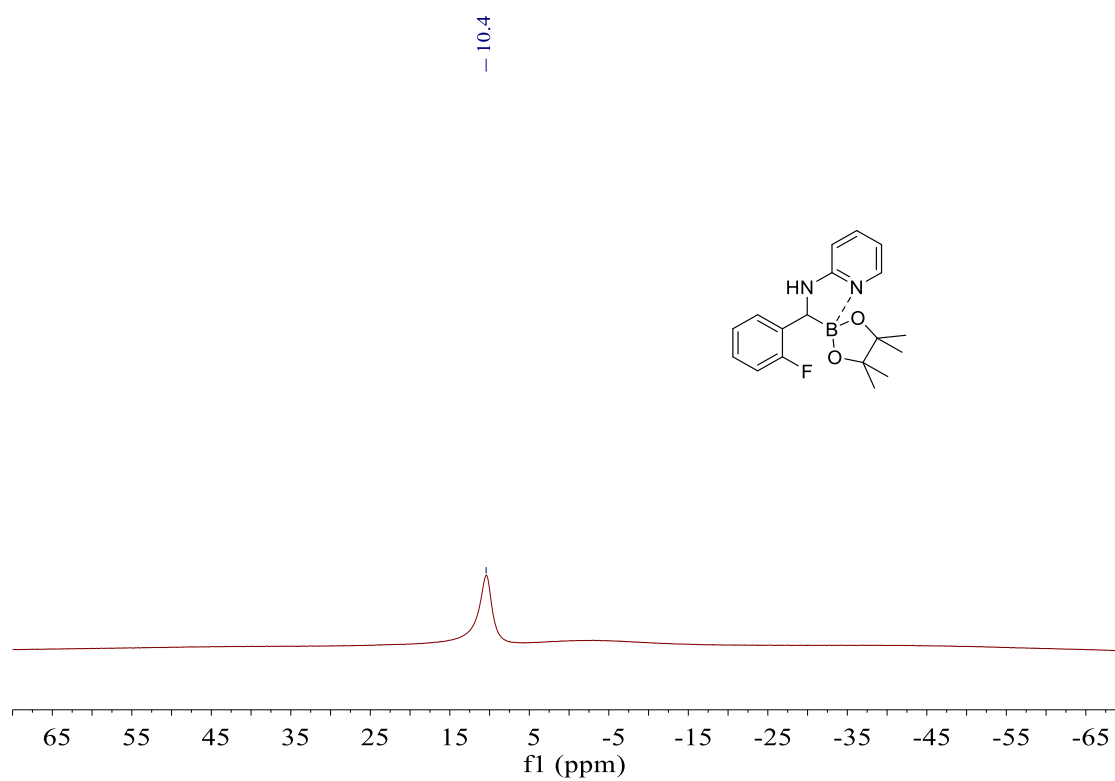
^{11}B NMR spectrum (160 MHz, CDCl_3) of **2-3I** ^1H NMR spectrum (300 MHz, CDCl_3) of **2-3m**

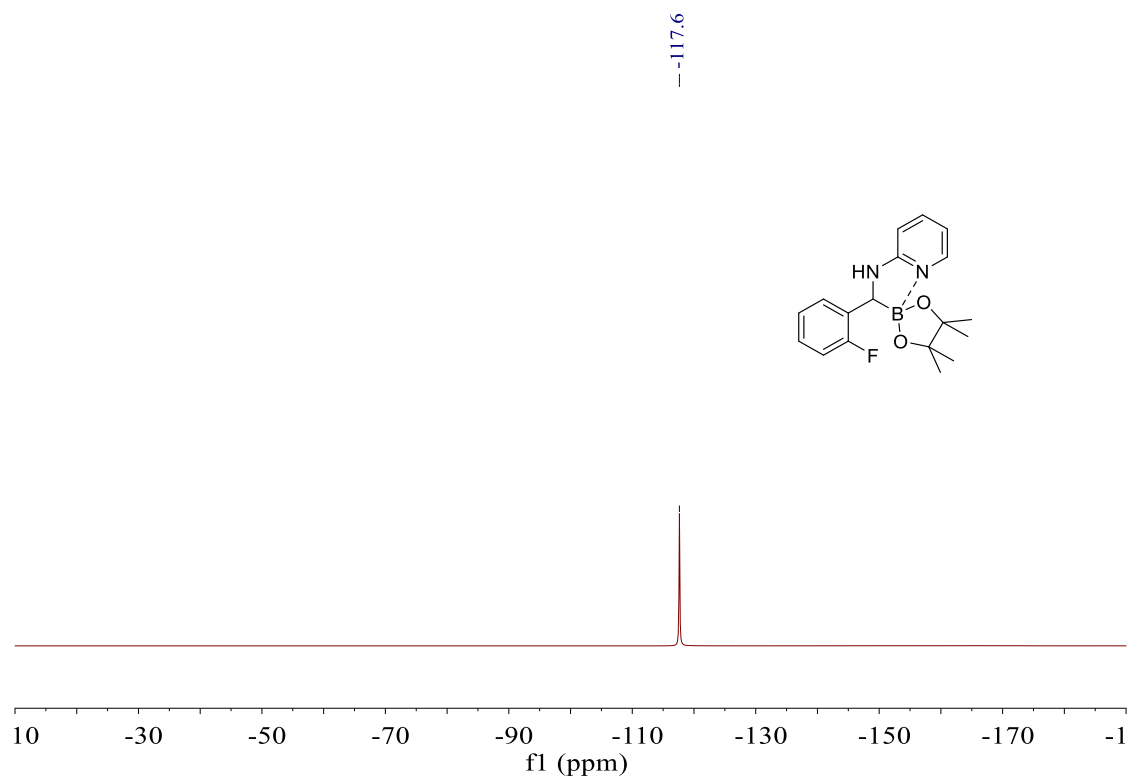
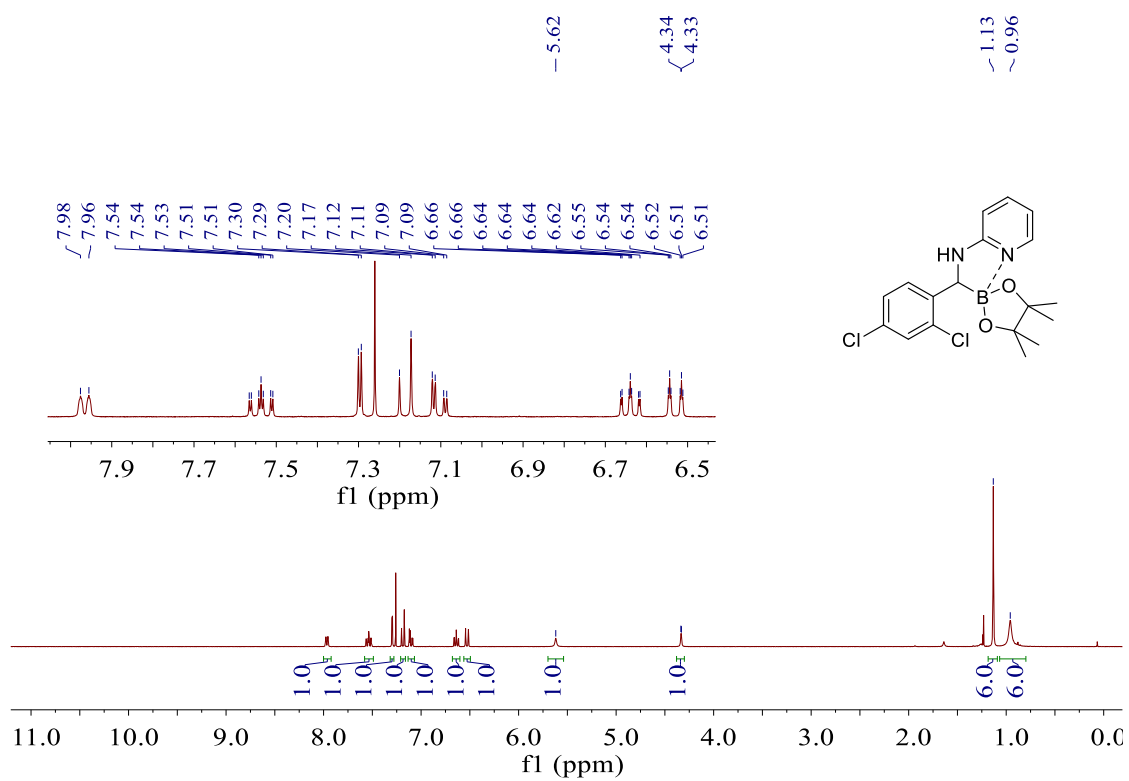
Appendix

$^{13}\text{C}\{^1\text{H}\}$ NMR spectrum (75 MHz, CDCl_3) of **2-3m**



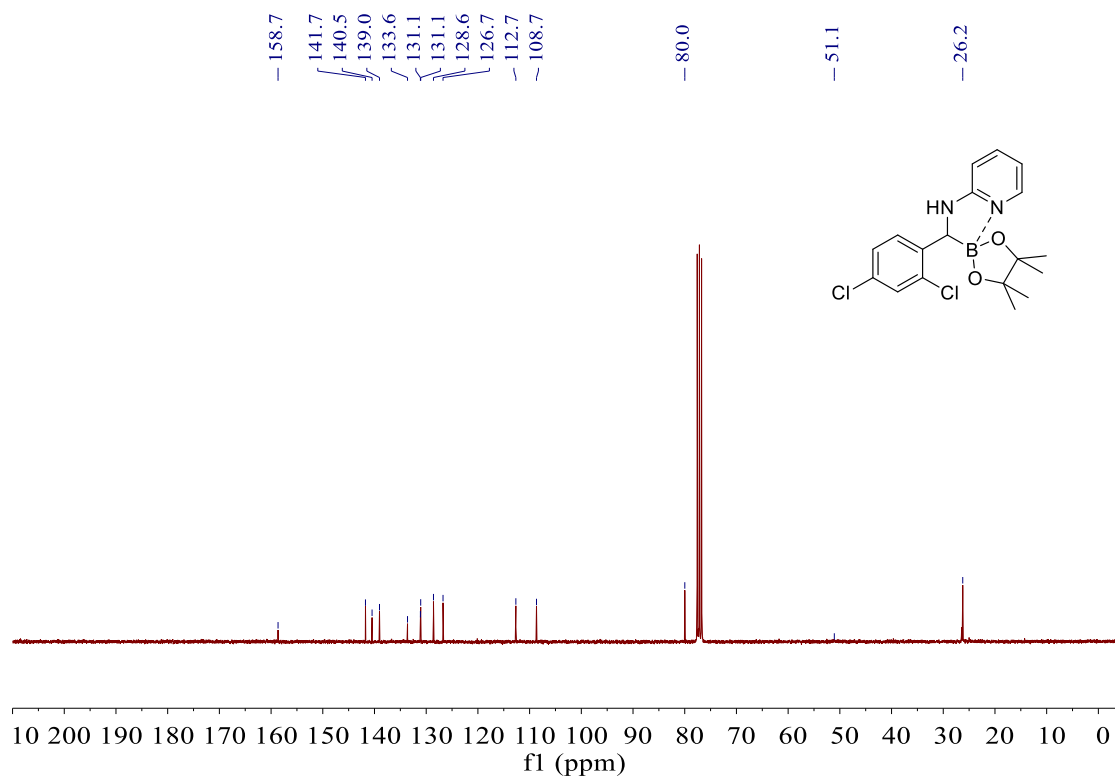
^{11}B NMR spectrum (96 MHz, CDCl_3) of **2-3m**



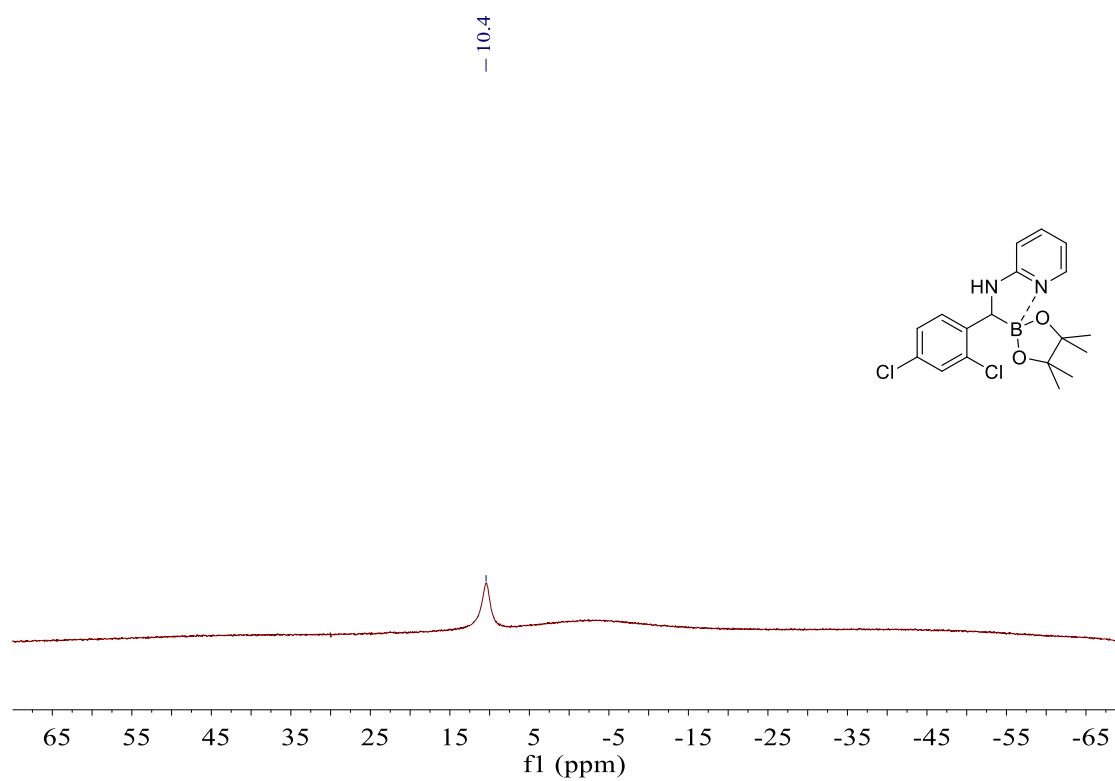
$^{19}\text{F}\{^1\text{H}\}$ NMR spectrum (471 MHz, CDCl_3) of **2-3m** ^1H NMR spectrum (300 MHz, CDCl_3) of **2-3n**

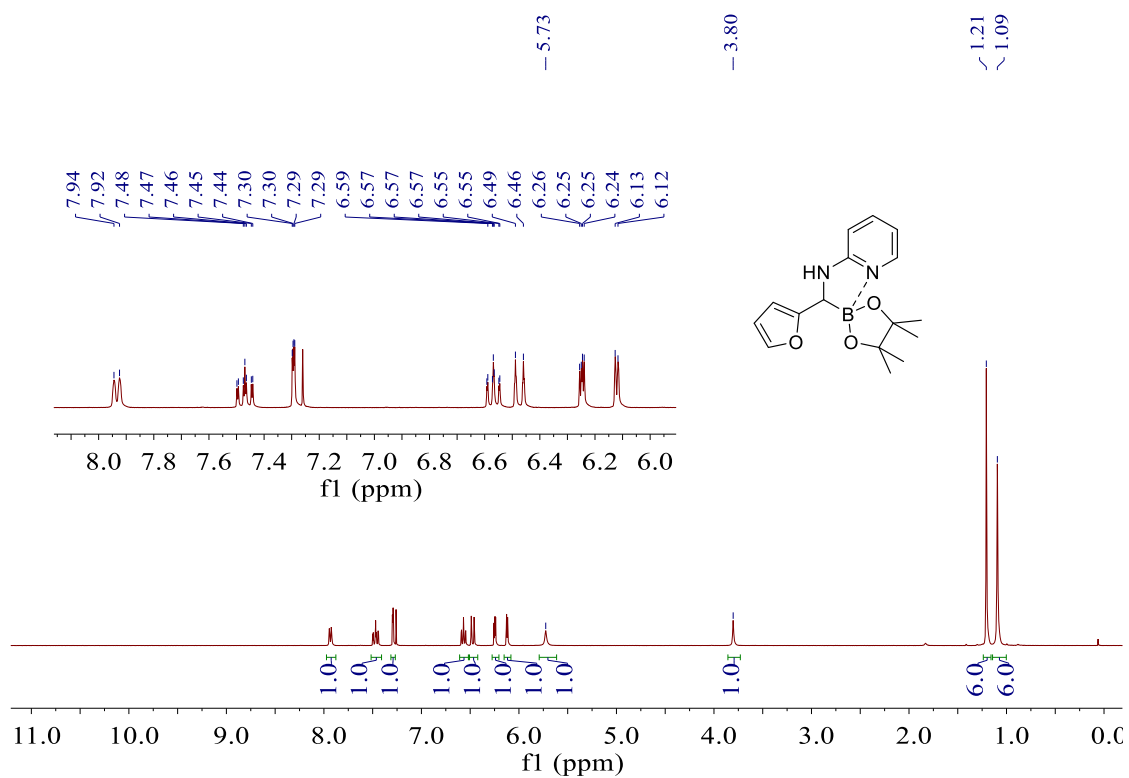
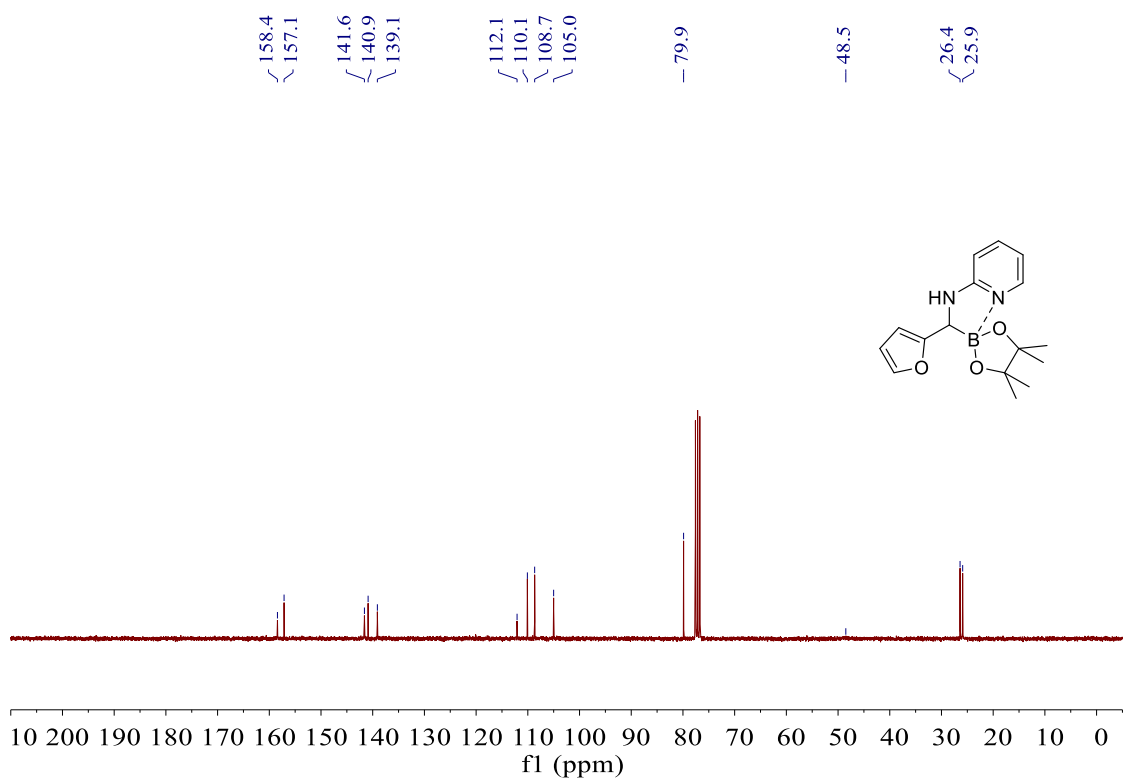
Appendix

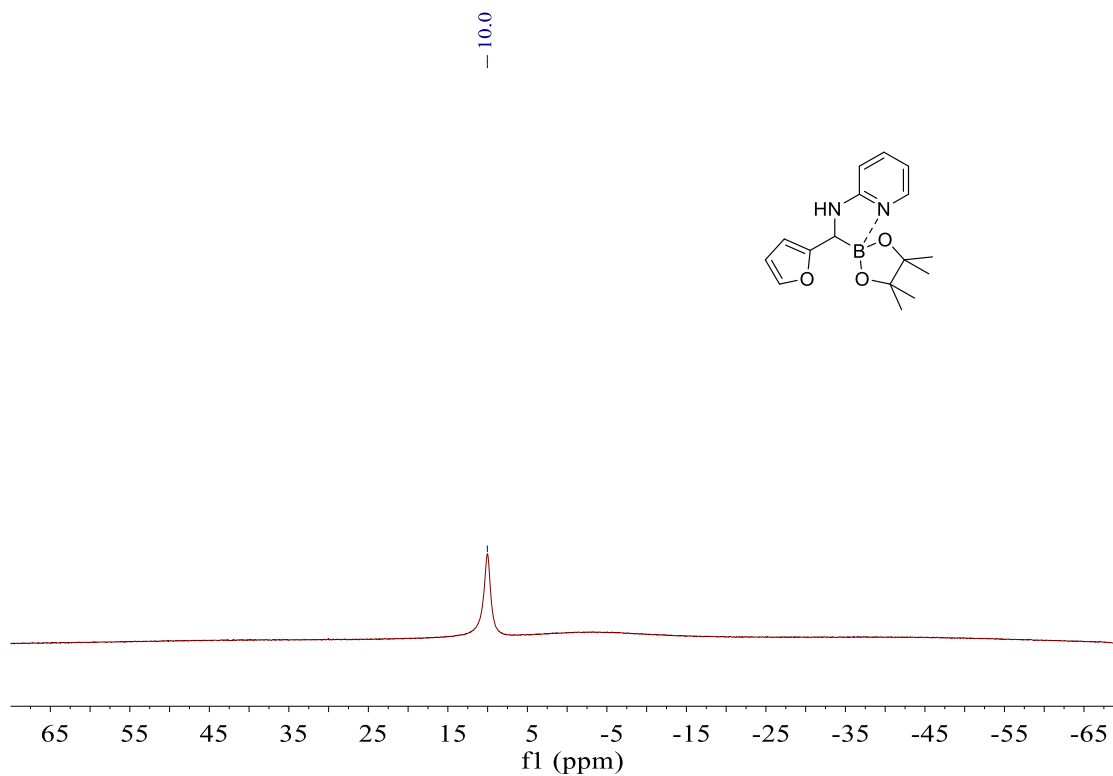
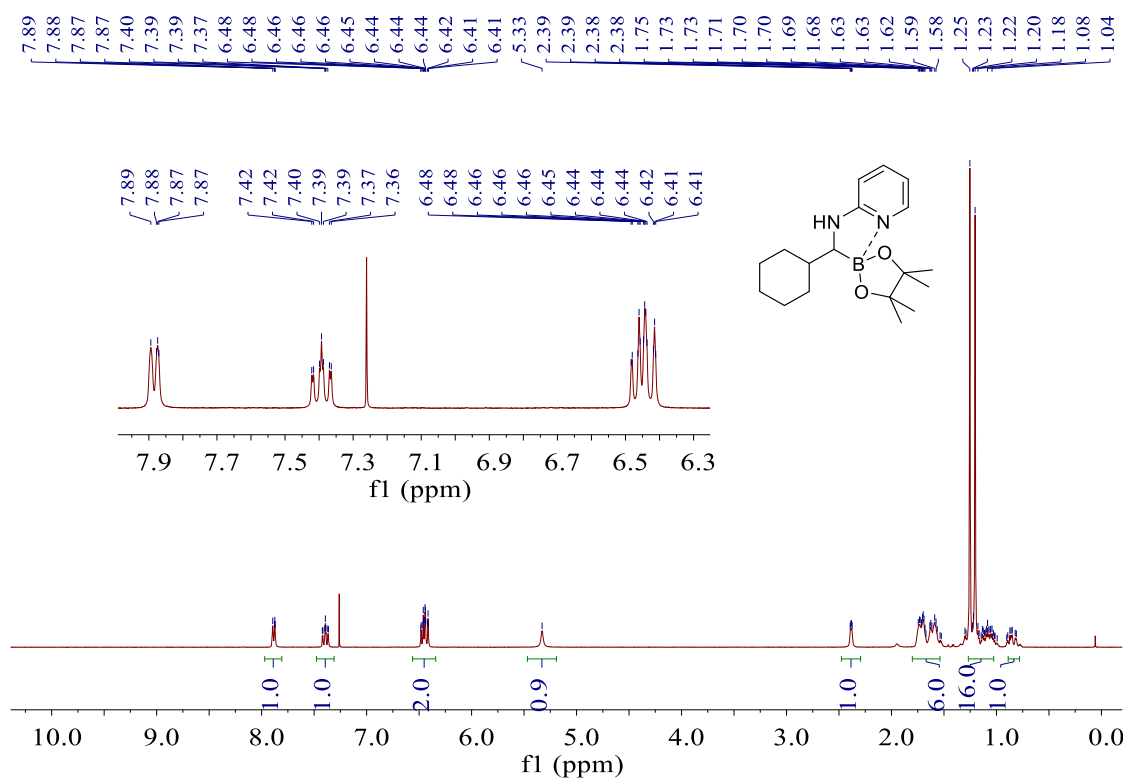
$^{13}\text{C}\{^1\text{H}\}$ NMR spectrum (75 MHz, CDCl_3) of **2-3n**

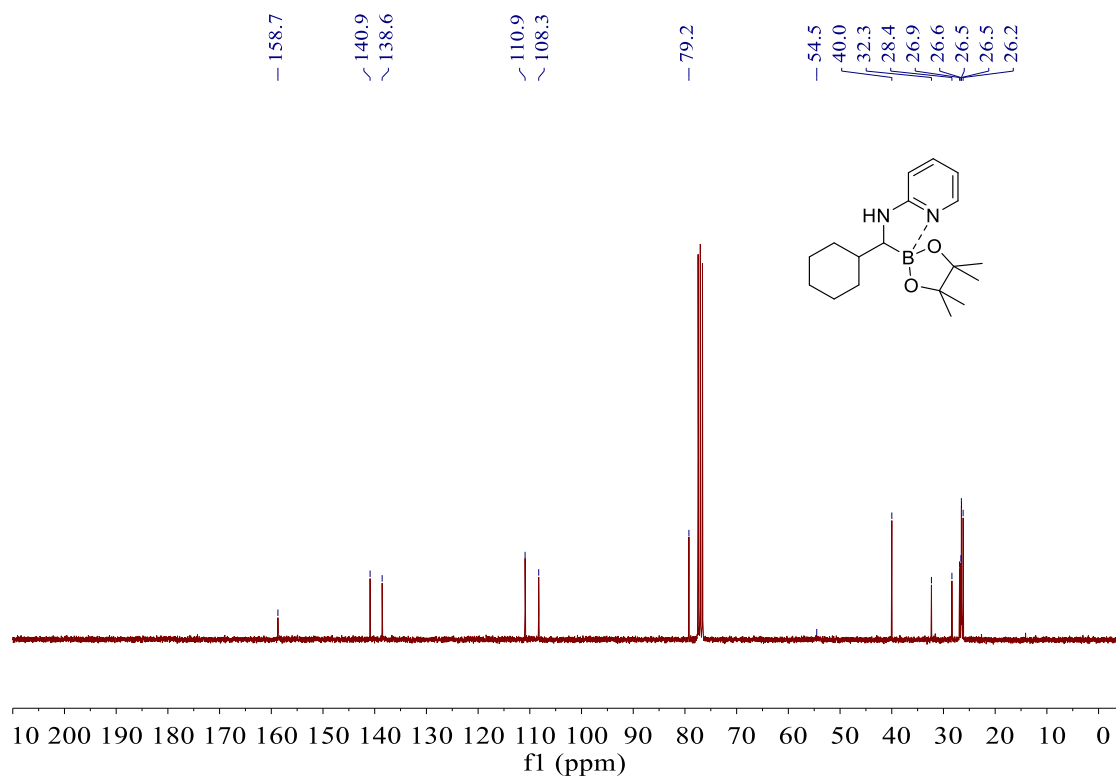
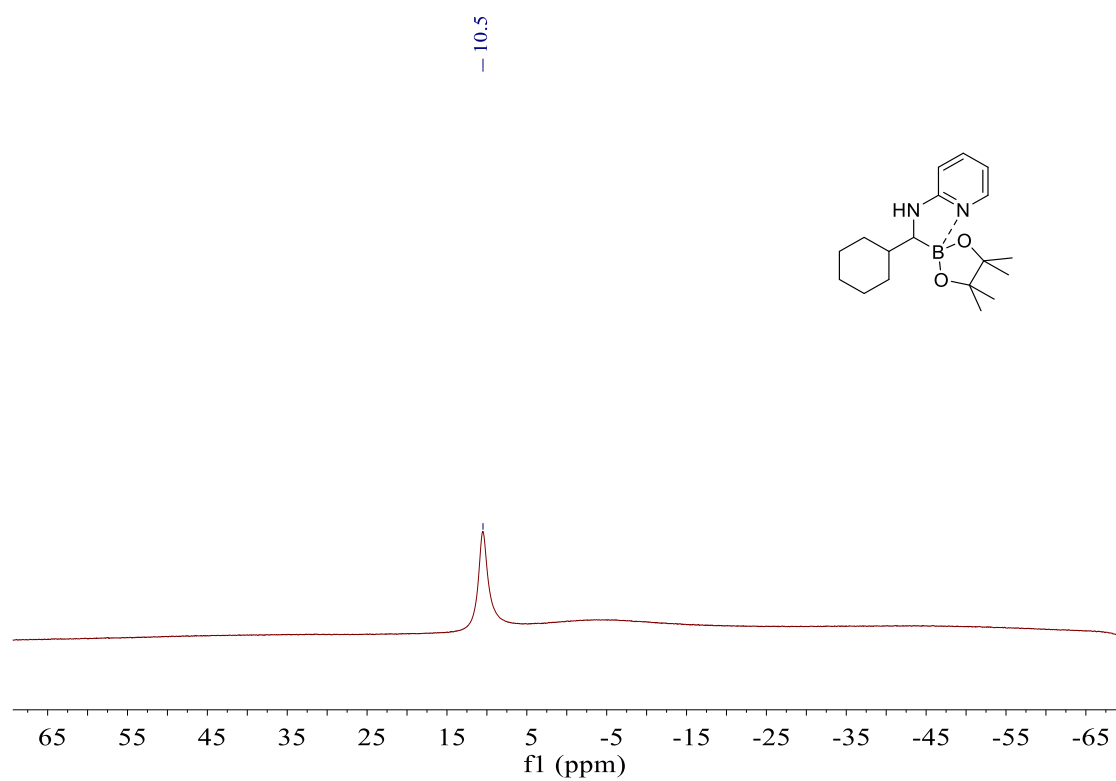


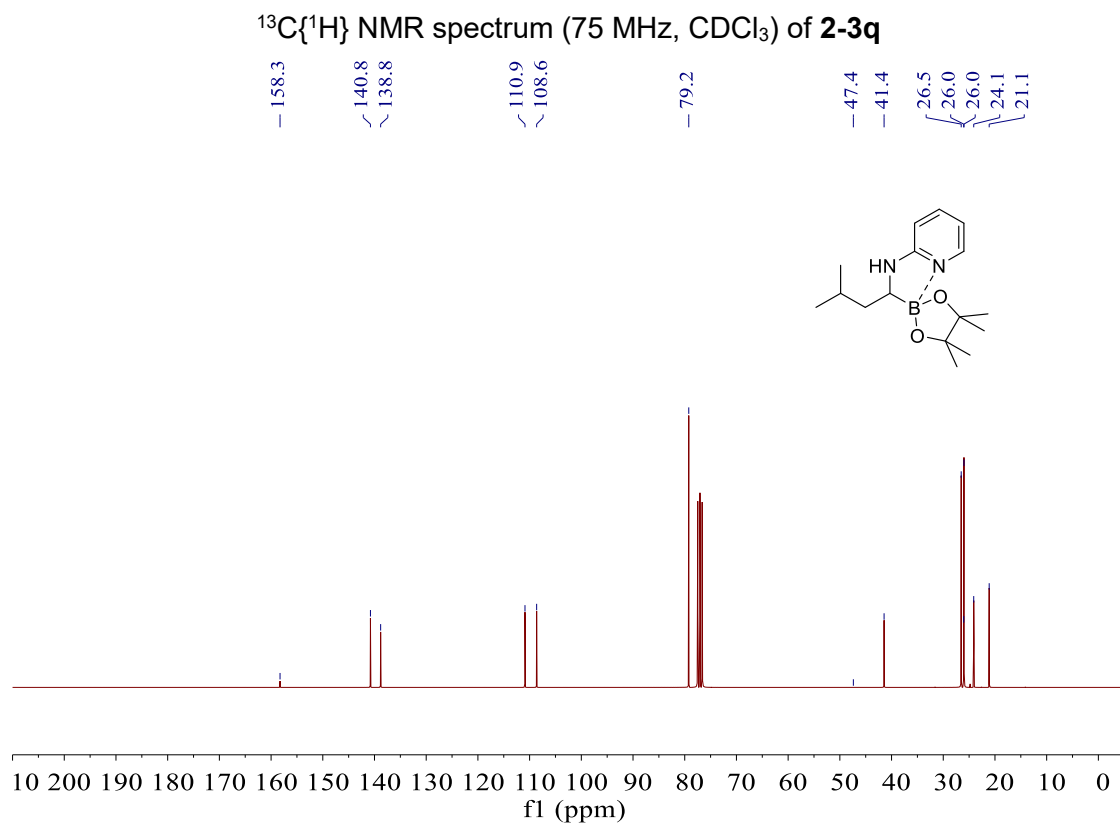
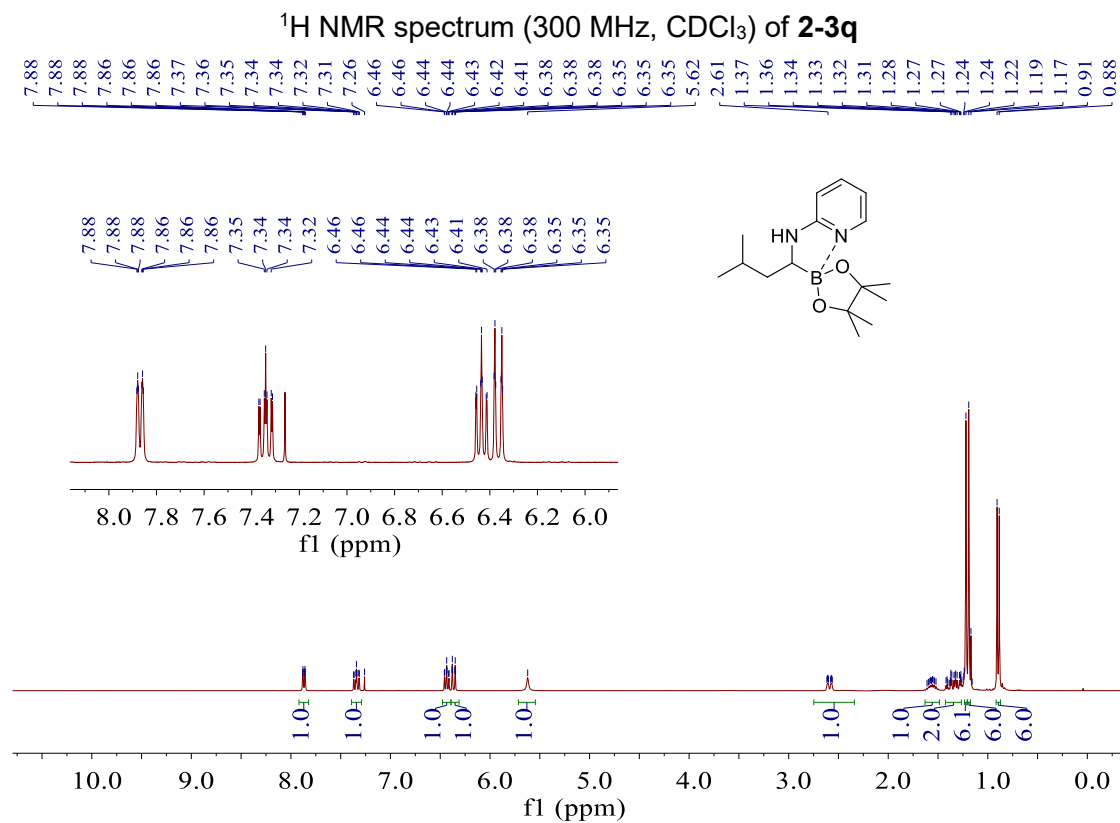
^{11}B NMR spectrum (96 MHz, CDCl_3) of **2-3n**

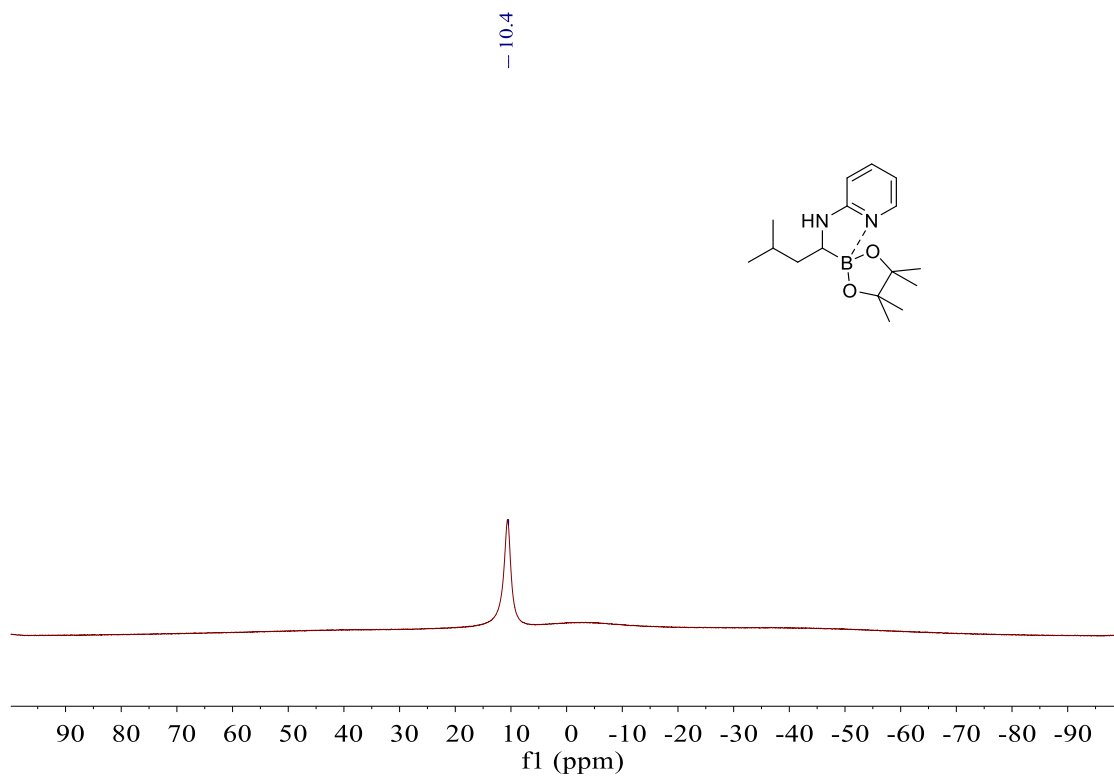
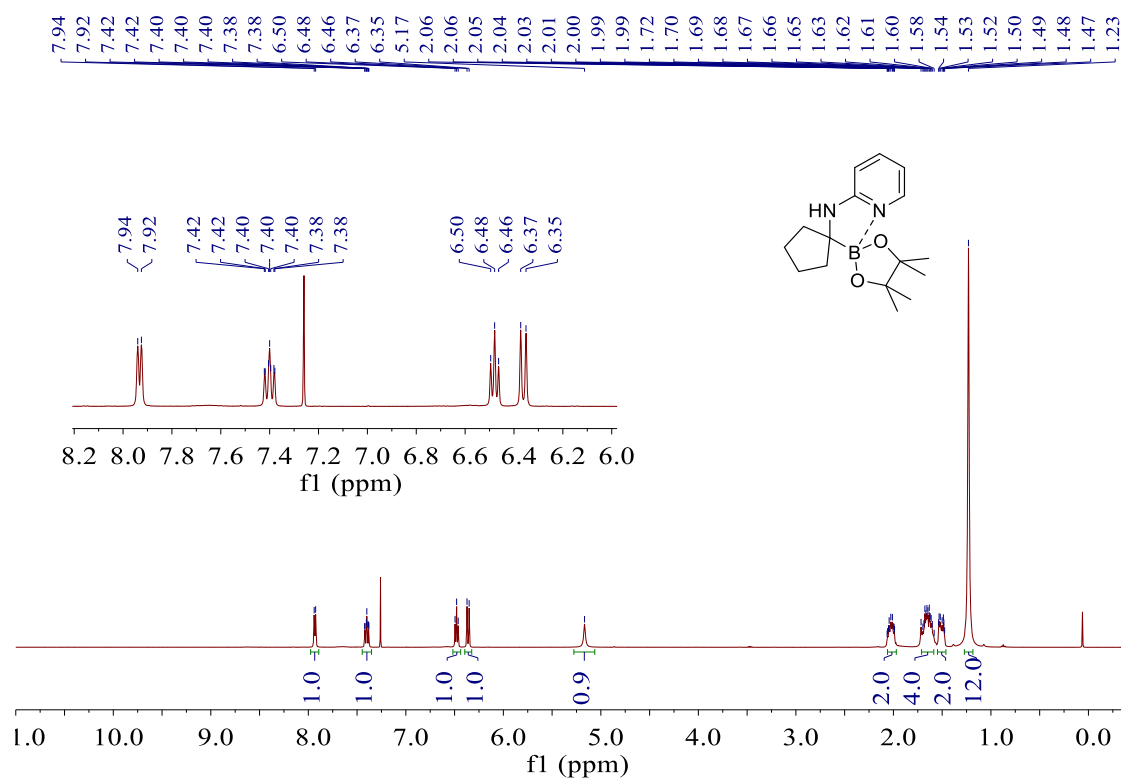


^1H NMR spectrum (300 MHz, CDCl_3) of **2-3o** $^{13}\text{C}\{^1\text{H}\}$ NMR spectrum (75 MHz, CDCl_3) of **2-3o**

^{11}B NMR spectrum (96 MHz, CDCl_3) of **2-3n** ^1H NMR spectrum (300 MHz, CDCl_3) of **2-3p**

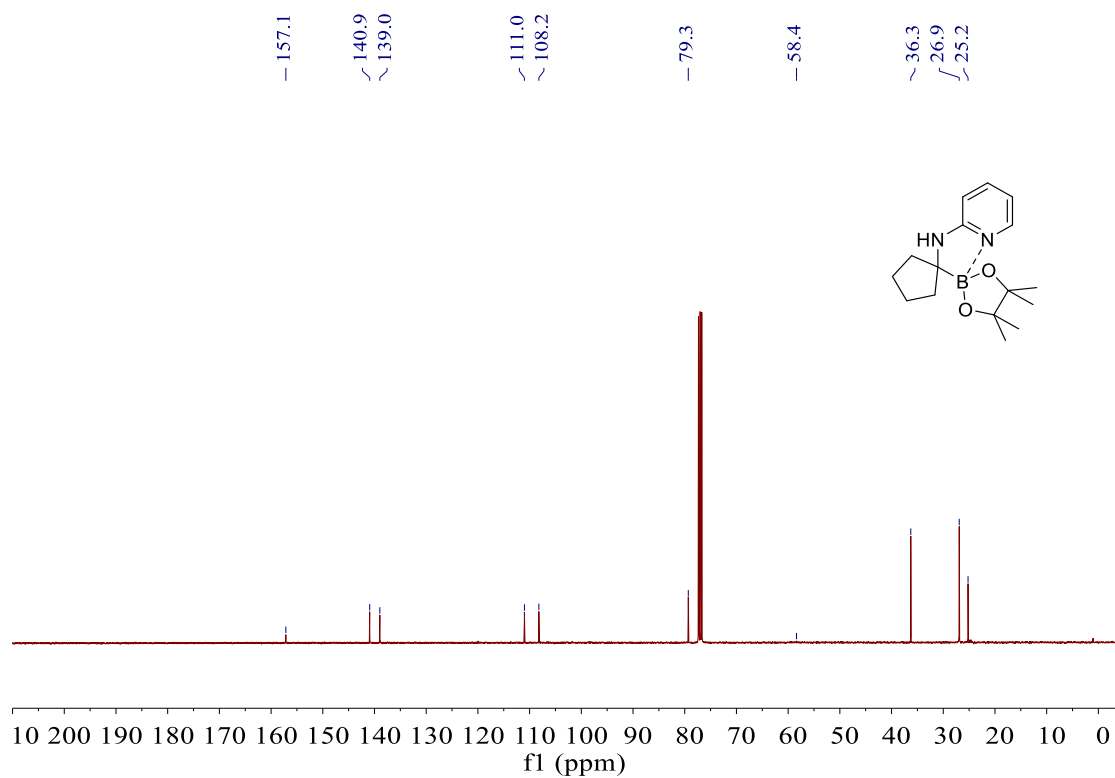
$^{13}\text{C}\{^1\text{H}\}$ NMR spectrum (75 MHz, CDCl_3) of **2-3p** ^{11}B NMR spectrum (96 MHz, CDCl_3) of **2-3p**



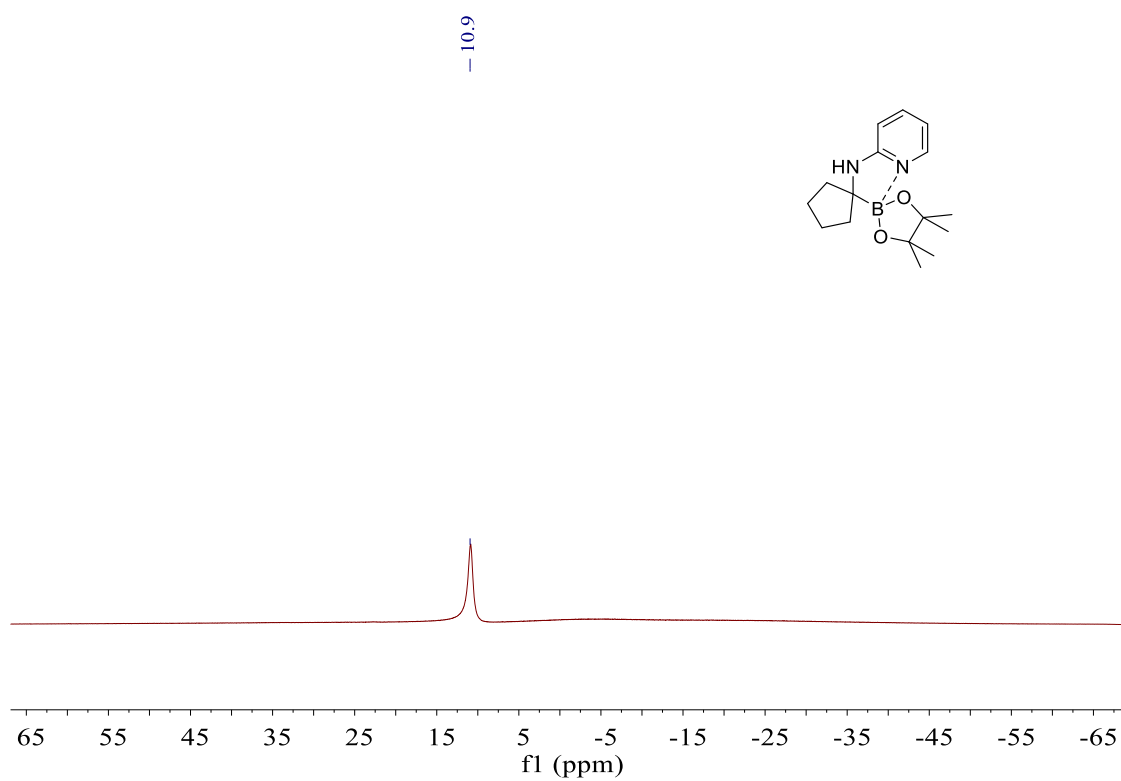
^{11}B NMR spectrum (96 MHz, CDCl_3) of **2-3q** ^1H NMR spectrum (400 MHz, CDCl_3) of **2-3r**

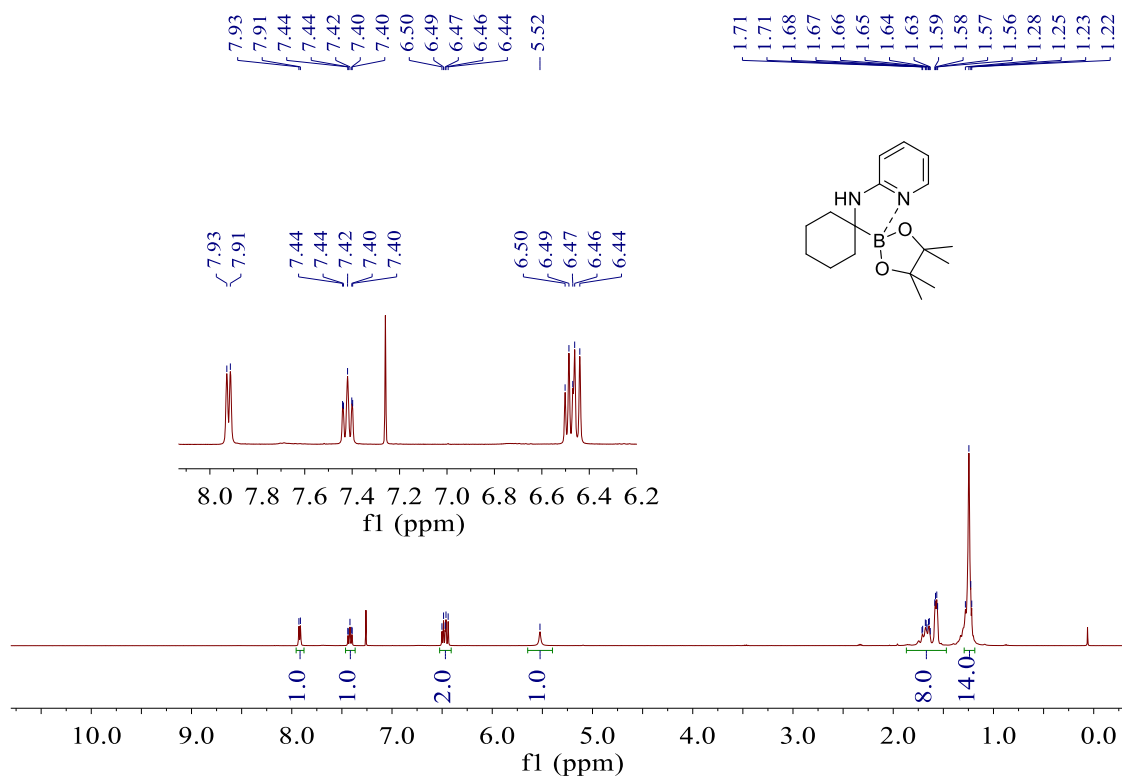
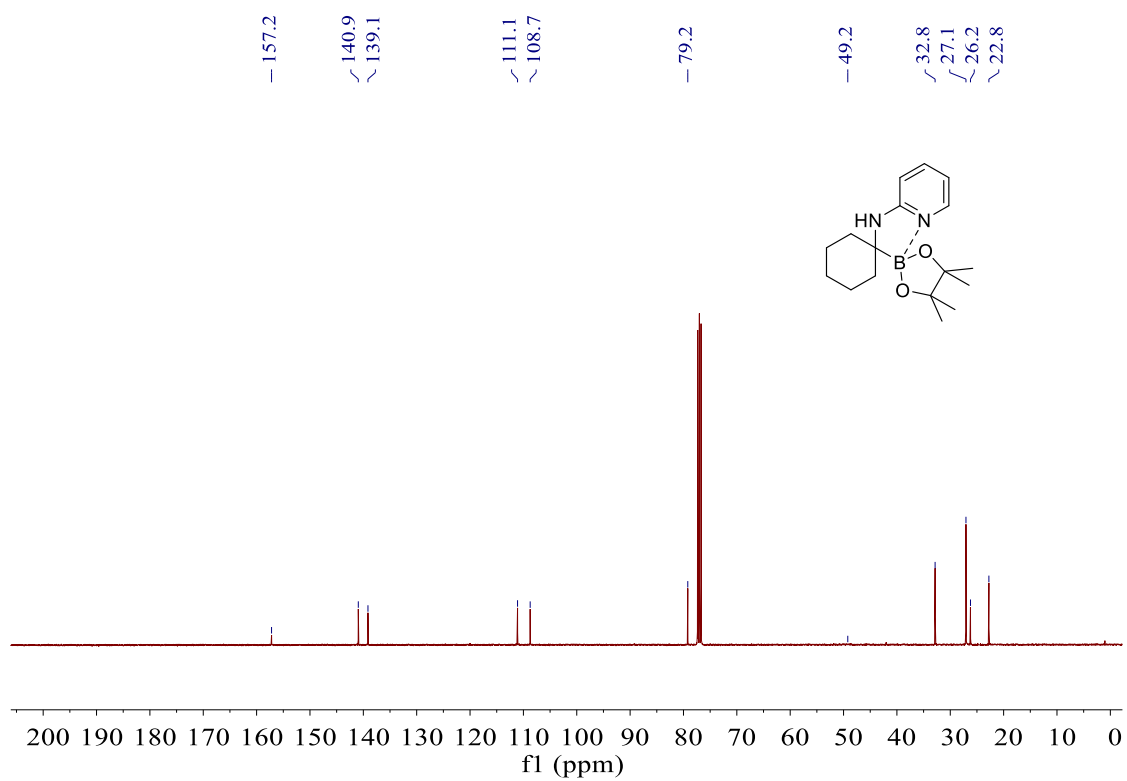
Appendix

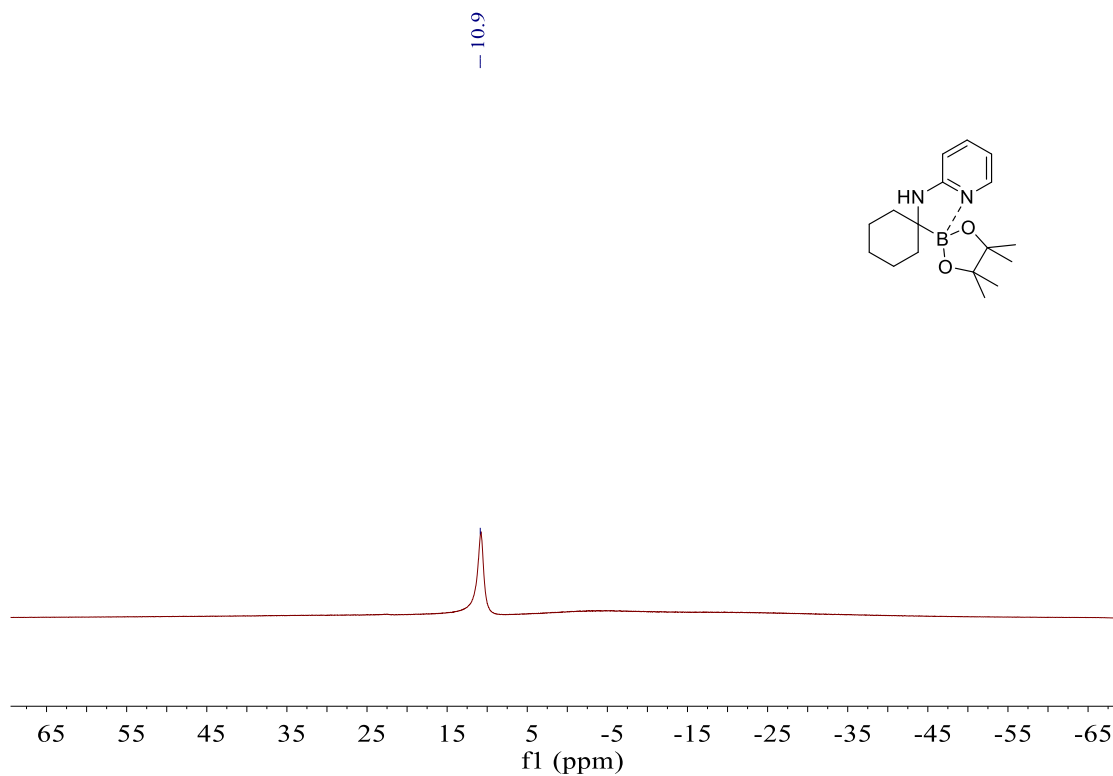
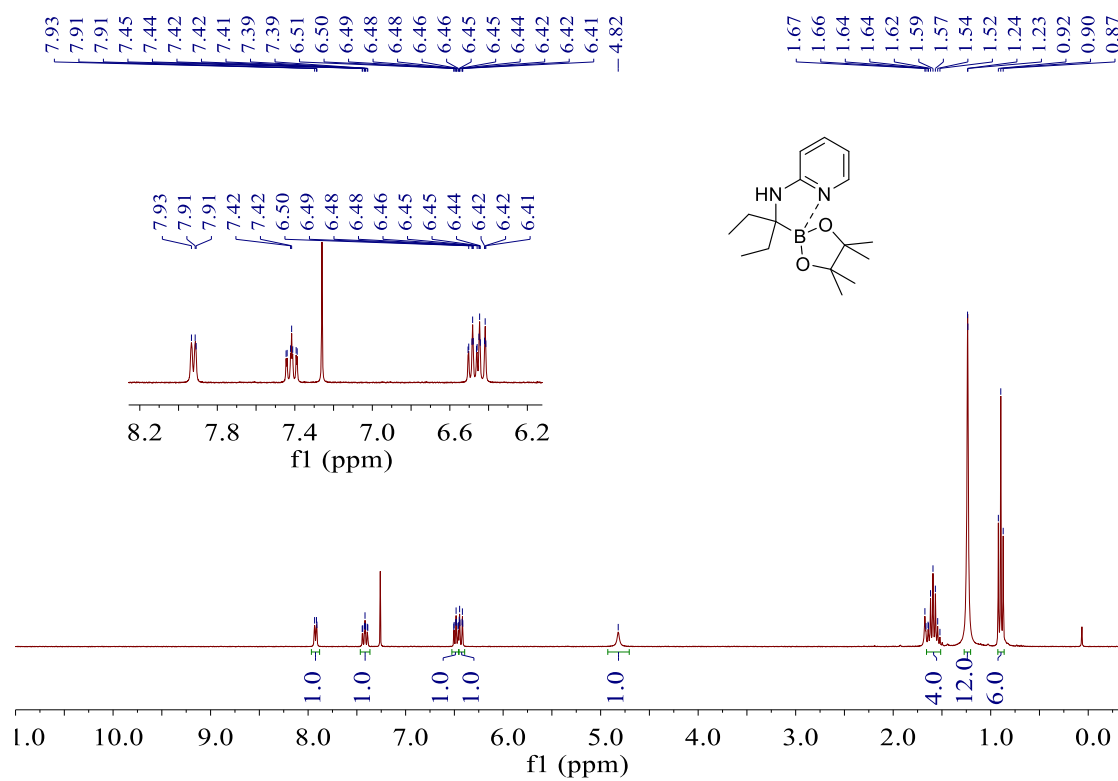
$^{13}\text{C}\{^1\text{H}\}$ NMR spectrum (101 MHz, CDCl_3) of **2-3r**

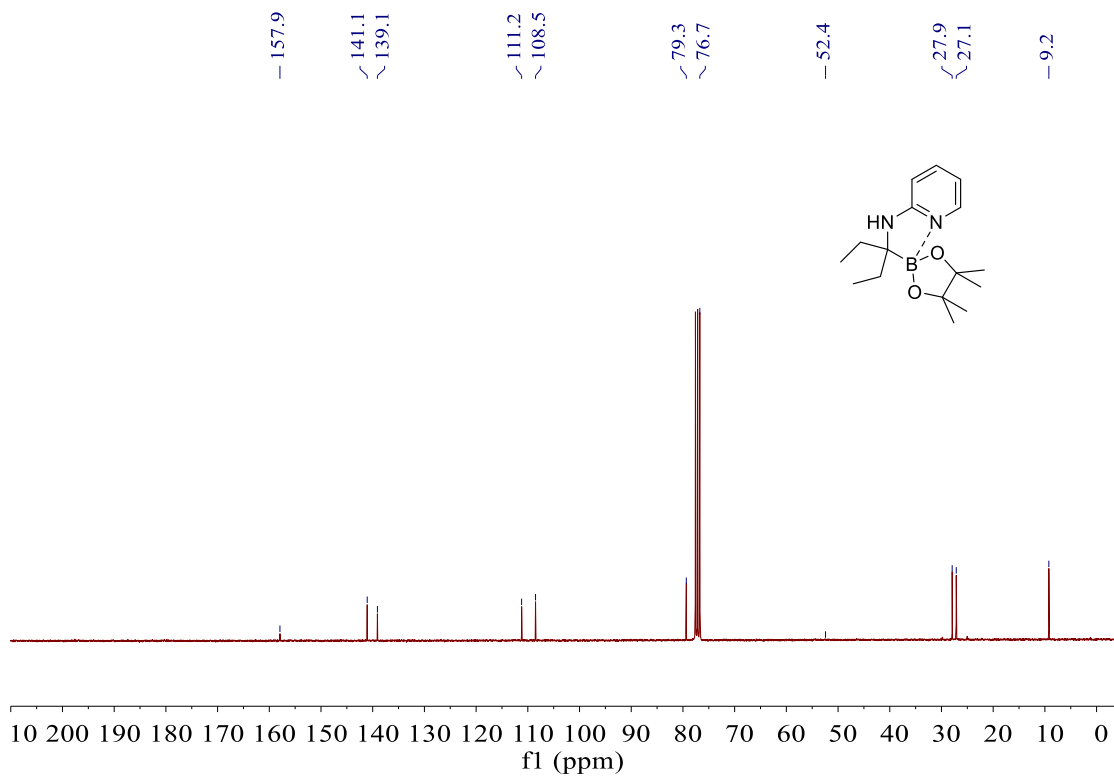
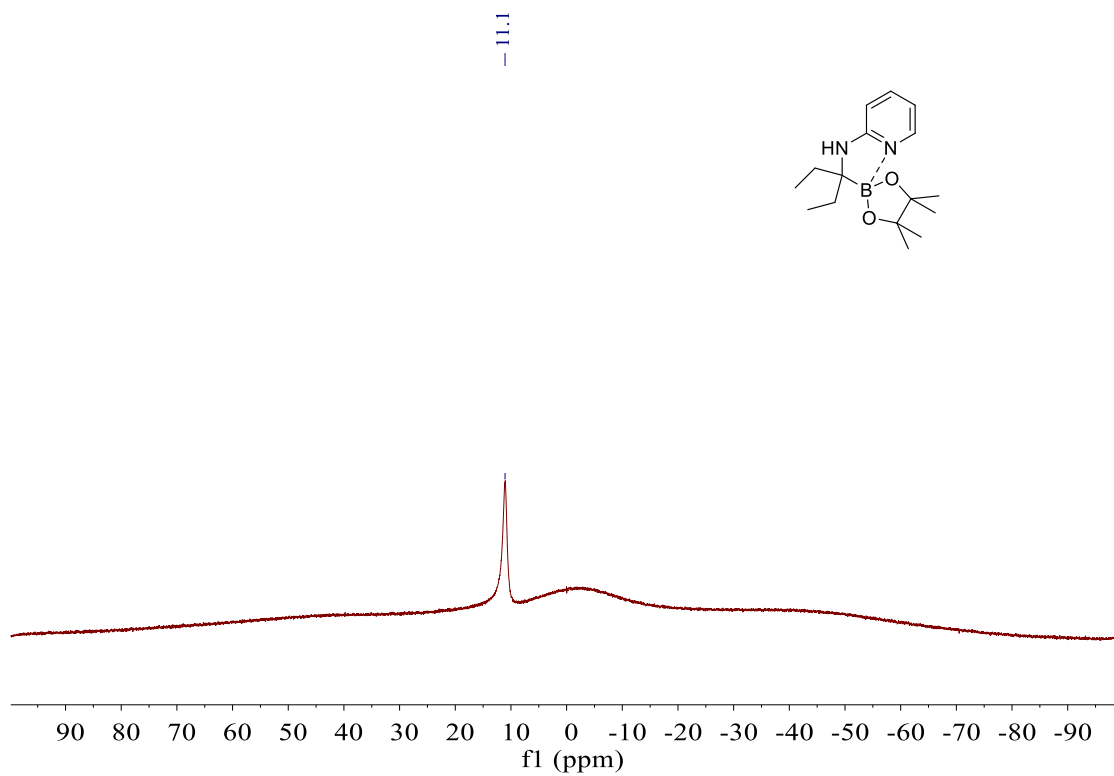


^{11}B NMR spectrum (128 MHz, CDCl_3) of **2-3r**



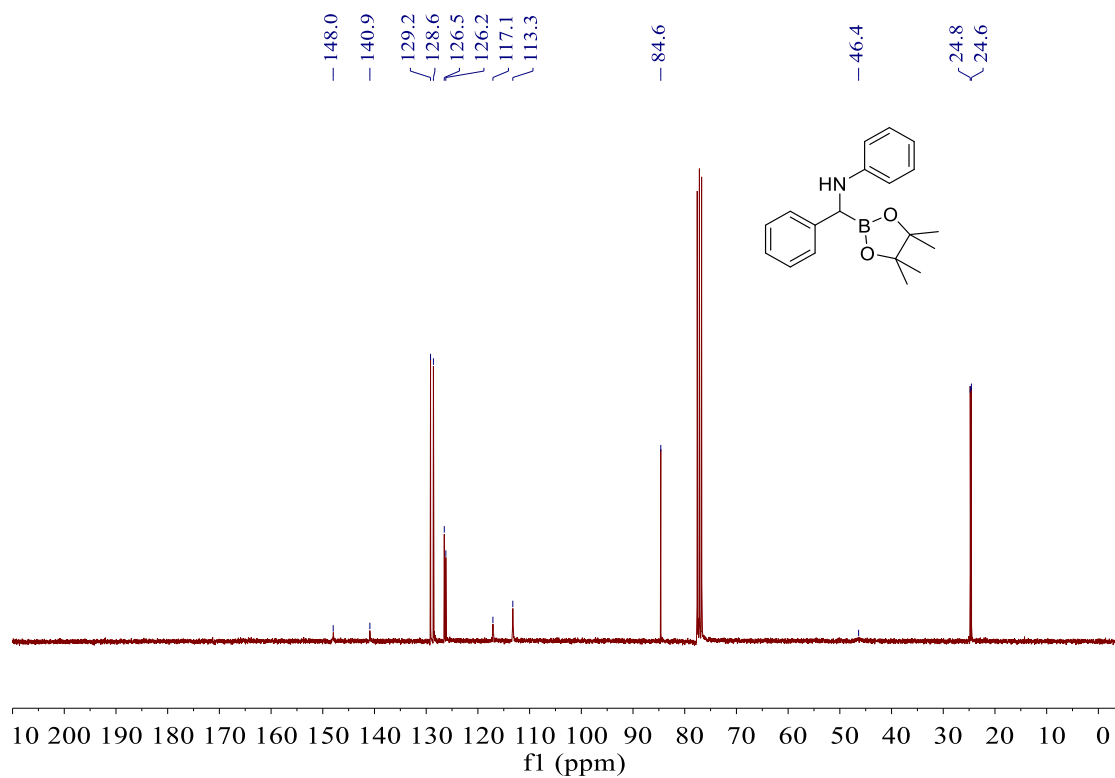
^1H NMR spectrum (400 MHz, CDCl_3) of **2-3s** $^{13}\text{C}\{^1\text{H}\}$ NMR spectrum (101 MHz, CDCl_3) of **2-3s**

^{11}B NMR spectrum (128 MHz, CDCl_3) of **2-3s** ^1H NMR spectrum (300 MHz, CDCl_3) of **2-3t**

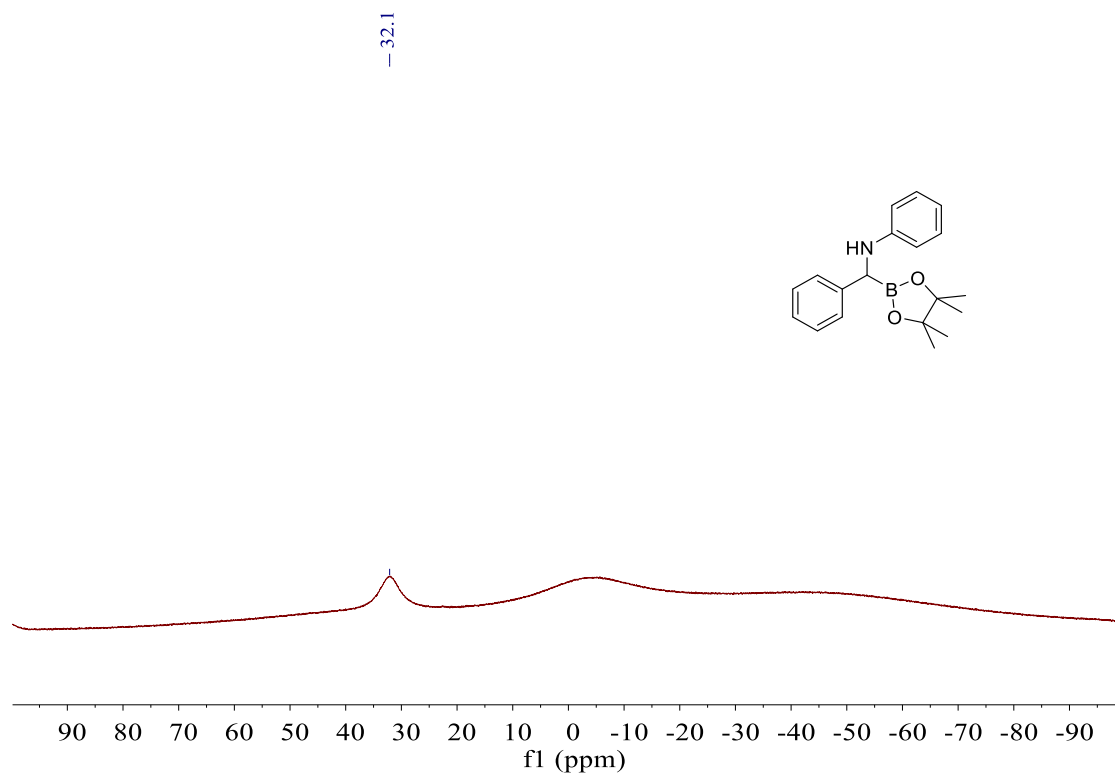
$^{13}\text{C}\{^1\text{H}\}$ NMR spectrum (75 MHz, CDCl_3) of **2-3t** ^{11}B NMR spectrum (96 MHz, CDCl_3) of **2-3t**

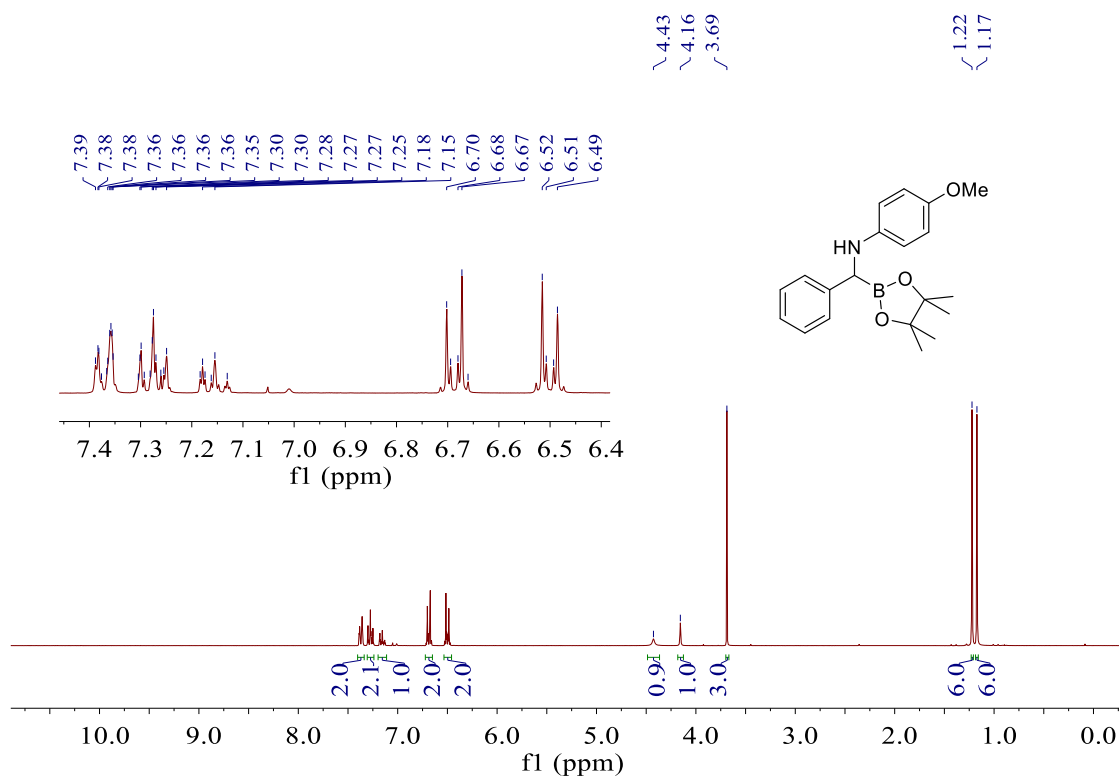
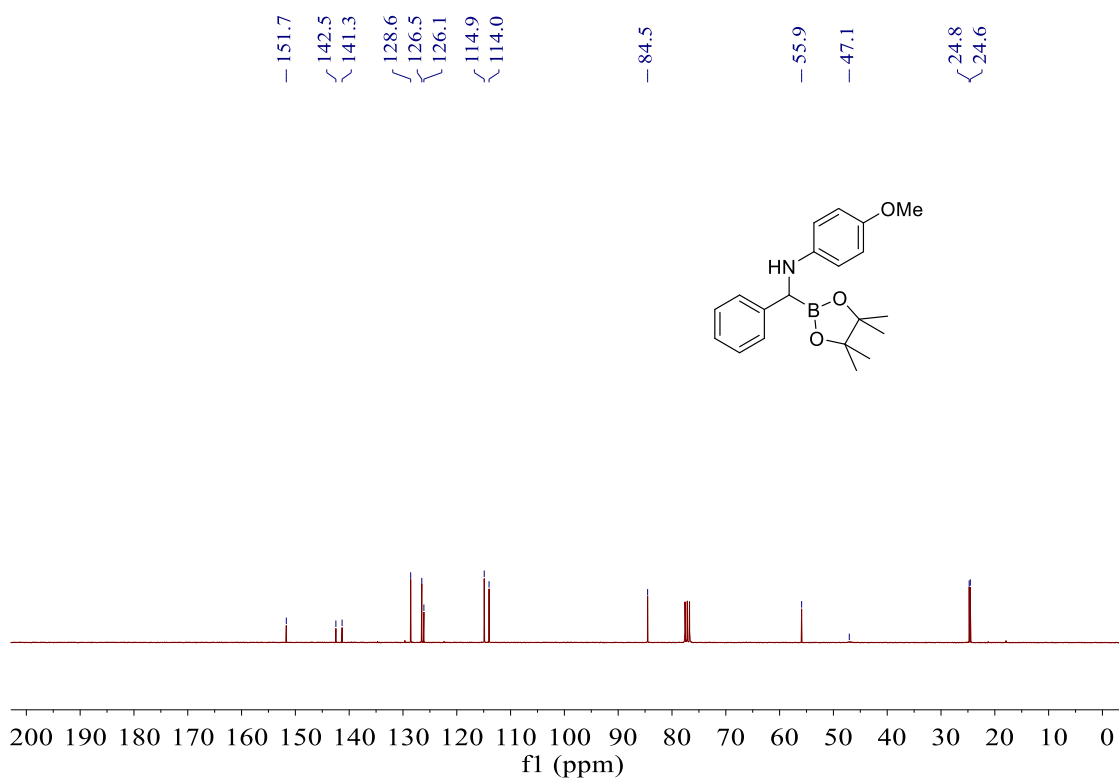
Appendix

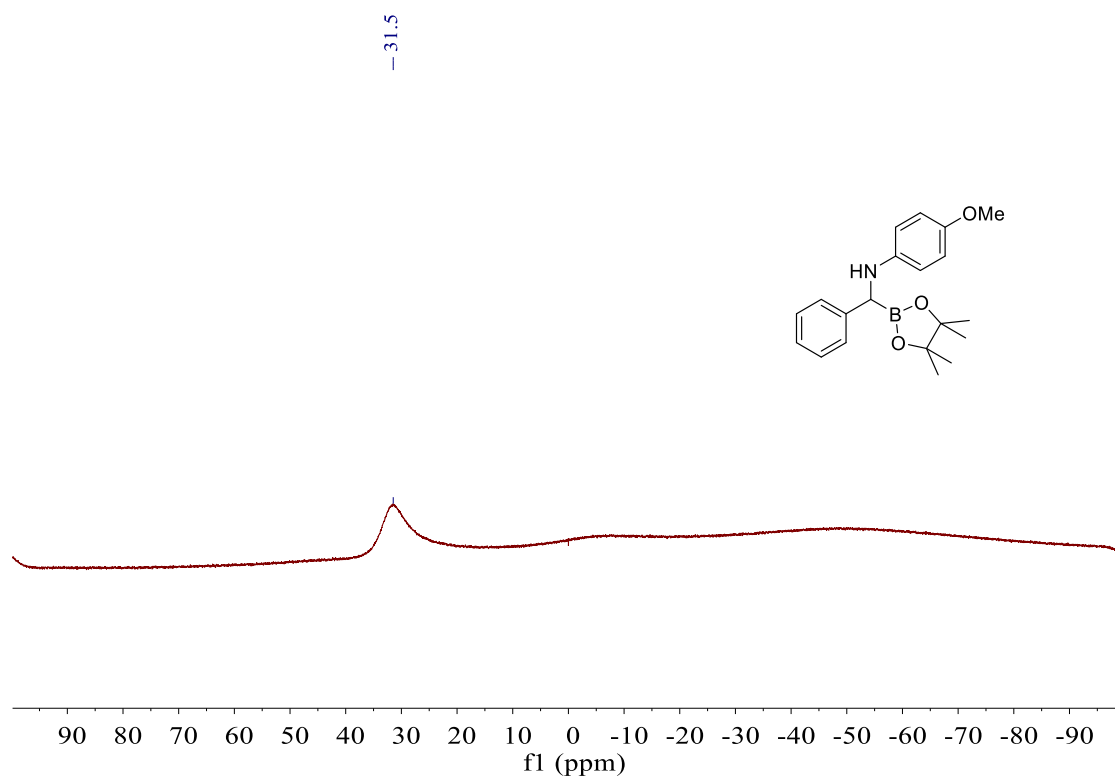
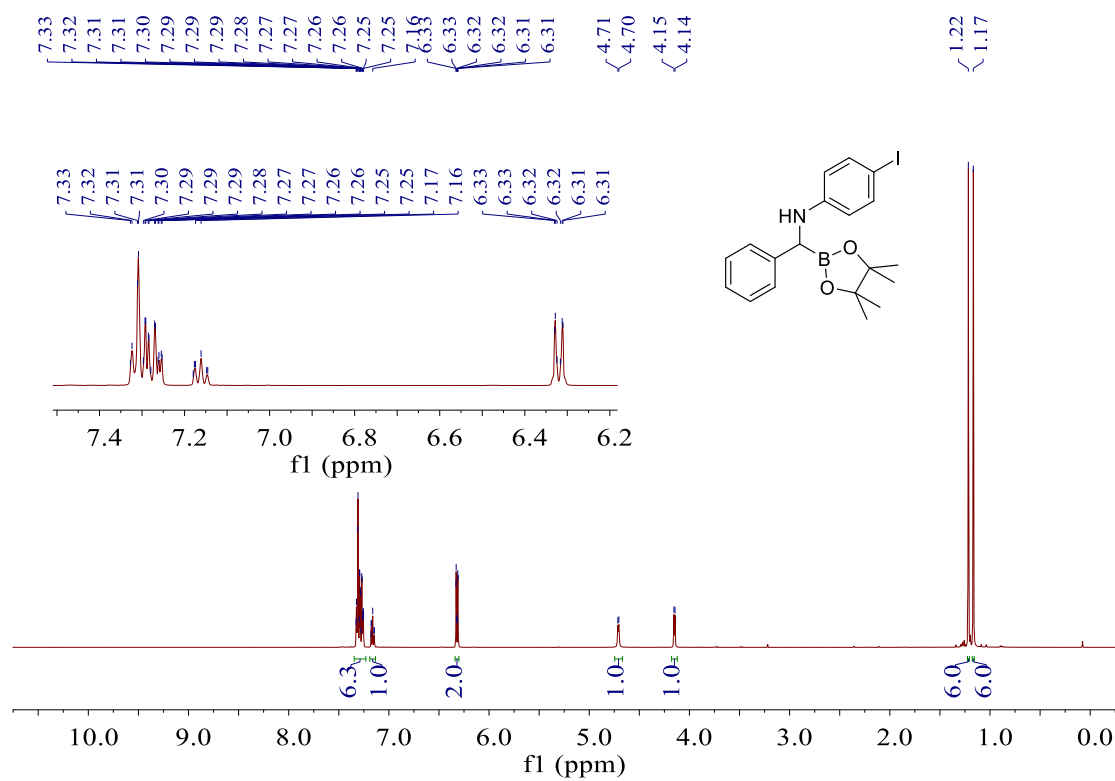
$^{13}\text{C}\{^1\text{H}\}$ NMR spectrum (75 MHz, CDCl_3) of **2-3v**

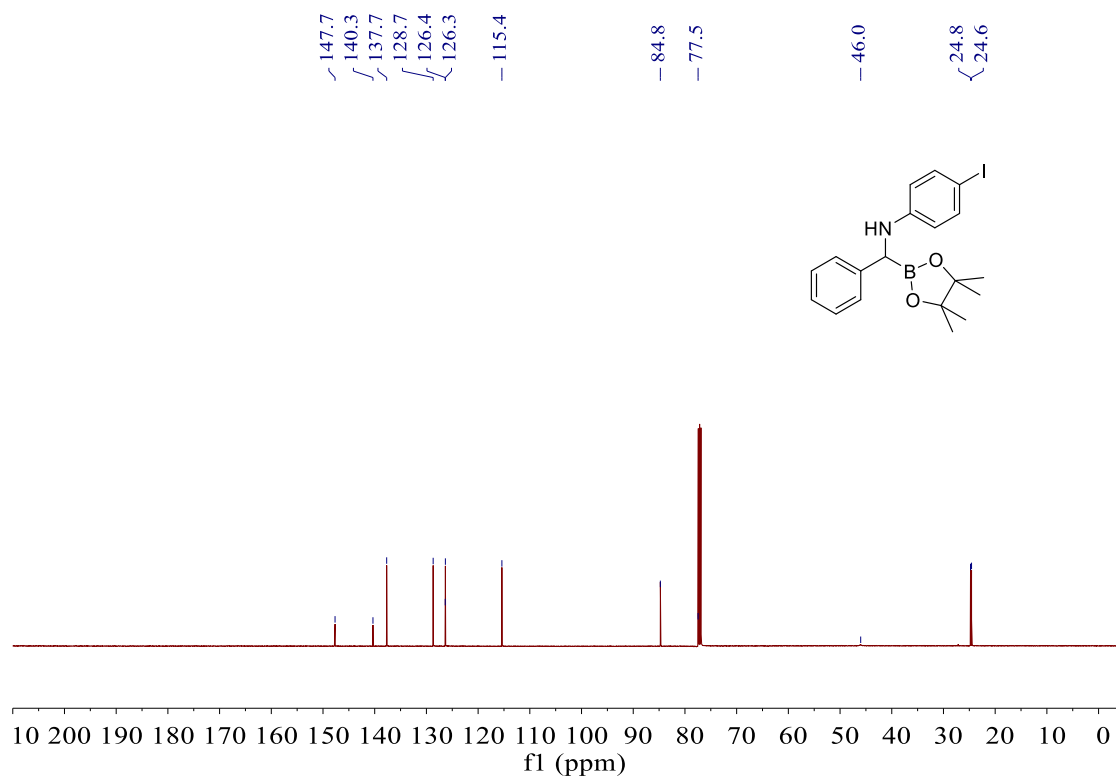
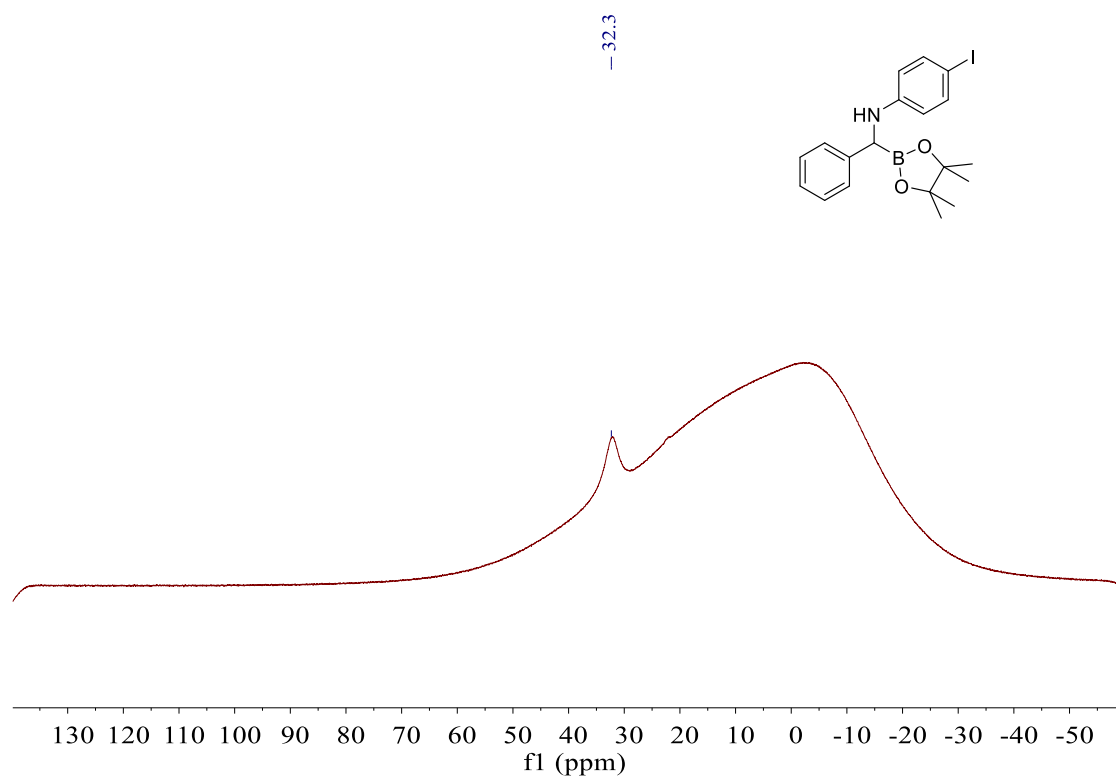


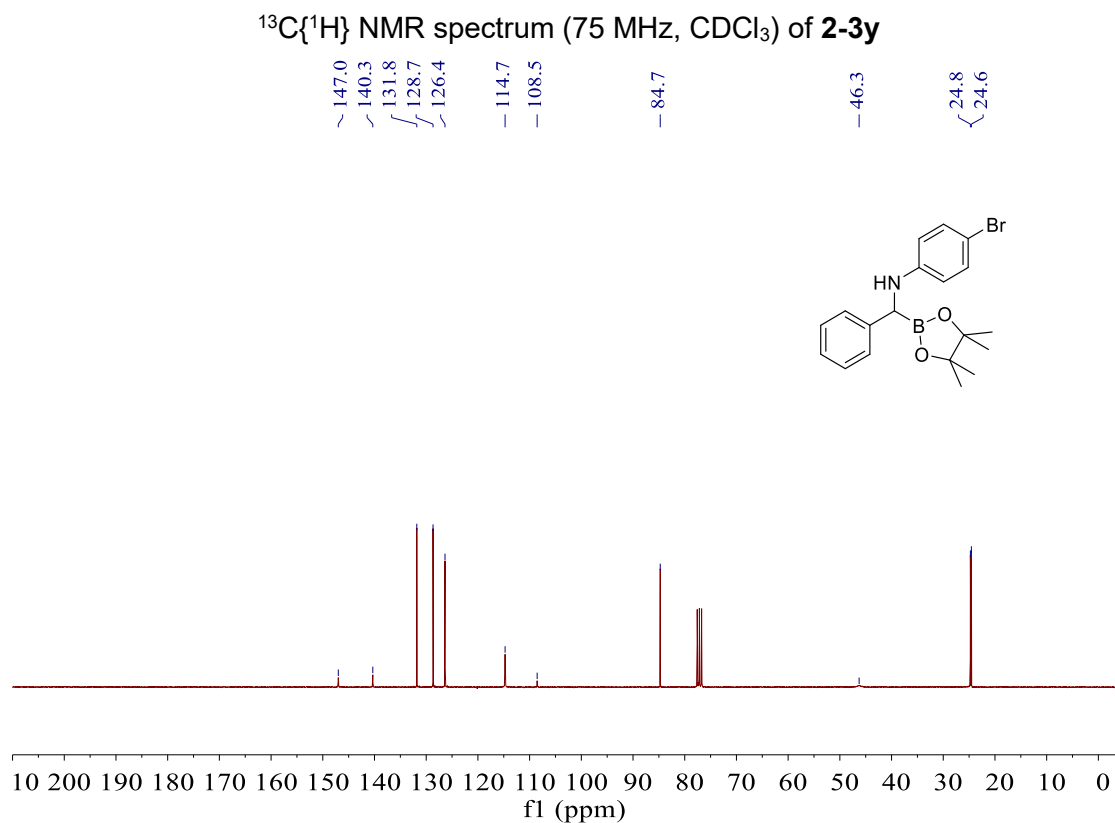
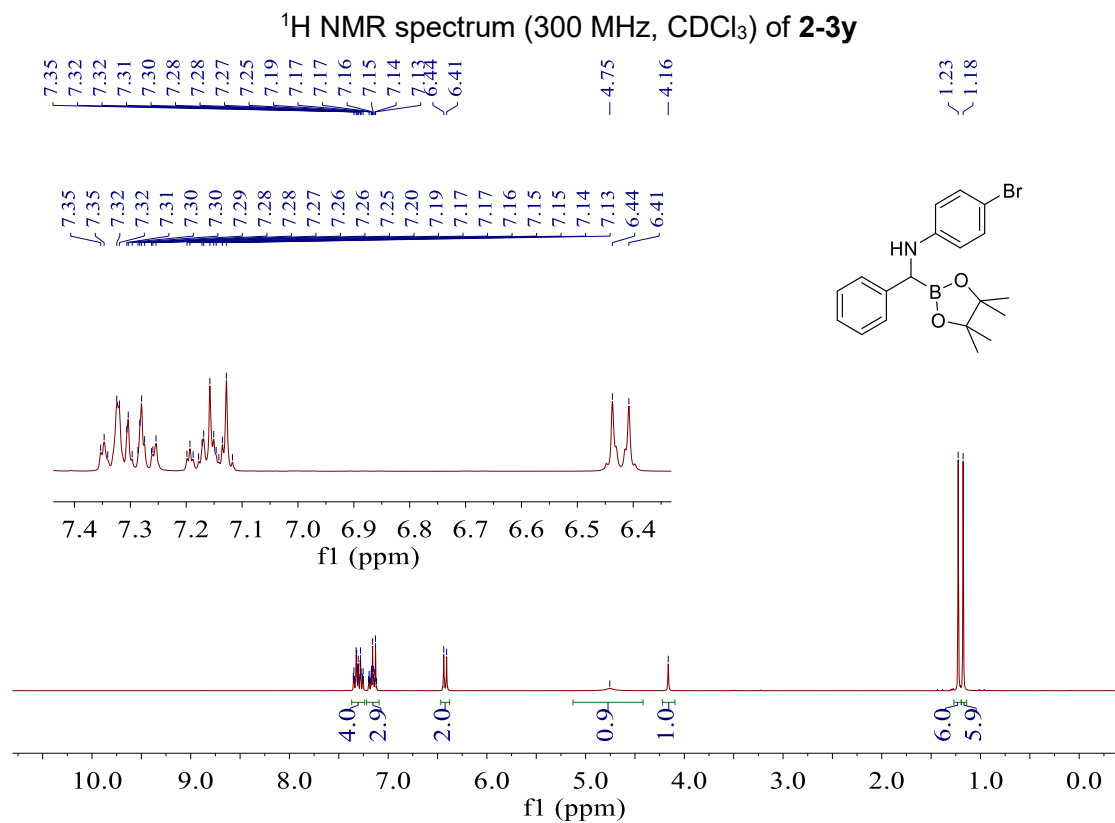
^{11}B NMR spectrum (96 MHz, CDCl_3) of **2-3v**

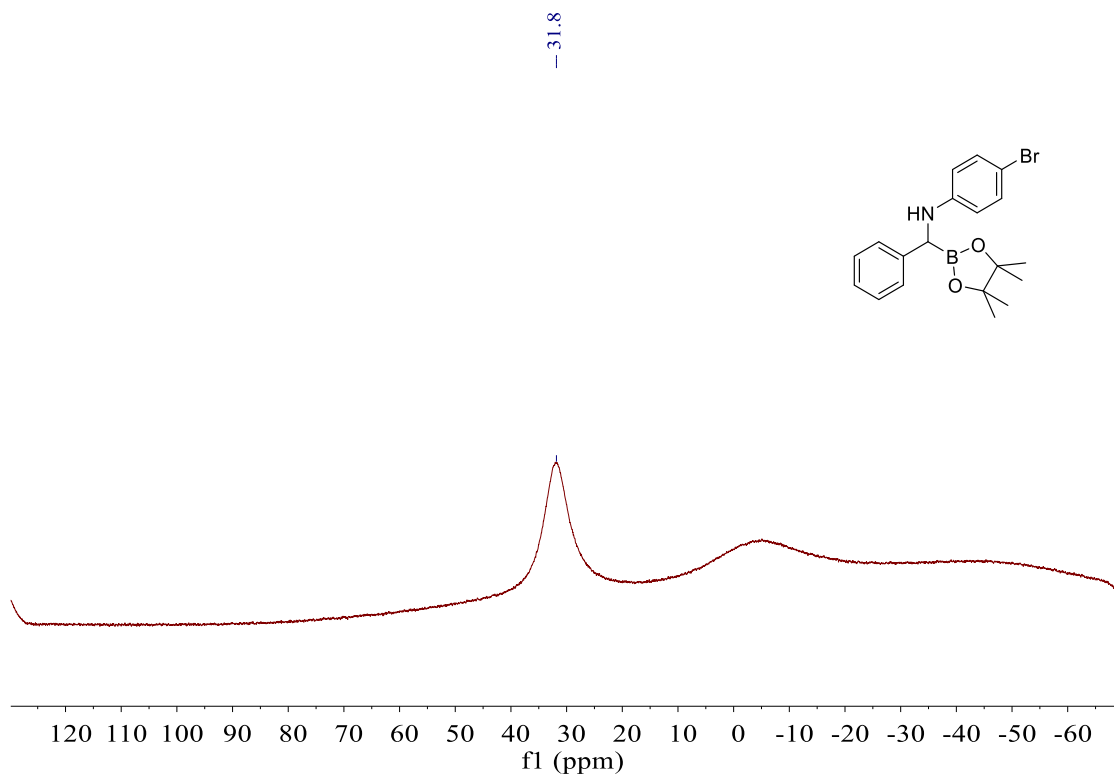
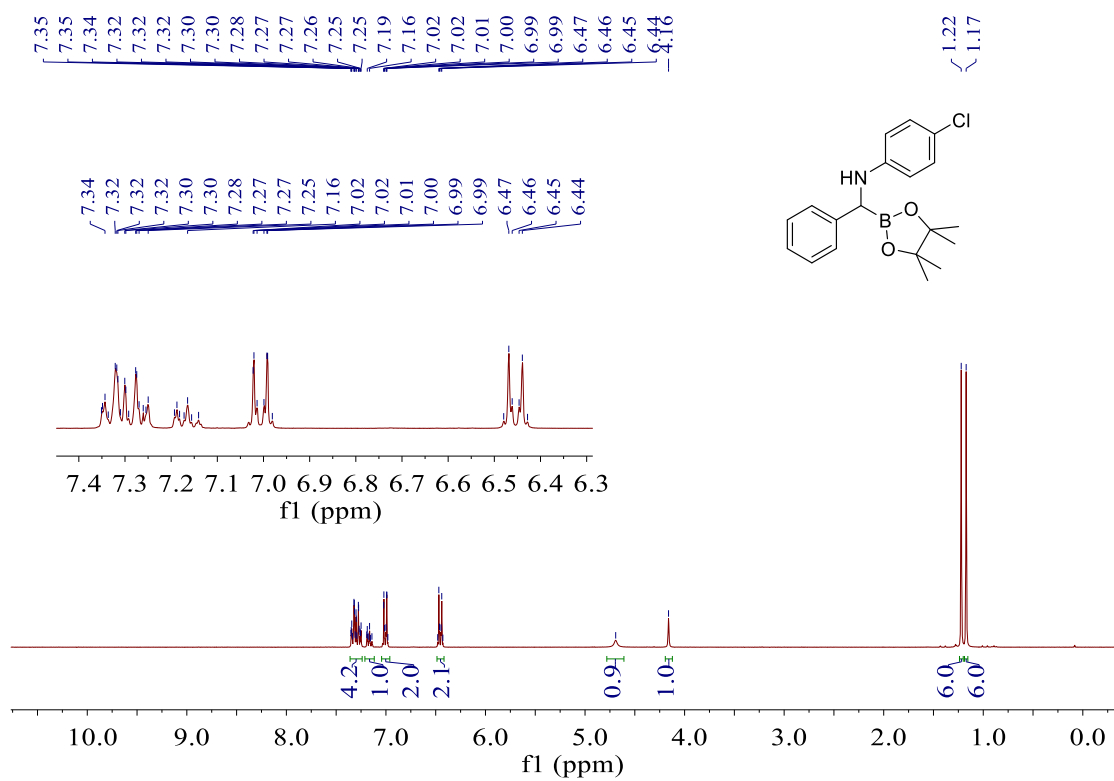


^1H NMR spectrum (300 MHz, CDCl_3) of **2-3w** $^{13}\text{C}\{^1\text{H}\}$ NMR spectrum (75 MHz, CDCl_3) of **2-3w**

^{11}B NMR spectrum (96 MHz, CDCl_3) of **2-3w** ^1H NMR spectrum (500 MHz, CDCl_3) of **2-3x**

$^{13}\text{C}\{^1\text{H}\}$ NMR spectrum (126 MHz, CDCl_3) of **2-3x** ^{11}B NMR spectrum (160 MHz, CDCl_3) of **2-3x**



^{11}B NMR spectrum (96 MHz, CDCl_3) of **2-3y** ^1H NMR spectrum (300 MHz, CDCl_3) of **2-3z**

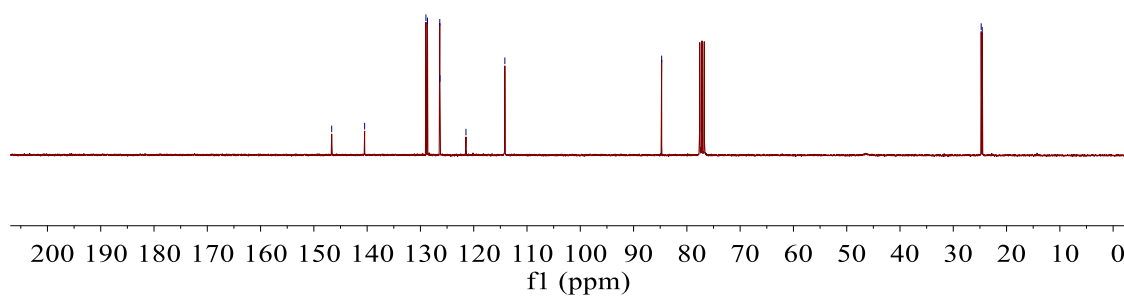
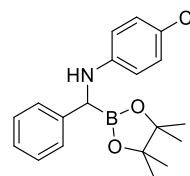
Appendix

$^{13}\text{C}\{^1\text{H}\}$ NMR spectrum (75 MHz, CDCl_3) of **2-3z**

-146.7
-140.5
129.0
128.7
126.4
126.3
121.5
114.2

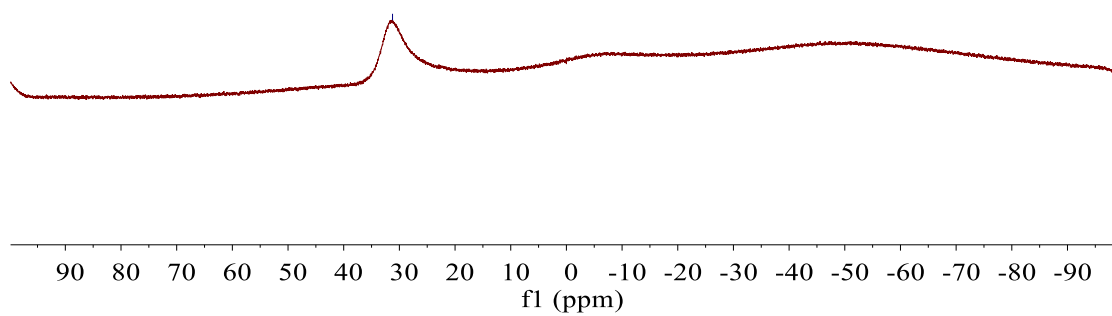
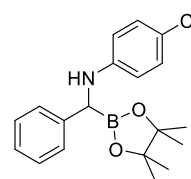
-84.7

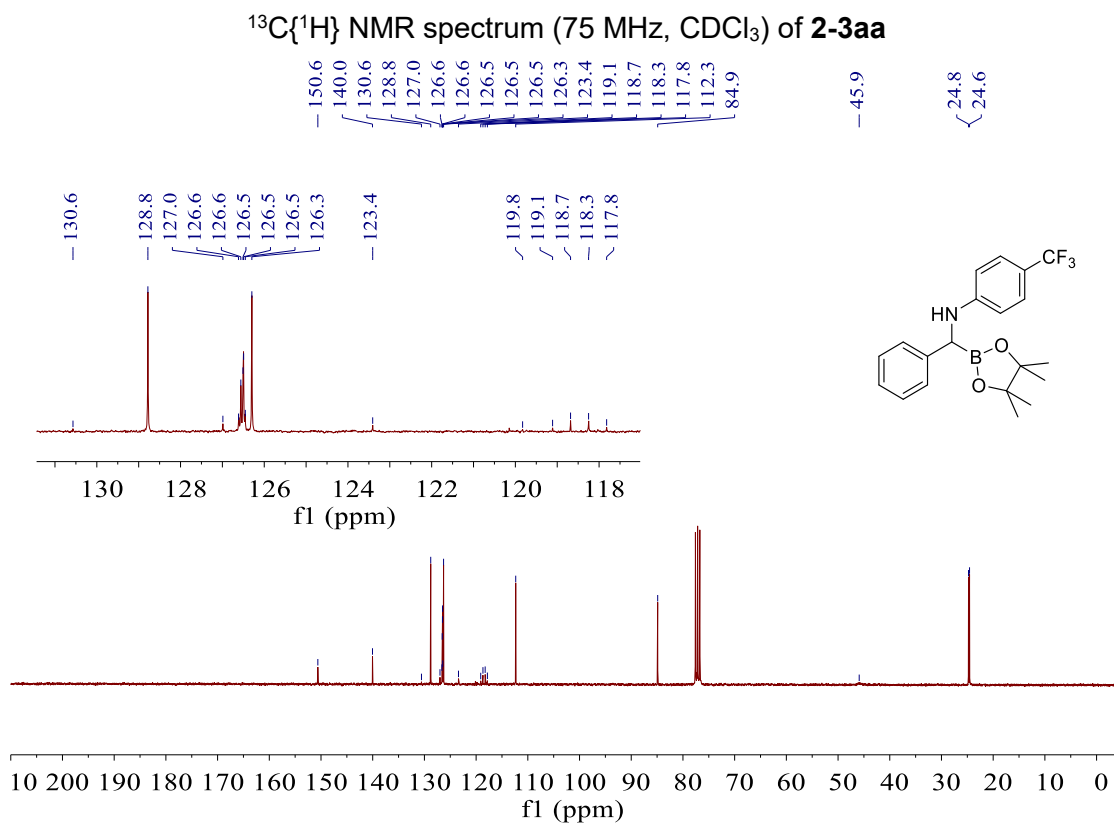
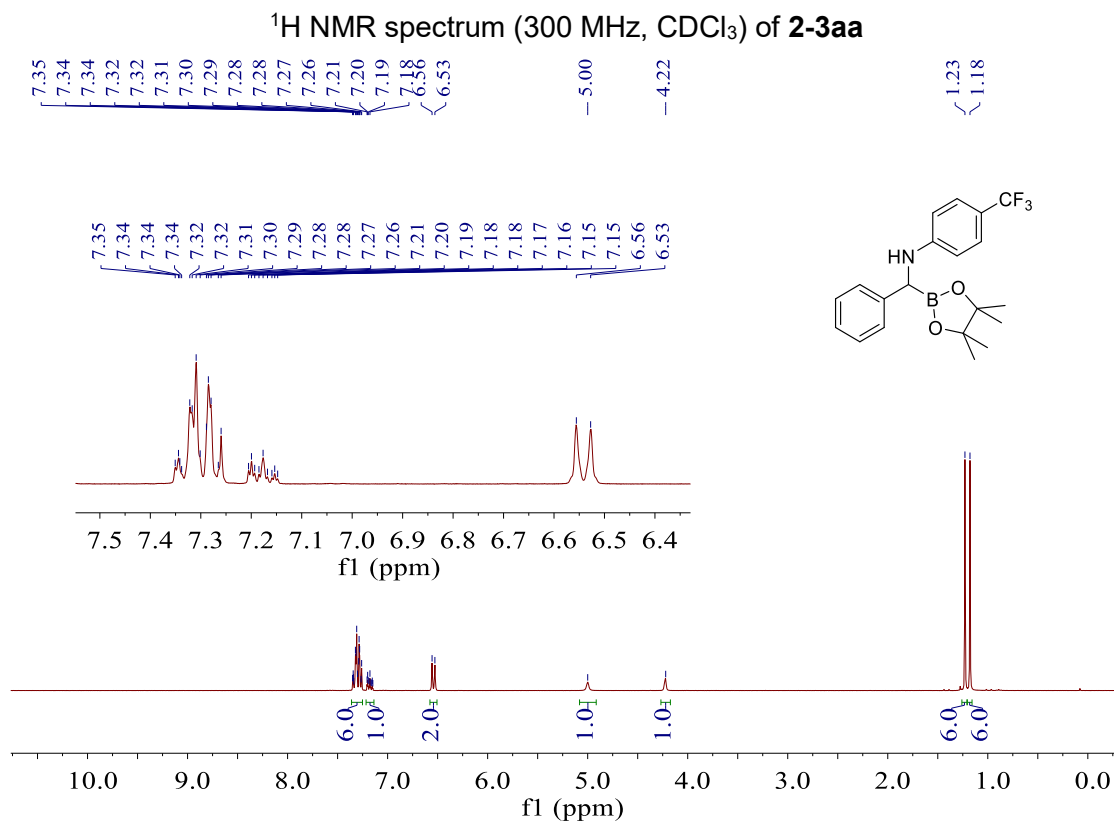
24.8
24.6

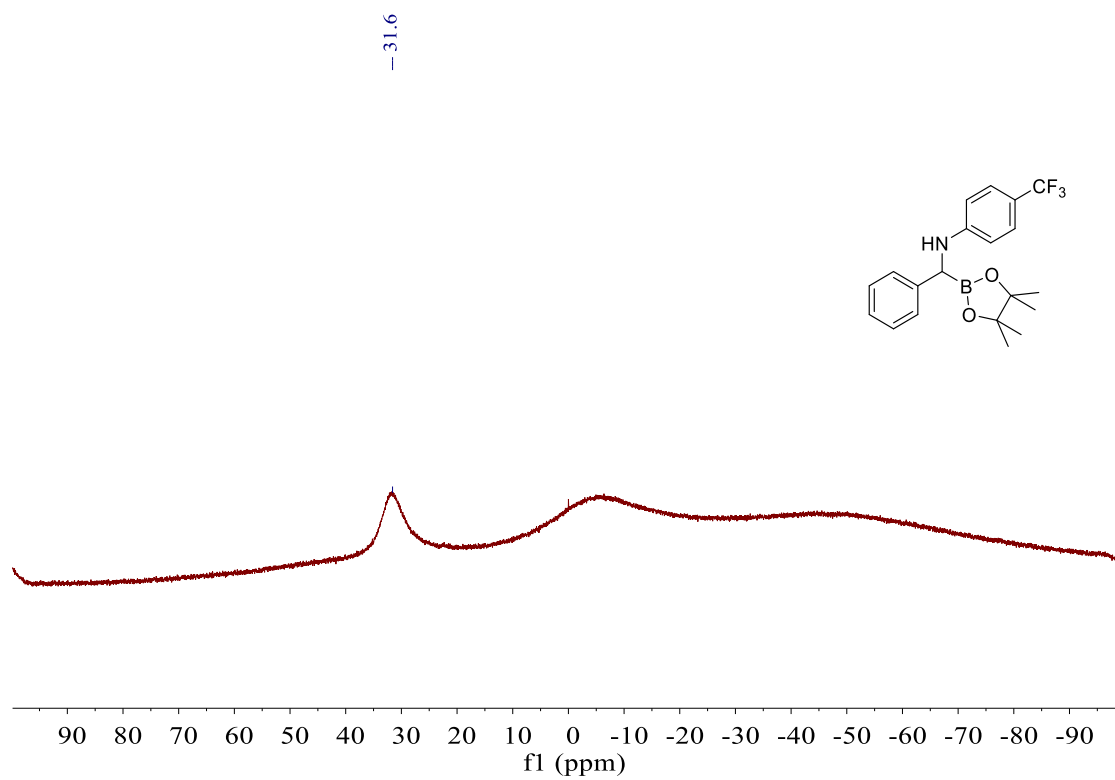
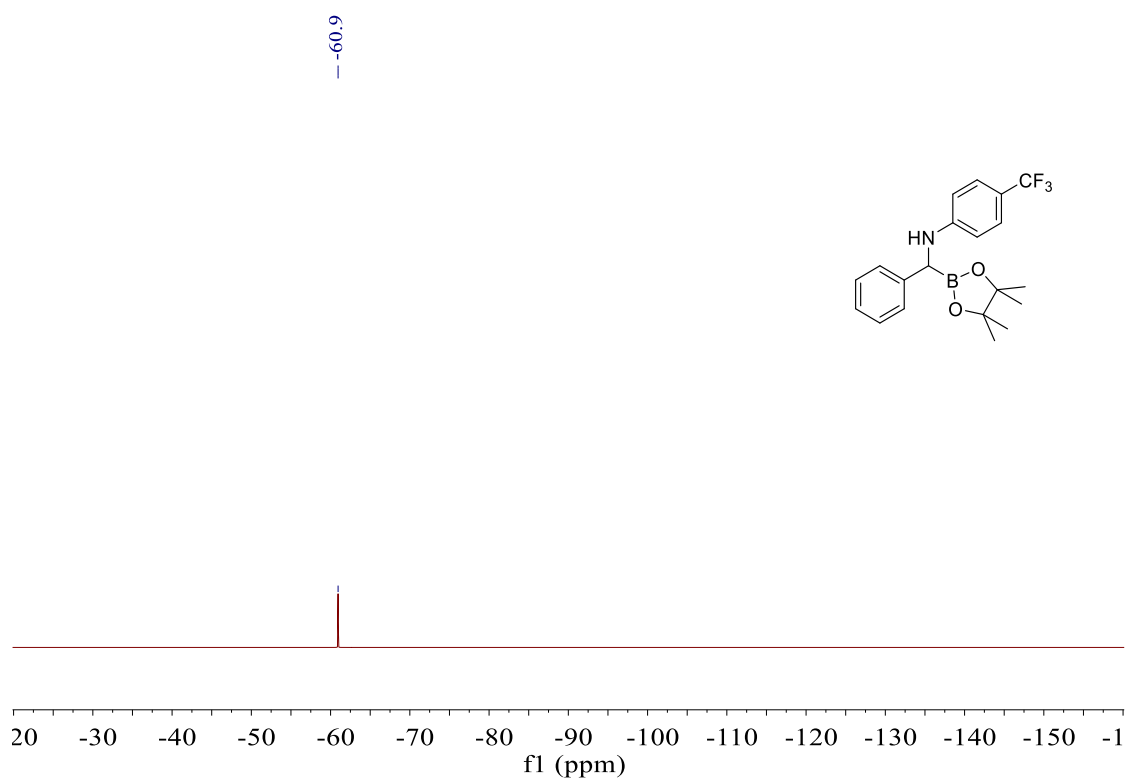


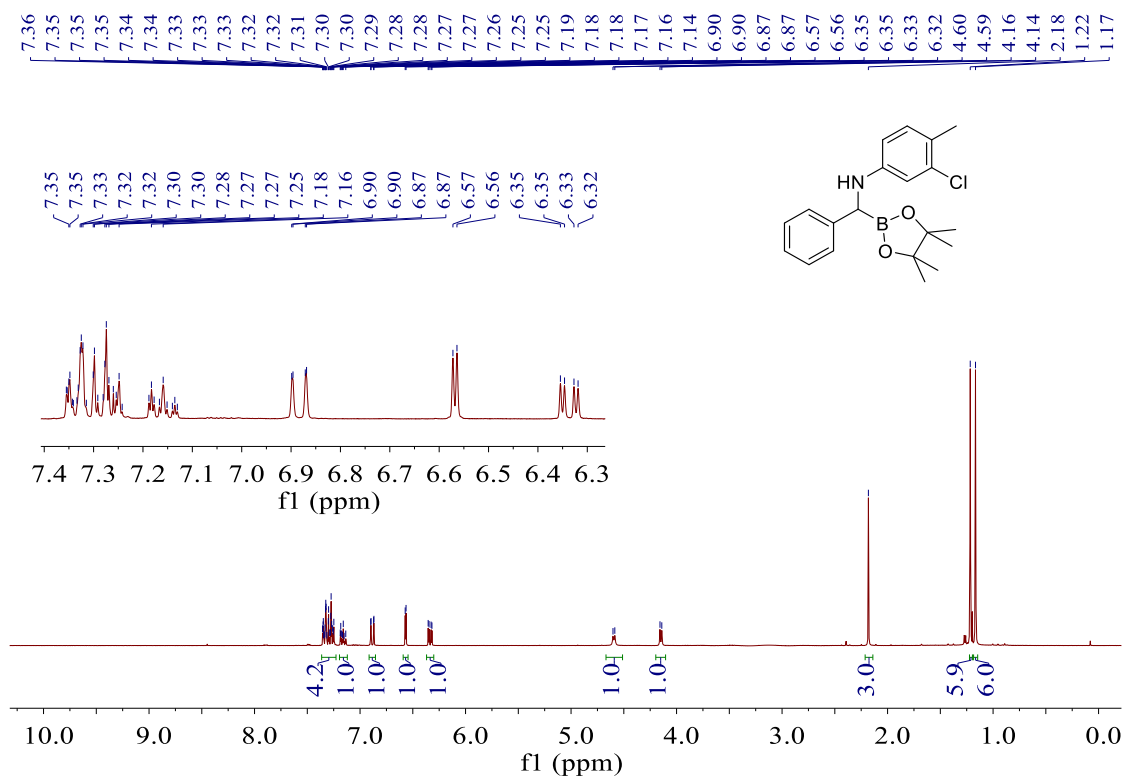
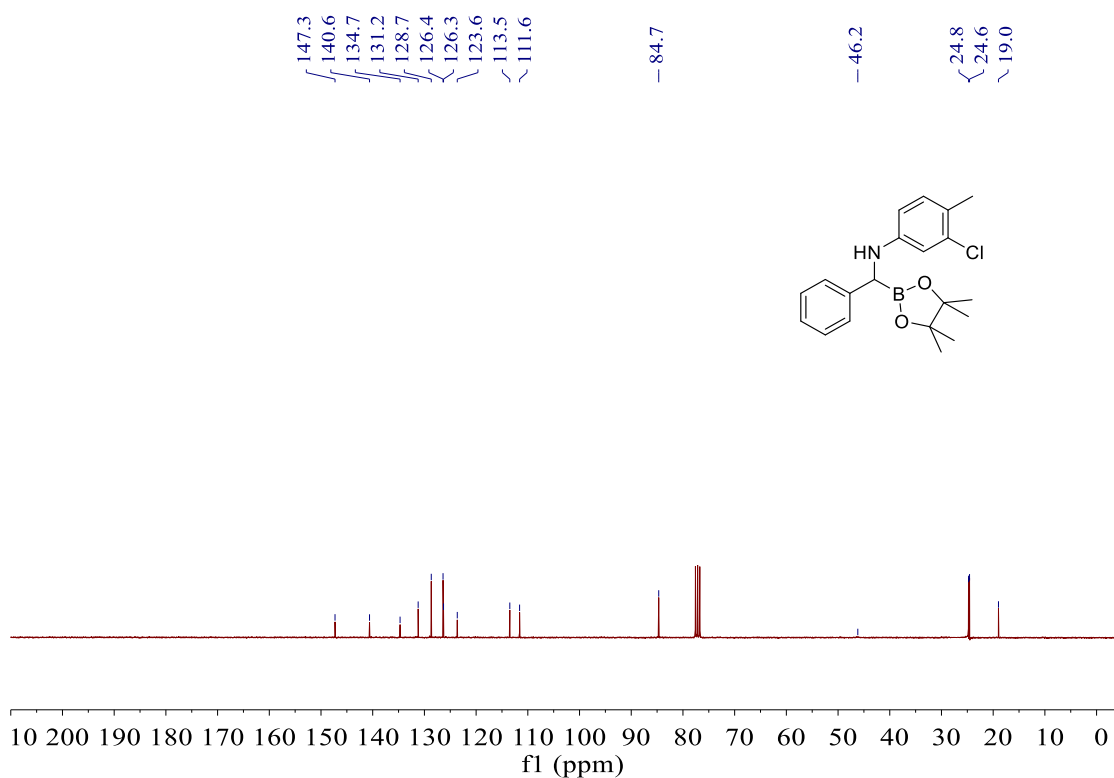
^{11}B NMR spectrum (96 MHz, CDCl_3) of **2-3z**

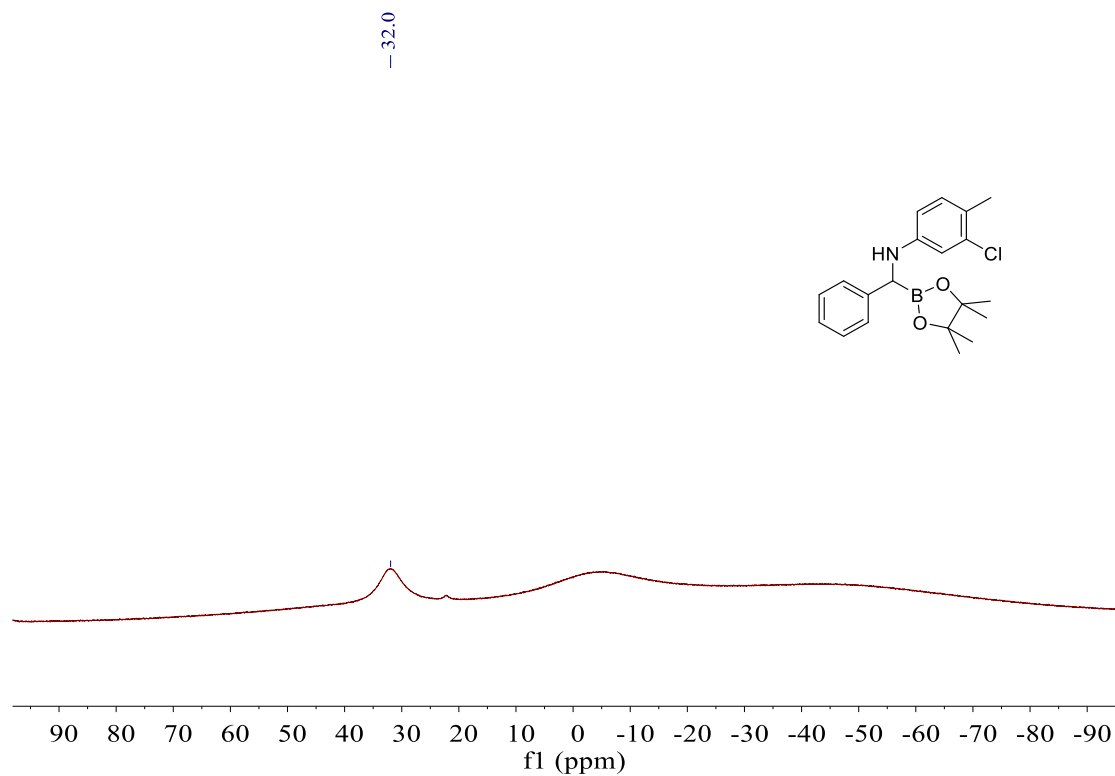
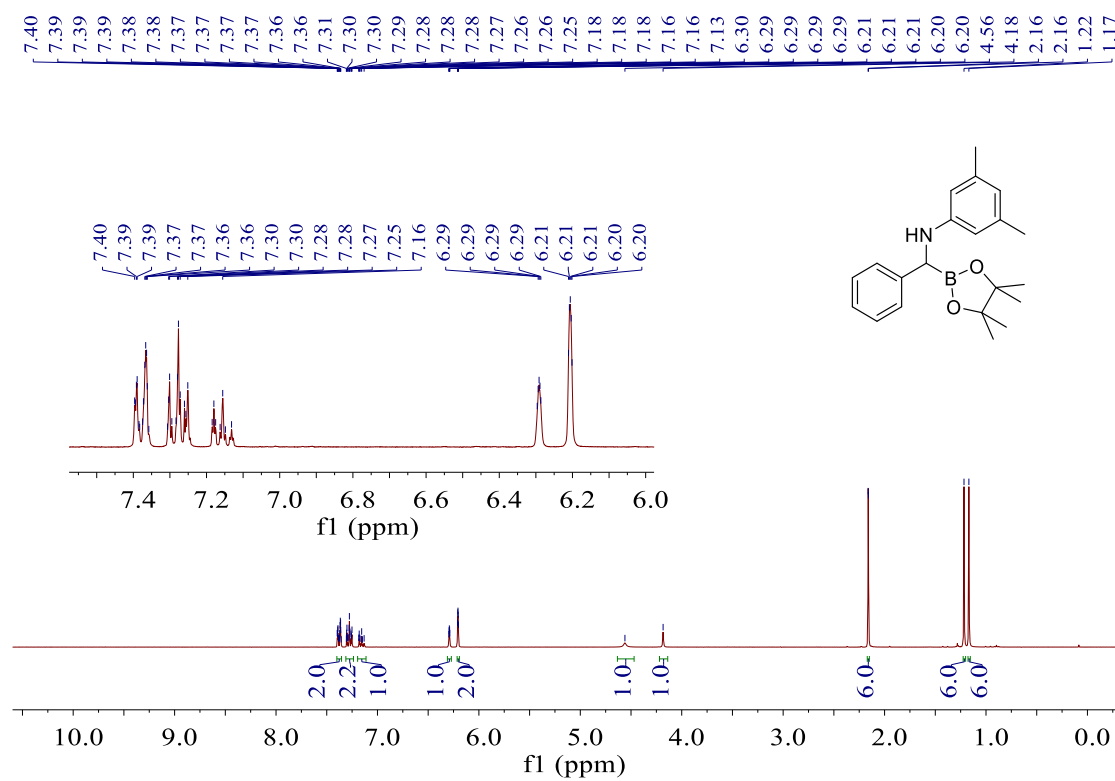
-31.2

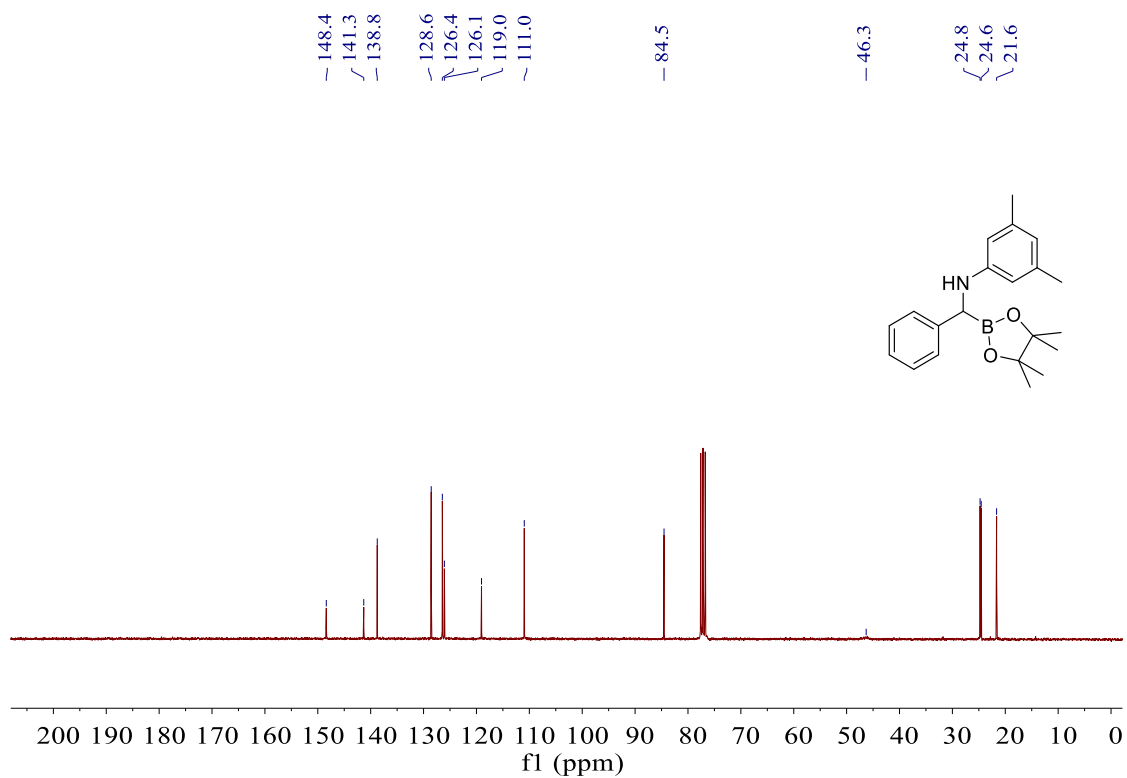
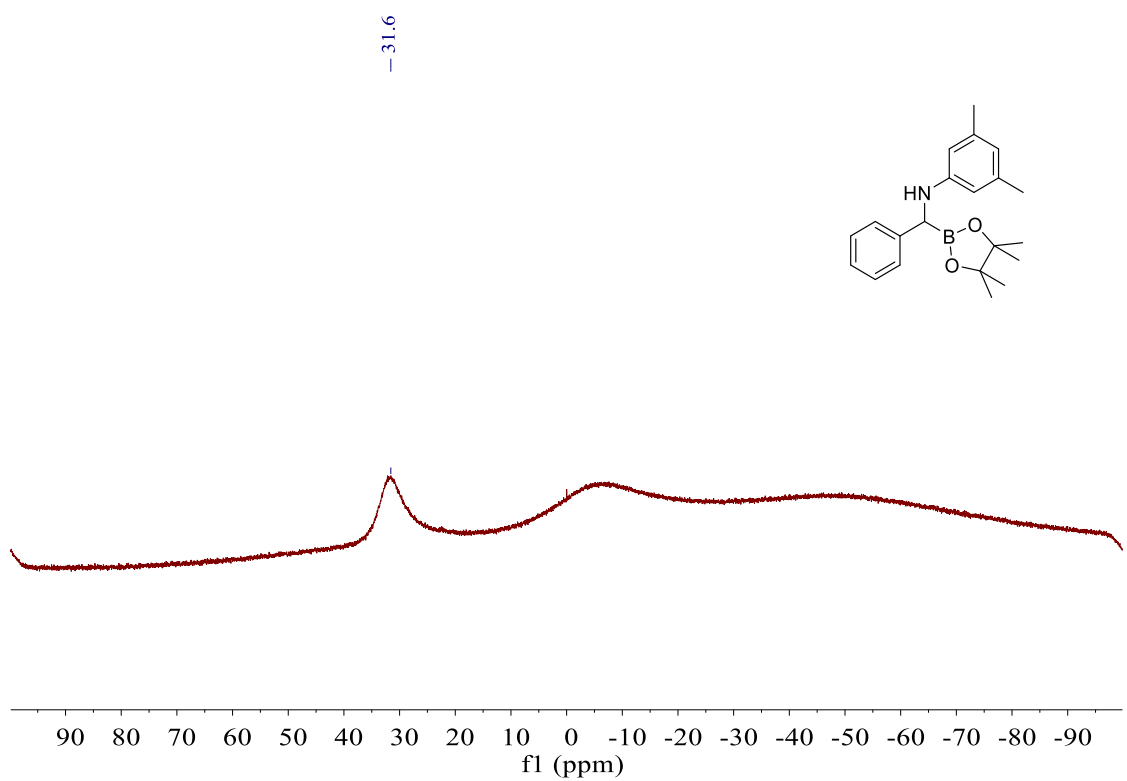


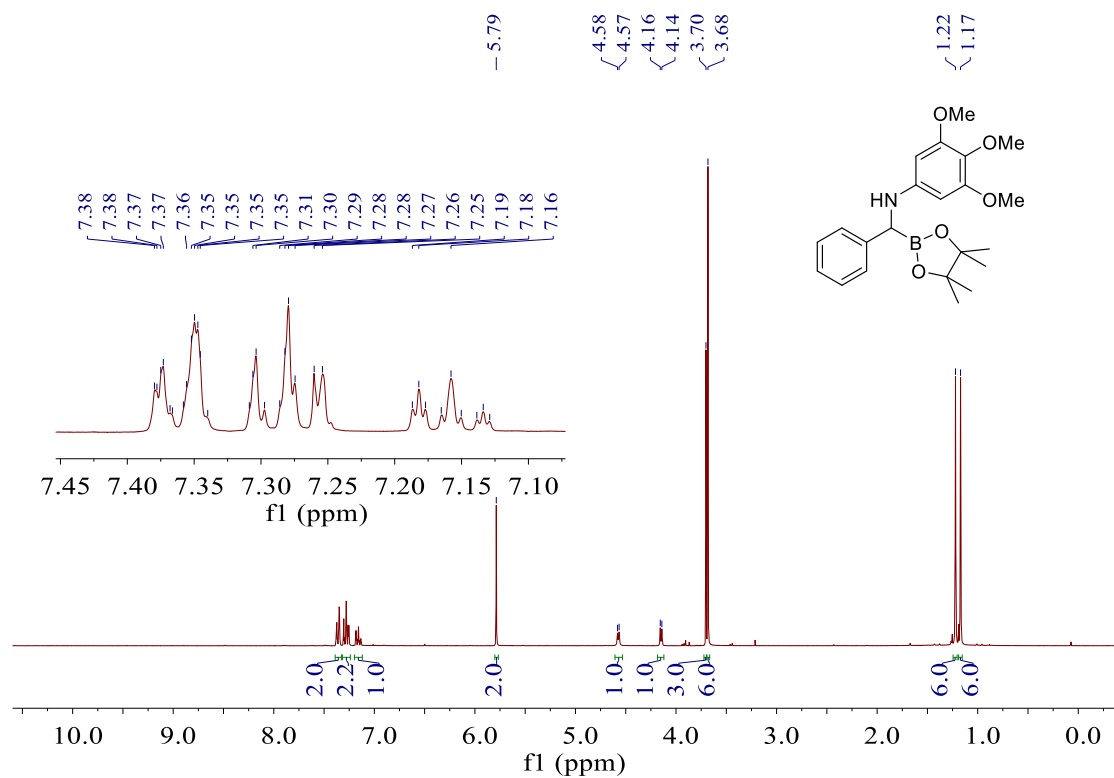
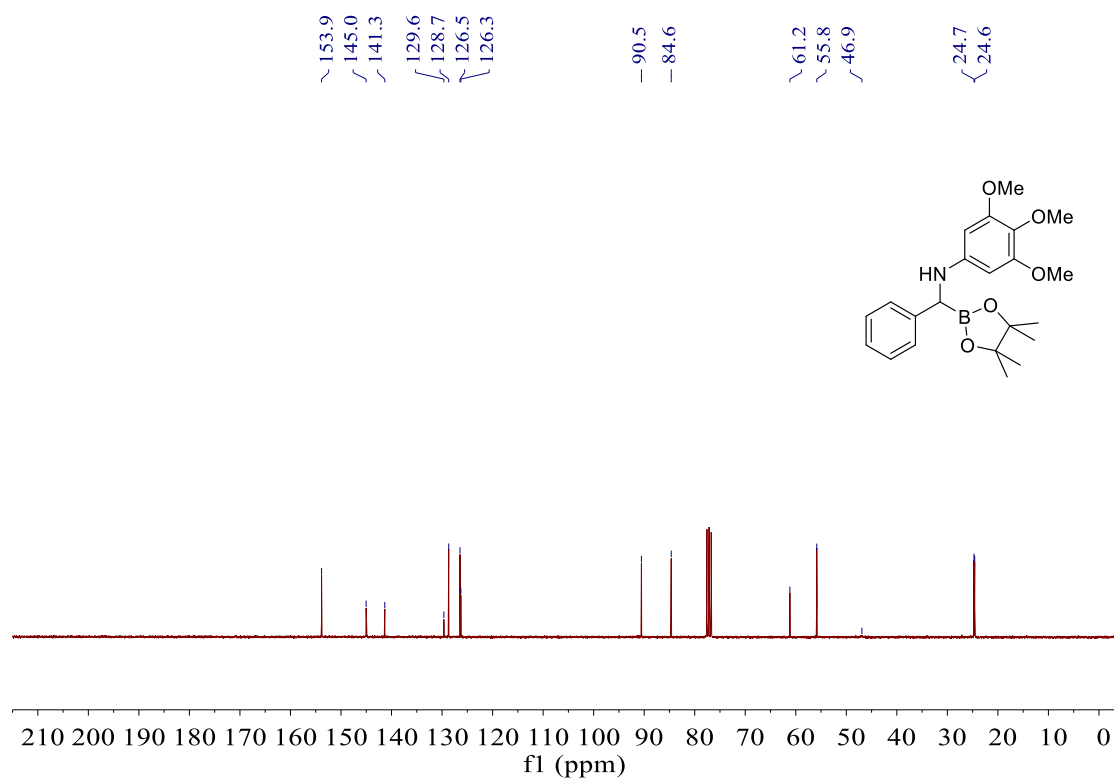


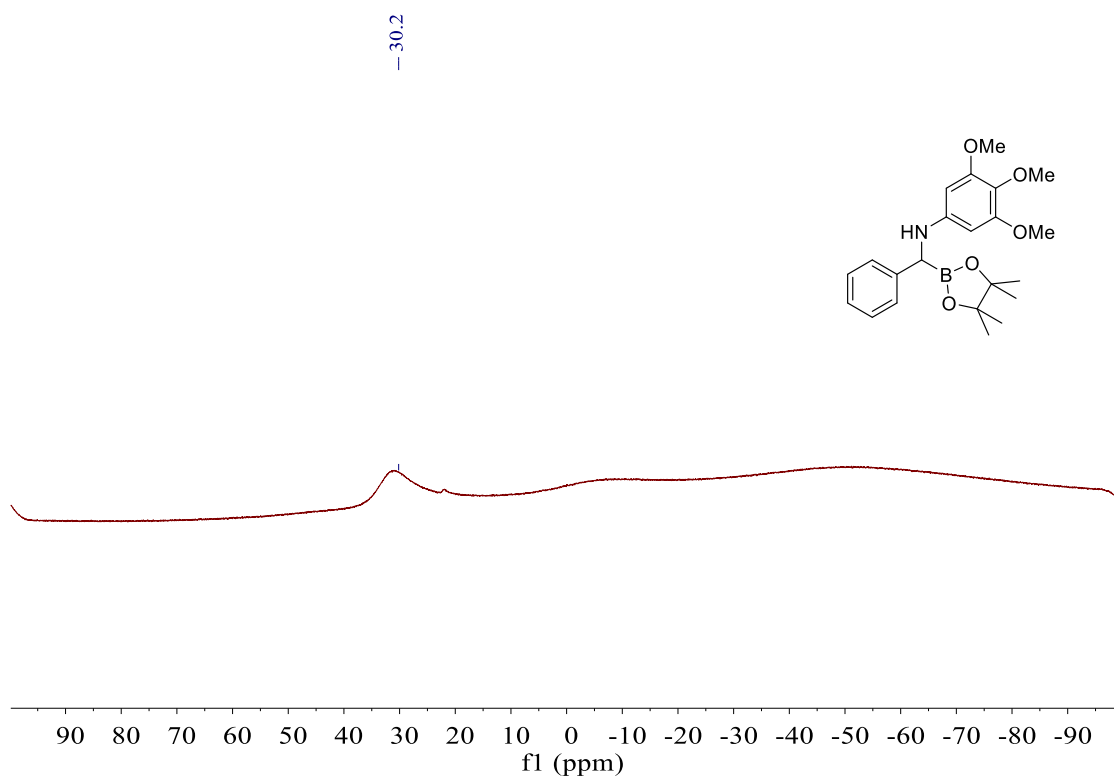
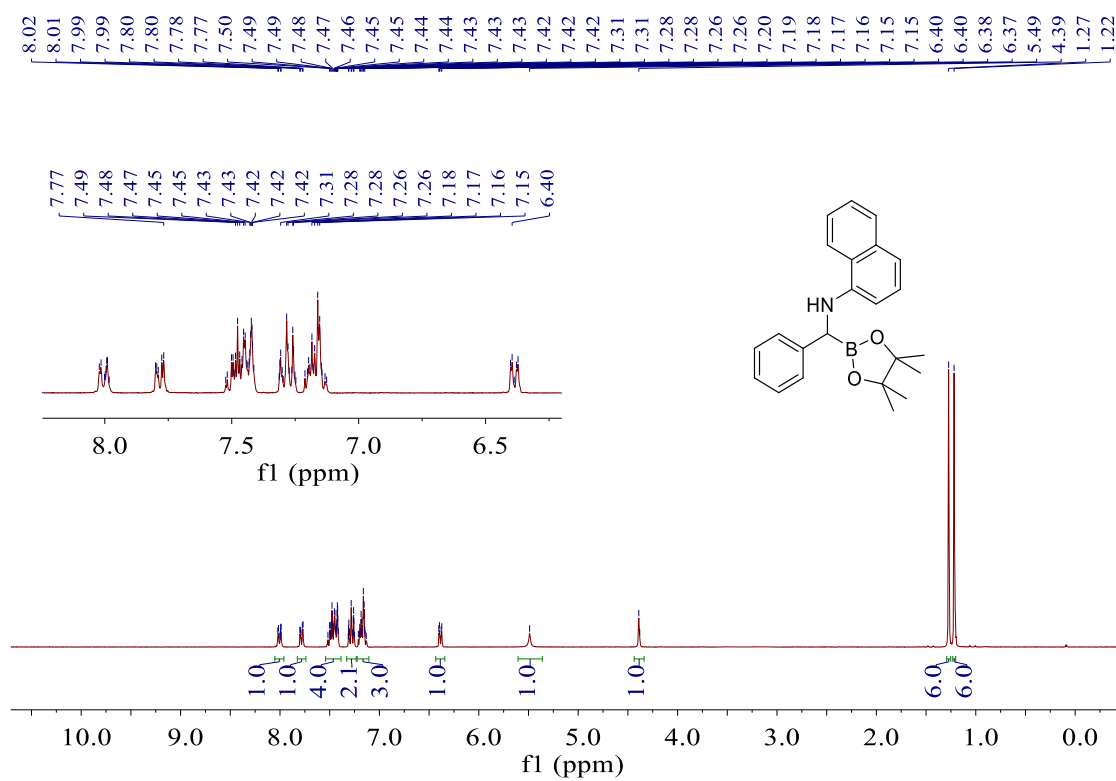
^{11}B NMR spectrum (96 MHz, CDCl_3) of **2-3aa** ^{19}F NMR spectrum (471 MHz, CDCl_3) of **2-3aa**

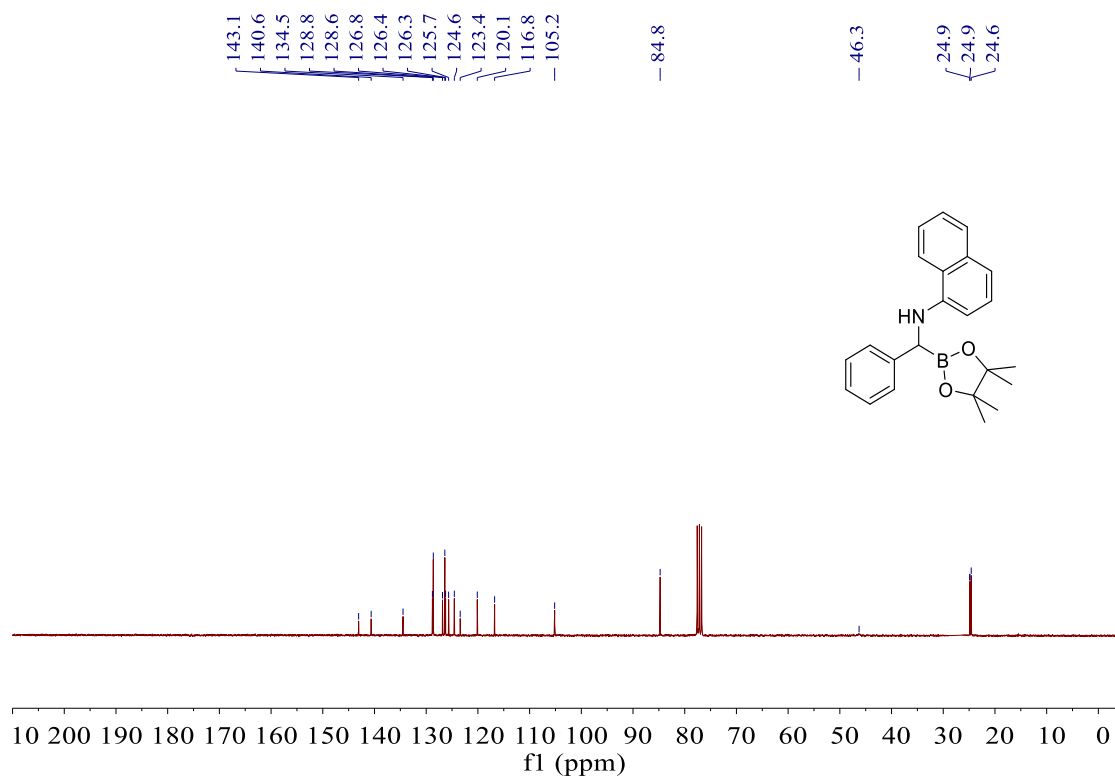
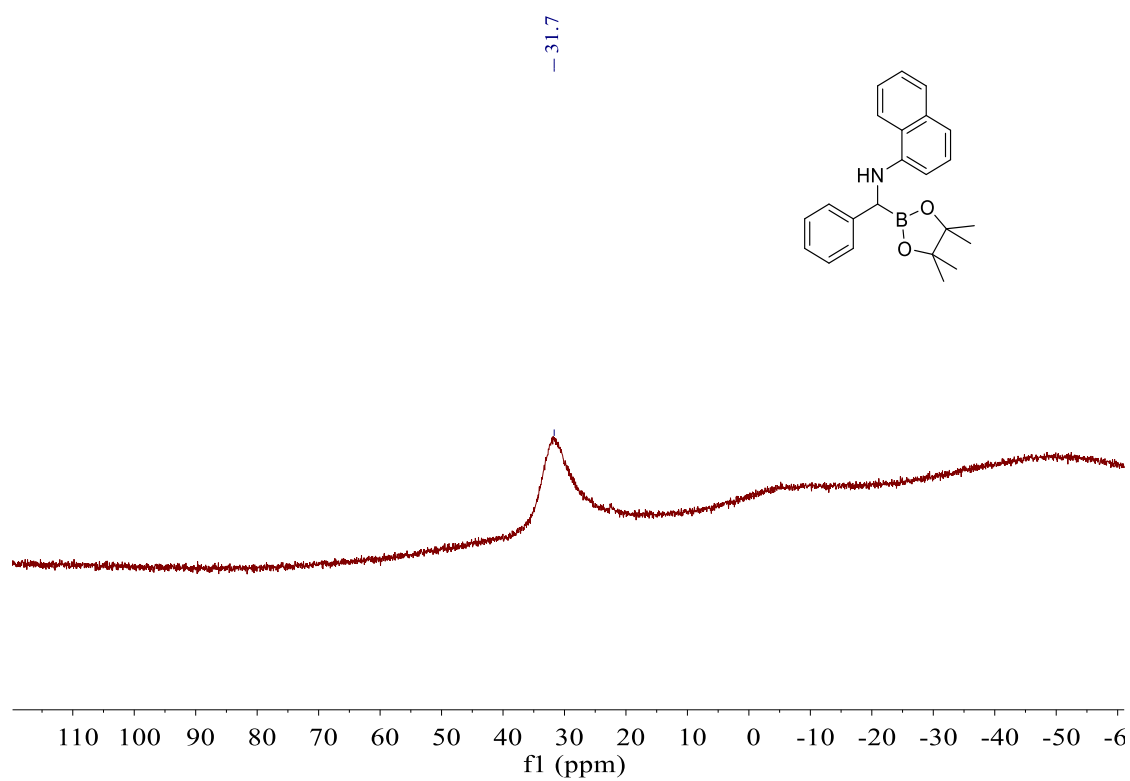
^1H NMR spectrum (300 MHz, CDCl_3) of **2-3ab** $^{13}\text{C}\{^1\text{H}\}$ NMR spectrum (75 MHz, CDCl_3) of **2-3ab**

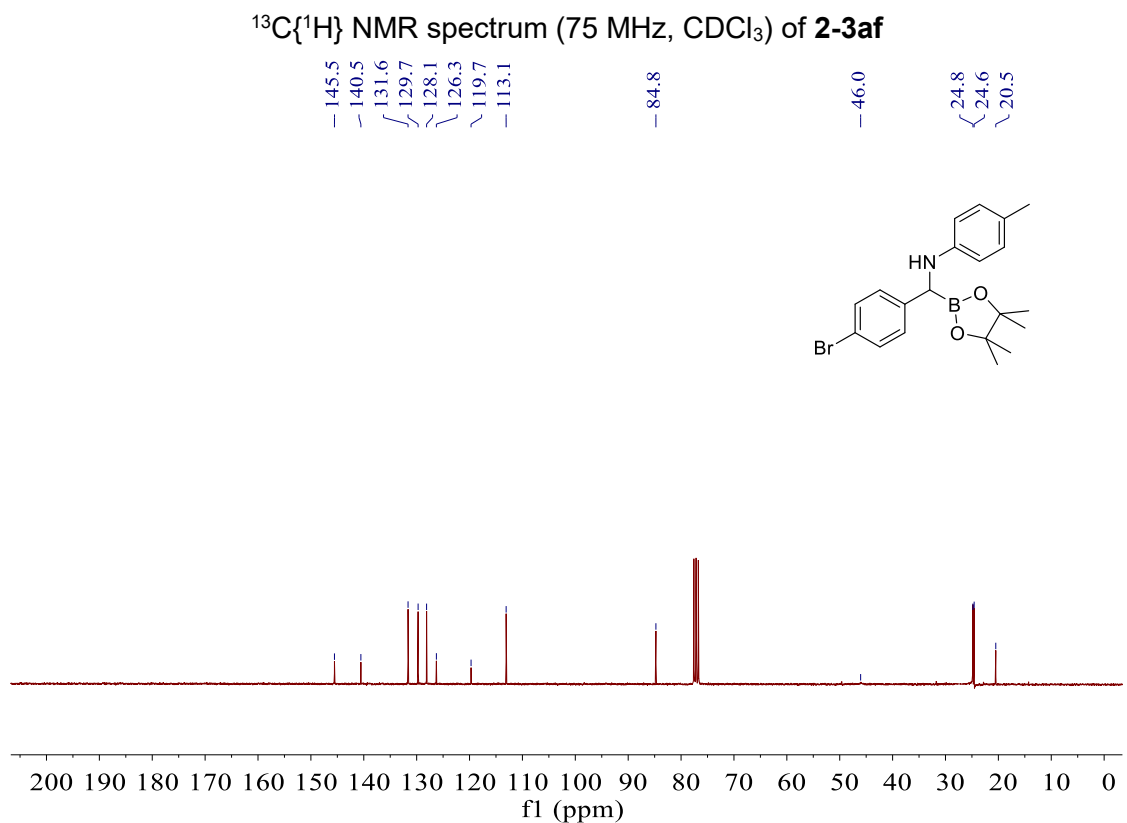
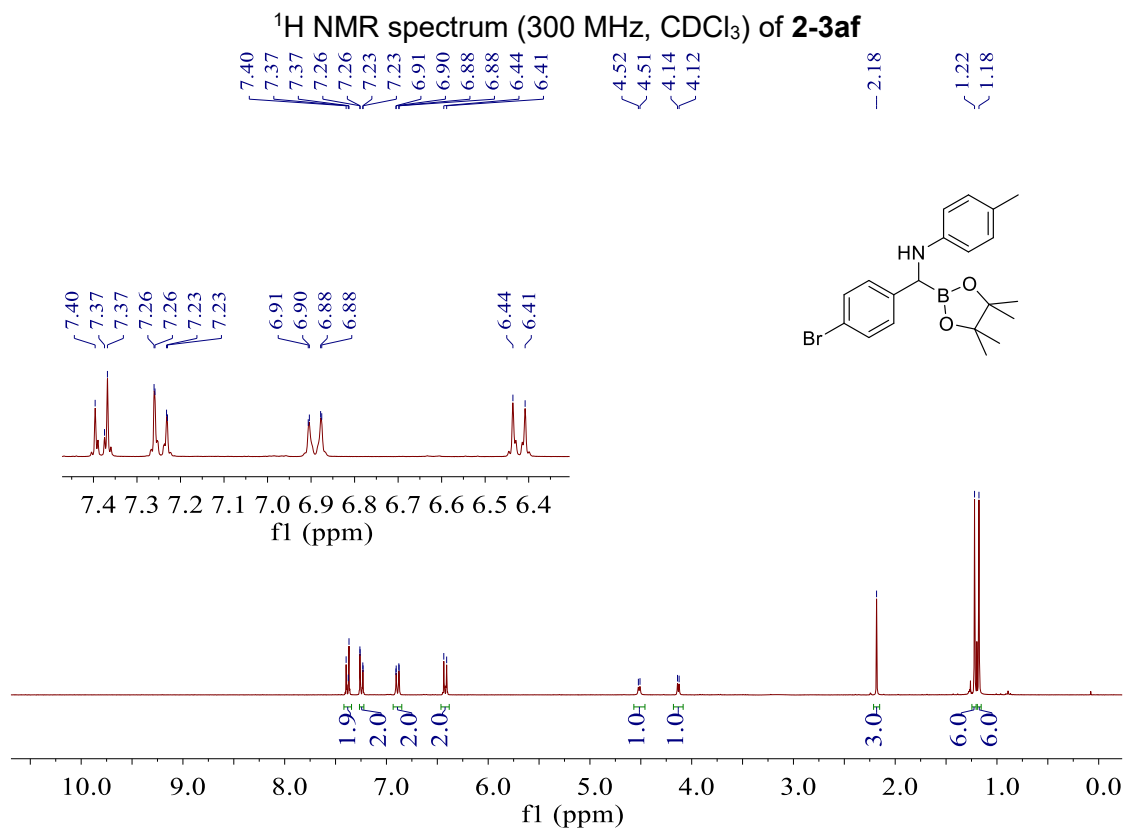
^{11}B NMR spectrum (96 MHz, CDCl_3) of **2-3ab** ^1H NMR spectrum (300 MHz, CDCl_3) of **2-3ac**

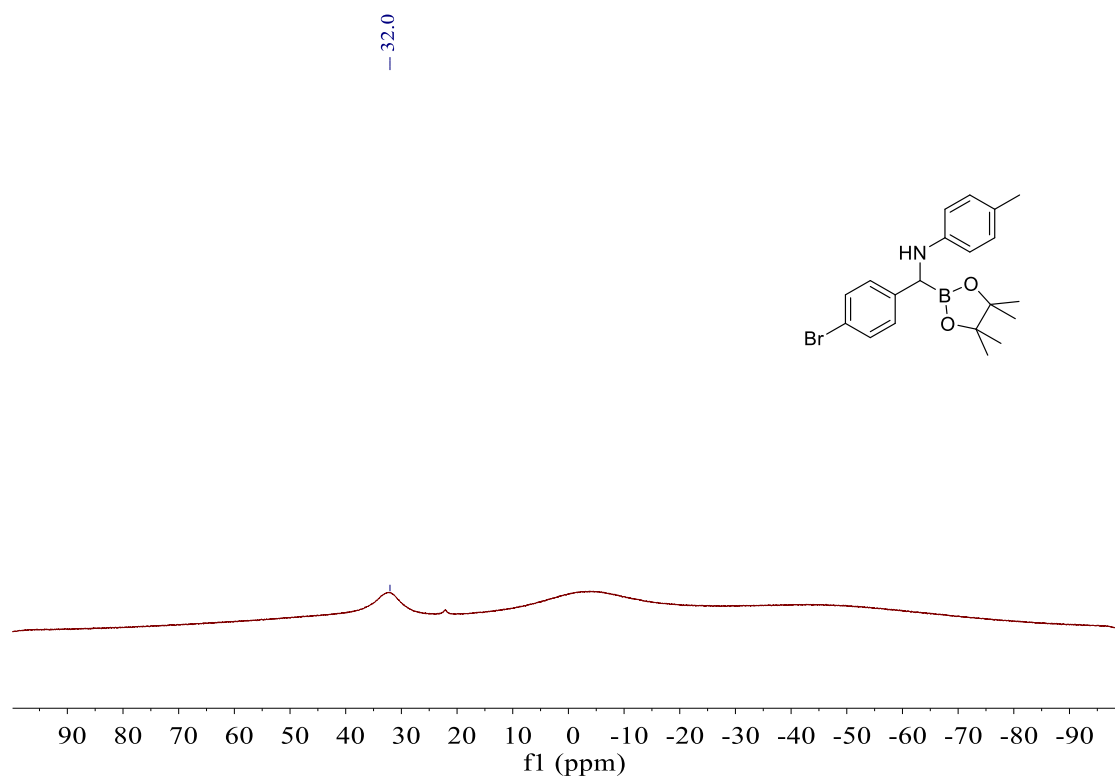
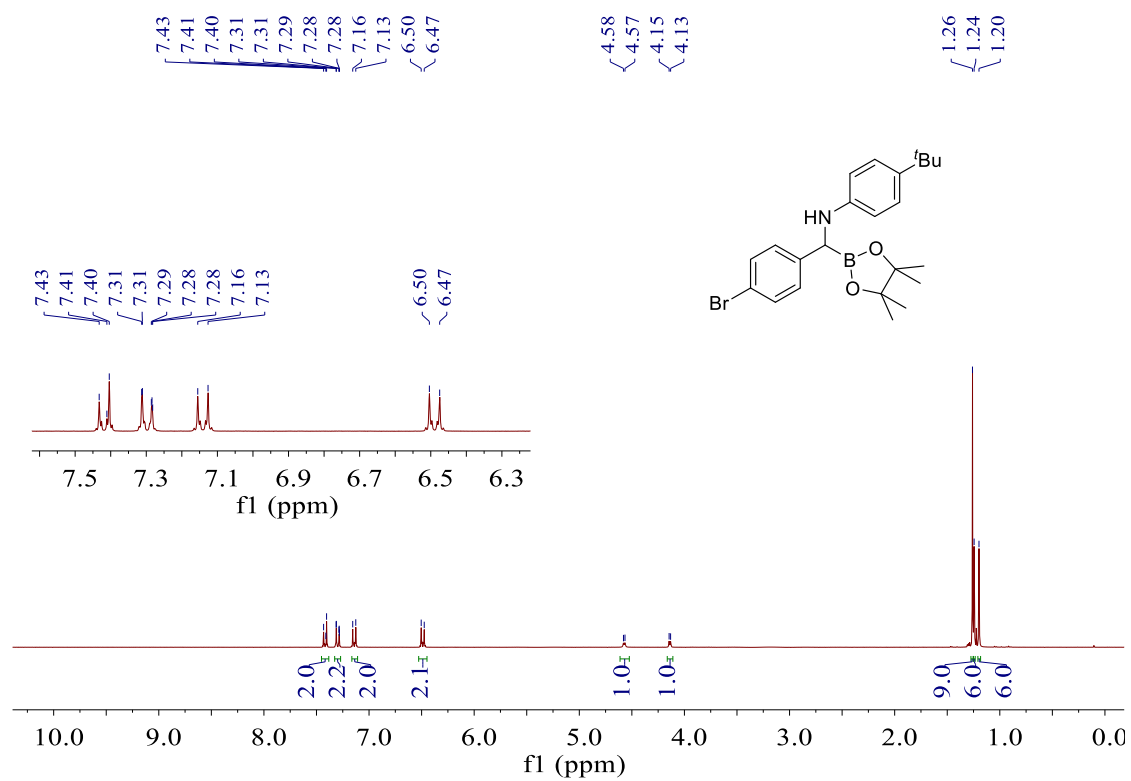
$^{13}\text{C}\{^1\text{H}\}$ NMR spectrum (75 MHz, CDCl_3) of **2-3ac** ^{11}B NMR spectrum (96 MHz, CDCl_3) of **2-3ac**

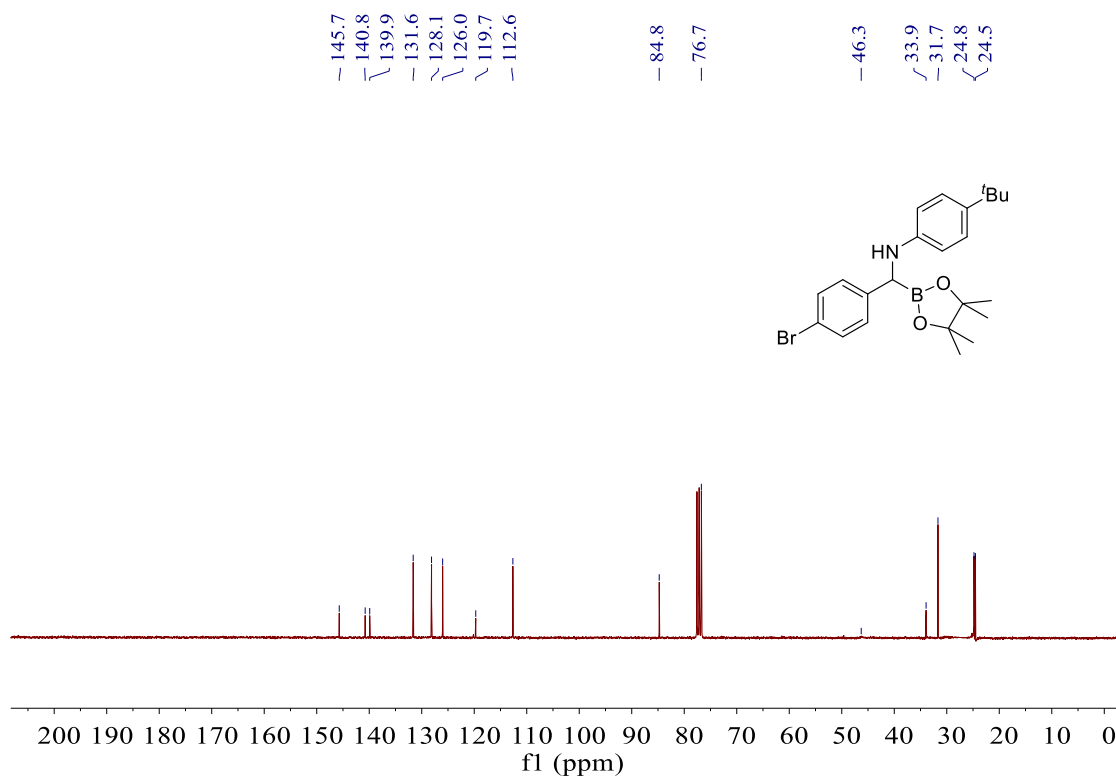
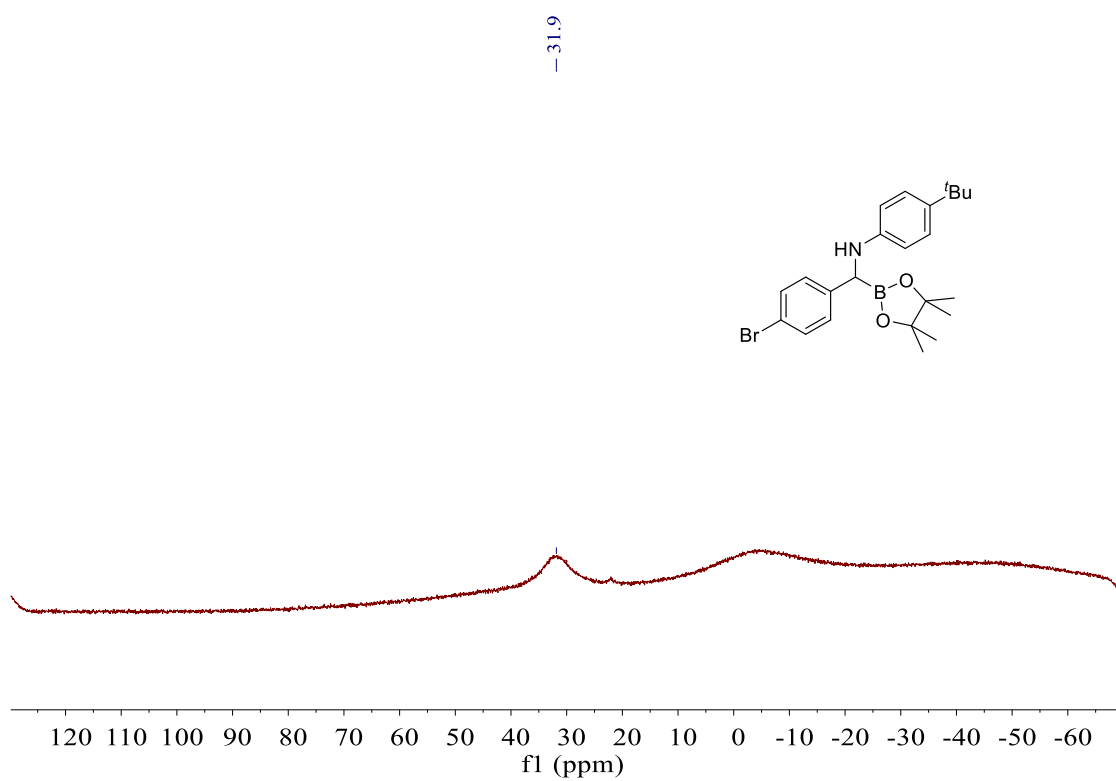
^1H NMR spectrum (300 MHz, CDCl_3) of **2-3ad** $^{13}\text{C}\{^1\text{H}\}$ NMR spectrum (75 MHz, CDCl_3) of **2-3ad**

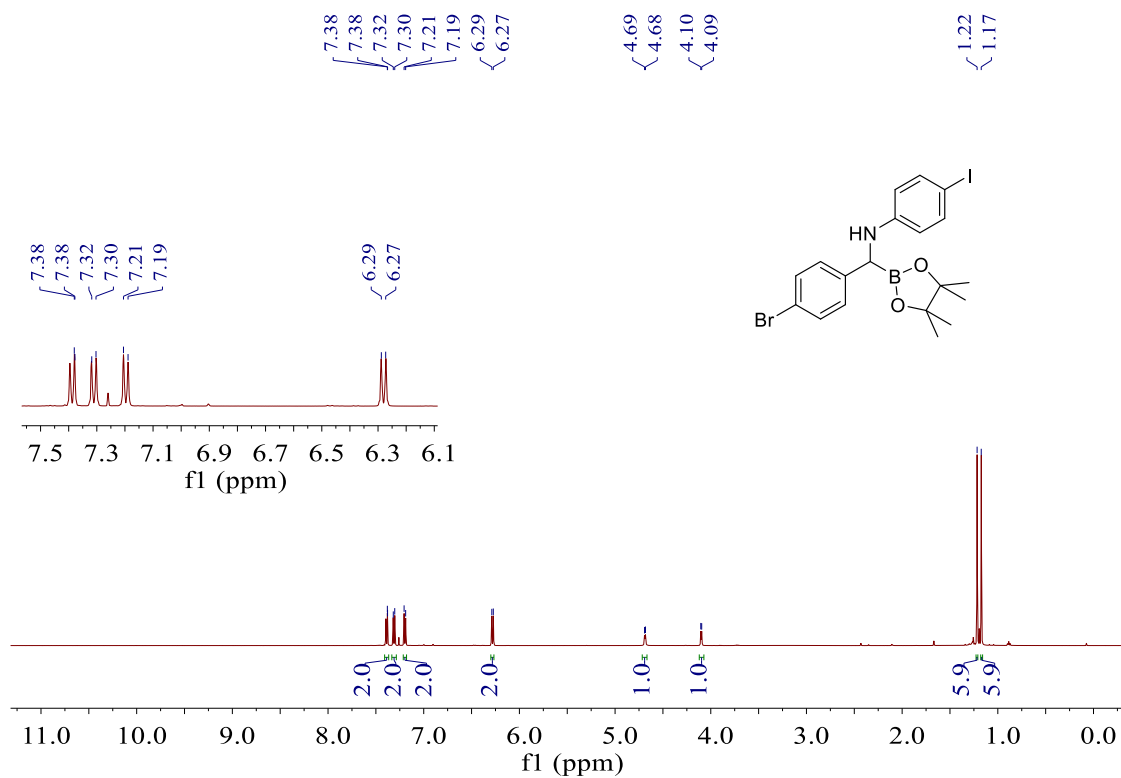
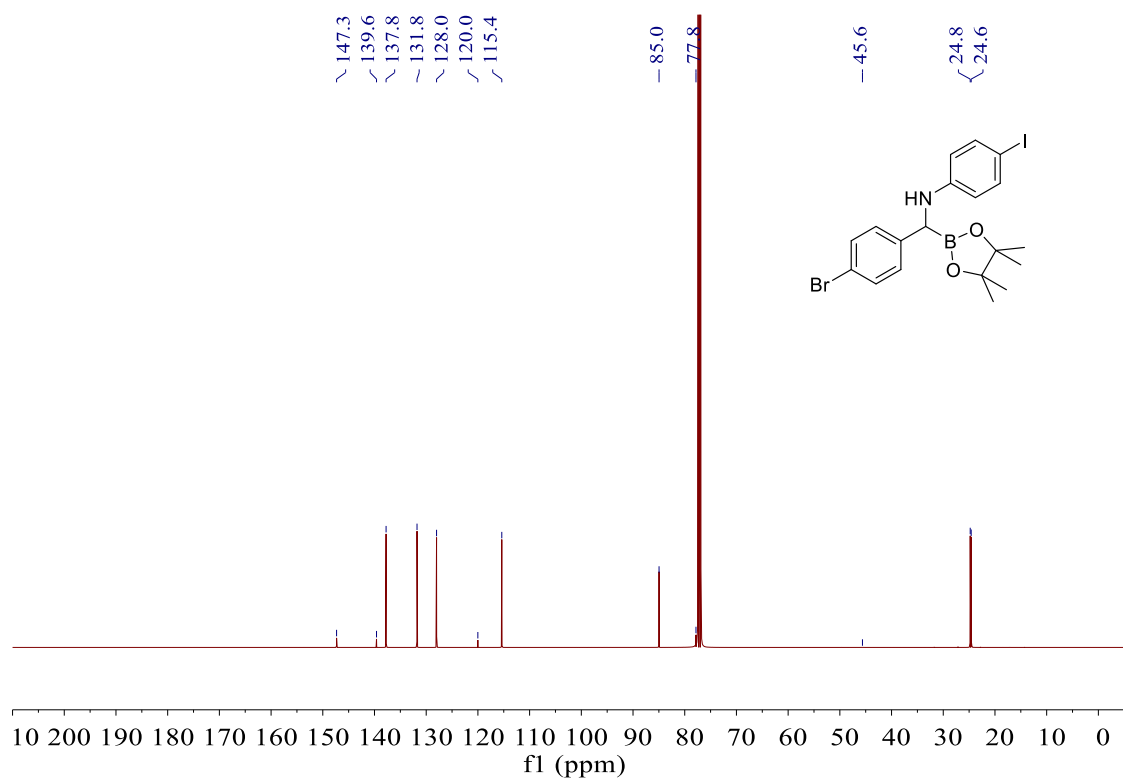
^{11}B NMR spectrum (96 MHz, CDCl_3) of **2-3ad** ^1H NMR spectrum (300 MHz, CDCl_3) of **2-3ae**

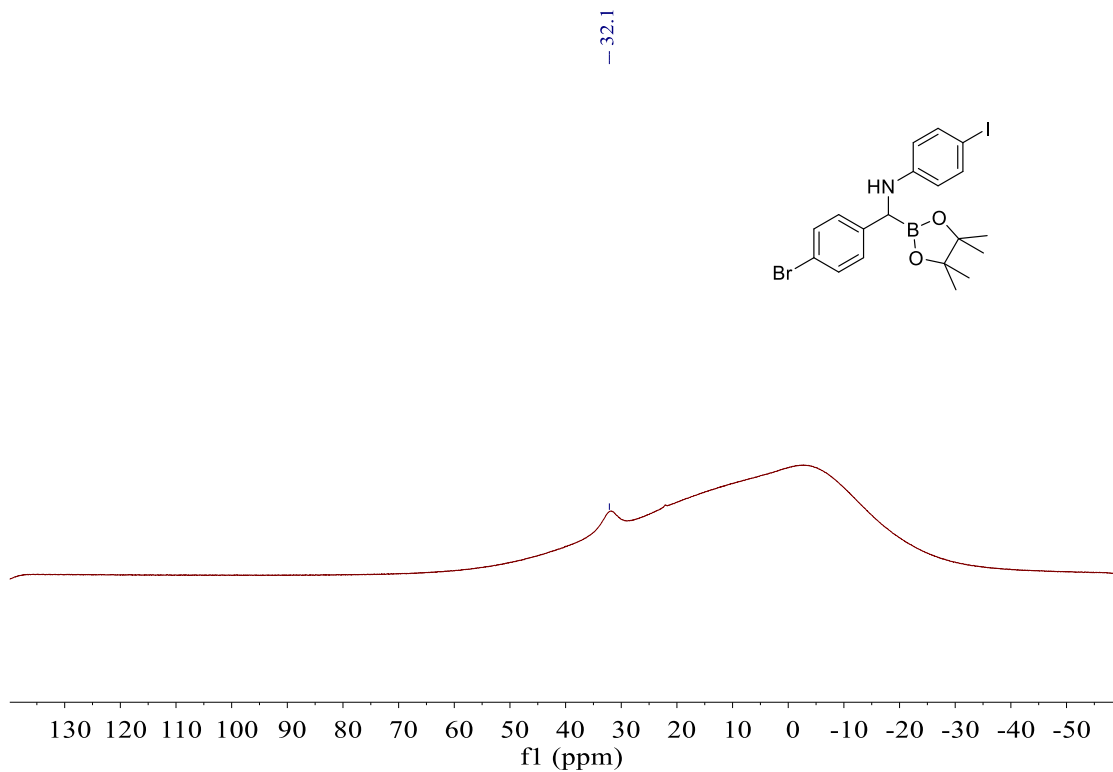
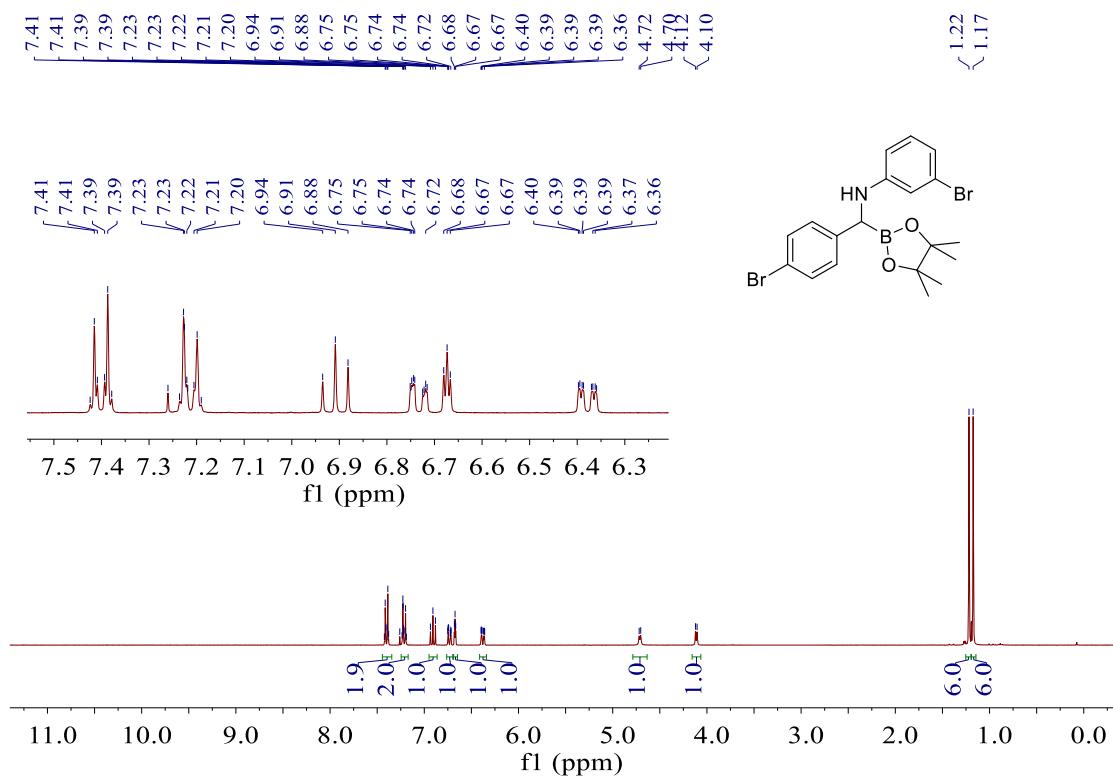
$^{13}\text{C}\{^1\text{H}\}$ NMR spectrum (75 MHz, CDCl_3) of **2-3ae** ^{11}B NMR spectrum (96 MHz, CDCl_3) of **2-3ae**

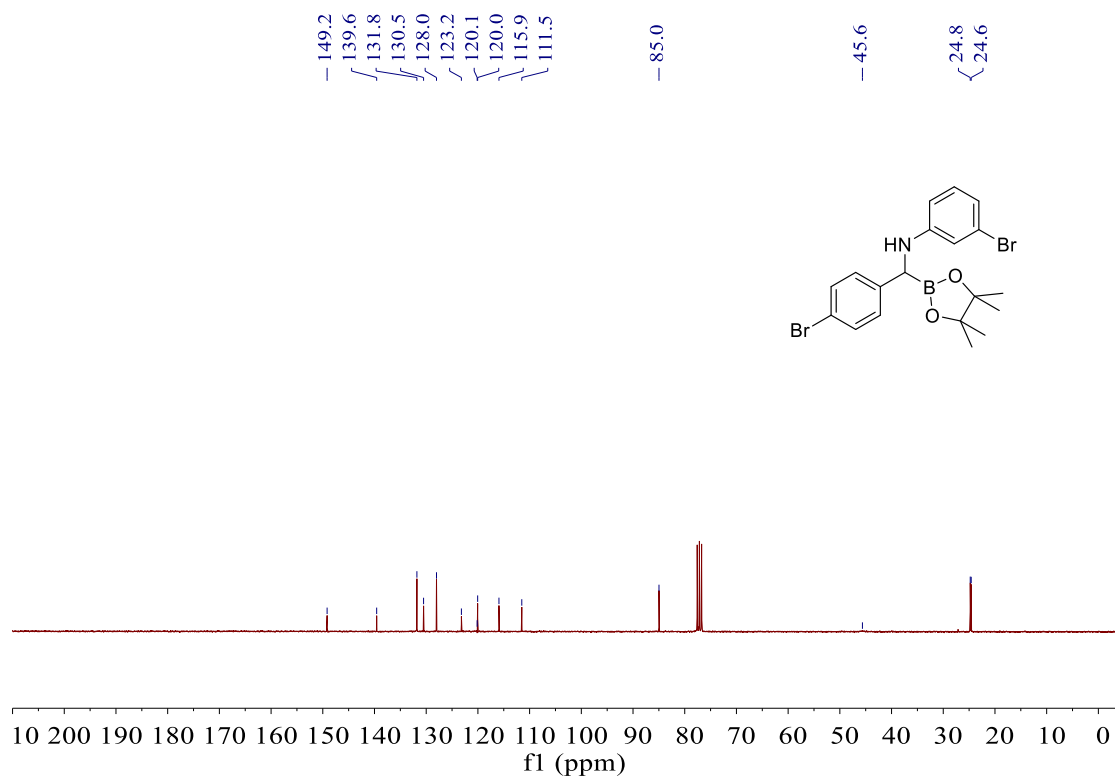
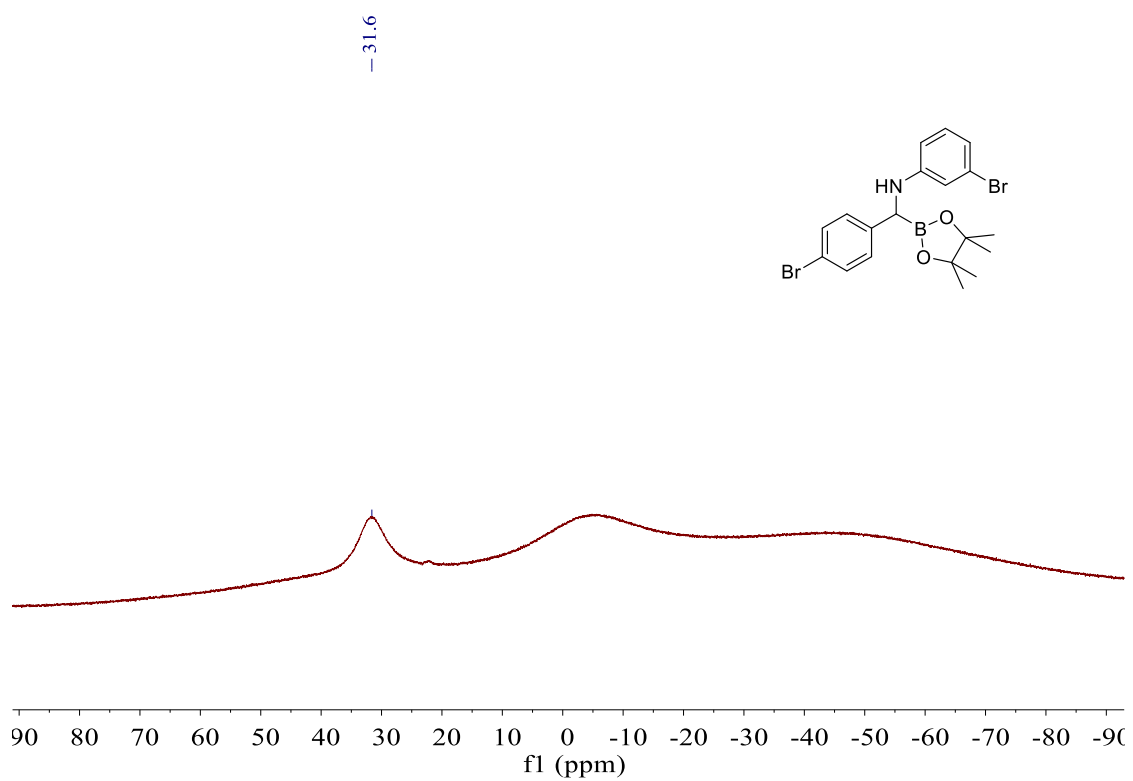


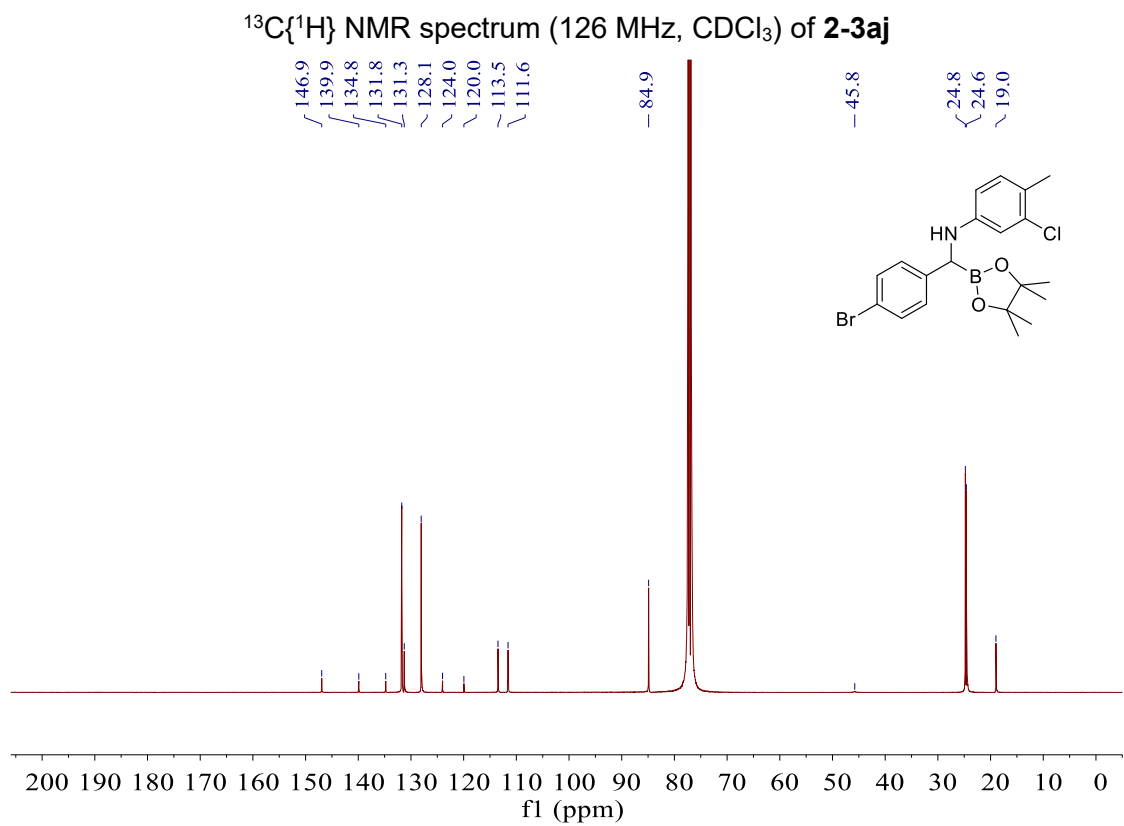
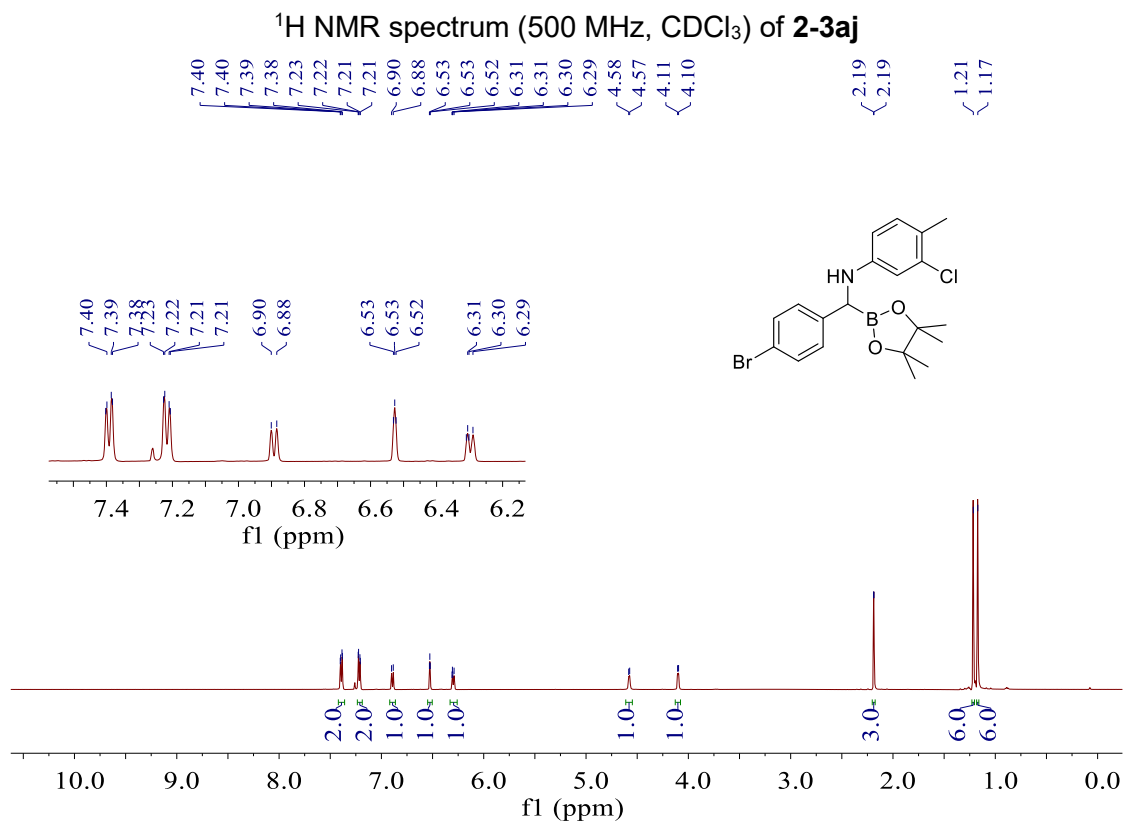
^{11}B NMR spectrum (96 MHz, CDCl_3) of **2-3af** ^1H NMR spectrum (300 MHz, CDCl_3) of **2-3ag**

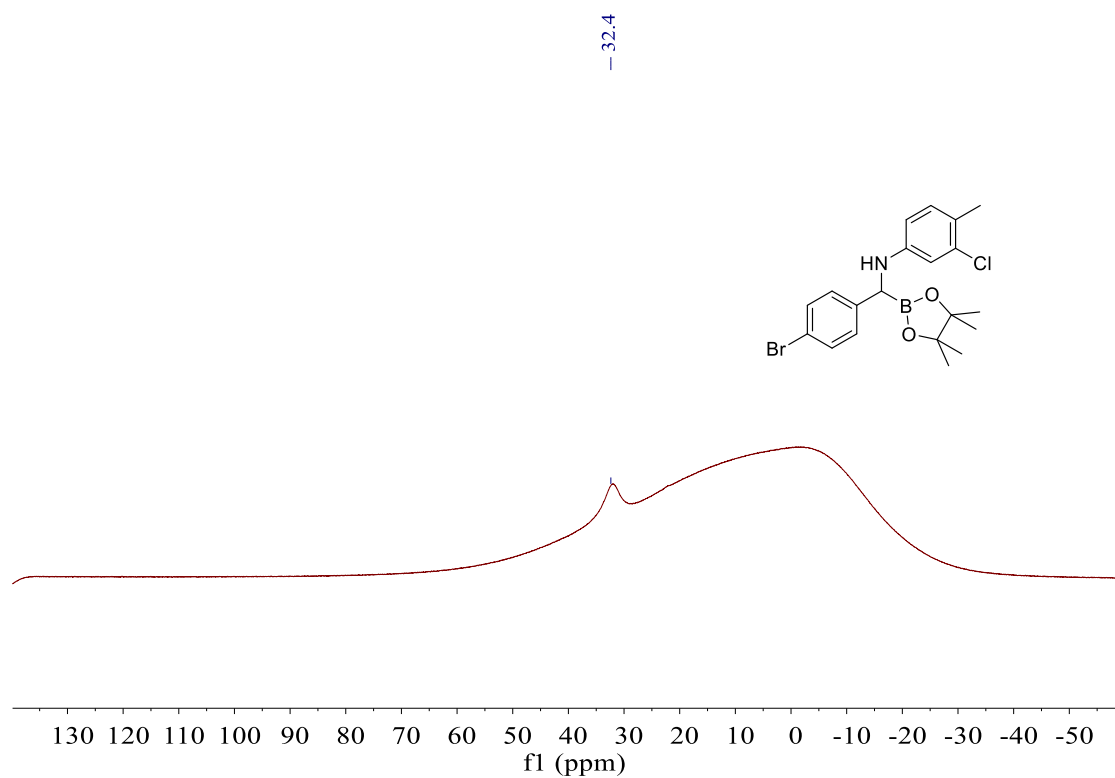
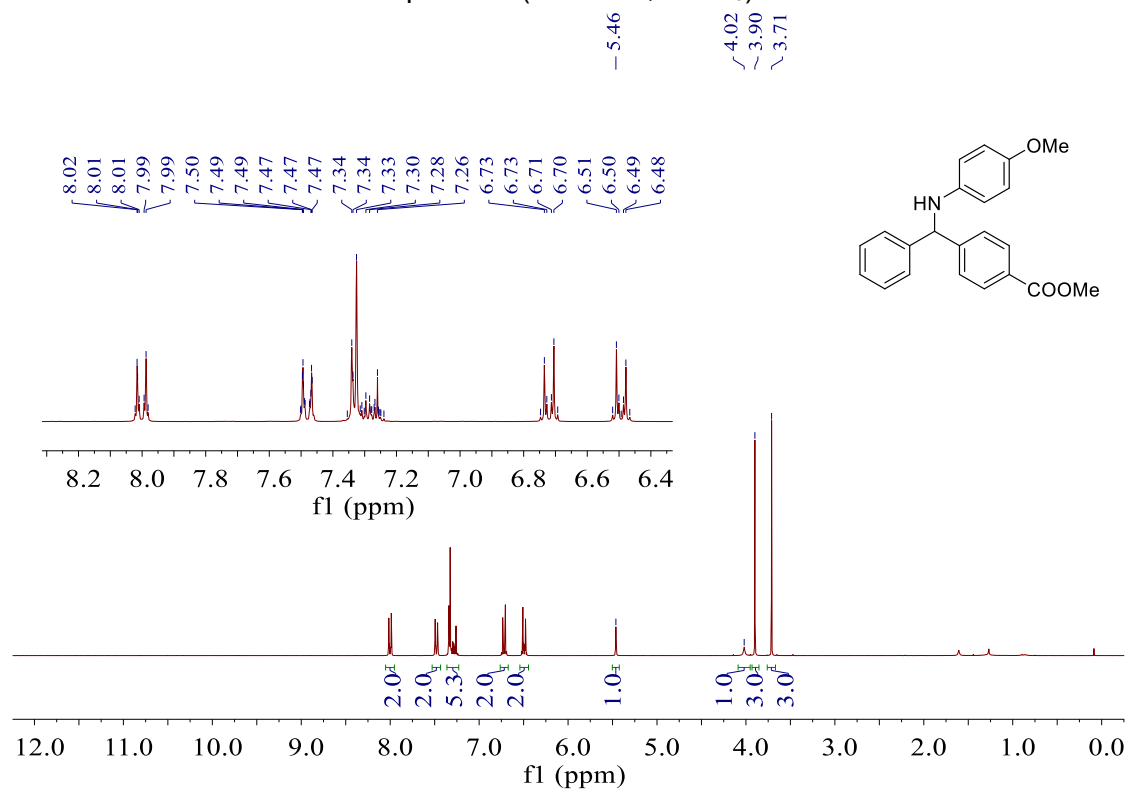
$^{13}\text{C}\{^1\text{H}\}$ NMR spectrum (75 MHz, CDCl_3) of **2-3ag** ^{11}B NMR spectrum (96 MHz, CDCl_3) of **2-3ag**

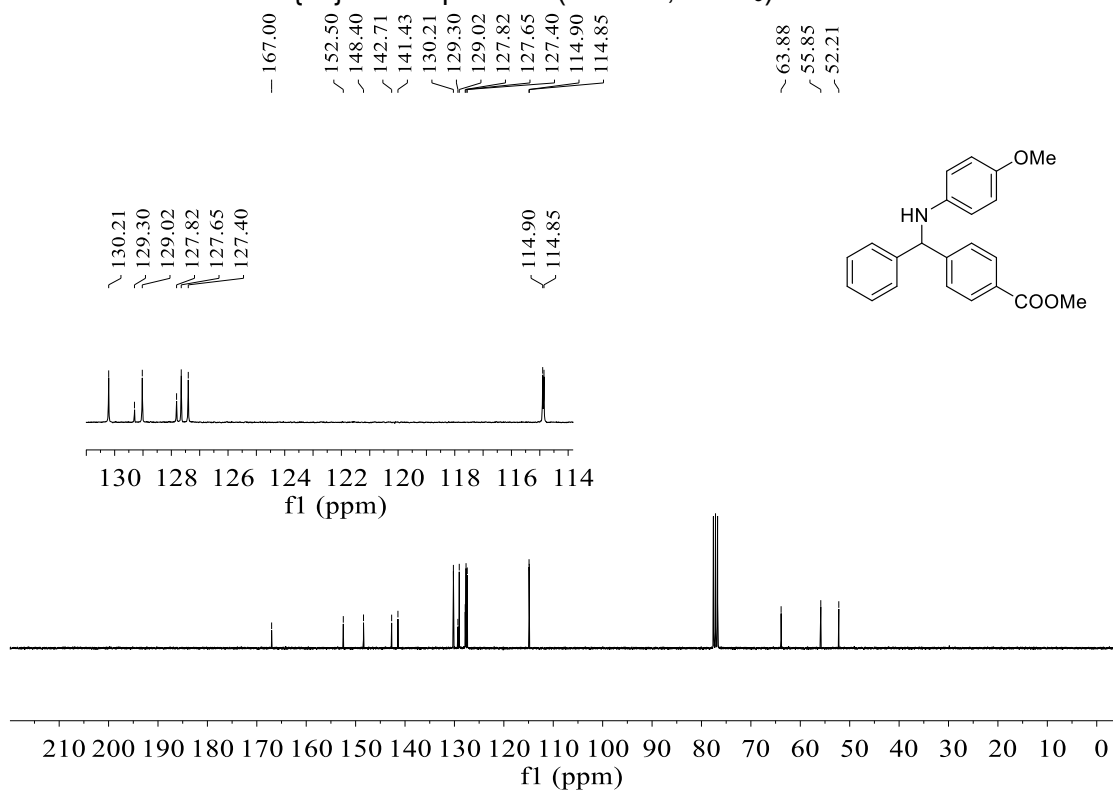
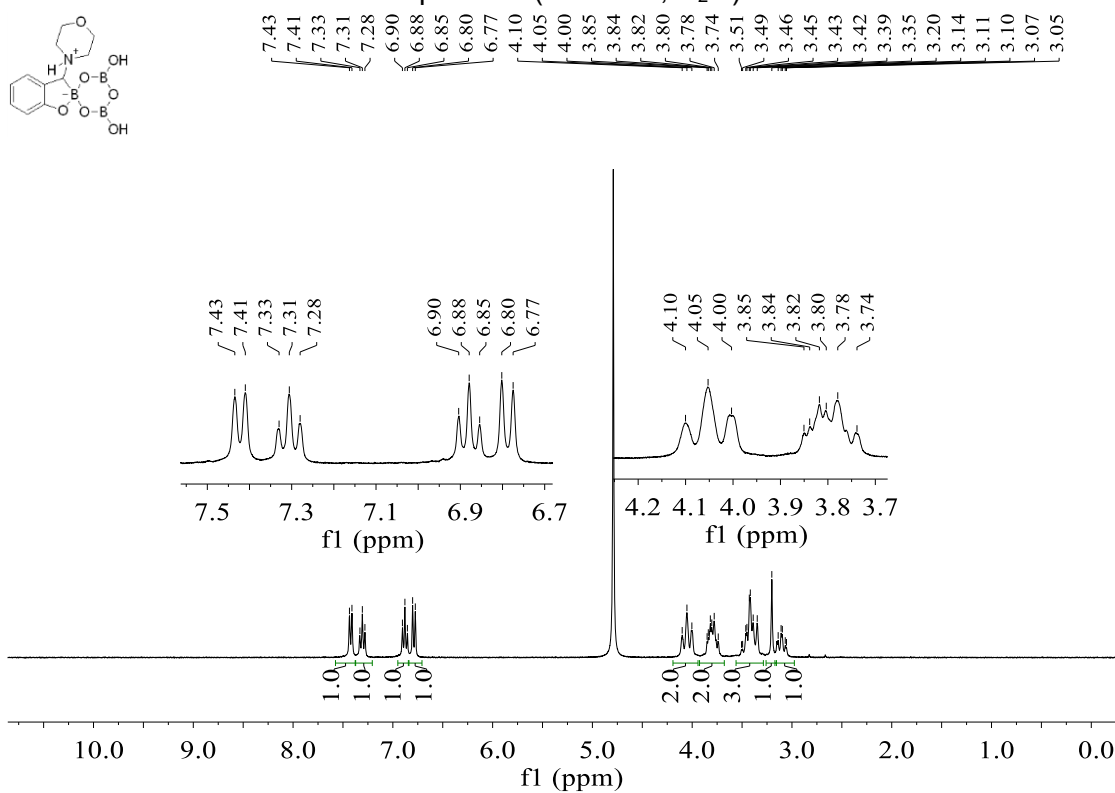
^1H NMR spectrum (500 MHz, CDCl_3) of **2-3ah** $^{13}\text{C}\{^1\text{H}\}$ NMR spectrum (126 MHz, CDCl_3) of **2-3ah**

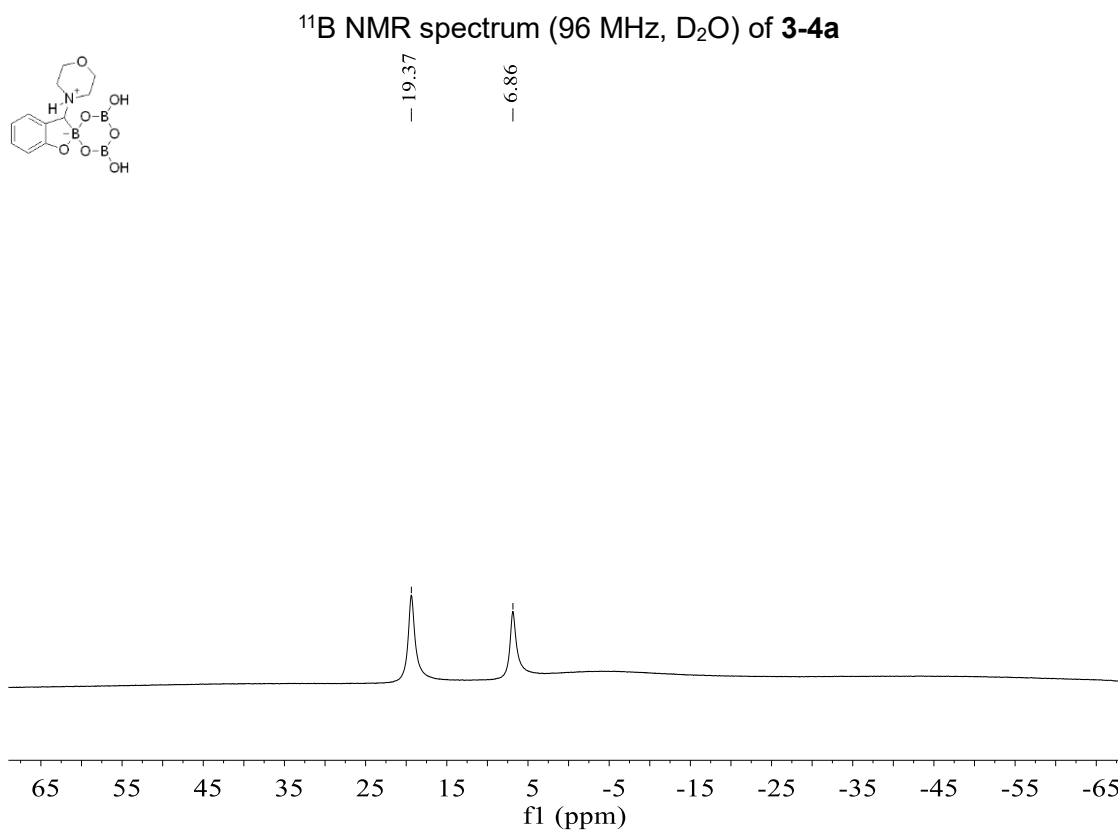
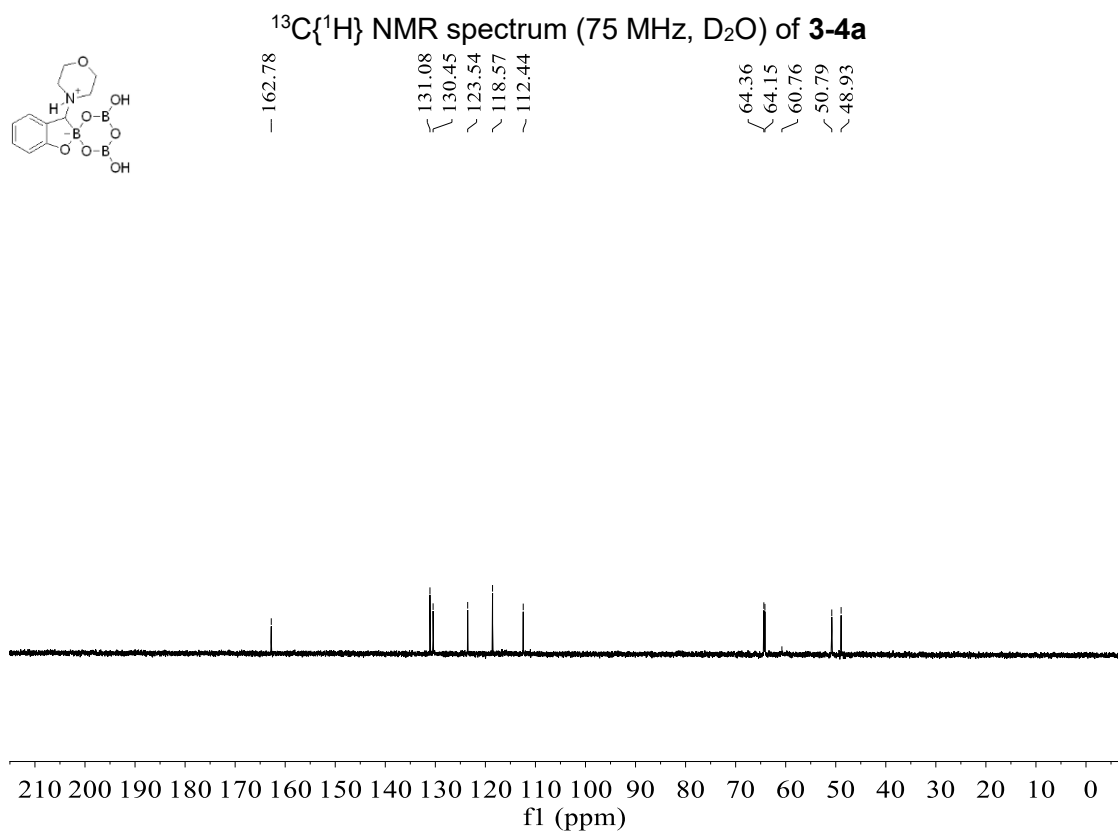
^{11}B NMR spectrum (160 MHz, CDCl_3) of **2-3ah** ^1H NMR spectrum (300 MHz, CDCl_3) of **2-3ai**

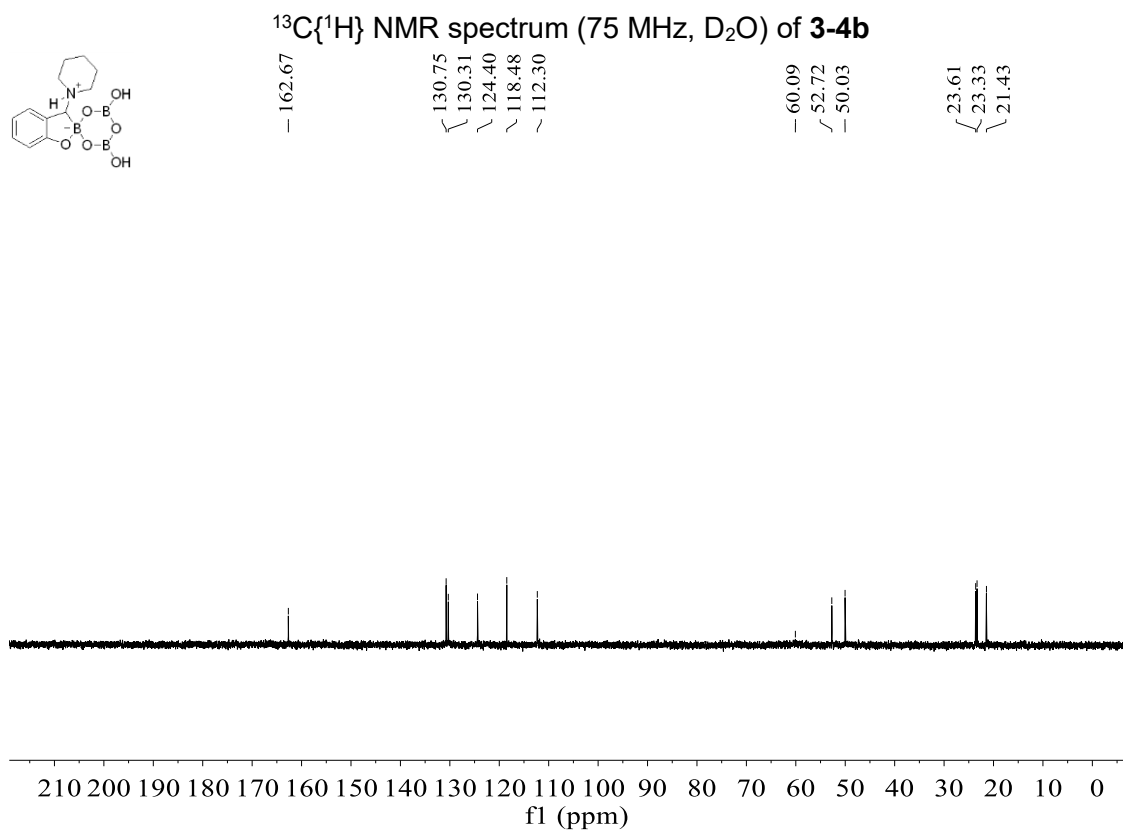
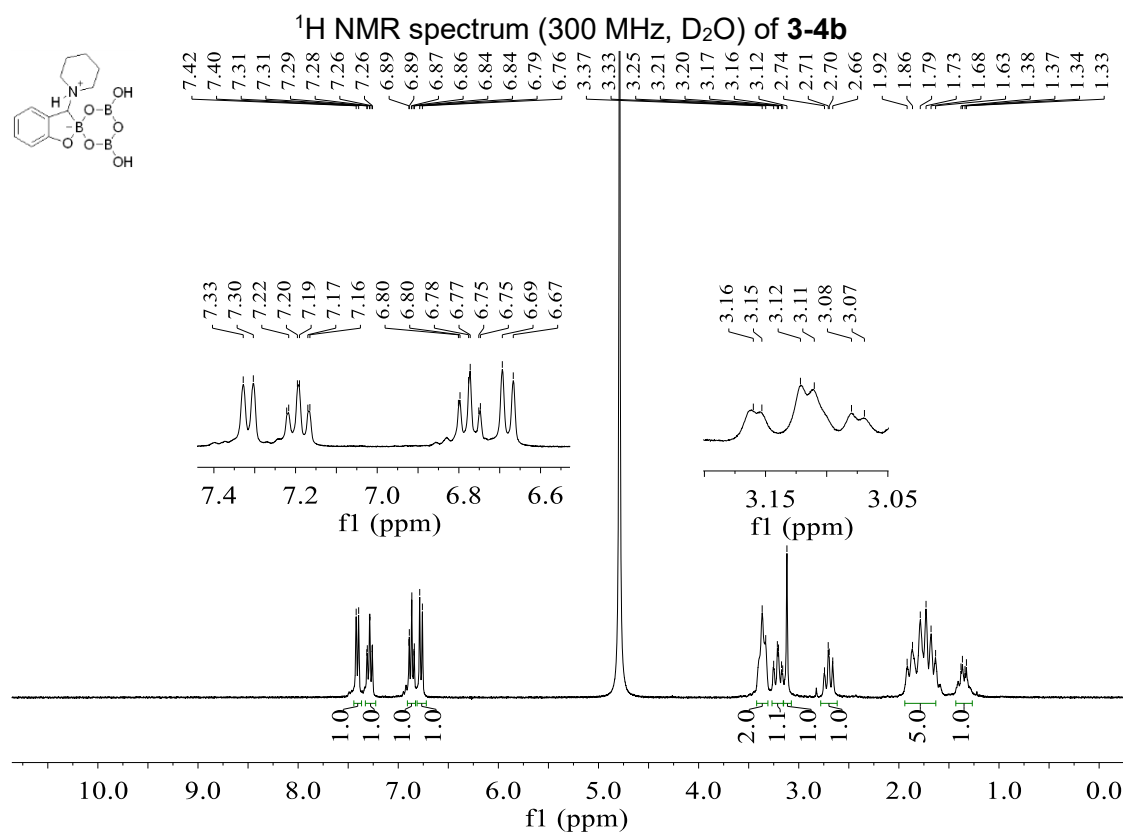
$^{13}\text{C}\{^1\text{H}\}$ NMR spectrum (75 MHz, CDCl_3) of **2-3ai** ^{11}B NMR spectrum (96 MHz, CDCl_3) of **2-3ai**



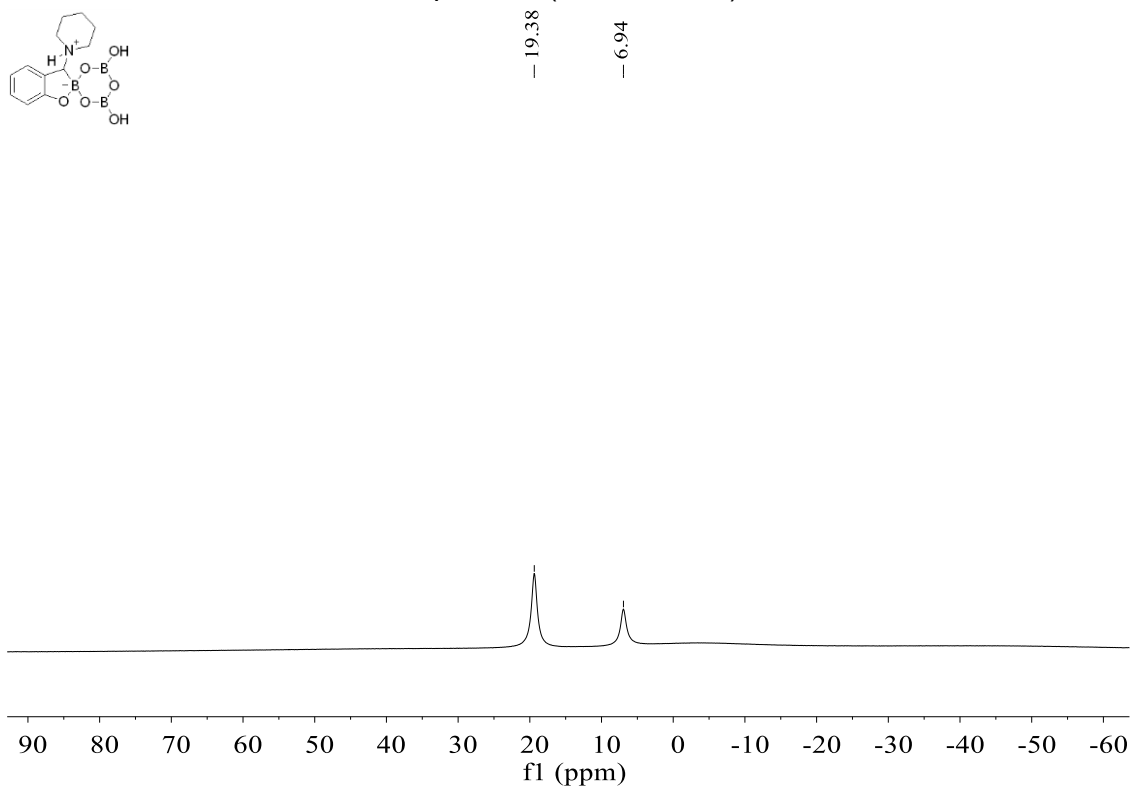
^{11}B NMR spectrum (160 MHz, CDCl_3) of **2-3aj** ^1H NMR spectrum (300 MHz, CDCl_3) of **2-6w**

$^{13}\text{C}\{^1\text{H}\}$ NMR spectrum (75 MHz, CDCl_3) of **2-6w** ^1H NMR spectrum (300 MHz, D_2O) of **3-4a**

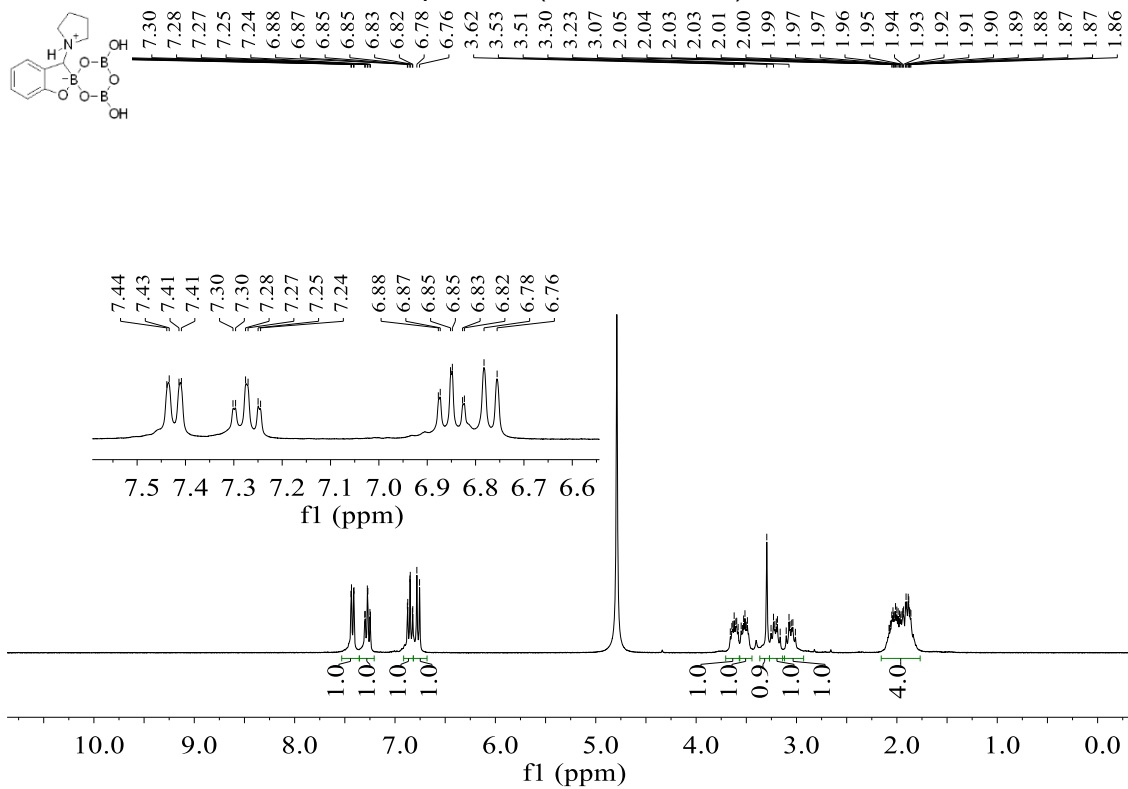


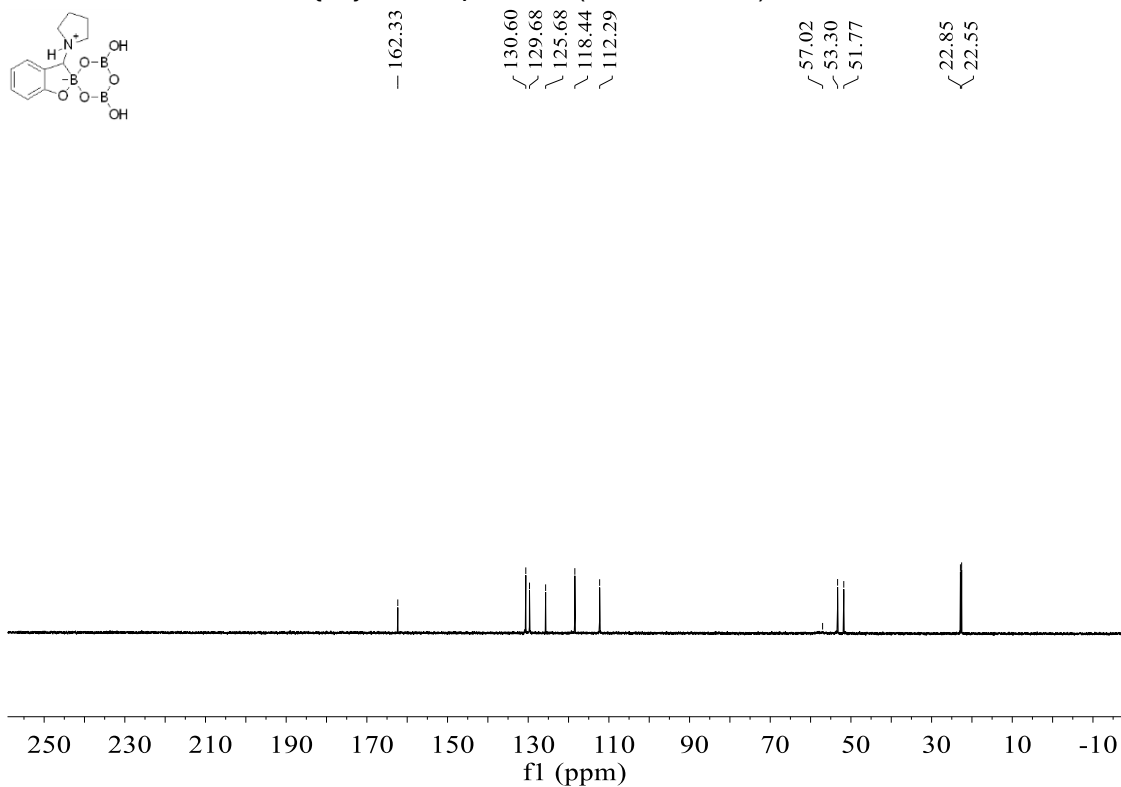
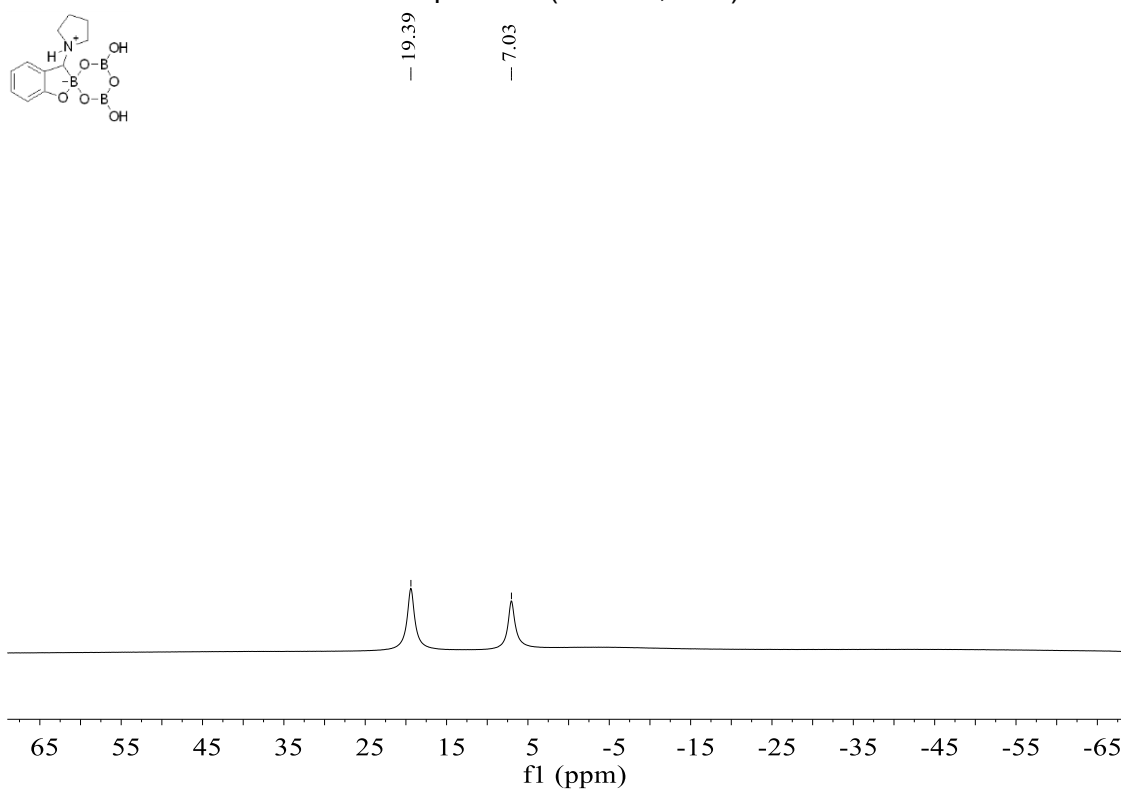


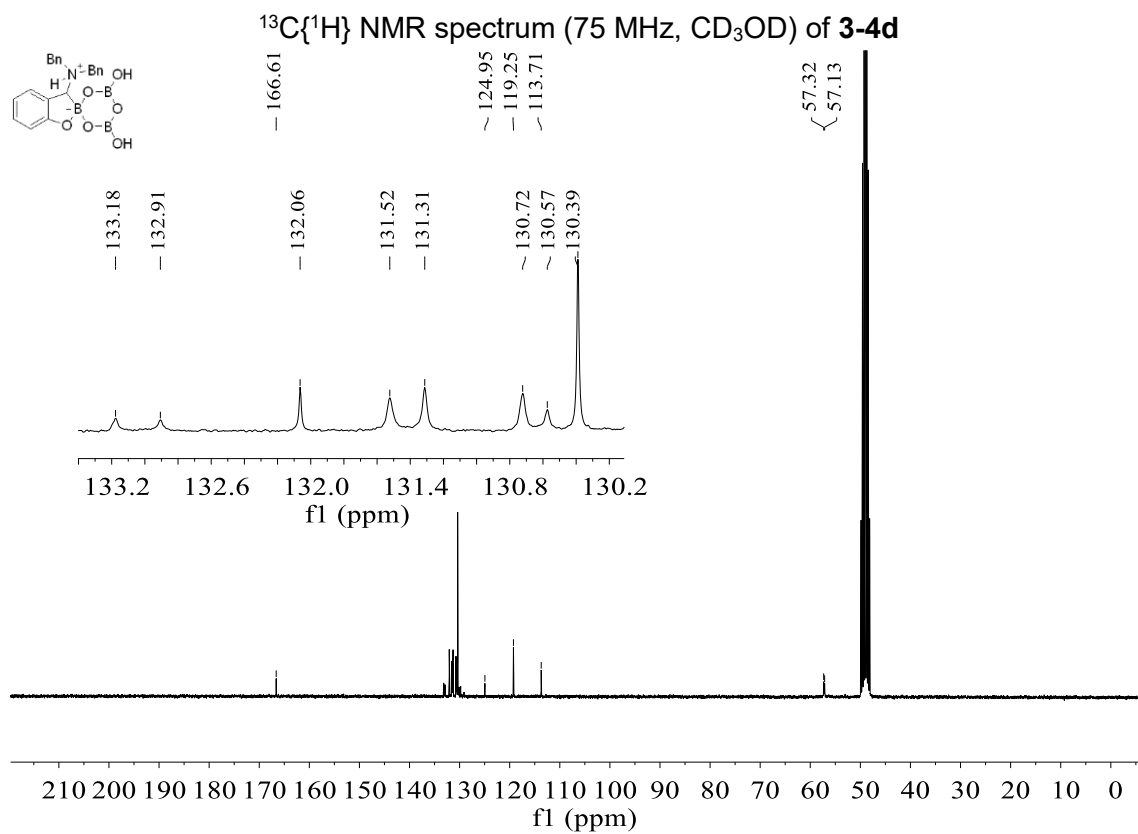
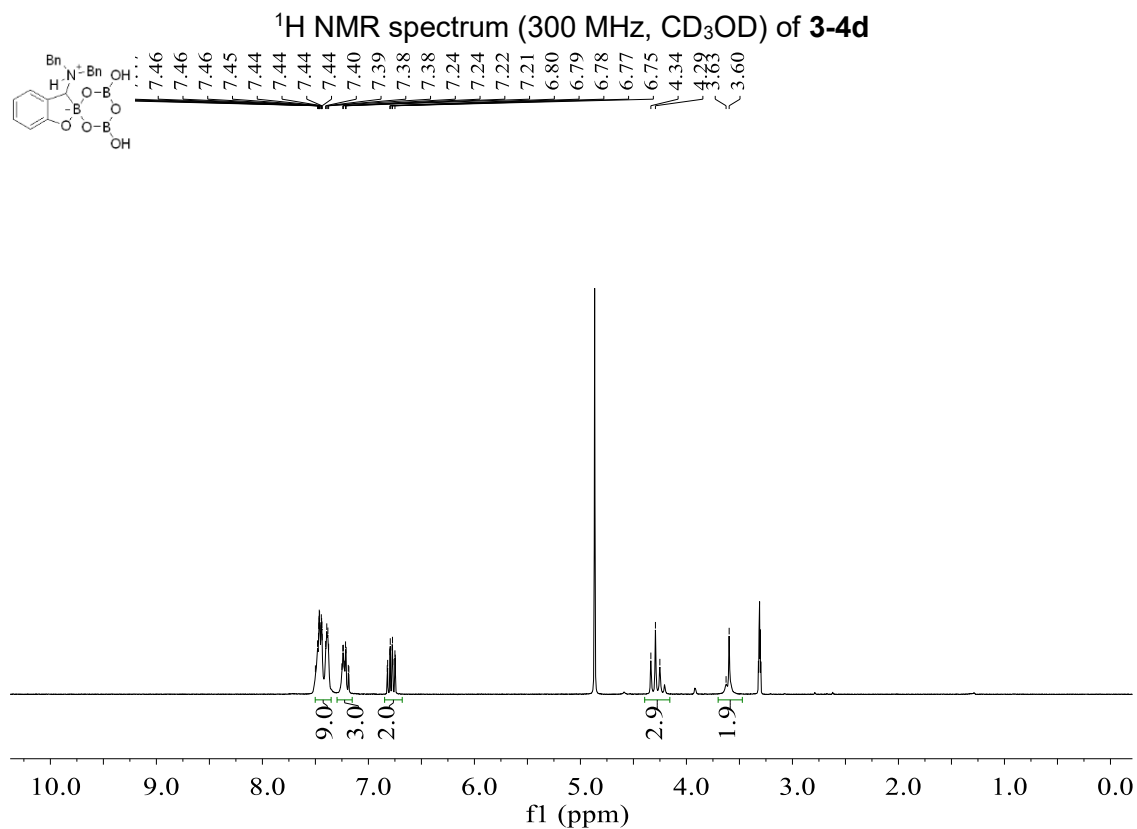
^{11}B NMR spectrum (96 MHz, D_2O) of **3-4b**

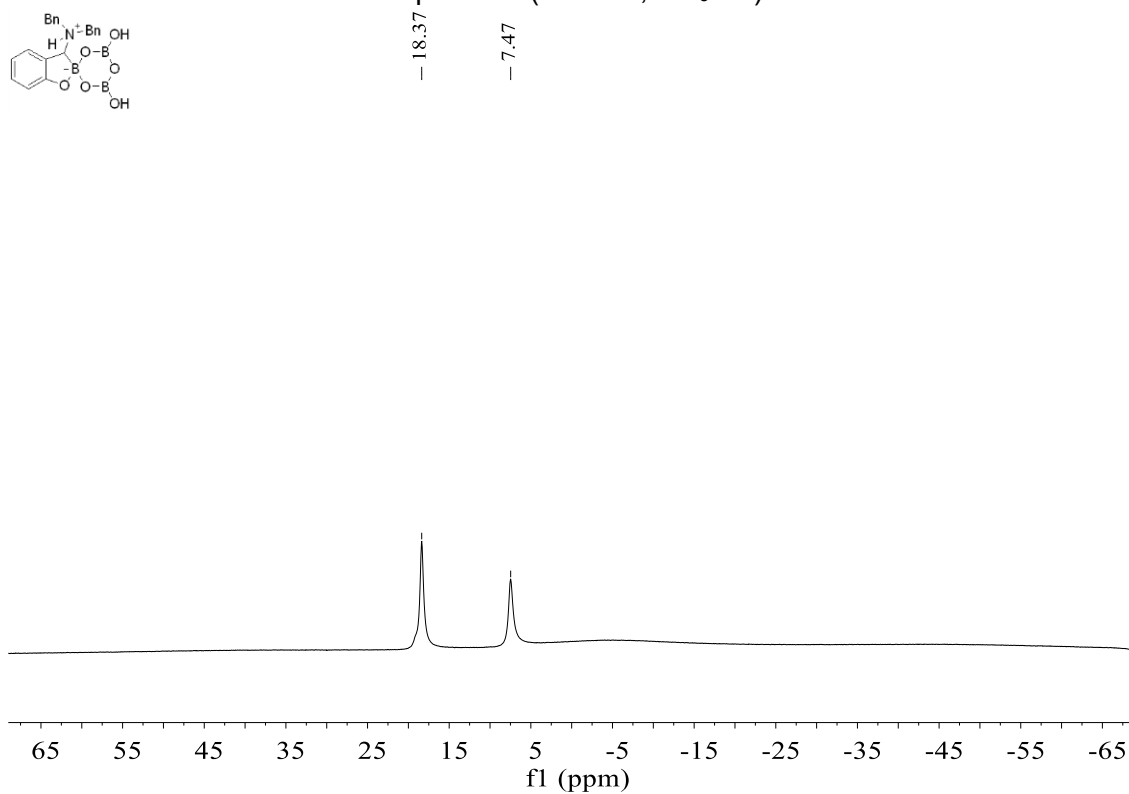
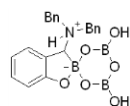
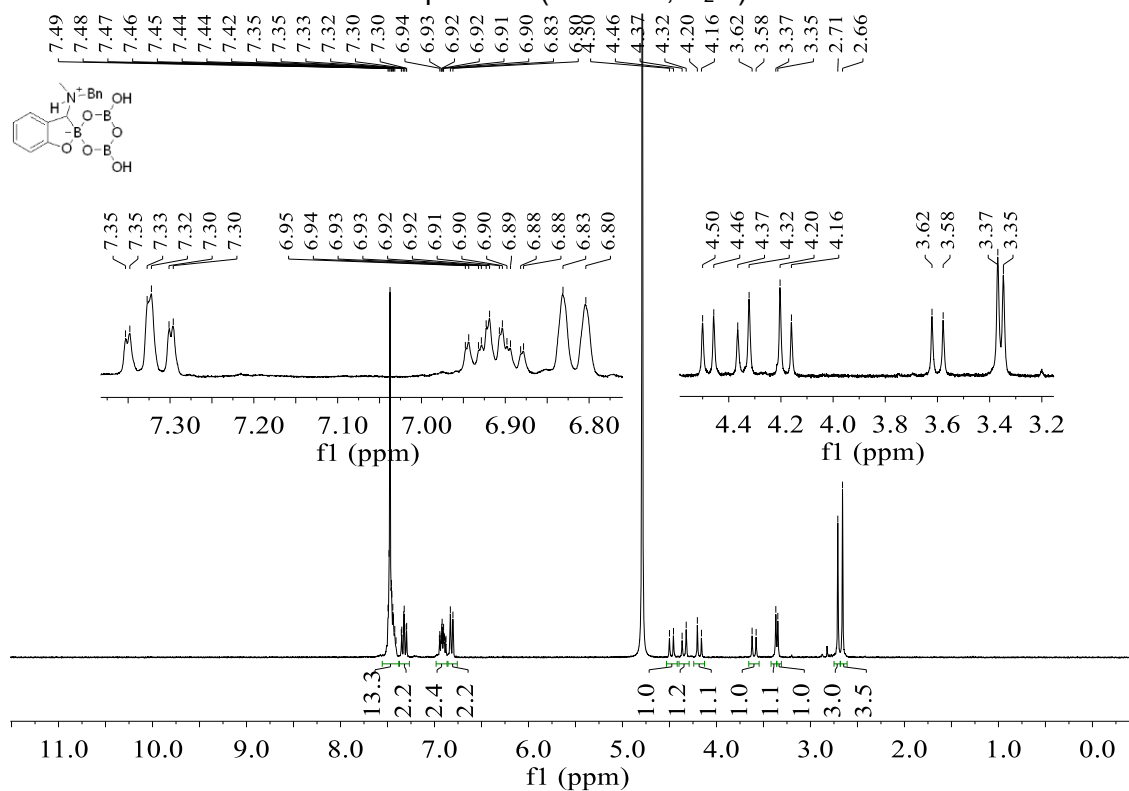


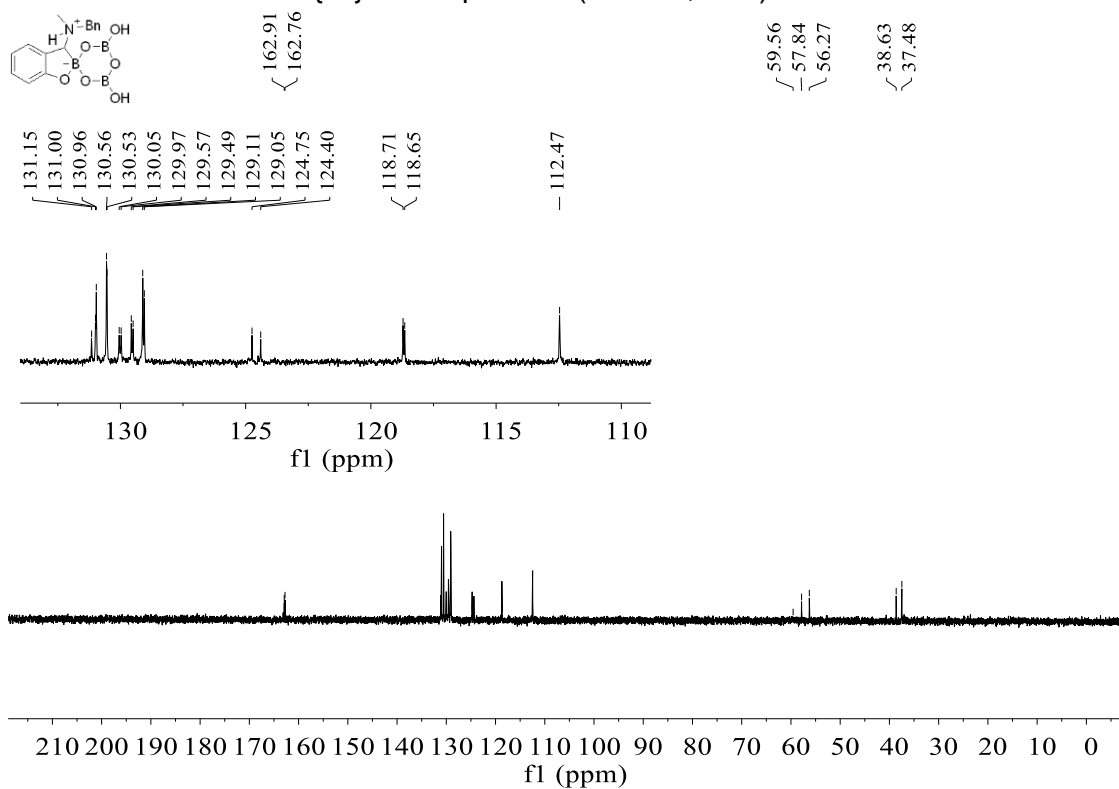
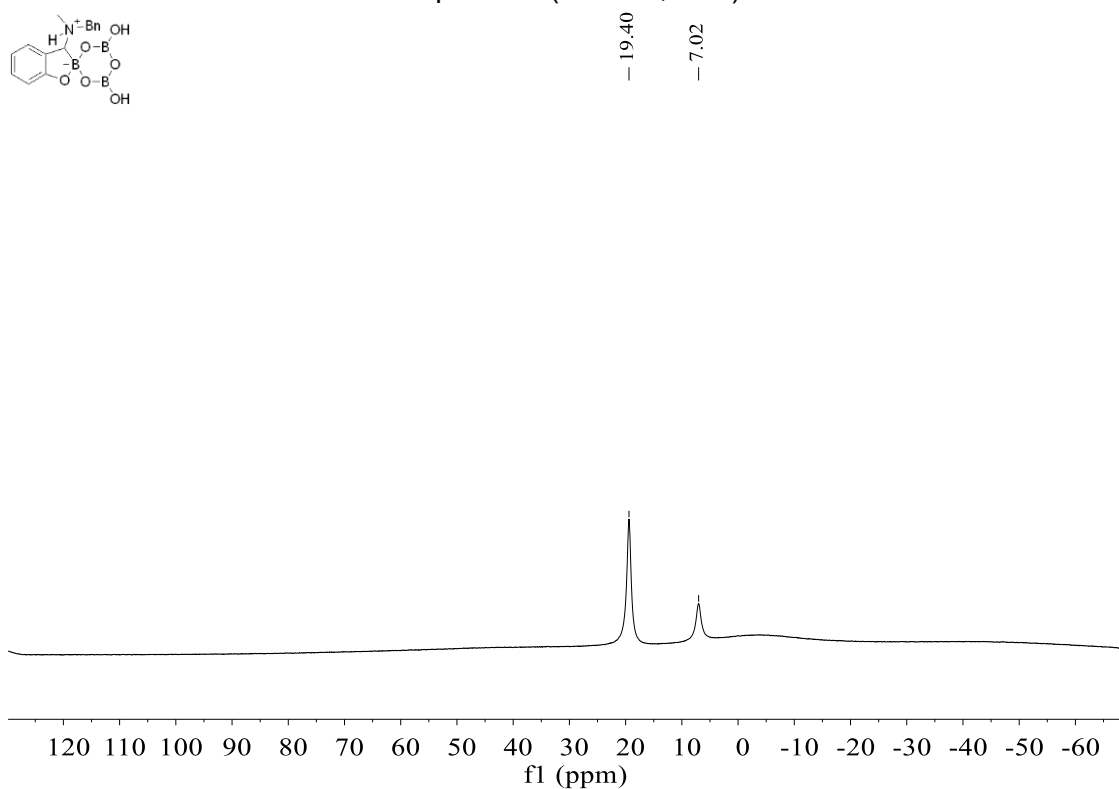
^1H NMR spectrum (300 MHz, D_2O) of **3-4c**

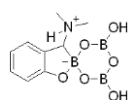


$^{13}\text{C}\{^1\text{H}\}$ NMR spectrum (75 MHz, D_2O) of **3-4c** ^{11}B NMR spectrum (96 MHz, D_2O) of **3-4c**

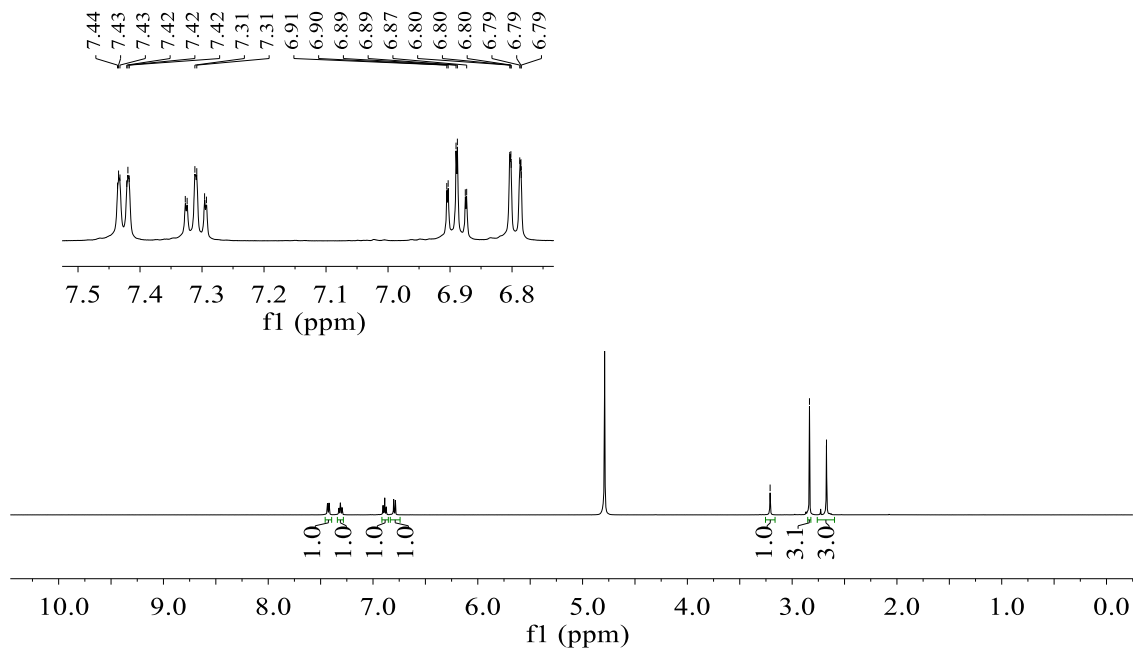
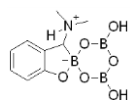


^{11}B NMR spectrum (96 MHz, CD_3OD) of **3-4d** ^1H NMR spectrum (300 MHz, D_2O) of **3-4e**

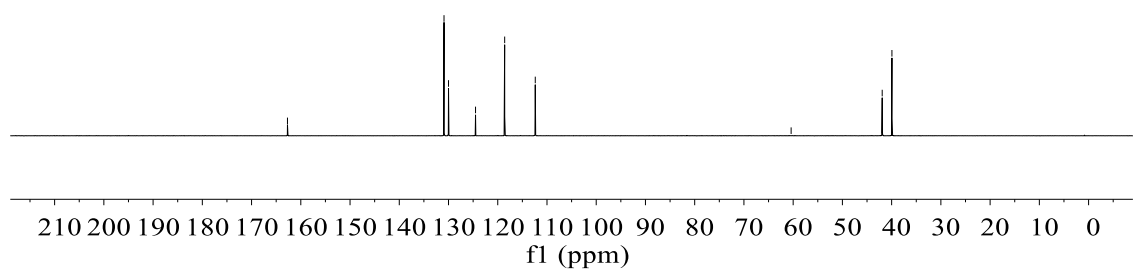
$^{13}\text{C}\{^1\text{H}\}$ NMR spectrum (75 MHz, D_2O) of **3-4e** ^{11}B NMR spectrum (96 MHz, D_2O) of **3-4e**

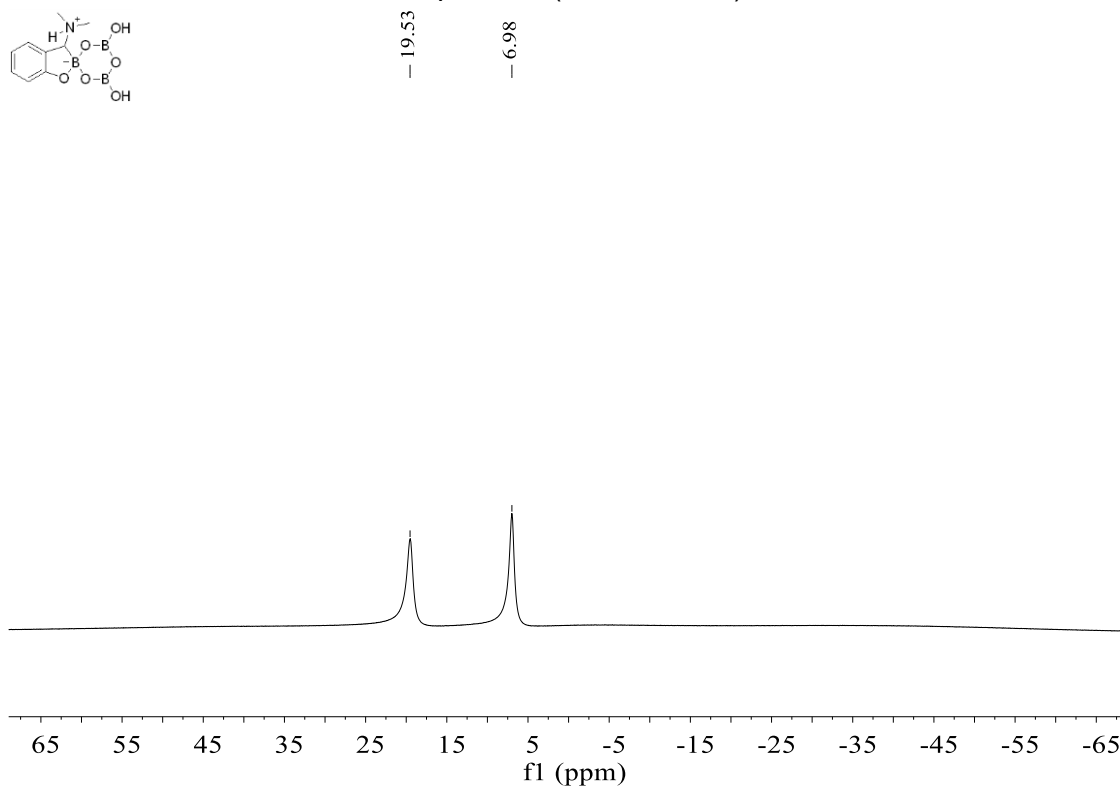
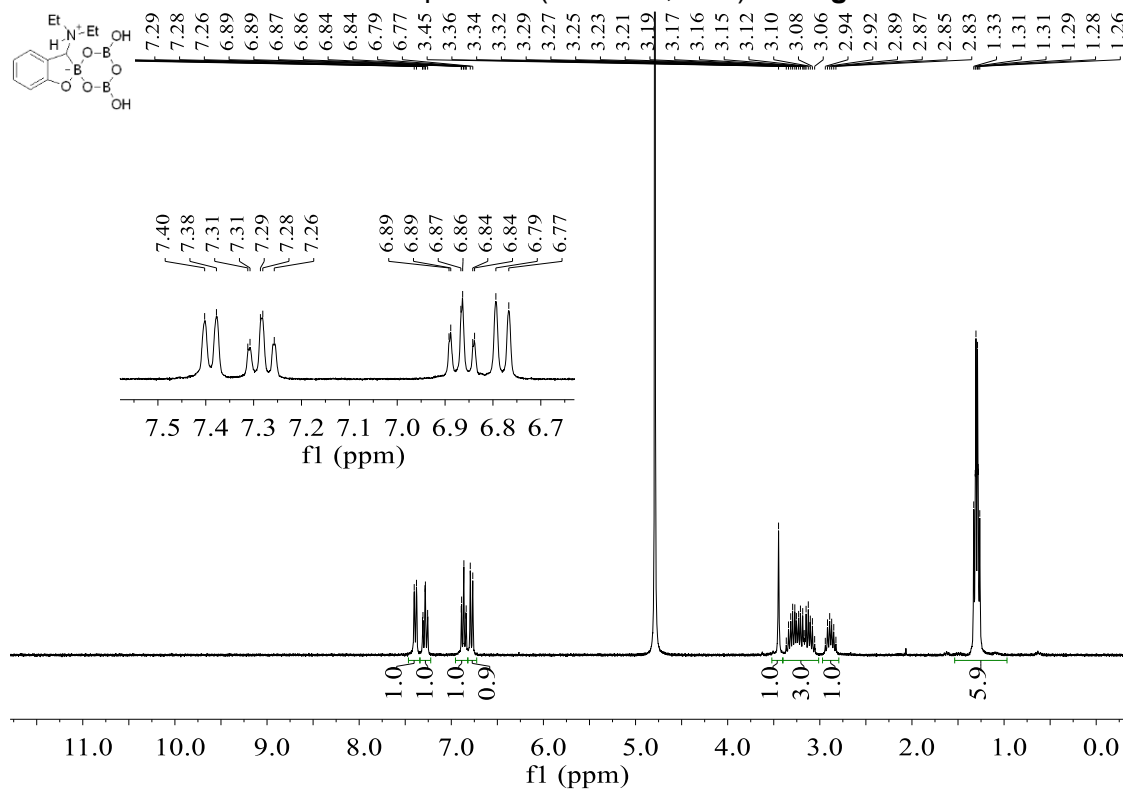
^1H NMR spectrum (300 MHz, D_2O) of **3-4f**

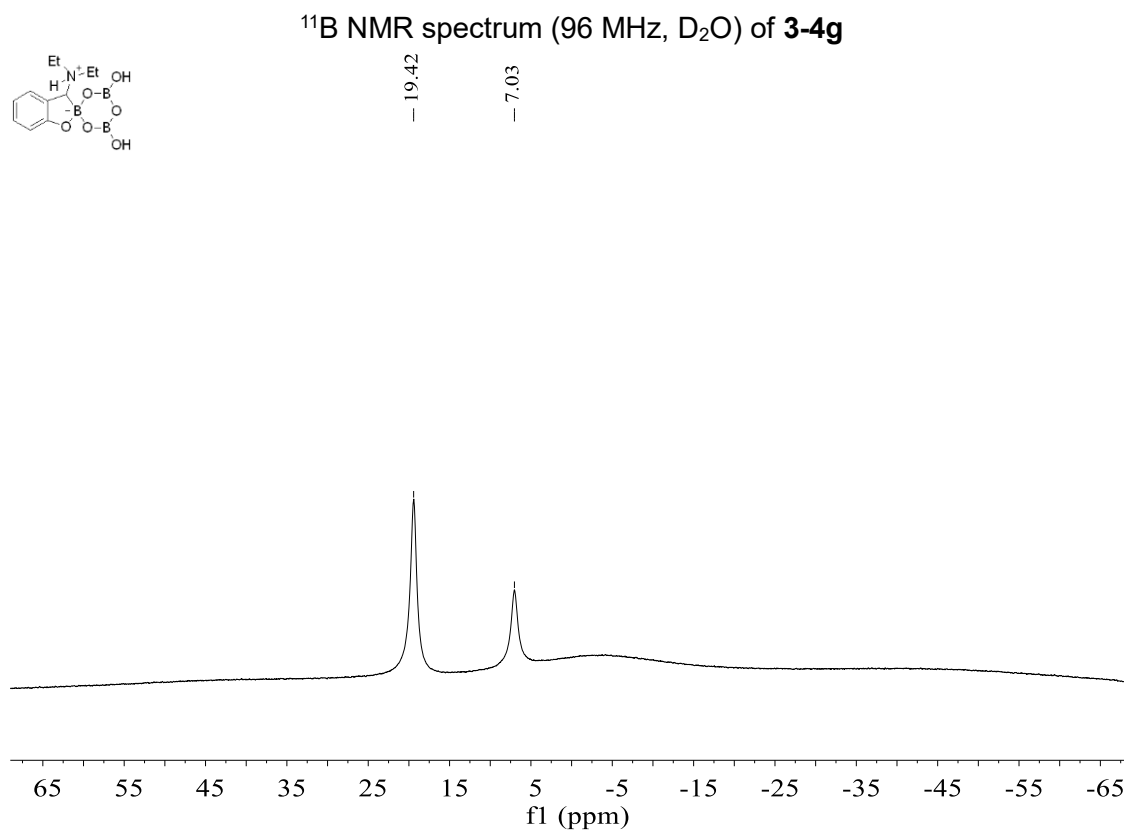
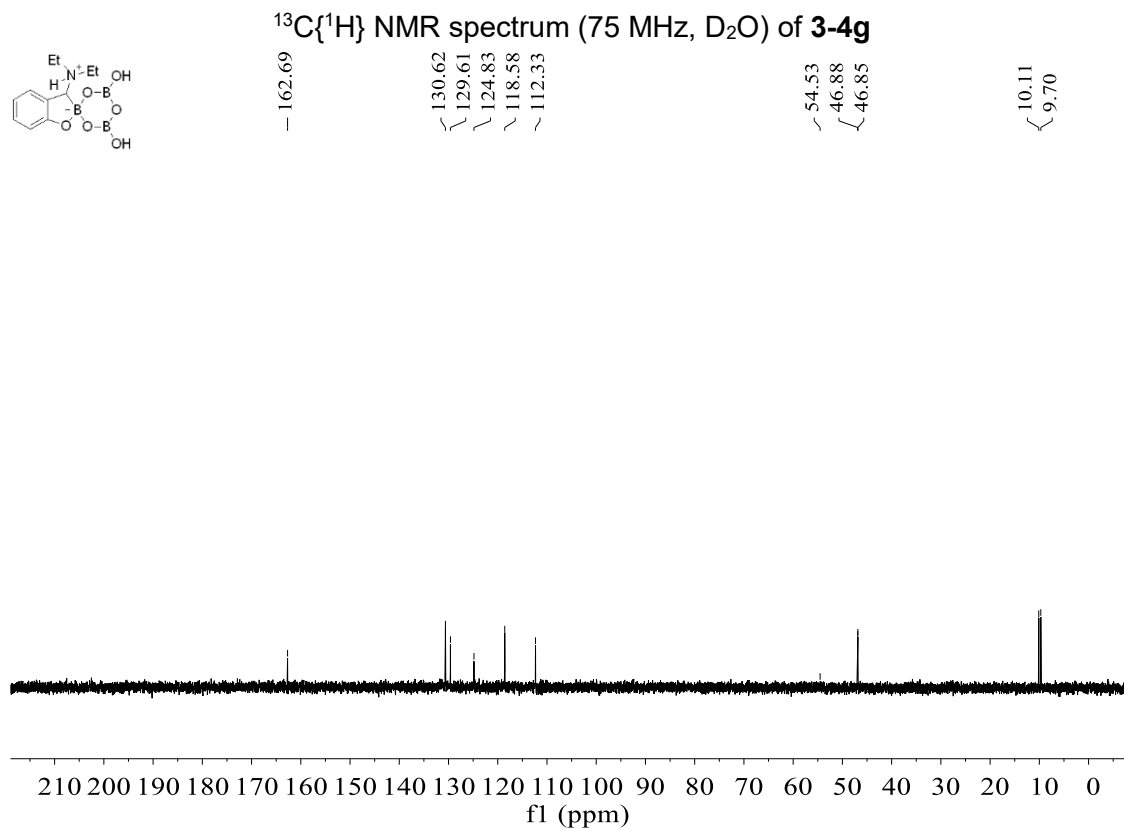
~ 3.21
~ 2.83
~ 2.67

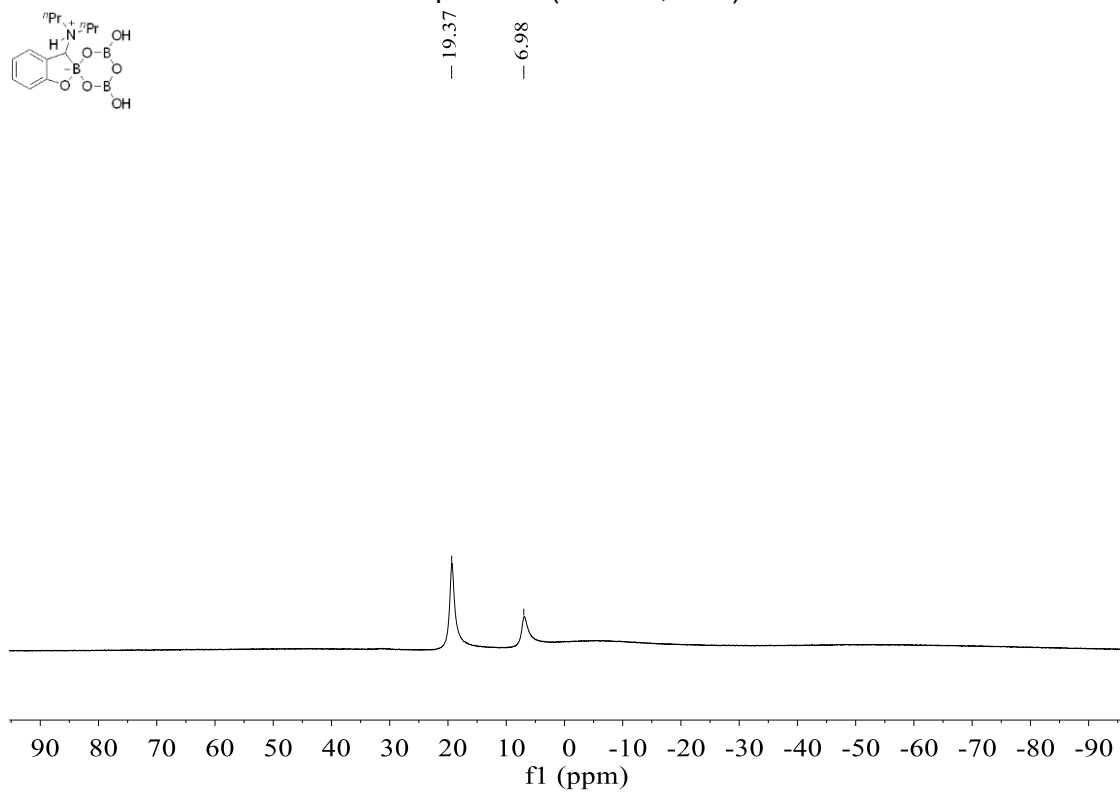
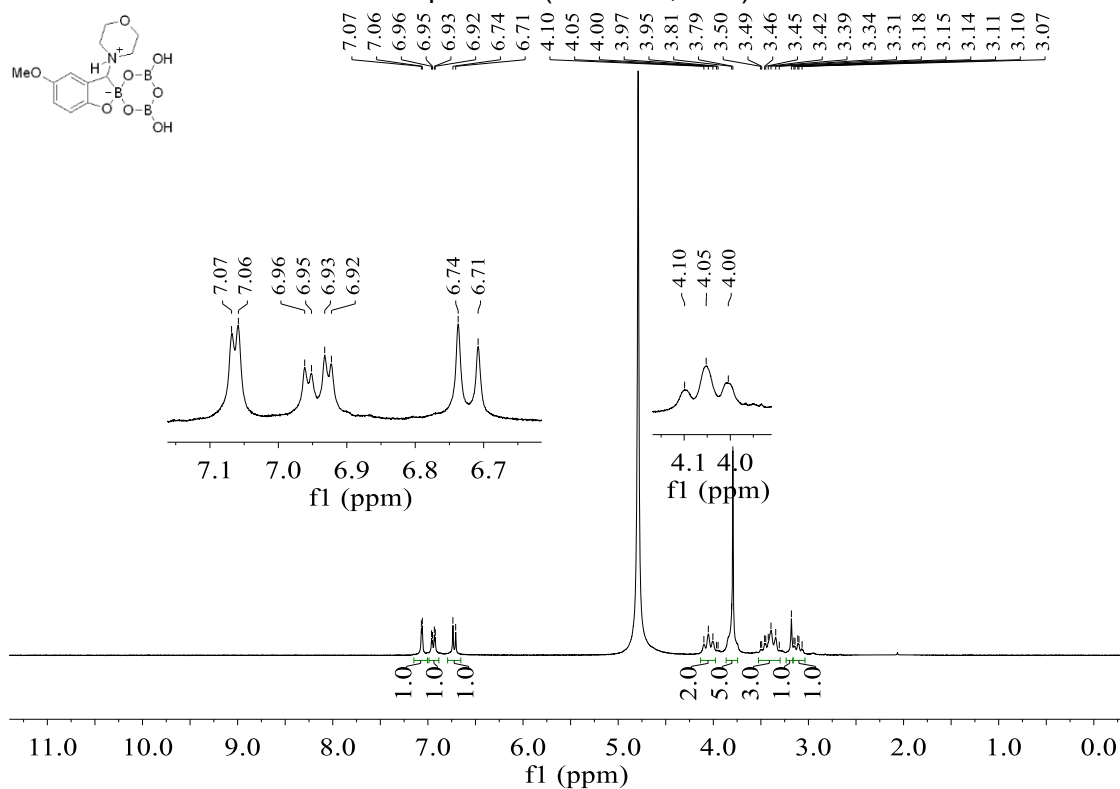
 $^{13}\text{C}\{^1\text{H}\}$ NMR spectrum (75 MHz, D_2O) of **3-4f**

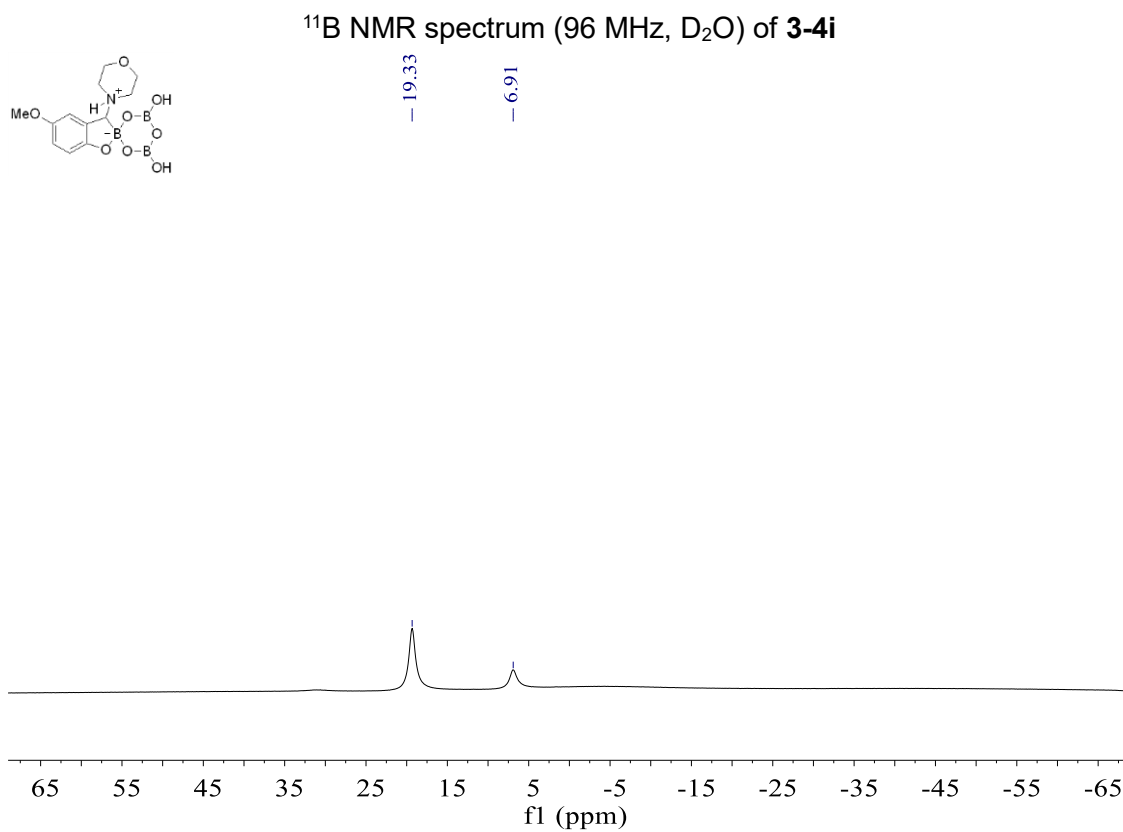
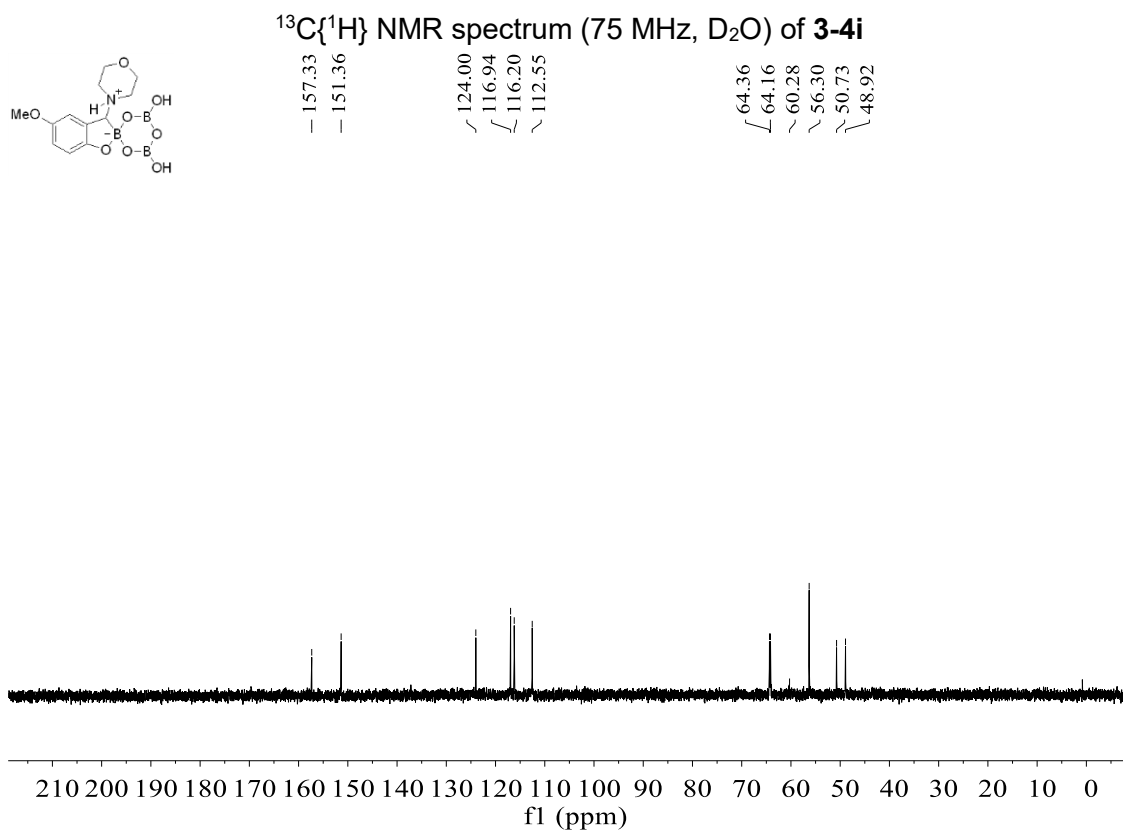
~ 162.71
~ 130.91
~ 130.00
~ 124.51
~ 118.59
~ 112.38
~ 60.41
~ 41.92
~ 39.94

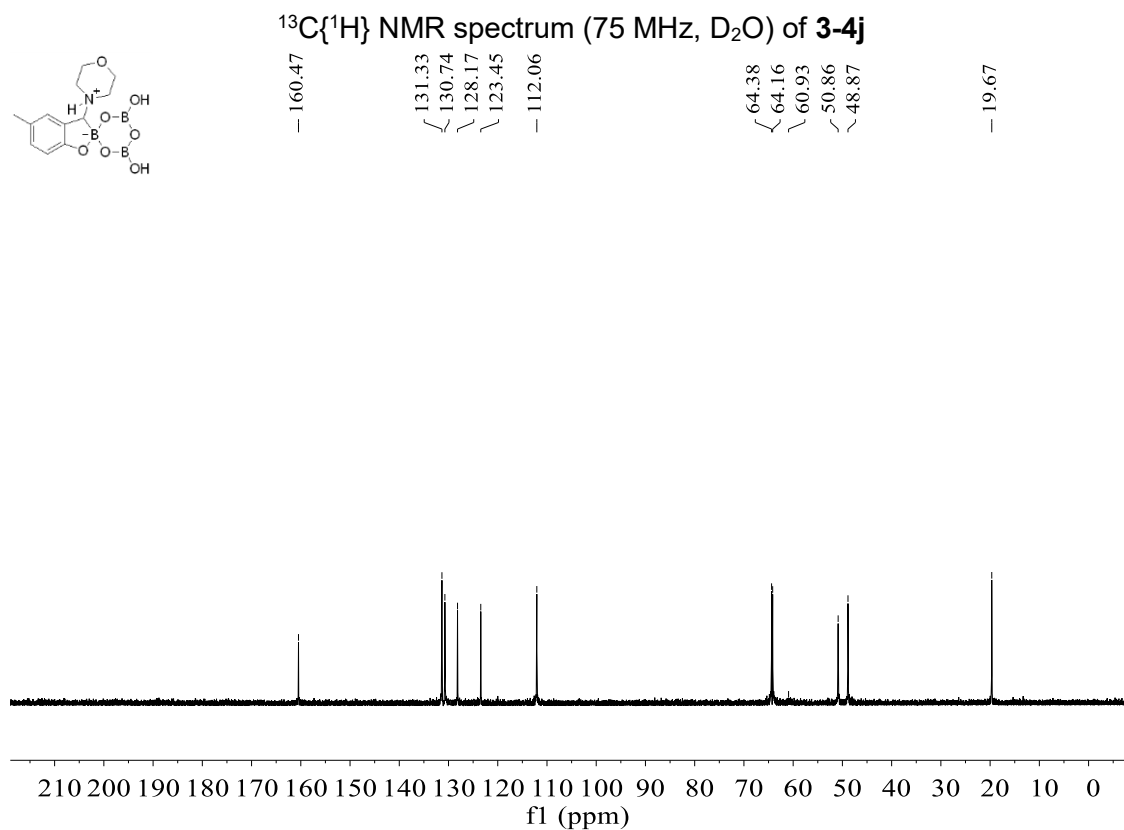
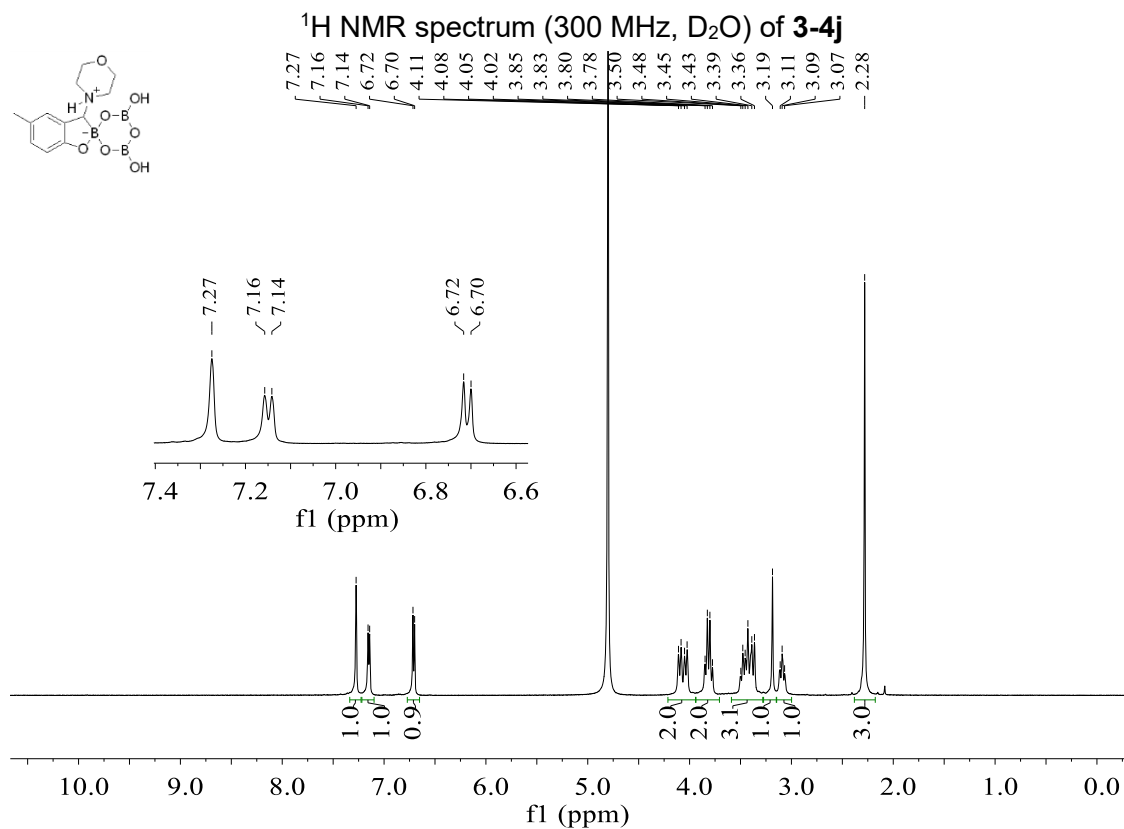


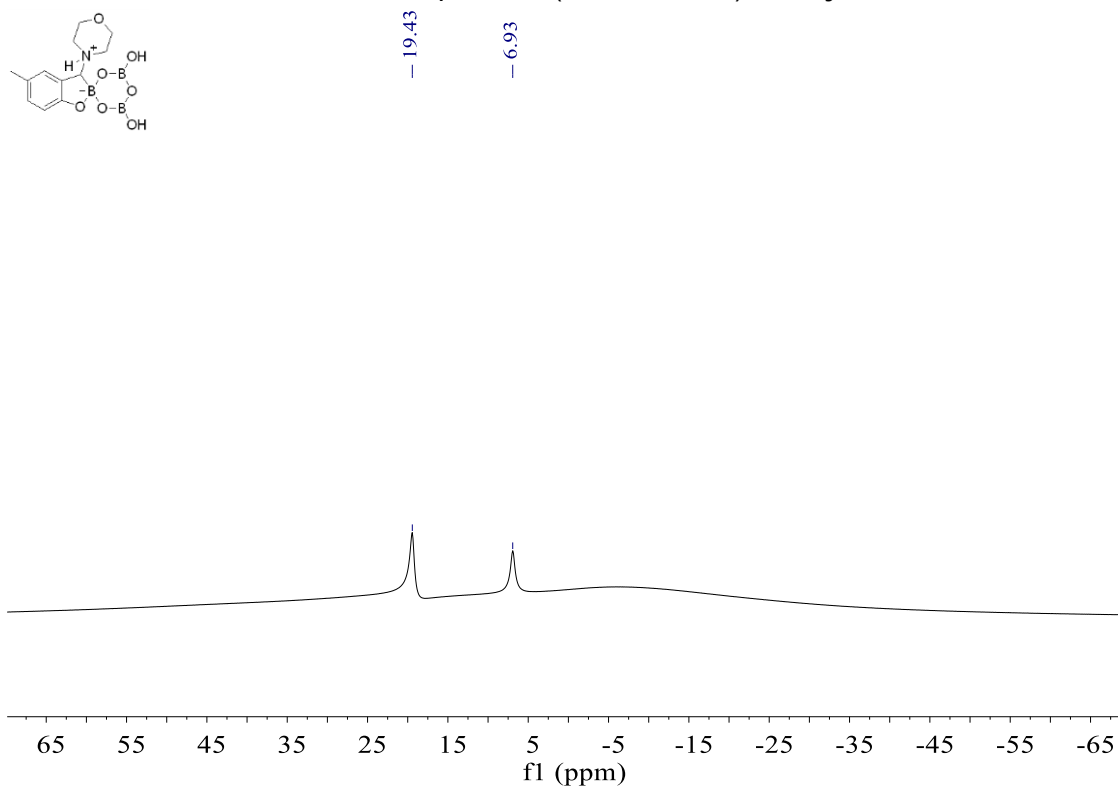
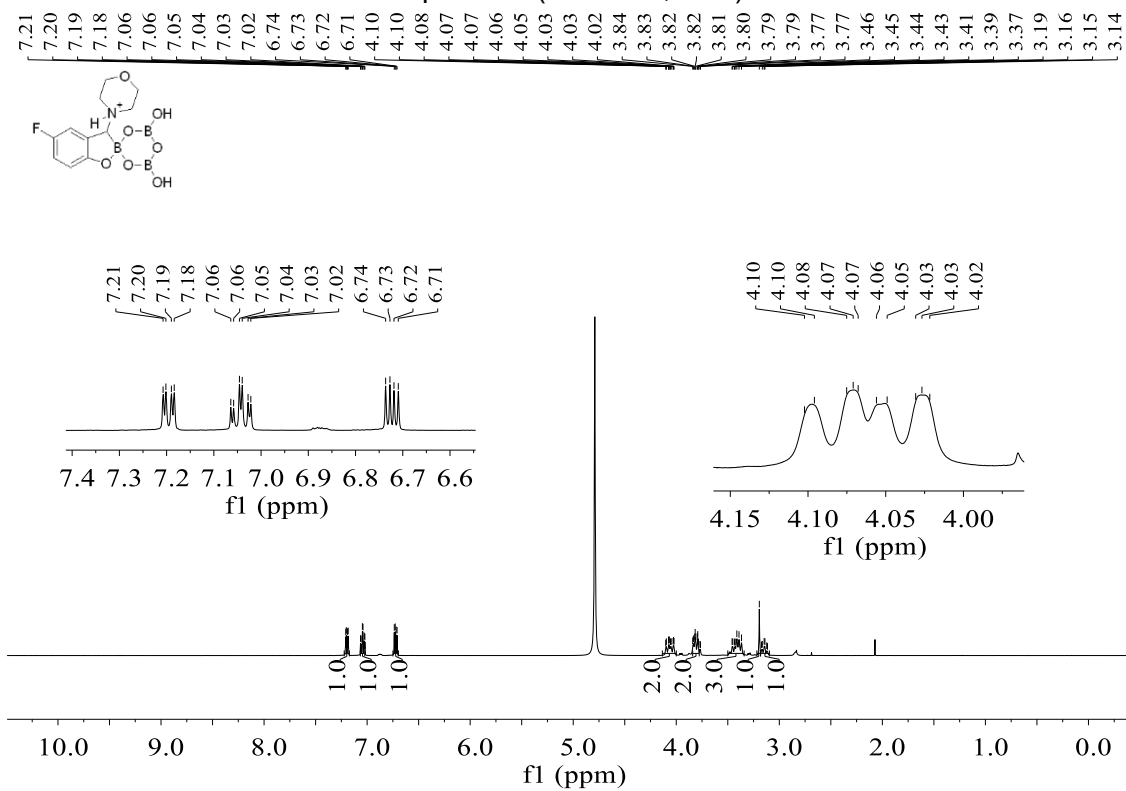
^{11}B NMR spectrum (96 MHz, D_2O) of **3-4f** ^1H NMR spectrum (300 MHz, D_2O) of **3-4g**

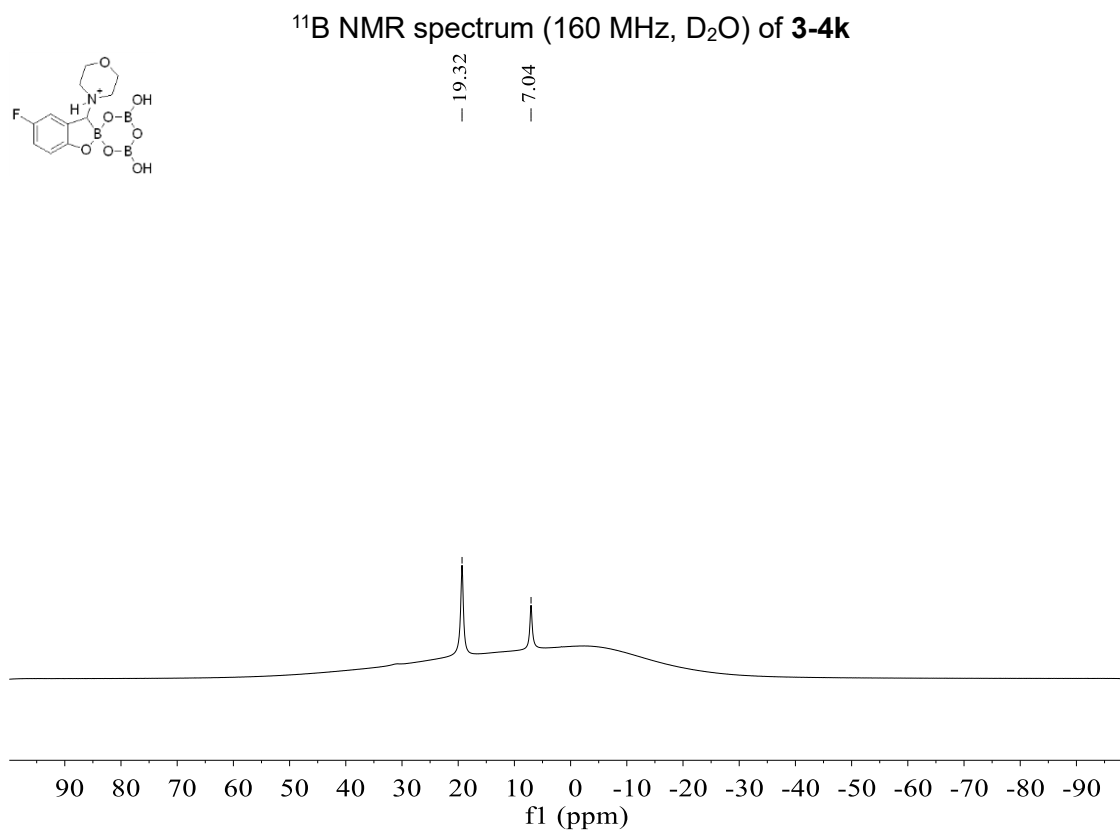
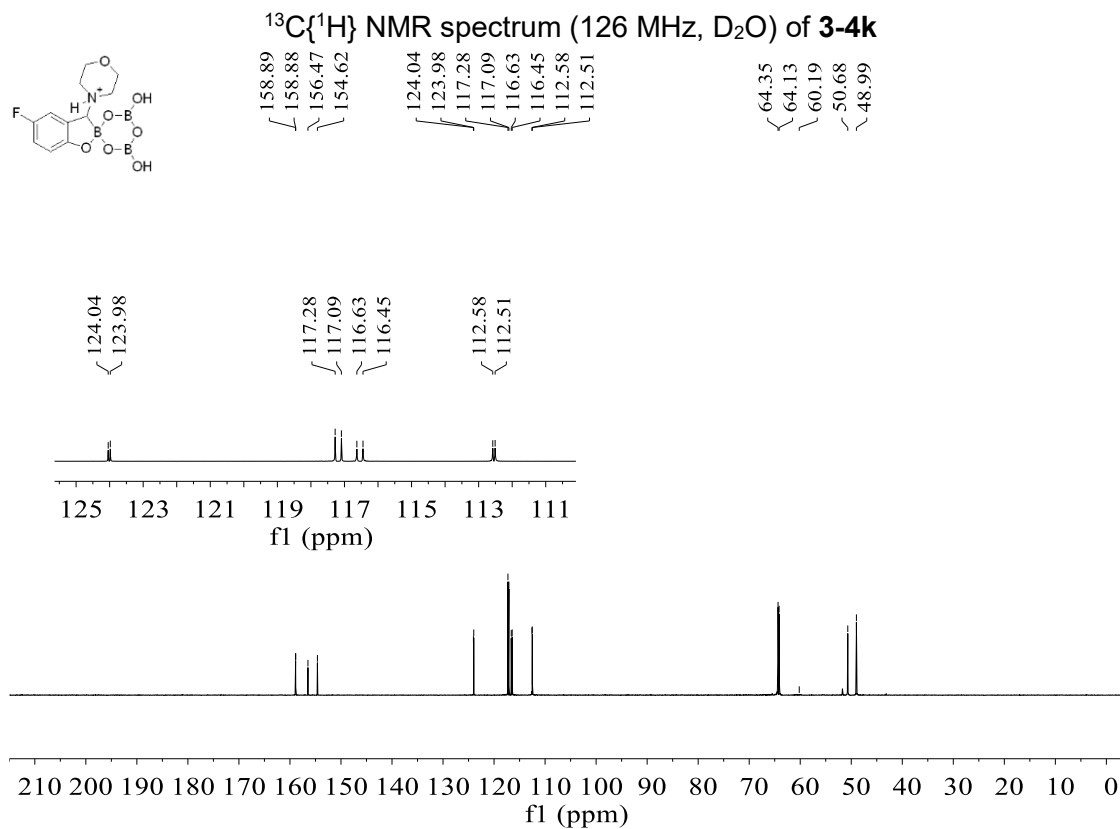


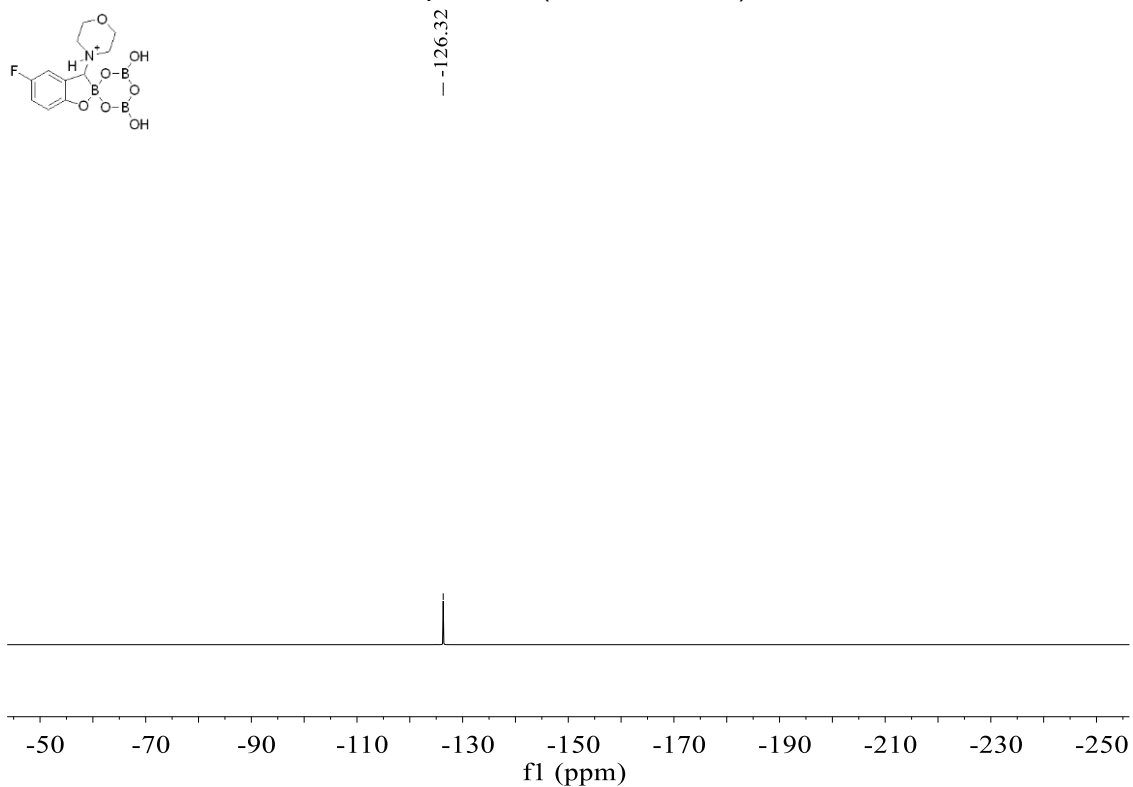
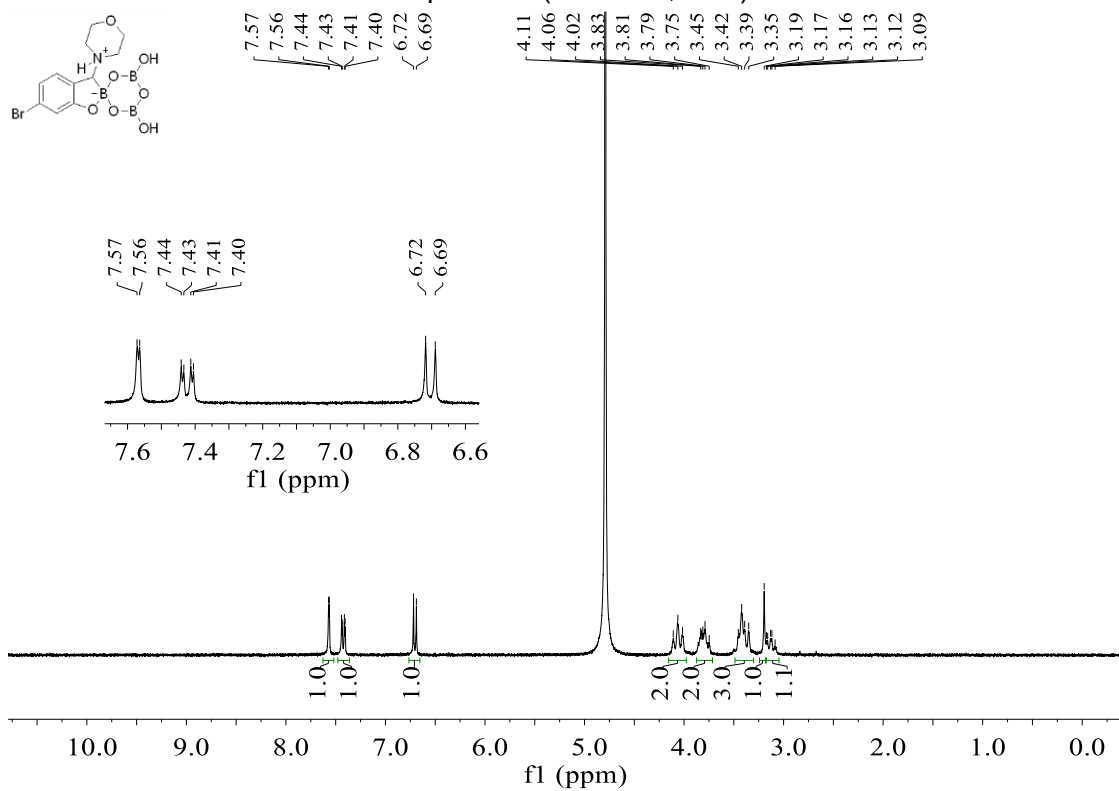
^{11}B NMR spectrum (96 MHz, D_2O) of **3-4h** ^1H NMR spectrum (300 MHz, D_2O) of **3-4i**

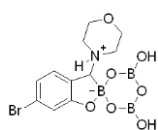




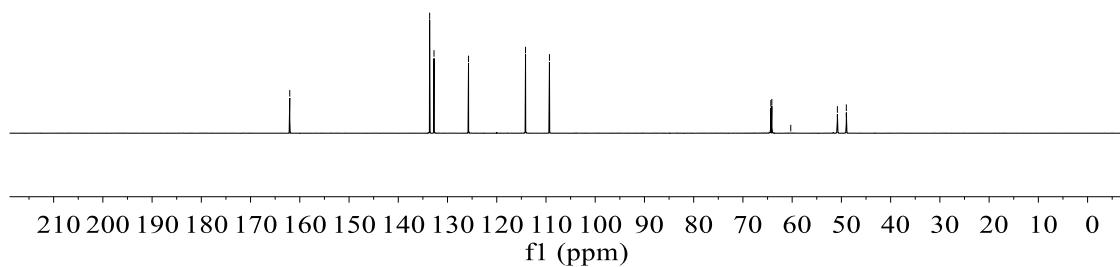
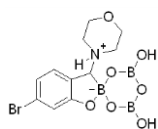
^{11}B NMR spectrum (96 MHz, D_2O) of **3-4j** ^1H NMR spectrum (500 MHz, D_2O) of **3-4k**



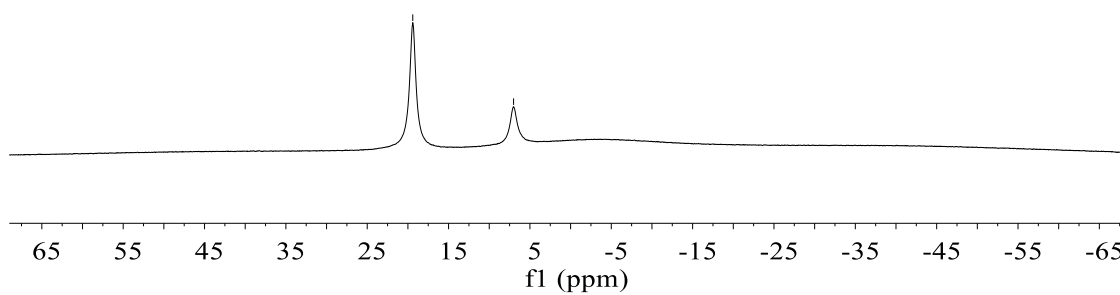
^{11}B NMR spectrum (160 MHz, D_2O) of **3-4k** ^1H NMR spectrum (300 MHz, D_2O) of **3-4l**

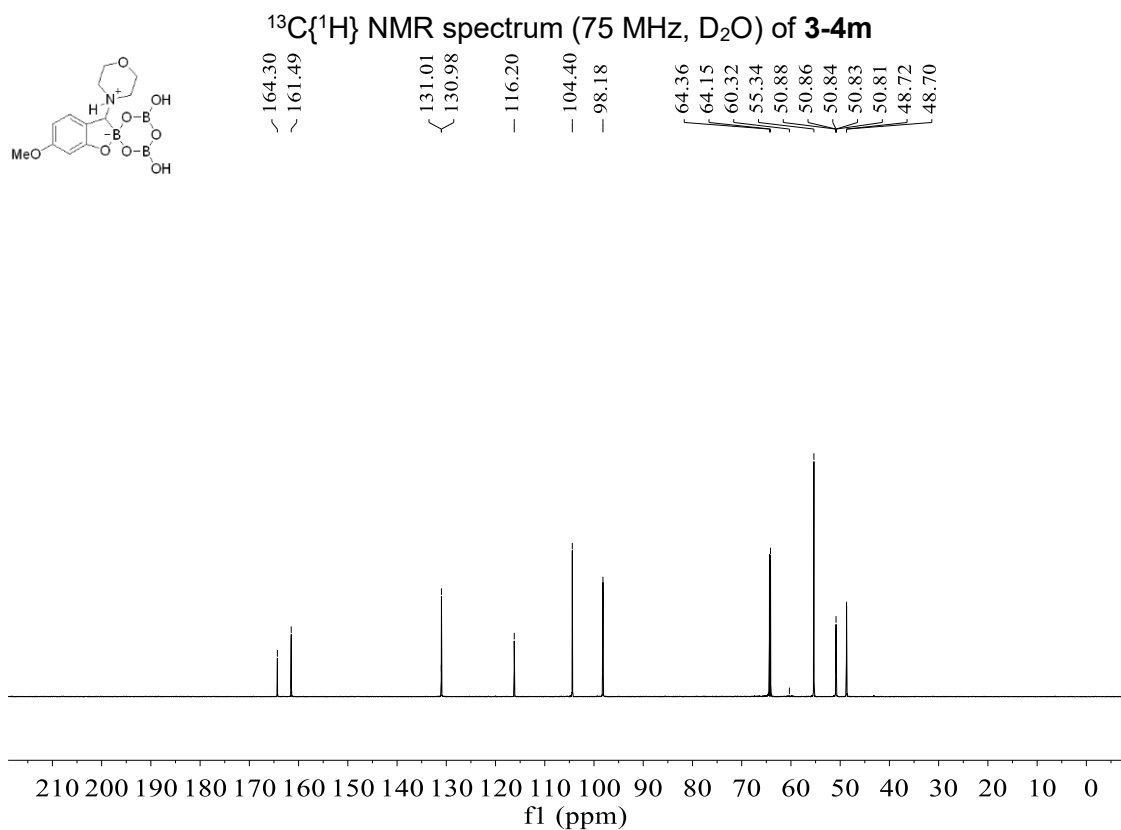
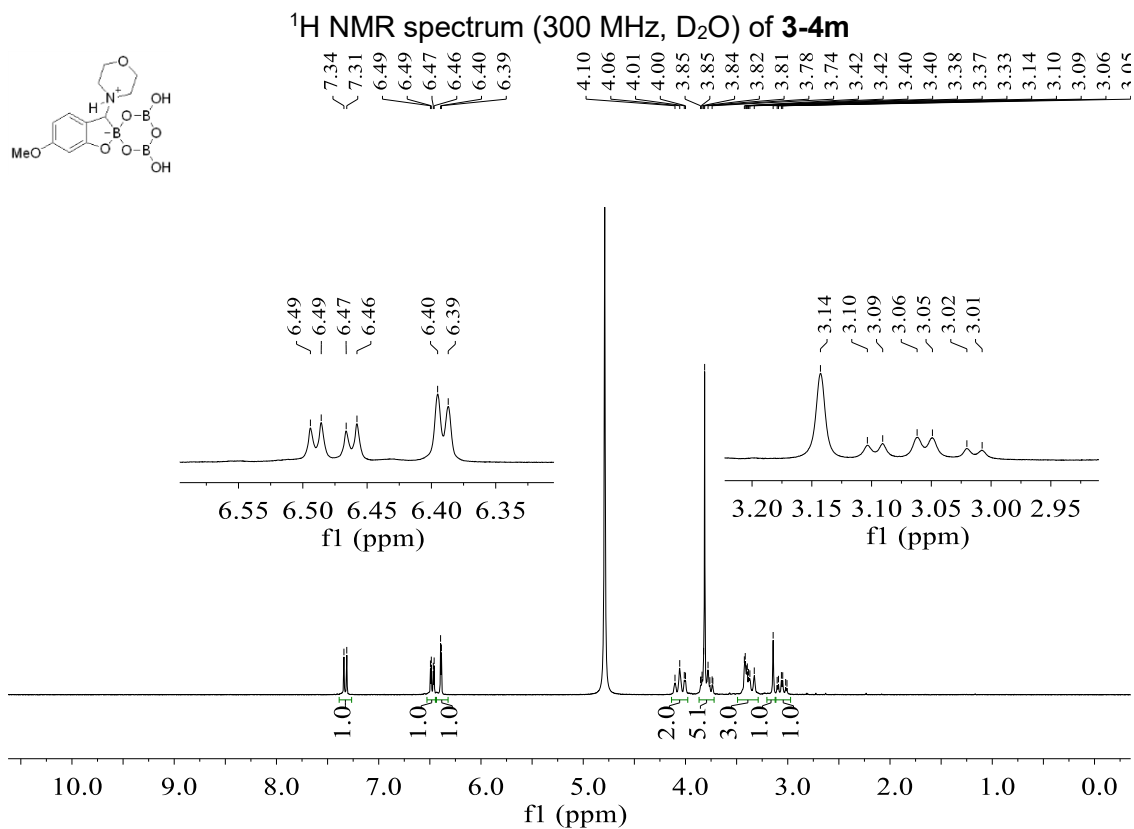
$^{13}\text{C}\{^1\text{H}\}$ NMR spectrum (75 MHz, D_2O) of **3-4I**

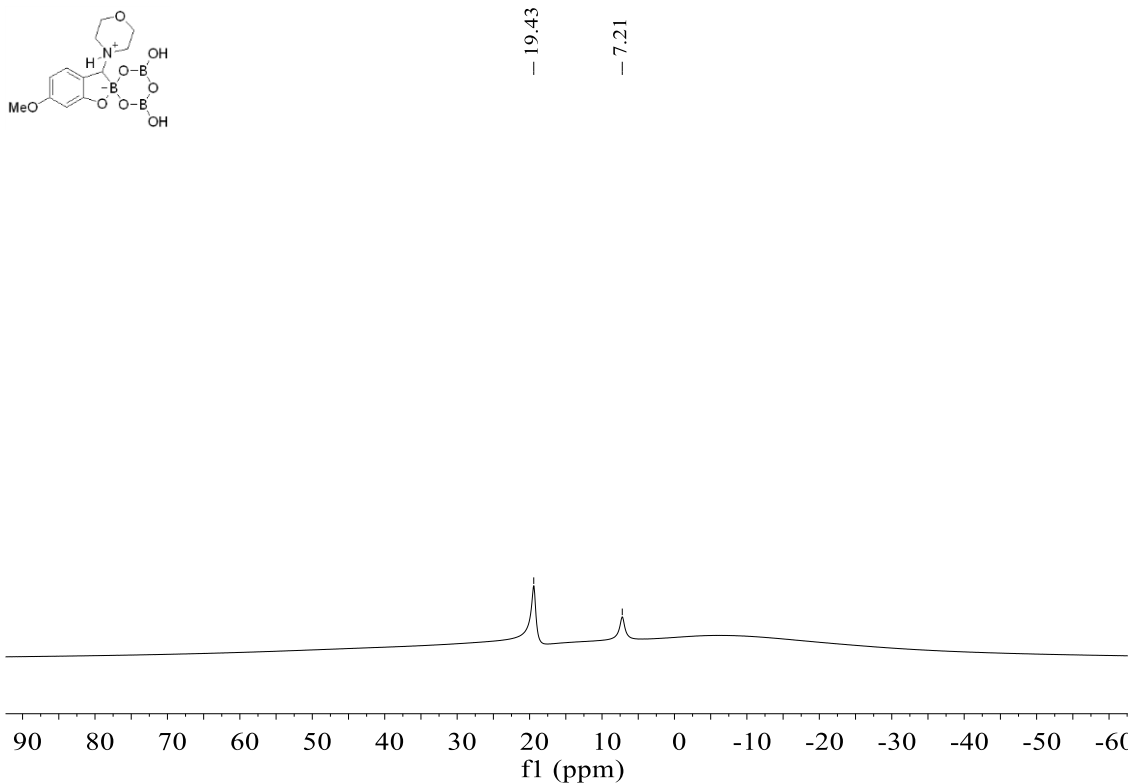
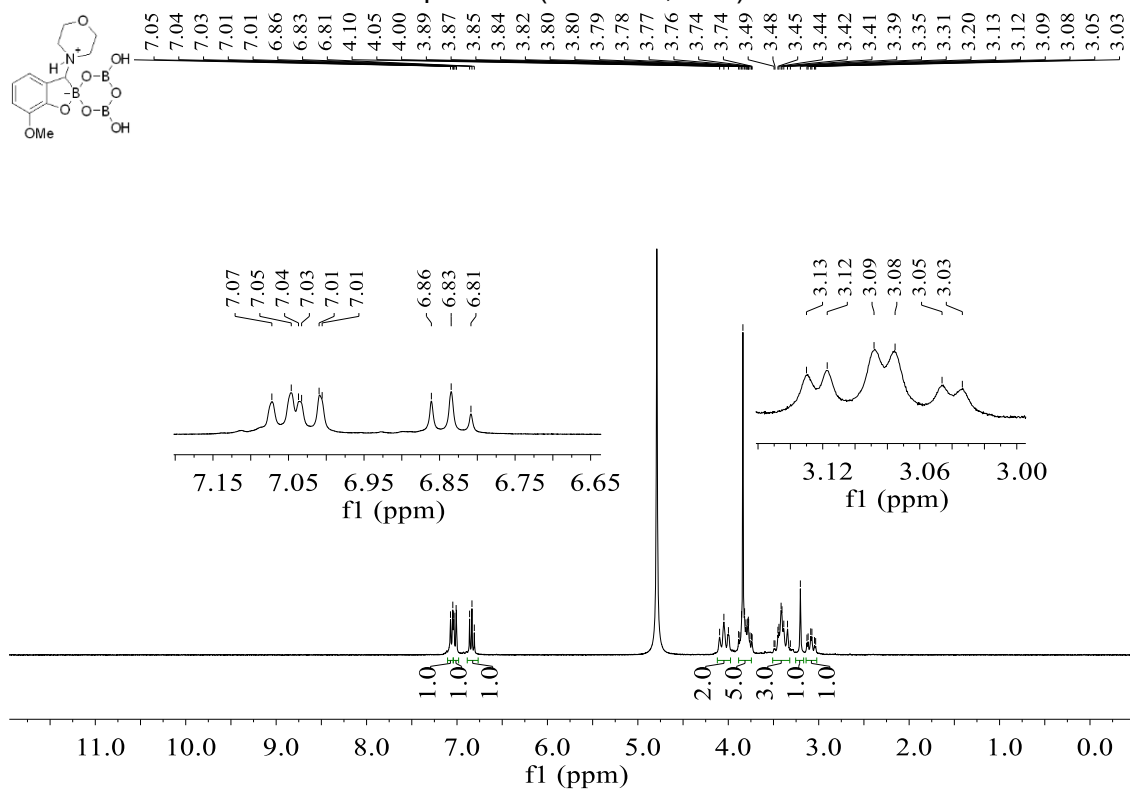
— 162.04
— 133.63
— 132.74
— 125.73
— 114.16
— 109.30
— 64.33
— 64.13
— 60.28
— 50.81
— 49.00

 ^{11}B NMR spectrum (96 MHz, D_2O) of **3-4I**

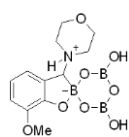
— 19.40
— 7.01



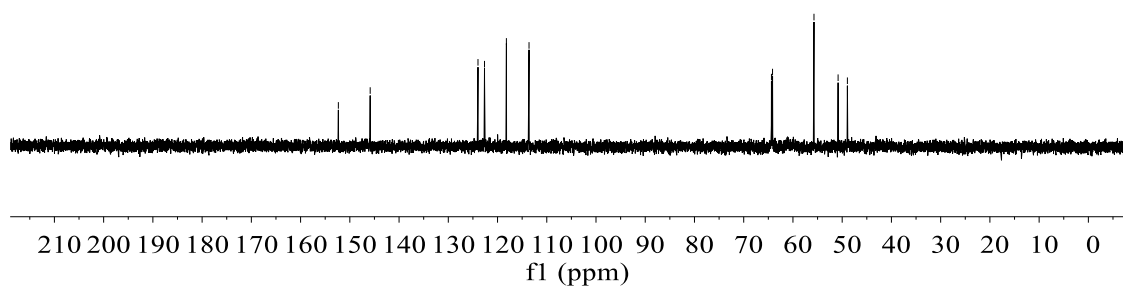


^{11}B NMR spectrum (96 MHz, D_2O) of **3-4m** ^1H NMR spectrum (300 MHz, D_2O) of **3-4n**

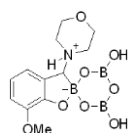
$^{13}\text{C}\{^1\text{H}\}$ NMR spectrum (75 MHz, D_2O) of **3-4n**



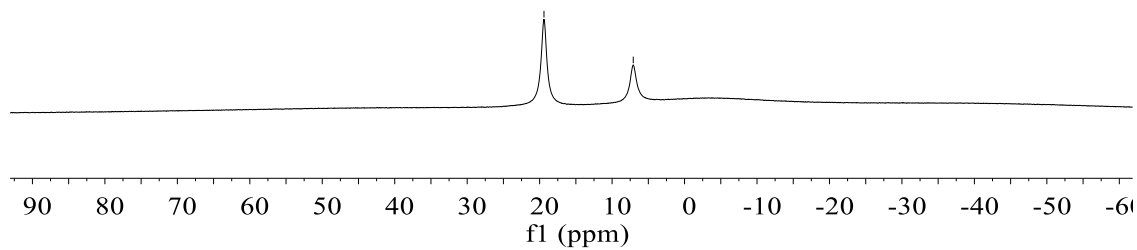
-152.33
 -145.86
 123.97
 122.65
 118.20
 113.60
 64.36
 64.15
 61.09
 55.73
 50.83
 48.94

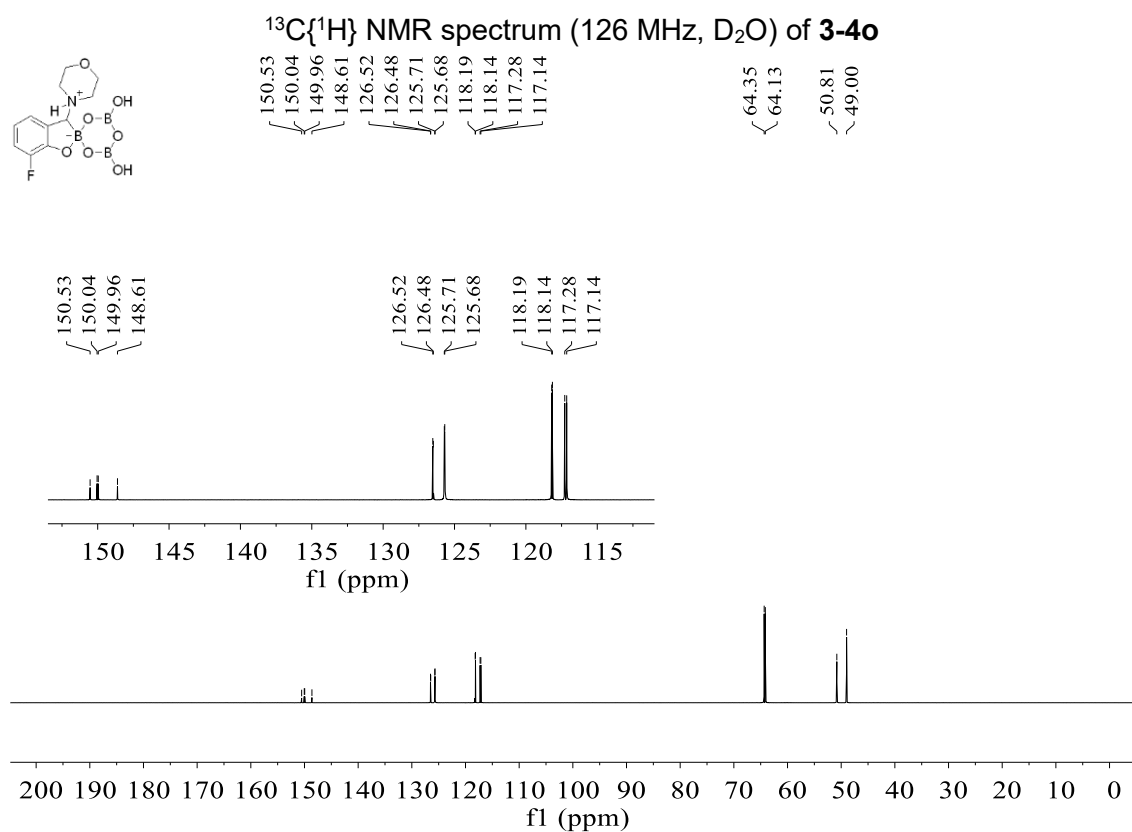
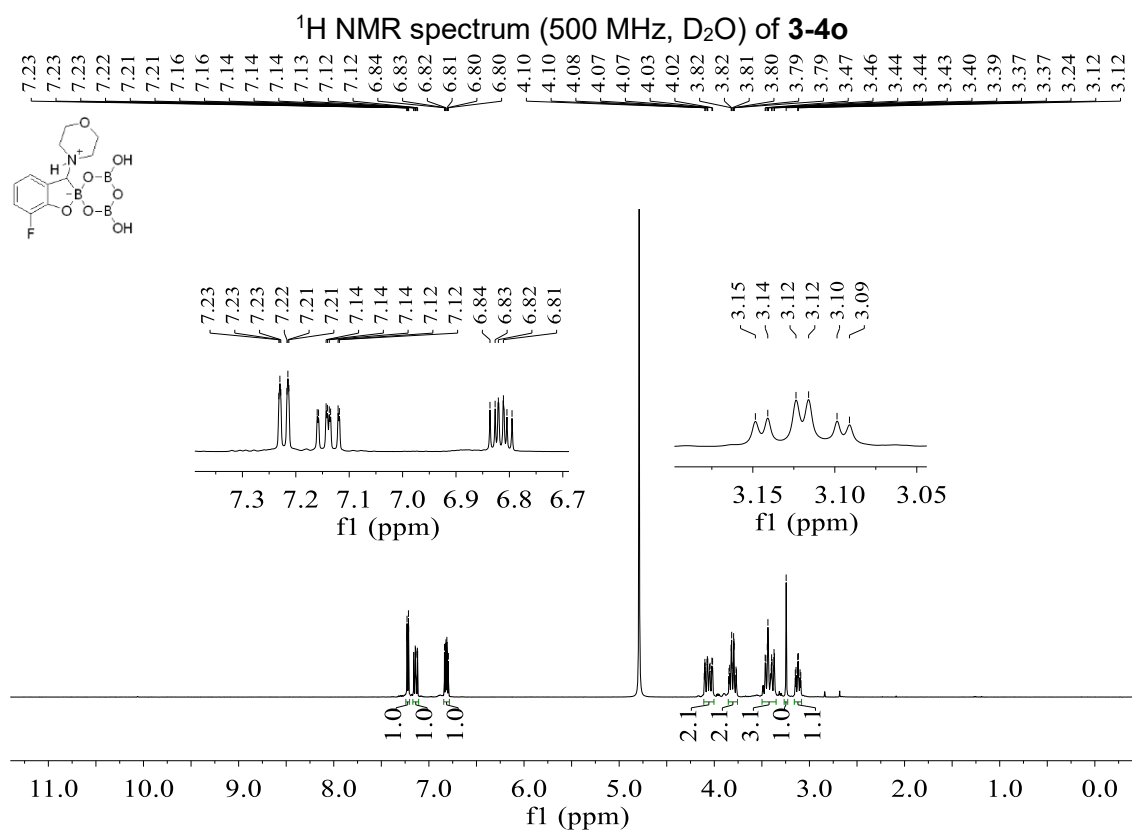


^{11}B NMR spectrum (96 MHz, D_2O) of **3-4n**



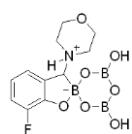
-19.40
 -7.08



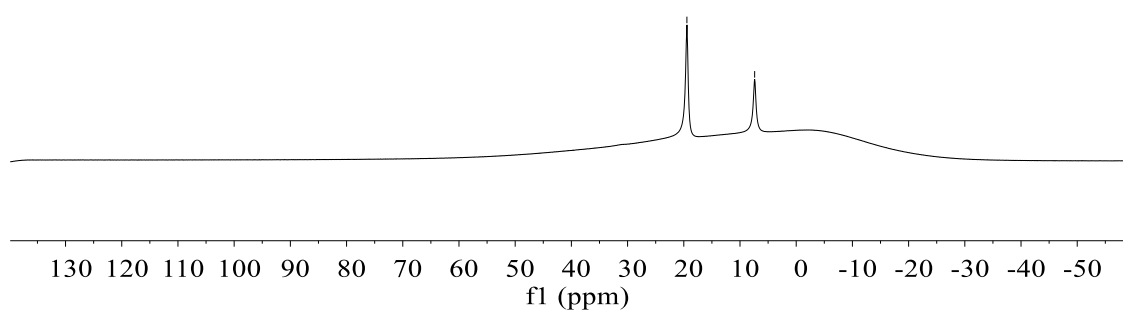


Appendix

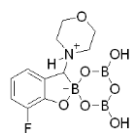
^{11}B NMR spectrum (160 MHz, D_2O) of **3-4o**



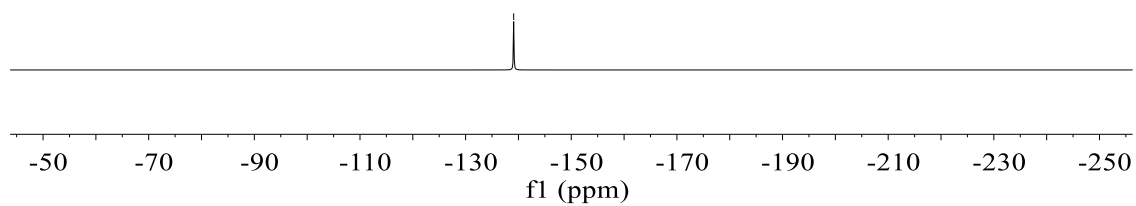
- 19.45
- 7.39

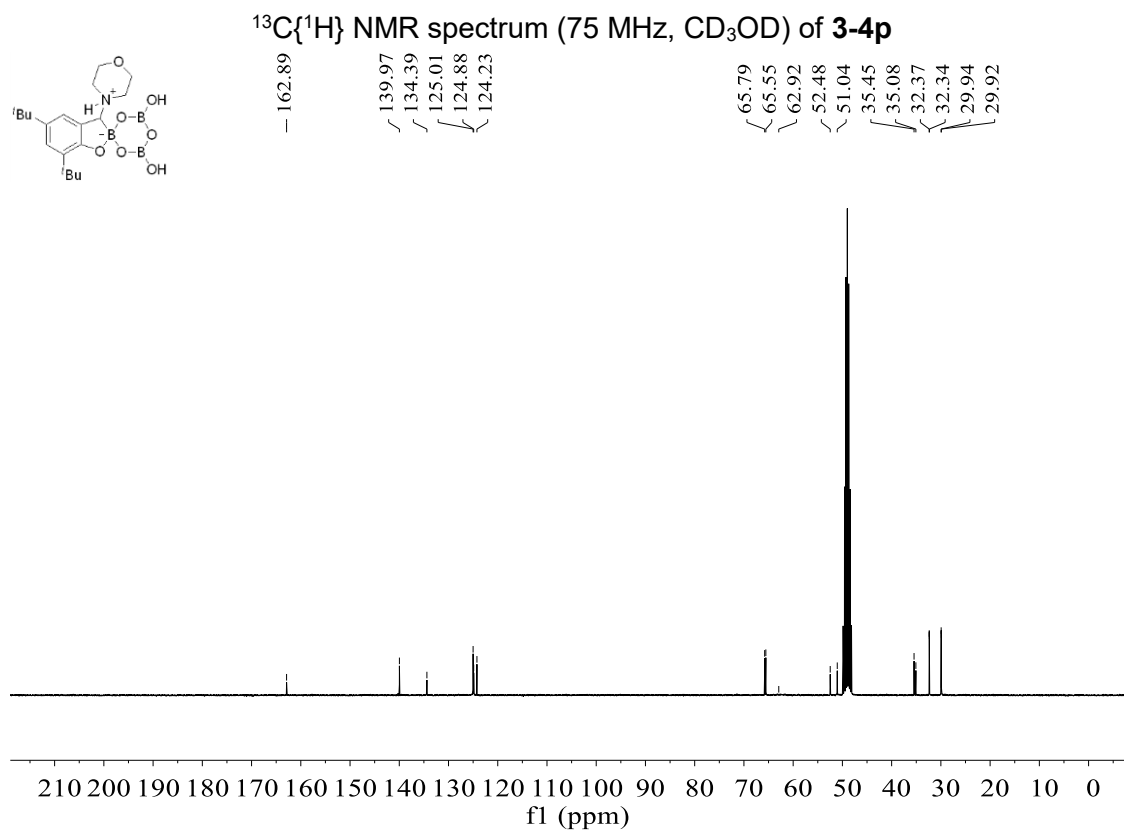
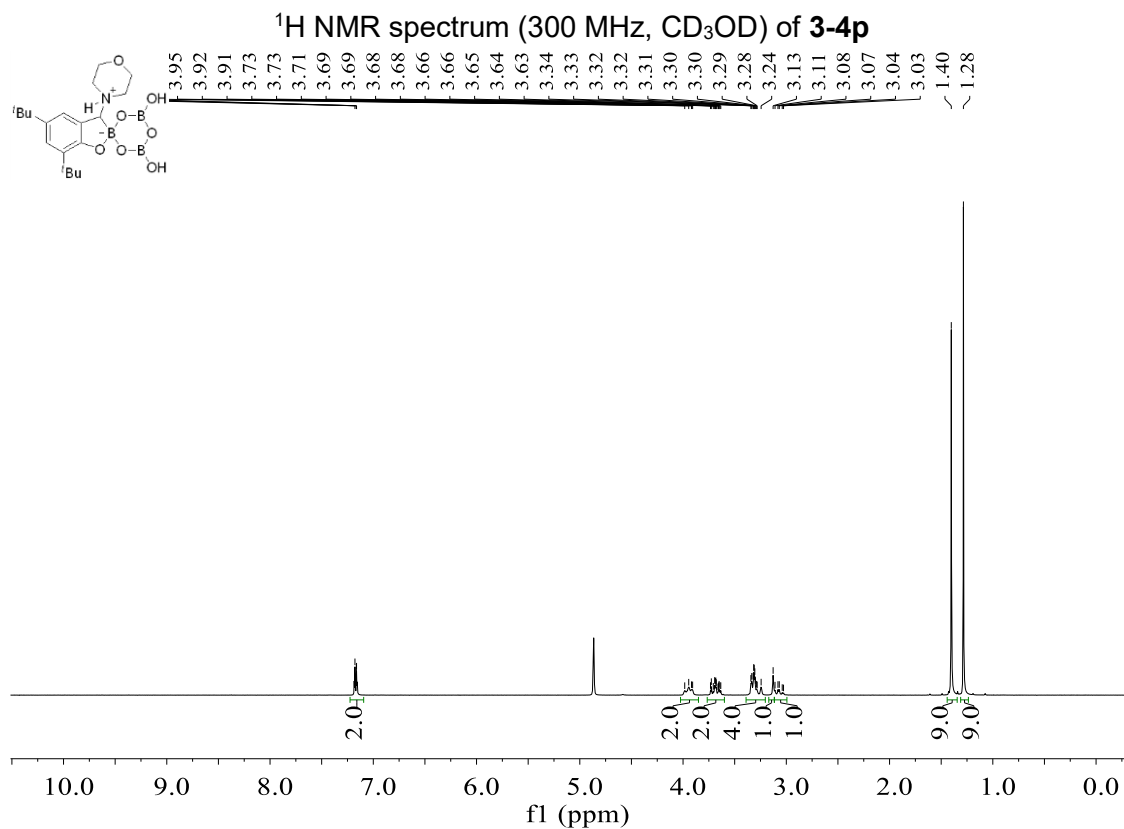


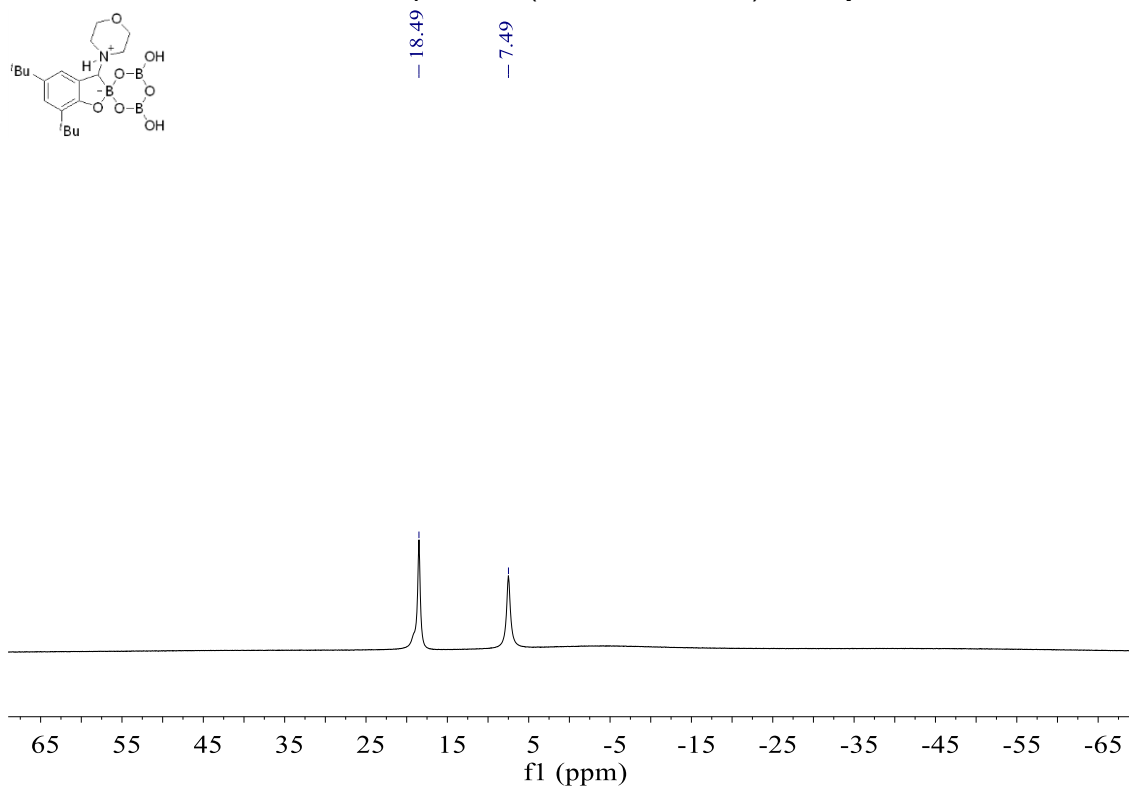
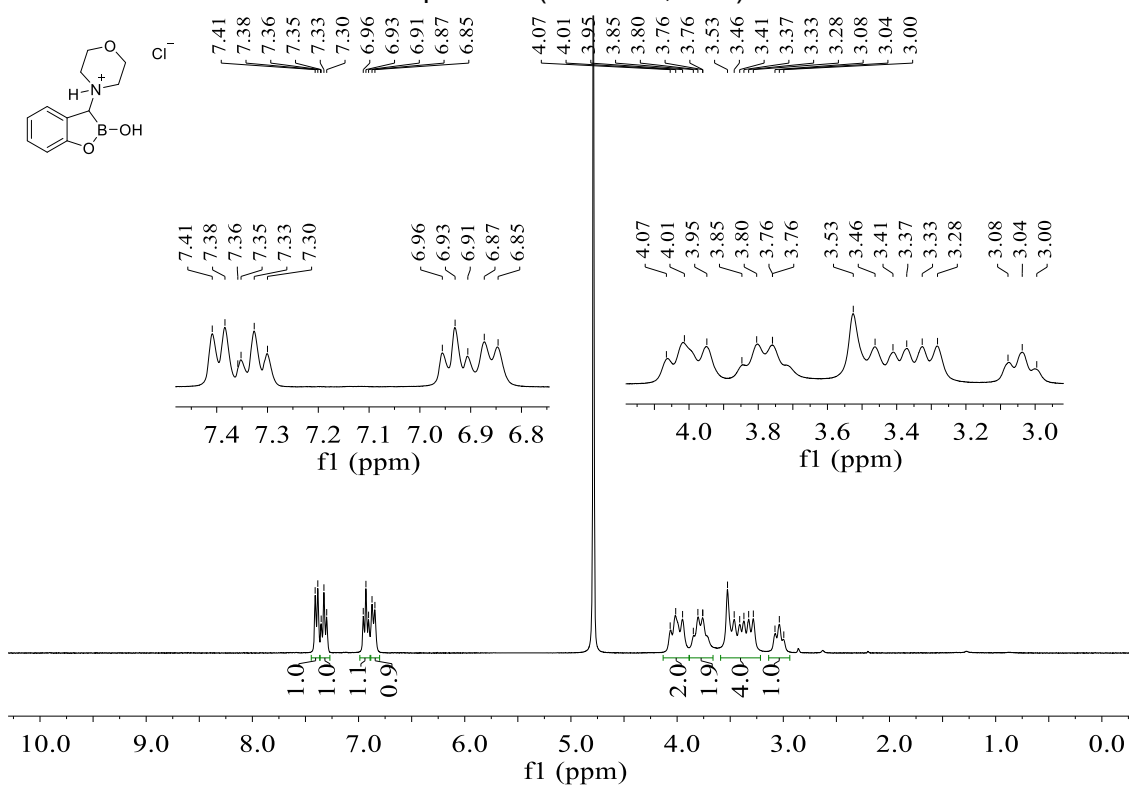
^{19}F NMR spectrum (471 MHz, D_2O) of **3-4o**

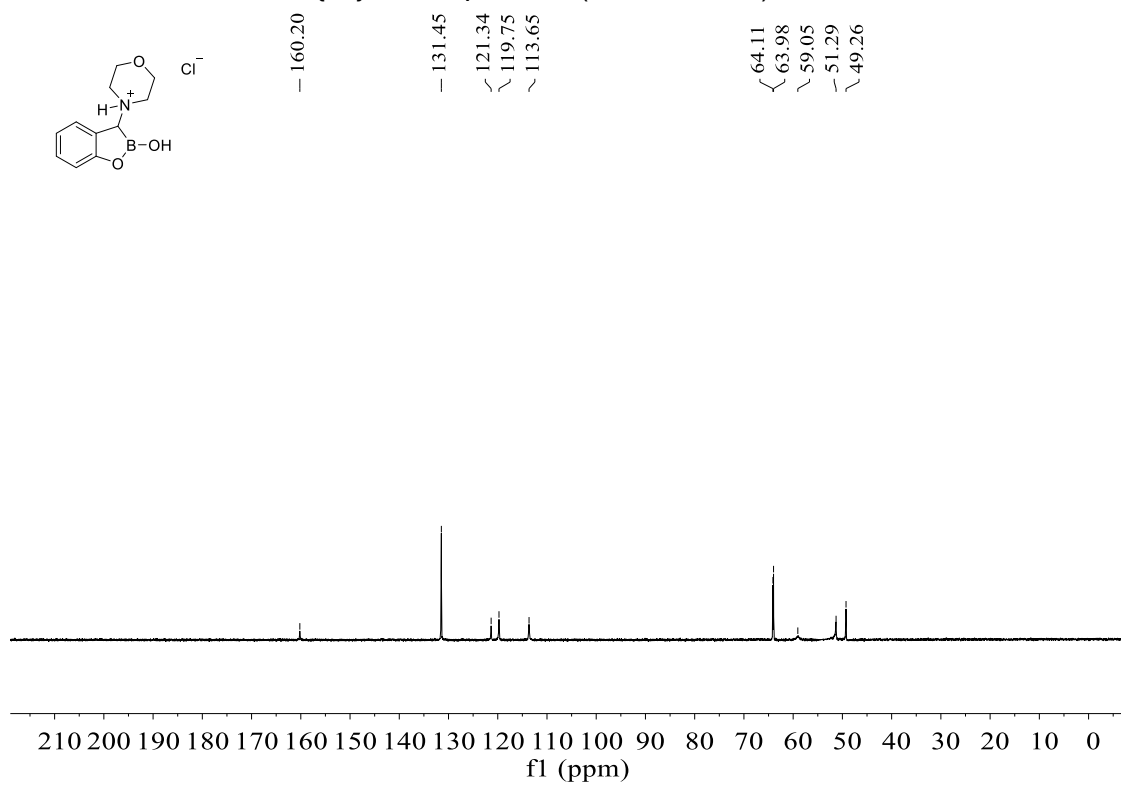
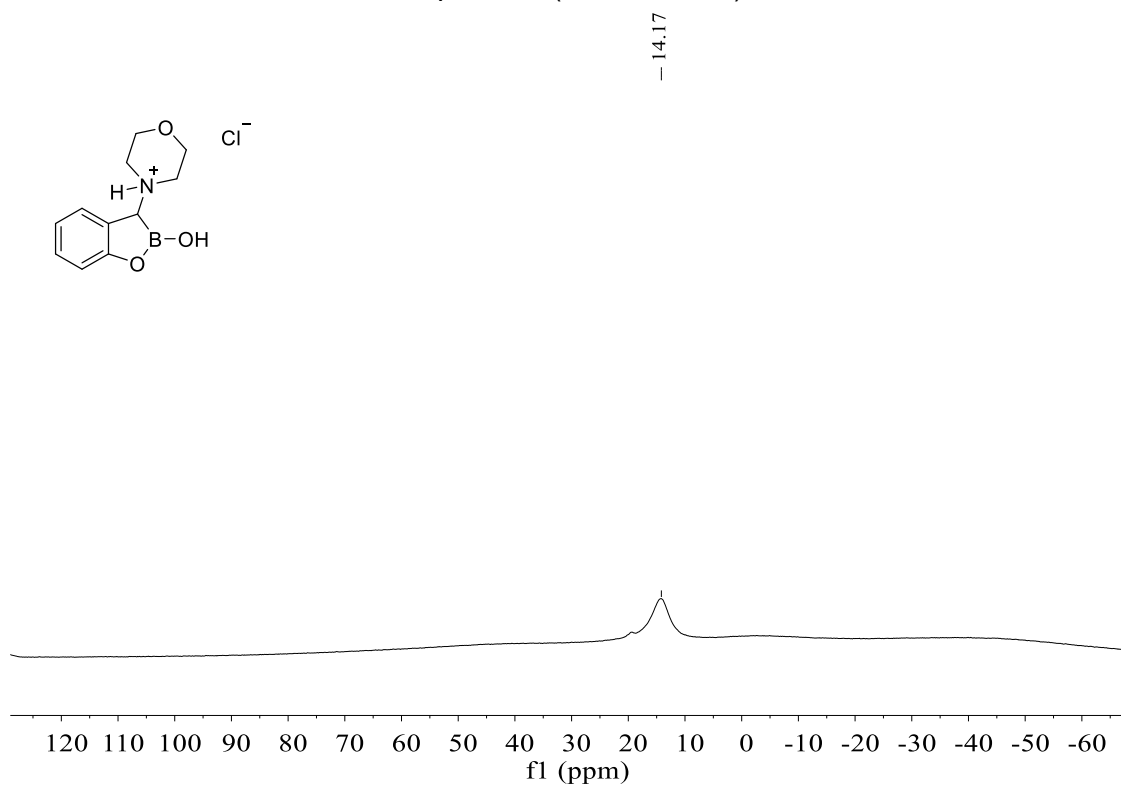


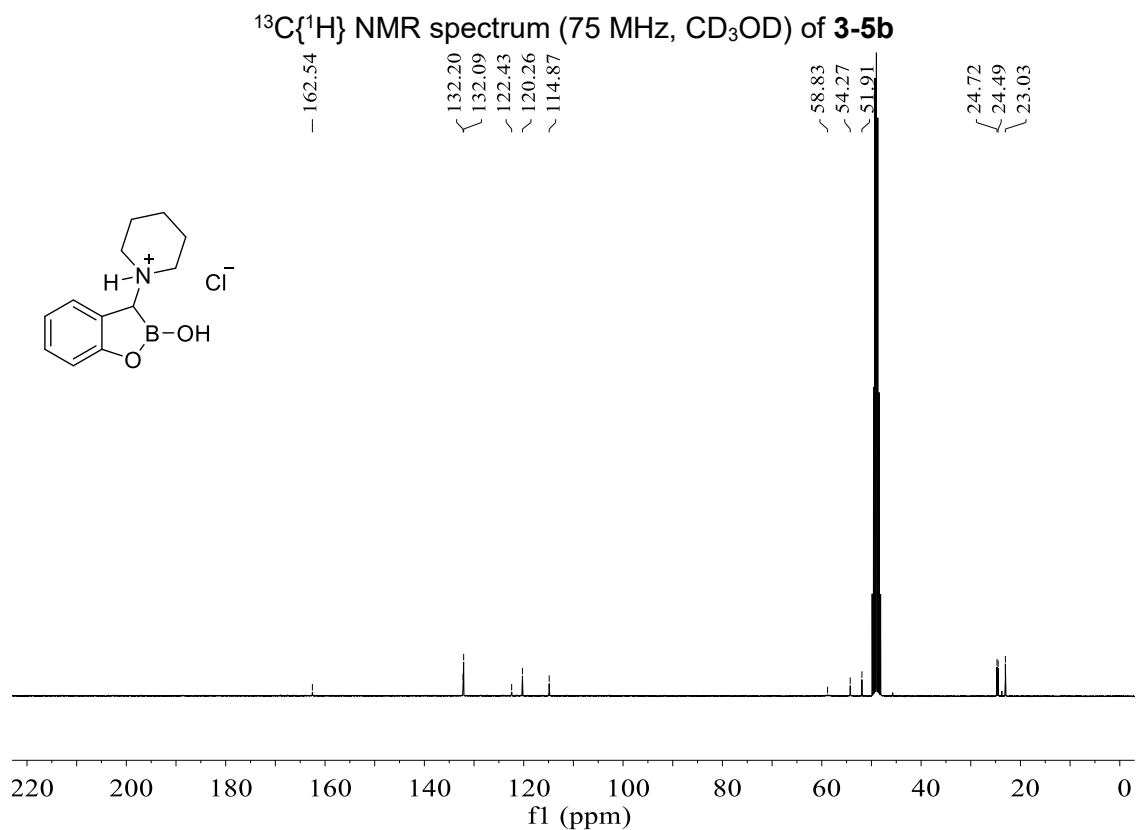
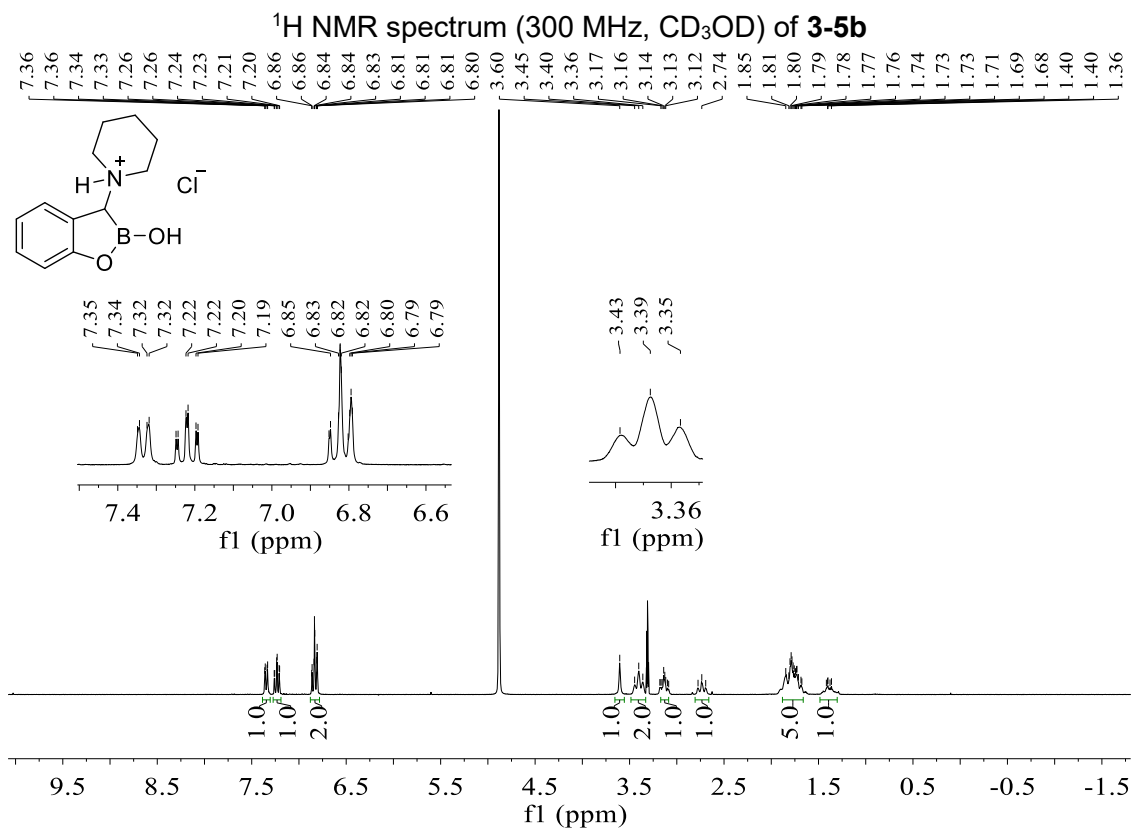
- -139.10

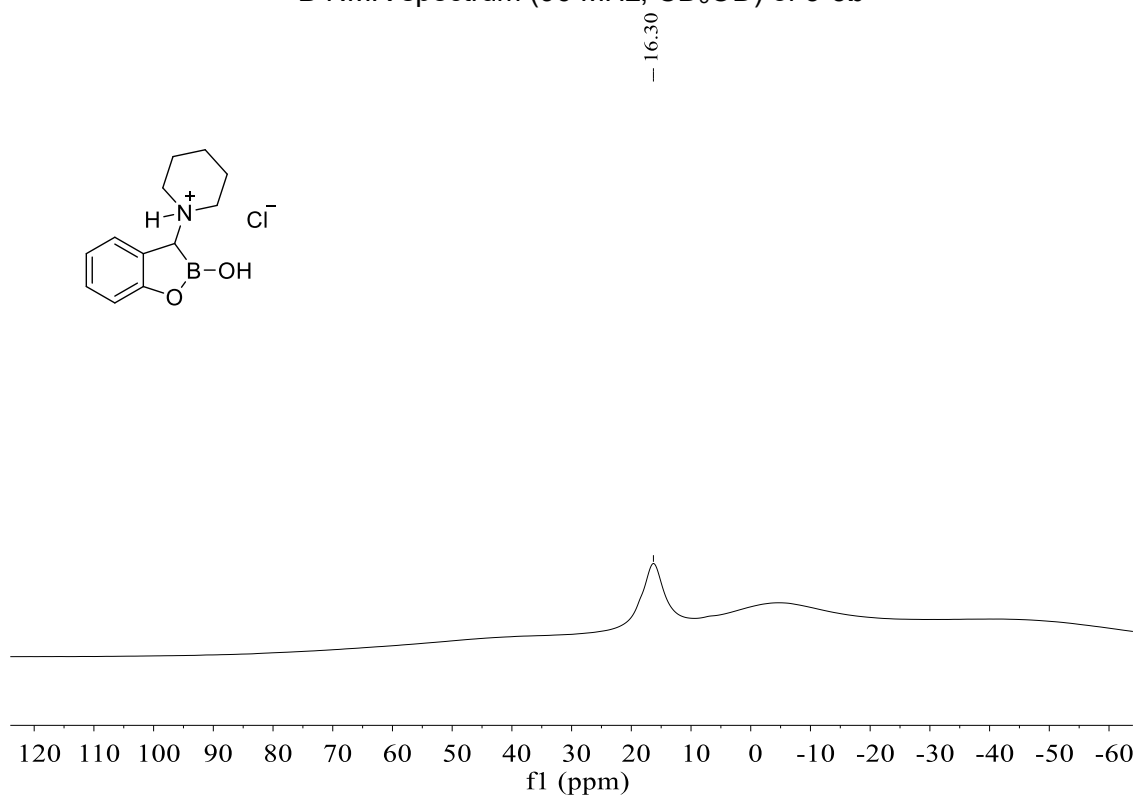
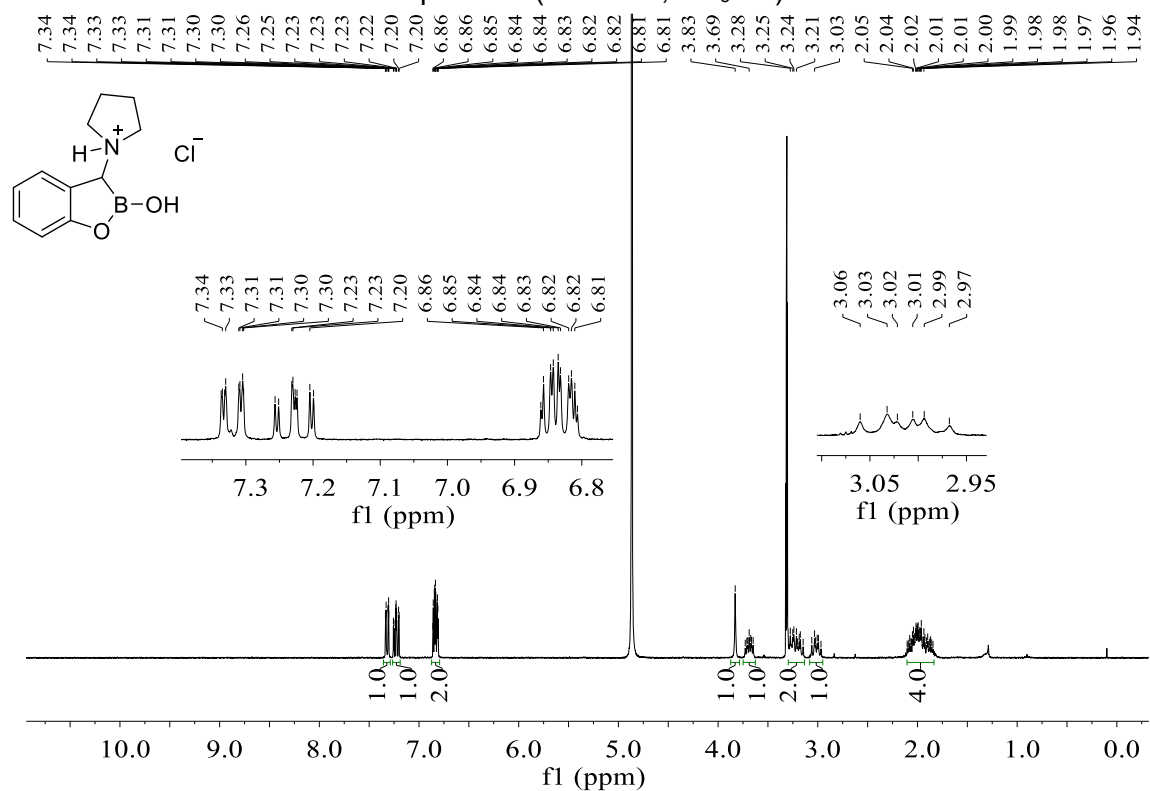


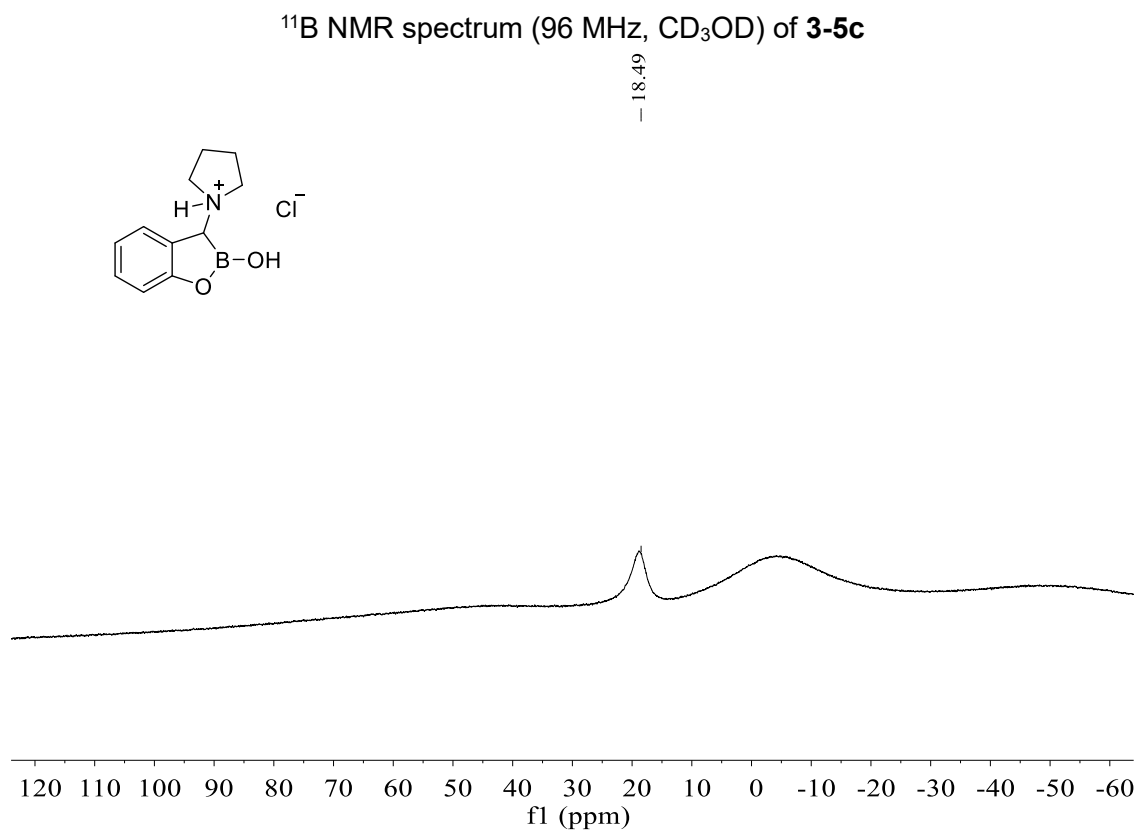
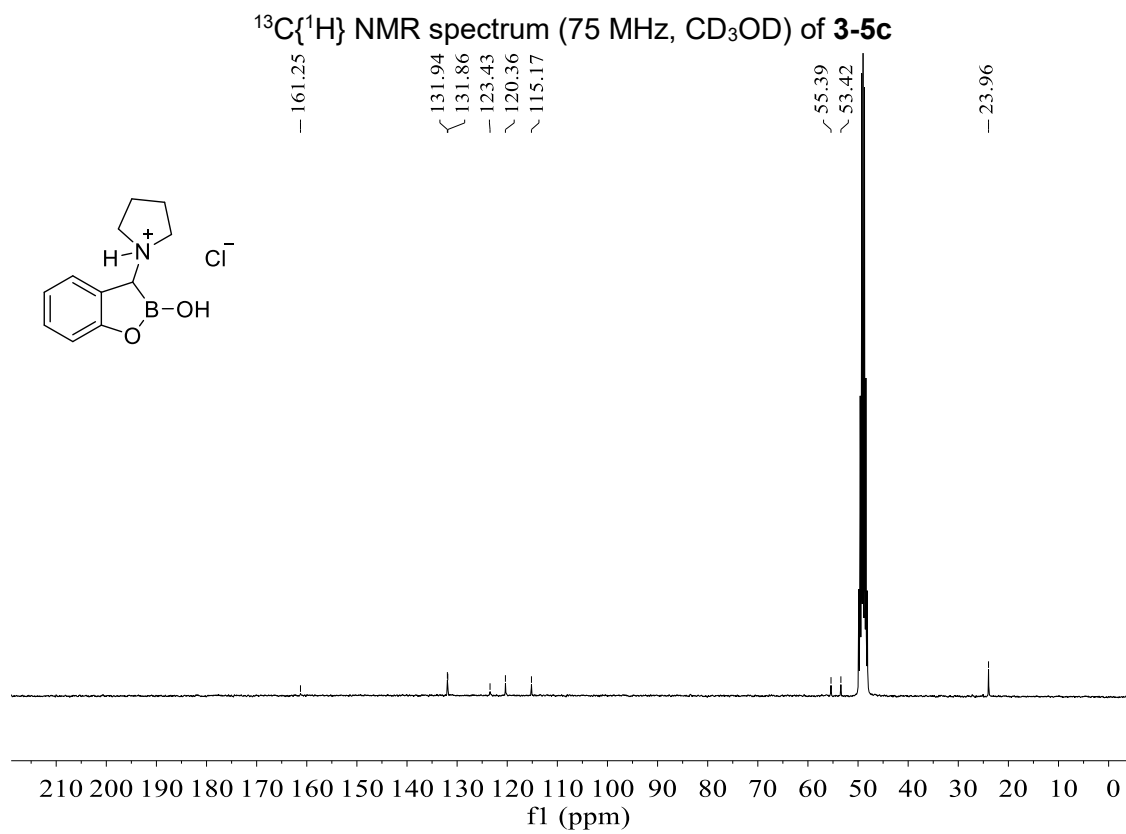


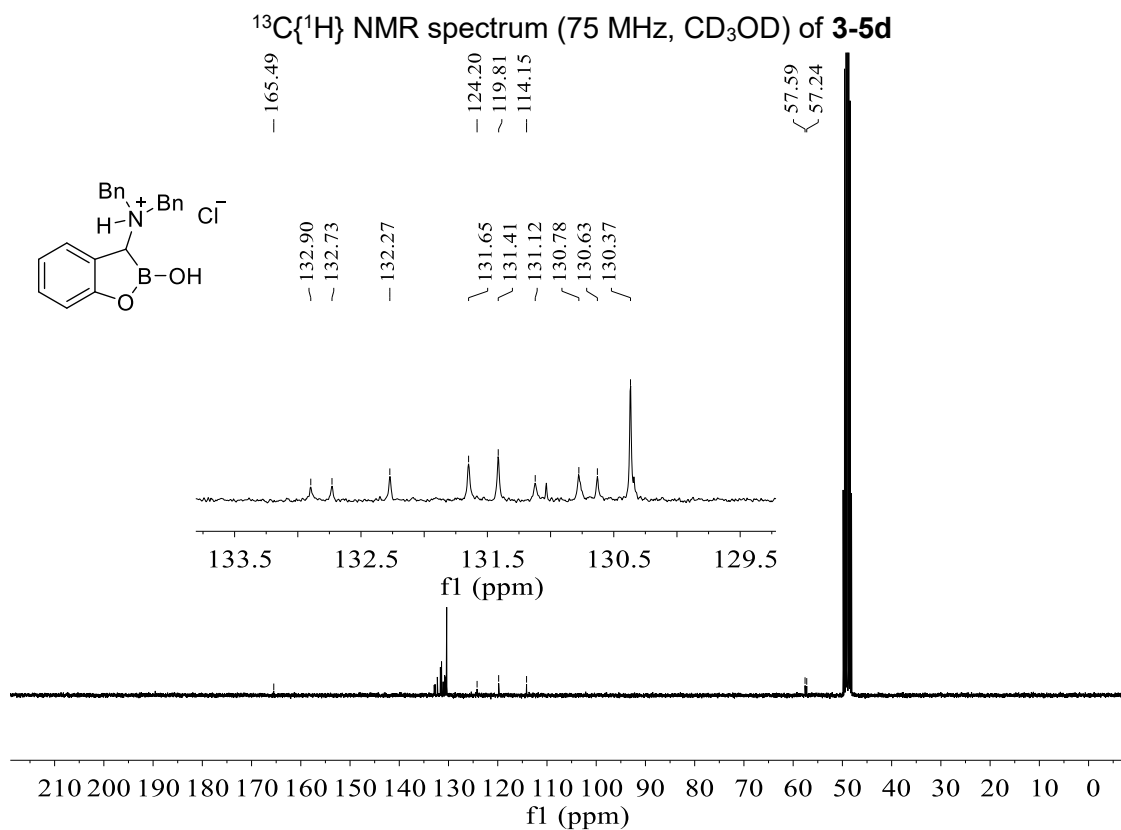
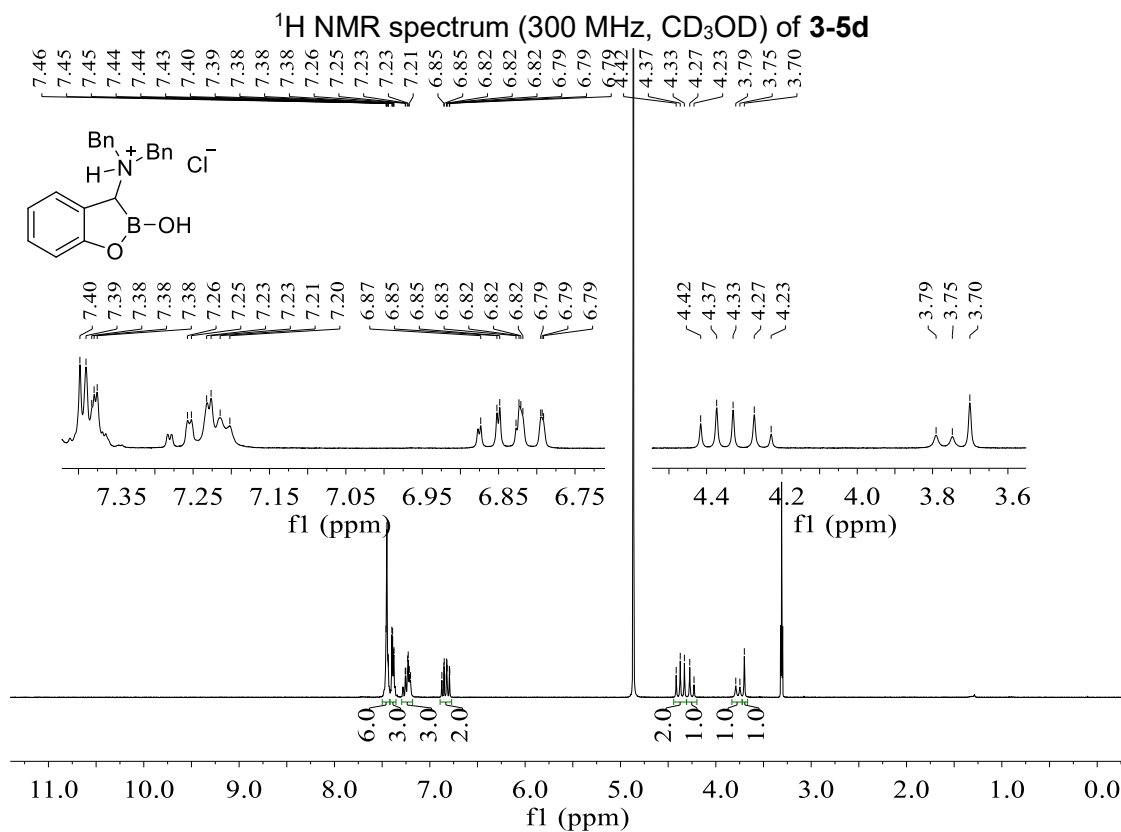
¹¹B NMR spectrum (96 MHz, CD₃OD) of **3-4p**¹H NMR spectrum (300 MHz, D₂O) of **3-5a**

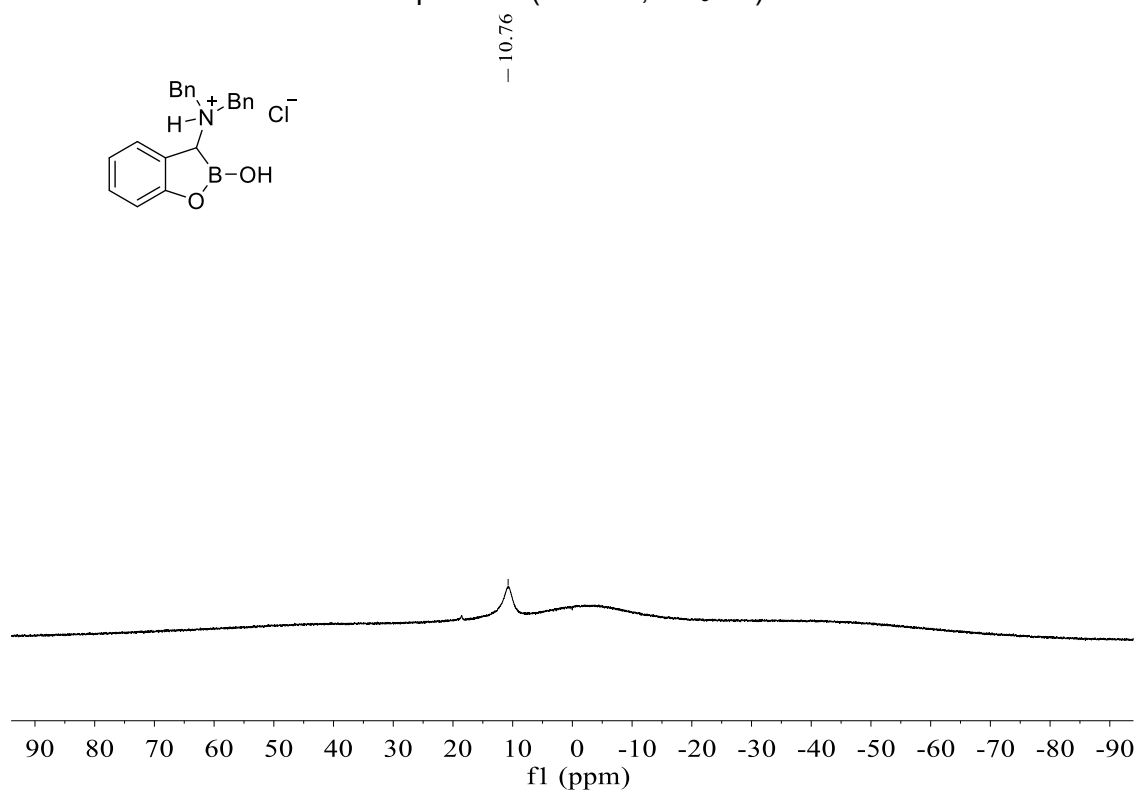
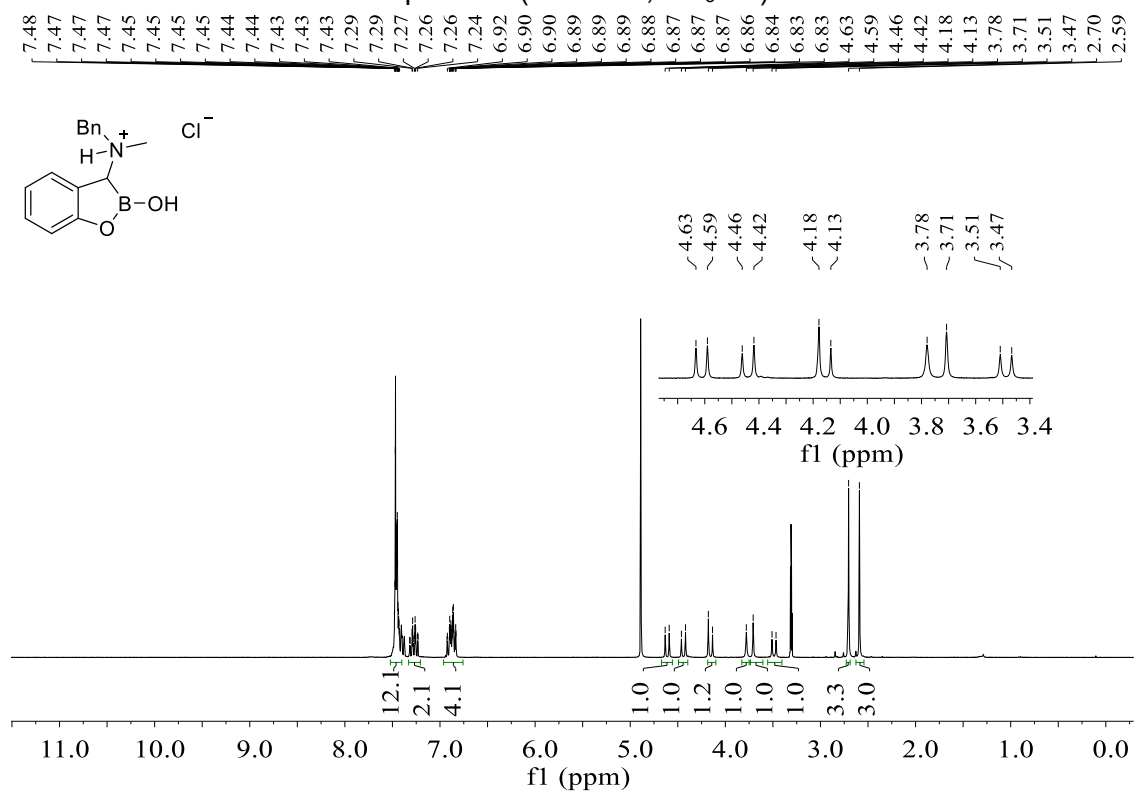
$^{13}\text{C}\{^1\text{H}\}$ NMR spectrum (75 MHz, D_2O) of **3-5a** ^{11}B NMR spectrum (96 MHz, D_2O) of **3-5a**

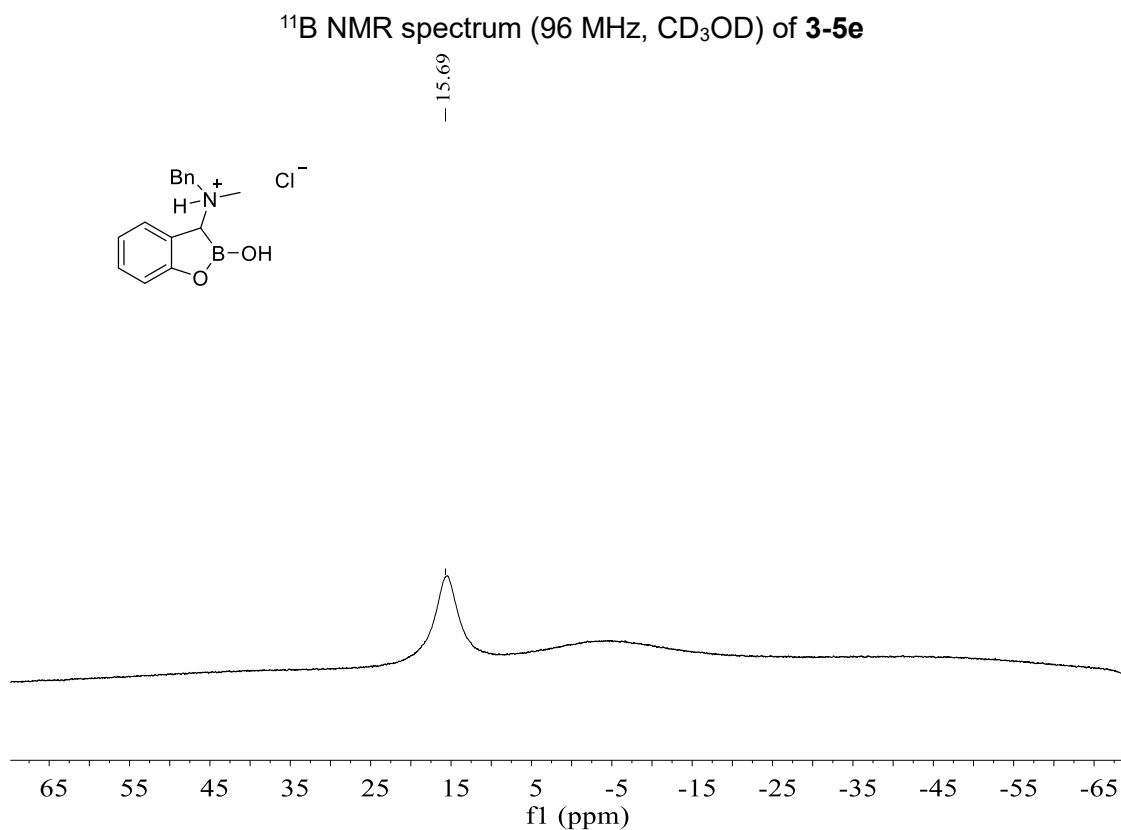
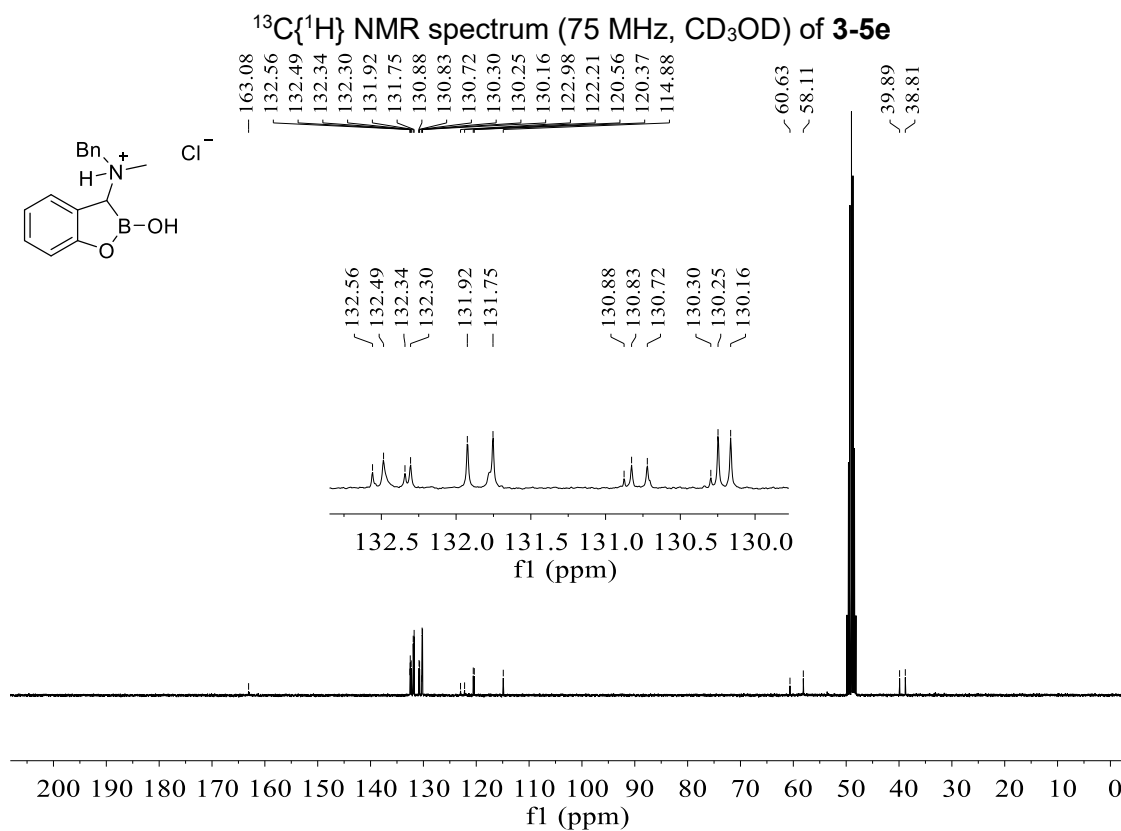


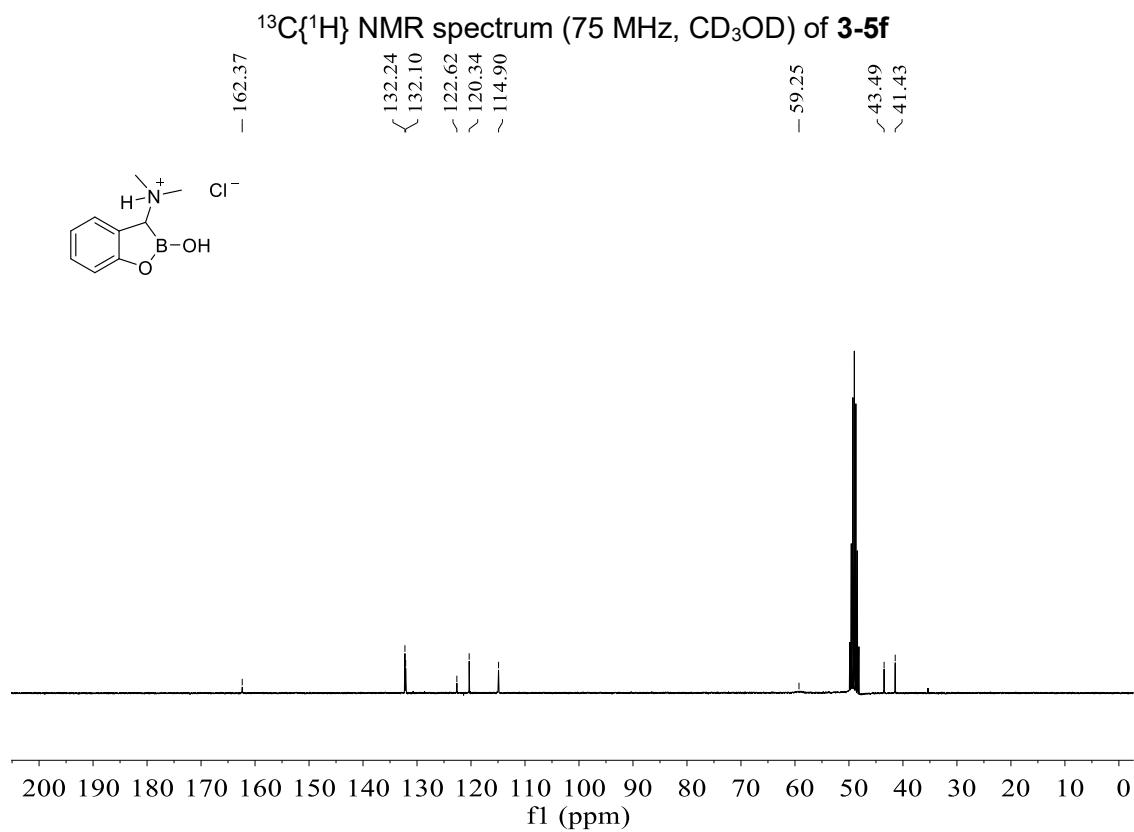
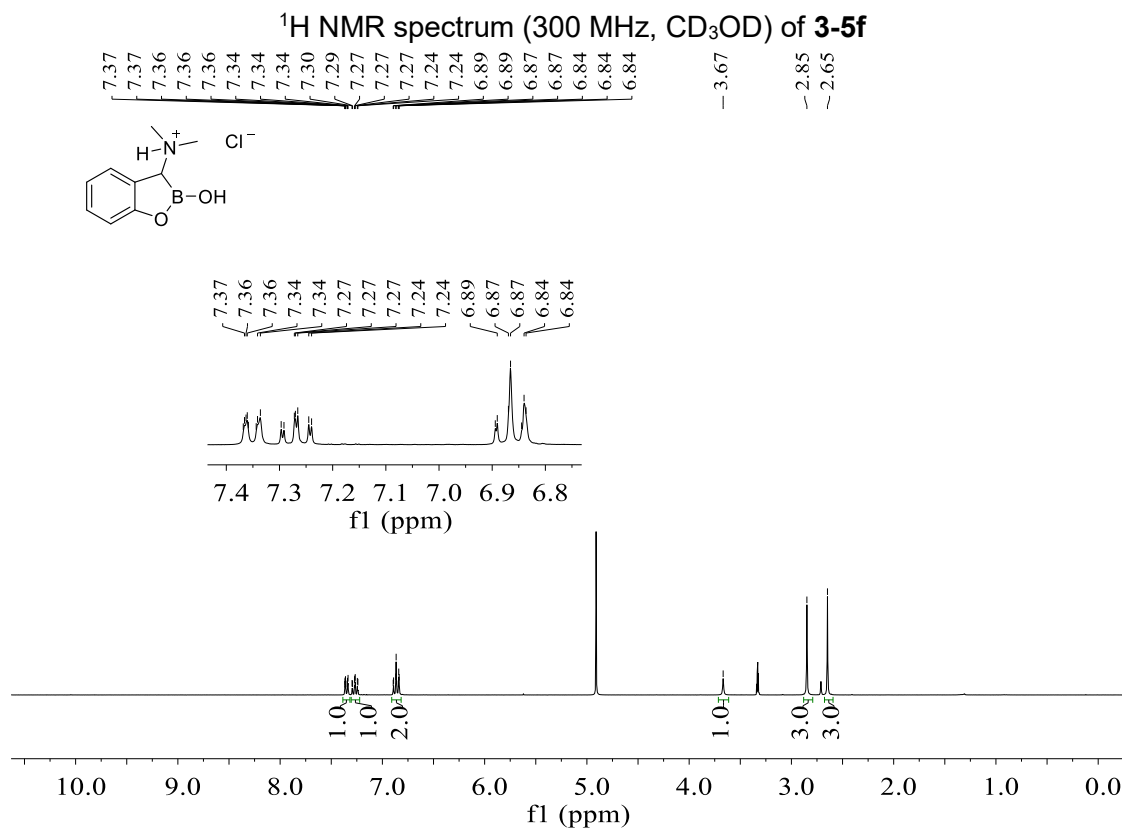
^{11}B NMR spectrum (96 MHz, CD_3OD) of **3-5b** ^1H NMR spectrum (300 MHz, CD_3OD) of **3-5c**

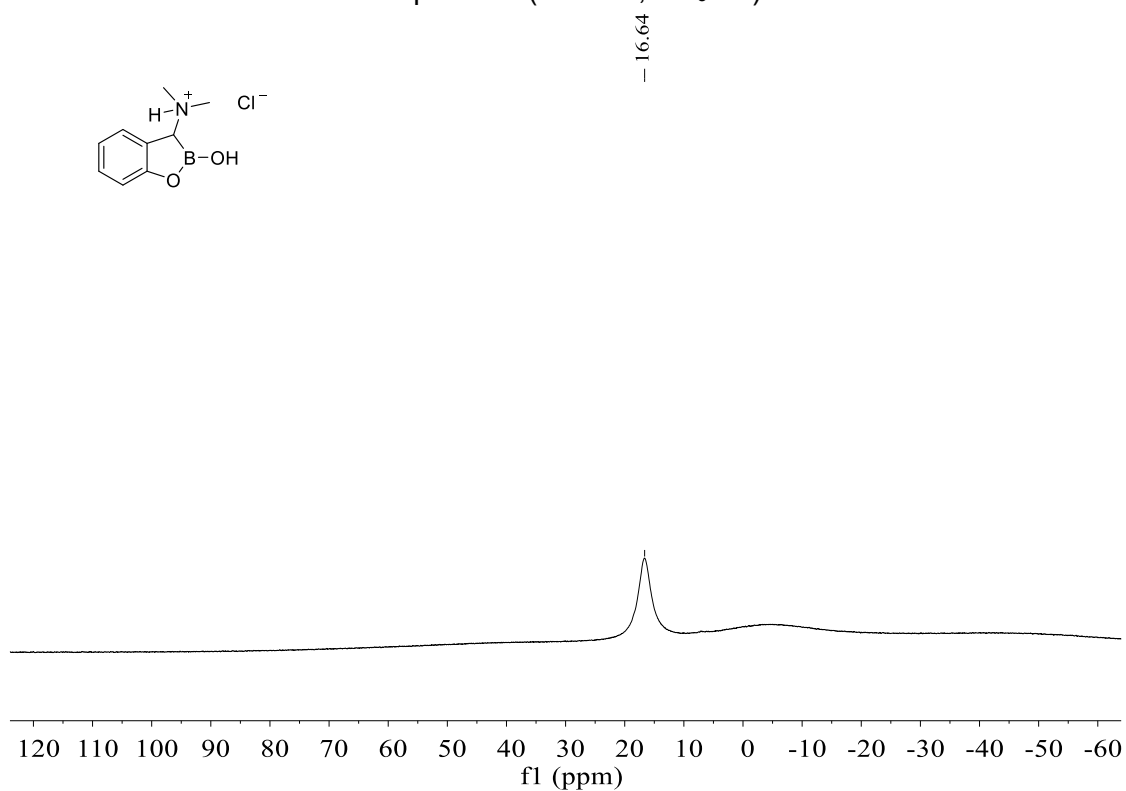
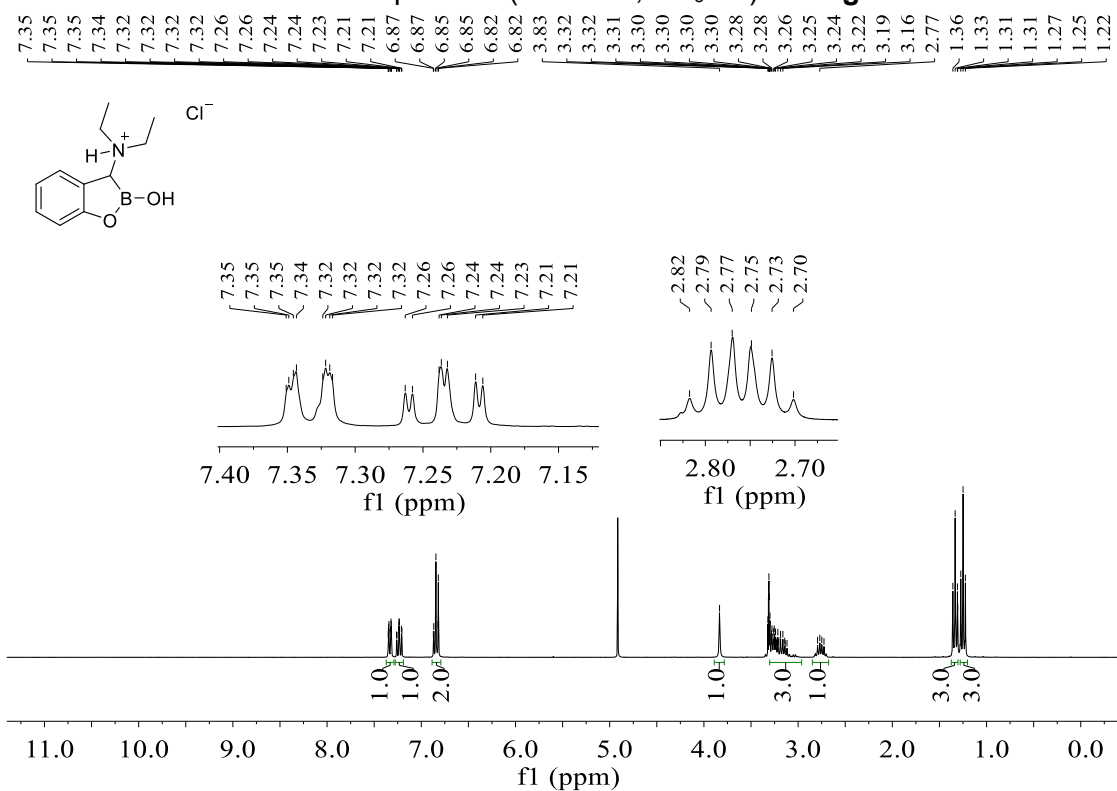




^{11}B NMR spectrum (96 MHz, CD_3OD) of **3-5d** ^1H NMR spectrum (300 MHz, CD_3OD) of **3-5e**

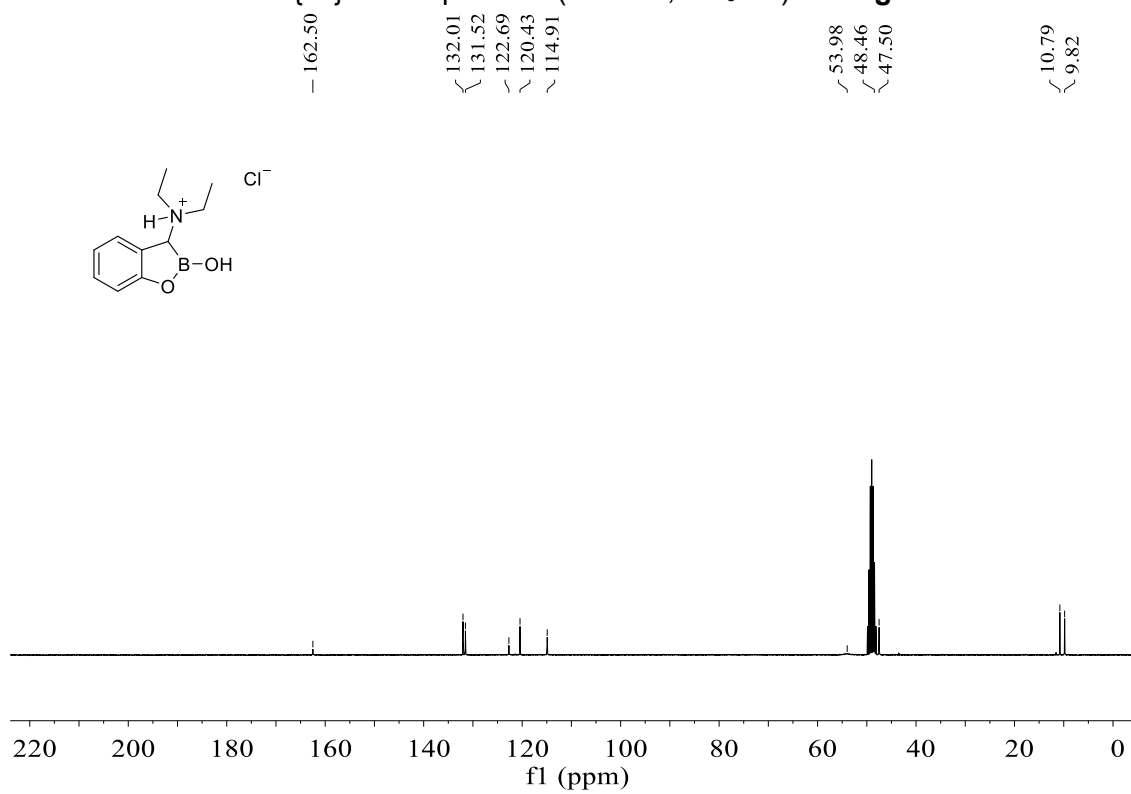




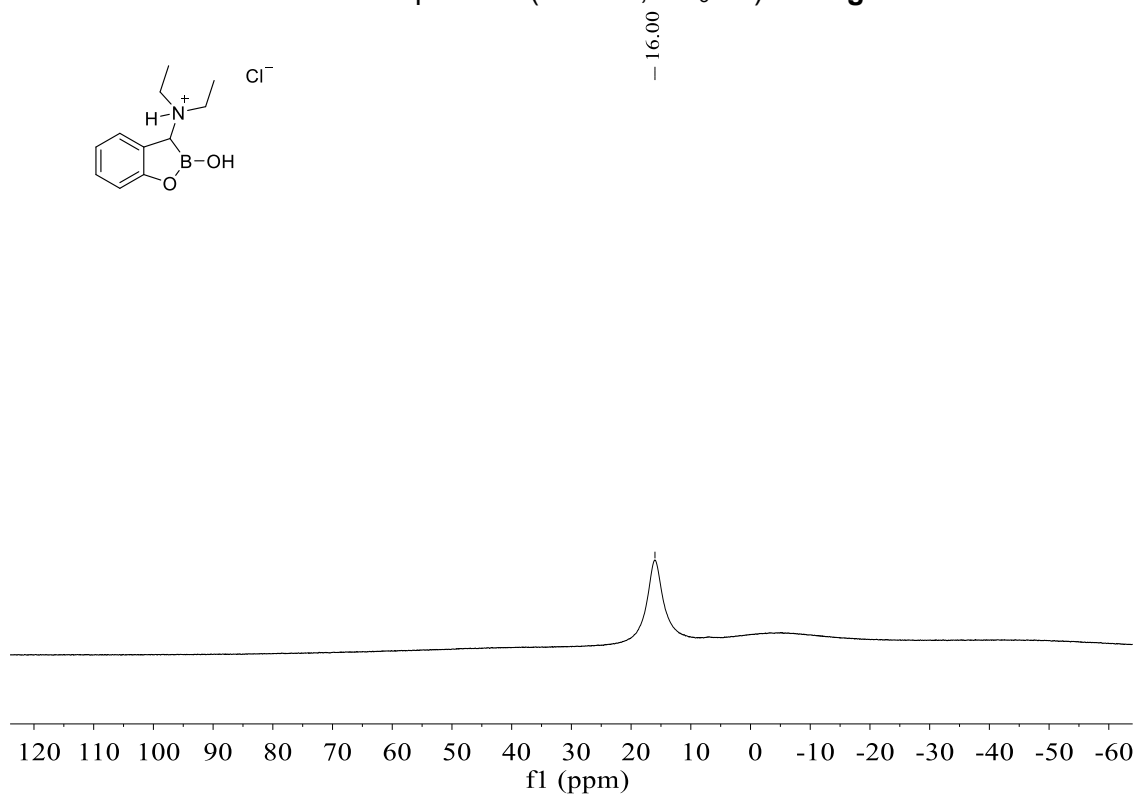
^{11}B NMR spectrum (96 MHz, CD_3OD) of **3-5f** ^1H NMR spectrum (300 MHz, CD_3OD) of **3-5g**

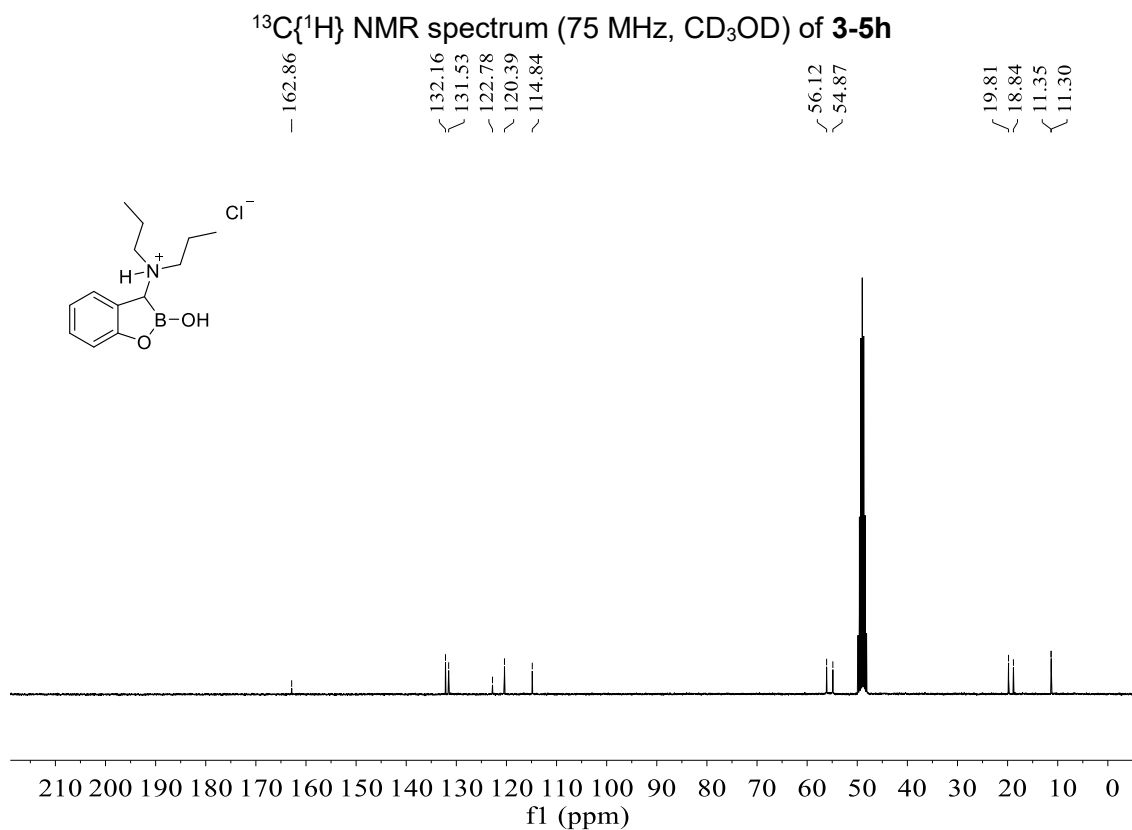
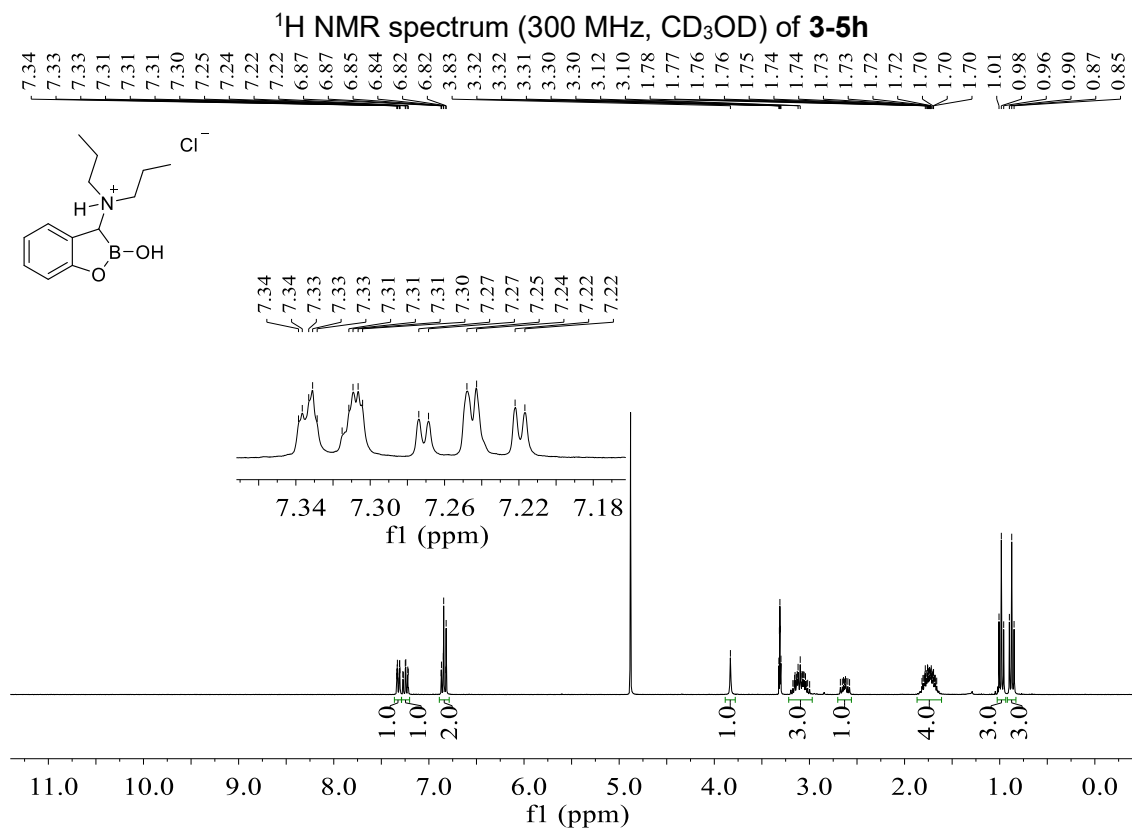
Appendix

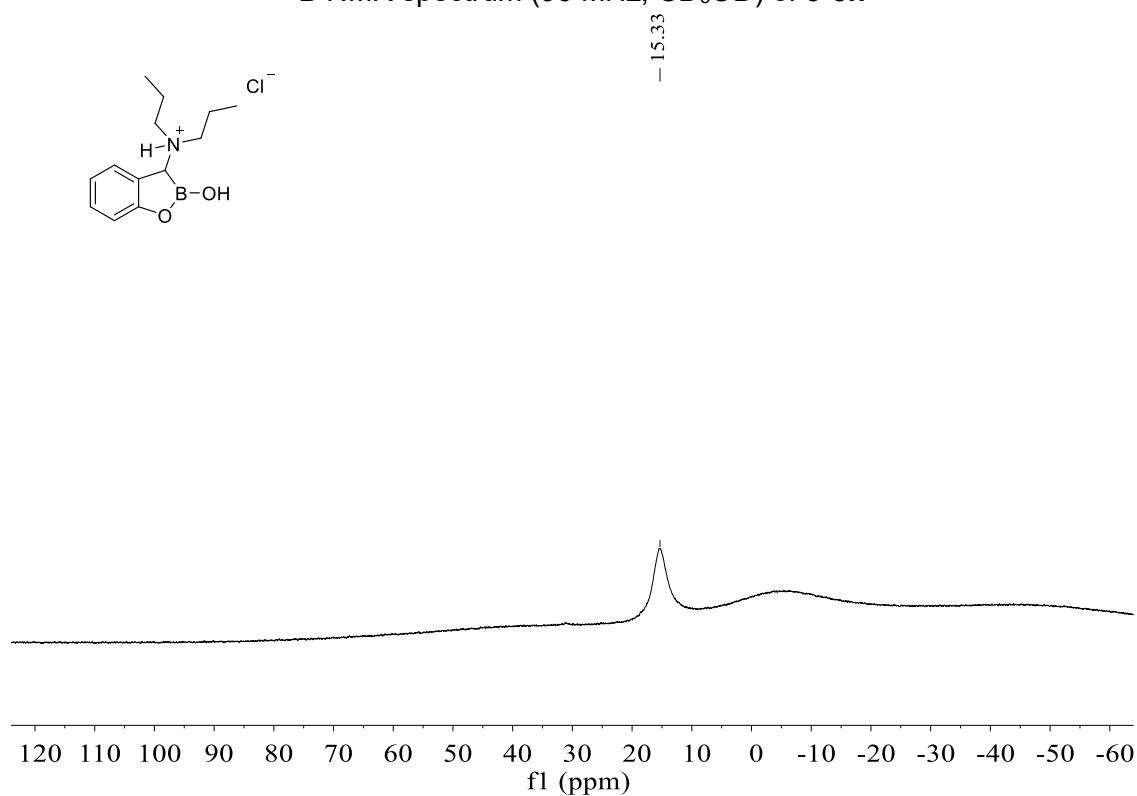
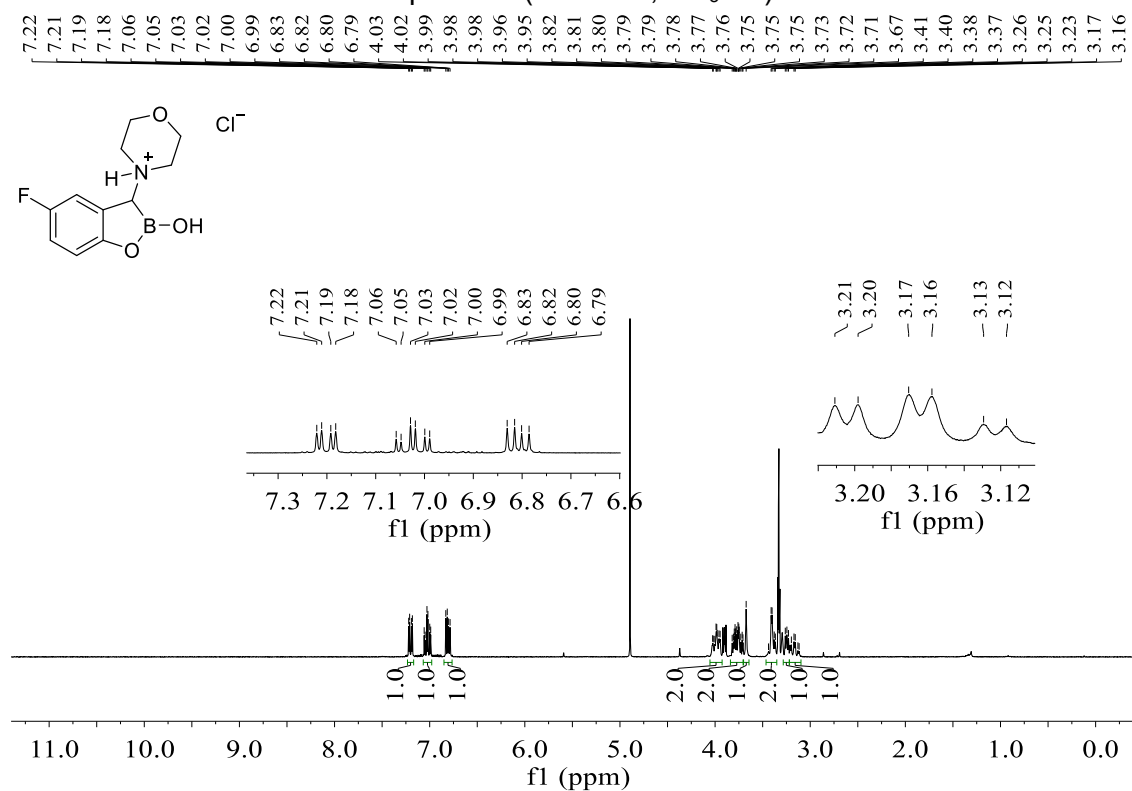
$^{13}\text{C}\{^1\text{H}\}$ NMR spectrum (75 MHz, CD_3OD) of **3-5g**

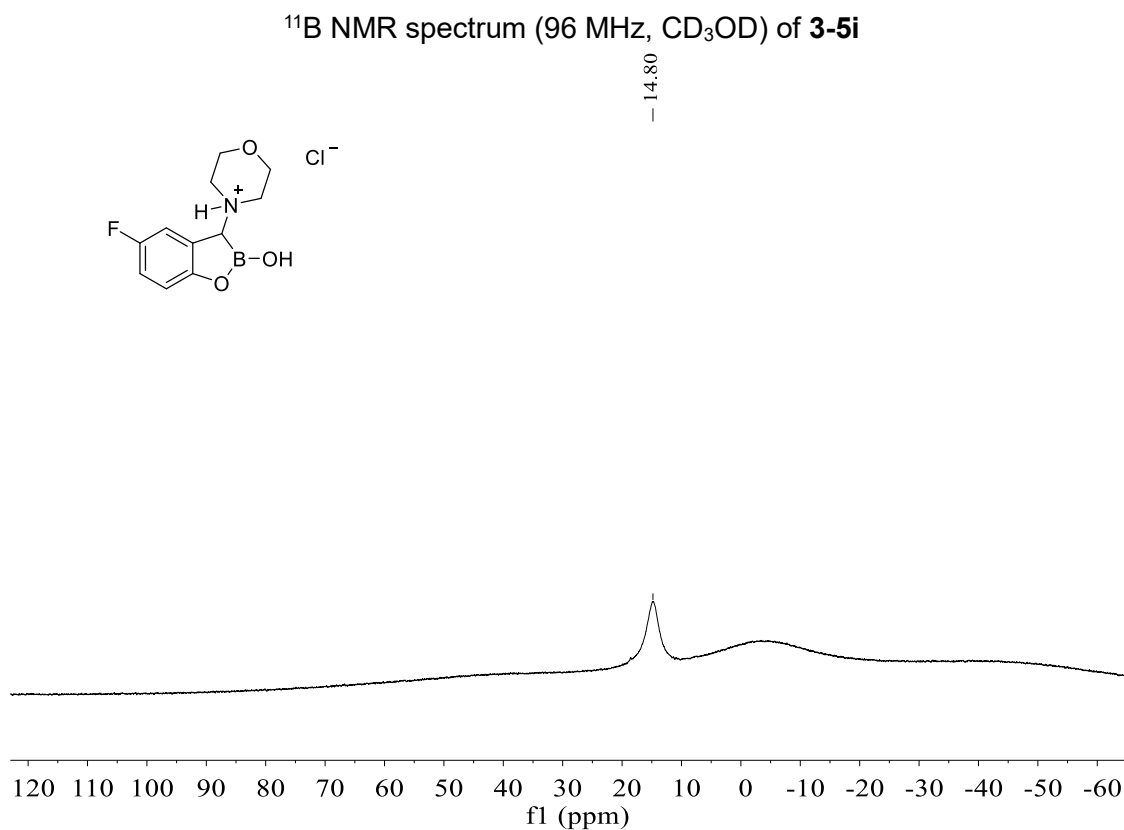
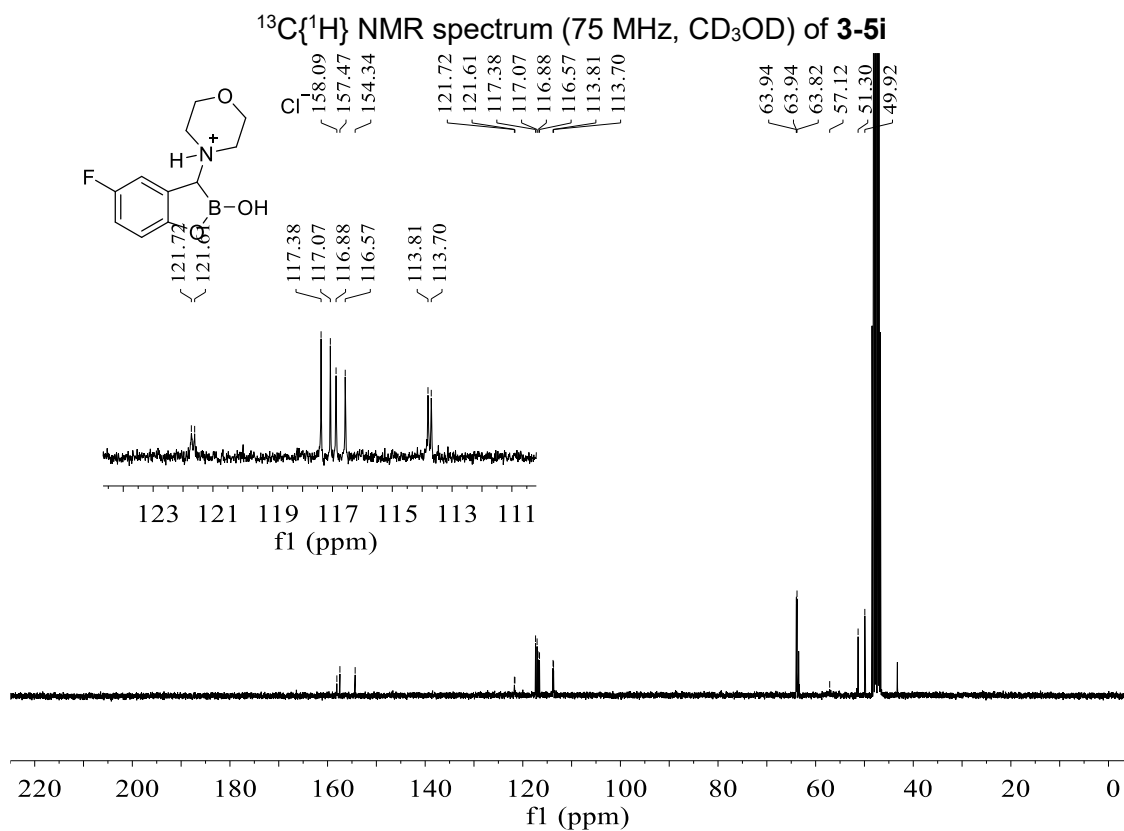


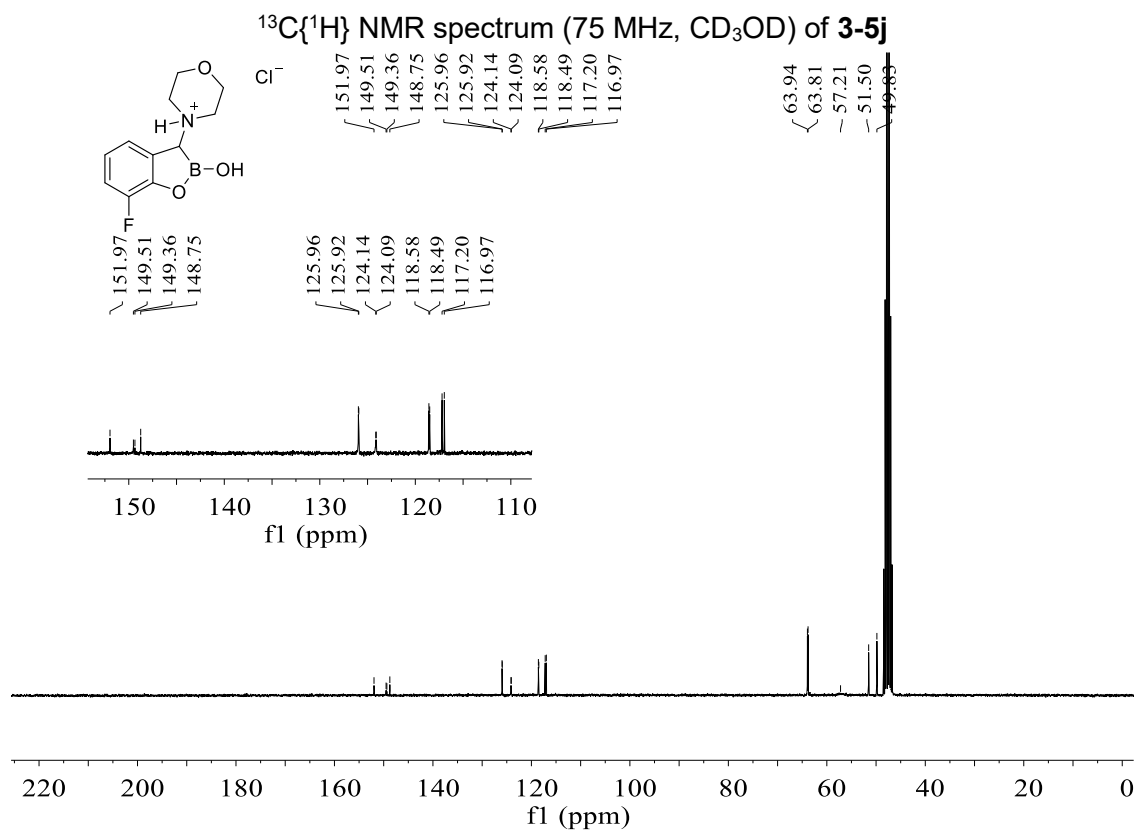
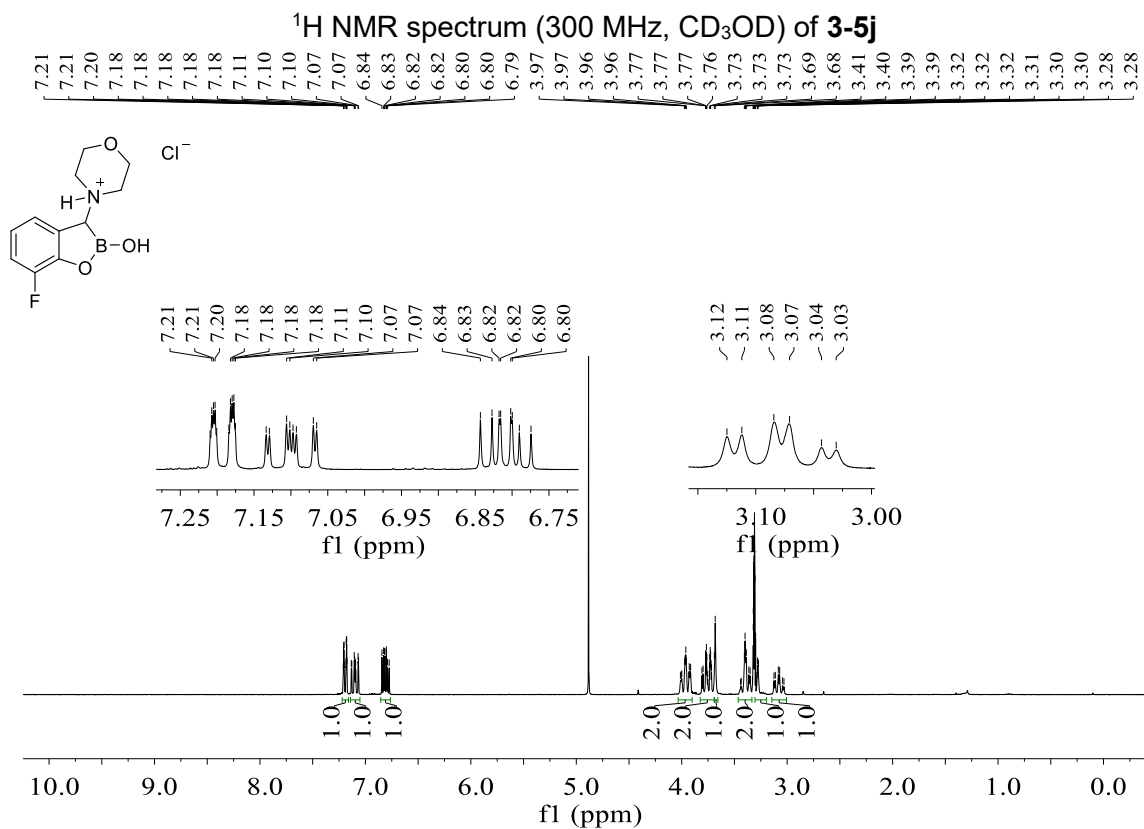
^{11}B NMR spectrum (96 MHz, CD_3OD) of **3-5g**

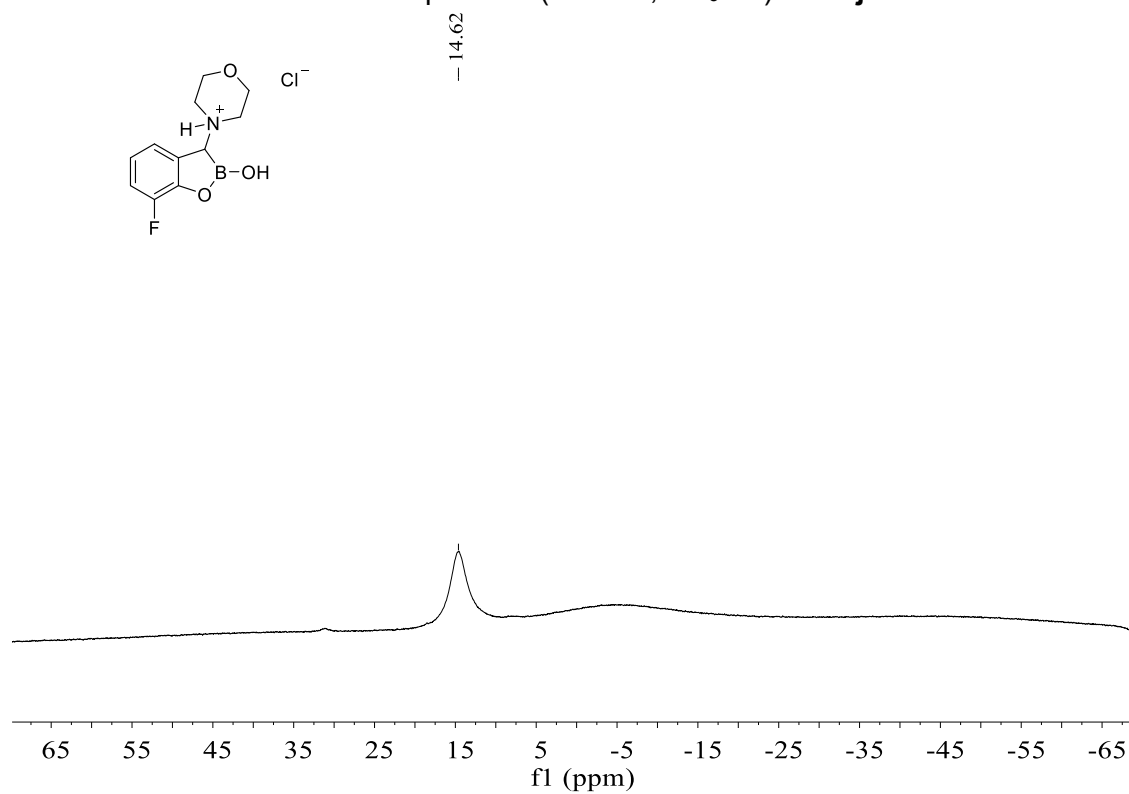
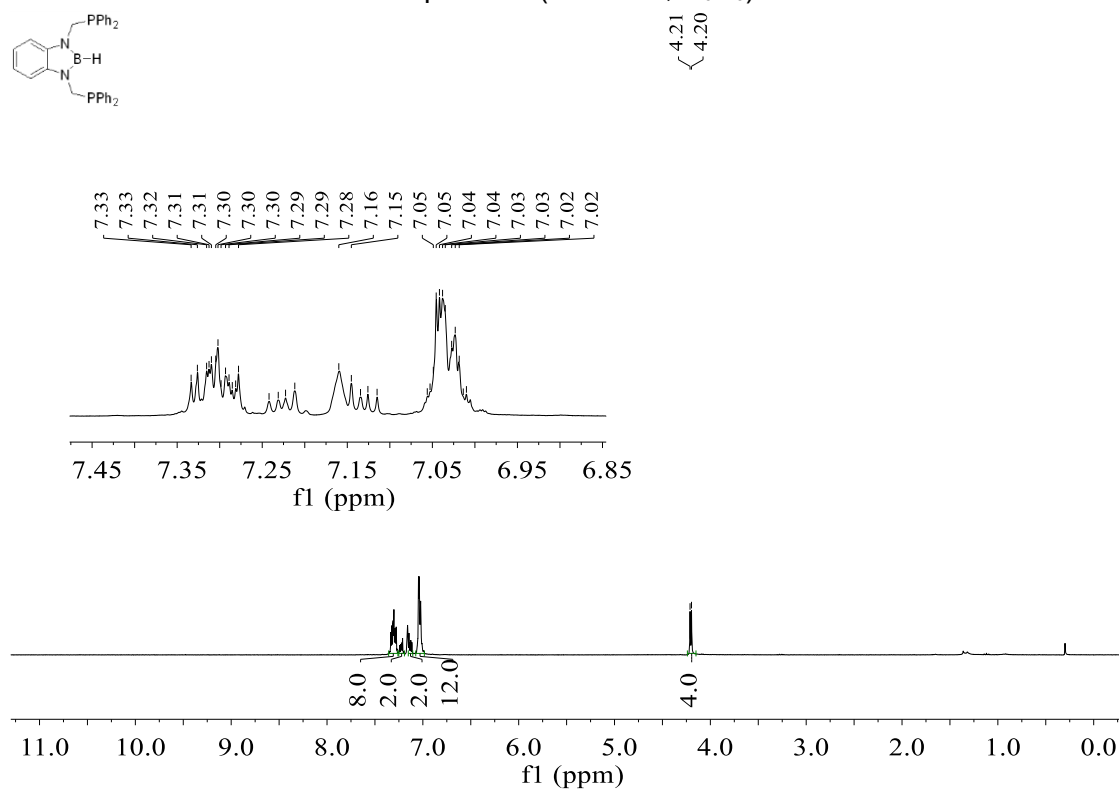


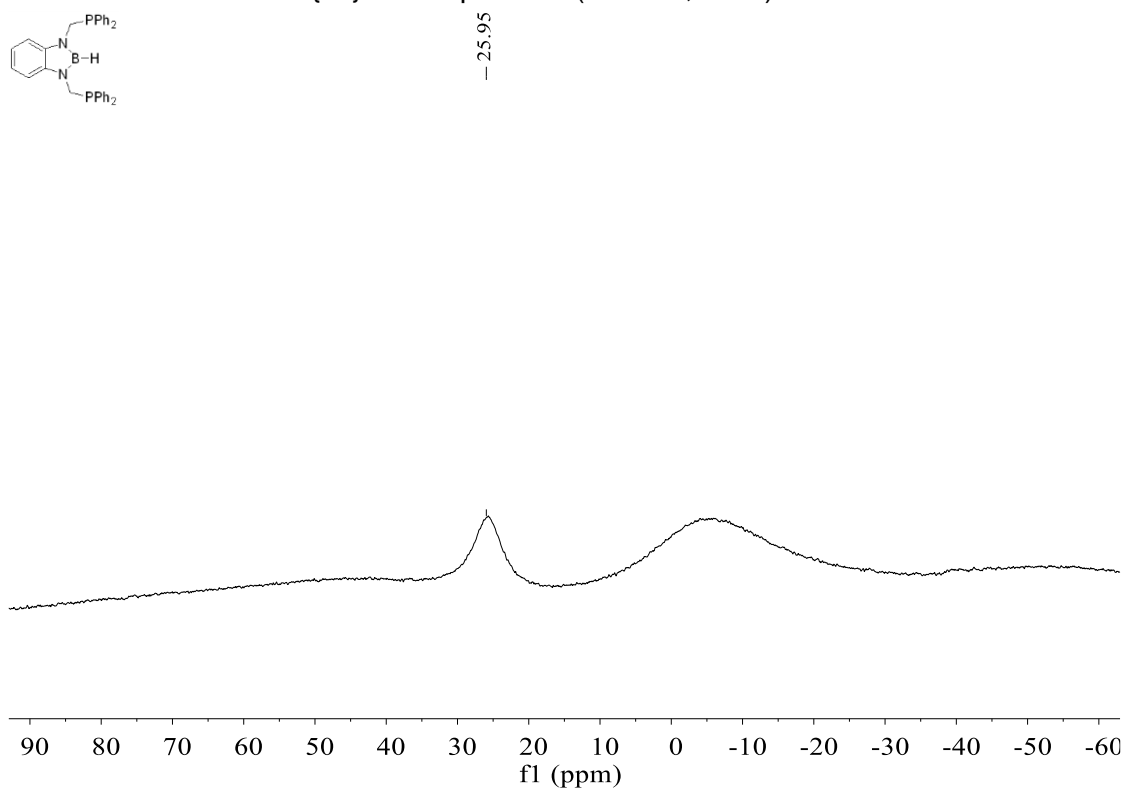
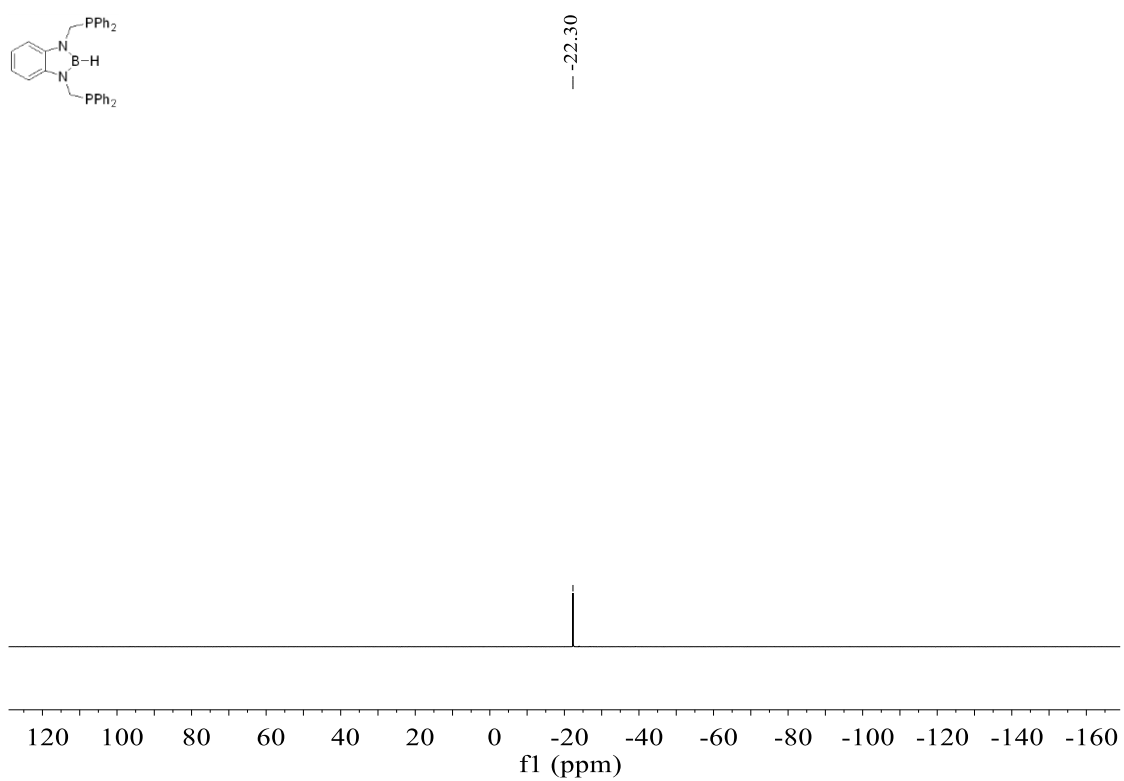


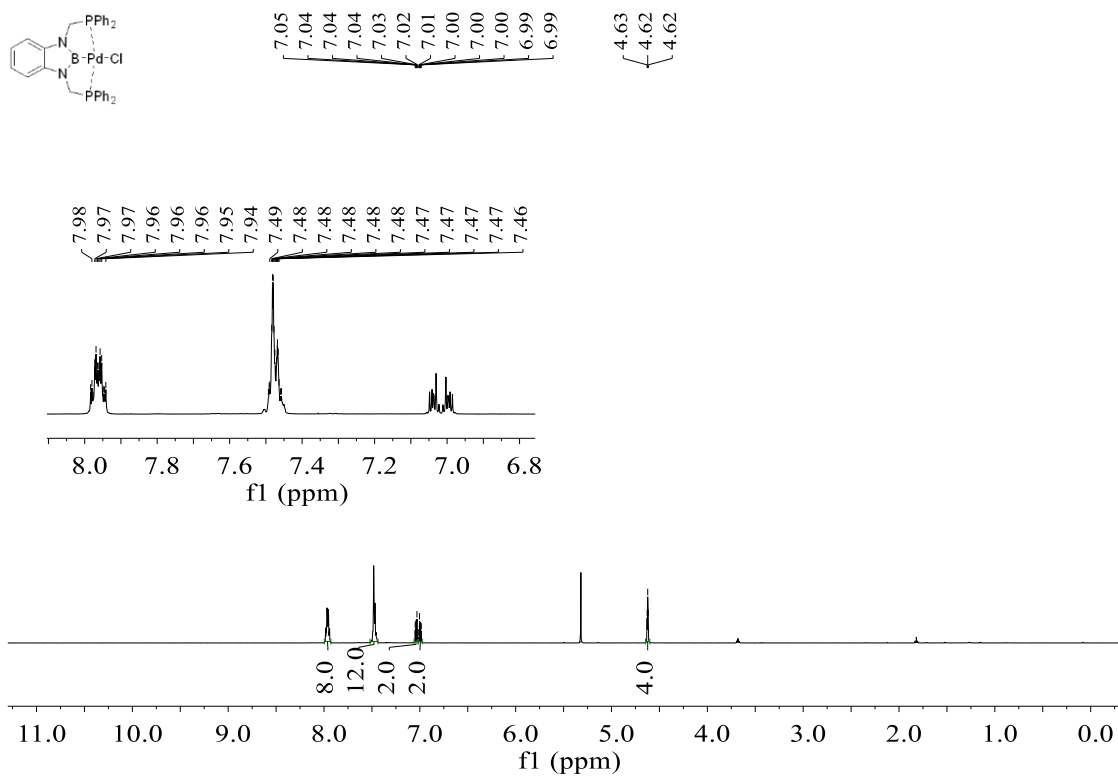
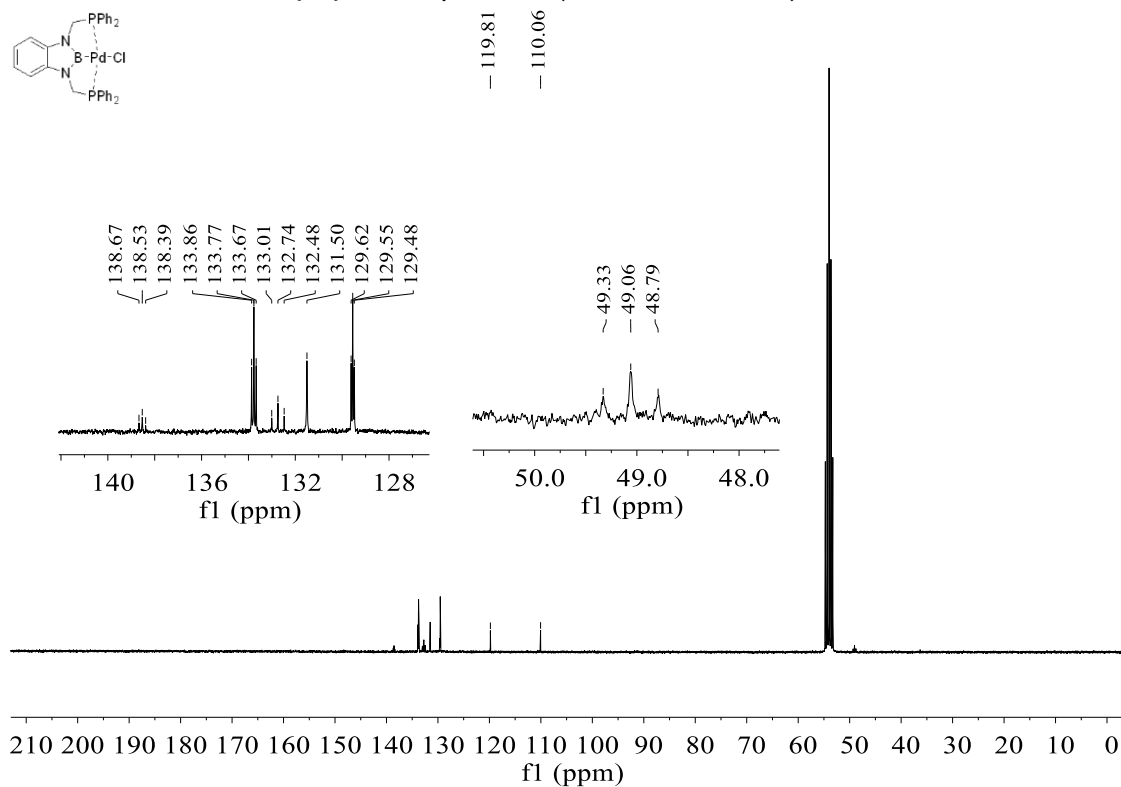
^{11}B NMR spectrum (96 MHz, CD_3OD) of **3-5h** ^1H NMR spectrum (300 MHz, CD_3OD) of **3-5i**

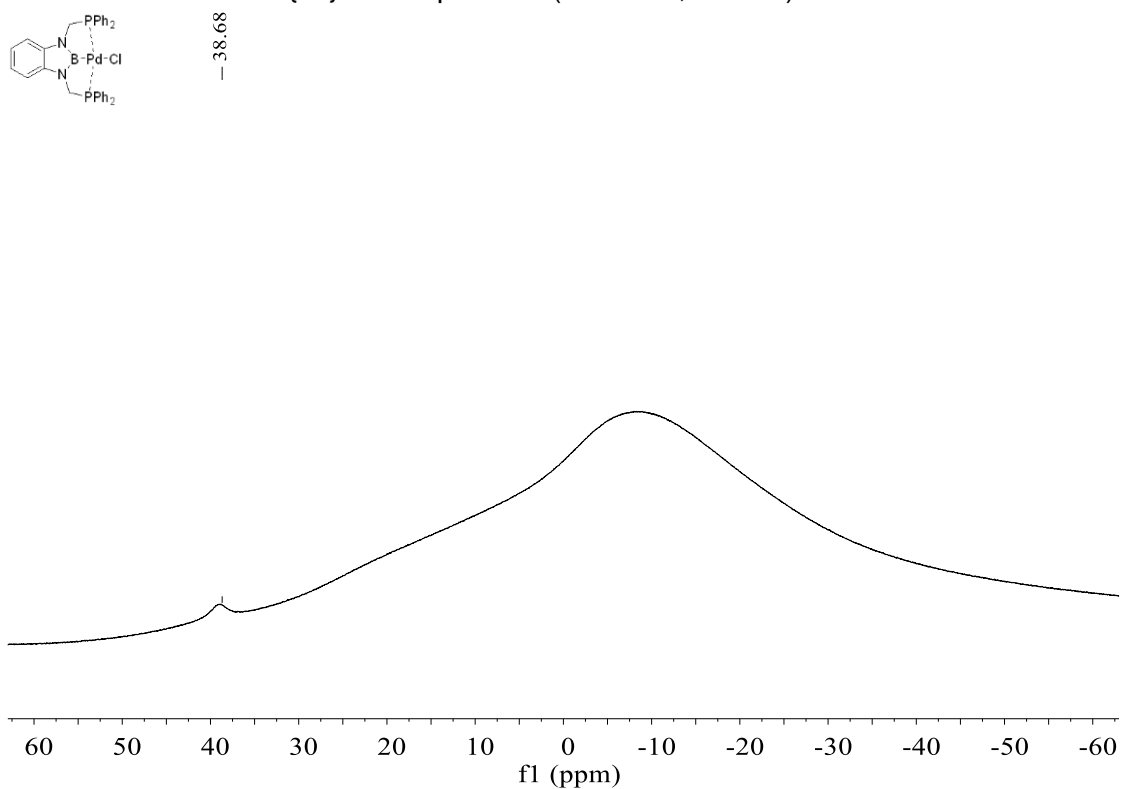
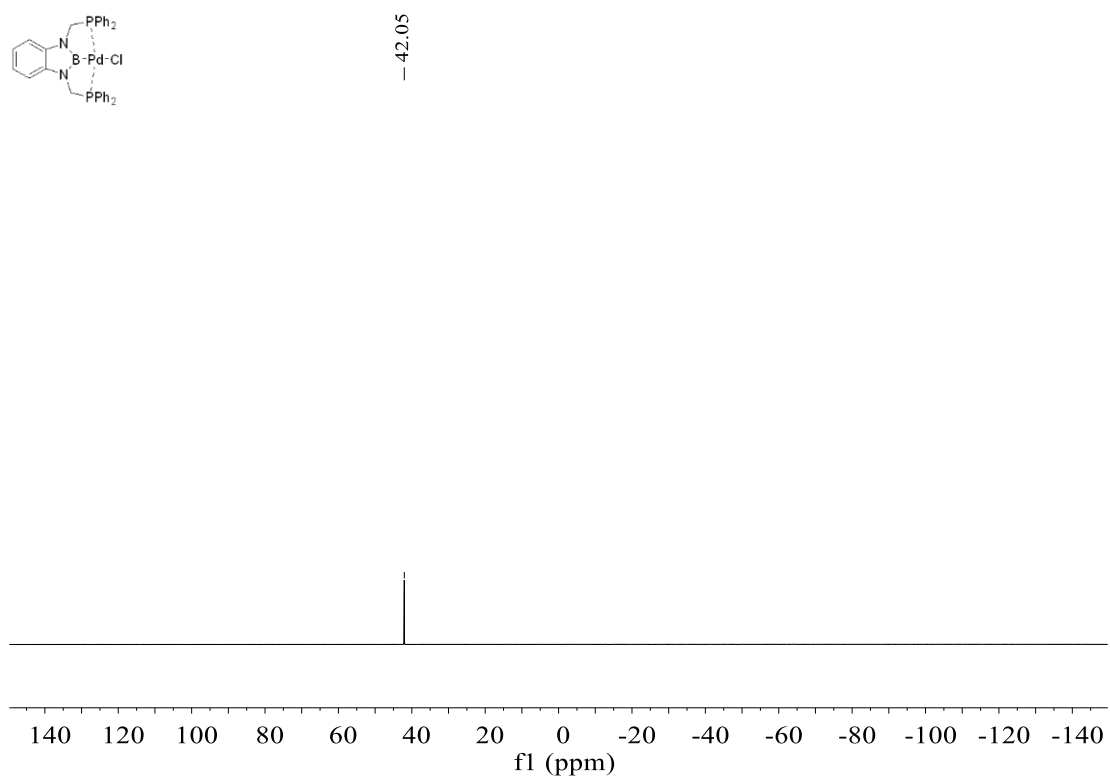


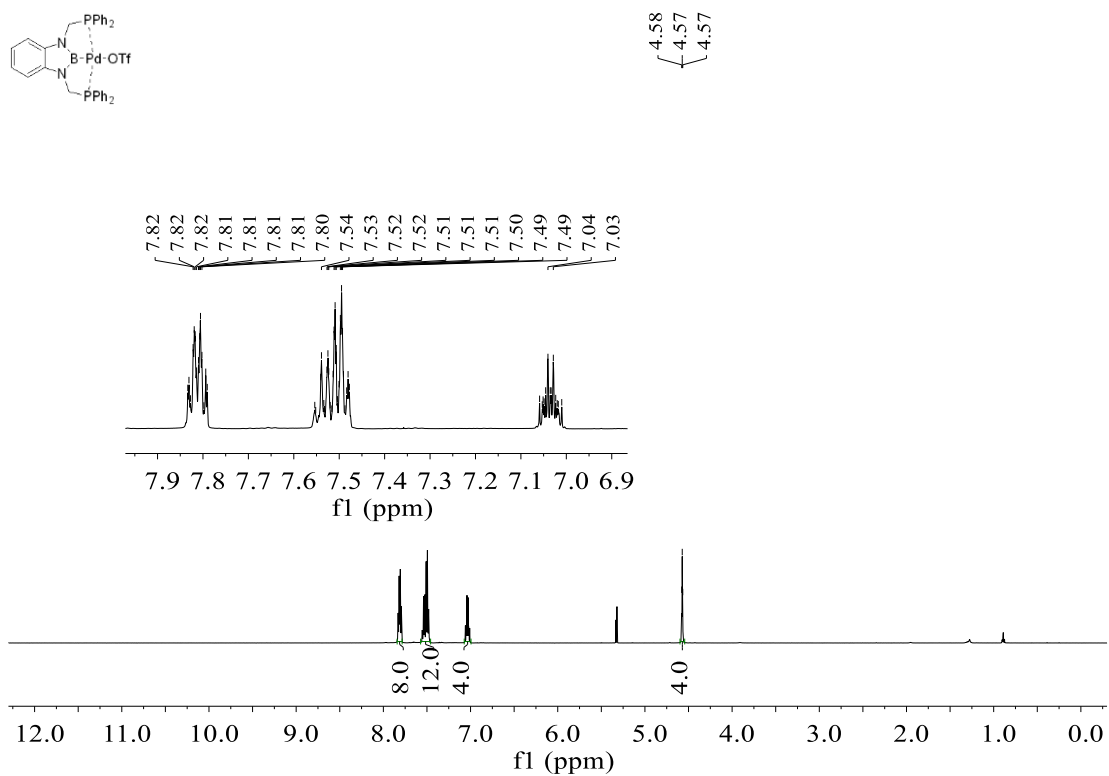
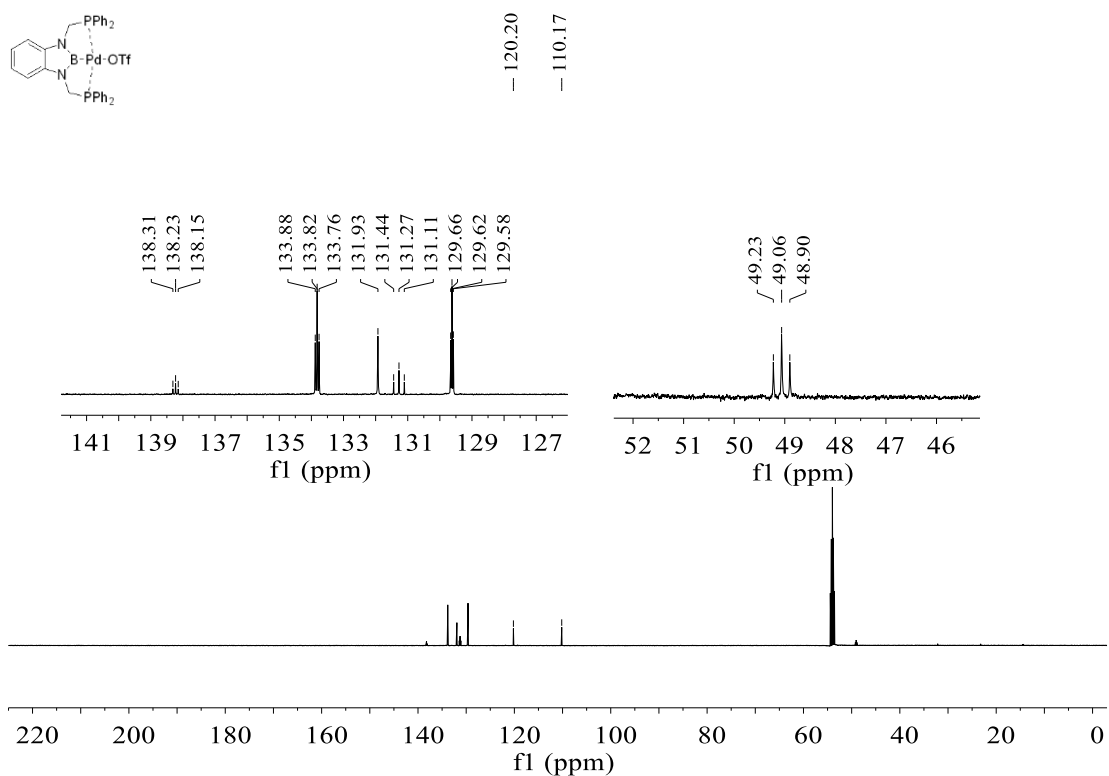


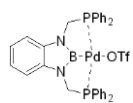
^{11}B NMR spectrum (96 MHz, CD_3OD) of **3-5j** ^1H NMR spectrum (300 MHz, C_6D_6) of **4-2**

$^{11}\text{B}\{^1\text{H}\}$ NMR spectrum (96 MHz, C_6D_6) of **4-2** $^{31}\text{P}\{^1\text{H}\}$ NMR spectrum (122 MHz, C_6D_6) of **4-2**

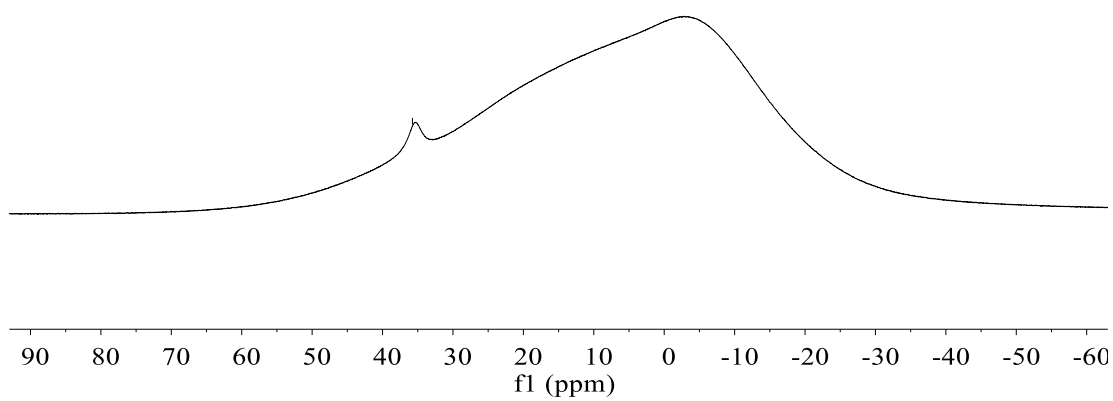
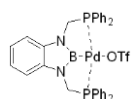
^1H NMR spectrum (500 MHz, CD_2Cl_2) of **4-3** $^{13}\text{C}\{^1\text{H}\}$ NMR spectrum (126 MHz, CD_2Cl_2) of **4-3**

$^{11}\text{B}\{^1\text{H}\}$ NMR spectrum (160 MHz, CD_2Cl_2) of **4-3** $^{31}\text{P}\{^1\text{H}\}$ NMR spectrum (202 MHz, CD_2Cl_2) of **4-3**

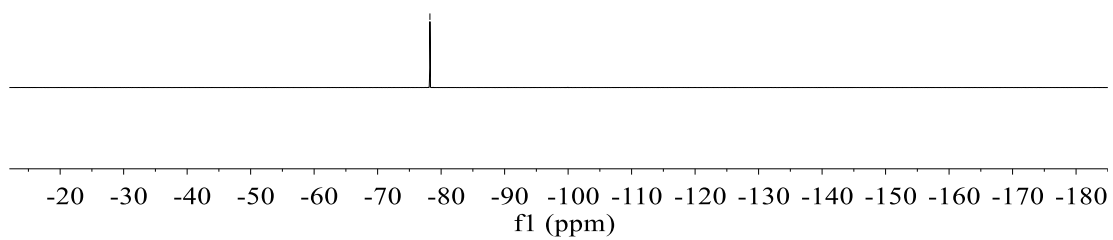
^1H NMR spectrum (500 MHz, CD_2Cl_2) of **4-4** $^{13}\text{C}\{^1\text{H}\}$ NMR spectrum (126 MHz, CD_2Cl_2) of **4-4**

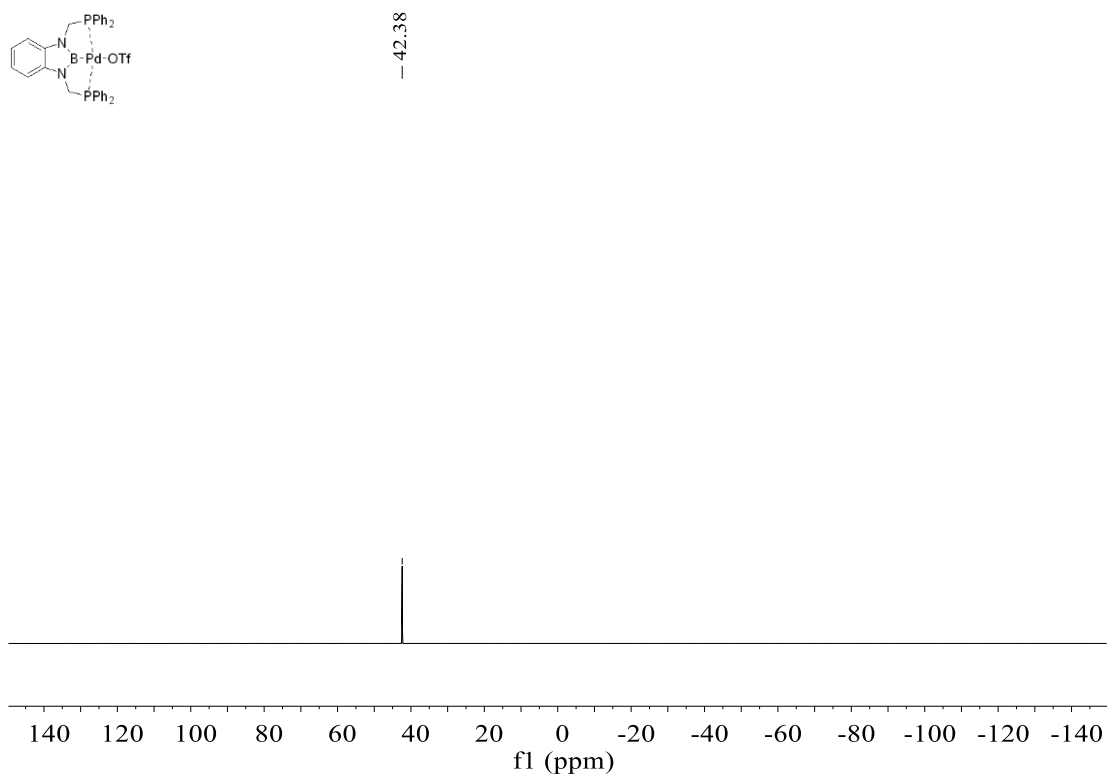
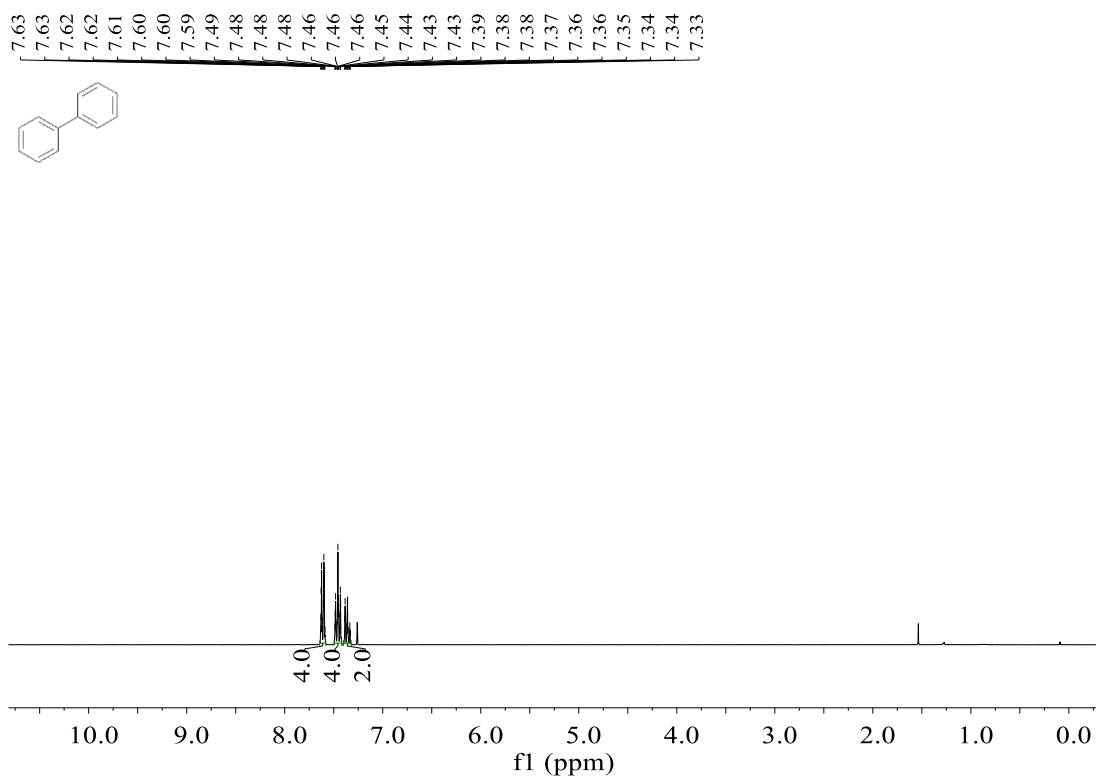
$^{11}\text{B}\{^1\text{H}\}$ NMR spectrum (160 MHz, CD_2Cl_2) of **4-4**

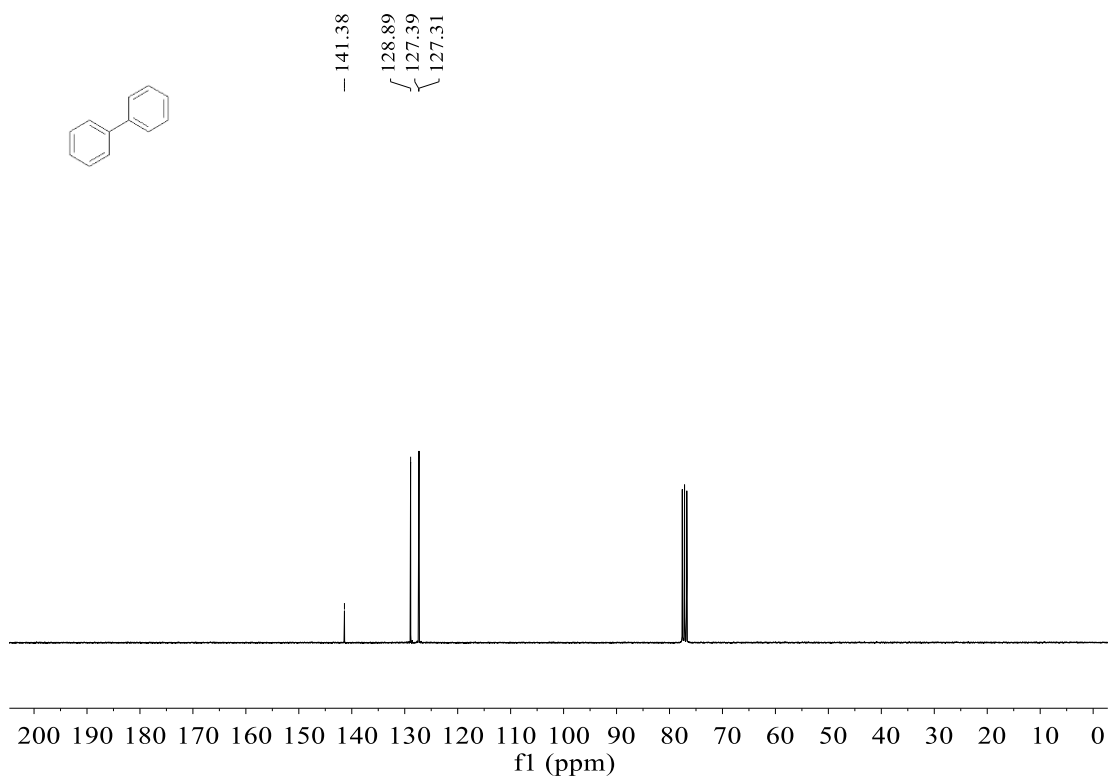
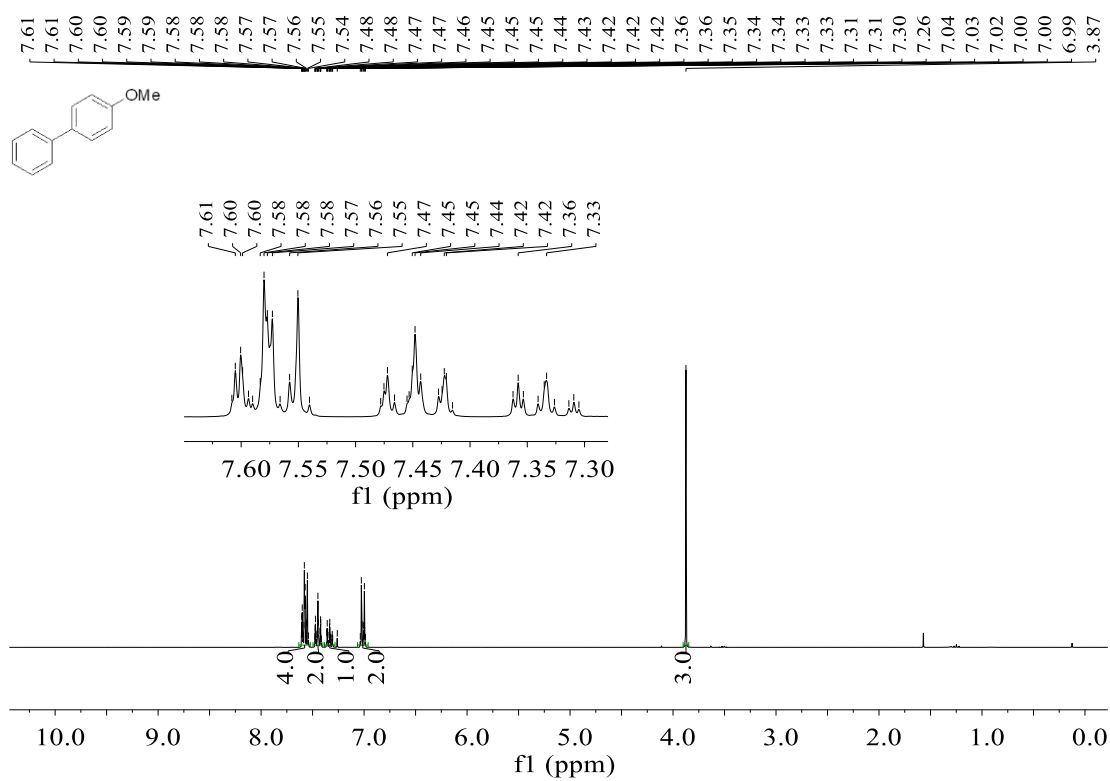
-35.75

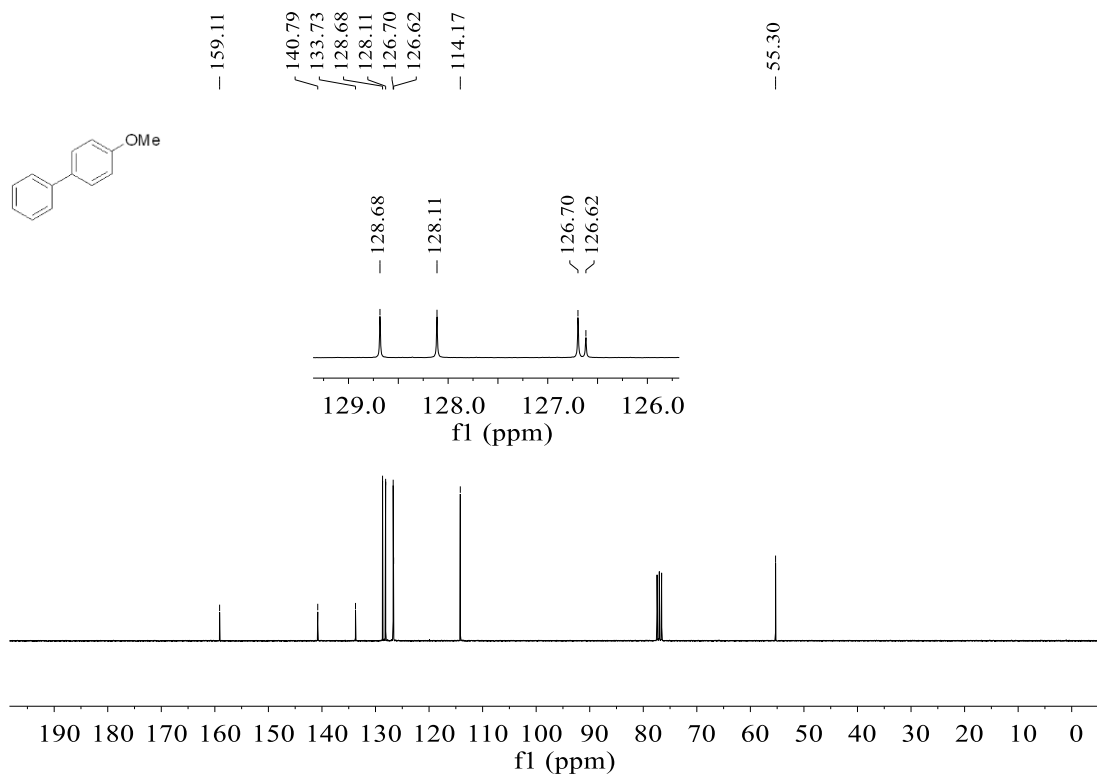
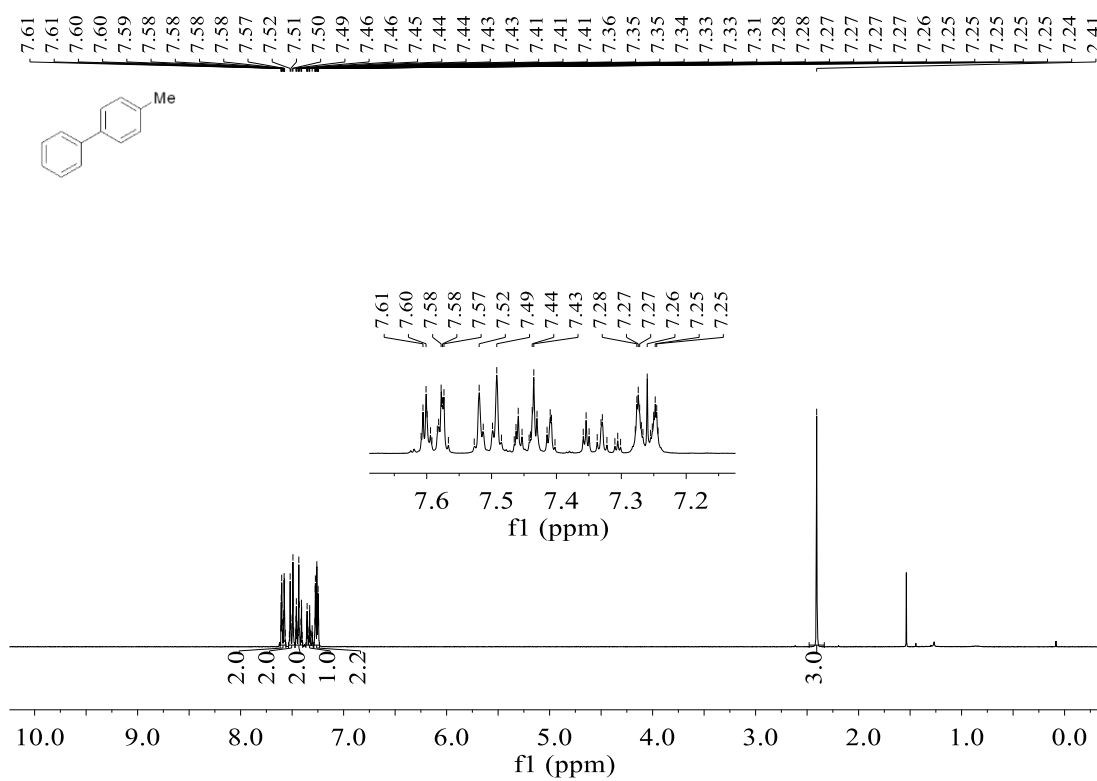
 ^{19}F NMR spectrum (471 MHz, CD_2Cl_2) of **4-4**

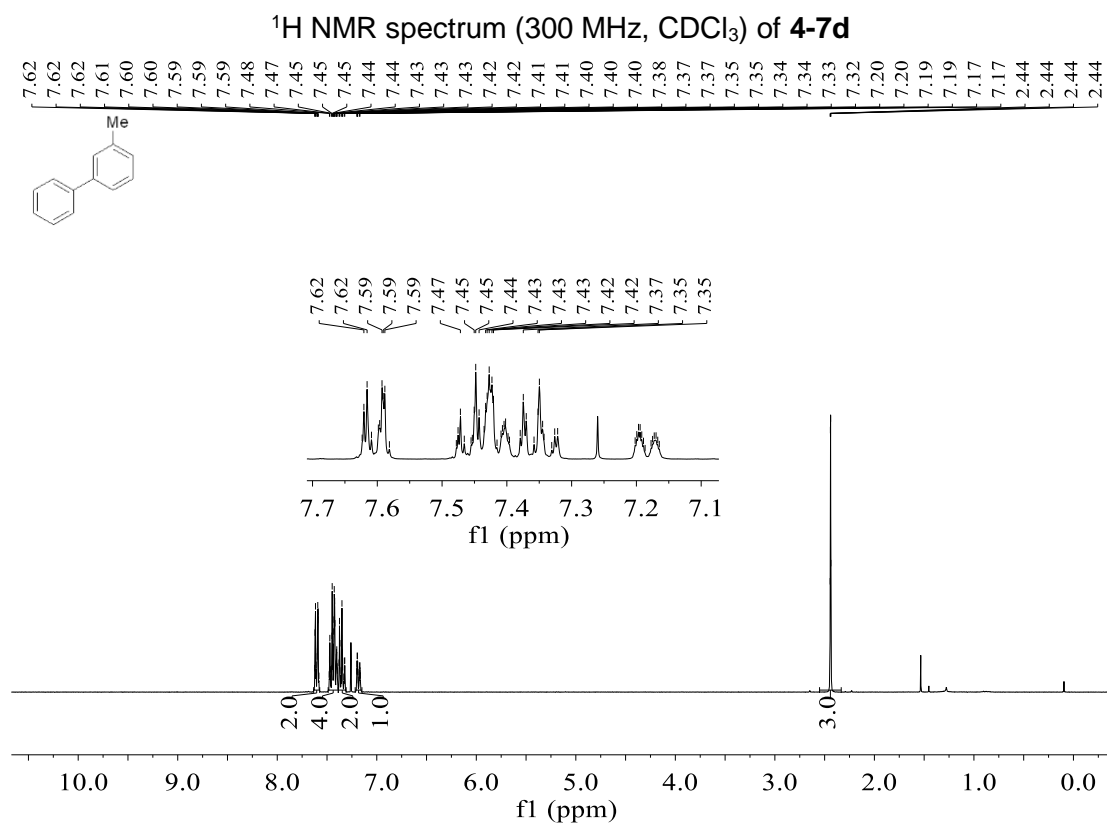
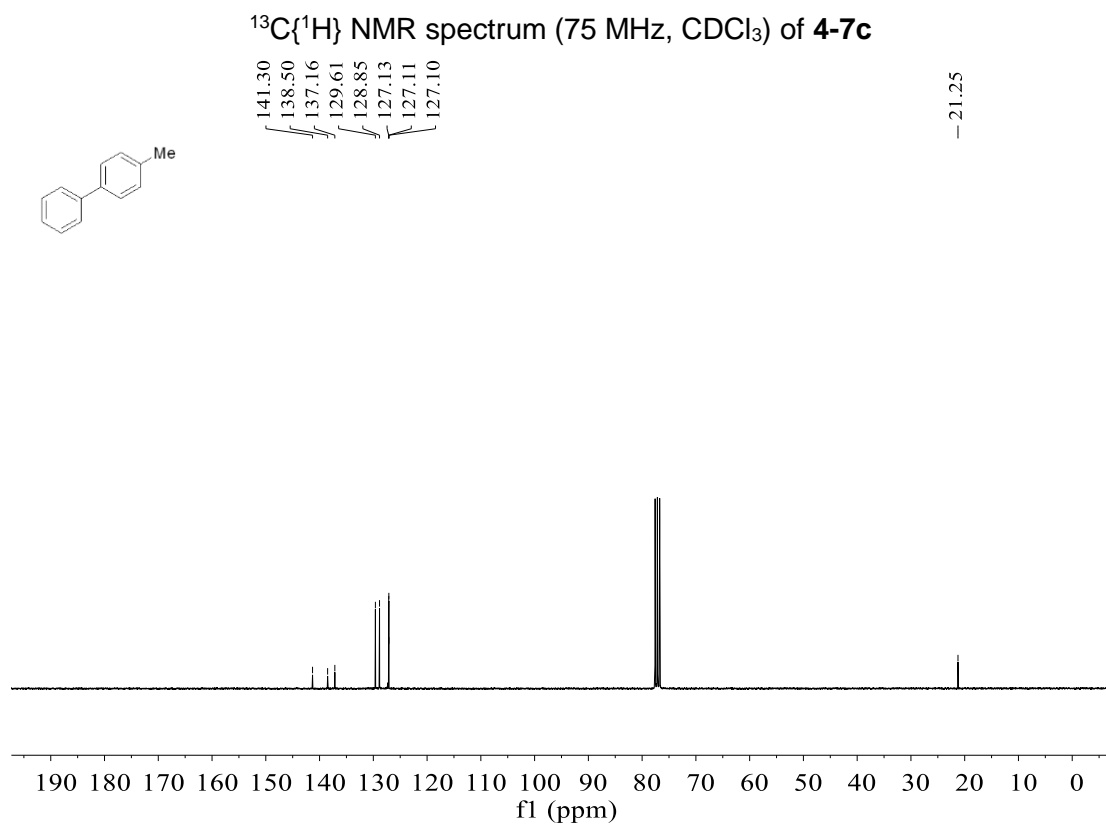
-78.24

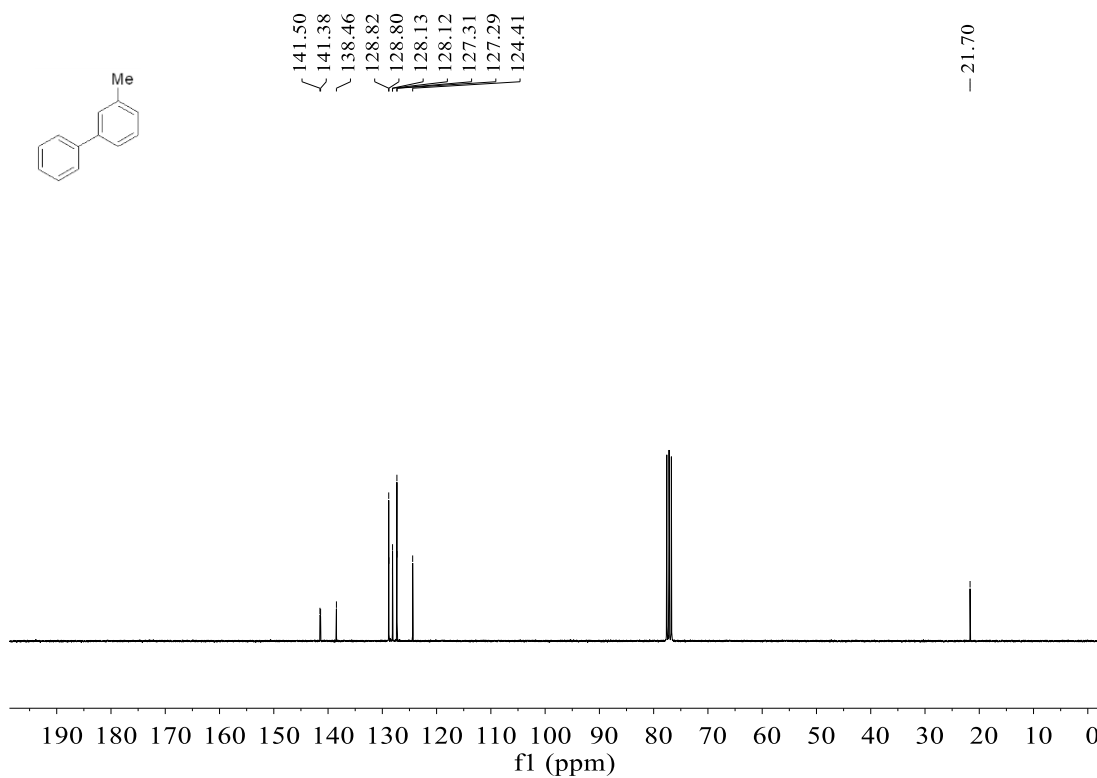
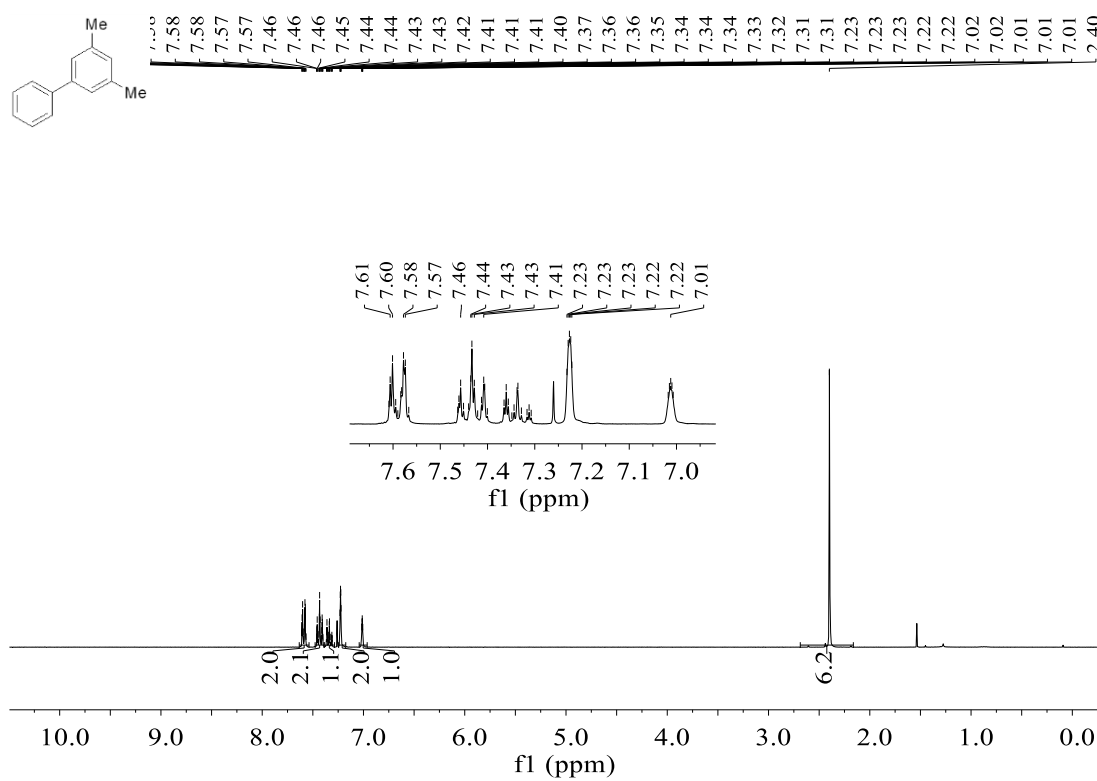


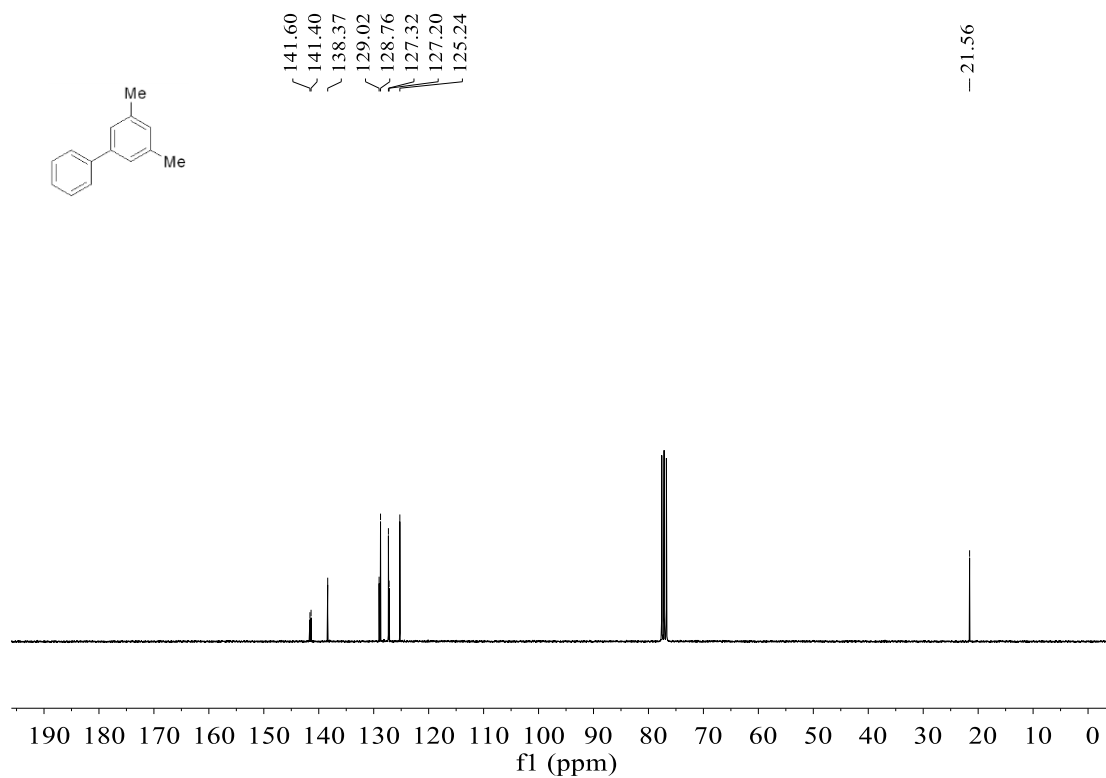
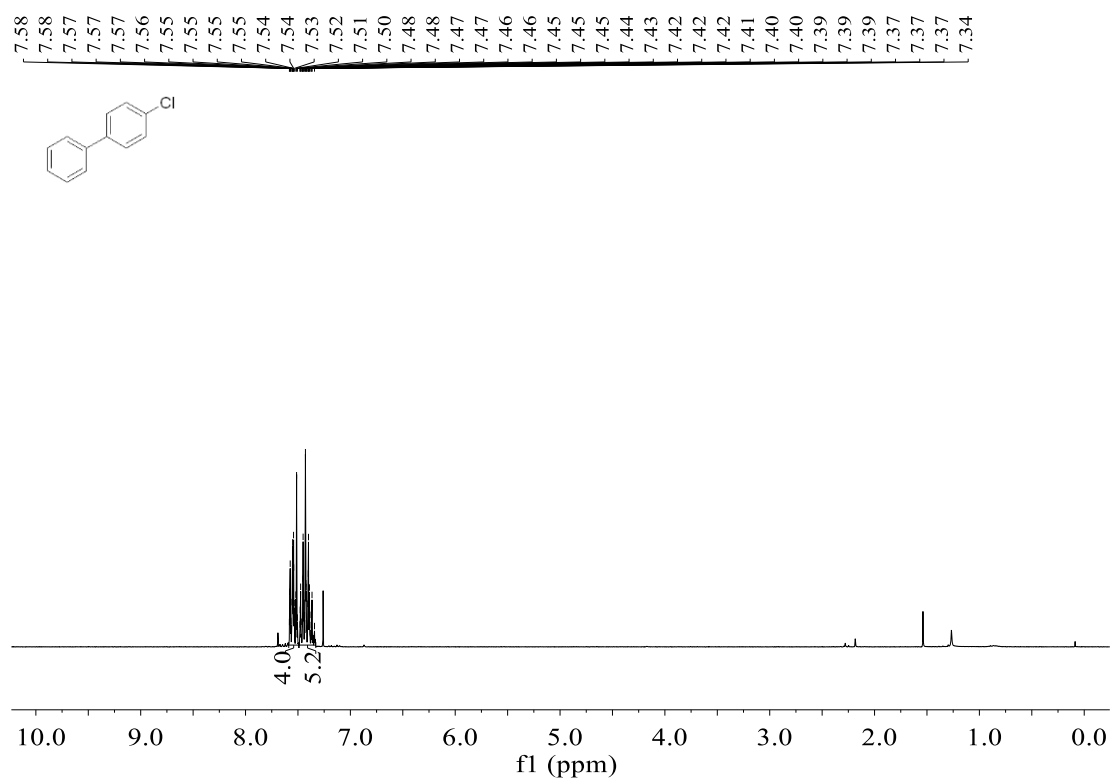
$^{31}\text{P}\{^1\text{H}\}$ NMR spectrum (202 MHz, CD_2Cl_2) of **4-4** ^1H NMR spectrum (300 MHz, CDCl_3) of **4-7a**

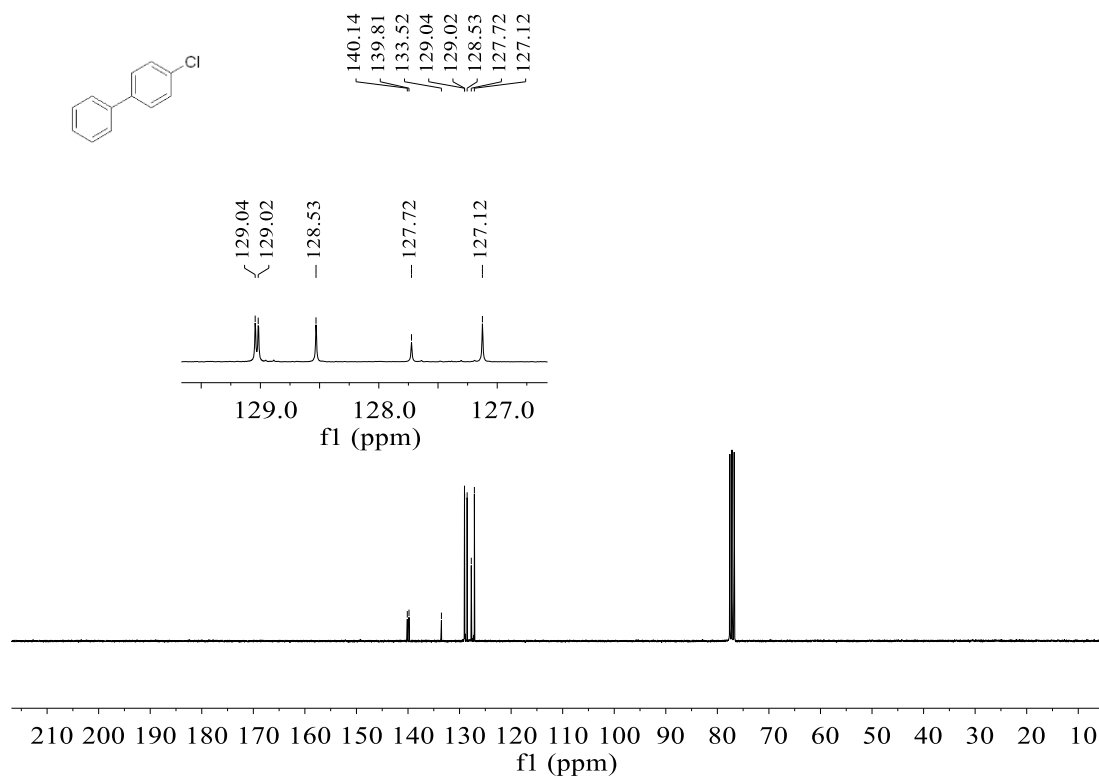
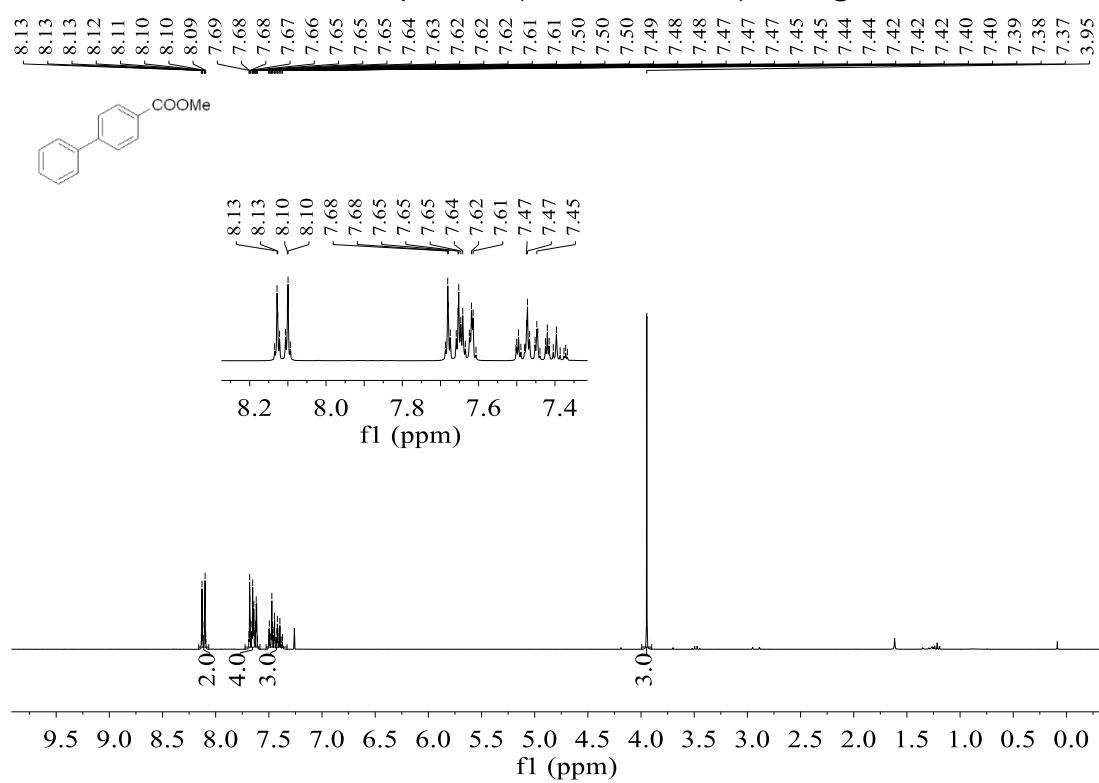
$^{13}\text{C}\{^1\text{H}\}$ NMR spectrum (75 MHz, CDCl_3) of **4-7a** ^1H NMR spectrum (300 MHz, CDCl_3) of **4-7b**

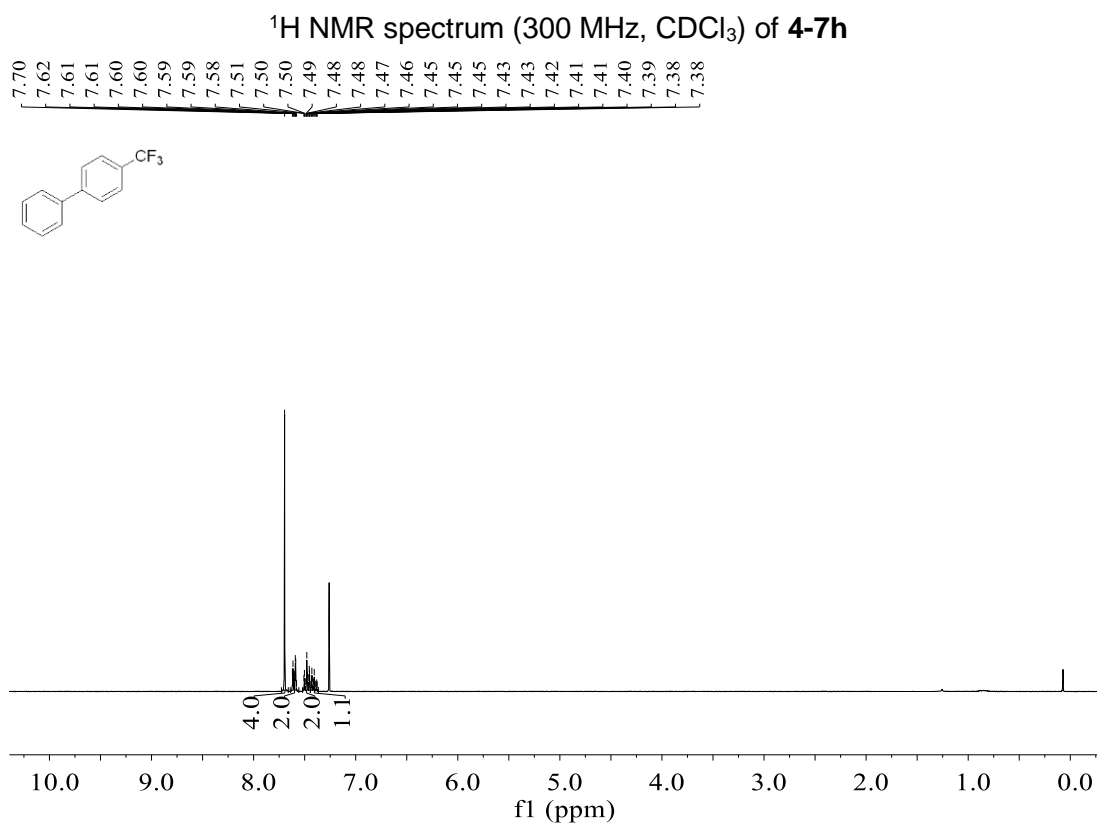
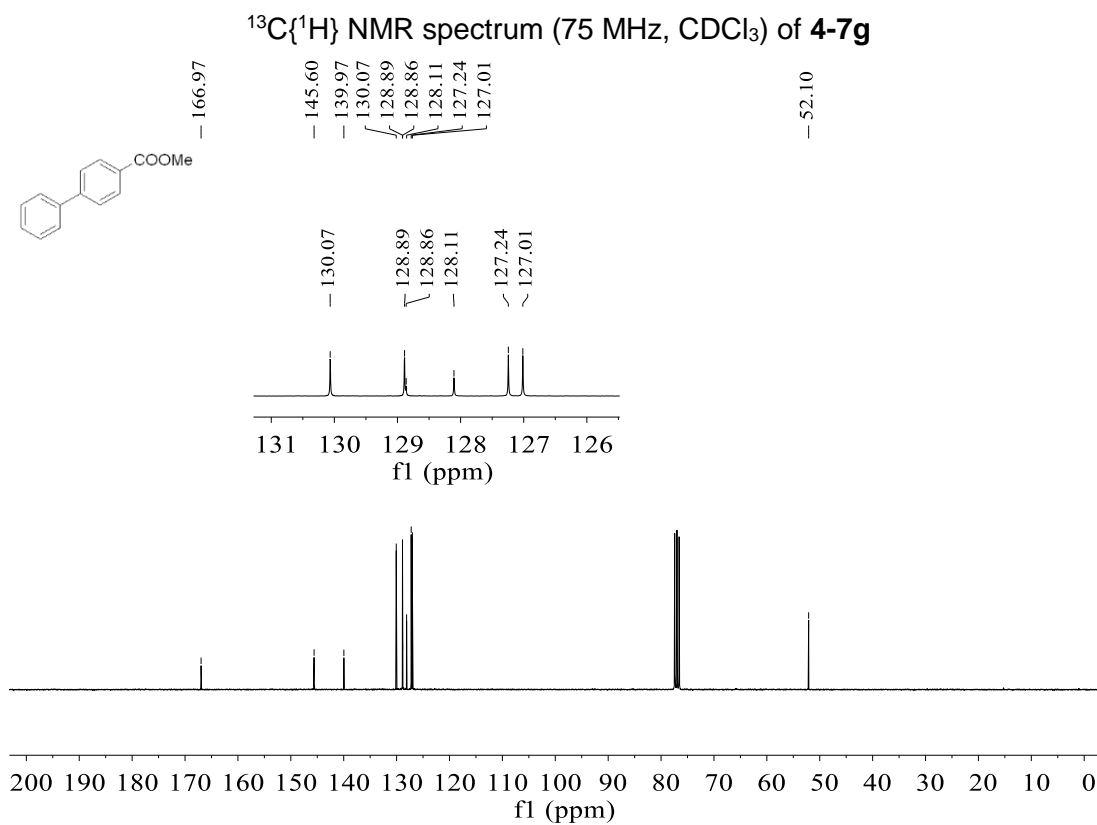
$^{13}\text{C}\{^1\text{H}\}$ NMR spectrum (75 MHz, CDCl_3) of **4-7b** ^1H NMR spectrum (300 MHz, CDCl_3) of **4-7c**

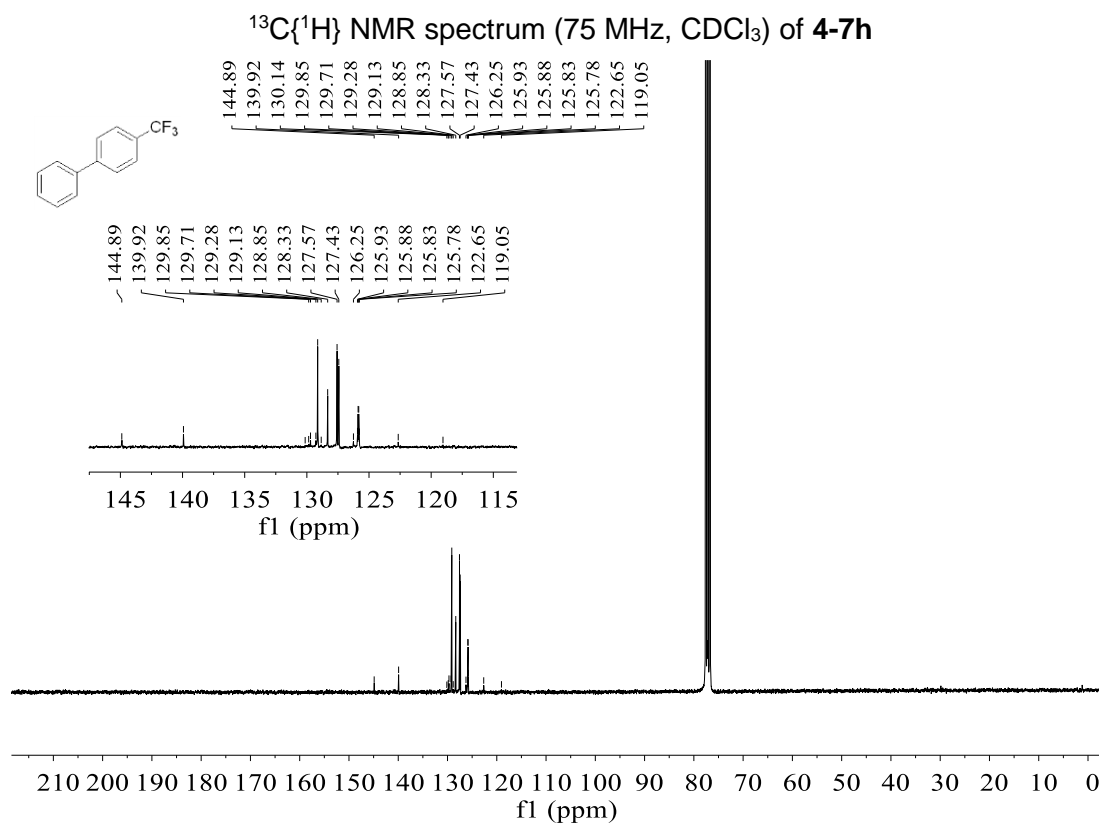


$^{13}\text{C}\{^1\text{H}\}$ NMR spectrum (75 MHz, CDCl_3) of **4-7d** ^1H NMR spectrum (300 MHz, CDCl_3) of **4-7e**


$^{13}\text{C}\{^1\text{H}\}$ NMR spectrum (75 MHz, CDCl_3) of **4-7e** ^1H NMR spectrum (300 MHz, CDCl_3) of **4-7f**

$^{13}\text{C}\{^1\text{H}\}$ NMR spectrum (75 MHz, CDCl_3) of **4-7f** ^1H NMR spectrum (300 MHz, CDCl_3) of **4-7g**






Permission of American Chemical Society



RightsLink

[Home](#)
[Help](#)
[Email Support](#)
[Sign in](#)
[Create Account](#)



The Borono–Strecker Reaction: Synthesis of α -Aminoboronates via a Multicomponent Reaction of Carbonyl Compounds, Amines, and B2pin2

Author: Wenbo Ming, Xiaocui Liu, Alexandra Friedrich, et al

Publication: Organic Letters

Publisher: American Chemical Society

Date: Dec 1, 2019

Copyright © 2019, American Chemical Society

Quick Price Estimate

This service provides permission for reuse only. If you do not have a copy of the article you are using, you may copy and paste the content and reuse according to the terms of your agreement. Please be advised that obtaining the content you license is a separate transaction not involving RightsLink.

Permission for this particular request is granted for print and electronic formats, and translations, at no charge. Figures and tables may be modified. Appropriate credit should be given. Please print this page for your records and provide a copy to your publisher. Requests for up to 4 figures require only this record. Five or more figures will generate a printout of additional terms and conditions. Appropriate credit should read: "Reprinted with permission from (COMPLETE REFERENCE CITATION). Copyright (YEAR) American Chemical Society." Insert appropriate information in place of the capitalized words.

I would like to...

Requestor Type

Portion

Format

Will you be translating?


Select your currency

Quick Price

To request permission for a type of use not listed, please contact the publisher directly.


© 2019 Copyright - All Rights Reserved | Copyright Clearance Center, Inc. | Privacy statement | Terms and Conditions

Comments? We would like to hear from you. E-mail us at customer@copyright.com



RightsLink

[Home](#)
[Help](#)
[Email Support](#)
[Sign in](#)
[Create Account](#)



The Borono–Strecker Reaction: Synthesis of α -Aminoboronates via a Multicomponent Reaction of Carbonyl Compounds, Amines, and B2pin2

Author: Wenbo Ming, Xiaocui Liu, Alexandra Friedrich, et al

Publication: Organic Letters

Publisher: American Chemical Society

Date: Dec 1, 2019

Copyright © 2019, American Chemical Society

PERMISSION/LICENSE IS GRANTED FOR YOUR ORDER AT NO CHARGE

This type of permission/license, instead of the standard Terms & Conditions, is sent to you because no fee is being charged for your order. Please note the following:

- Permission is granted for your request in both print and electronic formats, and translations.
- If figures and/or tables were requested, they may be adapted or used in part.
- Please print this page for your records and send a copy of it to your publisher/graduate school.
- Appropriate credit for the requested material should be given as follows: "Reprinted (adapted) with permission from (COMPLETE REFERENCE CITATION). Copyright (YEAR) American Chemical Society." Insert appropriate information in place of the capitalized words.
- One-time permission is granted only for the use specified in your request. No additional uses are granted (such as derivative works or other editions). For any other uses, please submit a new request.

© 2019 Copyright - All Rights Reserved | Copyright Clearance Center, Inc. | Privacy statement | Terms and Conditions

Comments? We would like to hear from you. E-mail us at customer@copyright.com

Affidavit

I hereby confirm that my theses entitled "*Synthesis of α -Aminoboronates and PBP Pincer Palladium Boryl Complexes*" is the result of my own work. I did not receive any help or support from commercial consultants. All sources and/or materials applied are listed and specified in the thesis. Furthermore, I confirm that this thesis has not yet been submitted as part of another examination process neither in identical nor similar form.

Würzburg, 01. 12. 2019

Signature

Eidesstaatliche Erklärung

Hiermit erkläre ich an Eides statt, die Dissertation „*Synthesis of α -Aminoboronates and PBP Pincer Palladium Boryl Complexes*“ eigenständig, d.h. insbesondere selbstständig und ohne Hilfe eines kommerziellen Promotionsberaters angefertigt und keinen anderen als die von mir angegebenen Quellen und Hilfsmittel verwendet zu haben. Ich erkläre außerdem, dass die Dissertation weder in gleicher noch ähnlicher Form bereits in einem anderen Prüfungsverfahren vorgelegen hat.

Würzburg, 01. 12. 2019

Unterschrift